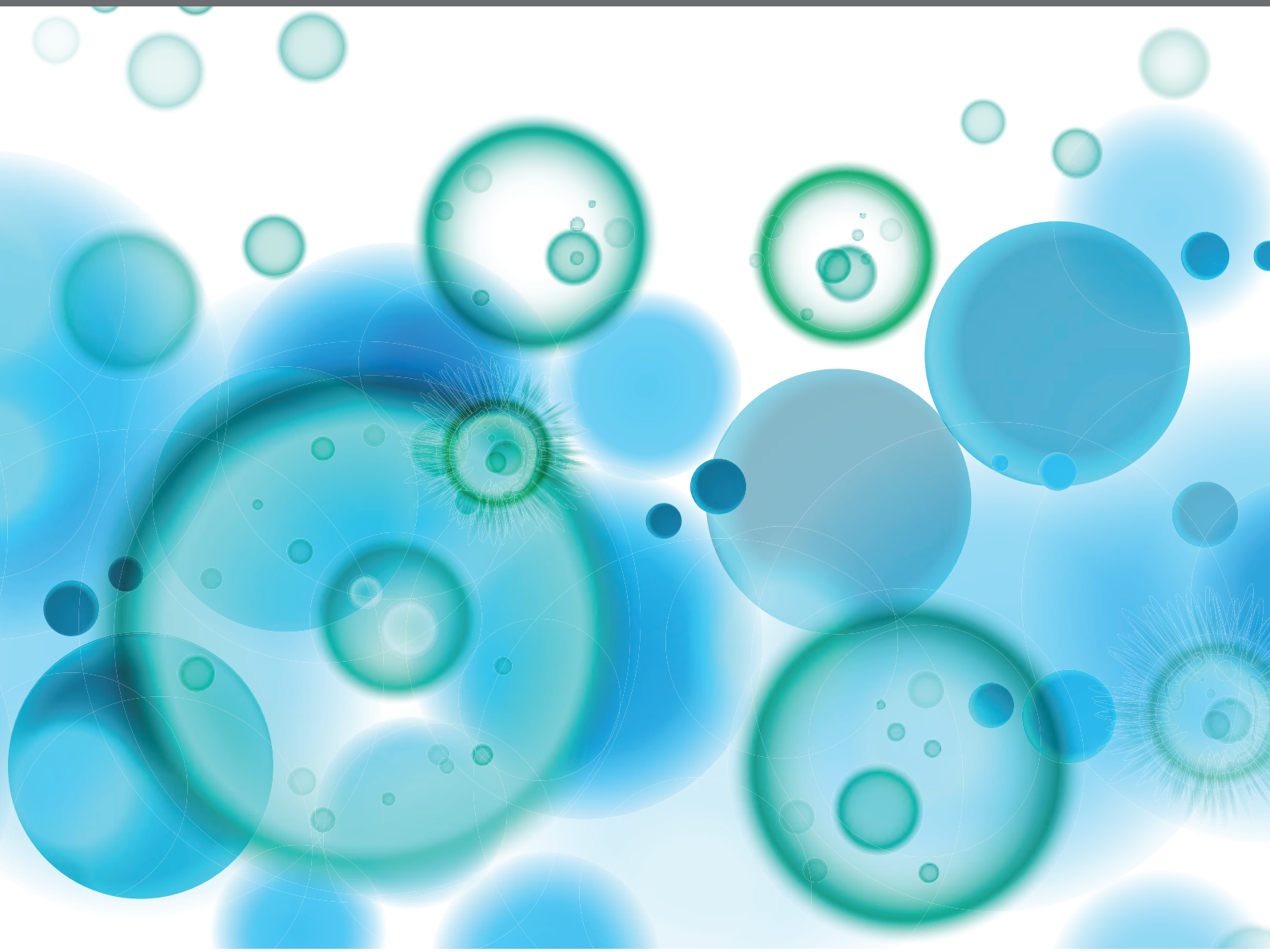
VACCINES AND IMMUNOSTIMULANTS FOR FINFISH

EDITED BY: Hetron Mweemba Munang'andu, Irene Salinas, Roy Ambli Dalmo and Carolina Tafalla

PUBLISHED IN: Frontiers in Immunology



frontiers Research Topics



frontiers

Frontiers eBook Copyright Statement

The copyright in the text of individual articles in this eBook is the property of their respective authors or their respective institutions or funders. The copyright in graphics and images within each article may be subject to copyright of other parties. In both cases this is subject to a license granted to Frontiers.

The compilation of articles constituting this eBook is the property of Frontiers.

Each article within this eBook, and the eBook itself, are published under the most recent version of the Creative Commons CC-BY licence. The version current at the date of publication of this eBook is CC-BY 4.0. If the CC-BY licence is updated, the licence granted by Frontiers is automatically updated to the new version.

When exercising any right under the CC-BY licence, Frontiers must be attributed as the original publisher of the article or eBook, as applicable.

Authors have the responsibility of ensuring that any graphics or other materials which are the property of others may be included in the CC-BY licence, but this should be checked before relying on the CC-BY licence to reproduce those materials. Any copyright notices relating to those materials must be complied with.

Copyright and source acknowledgement notices may not be removed and must be displayed in any copy, derivative work or partial copy which includes the elements in question.

All copyright, and all rights therein, are protected by national and international copyright laws. The above represents a summary only. For further information please read Frontiers' Conditions for Website Use and Copyright Statement, and the applicable CC-BY licence.

ISSN 1664-8714
ISBN 978-2-88966-173-2
DOI 10.3389/978-2-88966-173-2

About Frontiers

Frontiers is more than just an open-access publisher of scholarly articles: it is a pioneering approach to the world of academia, radically improving the way scholarly research is managed. The grand vision of Frontiers is a world where all people have an equal opportunity to seek, share and generate knowledge. Frontiers provides immediate and permanent online open access to all its publications, but this alone is not enough to realize our grand goals.

Frontiers Journal Series

The Frontiers Journal Series is a multi-tier and interdisciplinary set of open-access, online journals, promising a paradigm shift from the current review, selection and dissemination processes in academic publishing. All Frontiers journals are driven by researchers for researchers; therefore, they constitute a service to the scholarly community. At the same time, the Frontiers Journal Series operates on a revolutionary invention, the tiered publishing system, initially addressing specific communities of scholars, and gradually climbing up to broader public understanding, thus serving the interests of the lay society, too.

Dedication to Quality

Each Frontiers article is a landmark of the highest quality, thanks to genuinely collaborative interactions between authors and review editors, who include some of the world's best academicians. Research must be certified by peers before entering a stream of knowledge that may eventually reach the public - and shape society; therefore, Frontiers only applies the most rigorous and unbiased reviews.
Frontiers revolutionizes research publishing by freely delivering the most outstanding research, evaluated with no bias from both the academic and social point of view. By applying the most advanced information technologies, Frontiers is catapulting scholarly publishing into a new generation.

What are Frontiers Research Topics?

Frontiers Research Topics are very popular trademarks of the Frontiers Journals Series: they are collections of at least ten articles, all centered on a particular subject. With their unique mix of varied contributions from Original Research to Review Articles, Frontiers Research Topics unify the most influential researchers, the latest key findings and historical advances in a hot research area! Find out more on how to host your own Frontiers Research Topic or contribute to one as an author by contacting the Frontiers Editorial Office: researchtopics@frontiersin.org

VACCINES AND IMMUNOSTIMULANTS FOR FINFISH

Topic Editors:
Hetron Mweemba Munang'andu, Norwegian University of Life Sciences, Norway
Irene Salinas, University of New Mexico, United States
Roy Ambli Dalmo, Arctic University of Norway, Norway
Carolina Tafalla, National Institute for Agricultural and Food Research and Technology (INIA), Spain

Citation: Munang'andu, H. M., Salinas, I., Dalmo, R. A., Tafalla, C., eds. (2020). Vaccines and Immunostimulants for Finfish. Lausanne: Frontiers Media SA. doi: 10.3389/978-2-88966-173-2

Table of Contents

05 ***Editorial: Vaccines and Immunostimulants for Finfish***
Hetron M. Munang'andu, Irene Salinas, Carolina Tafalla and Roy Ambli Dalmo

09 ***Molecular Characterization, Phylogenetic, Expression, and Protective Immunity Analysis of OmpF, a Promising Candidate Immunogen Against* Yersinia ruckeri *Infection in Channel Catfish***
Erlong Wang, Zhenyang Qin, Zehui Yu, Xiaohui Ai, Kaiyu Wang, Qian Yang, Tao Liu, Defang Chen, Yi Geng, Xiaoli Huang, Ping Ouyang and Weimin Lai

24 ***A Novel Antigen-Sampling Cell in the Teleost Gill Epithelium With the Potential for Direct Antigen Presentation in Mucosal Tissue***
Goshi Kato, Haruya Miyazawa, Yumiko Nakayama, Yuki Ikari, Hidehiro Kondo, Takuya Yamaguchi, Motohiko Sano and Uwe Fischer

36 ***Origin of Public Memory B Cell Clones in Fish After Antiviral Vaccination***
Susana Magadan, Luc Jouneau, Maximilian Puelma Touzel, Simon Marillet, Wahiba Chara, Adrien Six, Edwige Quillet, Thierry Mora, Aleksandra M. Walczak, Frédéric Cazals, Oriol Sunyer, Simon Fillatreau and Pierre Boudinot

51 ***Studies on the Use of Flagellin as an Immunostimulant and Vaccine Adjuvant in Fish Aquaculture***
Eakapol Wangkahart, Christopher J. Secombes and Tiehui Wang

73 ***Trained Innate Immunity of Fish is a Viable Approach in Larval Aquaculture***
Zuobing Zhang, Heng Chi and Roy A. Dalmo

78 ***Profiling the Atlantic Salmon IgM$^+$ B Cell Surface Proteome: Novel Information on Teleost Fish B Cell Protein Repertoire and Identification of Potential B Cell Markers***
Ma. Michelle D. Peñaranda, Ingvill Jensen, Linn G. Tollersrud, Jack-Ansgar Bruun and Jorunn B. Jørgensen

97 ***Comparative Study of Immune Reaction Against Bacterial Infection From Transcriptome Analysis***
Shun Maekawa, Pei-Chi Wang and Shih-Chu Chen

110 ***Rainbow Trout (*Oncorhynchus Mykiss*) Intestinal Epithelial Cells as a Model for Studying Gut Immune Function and Effects of Functional Feed Ingredients***
Jie Wang, Peng Lei, Amr Ahmed Abdelrahim Gamil, Leidy Lagos, Yang Yue, Kristin Schirmer, Liv Torunn Mydland, Margareth Øverland, Åshild Krogdahl and Trond M. Kortner

127 ***Immunostimulatory Activities of CpG-Oligodeoxynucleotides in Teleosts: Toll-Like Receptors 9 and 21***
Chao-Yang Lai, Guann-Yi Yu, Yunping Luo, Rong Xiang and Tsung-Hsien Chuang

140 ***Comparative Extracellular Proteomics of* Aeromonas hydrophila *Reveals Iron-Regulated Secreted Proteins as Potential Vaccine Candidates***
Yuqian Wang, Xiaoyun Wang, Farman Ali, Zeqi Li, Yuying Fu, Xiaojun Yang, Wenxiong Lin and Xiangmin Lin

155 *Assessment of the Live Attenuated and Wild-Type* **Edwardsiella ictaluri-***Induced Immune Gene Expression and Langerhans-Like Cell Profiles in the Immune-Related Organs of Catfish*
Adef O. Kordon, Hossam Abdelhamed, Hamada Ahmed, Wes Baumgartner, Attila Karsi and Lesya M. Pinchuk

167 *CpGs Induce Differentiation of Atlantic Salmon Mononuclear Phagocytes Into Cells With Dendritic Morphology and a Proinflammatory Transcriptional Profile but an Exhausted Allostimulatory Activity*
Dimitar B. Iliev, Leidy Lagos, Hanna L. Thim, Sven M. Jørgensen, Aleksei Krasnov and Jorunn B. Jørgensen

179 *CpG Oligodeoxynucleotides Modulate Innate and Adaptive Functions of IgM$^+$ B Cells in Rainbow Trout*
Rocío Simón, Patricia Díaz-Rosales, Esther Morel, Diana Martín, Aitor G. Granja and Carolina Tafalla

193 *PACAP is Lethal to* **Flavobacterium psychrophilum** *Through Either Direct Membrane Permeabilization or Indirectly, by Priming the Immune Response in Rainbow Trout Macrophages*
Shawna L. Semple, Tania Rodríguez-Ramos, Yamila Carpio, John S. Lumsden, Mario P. Estrada and Brian Dixon

207 *Immunomodulatory Effects and Induction of Apoptosis by Different Molecular Weight Chitosan Oligosaccharides in Head Kidney Macrophages From Blunt Snout Bream (***Megalobrama amblycephala***)*
Changsong Wu, Yishan Dai, Gailing Yuan, Jianguo Su and Xiaoling Liu

220 *Evaluation of a Recombinant* **Flavobacterium columnare** *DnaK Protein Vaccine as a Means of Protection Against Columnaris Disease in Channel Catfish (***Ictalurus punctatus***)*
Miles D. Lange, Jason Abernathy and Bradley D. Farmer

233 *Recombinant ATPase of Virulent* **Aeromonas hydrophila** *Protects Channel Catfish Against Motile* **Aeromonas** *Septicemia*
Hossam Abdelhamed, Michelle Banes, Attila Karsi and Mark L. Lawrence

240 *Metabolites-Enabled Survival of Crucian Carps Infected by* **Edwardsiella tarda** *in High Water Temperature*
Ming Jiang, Zhuang-gui Chen, Jun Zheng and Bo Peng

254 *Detection of Salmonid IgM Specific to the* **Piscine Orthoreovirus** *Outer Capsid Spike Protein Sigma 1 Using Lipid-Modified Antigens in a Bead-Based Antibody Detection Assay*
Lena Hammerlund Teige, Subramani Kumar, Grethe M. Johansen, Øystein Wessel, Niccolò Vendramin, Morten Lund, Espen Rimstad, Preben Boysen and Maria K. Dahle

266 *Application of Outer Membrane Protein-Based Vaccines Against Major Bacterial Fish Pathogens in India*
Biswajit Maiti, Saurabh Dubey, Hetron Mweemba Munang'andu, Iddya Karunasagar, Indrani Karunasagar and Øystein Evensen

frontiers in Immunology

EDITORIAL
published: 29 September 2020
doi: 10.3389/fimmu.2020.573771

Editorial: Vaccines and Immunostimulants for Finfish

Hetron M. Munang'andu[1]*, *Irene Salinas*[2], *Carolina Tafalla*[3] and *Roy Ambli Dalmo*[4]

[1] Faculty of Veterinary Medicine, Norwegian University of Life Sciences, Oslo, Norway, [2] Biology Department, University of New Mexico, Albuquerque, NM, United States, [3] Animal Health Research Center (Centro de Investigación en Sanidad Animal - Instituto Nacional De Investigaciones Agrarias), Madrid, Spain, [4] Universitet i Tromsø – The Arctic University of Norway, Tromsø, Norway

Keywords: vaccines, immunostimulants, antigens, correlates of protection, immune training

Editorial on the Research Topic

Vaccines and Immunostimulants for Finfish

The expansion of intensive fish farming in recent decades has led to increase in the number of fish diseases (1, 2). This is partly because high stocking densities used in intensive farming cause stress making fish more susceptible to diseases and lead to high disease transmission index due increased contact among fish. These factors call for the need of protective vaccines (3). Understanding how the fish immune system responds to vaccines and immunostimulants/adjuvants is crucial for the rational development of efficient vaccines. These studies should guide the design and selection of effective immunostimulants and vaccine antigens that are efficiently taken up, processed and presented to cells of the adaptive immune system. Another priority of the field is the identification of optimal correlates of protective immunity that may be used as benchmarks in the design of long-term protective fish vaccines. This has traditionally been a challenge due to poor correlation between protection and antibody responses (4), but new emerging tools should complement traditional serological assays. The compilation of studies presented in this Special Issue provides an updated look on various immunostimulants and vaccine antigens relevant to farmed fish health. In addition, these papers also provide an update on recent discoveries in fish immunology that could aid in the design of highly protective vaccines for finfish, as well as to establish correlates of protection for these vaccines. Thus, we envisage that this Special Issue provides novel valuable insights essential for all researches working on the development and implementation of immune strategies that reduce the impact of infectious diseases in aquaculture.

IMMUNOSTIMULANTS AND INNATE IMMUNE RESPONSES

Immunostimulants (IMM) have historically been defined as substances that have the capacity to increase innate immune responses (5). But because innate responses have been shown to greatly influence adaptive responses, their administration along with vaccine antigens also influences the adaptive immune responses specifically mounted to the antigen. In this case, we refer to these immunostimulants as adjuvants. The term adjuvant is from the latin "adjuvare" meaning to help. As an example, immunostimulants such as certain oligosaccharides, CpGs, LPS, β-glucans, or flagellin can be administered parenterally or orally to fish without a vaccine to increase the general immune status of the fish (6) or they can be given together with a vaccine antigen (7). To date, commercial vaccines mostly use mineral oils as adjuvants (5). These mineral oils help induce a more robust immune response than the antigen alone by increasing the immunogenicity of weak antigens, prolonging the duration of antigen release at the injection site, and also stimulating and modulating adaptive immune responses. The use of IMM as adjuvants has been exclusively assayed experimentally, but they need to be more focused on specific immune functions that are beneficial

OPEN ACCESS

Edited and reviewed by:
Geert Wiegertjes, Wageningen University and Research, Netherlands

***Correspondence:**
Hetron M. Munang'andu
hetroney.mweemba.munangandu@nmbu.no

Specialty section:
This article was submitted to Comparative Immunology, a section of the journal Frontiers in Immunology

Received: *18 June 2020*
Accepted: *24 August 2020*
Published: *29 September 2020*

Citation:
Munang'andu HM, Salinas I, Tafalla C and Dalmo RA (2020) Editorial: Vaccines and Immunostimulants for Finfish. Front. Immunol. 11:573771. doi: 10.3389/fimmu.2020.573771

for a defined antigen, without provoking a massive pro-inflammatory response that can lead to unwanted side effects. Thus, IMM can for example promote expression and secretion of cytokines, soluble factors and enzymes that modulate migration of leukocytes to antigen deposition sites, enhance antigen uptake and the intracellular processing and presentation of antigen to cells of the adaptive immune systems (5). Among a broad range of IMM, chitosan oligosaccharides (COSs), synthetic pituitary adenylate cyclase-activating polypeptide (PACAP), CpGs, and flagellin have all been shown to stimulate the effector functions of monocytes, macrophages, dendritic-like, and B cells in fish. The study performed by Wu et al. showed that activation of macrophages using three different molecular weight COSs (∼500, ∼1,000, and 2,000∼3,000 Da) correlated with different chitosan oligosaccharides molecular weights (COS-MWs) of which the COS-MW with highest molecular weight had the highest activation of macrophages. In another study, Semple et al. showed that monocyte/macrophage- RTS11 cells pre-treated with PACAP 24 h before infection, severely inhibited *Flavobacterium psychrophilum* growth and increased expression of pro-inflammatory cytokines together with PACAP receptors in a dose-dependent manner. Simón et al. showed that CpGs increased the survival of IgM^+ B cells, induced their proliferation and differentiation to plasmablasts/plasma cells, upregulated MHC-II and co-stimulatory molecules, and increased their phagocytic capacity while Iliev et al. showed that CpG stimulation transformed the rainbow trout primary phagocytes into dendritic-like-cells exhibiting long branching pseudopodia. These dendritic-like cells expressed high pro-inflammatory genes belonging to a Th17 response (IL-17A/F1) and a Th2 response (IL-4/13) where IL-10 and IFNγ was downregulated. Both studies demonstrated that CpGs are capable of modulating both the innate and adaptive branches of the immune system in fish, thus pointing to these molecules as optimal vaccine adjuvants. To gain further insight on how these CpGs are recognized by the host, Lai et al. performed an in depth study that points out that recognition of CpGs in fish is carried out by two sensors, namely Toll-like receptor 9 (TLR9) and TLR21, consequently demonstrating that the signaling of CpGs is more complex in fish than in mammals that only use TLR9 as a CpG sensor. Wangkahart et al. showed that *Yersinia ruckeri* flagellin upregulated several pro-inflammatory cytokines, acute phase proteins, antimicrobial peptides and complement genes in multiple tissues after *in vivo* administration, results that point to flagellin as another potent immunostimulant/adjuvant for fish aquaculture.

Developing *in vitro* models for studying immune responses to vaccine antigens or to IMM, is of great interest, to reduce the use of animals and pre-evaluate the potential of these substances through an easy method. In this sense, Wang J. et al. developed an *in vitro* model for studying responses to immunostimulation in the gut using rainbow trout intestinal epithelial cells (RTgutGC) propagated on conventional culture plates and transwell membranes, which they used to evaluate gut responses to stimulation by LPS and three functional feed ingredients namely; (i) mannanoligosaccharides (MOS), (ii) β-glucans, and (iii) nucleotides. MOS was found to be the most potent immunostimulant that upregulated several inflammatory cytokines such IL-1β, IL-6, IL-8, TNFα, and TGFβ at similar levels with LPS while nucleotides and β-glucans only upregulated IL-1β and IL-8. Overall, RTgutGC cells had features characteristic of functional intestinal cells and therefore offer a useful *in vitro* model useful for evaluating the effects of IMM and feed ingredients on gut immune responses.

TRAINED IMMUNITY

Recent advances in innate immune studies show that both myeloid cells such as monocytes, macrophages and dendritic cells display changes in their metabolic and epigenetic programming to become hyperresponsive to second stimulation by the same antigen (8). This *de facto* "innate immune memory" is commonly referred to as "trained immunity" (8). The review by Zhang et al. discusses the role of IMMs such as β-glucans and TLR ligands in trained innate immunity in fish. Additionally, they describe how trained immunity can be introduced in brood stock fish and their offspring, highlighting its potential application as an alternative method to conventional vaccination.

ANTIGEN SAMPLING CELLS

Antigen uptake through mucosal surfaces by specific antigen sampling cells (ASCs) is well-documented in mammals where it is mainly done by M-cells (9). However, specific ASCs have not been described in fish despite the identification of several mucosal tissues that include the gills, skin, the digestive tract and the nose. To gain further insight on antigen uptake at mucosal surfaces, a key process for the optimization of mucosal vaccines, Kato et al. identified two phenotypes of ASCs able to take up antigens through rainbow trout gills. One phenotype had large vacuoles in the cytoplasm and expressed CD45, MHC-II, CD83, IL-1β, and IL-12p40b. Morphologically, this subset features of monocyte, macrophage and dendritic cells. The second phenotype exhibited features similar to mammalian M-cells that bind lectin UEA-1 but not WGA and expressed the surface marker Anxa5. Unlike mammalian M-cells, teleost M-like-cells possessed small vacuoles in the cytoplasm, but played a role in antigen sampling using mechanisms similar to the bona-fide M-cells and expressed genes linked to phagosome, lysosome, and antigen processing and presentation pathways seen in mammalian M-cells.

IDENTIFICATION OF PROTECTIVE ANTIGENS FOR VACCINE DESIGN

Pathogen diversity poses a challenge for the selection of vaccine candidates with broad protective ability across variant strains. To this aim, various techniques aimed at identifying vaccine antigen candidates with broad protective abilities are being sought. For example, Wang Y. et al. used the isobaric tag for relative and absolute quantification (iTRAQ), to identify protective biomarkers among 341 *Aeromonas hydrophila* genes expressed in response to iron starvation. By knocking out three genes that had low protease activity, they constructed three

avirulent mutants as live vaccines that produced high protection in zebrafish (*Danio rerio*). Another approach used to identify broadly protective antigens is by performing multiple sequence alignments to identify conserved antigenic proteins protective across variant strains. Wang E. et al. used this approach to design a *Yersinia ruckeri* outer membrane porin F (OmpF) vaccine after identifying a highly conserved motif among 15 sequences of *Yersinia* species, which confered increased protection and high antibody responses in channel catfish. Similarly, the paper by Maiti et al. provides a detailed account of various *in silico* and bioinformatics analytical tools used to identify outer membrane protein (OMP) antigens with broad protective abilities against variant strains of different bacterial species infecting major farmed fish species in India.

LIVE ATTENUATED AND RECOMBINANT VACCINES

Although there are many commercial antibacterial vaccines available for use in aquaculture, there are still some bacterial pathogens for which vaccines have not been developed or are deficient. In this Special Issue, different recombinant approaches have been explored. Abdelhamed et al. produced a recombinant *A. hydrophila* ATPase protein vaccine that showed increased survival and reduced bacterial concentrations in different tissues of catfish after challenge with virulent *A. hydrophila* ML09-119 strain. Lange et al. showed a progressive increase of systemic and mucosal IgM levels over a period of 2 years in catfish immunized by bath using a recombinant DnaK (rDnaK) vaccine made from the *Flavobacterium columnare* DnaK heat-shock-protein (Hsp70 protein). Finally, Maiti et al. reviewed the use of outer membrane proteins (OMPs) as subunit, DNA and nanoparticle vaccines against different pathogens infecting farmed fish in India. In the case of intracellular replicating bacteria, an efficient vaccine should be able to evoke both humoral and cell-mediated immune responses able to eliminate infected cells. To this end, Kordon et al. developed two live attenuated vaccines (LAVs) designated as *Ei*Δ*evpB*, and ESC-NDKL1 against *Edwardsiella ictaluri,* a facultative intracellular replicating bacterium. Both LAVs elevated IFN-γ expression in lymphoid organs that correlated with increased $CD207^+$ cells and polarization of T-helper genes in vaccinated catfish.

TEMPERATURE MANIPULATION AND HOST METABOLISM

Temperature manipulation is an important factor known to alter virulence of various fish pathogens (10) as well as the immune responses of the fish host (11). Although several studies have shown that virulence factors can be controlled by thermo-sensors in different bacterial pathogens (10, 12), little is known regarding how modulating temperature changes influence the ability of the host responses to mount protective immune responses against invading pathogens. The study undertaken by Jiang et al. showed that crucian carp (*Carassius carassiuss*) cultured at 30°C showed an increased tricarboxylic acid (TCA) cycle linked to reduced taurine and hypotaurine metabolism coupled with low unsaturated fatty acid biosynthesis, which enhanced bacterial infection in a dose-dependent manner in fish. Conversely, exogenous treatment of fish using these metabolites increased fish survival and rescued the decline of pro-inflammatory cytokine expression that included TNF-α1, TNF-α2, IL-1β1, IL-1β2, and lyz expression. This study shows that changes in the interplay between temperature and fish metabolism can be used to regulate immune protection against bacterial infection in fish.

B CELL IMMUNE RESPONSES IN VACCINATED FISH

Antibody production together with cell mediated immune responses constitute the hallmark of long-term protective immunity in vaccinated fish. As such, antibodies produced by B cells, are widely used as a measure of immune response to vaccination in fish (4). Along this line, Teige et al. developed a multiplexed bead antibody assay able to differentiate antibody responses induced by piscine reovirus (PRV) σ1, σ2, and σ3 antigens. In trying to elucidate factors driving the specificity of fish antibodies, Magadan et al. searched for "public" antibody clonotypes common to all individuals that may mediate universal protection against pathogens. Through CD3 spectratyping of splenic B cells 5 months after vaccination with an attenuated viral haemorrhagic septicaemia virus (VHSV) vaccine, they showed that the IgM repertoires of vaccinated fish had altered profiles for the heavy chain variables (VH) VH1, VH4, and VH5 families. The altered profile of VH5 was the only clonotype found in all vaccinated individuals, suggesting that it may contain a persisting public component, while responses associated with VH1 and VH4 varied from fish to fish. Further analysis of the variable (V), joining (J), and diversity (D) gene segments showed that the VH5 and JH5 clonotypes formed persistent public VH5JH5 IgM dominant antibodies common to all vaccinated individuals. In addition to these studies, Peñaranda et al. obtained a cell surface proteome of Atlantic salmon IgM^+ B cells by mass spectrometry and comparing it to that of two adherent salmon head kidney cell lines and used it to identify specific markers of B cells, namely CD22 and CD79A, in salmon. The identification of these molecules is very important to track B cell responses to vaccines and/or immunostimulants in the future.

MEASURES OF PROTECTIVE IMMUNITY FOR FISH VACCINES

To a large extent, the correlates of protective immunity for most fish vaccines are unknown. Moreover, whether common signatures of protective immunity across different fish species can be identified or not remains a challenge. However, novel high throughput sequencing (HTS) techniques such as RNA-seq that provide whole transcriptomes of immune genes expressed in response to different stimuli are beginning to unravel different molecular markers that could serve as signatures of protective immunity expressed by different fish species in response to different pathogens. The study performed by Maekawa et al.

describes the use of RNA-seq as a useful tool used to identify the universality and diversity of immune responses against different pathogens expressed in different fish species by comparing immune genes expressed in response to *Nocardia seriolae* in largemouth bass (*Micropterus salmoides*), *Lactococcus garvieae* in gray mullet (*Mugil cephalus*), *Vibrio harveyi* in orange-spotted grouper (*Epinephelus coioides*), and *Aeromonas sobria* in koi carp (*Cyprinus carpio*). They found 39 differentially expressed immune genes that were present in all fish species having the potential to serve as universal immunological markers of protective immunity. This study suggests that common signatures of protective immunity can be identified for use across different fish species.

Overall, the ccontributions gathered in this Special Issue provide a wide range of novel approaches and technologies being developed aimed at producing highly protective vaccines for finfish. What is now required is translation of these experimental findings to the fish farming industry with the objective of reducing the disease burden in aquaculture through vaccination.

AUTHOR CONTRIBUTIONS

All authors listed have made a substantial, direct and intellectual contribution to the work, and approved it for publication.

ACKNOWLEDGMENTS

We acknowledge the Frontiers Immunology Journal for allowing us to Serve as Guest editorson the Special Issue on Vaccines and Immunostimulants of finfish.

REFERENCES

1. FAO. *The State of World Fisheries and Aquaculture*. Food Agriculture Organization of the United Nations (2018).
2. Munang'andu HM, Mugimba KK, Byarugaba DK, Mutoloki S, Evensen Ø. Current advances on virus discovery and diagnostic role of viral metagenomics in aquatic organisms. *Front Microbiol.* (2017) 8:406. doi: 10.3389/fmicb.2017.00406
3. Gudding R, Lillehaug A, Evensen O. *Fish Vaccination.* South Gate; Chichester; West Sussex: John Wiley & Sons, Ltd.; The Atrium (2014). doi: 10.1002/9781118806913
4. Munang'andu HM, Evensen Ø. Correlates of protective immunity for fish vaccines. *Fish Shellfish Immunol.* (2019) 85:132–40. doi: 10.1016/j.fsi.2018.03.060
5. Tafalla C, Bøgwald J, Dalmo RA. Adjuvants and immunostimulants in fish vaccines: current knowledge and future perspectives. *Fish Shellfish Immunol.* (2013) 35:1740–50. doi: 10.1016/j.fsi.2013.02.029
6. Dawood MA, Koshio S, Esteban MÁ. Beneficial roles of feed additives as immunostimulants in aquaculture: a review. *Rev Aquac.* (2018) 10:950–74. doi: 10.1111/raq.12209
7. Anderson DP. Immunostimulants, adjuvants, and vaccine carriers in fish: applications to aquaculture. *Annu. Rev. Fish Dis.* (1992) 2:281–307. doi: 10.1016/0959-8030(92)90067-8
8. Netea MG, Joosten LA, Latz E, Mills KH, Natoli G, Stunnenberg HG, et al. Trained immunity: a program of innate immune memory in health and disease. *Science.* (2016) 352:aaf1098. doi: 10.1126/science.aaf1098
9. Neutra M. M cells in antigen sampling in mucosal tissues. In: Kraehenbuhl J-P, Neutra MR, editors. *Defense of Mucosal Surfaces: Pathogenesis, Immunity and Vaccines.* Berlin; Heidelberg: Springer (1999). p. 17–32. doi: 10.1007/978-3-642-59951-4_2
10. Mekalanos JJ. Environmental signals controlling expression of virulence determinants in bacteria. *J Bacteriol.* (1992) 174:1. doi: 10.1128/JB.174.1.1-7.1992
11. Bowden TJ. Modulation of the immune system of fish by their environment. *Fish Shellfish Immunol.* (2008) 25:373–83. doi: 10.1016/j.fsi.2008.03.017
12. Balado M, Lages MA, Fuentes-Monteverde JC, Martínez-Matamoros D, Rodríguez J, Jiménez C, et al. The siderophore piscibactin is a relevant virulence factor for *Vibrio anguillarum* favored at low temperatures. *Front Microbiol.* (2018) 9:1766. doi: 10.3389/fmicb.2018.01766

Conflict of Interest: The authors declare that the research was conducted in the absence of any commercial or financial relationships that could be construed as a potential conflict of interest.

Copyright © 2020 Munang'andu, Salinas, Tafalla and Dalmo. This is an open-access article distributed under the terms of the Creative Commons Attribution License (CC BY). The use, distribution or reproduction in other forums is permitted, provided the original author(s) and the copyright owner(s) are credited and that the original publication in this journal is cited, in accordance with accepted academic practice. No use, distribution or reproduction is permitted which does not comply with these terms.

frontiers in Immunology

ORIGINAL RESEARCH
published: 13 September 2018
doi: 10.3389/fimmu.2018.02003

Molecular Characterization, Phylogenetic, Expression, and Protective Immunity Analysis of OmpF, a Promising Candidate Immunogen Against *Yersinia ruckeri* Infection in Channel Catfish

Erlong Wang[1†], Zhenyang Qin[1†], Zehui Yu[1†], Xiaohui Ai[2†], Kaiyu Wang[1,3], Qian Yang[1], Tao Liu[1], Defang Chen[4], Yi Geng[1,3], Xiaoli Huang[4], Ping Ouyang[1] and Weimin Lai[1]*

[1] Department of Basic Veterinary, College of Veterinary Medicine, Sichuan Agricultural University, Chengdu, China, [2] Yangtze River Fisheries Research Institute, Chinese Academy of Fishery Sciences, Wuhan, China, [3] Key Laboratory of Animal Disease and Human Health of Sichuan Province, Sichuan Agricultural University, Chengdu, China, [4] Department of Aquaculture, College of Animal Science & Technology, Sichuan Agricultural University, Chengdu, China

Outer membrane porins, as the major components of Gram-negative bacterial membrane proteins, have been proven to be involved in interactions with the host immune system and potent protective antigen candidates against bacterial infection in fish. Outer membrane porin F (OmpF) is one of the major porins of *Yersinia ruckeri* (*Y. ruckeri*), the causative agent of enteric red mouth disease of salmonid and non-salmonid fish. In the present study, the molecular characterization and phylogenetic analysis of OmpF gene was studied, heterogenous expression, immunogenicity and protective immunity of OmpF were systemically evaluated as a subunit vaccine for channel catfish against *Y. ruckeri* infection. The results showed that OmpF gene was highly conserved among 15 known *Yersinia* species based on the analysis of conserved motifs, sequences alignment and phylogenetic tree, and was subjected to negative/purifying selection with global dN/dS ratios value of 0.649 throughout the evolution. Besides, OmpF was also identified to have immunogenicity by western blotting and was verified to be located on the surface of *Y. ruckeri* using cell surface staining and indirect immunofluorescence assays. Moreover, recombinant OmpF (rtOmpF) as a subunit vaccine was injected with commercial adjuvant ISA763, significantly enhanced the immune response by increasing serum antibody levels, lysozyme activity, complement C3 activity, total protein content, SOD activity, immune-related genes expression in the head kidney and spleen, and survival percent of channel catfish against *Y. ruckeri* infection. Thus, our present results not only enriched the information of molecular characterization and phylogenetics of OmpF, but also demonstrated that OmpF holds promise to be used as a potential antigen against *Y. ruckeri* infection in fish.

Keywords: ompF, molecular characterization, phylogenetic analysis, immunogenicity, immune effect, *Yersinia ruckeri*

OPEN ACCESS

Edited by:
Hetron Mweemba Munang'andu, Norwegian University of Life Sciences, Norway

Reviewed by:
Wenbin Zhan, Ocean University of China, China
Biswajit Maiti, Nitte University, India
Shih-Chu Chen, National Pingtung University of Science and Technology, Taiwan

***Correspondence:**
Kaiyu Wang
kywang1955@126.com

[†]These authors have contributed equally to this work

Specialty section:
This article was submitted to Comparative Immunology, a section of the journal Frontiers in Immunology

Received: *01 June 2018*
Accepted: *14 August 2018*
Published: *13 September 2018*

Citation:
Wang E, Qin Z, Yu Z, Ai X, Wang K, Yang Q, Liu T, Chen D, Geng Y, Huang X, Ouyang P and Lai W (2018) Molecular Characterization, Phylogenetic, Expression, and Protective Immunity Analysis of OmpF, a Promising Candidate Immunogen Against Yersinia ruckeri Infection in Channel Catfish. Front. Immunol. 9:2003. doi: 10.3389/fimmu.2018.02003

INTRODUCTION

Yersinia ruckeri (*Y. ruckeri*) is a Gram-negative rod-shaped enterobacterium and the causative agent of enteric red mouth disease (ERM), one of the most serious septicemic bacterial disease of salmonid fish species (1). It has been reported that *Y. ruckeri* has been increasingly widespread and been detected as an important pathogen of salmonid fish in many other countries (2–6) since its isolation in North American (7–10). Apart from salmonids, *Y. ruckeri* can also infect other non-salmonid fish species including common carp (11), whitefish (12), sturgeon (13–15), and channel catfish (16, 17). Alternative approaches to traditional control strategies include probiotics and vaccines, which may play greater significance in disease control due to the increasing antibiotic resistance of bacteria (18). Although vaccines against ERM have been widely used for more than 30 years, most of these vaccines are generally inactivated whole-cell vaccines (19–22) and live-attenuated vaccines (23), which have led to selective pressure leading to emergence of other serotypes (18). Moreover, concerns about the environmental safety restricted the commercial use of such live attenuated vaccines (18). Thus, genetically engineered vaccines based on conserved and potent protective antigen genes, are increasingly urgent and need to be developed.

Outer membrane proteins (OMPs) are the major components of Gram-negative bacterial membranes and essential in maintaining the integrity and selective permeability of the outer membrane (24). As one of the membrane surface molecules, OMPs are considered as the major targets of the membrane-environment interaction and easily recognized by the infected host compared with intracellular proteins (25). Bacterial porins, one of the most abundant OMPs (26), are the main channels for many hydrophilic nutrients and antibiotics (27), and are also involved in interactions with the host immune system due to their exposed antigen epitopes on bacterial surface (28). Many studies have reported that OMPs hold promise to serve as vaccine candidate and offer significant protection against bacterial infection in fish (29–39), including OmpA (31, 32), OmpC (33), OmpK (34), OmpN (35), OmpTS (36), OmpU (37), and OmpW (38, 39). OmpF is one of the major porins of *Enterobacteriaceae,* and has been reported to be the protective antigen and to provide desirable immunoprotection against pathogenic *Escherichia coli* (40) and *Salmonella enterica* (41). Besides, based on the perspective of structure and evolution, OmpF porin gene in genus *Yersinia* was comparably conserved in structure and homology and had putative antigenic epitopes located on several loops (42), indicating that it could be used as candidate protective antigen against *Y. ruckeri* infection.

Thus, in the present study, the molecular characterization and phylogenetic analysis of *Y. ruckeri* OmpF gene was studied, heterogenous expression was conducted to serve as a candidate immunogen, the immunogenicity and protective immunity of OmpF were also systemically evaluated as a subunit vaccine against *Y. ruckeri* infection in channel catfish, which was an excellent biological model for comparative immunology research in teleosts (43–45). Based on the results of this study, OmpF gene was inferred to be a novel protective antigen of *Y. ruckeri* and recombinant OmpF (rtOmpF) was a promising vaccine candidate for channel catfish against *Y. ruckeri* infection.

MATERIALS AND METHODS

Ethics Statement

The biosafety procedures of recombinant DNA technology and the use of laboratory animals in this study were carried out in strict accordance with the guidelines and recommendations of Chinese National Institute of Health. All the procedures of recombinant DNA technology and animal experiments were approved by the Institutional Animal Care and Use Committee of Sichuan Agricultural University (No. XF201418).

Bacterial Strains, Plasmids, Reagents, and Growth Conditions

Y. ruckeri YRWEL01, a fish pathogen isolated from dying channel catfish in Sichuan province of China, was cultured in Brain-Heart Infusion (BHI) medium at 28°C and stored at our laboratory (17). *Escherichia coli* strains DH5α and BL21 (DE3) competent cells (Takara; Dalian, China) served as cloning and protein expression host, respectively. Both strains were grown in Luria-Bertani medium containing 100 μg/ml of ampicillin (Amp) at 37°C. Plasmids pMD19-T (Takara) and pET32a (+) (Merck, Germany) served as cloning and expression vectors, respectively. Montanide™ ISA763 A VG (Seppic, France) was selected for use as an adjuvant for the experiment.

PCR Amplification and Molecular Cloning of OmpF

Y. ruckeri genomic DNA was extracted using a TIANamp Bacteria DNA extraction Kit (Tiangen, Beijing, China). The primers OmpF-F1/ OmpF-R1 of the target gene were designed using the Primer Premier 5.0 software based on the *Y. ruckeri* strain Nr34/85 OmpF gene sequence deposited in GenBank database (HM142671.1, corresponding OmpF protein accession no.: ADK27779.1). OmpF gene was amplified by PCR under the following conditions: 1 cycle of 94°C for 5 min, 30 cycles of 94°C for 1 min, 56°C for 30 s, and 72°C for 90 s, followed by a final extension of 72°C for 10 min. The product of PCR amplification was expected to be about 1098 bp and purified using the Agarose Gel DNA Extraction Kit (TaKaRa), ligated with the pMD19-T using T4 DNA ligase (TaKaRa) and transformed into *E. coli* DH5α competent cells. The positive recombinant clones were selected on the Amp/LB plate. The recombinant plasmid was identified by PCR under the aforementioned conditions, digested with restriction enzymes *Nco*I and *Sac*I, and fractionated on 1% agarose gels. DNA sequencing was conducted by TaKaRa Bio Inc. and the sequence was deposited in the NCBI GenBank to obtain accession number. The correct recombinant cloning plasmids were named as T-OmpF.

Sequence and Phylogenetic Analysis of OmpF

The opening reading frame of OmpF nucleotide sequence was analyzed using ORF Finder (46). The OmpF amino acid

sequences were derived from the nucleotide sequence. The signal peptide was predicted by SignalP 4.1 Server (47). To delineate the evolutionary dynamics of bacteria OmpF gene, the conserved domains and conserved motifs of OmpF in this study and other 25 reference bacteria OmpFs were searched using the Conserved Domain Database (CDD) in NCBI (48) and MEME software (49), respectively, their amino acid sequences identity were calculated using MegAlign program (DNASTAR, Madison, WI) (50), multiple sequences alignment was performed using MUSCLE (51), the phylogenetic tree was constructed using neighbor-joining method in MEGA 5 (52) with bootstrap test of 1000 replicates. To measure the selection pressures imposed on OmpF gene, the natural selection analysis was conducted based on the dN/dS ratios (the relative rates of non-synonymous (dN) and synonymous (dS) substitutions) which was calculated using Datamonkey (53).

Cloning, Expression, Purification, and Refolding of Truncate OmpF (tOmpF)

Based on the sequence analysis, the signal peptide was removed to obtain the mature OmpF by prokaryotic expression with *E. coli* BL21 (DE3). The truncated OmpF (tOmpF) gene was amplified using primers OmpF-F2/ OmpF-R2 (**Table 1**), which contained *Nco*I and *Sac*I restriction enzyme sites. The resultant amplicons were purified, ligated, transformed, and sequenced as described above, and the positive recombinant cloning plasmid was named as T-tOmpF.

The expression, purification, and refolding of recombinant tOmpF protein were performed as described in our previous studies (54, 55). Briefly, the cloned plasmid T-tOmpF was digested with *Nco*I and *Sac*I, and the resultant products and the *Nco*I /*Sac*I -digested pET32a (+) were ligated to construct the recombinant expression plasmid, named as P-tOmpF. Then, the plasmid P-tOmpF was transformed into *E. coli* BL21 and induced using 1.0 mM IPTG at 37°C for 4 h. Bacterial cells were harvested and resuspended with sterile phosphate buffer saline (PBS), followed by ultrasonication, and detection using 12.5% SDS-PAGE. The purification of recombinant tOmpF (rtOmpF), which was expressed in the form of inclusion bodies in the sediment was conducted using Ni-NTA-Sefinose Column (Sangon Biotech, Shanghai, China). The refolded tOmpF protein was obtained by gradient dialysis and analyzed using 12.5% SDS-PAGE. To rule out the potential bystander effects of LPS/or other impurities, endotoxin in recombinant protein was removed using ToxinEraserTM Endotoxin Removal kit (GenScript Corp. Nanjing, China), and the remaining endotoxin levels were measured using the Chromogenic End-point Endotoxin Assay kit (Limulus reagent biotechnology, Xiamen, China). Less than 0.1 EU/ml was detected in the final protein preparations. The protein was quantified using a NanoDrop spectrophotometer (Thermo Scientific) according to the manufacturer's instructions. Purified protein rtOmpF was stored at −20°C until further use.

Preparation of Rabbit Anti-*Y. ruckeri* and Anti-rtOmpF Antisera

Rabbit anti-*Y. ruckeri* and anti-rtOmpF antisera were prepared according to the method described previously (56) using formaldehyde-killed *Y. ruckeri* (3.0×10^9 CFU/ml) (57) and purified protein rtOmpF as the antigens, respectively. Briefly, New Zealand white rabbits were divided into three groups, one control group and two experimental groups. The purified rtOmpF (2 mg/ml) used as the antigen was emulsified with an equal volume of Freund's Complete Adjuvant (FCA, Sigma, USA) and injected intravenously into rabbits, followed by three intravenous booster injections of rtOmpF-FIA (Freund's Incomplete Adjuvant, Sigma) at 1-week intervals. Similarly, the rabbits in other two groups were immunized on the same day with PBS (control group) and formaldehyde-killed *Y. ruckeri*, respectively. After the last injection, blood was sampled from the rabbits in all three groups and centrifuged to obtain the antisera at 3,000 × g for 15 min. The antisera (Immunoglobulin G, IgG) were purified by the ammonium sulfate precipitation method (58) and stored at −20°C until required.

TABLE 1 | Primers used in this study.

Primers	Sequences (5′ → 3′)[a]	Accession no.	Application
OmpF-F1	CCATGGATGAAGCGCAATATT CTTGCAGTAGTA (*Nco*I)	HM142671.1	PCR and molecular cloning
OmpF-R1	GAGCTCTTAGAACTGATAAACC AAGCCAACA (*Sac*I)		
OmpF-F2	CATGCCATGGCAGAAATCTA CAACAAAG (*Nco*I)	HM142671.1	rtOmpF expression
OmpF-R2	CGAGCTCTTAGAACTGATA AACCAAGC (*Sac*I)		
18S-F	GGACACGGAAAGGATTGACAGA	AF021880.1	qRT-PCR
18S-R	GAGGAGTCTCGTTCGTTATCGG		
EF1α-F	CTGGAGATGCTGCCATTGTTG	DQ353797.1	qRT-PCR
EF1α-R	ACAGCAACGGTCTGCCTCAT		
IL-1β1-F	GCCATGTTGCTAATGTTGTAATCG	DQ160229.1	qRT-PCR
IL-1β1-R	TGTCTTGCAGGCTGTAACTCTTG		
TNF-α-F	CGCACAACAAACCAGACGAGAC	AJ417565.2	qRT-PCR
TNF-α-R	ACCACTGCATAGATACGCTCGAA		
IFN-γ-F	TGCACGAAGTGAAAGACCAAA	DQ124251.1	qRT-PCR
IFN-γ-R	TTAAGGTCCAGCAGCTCAGTGA		
CD4-L2-F	GCAGGGCACGGATAGATGGA	DQ435304.1	qRT-PCR
CD4-L2-R	TGGGTTCGCAGAGGCTGATAC		
CD8α-F	CCGACAGTGCCTACGACTAAAGC	GQ179649.1	qRT-PCR
CD8α-R	CCAGCAGCCAAAGGAATGAAG		
MHC Iα-F	GGTATCATCGTTGGTGTAGCCG	AF053547.1	qRT-PCR
MHC Iα-R	GGACAGGTTTGAAGCCAGAGTT		
MHC IIβ-F	CGGGAAGGAGATTAAAGGAGGT	U77598.1	qRT-PCR
MHC IIβ-R	GTTTGGTGAAGCTGGCGTGT		

[a] *Underlined nucleotides are restriction sites of the enzymes indicated in the brackets.*

Western Blotting

The western blotting analysis of recombinant proteins was carried out as previously described with slight modifications (54, 55). Briefly, the purified proteins were separated using 12.5% SDS-PAGE and transferred onto two PVDF membranes at 150 V for 2 h. The membranes were pre-blocked with TBST containing 3% Bovine Serum Albumin (BSA, Sangon Biotech)

for 1 h at 37°C, then incubated with rabbit anti-6×His antibody (1:1000, Sangon Biotech) and rabbit anti-*Y. ruckeri* antisera (1:200) respectively for 12 h at 4°C. After washing three times with TBST, the membranes were incubated with goat-anti-rabbit IgG-HRP (1:5000, Sangon Biotech) for 1h at 37°C. The reaction was visualized using DAB (Sigma) for 5 to 15 min, and terminated by rinsing with distilled water.

To verify the cross-protection of OmpF in *Yersiniaceae* species, *Y. ruckeri* YRWEL01 (used in this study), *Yersinia enterocolitica,* and *Yersinia pestis* were cultured overnight and homogenized as protein sources for Western blotting. They were incubated with rabbit anti-rtOmpF sera.

Surface Display of *Y. ruckeri* OmpF

Cell Surface Staining of Bacteria

The OmpF protein on the surface of *Y. ruckeri* was detected and verified using the cell surface staining method described previously (56). Briefly, *Y. ruckeri* was distributed uniformly on poly-L-lysine-treated slides (Boster, Wuhan, China) after culturing overnight on BHI agar plates. After air drying, flame fixation, and fixation in 100% methanol for 10 min at −20°C, *Y. ruckeri* coated on the slides were incubated with rabbit anti-rtOmpF sera (1:200), anti-*Y. ruckeri* sera (positive control), and rabbit negative sera (PBS group, negative control) respectively for 1 h at 37°C. After washing three times with PBST, goat anti-rabbit IgG-HRP (1:5000) was applied and incubated for 1 h at 37°C. The reaction wase visualized using DAB for 5 to 15 min and stopped by rinsing with distilled water. Then the slides were covered by cover glasses and observed using a Nikon microscope (Japan) at a ×1000 magnification.

Indirect Immunofluorescence

To verify the surface localization of OmpF protein on *Y. ruckeri,* indirect immunofluorescence assay was also carried out as described previously with minor modification (59). Briefly, *Y. ruckeri* was distributed uniformly on poly-L-lysine-treated slides (Boster, Wuhan, China) after culturing overnight on BHI agar plates. After air drying, flame fixation, and fixation in 100% methanol for 10 min at −20°C, *Y. ruckeri* coated on the slides were incubated with rabbit anti-rtOmpF sera (1:200), anti-*Y. ruckeri* sera (positive control), and rabbit negative sera (negative control) respectively for 1 h at 37°C. After washing three times with PBS, each slide was incubated with fluorescein isothiocyanate (FITC) conjugated goat anti rabbit IgG-FITC (1:64, Sangon Biotech) for 1 h at 37°C. The reaction was stopped by rinsing with PBS and cover glasses were covered in a solution containing glycerol and PBS (1:1). The slides were observed using a fluorescence microscope (Nikon Eclipse 80i).

Preparation of Fish and Vaccines

Channel catfish (50.0 ± 5.0 g) were purchased from a fish farm in Chengdu (Sichuan, China) and acclimatized in the laboratory for 2 weeks at 28 ± 1°C before any experimental manipulation. Fish were fed a commercial diet daily and water was partially replaced every day. Before the experiments, blood and tissues including liver, kidney, and spleen were sampled to detect the bacteria. No bacteria was recovered and agglutination tests showed no reaction between the serum and *Y. ruckeri*. Fish were anesthetized using MS-222 (Sigma) before any experimental manipulation. The recombinant antigen rtOmpF was diluted in PBS to obtain appropriate concentration. To obtain PBS+ISA763 and rtOmpF+ISA763, the PBS and rtOmpF were emulsified respectively with commercial adjuvant Montanide™ ISA763 at a ratio of 3:7 by ultrasonic disruption (JY92-IIDN, Ningbo Scientz, China). The effective concentration of rtOmpF injected into fish was set as 1.0 mg/ml, which was determined using BCA Protein Assay Kit (Nanjing Jiancheng Bioengineering Institute, Nanjing, China), according to the manufacturer's description.

Vaccination and Bacterial Challenge

Healthy channel catfish were divided randomly into four groups (100 fish /group) including one control group and three test groups. The vaccination protocol was carried out as described previously with some modification (55). Briefly, fish were injected intraperitoneally (i.p.) with 0.2 ml of PBS (control group), PBS+ISA763, rtOmpF, and rtOmpF+ISA763 respectively, i.e., effective dose of rtOmpF was 4 μg/g fish, which was determined to be an optimal dose in our preliminary experiments. To obtain an optimal immune response, booster vaccination were conducted with the same method and dosage of first vaccination at 2 weeks later. At 4 weeks post-secondary vaccination (psv), 30 fish from each group were randomly selected and challenged by i.p. injection with 0.2 ml of *Y. ruckeri* YRWEL01 which was resuspended in PBS to 3.5×10^8 CFU/ml (57). Mortality was monitored over a period of 14 days after the challenge, and dying fish were randomly selected for the examination of bacterial recovery from liver, kidney, and spleen. Relative percent of survival (RPS) was calculated according to the following formula: RPS = [1– (% mortality of vaccinated fish/% mortality of control fish)] × 100 (60). Serum samples of five fish in each group were collected for the detection of immune related indexes at 1-8 week psv. Head-kidney and spleen tissues of five fish were taken for qRT-PCR analysis at 24 h post-challenge. Vaccination experiments were performed in duplicate.

Enzyme-Linked Immunosorbent Assay (ELISA)

Sera were collected from the caudal vein of vaccinated fish at 1–8 weeks psv to detect the specific antibody against rtOmpF by ELISA as described perviously (54). Briefly, rtOmpF was diluted to 50 μg/ml in a carbonate buffer (pH = 9.6). Each well of 96-well microplate was coated using 100 μL diluted rtOmpF overnight at 4°C, followed by washing three times with PBST (0.1% Tween-20 in PBS), and then blocking with 3% BSA in PBST for 2 h at 37°C. The sera were added into the wells in triplicate and subsequently incubated for 2 h at 37°C. Rabbit anti-channel catfish IgM antiserum (1:200, prepared in our laboratory) and goat-anti-rabbit IgG-HRP (1:2000) were used as primary and secondary antibodies, respectively. The reaction was visualized using the TMB kit (Tiangen, Beijing, China) and terminated with

2 M H_2SO_4. The absorbance was measured at 450 nm with a microplate reader (Bio-Rad, Hercules, USA).

Measurement of Innate Immune Parameters

The serum lysozyme activity, complement C3 activity, total protein content, and superoxide dismutase (SOD) activity were measured at 1–8 week psv to evaluate the innate immune responses using the commercial kits (lysozyme kit Cat. No: A050-01; complement C3 kit Cat. No: E032; total protein kit Cat. No: A045-3; SOD kit Cat. No: A001-01) according to the manufacturer's instructions (Nanjing Jiancheng Bioengineering Institute, Nanjing, China). The absorbance of lysozyme, complement C3, total protein, and SOD were measured at 530, 340, 562, and 550 nm, respectively, under a microtiter plate reader (Thermo, Varioskan Flash, USA).

qRT-PCR Analysis of Immune-Related Genes Expression

Head kidney and spleen were taken at 24 h post-challenge. Total RNA extraction and cDNA synthesis were performed as described in our previous study (54). qRT-PCR was carried out using SYBR® Premix Ex Taq™ II (Tli RNaseH Plus) (TaKaRa) in an ABI StepOnePlus™ System (Applied Biosystems, USA) as described previously (54). Each assay was performed in triplicate, two housekeeping genes 18S ribosomal RNA (18S) and elongation factor-1 alpha (EF1α) were used as internal control genes (reference genes). The primers used to amplify reference genes and immune-related genes were shown in **Table 1**. The relative expression levels of these genes were analyzed by the $2^{-\Delta\Delta CT}$ method with the geometric mean of the expression levels of 18S and EF1α. All data are presented as relative mRNA expression.

Statistical Analysis

Statistical analysis was performed using SPSS 19.0 software (SPSS Inc., USA). Survival data of bacterial challenge experiment were analyzed by the Kaplan-Meier methods and log-rank tests. The data differences among groups were detected using a one-way analysis of variance (ANOVA). In all cases, the significance level was defined as $P < 0.05$ and the results were presented as mean ± SE (standard error).

RESULTS

Molecular Characterization and Sequence Analysis of OmpF

The coding sequence length of *Y. ruckeri* YRWEL01 OmpF gene was 1095 bp (GenBank accession No: KP159420) (**Figures 1A,B**), which was 3 bp shorter than reference OmpF gene (Accession No.: HM142671.1). The OmpF gene in this study contained a complete open reading frame and encoded 364 amino acid (a.a.), which was predicted to contain a 21 a.a. signal peptide (1-21 a.a.) and a 351 a.a. OM_channels superfamily conserved domain (14-364 a.a.) (**Figures 1C,D**). Comparing with reference OmpF amino acid sequence (Accession No.: ADK27779.1), although there were 3 a.a. differences between them, both possessed 39 trimer interface polypeptide binding sites and 5 channel eyelet sites (**Figure 1C**).

Phylogenetic Analysis of OmpF

Figure 2 presented the logos of top five conserved motifs with length ranging from five to fifty (**Figure 2A**), as well as their corresponding locations in bacteria OmpF proteins (**Figure 2C**). All these reference bacteria OmpFs possessed all these five conserved motifs (**Figure 2C**) which constituted about 60% of the OmpF length, indicating OmpF remained comparatively conserved in different bacteria species. Besides, the two-dimensional topology structures of *Y. ruckeri* OmpF showed that OmpF located extracellular without any transmembrane regions and the signal peptide sequences located into the Motif 1 domain (**Figure 2B**).

The results of amino acid sequences identity indicated that OmpF in this study shared 99.2% identity with *Y. ruckeri* strain Nr34/85 OmpF, shared relative high identity (80.8–86.8%) with other 14 *Yersiniaceae* species OmpFs and relative low identity (58.8–76.4%) with other *Enterobacteriaceae* species OmpFs (**Figure 3A**). The phylogenetic analysis showed that OmpF in this study clustered one clade with *Y. ruckeri* OmpF with the bootstrap values 100, displayed a closer relationship with other bacteria of *Yersiniaceae* family and a distant relationship with other *Enterobacteriaceae* bacteria (**Figure 3B**). In addition, the result of natural selection pressure analysis indicated that the global dN/dS ratios of bacteria OmpFs was 0.649 with 13 positive/diversifying selection sites and 53 negative/purifying selection sites, which was well below 1.0, a theoretical boundary for positive and negative selection.

Expression, Purification and Western Blotting Analysis of Recombinant tOmpF

To obtain the mature peptide of *Y. ruckeri* OmpF, the truncated OmpF (∼1032 bp) removing the signal peptide sequence was successfully amplified using PCR and cloned into pMD19-T to obtain recombinant cloned plasmid T-tOmpF (**Figures 4A,B**), followed by constructing recombinant expression plasmid P-tOmpF (**Figure 4C**) using vector pET32a, expectedly expressed in induced *E. coli* BL21 (P-tOmpF) sediment and purifying using Ni-NTA metal affinity chromatography. After expression, purification, and refolding, recombinant proteins rtOmpF with about 55 kDa were observed using SDS-PAGE (**Figure 4D**). Western blotting analysis indicated that the 55 kDa band of rtOmpF specifically reacted with the rabbit anti-6×His antisera (**Figure 4E**) and rabbit anti-*Y. ruckeri* antisera, respectively (**Figure 4F**). Furthermore, the proteins from *Y. ruckeri* YRWEL01, *Y. enterocolitica,* and *Y. pestis* were also detected by anti-rtOmpF sera with about 38 kDa (**Figure 4G**). Thus, we infer that rtOmpF may confer cross-protection in *Yersiniaceae* species.

Surface Display of *Y. ruckeri* OmpF

The rabbit anti-*Y. ruckeri* antisera and rabbit negative antisera were employed as positive and negative controls, respectively. After staining with DAB, the target bacteria was recognized

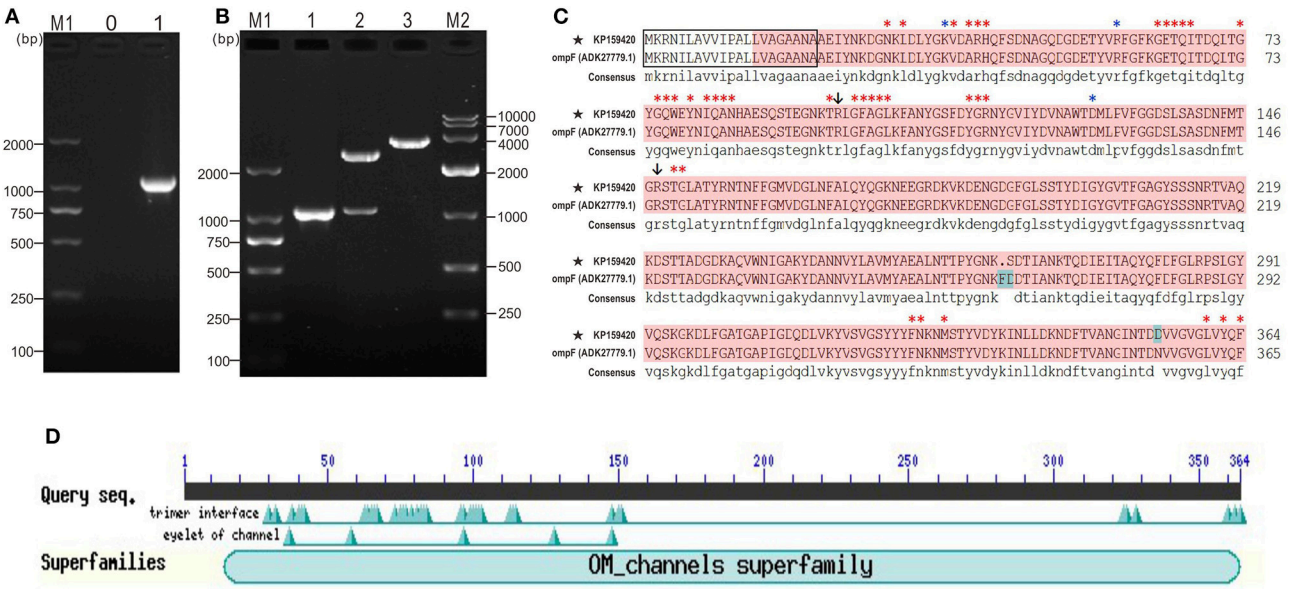


FIGURE 1 | PCR, cloning, alignment and conserved domains analyses of OmpF. **(A)** PCR amplification of OmpF gene. M1: DNA marker (DL2000); lane 0: negative control; lane 1: PCR product of OmpF gene with 1095 bp. **(B)** Identification of cloning plasmid T-OmpF. M1: DNA marker (DL2000); lane 1: PCR identification of T-OmpF; lane 2: digestion of T-OmpF with NcoI and SacI; lane 3: digestion of T-OmpF with SacI [A and B are Figures 1A,B from Wang et al. (61) reproduced with permission from South China Fisheries Science]. **(C)** Amino acid sequence alignment of OmpF in this study with reference *Y. ruckeri* OmpF deposited in NCBI (ADK27779.1), black box presented the signal peptide sequences (1–22 a.a.), red shade regions presented the OM_channels superfamily conserved domain, red "*" indicated the trimer interface polypeptide binding sites, blue "*" indicated the eyelet of channel, "↓" indicated both trimer interface polypeptide binding sites and eyelet of channel. **(D)** Conserved domains of OmpF.

by rabbit anti-rtOmpF antisera and showed in brown color, which was consistent with the result of positive control, while the negative control showed no color (**Figure 5A**). Similarly, in indirect immunofluorescence assay, the target bacteria incubated with anti-rtOmpF antisera showed fluorescence signal, although the signal was a little weak compared with that in positive control, and the negative control showed dark without fluorescence signal (**Figure 5B**).

Serum Antibody Production

Serum specific-antibody was detected continuously using ELISA from 1st to 8th week psv (**Figure 6**). The results showed that antibody levels in fish vaccinated with rtOmpF and rtOmpF+ISA763 were both significantly higher ($P < 0.05$) than that of fish vaccinated with PBS and PBS+ ISA763 at 1st−8th weeks psv. Compared with vaccine rtOmpF alone, rtOmpF+ISA763 induced significantly higher ($P < 0.05$) antibody levels at 4th, 5th and 6th weeks psv, and slightly higher antibody levels at other time points. The antibody peaks of fish vaccinated with rtOmpF and rtOmpF+ISA763 were located at 3rd and 4th week psv, respectively. During whole experimental period, the absorbance values of fish in group PBS+ ISA763 were just slight higher than that in PBS group.

Measurement of Innate Immune Parameters

Serum Lysozyme Activity

The serum lysozyme activity of fish vaccinated with rtOmpF and rtOmpF+ISA763 increased significantly ($P < 0.05$) compared with that of fish in PBS and PBS+ ISA763 groups from 1st to 8th week psv (**Figure 7A**). During the whole experimental period, rtOmpF+ISA763 induced significantly higher ($P < 0.05$) lysozyme activity than rtOmpF alone except at 5th week psv with slight higher. The highest lysozyme activities of rtOmpF and rtOmpF+ISA763 groups were both detected at 4th week psv. Moreover, the lysozyme activity of fish in PBS+ ISA763 group was just slight higher than that in PBS group except 2nd week psv with significantly higher ($P < 0.05$).

Serum Complement C3

Figure 7B showed the complement C3 content in serum of fish vaccinated with PBS and vaccines. The results suggested that compared with complement C3 content of fish in PBS and PBS+ ISA763 groups, the complement C3 content of fish vaccinated with rtOmpF and rtOmpF+ISA763 were significantly ($P < 0.05$) higher throughout whole detection period. Compared with rtOmpF alone, rtOmpF+ISA763 enhanced significantly higher ($P < 0.05$) complement C3 at 1st, 2nd, 3rd, and 5th weeks psv. The highest complement C3 content of fish vaccinated with rtOmpF and rtOmpF+ISA763 were detected at 4th and 5th weeks psv, respectively. Besides, the differences of complement C3 content of fish in PBS and PBS+ ISA763 were not significant from 1st to 8th week psv.

Serum Total Protein

As shown in **Figure 8A,** the vaccines rtOmpF and rtOmpF+ISA763 both induced significantly higher ($P < 0.05$) serum total protein than PBS and PBS+ ISA763 from 1st to 8th

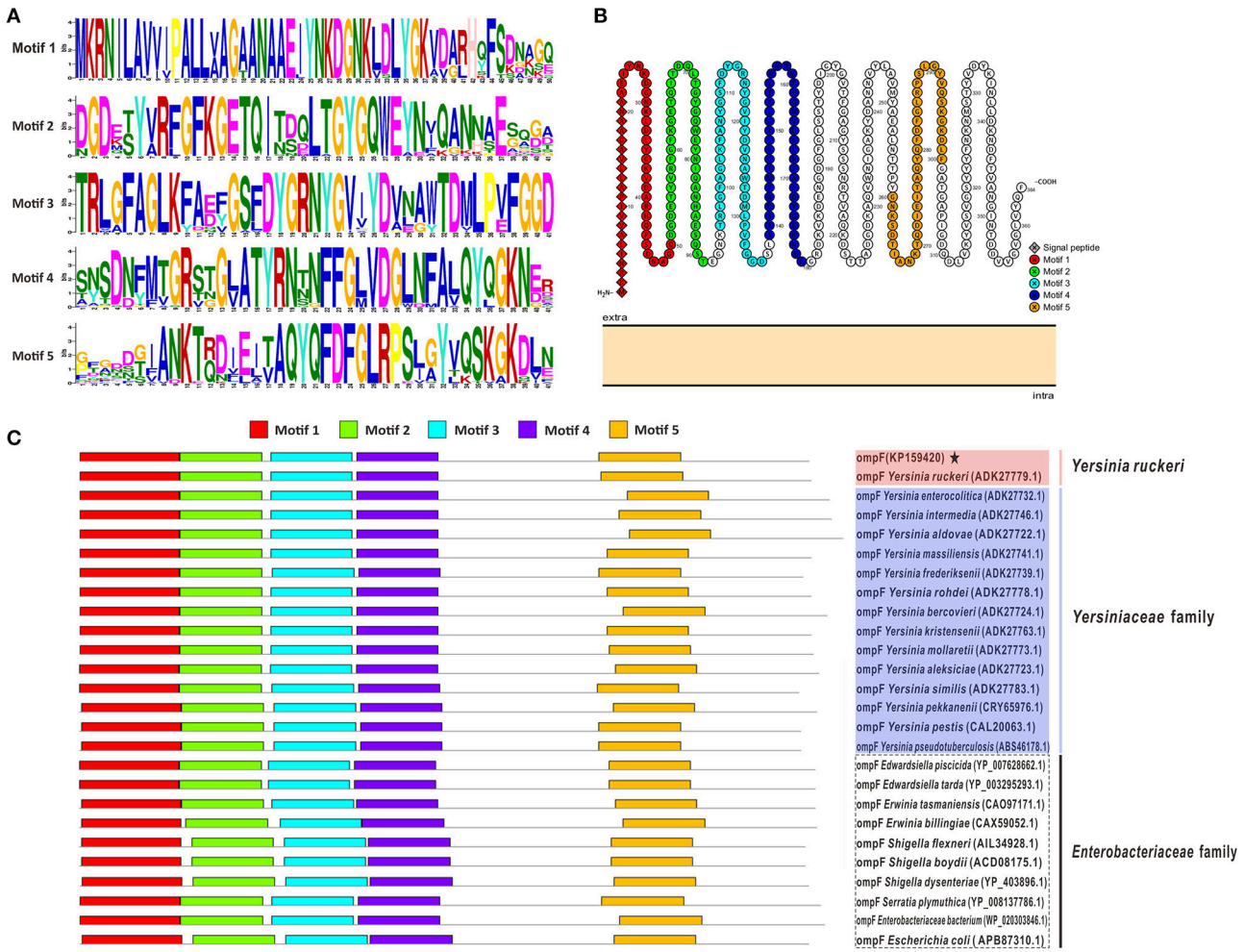


FIGURE 2 | Conserved motifs analysis of OmpF with other 25 reference OmpFs. **(A)** The logos of top five conserved motifs with length ranging from five to fifty in OmpF amino acid sequences. **(B)** The distribution of these five motifs in the two-dimensional topology structures of OmpF (used OmpF in this study as an example). **(C)** The location of these five motifs in bacteria OmpFs. Red shades presented *Y. ruckeri*, blue shades presented other *Yersiniaceae* species, dotted box presented other *Enterobacteriaceae* species.

week psv. Throughout whole detection period, the total protein levels induced by rtOmpF+ISA763 was significantly higher ($P < 0.05$) than rtOmpF alone, and the total protein levels of fish in PBS+ ISA763 group were significantly higher than that in PBS group except 1st week psv. Furthermore, the total protein peaks of fish in rtOmpF and rtOmpF+ISA763 were both observed at 4th week psv.

Serum SOD Activity

Compared with PBS and PBS+ ISA763 groups, a significant ($P < 0.05$) increase of serum SOD activity was measured in rtOmpF and rtOmpF+ISA763 groups from 1st to 8th week psv (**Figure 8B**). During whole detection period, the SOD activity of fish in rtOmpF+ISA763 group was significantly ($P < 0.05$) higher than that in rtOmpF group, and the SOD activity of fish in PBS+ ISA763 group increased significantly ($P < 0.05$) compared with that in PBS group. Moreover, the highest SOD activity of vaccine groups (rtOmpF and rtOmpF+ISA763) were both detected at 4th week psv.

Expression of the Immune-Related Genes

The immune-related genes expression in the head kidney and spleen at 24 h post-challenge were detected by qRT-PCR with two housekeeping genes 18S and EF1α. The results of melting curve analysis indicated that there was only one peak for the PCR product of each gene (**Figure 9A**). The results (**Figure 9B**) of relative expression analysis showed that in the head kidney, the mRNA expression levels of all detected immune-related genes in rtOmpF and rtOmpF+ISA763 groups were significantly increased ($P < 0.05$) compared with those in PBS and PBS+ ISA763 groups, especially CD8α gene (more than 4.2 fold change) in rtOmpF group, CD4-L2, CD8α and MHC Iα genes (more than 4.8 fold change) in rtOmpF+ISA763 groups. Moreover, the fold changes of all these genes in rtOmpF+ISA763 group

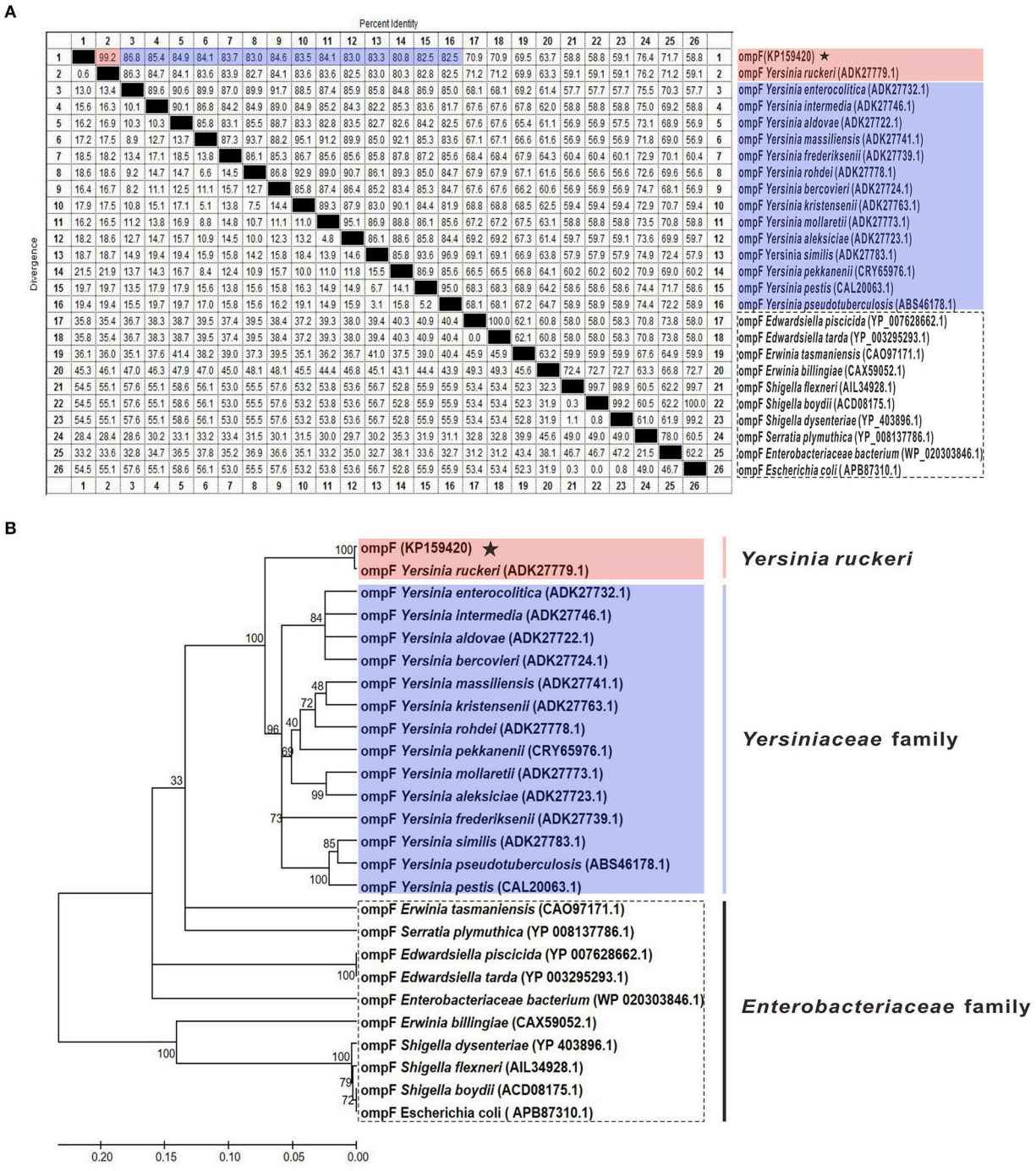


FIGURE 3 | Multiple sequences alignment and phylogenetic tree of OmpF with other 25 reference OmpFs. **(A)** Multiple sequences alignment of OmpF with other 25 reference OmpFs. Red shades indicated OmpF in this study was consistent with *Y. ruckeri* OmpF with 99.2% identities, blue shades indicated other *Yersiniaceae* species OmpFs, dotted box presented other *Enterobacteriaceae* species. **(B)** Phylogenetic tree of OmpF with other 25 reference OmpFs. The numbers at each branch represent the bootstrap values obtained with 1000 replicates. "KP159420" represent the OmpF in this study.

were significantly higher ($P < 0.05$) than that in rtOmpF group. In addition, similar trends were observed in spleen. Compared with PBS group, rtOmpF and rtOmpF+ISA763 induced notably higher ($P < 0.05$) relative expression of these genes, especially CD8α and MHC IIβ genes (more than 4 fold change) in rtOmpF+ISA763 group. Interestingly, the fold change of each gene in spleen was lower than that in head kidney at the same time.

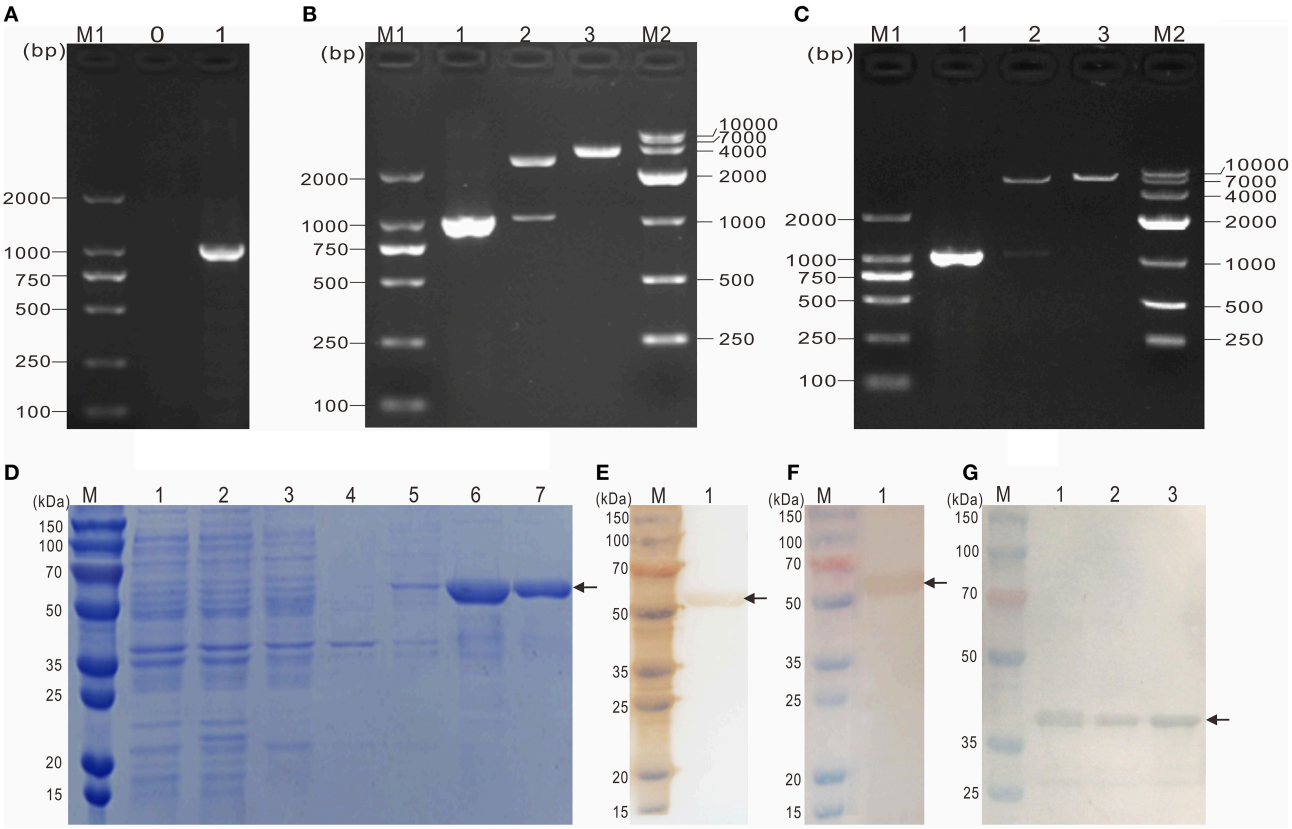


FIGURE 4 | Molecular cloning, expression, purification and western blotting analysis of rtOmpF. **(A)** PCR amplification of tOmpF gene. M1: DNA Marker (DL2000); lane 0: negative control; lane 1: PCR product of tOmpF gene with 1032 bp. **(B)** Identification of recombinant cloning plasmid T-tOmpF. M1: DNA Marker (DL2000); lane 1: PCR product of T-tOmpF; lane 2: digestion of T-tOmpF with NcoI and SacI; lane 3: digestion of T-tOmpF with SacI; M2: DNA Marker (DL10000). **(C)** Identification of recombinant expression plasmid P-tOmpF. M1: DNA Marker (DL2000); lane 1: PCR product of P-tOmpF; lane 2: digestion of P-tOmpF with NcoI and SacI; lane 3: digestion of P-tOmpF with SacI; M2: DNA Marker (DL10000) [C is Figure 1C from Wang et al. (61) reproduced with permission from South China Fisheries Science]. **(D)** SDS-PAGE analysis of recombinant protein rtOmpF. M: protein marker; lane 1∼6: uninduced BL21 (pET32a), induced BL21 (pET32a), uninduced BL21 (P-tOmpF) supernatant, uninduced BL21 (P-tOmpF) sediment, induced BL21 (P-tOmpF) supernatant, induced BL21 (P-tOmpF) sediment, lane 7: purified rtOmpF. **(E)** Western blotting analysis of rtOmpF with rabbit anti-6×His antisera. M: protein marker; lane 1: specific binding between rtOmpF and rabbit anti-6×His antisera. **(F)** Western blotting analysis of rtOmpF with rabbit anti-*Y. ruckeri* antisera. M: protein marker; lane 1: specific binding between rtOmpF and rabbit anti-*Y. ruckeri* antisera [D, E and F are Figure 10 from Wang et al. (61) reproduced with permission from South China Fisheries Science]. **(G)** The cross-protection of OmpF in *Yersiniaceae* species was analyzed by Western blotting with rabbit anti-rtOmpF sera. M: protein marker; lane 1∼3: *Y. ruckeri* YRWEL01, *Y. enterocolitica* and *Y. pestis*, respectively.

Immunoprotection Efficacy Against *Y. ruckeri*

The results of survival data analyzed using the Kaplan-Meier methods indicated that the percent survivals of fish were 3.33% in PBS group, 10.0% in PBS+ISA763, 66.67% in rtOmpF group, and 76.67% in rtOmpF+ISA763 group during the challenge test with pathogenic *Y. ruckeri* YRWEL01 at 4th week psv (**Figure 10**). The results of log-rank analysis suggested that the survivals of fish in rtOmpF and rtOmpF+ISA763 groups were both significantly higher ($P < 0.05$) than that in PBS and PBS+ ISA763 groups. Moreover, the survival of fish vaccinated with rtOmpF+ISA763 was remarkably higher ($P < 0.05$) than that of fish vaccinated with rtOmpF alone, and the survival of fish vaccinated with PBS+ ISA763 was significantly higher ($P < 0.05$) than that of fish vaccinated with PBS alone. Besides, compared with PBS group, the immunoprotective efficacy (in terms of RPS) of PBS+ ISA763, rtOmpF and rtOmpF+ISA763 were 6.90, 65.52, 75.86%, respectively. Furthermore, *Y. ruckeri* YRWEL01 was the only type of bacterial strain detected in the liver, and kidney of moribund fish, suggesting that mortality was indeed caused by *Y. ruckeri* YRWEL01 infection.

DISCUSSION

With the continuous expansions of aquaculture and yield and the increasing of fish breeding density, many aquatic diseases have appeared and seriously damaged the economic productivity of aquaculture, especially bacterial diseases (62–64). Nowadays, based on the consideration of safety and antimicrobial resistance, traditional control strategies including antibiotics and chemicals are more and more questioned. By contrast, vaccines have become a more effective, safe and green intervention to control bacterial infection in aquaculture. As one of the most promising vaccines, genetically engineered vaccines such as subunit vaccines

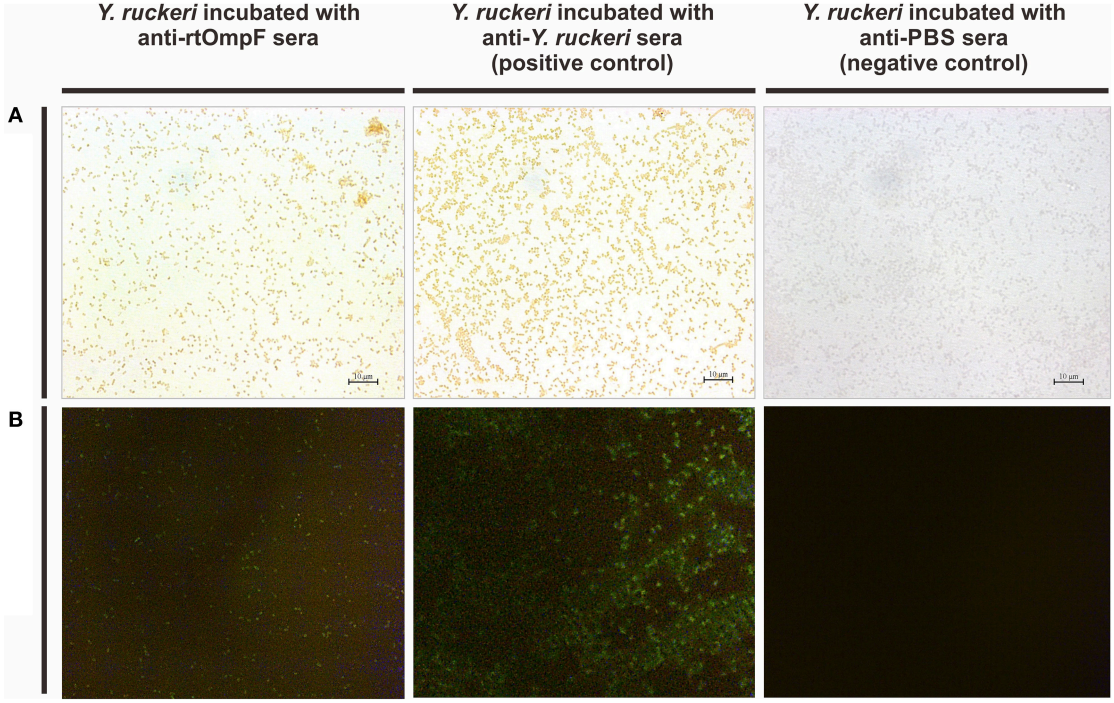


FIGURE 5 | Detection of OmpF localization using bacteria cell surface staining and indirect immunofluorescence. **(A)** Cell surface staining of *Y. ruckeri*. *Y. ruckeri* incubated with rabbit negative antisera (negative control) showed no color. **(B)** Indirect immunofluorescence assay. *Y. ruckeri* incubated with rabbit negative antisera (negative control) showed no fluorescence signal.

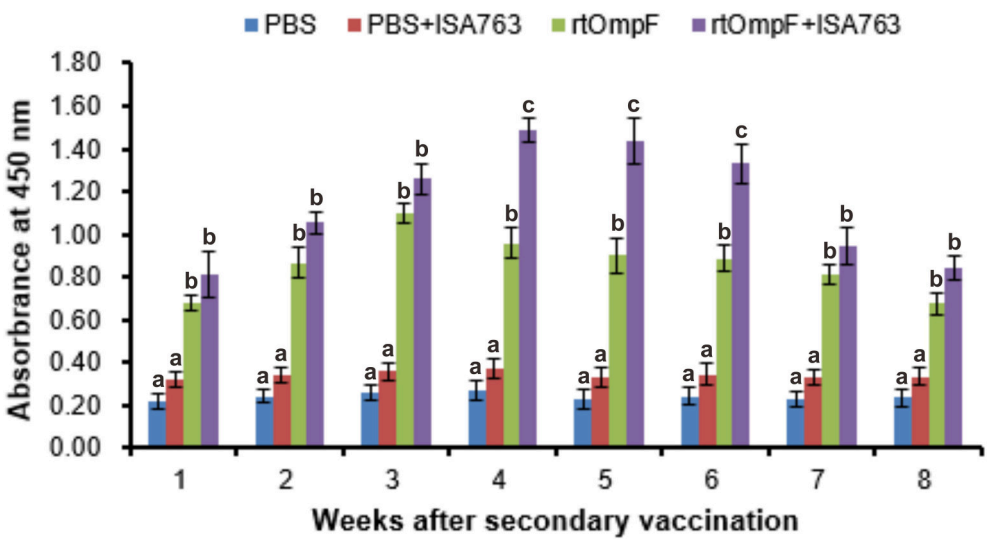


FIGURE 6 | The detection of specific serum antibody in vaccinated fish using ELISA. Channel catfish were vaccinated twice at 2-week intervals, with PBS, PBS+ISA763, rtOmpF and rtOmpF+ISA763 respectively. Sera were collected from 1st to 8th week psv. Data are presented as means ± SE ($n = 5$). Different letters above a bar denoted significant difference ($P < 0.05$).

and DNA vaccines are more safe and serotype-independent due to the basis of protective immunogens (65–67). Therefore, the identification of conserved and protective immunogens is vital for the development of effective genetically engineered vaccines.

As the major components and one of the most abundant proteins in the outer membrane, bacterial porin proteins play a critical role in bacterial pathogenesis and interactions with the host immune system (68, 69). OmpF, as one of the best-studied

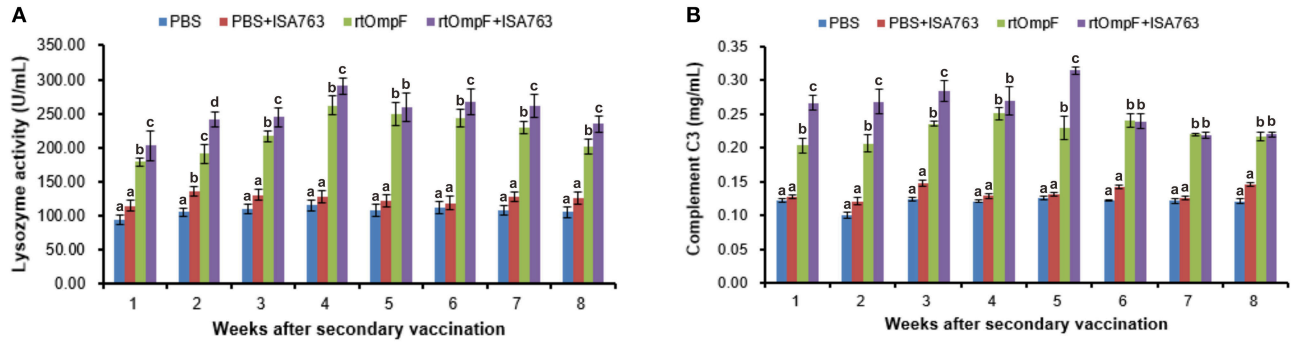


FIGURE 7 | Serum lysozyme activity **(A)** and complement C3 **(B)** of vaccinated fish. Channel catfish were vaccinated twice at 2-week intervals, with PBS, PBS+ISA763, rtOmpF and rtOmpF+ISA763 respectively. Sera were collected from 1st to 8th week psv. Data are presented as means ± SE ($n = 5$). Different letters above a bar denoted significant difference ($P < 0.05$).

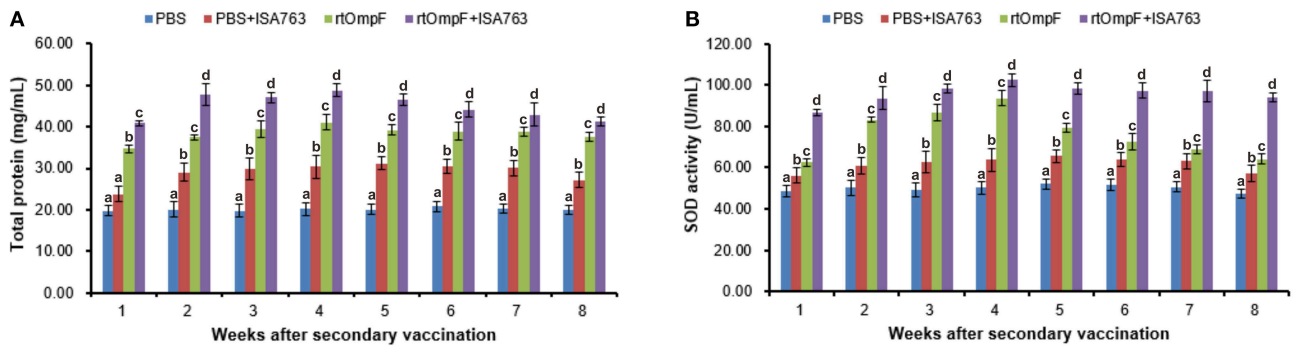


FIGURE 8 | Serum total protein content **(A)** and SOD activity **(B)** of vaccinated fish. Channel catfish were vaccinated twice at 2-week intervals, with PBS, PBS+ISA763, rtOmpF and rtOmpF+ISA763 respectively. Sera were collected from 1st to 8th week psv. Data are presented as means ± SE ($n = 5$). Different letters above a bar denoted significant difference ($P < 0.05$).

bacterial porins on structural and functional characteristics (70–74), has been reported to be a protective antigen against some bacterial infections (40, 74–77) and been predicted to be a conserved porin located on the surface of *Yersinia* (42), which suggests it is possible to use as an immunogen candidate providing immunoprotection against *Yersinia* infection.

In this study, the molecular characteristic results of *Y. ruckeri* OmpF a.a. sequence suggested OmpF was a member of OM_channels porin superfamily, a β-barrel nonspecific channels consisting of 16 antiparallel β-strands for the transportation of small hydrophillic molecules (78, 79). There were 39 trimer interface polypeptide binding sites located in OM_channels domain, which was related with the typical homotrimer structure of bacterial porins (80, 81). Conserved motifs analysis of *Y. ruckeri* OmpF with 25 reference OmpFs revealed that even though the sequence divergences existed among different bacterial OmpFs, the components and positions of conserved motifs of bacterial OmpFs remained highly conserved. Besides, multiple sequences alignment and phylogenetic analysis also indicated that OmpF remained comparatively conserved in different *Enterobacteriaceae* species, especially in *Yersiniaceae* species (sharing 80.8–86.8% identity in 14 *Yersiniaceae* species OmpFs). Moreover, the dN/dS ratio was calculated to determine the natural selection pressure imposed on OmpF gene throughout the evolution process. If a ratio dN/dS = 1, a theoretical boundary for positive/diversifying and negative/purifying selection, indicated the absence of selection. A ratio dN/dS > 1 indicated the positive/diversifying selection had occurred. By contrast, negative/purifying selection occurring on the gene should generate dN/dS <1. In the present study, the global dN/dS ratios of bacterial OmpFs was 0.649, implying that negative/purifying selection played a critical role to remove nonsynonymous substitutions from OmpF genes and OmpFs remained comparatively conserved during the evolution process and the interactions with the host immune system, which agreed with the conclusion of Stenkova et al. (42).

To verify the surface location of OmpF protein on *Y. ruckeri,* bacteria cell surface staining and indirect immunofluorescence assays were conducted with specific anti-rtOmpF antibody. Rabbit anti-*Y. ruckeri* antisera and rabbit negative antisera were employed as positive and negative controls respectively. The results suggested that positive signals were observed on the surface of *Y. ruckeri* incubated with rabbit anti-rtOmpF sera, which was consistent with the results of positive control groups,

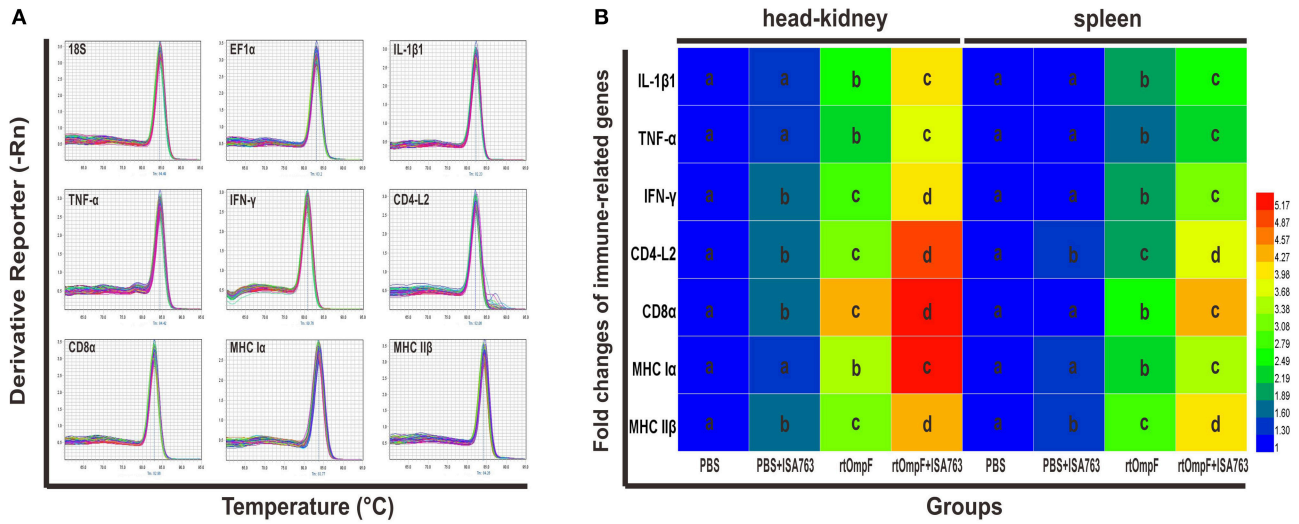


FIGURE 9 | The melt curves and relative expression levels of immune-related genes in the head kidney and spleen of vaccinated fish. **(A)** The melt curves analysis of two reference genes and seven immune-related genes. **(B)** Heatmap analysis of the fold changes of immune-related genes determined by qRT-PCR in the head kidney and spleen. For each gene, the mRNA level of the PBS-vaccinated fish was set as 1. Data were presented as means ($n = 5$). Different letters in the same tissues denoted significant difference ($P < 0.05$) of the same gene in different groups. The color scale was shown at right of the figure, with blue color indicating low fold changes and red color indicating high fold changes.

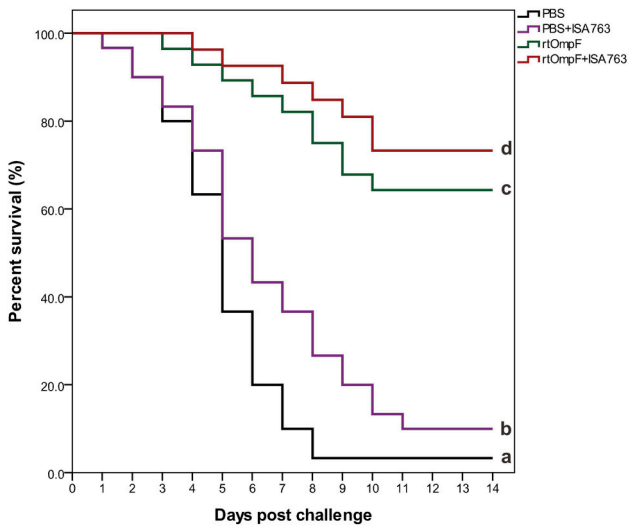


FIGURE 10 | Percent survival analysis of vaccinated fish using Kaplan-Meier method. The differences among groups were analyzed by log-rank test. Different letters denoted significant difference ($P < 0.05$).

indicating that OmpF was located on the surface of *Y. ruckeri* and the polyclonal antibody against rtOmpF was successfully generated and had the desirable affinity to *Y. ruckeri*. Besides, the results of western blotting showed rtOmpF specifically reacted with the rabbit anti-6×His antiserum and rabbit anti-*Y. ruckeri* antiserum respectively, and displayed a single predicted band with 55 kDa, which consisted of the OmpF sequence, the His-tag sequences and some sequences of expression plasmid pET32a. Furthermore, the proteins from *Y. ruckeri* YRWEL01, *Y. enterocolitica,* and *Y. pestis* can also be detected by anti-rtOmpF sera with about 38 kDa (**Figure 4G**), which only consisted of the OmpF sequence in strains. Taken together, these results suggested that recombinant proteins rtOmpF was expressed correctly *in vitro* and able to confer cross-protection in *Yersiniaceae* species, and harbored antigenicity properties to serve as candidate immunogen for vaccine development.

Recently, increasing studies haveshown that reference genes might not be stably expressed in different host tissues and one reference gene is not reliable enough for the accurate normalization of target genes expression (82–88). Thus, in the present study, 18S and EF1α genes, two most suitable and stably expressed genes observed in the head kidney and spleen tissues of channel catfish (89), was employed as reference genes. The geometric mean of the expression levels of 18S and EF1α was used for the accurate normalization of immune-related genes expression in qRT-PCR analysis, which was better than arithmetic mean to control the possible outlying values and abundance differences between the different genes (82). The results indicated that compared with control group, rtOmpF significantly enhanced the expression of immune-related genes involved in inflammatory response (IL-1β1, TNF-α), humoral immunity (MHC II β and CD4-L2) and cellular immunity (MHC Iα, CD8α, and IFN-γ) in the head kidney and spleen, especially co-injection of rtOmpF+ISA763, implying rtOmpF had potential as the antigen to induce a series of immune responses for channel catfish against bacterial infection, and ISA763 as the adjuvant improved the immune response. Moreover, we found that the immune-related gene expression levels in head kidney were higher than that in spleen, which may be due to their different roles and functions in fish immune response (90, 91), since head kidney served as not only the site of hematopoiesis, but also

both a primary and secondary lymphoid organ, while spleen just served as a secondary peripheral lymphoid organ in fish (45).

In addition, the measurement of immune parameters including adaptive and innate immunity is the direct method to evaluate the vaccine effect. In the present study, serum specific antibody levels, lysozyme activity, complement C3 activity, total protein content, and SOD activity were detected in the control group and treatment groups. The results indicated that rtOmpF significantly enhanced the levels of above five immune parameters compared with PBS. Moreover, commercial adjuvant ISA 763 notably enhanced the immune effects induced by rtOmpF. Furthermore, survival percent and PRS were also calculated to assess the vaccine efficacy against *Y. ruckeri* infection. It was shown that the percent survival of fish in rtOmpF+ISA763 group was significantly higher than that of rtOmpF group which was remarkably higher than that of control group, and the PRS of rtOmpF and rtOmpF+ISA763 groups was 65.52 and 75.86% respectively, both were higher than that of inactive *Y. ruckeri* vaccine (RPS with 13.8%) shown in our previous study (57), mainly because of difference types, functions and mechanisms of different antigens.

In conclusion, OmpF gene was shown to be highly conserved among 15 known *Yersinia* species even in *Enterobacteriaceae* species based on the analysis of conserved motifs, sequences alignment and phylogenetic tree, and was subjected to negative/purifying selection with global dN/dS ratios value of 0.649 throughout the evolution. Besides, rtOmpF served as a candidate antigen could enhance the immune response by increasing antibody levels, lysozyme activity, complement C3 activity, total protein content, SOD activity, immune-related genes expression, and survival percent against *Y. ruckeri* infection. Moreover, co-injection of rtOmpF+ISA763 significantly improved the immune effect and immunoprotection induced by rtOmpF. Thus, our present results enriched the information of *Y. ruckeri* OmpF molecular characterization and phylogenetics, and demonstrated that OmpF holds promise to be used as a potential antigen against *Y. ruckeri* infection in fish. However, further studies are still required to understand the detailed mechanisms of OmpF used as immunogen and seek for more effective vaccine types like DNA vaccines to enhance and extend the immunoprotection.

AUTHOR CONTRIBUTIONS

EW, ZQ, ZY, and KW designed the experiment; EW, ZQ, ZY, and XA performed the experimental work. EW, ZQ, and XA analyzed the data, EW and ZY prepared all figures, and EW drafted the paper. QY, TL, DC, and YG participated in fish vaccination and sample collection. XH, PO, and WL contributed to the discussion and revision. All authors reviewed the manuscript.

FUNDING

This work was supported by the Program for Changjiang Scholars and Innovative Research Team in University (No. IRT0848), Sichuan Technology Support Planning (No. 2014JY0143).

REFERENCES

1. Furones MD, Rodgers CJ, Munn CB. *Yersinia ruckeri,* the causal agent of enteric redmouth disease (ERM) in fish. *Ann Rev Fish Dis.* (1993) 3:105–25. doi: 10.1016/0959-8030(93)90031-6
2. Horne MT, Barnes AC. Enteric Redmouth Disease (*Yersinia ruckeri*). In: Woo PTK, Bruno DW, editors. *Fish Diseases and Disorders, Vol. 3: Viral, Bacterial and Fungal Infections*. Oxfordshire: CABI Publishing (1999). p. 455–77.
3. Carson J, Wilson T. *Yersiniosis in Fish. Australian New Zealand Standard Diagnostic Procedures*. Canberra, ACT: Sub-Committee on Animal Health Laboratory Standards, Commonwealth of Australia (2009). p. 1–19.
4. Bastardo A, Bohle H, Ravelo C, Toranzo AE, Romalde JL. Serological and molecular heterogeneity among Yersinia ruckeri strains isolated from farmed Atlantic salmon Salmo salar in Chile. *Dis Aquat Organ.* (2011) 93:207–14. doi: 10.3354/dao02296
5. Shah SQA, Karatas S, Nilsen H, Steinum TM, Colquhoun DJ, Sorum H. Characterization and expression of the gyrA gene from quinolone resistant Yersinia ruckeri strains isolated from Atlantic salmon (*Salmo salar* L.) in Norway. *Aquaculture* (2012) 350:37–41. doi: 10.1016/j.aquaculture.2012.04.022
6. Ormsby MJ, Caws T, Burchmore R, Wallis T, Verner-Jeffreys DW, Davies RL. Yersinia ruckeri isolates recovered from diseased atlantic salmon (*Salmo salar*) in scotland are more diverse than those from rainbow trout (*Oncorhynchus mykiss*) and represent distinct subpopulations. *Appl Environ Microbiol.* (2016) 82:5785–94. doi: 10.1128/AEM.01173-16
7. Ross AJ, Rucker RR, Ewing WH. Description of a bacterium associated with redmouth disease of rainbow trout (*Salmo Gairdneri*). *Can J Microbiol.* (1966) 12:763. doi: 10.1139/m66-103
8. Bullock GL, Stuckey HM, Shotts EB. Enteric redmouth bacterium: comparison of isolates from different geographic areas. *J Fish Dis*. (1978) 1:351–6. doi: 10.1111/j.1365-2761.1978.tb00039.x
9. Busch RA. Enteric redmouth disease (*Hagerman strain*). *Marine Fish Rev*. (1978) 40:42–51.
10. Stevenson R, Daly JG. Biochemical and serological characteristics of Ontario isolates of Yersinia ruckeri. *Can J Fish Aquatic Sci.* (1982) 39:870–6. doi: 10.1139/f82-118
11. Berc A, Petrinec Z, Matasin Z, Kozaric Z. Yersinia ruckeri septicaemia in experimentally infected carp (*Cyprinus carpio* L.) fingerlings. *Acta Vet Hung* (1999) 47:161–72. doi: 10.1556/004.47.1999.2.2
12. Rintamaki P, Valtonen ET, Frerichs GN. Occurrence of Yersinia ruckeri infection in farmed whitefish, *Coregonus peled Gmelin* and *Coregonus muksun Pallas*, and Atlantic salmon, *Salmo salar* L., in northern Finland. *J Fish Dis*. (1986) 9:137–40. doi: 10.1111/j.1365-2761.1986.tb00993.x
13. Vuillaume A, Brun R, Chene P, Sochon E, Lesel R. First isolation of Yersinia ruckeri from sturgeon, *Acipenser baeri Brandt*, in south west of France. *B Eur Assoc Fish Pat*. (1987) 7:18–9.
14. Shaowu L, Di W, Hongbai L, Tongyan L. Isolation of Yersinia ruckeri Strain H01 from Farm-Raised Amur Sturgeon Acipenser schrencki in China. *J Aquat Anim Health* (2013) 25:9–14. doi: 10.1080/08997659.2012.728169
15. Li S, Zhang Y, Cao Y, Wang D, Liu H, Lu T. Trancriptome profiles of Amur sturgeon spleen in response to Yersinia ruckeri infection. *Fish Shellfish Immunol*. (2017) 70:451–60. doi: 10.1016/j.fsi.2017.09.033
16. Danley ML, Goodwin AE, Killian HS. Epizootics in farm-raised channel catfish, Ictalurus punctatus (*Rafinesque*), caused by the enteric redmouth bacterium Yersinia ruckeri. *J Fish Dis*. (1999) 22:451–6. doi: 10.1046/j.1365-2761.1999.00196.x
17. Fan F, Wang K, Geng Y, Huang X, Chen D. Isolation, identification and phylogenetic analysis of *Yersinia ruckeri* in channel catfish *Ictalunes punctatus. Oceanol Limnol Sin*. (2010) 41:862–8. doi: 10.11693/hyhz201006010010
18. Ormsby M, Davies R. *Yersinia ruckeri* In: Woo PTK, Cipriano RC, editors. *Fish Viruses and Bacteria: Pathobiology and Protection.* Oxfordshire: CABI Publishing (2017). p. 339–51.

19. Tinsley JW, Austin DA, Lyndon AR, Austin B. Novel non-motile phenotypes of Yersinia ruckeri suggest expansion of the current clonal complex theory. *J Fish Dis*. (2011) 34:311–7. doi: 10.1111/j.1365-2761.2011.01237.x
20. Costa AA, Leef MJ, Bridle AR, Carson J, Nowak BF. Effect of vaccination against yersiniosis on the relative percent survival, bactericidal and lysozyme response of Atlantic salmon, Salmo salar. *Aquaculture* (2011) 315:201–6. doi: 10.1016/j.aquaculture.2011.02.031
21. Deshmukh S, Raida MK, Dalsgaard I, Chettri JK, Kania PW, Buchmann K. Comparative protection of two different commercial vaccines against Yersinia ruckeri serotype O1 and biotype 2 in rainbow trout (*Oncorhynchus mykiss*). *Vet Immunol Immunop*. (2012) 145:379–85. doi: 10.1016/j.vetimm.2011.12.014
22. Kumar G, Menanteau-Ledouble S, Saleh M, El-Matbouli M. Yersinia ruckeri, the causative agent of enteric redmouth disease in fish. *Vet Res*. (2015) 46:103. doi: 10.1186/s13567-015-0238-4
23. Temprano A, Riano J, Yugueros J, Gonzalez P, de Castro L, Villena A, et al. Potential use of a Yersinia ruckeri O1 auxotrophic aroA mutant as a live attenuated vaccine. *J Fish Dis*. (2005) 28:419–27. doi: 10.1111/j.1365-2761.2005.00646.x
24. Nikaido H. Molecular basis of bacterial outer membrane permeability revisited. *Microbiol Mol Biol R* (2003) 67:593. doi: 10.1128/MMBR.67.4.593-656.2003
25. Ellis TN, Kuehn MJ. Virulence and immunomodulatory roles of bacterial outer membrane vesicles. *Microbiol Mol Biol Rev*. (2010) 74:81–94. doi: 10.1128/MMBR.00031-09
26. Nikaido H, Nakae T. The outer membrane of Gram-negative bacteria. *Adv Microb Physiol*. (1980) 20:163–250. doi: 10.1016/S0065-2911(08)60208-8
27. Pages JM, James CE, Winterhalter M. The porin and the permeating antibiotic: a selective diffusion barrier in Gram-negative bacteria. *Nat Rev Microbiol*. (2008) 6:893–903. doi: 10.1038/nrmicro1994
28. Benz R. Structure and function of porins from gram-negative bacteria. *Annu Rev Microbiol*. (1988) 42:359–93. doi: 10.1146/annurev.mi.42.100188.002043
29. Tang X, Zhan W, Sheng X, Chi H. Immune response of Japanese flounder Paralichthys olivaceus to outer membrane protein of Edwardsiella tarda. *Fish Shellfish Immun*. (2010) 28:333–43. doi: 10.1016/j.fsi.2009.11.015
30. Phuong PTM. *Expression of Recombinant Outer Membrane Protein 48 (OMP48) Developing Vaccine Against Aeromonas hydrophila Infection*. Dissertation thesis, HCMC International University, Vietnam (2014).
31. Maiti B, Shetty M, Shekar M, Karunasagar I, Karunasagar I. Recombinant outer membrane protein A (OmpA) of *Edwardsiella tarda*, a potential vaccine candidate for fish, common carp. *Microbiol Res*. (2011) 167:1–7. doi: 10.1016/j.micres.2011.02.002
32. Abdelhamed H, Ibrahim I, Nho SW, Banes MM, Wills RW, Karsi A, et al. Evaluation of three recombinant outer membrane proteins, OmpA1, Tdr, and TbpA, as potential vaccine antigens against virulent *Aeromonas hydrophila* infection in channel catfish (*Ictalurus punctatus*). *Fish Shellfish Immunol*. (2017) 66:480–6. doi: 10.1016/j.fsi.2017.05.043
33. Yadav SK, Meena JK, Sharma M, Dixit A. Recombinant outer membrane protein C of *Aeromonas hydrophila* elicits mixed immune response and generates agglutinating antibodies. *Immunol Res*. (2016) 64:1087–99. doi: 10.1007/s12026-016-8807-9
34. Ningqiu L, Junjie B, Shuqin W, Xiaozhe F, Haihua L, Xing Y, et al. An outer membrane protein, OmpK, is an effective vaccine candidate for Vibrio harveyi in Orange-spotted grouper (*Epinephelus coioides*). *Fish Shellfish Immun*. (2008) 25:829–33. doi: 10.1016/j.fsi.2008.09.007
35. Yang Q, Pan YL, Wang KY, Wang J, He Y, Wang EL, et al. OmpN, outer membrane proteins of Edwardsiella ictaluri are potential vaccine candidates for channel catfish (*Ictalurus punctatus*). *Mol Immunol*. (2016) 78:1–8. doi: 10.1016/j.molimm.2016.08.011
36. Khushiramani R, Girisha SK, Karunasagar I, Karunasagar I. Cloning and expression of an outer membrane protein ompTS of *Aeromonas hydrophila* and study of immunogenicity in fish. *Protein Expr Purif*. (2007) 51:303–7. doi: 10.1016/j.pep.2006.07.021
37. Wang Q, Chen J, Liu R, Jia J. Identification and evaluation of an outer membrane protein OmpU from a pathogenic Vibrio harveyi isolate as vaccine candidate in turbot (*Scophthalmus maximus*). *Lett Appl Microbiol*. (2011) 53:22–9. doi: 10.1111/j.1472-765X.2011.03062.x
38. Maiti B, Shetty M, Shekar M, Karunasagar I, Karunasagar I. Evaluation of two outer membrane proteins, Aha1 and OmpW of *Aeromonas hydrophila* as vaccine candidate for common carp. *Vet Immunol Immunopathol*. (2012) 149:298–301. doi: 10.1016/j.vetimm.2012.07.013
39. Neema M, Karunasagar I. *In silico* homology modeling and epitope prediction of outer membrane protein OMP W, a potential vaccine candidate against *Edwardsiella tarda*. *Int. J. Curr. Microbiol. App. Sci*. (2018) 7:2762–73. doi: 10.20546/ijcmas.2018.703.319
40. Liu C, Chen Z, Tan C, Liu W, Xu Z, Zhou R, et al. Immunogenic characterization of outer membrane porins OmpC and OmpF of porcine extraintestinal pathogenic *Escherichia coli*. *Fems Microbiol Lett*. (2012) 337:104–11. doi: 10.1111/1574-6968.12013
41. Verma SK, Gautam V, Balakrishna K, Kumar S. Overexpression, purification, and immunogenicity of recombinant porin proteins of *Salmonella enterica Serovar Typhi* (S. Typhi). *J Microbiol Biotechn*. (2009) 19:1034–40. doi: 10.4014/jmb.0812.675
42. Stenkova AM, Isaeva MP, Shubin FN, Rasskazov VA, Rakin AV. Trends of the major porin gene (OmpF) evolution: insight from the genus Yersinia. *Plos ONE* (2011) 6:e20546. doi: 10.1371/journal.pone.0020546
43. Clem LW, Bly JE, Ellsaesser CF, Lobb CJ, Miller NW. Channel catfish as an unconventional model for immunological studies. *J Exp Zool*. (1990) 4:123–5. doi: 10.1002/jez.1402560420
44. Liu Z, Liu S, Yao J, Bao L, Zhang J, Li Y, et al. The channel catfish genome sequence provides insights into the evolution of scale formation in teleosts. *Nat Commun*. (2016) 7:11757. doi: 10.1038/ncomms11757
45. Dickerson HW, Findly RC. Vertebrate adaptive immunity-comparative insights from a teleost model. *Front Immunol*. (2017) 8:1379. doi: 10.3389/fimmu.2017.01379
46. Rombel IT, Sykes KF, Rayner S, Johnston SA. ORF-FINDER: a vector for high-throughput gene identification. *Gene* (2002) 282:33–41. doi: 10.1016/S0378-1119(01)00819-8
47. Petersen TN, Brunak S, von Heijne G, Nielsen H. SignalP 4.0: discriminating signal peptides from transmembrane regions. *Nat Methods* (2011) 8:785–6. doi: 10.1038/nmeth.1701
48. Marchlerbauer A, Derbyshire MK, Gonzales NR, Lu S, Chitsaz F, Geer LY, et al. CDD: NCBI's conserved domain database. *Nucleic Acids Res*. (2015) 43:D222. doi: 10.1093/nar/gku1221
49. Bailey TL, Boden M, Buske FA, Frith M, Grant CE, Clementi L, et al. MEME Suite: tools for motif discovery and searching. *Nucleic Acids Res*. (2009) 37:202–8. doi: 10.1093/nar/gkp335
50. Clewley JP, Arnold C. MEGALIGN. The multiple alignment module of LASERGENE. *Methods Mol Biol*. (1997) 70:119–29. doi: 10.1385/0-89603-358-9:119
51. Edgar RC. MUSCLE: multiple sequence alignment with improved accuracy and speed. In: *Proceedings of the 2004 IEEE Computational Systems Bioinformatics Conference (CSB 2004)*. Washington, DC: The IEEE Computer Society (2004). p. 728–9.
52. Tamura K, Peterson D, Peterson N, Stecher G, Nei M, Kumar S. MEGA5: molecular evolutionary genetics analysis using maximum likelihood, evolutionary distance, and maximum parsimony methods. *Mol Biol Evol*. (2011) 28:2731. doi: 10.1093/molbev/msr121
53. Delport W, Poon AF, Frost SD, Kosakovsky Pond SL. Datamonkey 2010: a suite of phylogenetic analysis tools for evolutionary biology. *Bioinformatics* (2010) 26:2455–7. doi: 10.1093/bioinformatics/btq429
54. Wang E, Wang J, Long B, Wang K, Yang H, Yang Q, et al. Molecular cloning, expression and the adjuvant effects of interleukin-8 of channel catfish (*Ictalurus Punctatus*) against *Streptococcus iniae*. *Sci Rep*. (2016) 6:29310. doi: 10.1038/srep29310
55. Wang Y, Wang E, He Y, Wang K, Yang Q, Wang J, et al. Identification and screening of effective protective antigens for channel catfish against *Streptococcus iniae*. *Oncotarget* (2017) 8:30793. doi: 10.18632/oncotarget.16475
56. He Y, Wang K, Xiao D, Chen D, Huang L, Liu T, et al. A recombinant truncated surface immunogenic protein (tSip) plus adjuvant FIA confers active protection against Group B streptococcus infection in tilapia. *Vaccine* (2014) 32:7025–32. doi: 10.1016/j.vaccine.2014.08.017

57. Yang L, Wang KY, Zhou Y, Wang EL, Wang J, Chen DF, et al. The characteristics and immune efficacy of an oral microspheres vaccine of *Yersinia ruckeri*. *Acta Hydrobiologica Sinica* (2015) 39:1149–56. doi: 10.7541/2015.151
58. Page M, Thorpe R. Purification of IgG by precipitation with sodium sulfate or ammonium sulfate. In: Walker JM, editor. *The Protein Protocols Handbook*. Totowa, NJ: Humana Press (2009). p. 1749–51.
59. Wang J, Wang K, Chen D, Geng Y, Huang X, He Y, et al. Cloning and characterization of surface-localized α-Enolase of *Streptococcus iniae*, an effective protective antigen in mice. *Int J Mol Sci*. (2015) 16:14490–510. doi: 10.3390/ijms160714490
60. Amend DF. Potency testing of fish vaccines. *Fish Biol*. (1981) 49:447–54.
61. Wang E, Qin Z, Wang K, Chen D, Wang J, He Y. Molecular cloning, bioinformatics and immunogenicity analyses of outer membrane protein ompF gene of *Yersinia ruckeri*. *South China Fish Sci*. (2016) 12:24–34. doi: 10.3969/j.issn.2095-0780.2016.03.004
62. Austin B, Austin DA. *Bacterial Fish Pathogens: Disease of Farmed and Wild Fish*. Cham: Springer.(2012)
63. Kumagai A. Bacterial Cold-water Disease in Salmonid Fish and Ayu. *Fish Pathol*. (2016) 51:153–7. doi: 10.3147/jsfp.51.153
64. Haditomo AHC, Ariyati RW, Prayitno SB. The diversity of causative agent associated with bacterial diseases on catfish (*Clarias gariepinus*) with molecular based from Kendal, Indonesia. *Adv Sci Lett*. (2017) 23:6479–82. doi: 10.1166/asl.2017.9659
65. Moyle PM, Toth I. Modern subunit vaccines: development, components, and research opportunities. *Chemmedchem*. (2013) 8:360–76. doi: 10.1002/cmdc.201200487
66. Karch CP, Burkhard P. Vaccine technologies: From whole organisms to rationally designed protein assemblies. *Biochem Pharmacol*. (2016) 120:1–14. doi: 10.1016/j.bcp.2016.05.001
67. Moyle PM. Biotechnology approaches to produce potent, self-adjuvanting antigen-adjuvant fusion protein subunit vaccines. *Biotechnol Adv*. (2017) 35:375–89. doi: 10.1016/j.biotechadv.2017.03.005
68. Achouak W, Heulin T, Pages JM. Multiple facets of bacterial porins. *Fems Microbiol Lett*. (2001) 199:1–7. doi: 10.1111/j.1574-6968.2001.tb10642.x
69. Massari P, Ram S, Macleod H, Wetzler LM. The role of porins in neisserial pathogenesis and immunity. *Trends Microbiol*. (2003) 11:87–93. doi: 10.1016/S0966-842X(02)00037-9
70. Williams KM, Bigley EC, Raybourne RB. Identification of murine B-cell and T-cell epitopes of *Escherichia coli* outer membrane protein F with synthetic polypeptides. *Infect Immun*. (2000) 68:2535–45. doi: 10.1128/IAI.68.5.2535-2545.2000
71. Guzev KV, Isaeva MP, Novikova OD, Solov'Eva TF, Rasskazov VA. Molecular characteristics of OmpF-Like porins from pathogenic Yersinia. *Biochemistry* (2005) 70:1104–10. doi: 10.1007/s10541-005-0231-z
72. Novikova OD, Vakorina TI, Khomenko VA, Likhatskaya GN, Kim NY, Emelyanenko VI, et al. Influence of cultivation conditions on spatial structure and functional activity of OmpF-like porin from outer membrane of *Yersinia pseudotuberculosis*. *Biochemistry* (2008) 73:139–48. doi: 10.1134/S0006297908020041
73. Chistyulin DK, Novikova OD, Portnyagina OY, Khomenko VA, Vakorina TI, Kim NY, et al. Isolation and characterization of OmpF-like Porin from *Yersinia ruckeri*. *Biochemistry* (2012) 6:235–42. doi: 10.1134/S1990747812030038
74. Sidorova OV, Khomenko VA, Portnyagina OY, Likhatskaya GN, Vakorina TI, Kim NY, et al. Mutant OmpF porins of *Yersinia pseudotuberculosis* with deletions of external loops: structure–functional and immunochemical properties. *Biochem Bioph Res Co*. (2014) 445:428–32. doi: 10.1016/j.bbrc.2014.02.018
75. Hughes EE, Gilleland HE. Ability of synthetic peptides representing epitopes of outer membrane protein F of Pseudomonas aeruginosa to afford protection against P. aeruginosa infection in a murine acute pneumonia model. *Vaccine* (1995) 13:1750–3. doi: 10.1016/0264-410X(95)00166-X
76. Portnyagina O, Sidorova O, Khomenko V, Novikova O, Issaeva M, Solovev T. Immunochemical properties of recombinant Ompf Porin from outer membrane of *Yersinia pseudotuberculosis*. In: Abuelzein E, editor. *Trends in Immunolabelled and Related Techniques*. Rijeka: InTech Open Access Publisher (2012). p. 243–58.
77. Sharma M, Dixit A. Identification and immunogenic potential of B cell epitopes of outer membrane protein OmpF of *Aeromonas hydrophila* in translational fusion with a carrier protein. *Appl Microbiol Biotechnol*. (2015) 99:6277–91. doi: 10.1007/s00253-015-6398-3
78. Gromiha MM, Majumdar R, Ponnuswamy PK. Identification of membrane spanning beta strands in bacterial porins. *Protein Eng*. (1997) 10:497–500. doi: 10.1093/protein/10.5.497
79. Schulz GE. The structure of bacterial outer membrane proteins. *Biochimica et Biophysica Acta Biomembranes* (2002) 1565:308–17. doi: 10.1016/S0005-2736(02)00577-1
80. Cowan SW, Schirmer T, Rummel G, Steiert M, Ghosh R, Pauptit RA, et al. Crystal structures explain functional properties of two *E. coli* porins. *Nature* (1992) 358:727–33. doi: 10.1038/358727a0
81. Basle A, Rummel G, Storici P, Rosenbusch JP, Schirmer T. Crystal structure of osmoporin OmpC from *E. coli* at 2.0 A. *J Mol Biol*. (2006) 362:933–42. doi: 10.1016/j.jmb.2006.08.002
82. Vandesompele J, De Preter K, Pattyn F, Poppe B, Van Roy N, De Paepe A, et al. Accurate normalization of real-time quantitative RT-PCR data by geometric averaging of multiple internal control genes. *Genome Biol*. (2002) 3:H34. doi: 10.1186/gb-2002-3-7-research0034
83. Peters IR, Peeters D, Helps CR, Day MJ. Development and application of multiple internal reference (housekeeper) gene assays for accurate normalisation of canine gene expression studies. *Vet Immunol Immunopathol*. (2007) 117:55–66. doi: 10.1016/j.vetimm.2007.01.011
84. Chen H, Yang Z, Hu Y, Tan J, Jia J, Xu H, et al. Reference genes selection for quantitative gene expression studies in *Pinus massoniana* L. *Trees-Struct Funct*. (2016) 30:685–96. doi: 10.1007/s00468-015-1311-3
85. Jiang M, Lee JN, Bionaz M, Deng XY, Wang Y. Evaluation of suitable internal control genes for RT-qPCR in yak mammary tissue during the lactation cycle. *PLoS ONE* (2016) 11:e147705. doi: 10.1371/journal.pone.0147705
86. Gütling H, Bionaz M, Sloboda DM, Ehrlich L, Braun F, Gramzow AK, et al. The importance of selecting the right internal control gene to study the effects of antenatal glucocorticoid administration in human placenta. *Placenta* (2016) 44:19–22. doi: 10.1016/j.placenta.2016.05.011
87. Marcial-Quino J, Fierro F, De la Mora-De LMI, Enriquez-Flores S, Gomez-Manzo S, Vanoye-Carlo A, et al. Validation of housekeeping genes as an internal control for gene expression studies in Giardia lamblia using quantitative real-time PCR. *Gene* (2016) 581:21–30. doi: 10.1016/j.gene.2016.01.018
88. Palve V, Pareek M, Krishnan NM, Siddappa G, Suresh A, Kuriakose MA, et al. A minimal set of internal control genes for gene expression studies in head and neck squamous cell carcinoma. *bioRxiv [Preprint]* (2017). doi: 10.1101/108381
89. Small BC, Murdock CA, Bilodeau-Bourgeois AL, Peterson BC, Waldbieser GC. Stability of reference genes for real-time PCR analyses in channel catfish (*Ictalurus punctatus*) tissues under varying physiological conditions. *Comp Biochem Physiol B Biochem Mol Biol*. (2008) 151:296–304. doi: 10.1016/j.cbpb.2008.07.010
90. Dickerson H, Clark T. Ichthyophthirius multifiliis: a model of cutaneous infection and immunity in fishes. *Immunol Rev*. (1998) 166:377–84. doi: 10.1111/j.1600-065X.1998.tb01277.x
91. Rauta PR, Nayak B, Das S. Immune system and immune responses in fish and their role in comparative immunity study: a model for higher organisms. *Immunol Lett*. (2012) 148:23–33. doi: 10.1016/j.imlet.2012.08.003

Conflict of Interest Statement: The authors declare that the research was conducted in the absence of any commercial or financial relationships that could be construed as a potential conflict of interest.

Copyright © 2018 Wang, Qin, Yu, Ai, Wang, Yang, Liu, Chen, Geng, Huang, Ouyang and Lai. This is an open-access article distributed under the terms of the Creative Commons Attribution License (CC BY). The use, distribution or reproduction in other forums is permitted, provided the original author(s) and the copyright owner(s) are credited and that the original publication in this journal is cited, in accordance with accepted academic practice. No use, distribution or reproduction is permitted which does not comply with these terms.

frontiers in Immunology

ORIGINAL RESEARCH
published: 20 September 2018
doi: 10.3389/fimmu.2018.02116

A Novel Antigen-Sampling Cell in the Teleost Gill Epithelium With the Potential for Direct Antigen Presentation in Mucosal Tissue

Goshi Kato[1], Haruya Miyazawa[1], Yumiko Nakayama[1], Yuki Ikari[1], Hidehiro Kondo[1], Takuya Yamaguchi[2], Motohiko Sano[1] and Uwe Fischer[2]*

[1] *Department of Marine Biosciences, Tokyo University of Marine Science and Technology, Tokyo, Japan,* [2] *Institute of Infectology, Friedrich-Loeffler-Institute, Federal Research Institute for Animal Health, Greifswald-Insel Riems, Germany*

In mammals, M cells can take up antigens through mucosal surfaces of the gut and the respiratory tract. Since M cells are deficient of lysosomes and phagosomes, the antigens are directly delivered to the mucosa-associated lymphoid tissue (MALT) without degradation. In teleost fish, the entire body surface (gills, skin, and intestinal system) is covered by mucus; however, specific antigen-sampling cells have not yet been identified in their mucosal tissues. Here, we show that two phenotypes of antigen-sampling cells take up antigens through epithelial surfaces of the rainbow trout gill. One phenotype of antigen-sampling cells has features of monocyte/macrophage/dendritic cell-type cells; they have large vacuoles in the cytoplasm and express PTPRC (CD45), CD83, IL-1β, and IL-12p40b. The second phenotype exhibits similar characteristics to mammalian M cells; the corresponding cells bind the lectin UEA-1 but not WGA and show expression of M cell marker gene Anxa5. In contrast to mammalian M cells, teleost M-type cells were found to exhibit small vacuoles in their cytoplasm and to express almost all genes related to the "phagosome", "lysosome," and "antigen processing and presentation" pathways. Furthermore, MHC class II was constitutively expressed on a fraction of M-type cells, and this expression was significantly increased after antigen uptake, suggesting that the MHC class II is inducible by antigen stimulation. Here, we suggest that teleost M-type cells play a role in the phylogenetically primitive teleost immune system, similar to bona-fide M cells. In addition, the presence of MHC class II expression suggests an additional role in antigen presentation in the gills, which are an organ with high T cell abundance, especially in interbranchial lymphoid tissue. The present results suggest an unconventional antigen presentation mechanism in the primitive mucosal immune system of teleosts, which generally lack highly organized lymphoid tissues. Moreover, the results of this work may be valuable for the development of mucosal vaccines that specifically target M-type cells; mucosal vaccines significantly reduce working costs and the stress that is usually induced by vaccination via injection of individual fish.

Keywords: ***Oncorhynchus mykiss*****, comparative immunology, mucosal vaccination, atypical antigen presenting cell, lower vertebrate**

OPEN ACCESS

Edited by:
Hetron Mweemba Munang'andu, Norwegian University of Life Sciences, Norway

Reviewed by:
Chiu-Ming Wen, National University of Kaohsiung, Taiwan
Heidrun Wergeland, University of Bergen, Norway

****Correspondence:***
Goshi Kato
gkato00@kaiyodai.ac.jp

Specialty section:
This article was submitted to Comparative Immunology, a section of the journal Frontiers in Immunology

Received: *06 June 2018*
Accepted: *28 August 2018*
Published: *20 September 2018*

Citation:
Kato G, Miyazawa H, Nakayama Y, Ikari Y, Kondo H, Yamaguchi T, Sano M and Fischer U (2018) A Novel Antigen-Sampling Cell in the Teleost Gill Epithelium With the Potential for Direct Antigen Presentation in Mucosal Tissue. Front. Immunol. 9:2116. doi: 10.3389/fimmu.2018.02116

INTRODUCTION

The mucosal surfaces of the digestive and respiratory systems are continuously exposed to the external environment and therefore represent potential ports of pathogen entry. The immune system has evolved to prevent pathogen entry in mucosal tissues, and if an entry is unavoidable, to mount a local immune response. In mammals, recognition of pathogens, and initialization of the immune response occurs in mucosa-associated lymphoid tissue (MALT). MALT consists of germinal centers, lymphoid follicles, and T cell regions and harbors professional antigen-presenting cells (APCs), such as macrophages and dendritic cells (1). M (membranous epithelial, microfold, or microvillous) cells (2) are atypical epithelial cells that phagocytize antigens and macromolecules in the follicle-associated (dome) epithelium (FAE) of gut-associated lymphoid tissue (GALT) and nasopharynx-associated lymphoid tissue (NALT) in mammals. In mice, the lectin *Ulex europaeus* agglutinin-1 (UEA-1), which specifically binds to α (1, 2) fucose and it has been established as an excellent marker for human endothelial cells, is routinely used to identify M cells. In contrast, M cells do not test positive for the lectin wheat germ agglutinin (WGA), which binds to UEA-1$^+$ goblet cells in FAE (3). Molecules on the surface of M cells such as glycoprotein 2 (4), integrin β1 (5), and α2-3-linked sialic acid (6) have been identified as receptors involved in the uptake of FimH$^+$ bacteria, *Yersinia enterocolitica* and type 1 reovirus, respectively. Following their capture by the corresponding receptors, M cells mainly transcytose the respective antigens and deliver them to subjacent APCs (7), and the APCs then present antigens to T lymphocytes in MALT. Finally, antigen-specific immune responses, such as production of IgA by B cells, are induced in mucosal tissues.

Fish inhabit aquatic environments, in which microorganisms are more abundant than in terrestrial environments. The entire body surface of fish (gills, intestine, and skin) is covered by mucus, which is one of the initial immune barriers preventing the invasion of pathogens. Unlike mammals, teleost fish lack lymphoid structures such as germinal centers, B-cell follicles, lymph nodes, and structured MALT. Zapata and Amemiya (8) described the teleost GALT as diffuse subepithelial lymphoid aggregates. Another lymphoid structure that complies with the definition of a tissue is found in the gill epithelium and is referred to as interbranchial lymphoid tissue (ILT). Although the function of ILT is yet to be elucidated, it is considered to represent a phylogenetically early form of leukocyte accumulation in a respiratory organ (9–11). Another special feature of teleost fish is the production of a unique immunoglobulin, IgT, that is suggested to be specialized for mucosal immunity and to possess similar functions to mammalian IgA, although IgT, and IgA are phylogenetically distant immunoglobulins (12).

Mucosal delivery of vaccines, for example, via immersion or oral immunization, is the preferred vaccination method for preventing infectious diseases in aquaculture (13). These vaccination methods significantly decrease the working cost of vaccination in aquaculture since they are suitable approaches for mass vaccination. Vaccine antigens that are administered via the oral route are taken up by the intestinal epithelium of teleost fish (14). The first evidence for the existence of M cells in fish was found in rainbow trout, in which the M-like cells were shown to exhibit similar characteristics to mammalian M cells, exemplified by their morphology (with openly arranged microvilli) and their affinity for the lectin UEA-1 but not WGA (15). In zebrafish, M-like cells have not been yet described, but nanoparticles, and bacteria (*Mycobacterium marinum*) are taken up in the intestinal epithelium when administered via an oral route (16). Bath vaccination of teleost fish is effective against pathogenic bacteria such as *Aeromonas salmonicida* subsp. *salmonicida* (*Ass*) (17), *Vibrio anguillarum* (18), and *Yersinia ruckeri* (19). Large numbers of fish are dipped into a vaccine solution that is traditionally composed of formalin-killed bacteria. While soluble antigens in the vaccine solution are mainly taken up via the skin (20), particulate antigens, such as bacterins from *Y. ruckeri*, are taken up not only via the gill epithelium but also via the gastrointestinal tract, probably after ingestion of the vaccine solution (21, 22). Kato et al. (23) showed that *V. anguillarum* bacterin was taken up primarily via gill epithelial cells, inducing the up-regulation of inflammatory cytokine genes. However, little is known about the exact antigen-sampling mechanisms in the gill epithelium of teleost fish or about the cell populations involved and the resulting local and systemic immune responses.

In this study, we identified and characterized two types of antigen-sampling cells in the rainbow trout gill epithelium that are involved in bacterin uptake during bath vaccination: resident DC/macrophage-type cells in the gill epithelium and another group of antigen-sampling cells that exhibit phenotypic characteristics of M cells, expressing MHC class II molecules on their surface. The M-type antigen-sampling cells showing MHC class II expression were significantly increased in the gill epithelium after bath vaccination. Thus, we hypothesize that antigen-sampling cells are involved in direct antigen presentation to T cells in the gill mucosal tissue of teleosts, which lack highly organized lymphoid organs.

MATERIALS AND METHODS

Fish Rearing and Bacterial Propagation

Rainbow trout (56–126 g body weight) were reared in 400 L tanks at 15°C in a recirculating water system at the Friedrich-Loeffler-Institut and the Tokyo University of Marine Science and Technology. Fish were anesthetized with benzocaine or 2-phenoxyethanol prior to dissection. All animal experiments were approved by the Institutional Animal Care and Use Committee in TUMSAT and FLI. *Ass* bacteria isolated from diseased rainbow trout were cultured in veal infusion broth (VIB) or tryptic soy broth (TSB). *V. anguillarum* (serotype J-O-1, J-O-2, and J-O-3) isolated from diseased ayu *Plecoglossus altivelis* were cultured in TSB. The cultured bacteria were inactivated in 0.3% formalin overnight and then washed.

Immunohistochemistry

Rainbow trout were dipped into a vaccine solution initially corresponding to 2.6–4.4 × 10^8 CFU/ml of *Ass* bacterin,

followed by incubation for 30 min. The gills of the bath-vaccinated fish were fixed overnight in Davidson's solution, embedded in paraffin and sectioned at a 3 μm thickness. The sections were subsequently incubated with polyclonal rabbit antiserum raised against *Ass* (1:1000 dilution) for 1 h at 4°C. After being washed three times with 1 × tris buffered saline (TBS), the sections were treated with a VECTASTAIN ABC Rabbit IgG kit (VECTOR Laboratories) following the manufacturer's instructions. Next, the sections were washed again, treated with 50 mM Tris-HCl (pH 7.6) containing 0.02% 3,3′-diaminobenzidine tetrahydrochloride (Dojindo) and 0.03% H_2O_2 for 3 min, and counterstained with hematoxylin. For immunofluorescence assays, sections stained with the anti-*Ass* serum were incubated with a UEA-1 TRITC conjugate (final concentration, 10 μg/ml; Sigma-Aldrich) or WGA rhodamine conjugate (10 μg/ml, VECTOR Laboratories) for 30 min at 4°C. A goat anti-rabbit IgG (H+L) Alexa Fluor 488 conjugate (4 μg/ml, Thermo Fisher Scientific) was used as a secondary antibody to detect the *Ass* bacterin. Paraffin sections of gills from unvaccinated fish were also stained with UEA-1 FITC conjugate (10 μg/ml, Sigma-Aldrich) and WGA rhodamine conjugate, as above. Cryosections of gills sampled 3 h after *ex vivo* bath vaccination were fixed with acetone for 10 min and incubated with an anti-rainbow trout MHC class II mAb (24) (a gift from Dr. C. Tafalla) for 30 min at 4°C. The slides were then washed three times and incubated with goat anti-mouse IgG (H+L) Alexa Fluor 555 (2 μg/ml, Thermo Fisher Scientific) for 30 min at 4°C. The sections were finally stained with Hoechst 33342 (Thermo Fisher Scientific) and mounted with ProLong Gold Antifade Mountant (Thermo Fisher Scientific), and digital images were captured and analyzed with a Nikon ECLIPSE Ti S fluorescence microscope and NIS Elements software (Nikon).

Flow Cytometry

Formalin-inactivated *Ass* and *V. anguillarum* J-O-1, J-O-2, and J-O-3 were stained with SYTO 61 (Thermo Fisher Scientific). The gills were treated with bacterins *ex vivo* as described by Torroba et al. (25). Briefly, the gills were removed from anesthetized naïve fish and washed twice using RPMI 1640 medium for 5 min with a stirring at 400 rpm. Four pieces of the gills were dipped into SYTO 61-stained bacterin (1.0–2.0 × 10^8 CFU/ml) or 1.0 × 10^7 particles/ml of Fluoresbrite YG Carboxylate microspheres (0.97 μm, Polysciences) suspended in RPMI 1640 medium (Nissui) for 30 min with a stirring at 400 rpm. The other four pieces of the gills were incubated in RPMI 1640 as above and used as a negative control. It was confirmed that the data obtained using the *ex vivo* method were equivalent to those from *in vivo* bath vaccination.

After *ex vivo* bath vaccination with SYTO 61-stained bacterin, gills were washed twice with RPMI 1640 medium. For separation of the gill epithelial cells, the gills were incubated in PBS containing 10 mM EDTA with a stirring at 400 rpm for 20 min at 4°C. The cells were then washed three times with RPMI 1640, counted, and resuspended in RPMI 1640 at 0.84–1.64 × 10^8 cells/ml (>85% viability). One-hundred microliter of the cell suspension was incubated with FITC-labeled UEA-1 diluted in the cell culture medium (10 μg/ml). Further, UEA-1-treated cells were also stained with a mAb against rainbow trout MHC class II (1: 1,000 dilutions in the cell culture medium) for 1 h at 4°C, and a goat anti-mouse IgG PE/Cy 5.5 conjugate (0.25 μg/ml, Abcam) diluted in RPMI 1640 was used as secondary antibodies. The epithelial cells from the gills dipped into the microspheres were stained with UEA-1 (10 μg/ml in RPMI 1640, without fluorescent conjugation). A rabbit anti-UEA-1 polyclonal antibody (5 μg/ml in RPMI 1640, Bioss Antibodies) and goat anti-rabbit IgG (H+L) Alexa 647 (2 μg/ml in RPMI 1640, Abcam) were used as secondary and tertiary antibodies to detect UEA-1, respectively. Afterbeing washed three times with RPMI 1640, the cells were re-suspended in the cell culture medium and stained with DAPI (4',6-diamidino-2-phenylindole, 1 μg/ml in RPMI 1640; Life Technologies). The epithelial cells collected from the gills exposed to RPMI 1640 were incubated with the secondary antibodies and used as negative controls. Flow cytometry analyses of 10,000 cells in each group were performed using a CytoFlex (Beckman Coulter). Data from the cytometers were analyzed with Kaluza Flow Cytometry Analysis Software (Beckman Coulter).

Cell Sorting by Flow Cytometry

Formalin-inactivated *Ass* were stained with SYTO 61 (Thermo Fisher Scientific) and used for bath vaccination. Rainbow trout were dipped into a vaccine solution initially corresponding to 1.0–2.0 × 10^8 CFU/ml of SYTO 61-stained bacterins, followed by incubation for 30 min. After *in vivo* bath vaccination with SYTO 61-stained bacterin, gills were washed twice with the ZB28 cell culture medium (50/50 mixture of Iscove's and Ham's F12 medium). The gill epithelial cells were prepared and stained with FITC-labeled UEA-1 (10 μg/ml in ZB28), as above. After being washed three times with ZB28, the cells were re-suspended in the cell culture medium and stained with propidium iodide (PI, 2 μg/ml; Life Technologies) or DAPI (4',6-diamidino-2-phenylindole, 1 μg/ml; Life Technologies). The gill epithelial cells collected from rainbow trout dipped into rearing water without SYTO61-stained bacterin were prepared and used as negative control. Cell sorting was performed with a MoFlo high-speed cell sorter (Dako Cytomation) or a FACSAria Fusion cell sorter (BD Biosciences). First, PI^+ or $DAPI^+$ cells were gated to exclude sorting dead cells. Then, 30,000 cells of UEA-1^- *Ass*$^-$ population as a negative control, UEA-1^- *Ass*$^+$ population and UEA-1^+ *Ass*$^+$ population were sorted. Data from the cytometers were analyzed with Kaluza Flow Cytometry Analysis Software (Beckman Coulter).

Gene Expression Analysis

Total RNA was extracted from sorted cells using a NucleoSpin RNA XS kit (Machery-Nagel), following the manufacturer's instructions. Equal amounts of total RNA from each sorted cell population of three fish individuals were pooled prior to library construction. RNA libraries were constructed using the Illumina TruSeq Stranded mRNA Sample Preparation Kit (Illumina), following the manufacturer's instructions. Sequencing was performed using the Illumina MiSeq platform, employing the MiSeq Reagent Kit v2 (Illumina), with 151 paired-end reads. The whole transcriptome sequence raw data were deposited in the DDBJ Sequence Read Archive (Accession Number: DRA006692). *De novo* assembly of the MiSeq reads and gene expression analysis using the fragments per kilobase of exon

per million mapped reads (FPKM) model was performed with Trinity v2.1.1 software (https://github.com/trinityrnaseq/trinityrnaseq). The assembled sequences were annotated using the BLAST program at the UniProtKB database (http://www.uniprot.org/help/uniprotkb) and using Blast2GO software (https://www.blast2go.com/). The UniProtKB accession numbers of the expressed genes of each library were submitted to Venny 2.1 software (http://bioinfogp.cnb.csic.es/tools/venny/) to construct a Venn diagram. The KAAS (http://www.genome.jp/tools/kaas/) was employed for orthologue assignment and pathway mapping.

Total RNA was extracted from each sorted cell population using Nucleospin RNA XS kit (Machery-Nagel), following manufacturer's instructions. First-strand cDNAs were synthesized using 100 ng of total RNA using M-MLV reverse transcriptase (Thermo Fisher Scientific). The primers employed for qRT-PCR are shown in **Table S3**. The expression levels of several genes of interest in each sorted cell population from three individuals were analyzed by quantitative RT-PCR (qRT-PCR) using THUNDERBIRD SYBR qPCR Mix (TOYOBO), following the manufacturer's instructions. Since the PCR efficiency of all primer sets for qPCR were higher than 95%, the relative values for expression levels were calculated using the $2^{-\Delta\Delta Ct}$ method, taking into account the expression of elongation factor 1α (Accession No. AF498320) as an internal control. Significant differences among samples were assessed using one-way analysis of variance (ANOVA) and Tukey's *post-hoc* test. $P < 0.05$ were considered statistically significant.

RESULTS

Identification of Two Phenotypes of Antigen-Sampling Cells in the Gill Epithelium of Rainbow Trout

Since in antigen sampling in rainbow trout has been studied only using live *Ass* (26), and the site of *Ass* bacterin uptake is still unknown, we first aimed to determine the localization of the respective antigen-sampling cells. Immunohistochemistry analysis showed that inactivated *Ass* bacteria were frequently taken up by gill epithelial cells after bath vaccination (**Figure 1A**). Lectin staining revealed numerous UEA-1$^+$ WGA$^-$ cells in the epithelial cells of the primary and secondary lamellae. This UEA1$^+$ WGA$^-$ phenotype, which is typical of mouse M cells, was found both in the epithelia of the outer lamellae and close to the base of the gill filament's septae, where ILT is located (**Figure 1B**). UEA-1$^+$ WGA$^+$ staining, which is typical of mammalian goblet cells, was scarcely observed in the gill epithelial cells of rainbow trout. Double staining with an anti-*Ass* polyclonal antibody and either of the lectins after bath vaccination revealed that both UEA-1$^+$ and UEA-1$^-$ cells were able to take up *Ass* bacterin (**Figure 1C**), while WGA$^+$ cells were not (**Figure 1D**). To further characterize the antigen-sampling cells, gill epithelial cells were isolated and analyzed via flow cytometry. Similar to the immunohistochemistry analysis, flow cytometry revealed two cell populations that take up *Ass* bacterin in the gill epithelium: UEA-1$^+$ cells and UEA-1$^-$ cells (**Figure 2A** left panel). These two populations showed distinct side scatter characteristics, with higher side scatter being observed in UEA-1$^+$ *Ass*$^+$ cells than in UEA-1$^-$ *Ass*$^+$ cells, suggesting that UEA-1$^+$ *Ass*$^+$ cells are more highly granulated than UEA-1$^-$ *Ass*$^+$ cells (**Figure 2A** right panel). Since Kato et al. (23) showed previously that *V. anguillarum* bacterin is taken up by the gill epithelium in bath-vaccinated Japanese flounder, we further analyzed gill epithelial cells of rainbow trout that were bath vaccinated with *V. anguillarum* (J-O-1, J-O-2, and J-O-3 serotype) bacterin. Similar to *Ass* bacterin, *V. anguillarum* bacterin was taken up by UEA-1$^+$ cells (**Figures 2B–D** left panels). Additionally, UEA-1$^-$ *V. anguillarum*$^+$ cells were observed in the gill epithelium of fish that were bath vaccinated with *V. anguillarum* bacterin (**Figures 2B–D** right panels). However, fluorescence microbeads were taken up neither by UEA-1$^+$ nor UEA-1$^-$ cells (**Figure 2E**). In addition, the gill epithelial cells that took up *Ass* bacterin (**Figure S1A**) did not react with mAbs against CD8α, IgM, and thrombocytes (**Figures S1B–D**). Based on these results, we

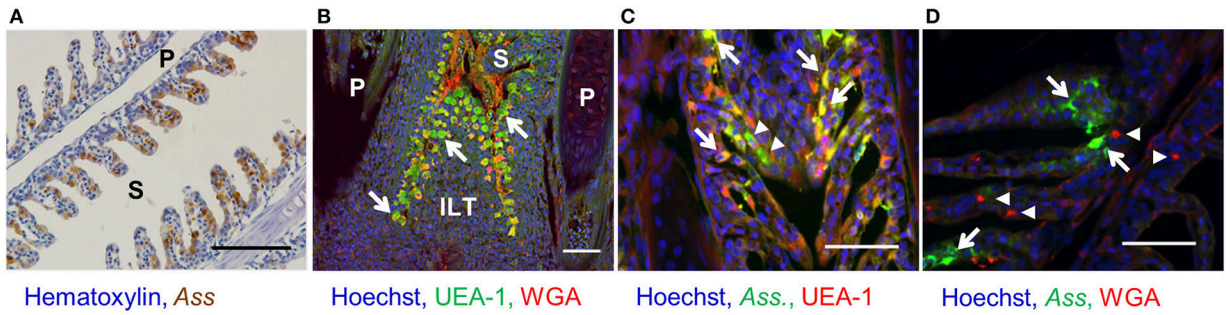


FIGURE 1 | Bacterin uptake by UEA-1$^+$ and UEA-1$^-$ gill epithelial cells after bath vaccination. **(A)** Immunohistochemistry for the detection of *Ass* bacterin in paraffin section of gills from bath-vaccinated fish. Scale bars, 100 μm. **(B)** Lectin staining in a paraffin gill section. White arrows indicate UEA-1$^+$ WGA$^-$ cells. Scale bars, 50 μm. **(C)** Fluorescent staining with an anti-*Ass* polyclonal antibody (in green) and the lectin UEA-1 (in red) in gill paraffin section from bath-vaccinated fish. White arrows and white arrowheads indicate UEA-1$^+$ and UEA-1$^-$ antigen-sampling cells, respectively. Scale bars, 50 μm. **(D)** Fluorescent staining with an anti-*Ass* polyclonal antibody (in green) and the lectin WGA (in red) in gill paraffin section from bath-vaccinated fish. White arrows and arrowheads indicate antigen-sampling cells and WGA-stained cells, respectively. Scale bars, 50 μm. P, primary lamellae; S, secondary lamellae; ILT, interbrachial lymphoid tissue. Experiments were done by *in vivo* bath vaccination and data are from one experiment **(A)** and representative of three experiments **(B–D)**.

identified two cell populations that take up bacterins in the gill epithelium of bath-vaccinated rainbow trout.

Characterization of the Two Phenotypes of Antigen-Sampling Cells

To characterize the two antigen-sampling cell populations in the gill epithelium, the UEA-1$^+$ *Ass*$^+$ and UEA-1$^-$ *Ass*$^+$ cell populations and the negative cell population were sorted via flow cytometry (**Figure S2**). May-Grünwald-Giemsa (MGG) staining of the sorted cells confirmed that UEA-1$^+$ *Ass*$^+$ cells exhibited round nuclei, with reddish-purple granules and small vacuoles in the cytoplasm (**Figure 3A**). Most of the UEA-1$^-$ *Ass*$^+$ cells showed typical monocyte/macrophage morphologies, including oval nuclei with a homogenous chromatin pattern and pale-blue cytoplasm with vacuoles (**Figure 3B**). Negative cell population included many cell phenotypes such as erythrocytes, monocyte-like cells and others (**Figure 3C**). Total RNA samples from the sorted cells were subjected to transcriptome analysis. Deep sequencing yielded 174,245 contigs from sixty-five million total reads (**Table S1**) and revealed clear differences in gene expression patterns among the three cell populations (**Figure 3D**). Venn diagrams of the three RNA libraries showed that there were 5,002, 30,290, and 39,260 unique genes expressed in the negative, UEA-1$^+$ *Ass*$^+$ and UEA-1$^-$ *Ass*$^+$ cell populations, respectively, (**Figure 3E**). Pathway analysis using the Kyoto Encyclopedia of Genes and Genome Automatic Annotation Server (KAAS)

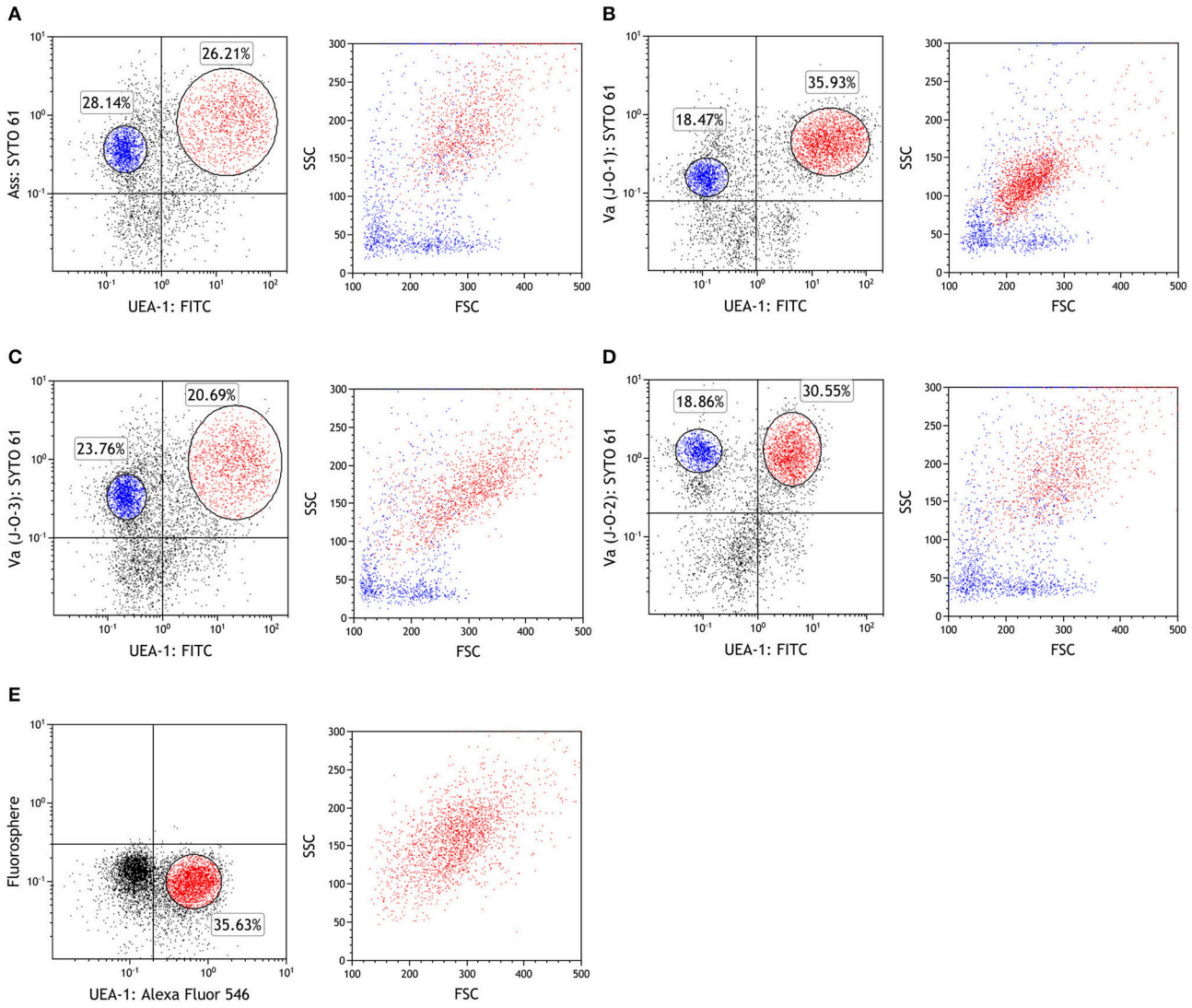


FIGURE 2 | UEA-1$^+$ and UEA-1$^-$ gill epithelial cells take up bacterins but not microbeads during bath administration. **(A–D)** Flow cytometry of fish gill epithelial cells bath vaccinated with *Ass* bacterin in **(A)**, with *V. anguillarum* J-O-1 serotype bacterin in **(B)**, with *V. anguillarum* J-O-2 serotype bacterin in **(C)**, and with *V. anguillarum* J-O-3 serotype bacterin in **(D)**. **(E)** Flow cytometry of gill epithelial cells from fish immersed with fluorescent microbeads (diameter: 1 μm). Left panels show dot plots of depicting antigen or bead staining on the Y-axis against UEA-1 staining on the X-axis. Red dots represent UEA-1$^+$ bacterin$^+$ cells, while blue dots represent UEA-1$^-$ bacterin$^+$ cells in the right panels. Experiments were done by *ex vivo* bath vaccination and data are representative of two experiments.

revealed that the RNA libraries from both UEA-1$^+$ *Ass*$^+$ and UEA-1$^-$ *Ass*$^+$ cells contained an almost full set of genes related to the "lysosome," "phagosome," and "antigen processing and presentation" pathways (**Table S2**, and **Figures S3**, **S4**). Genes of interest that were highly expressed in UEA-1$^+$ *Ass*$^+$ and UEA-1$^-$ *Ass*$^+$ cells are shown in **Table 1**. Several genes encoding epithelial cell markers, *CDH1, Cldn3, KRT13, KRTS8, KRTE1, KRTE3,* and *IL-17R*, were highly expressed in UEA-1$^+$ *Ass*$^+$ cells. Several genes that are highly expressed in mammalian M cells, such as *Anxa5*, *Ctsh*, *CCL20*, *Dnclc,* and *Gpx I,* were highly expressed in UEA-1$^+$ *Ass*$^+$ cells as well. However, UEA-1$^+$ *Ass*$^+$ cells also expressed *MHC-IIA*, *MHC-IIB,* and *MHC-II Ii* at high levels. Macrophage, monocyte and dendritic cell makers such as *CD83*, *IL-1β*, *IL-10R,* and *IL-12 p40* were highly expressed in the UEA-1$^-$ *Ass*$^+$ cell population, while these genes were not expressed or negligibly expressed in UEA-1$^+$ *Ass*$^+$ cells. Gene expression levels determined via MiSeq sequencing in the negative, UEA-1$^+$ *Ass*$^+$ and UEA-1$^-$ *Ass*$^+$ cell populations were confirmed using qRT-PCR. The expression level of the M cell marker gene *Anxa5* was significantly higher in UEA-1$^+$ *Ass*$^+$ cells than in the negative and UEA-1$^-$ *Ass*$^+$ cell populations ($p < 0.05$, **Figure 4A**). The epithelial cell markers *Cldn3, CDH1, KRT13, KRTE1,* and *IL-17R* also showed significantly higher expression in UEA-1$^+$ *Ass*$^+$ cells than in the other two cell populations ($p < 0.01$, **Figures 4B–F**). In contrast, the gene expression levels of *CD83*, *IL-1β,* and *IL-12 p40* were significantly higher in UEA-1$^-$ *Ass*$^+$ cells ($p < 0.05$, **Figures 4G–I**). In addition, the gene expression level of *PTPRC* (*CD45*), a lineage maker for hematopoietic origin, was significantly higher in UEA-1$^-$ *Ass*$^+$ cells ($p < 0.05$, **Figure 4J**). qRT-PCR analyses further confirmed the significantly higher expression level of *MHC-IIB* and *MHC-II Ii* in UEA-1$^+$ *Ass*$^+$ cells and UEA-1$^-$ *Ass*$^+$ cells than in the negative cell population ($p < 0.05$, **Figures 4K–L**). Despite the high

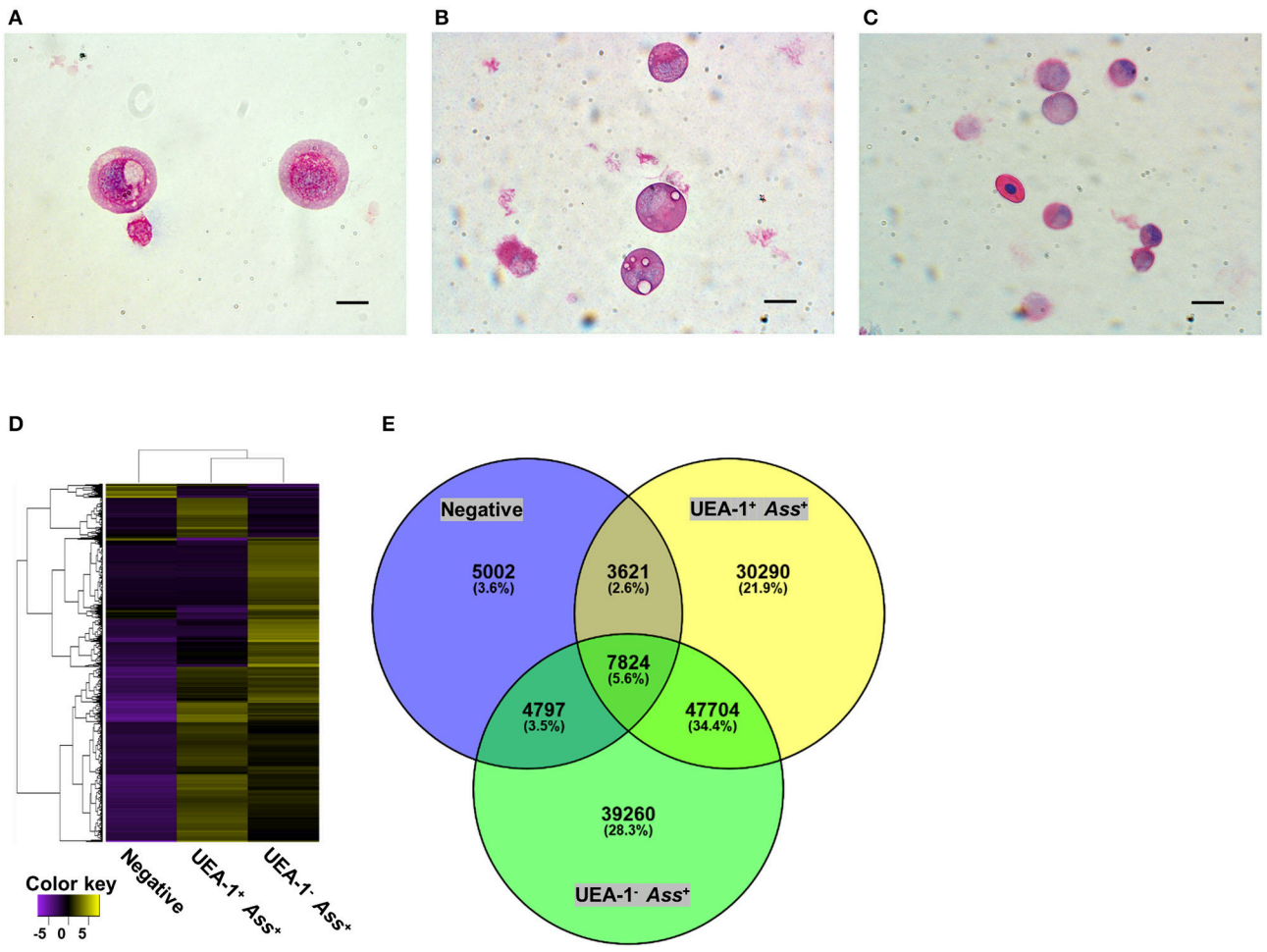


FIGURE 3 | The two antigen-sampling cell populations in the gill epithelium show distinct morphologies and gene expression profiles. **(A–C)** May-Grünwald-Giemsa staining of sorted UEA-1$^+$ *Ass*$^+$ cells in **(A)**, UEA-1$^-$ *Ass*$^+$ cells in **B**, and negative cell population in **(C)**. scale bars, 10 μm. **(D)** Heat map of differentially expressed genes in each sample, constructed with the Trinity program. **(E)** Venn diagram summary of differentially expressed genes in the UEA-1$^+$ *Ass*$^+$, UEA-1$^-$ *Ass*$^+$ and negative cell populations. Experiments were done by *in vivo* bath vaccination and data are representative of two experiments **(A–C)** or come from one experiment involving three individuals **(D,E)**.

TABLE 1 | Genes of interest expressed in UEA-1$^+$ Ass$^+$ cell and UEA-1$^-$ Ass$^+$ cell population.

Description (gene symbol)	Accession (UniProtKB)	Blast Hit Acc (nr), Matched species	*E*-value	FPKM		
				negative	UEA-1$^+$ Ass$^+$	UEA-1$^-$ Ass$^+$
EPITHELIAL CELL						
Claudin 3 (*Cldn3*)	A0A060WMH8_ONCMY	XP_013985100, *S. salar*	2.2E-30	0.0	119.8	26.7
E-cadherin (*CDH1*)	M1VNS4_ONCMY	BAM84263, *O. mykiss*	6.0E-71	0.0	154.1	34.8
Interleukin-17 receptor precursor (*IL-17R*)	A1IMH6_ONCMY	NP_001117885, *O. mykiss*	7.5E-35	35.5	111.2	0.0
Type I keratin13 (*KRT13*)	K1C13_ONCMY	NP_001117848, *O. mykiss*	2.0E-153	22.7	99.5	17.5
Type I keratin S8 (*KRTS8*)	Q90W73_ONCMY	NP_001117826, *O. mykiss*	0.0E+00	0.0	354.8	106.7
Type II keratin E1 (*KRTE1*)	Q90W76_ONCMY	NP_001118215, *O. mykiss*	0.0E+00	0.0	151.1	33.2
Type II keratin E3 (*KRTE3*)	Q8JFG4_ONCMY	NP_001123458, *O. mykiss*	0.0E+00	0.0	587.7	198.9
M CELL						
Annexin A5 (*Anxa5*)	A0A060W4V6_ONCMY	NP_001134508, *S. salar*	0.0E+00	0.0	222.2	66.7
Cathepsin H (*CtsH*)	A0A060YPS5_ONCMY	XP_021427100, *O. mykiss*	0.0E+00	69.4	412.6	999.5
C-C motif chemokine 20 (*CCL20*)	A0A060Z5E6_ONCMY	XP_020314768, *O. mykiss*	3.8E-50	0.0	325.5	88.4
Dynein light chain cytoplasmic (*Dnclc*)	A0A060W6Y3_ONCMY	XP_021477488, *O. mykiss*	5.4E-62	0.0	91.4	46.9
Glutathione peroxidase 1 (*Gpxl*)	W8W106_ONCMY	CCG28020, *O. mykiss*	4.7E-135	0.0	177.1	72.4
MACROPHAGE AND DENDRITIC CELL						
CD83	Q6WZ85_ONCMY	AAP93909, *O. mykiss*	6.1E-23	0.0	63.12	1181.6
Interleukin-1 beta 3 (*IL-1β3*)	A0A060YIQ8_ONCMY	CAD89533, *O. mykiss*	0.0E+00	0.0	11.6	107.9
Interleukin-10 receptor subunit beta (*IL-10R*)	A0A060ZFQ5_ONCMY	XP_020338312, *O. kisutch*	0.0E+00	16.2	2.02	85.3
Interleukin 12 subunit beta (*IL-12 p40b*)	X5J4B0_ONCMY	CCH10517, *O. mykiss*	0.0E+00	3.3	0.0	390.5
MHC class II alpha partial (*MHC-IIA*)	E0WN08_ONCMY	CBX11163, *O. mykiss*	7.5E-57	0.0	723.1	1995.4
MHC class II beta partial (*MHC-IIB*)	E0WN21_ONCMY	CBX11176, *O. mykiss*	0.0E+00	0.0	1732.4	3760.0
MHC class II invariant chain (*MHC-II Ii*)	Q8MHB9_ONCMY	AAL91669, *O. mykiss*	1.2E-143	0.0	1241.8	8911.1

mRNA levels of MHC class II-related genes observed in UEA-1$^+$ *Ass*$^+$ cells, we conclude that these cells do not belong to the macrophage/monocyte/dendritic cell lineage but to a cell type that is reminiscent of M cells. The second class of antigen-sampling cells, the UEA-1$^-$ *Ass*$^+$ cell population, is suggested to be gill epithelium-resident macrophages, monocytes or dendritic cells.

MHC Class II Expression in the Two Phenotypes of Antigen-Sampling Cells

Since almost all UEA-1$^+$ gill epithelial cells were M-type antigen-sampling cells, the fraction of MHC class II$^+$ cells among UEA-1$^+$ population was compared between mock-vaccination and *ex vivo*-vaccination. In the mock-vaccination, 17.7% of UEA-1$^+$ cells showed MHC class II expression on their surface (**Figure 5A**), while the percentage of MHC class II$^+$ UEA-1$^+$ cells in the *ex vivo*-vaccination was 26.2% (**Figure 5B**). The difference was statistically significant between mock-vaccination and *ex vivo*-vaccination ($p < 0.05$, **Figure 5C**). The presence of UEA-1$^+$ MHC class II$^+$ cells in the gill epithelium after *ex vivo*-vaccination was confirmed by fluorescence microscopy (**Figure 5D**).

DISCUSSION

The mechanisms of antigen sampling in the mucosal epithelium of teleost fish are mostly unknown. In mammals, M cells in the gut mucosal epithelium take up antigens and deliver them to MALT, where antigen presentation by APCs occurs, and a local immune response is induced. Although teleost fish possess an acquired immune system, they lack highly organized lymphoid structures consisting of lymphoid follicles and germinal centers (8). In this study, we identified two phenotypes of gill epithelial antigen-sampling (GAS) cells in rainbow trout: M-type GAS cells with similar characteristics to mammalian M cells; and macrophage/DC-type GAS cells. Furthermore, we demonstrated that the M-type GAS cells

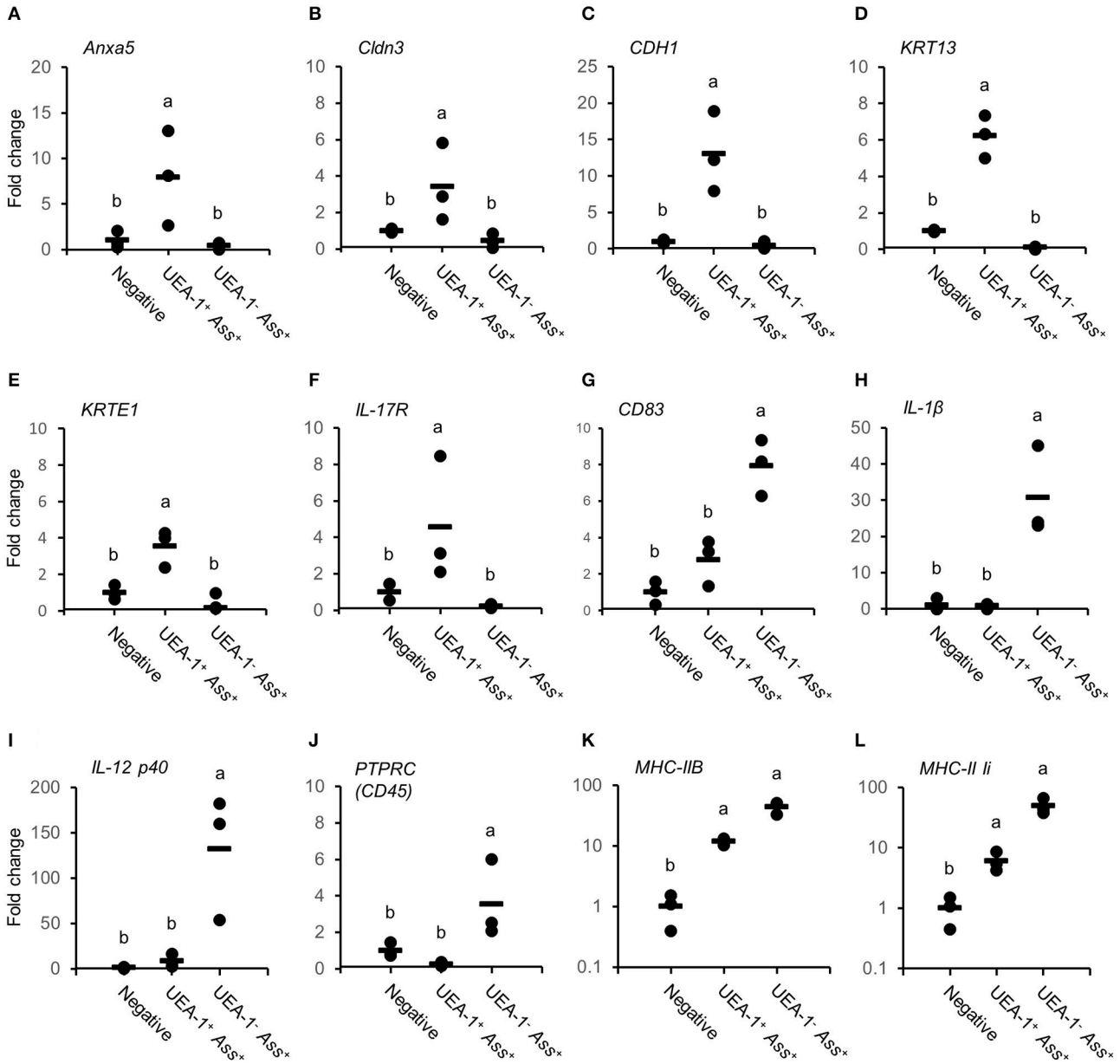


FIGURE 4 | Expression levels of genes expressed in UEA-1^{+} *Ass*$^{+}$ and in UEA-1^{-} *Ass*$^{+}$ cells. **(A–L)** Gene expression levels of *Anxa5* in **(A)**, *Cldn3* in **(B)**, *CDH1* in **(C)**, *KRT13* in **(D)**, *KRTE1* in **(E)**, *IL-17R* in **(F)**, *CD83* in **(G)**, *IL-1β3* in **(H)**, *IL-12p40b* in **(I)**, *PTPRC (CD45)* in **(J)**, *MHC-IIB* in **(K)**, and *MHC-II Ii* in **(L)**, in the three sorted cell populations after bath vaccination. Each dot indicates the gene expression level relative to the mean expression level in the negative cell population, which was set as 1. Horizontal lines indicate the mean expression levels ($n = 3$). Different letters represent significant differences between cell populations ($p < 0.05$, one-way ANOVA with Tukey's *post-hoc* test). Experiments were done by *in vivo* bath vaccination and Data are from one experiment with three individual fish.

show the potential for direct antigen presentation in the gill epithelium. These results suggest an unconventional system of antigen sampling and presentation in the teleost gill epithelium. Our findings may shed light on the mechanisms of local mucosal immune response induction in gill-breathing vertebrates.

It was shown in this work that M-type GAS cells are able to take up bacterins but not fluorescence microbeads during bath administration, suggesting a receptor-based mechanism. The engulfment of bacteria by M cells is dependent on the recognition of bacteria by several receptors. For example, mammalian M cells are able to take up wild-type *Escherichia coli* but not FimH-deficient *E. coli* since glycoprotein 2, a receptor expressed on M cells, selectively binds to FimH on the outer membrane of the bacteria (4). The gill epithelium is the major route for the entry of bacterins of species

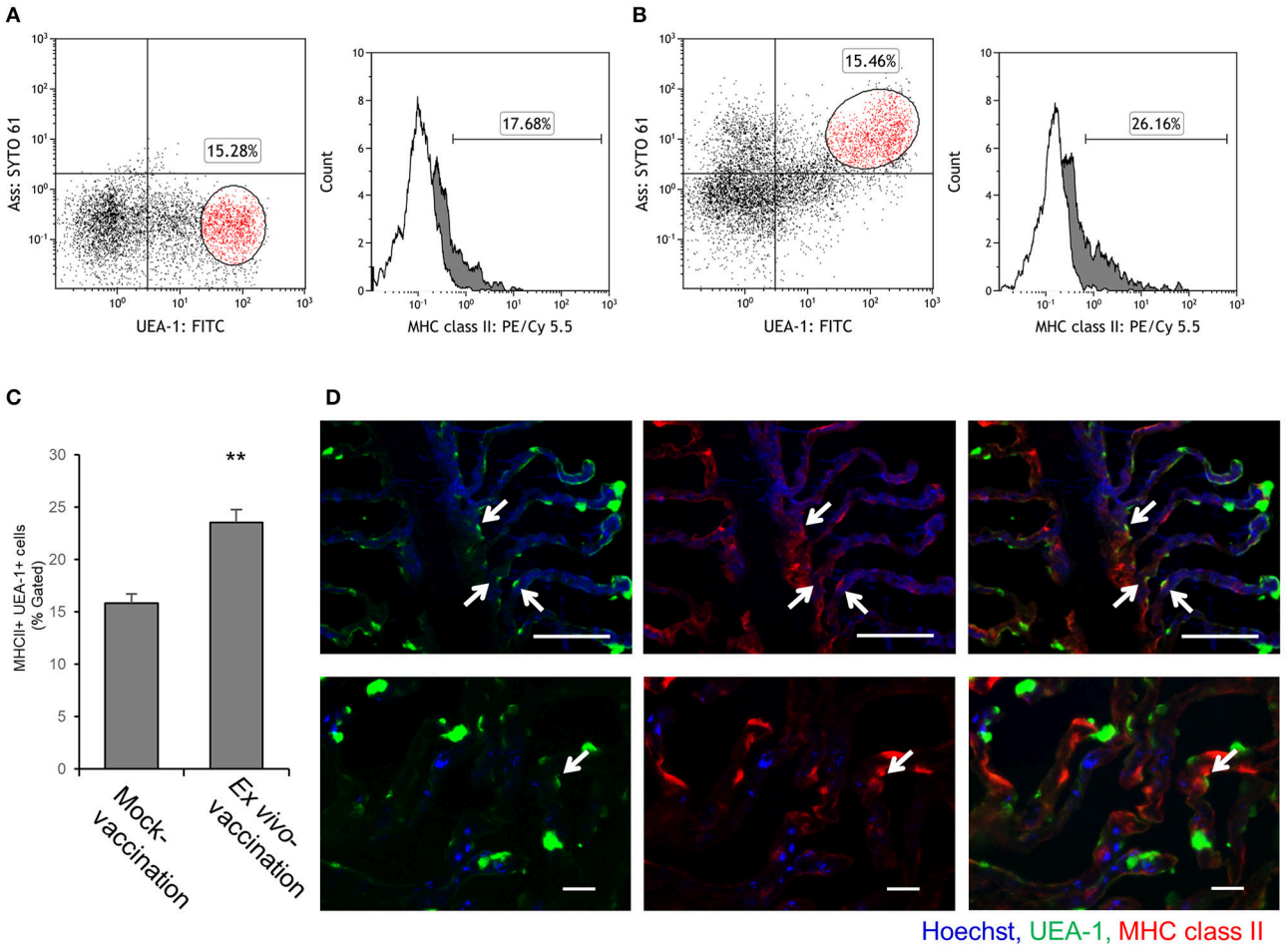


FIGURE 5 | MHC class II expression on UEA-1$^+$ cells after *ex vivo* bath vaccination with *Ass* bacterin. **(A,B)** Flow cytometry for UEA-1, *Ass* and MHC class II staining of gill epithelial cells from the gills *ex vivo* bath-vaccinated with *Ass* bacterin in **A** and mock-vaccinated in **B**. Left panels show dot plots for UEA-1 and *Ass* staining of gill epithelial cells. Right panels show the percentage of MHC class II$^+$ cells, gated on the UEA-1$^+$ cell population. White areas show cells treated only with secondary antibodies (conjugate control), and gray areas show cells positive for MHC class II. **(C)** Mean values for the percentage of MHC class II$^+$ cells gated for UEA-1$^+$ gill epithelial cells of mock-vaccination and *ex vivo* bath-vaccination ($n = 3$). ** $p < 0.01$, Student's *t*-test (two-sided). **(D)** MHC class II$^+$ UEA-1$^+$ gill epithelium cells in the gills *ex vivo* bath-vaccinated with *Ass* bacterin in lower magnification (upper panels) and higher magnification (lower panels). Arrows indicate MHC class II$^+$ UEA-1$^+$ cells. P, primary lamellae; S, secondary lamellae; scale bar, 50 μm (upper panels) and 20 μm (lower panels). Experiments were done by *ex vivo* bath vaccination. Data are representative of three experiments **(A,B)**, or one experiment with three individuals **(C)**, or representative of three experiments **(D)**.

such as *Y. ruckeri* (21) and *V. anguillarum* (23) during bath vaccination. Immunohistochemistry analyses revealed that the gill epithelial cells actively sample vaccine antigens during bath vaccination (21, 23, 25, 27), while fluorescent microbeads administered by bath immersion are rarely taken up (28). These data suggest that M-type GAS cells take up antigens with a certain pattern through receptor-based mechanisms.

The M-type GAS cells showed similar characteristics to mammalian M cells, exemplified by their affinity for lectins (UEA-1$^+$ WGA$^-$) and by high expression of *Anxa5*. Other typical gene markers of mammalian M cells, such as *CCL20, Ctsh*, *Dnclc,* and *Gpx I* (29, 30), were also expressed in M-type GAS cells, although at similar levels to those in negative and macrophage/DC-type GAS cells, based on qRT-PCR analysis (data not shown). The α (1, 2) fucose carbohydrate moiety recognized by UEA-1 has been suggested to play a role in antigen trapping by M cells (31). A role for annexin V, which is important in endocytic transport and membrane scaffolding, has been suggested in M cell-mediated transcytosis (30). The gene expression patterns of M-type GAS cells suggest that they are closely related to mammalian M cells.

The main function of M cells is transcytosis of antigens to dendritic cells and macrophages in mammalian MALT (7). Although there are several reports suggesting that MHC class II is expressed on M cells (32, 33), the general view is that these cells are unable to process and present antigens to T cells since they are markedly deficient in lysosomes (34). In contrast, M-type GAS cells were found to exhibit small vacuoles

in their cytoplasm and to express almost all genes related to the "phagosome," "lysosome," and "antigen processing and presentation" pathways. Further, MHC class II was constitutively expressed on a fraction of M-type GAS cells, which was significantly increased after bath vaccination, suggesting that the MHC class II expression is inducible by antigen stimulation. Similar to our results, MHC class II expression in the gill epithelium has also been reported in Atlantic salmon infected with *Neoparamoeba* sp. amoebae, although the corresponding cells have not been fully characterized (35). Thus, M-type GAS cells are more likely to present antigens in the gill epithelium than bona-fide mammalian M cells in the intestinal epithelium.

In mammals, cells other than M cells in mucosal tissues are able to take up antigens. These cells include type II alveolar epithelial cells, keratinocytes and goblet cells. Multiple reports suggest that most of these epithelial cells show constitutive MHC class II expression and present antigens to T cells (36). Debbabi et al. (37) reported that type II alveolar epithelial cells present exogenous antigens from *Mycobacterium tuberculosis* through MHC class II and that they can prime antigen-specific $CD4^+$ T cells. Keratinocytes are also able to efficiently process and present soluble antigens only to $CD4^+$ memory T cells, resulting in Th1 and Th2 cytokine secretion (38). However, in the present study, no genes characteristic of type II alveolar epithelial cells and keratinocytes, such as surfactant protein A, cytokeratin-8, keratin-6, and aquaporin-3 (39), were found in the mRNA library from M-type GAS cells. Due to the unique gene expression pattern observed in this phenotype of GAS cells and the fact that this cell population constitutively expresses MHC class II in teleosts, M-type GAS cells should be a different cell type from mammalian intestinal M cells.

It has been shown in the past that after bath vaccination with bacterins, the corresponding antigens are transported to the head kidney, trunk kidney and spleen via the blood circulation (21). It has been proposed that vaccine components are processed primarily at the site of melano-macrophage centers in lymphoid organs (40). The spleen and head kidney are the major lymphoid organs of teleost fish (41), and their melano-macrophage centers are considered to be the phylogenetic precursors of germinal centers in higher vertebrates (42). Mammalian macrophages and dendritic cells play an important role in antigen transportation. Rességuier et al. (43) showed that dendritic cells take up surfactant-free poly (lactic acid) nanoparticles in the gill epithelium. In the present work, numerous gill epithelium-resident macrophage/DC-like GAS cells that contained bacterin were found following bath vaccination. This second type of GAS cells might be important for the transportation of vaccine antigens into the lymphoid organs and for the subsequent induction of systemic immune responses, such as the production of specific antibodies (44).

Antigen-specific mucosal immune responses have been frequently reported in mammals (45). Recently, Xu et al. (46) further showed that rainbow trout survived an infection with the parasite *Ichthyophthirius multifiliis* by inducing local proliferation of IgT^+ B cells and IgT production in the gills. In addition, Kai et al. demonstrated that high IgT levels are induced by bath and immersion vaccination, whereas injection vaccination induces high IgM levels (47). These reports suggest that distinct local mucosal immune responses have evolved during the course of vertebrate evolution. Here, we suggest that teleost M-type GAS cells represent a primitive type of epithelial antigen-sampling cells. Bona-fide M cells are critical in terms of inducing local mucosal immune responses in mammalian MALTs, mainly via the transcytosis of antigens (7). Teleost M-type GAS cells may play a similar role in the phylogenetically primitive teleost immune system. In addition, the presence of MHC class II expression suggests an additional role in antigen presentation in the gills, which are an organ with high T cell abundance, especially in ILT (9, 10). Moreover, the results of this work may be valuable for the development of mucosal vaccines that specifically target GAS cells. Due to the rapidly growing aquaculture industry and declining capture fishery resources, effective mucosal vaccines for farmed fish are urgently needed. Bath vaccines significantly reduce working costs and the stress that is usually induced by vaccination via injection of individual fish.

AVAILABILITY OF DATA AND MATERIAL

The whole transcriptome sequence raw data were deposited in the DDBJ Sequence Read Archive (Accession Number: DRA006692).

AUTHOR CONTRIBUTIONS

GK and UF designed the study. GK wrote the manuscript. GK, UF, HM, YN, YI, and TY performed the experiments. HK analyzed the RNA-seq data. MS, UF, and TY edited the manuscript.

FUNDING

This work was supported in part by KAKENHI (26850128 and 16H06201) and by the FP7 EU project TargetFish (311993).

ACKNOWLEDGMENTS

We thank Dr. C. Tafalla for giving us the monoclonal antibody against rainbow trout MHC class II. Ms. G. Czerwinski for assistance with immunohistochemistry. and Ms. S. Schares for assistance with bacterial propagation and cell preparation.

SUPPLEMENTARY MATERIAL

The Supplementary Material for this article can be found online at: https://www.frontiersin.org/articles/10.3389/fimmu.2018.02116/full#supplementary-material

REFERENCES

1. Hein WR. Organization of mucosal lymphoid tissue. *Curr Top Microbiol Immunol*. (1999) 236:1–15. doi: 10.1007/978-3-642-59951-4_1
2. Bockman DE, Cooper MD. Pinocytosis by epithelium associated with lymphoid follicles in the bursa of Fabricius, appendix, and Peyer's patches. An electron microscopic study. *Am J Anat*. (1973) 136:455–77. doi: 10.1002/aja.1001360406
3. Clark MA, Jepson MA, Simmons NL, Booth TA, Hirst BH. Differential expression of lectin-binding sites defines mouse intestinal M-cells. *J Histochem Cytochem*. (1993) 41:1679–87. doi: 10.1177/41.11.7691933
4. Hase K, Kawano K, Nochi T, Pontes GS, Fukuda S, Ebisawa M, et al. Uptake through glycoprotein 2 of FimH (+) bacteria by M cells initiates mucosal immune response. *Nature* (2009) 462:226–30. doi: 10.1038/nature08529
5. Clark MA, Hirst BH, Jepson MA. M-cell surface beta1 integrin expression and invasin-mediated targeting of *Yersinia pseudotuberculosis* to mouse Peyer's patch M cells. *Infect Immun*. (1998) 66:1237–43.
6. Helander A, Silvey KJ, Mantis NJ, Hutchings AB, Chandran K, Lucas WT, et al. The viral σ1 protein and glycoconjugates containing α2-3-linked sialic acid are involved in type 1 reovirus adherence to M cell apical surfaces. *J Virol*. (2003) 77:7964–77. doi: 10.1128/JVI.77.14.7964-7977.2003
7. Mabbott NA, Donaldson DS, Ohno H, Williams IR, Mahajan A. Microfold (M) cells: important immunosurveillance posts in the intestinal epithelium. *Mucosal Immunol*. (2013) 6:666–77. doi: 10.1038/mi.2013.30
8. Zapata A, Amemiya CT. Phylogeny of lower vertebrates and their immunological structures. *Curr Top Microbiol Immunol*. (2000) 248:67–107. doi: 10.1007/978-3-642-59674-2_5
9. Haugarvoll E, Bjerkås I, Nowak BF, Hordvik I, Koppang EO. Identification and characterization of a novel intraepithelial lymphoid tissue in the gills of Atlantic salmon. *J Anat*. (2008) 213:202–9. doi: 10.1111/j.1469-7580.2008.00943.x
10. Koppang EO, Fischer U, Moore L, Tranulis MA, Dijkstra JM, Köllner B, et al. Salmonid T cells assemble in the thymus, spleen and in novel interbranchial lymphoid tissue. *J Anat*. (2010) 217:728–39. doi: 10.1111/j.1469-7580.2010.01305.x
11. Aas IB, Austbø L, König M, Syed M, Falk K, Hordvik I, et al. Transcriptional characterization of the T cell population within the salmonid interbranchial lymphoid tissue. *J Immunol*. (2014) 193:3463–9. doi: 10.4049/jimmunol.1400797
12. Zhang YA, Salinas I, Li J, Parra D, Bjork S, Xu Z, et al. IgT, a primitive immunoglobulin class specialized in mucosal immunity. *Nat Immunol*. (2010) 11:827–35. doi: 10.1038/ni.1913
13. Gudding R, Van Muiswinkel WB. A history of fish vaccination: science-based disease prevention in aquaculture. *Fish Shellfish Immunol*. (2013) 35:1683–8. doi: 10.1016/j.fsi.2013.09.031
14. Adelmann M, Köllner B, Bergmann SM, Fischer U, Lange B, Weitschies W, et al. Development of an oral vaccine for immunisation of rainbow trout (*Oncorhynchus mykiss*) against viral haemorrhagic septicaemia. *Vaccine* (2008) 26:837–44. doi: 10.1016/j.vaccine.2007.11.065
15. Fuglem B, Jirillo E, Bjerkås I, Kiyono H, Nochi T, Yuki Y, et al. Antigen-sampling cells in the salmonid intestinal epithelium. *Dev Comp Immunol*. (2010) 34:768–74. doi: 10.1016/j.dci.2010.02.007
16. Løvmo SD, Speth MT, Repnik U, Koppang EO, Griffiths GW, Hildahl JP. Translocation of nanoparticles and *Mycobacterium marinum* across the intestinal epithelium in zebrafish and the role of the mucosal immune system. *Dev Comp Immunol*. (2017) 67:508–18. doi: 10.1016/j.dci.2016.06.016
17. Villumsen KR, Raida MK. Long-lasting protection induced by bath vaccination against *Aeromonas salmonicida* subsp. salmonicida in rainbow trout. *Fish Shellfish Immunol*. (2013) 35:1649–53. doi: 10.1016/j.fsi.2013.09.013
18. Horne MT, Tatner M, McDerment S, Agius C, Ward P. Vaccination of rainbow trout, *Salmo gairdneri* Richardson, at low temperatures and the long-term persistence of protection. *J Fish Dis*. (1982) 5:343–5. doi: 10.1111/j.1365-2761.1982.tb00490.x
19. Tebbit GL, Erickson JD, Van de Water RB. Development and use of *Yersinia ruckeri* bacterins to control enteric redmouth disease. *Dev Biol Stand.* (1981) 49:395–401.
20. Ototake M, Iwama GK, Nakanishi T. The uptake of bovine serum albumin by the skin of bath-immunised rainbow trout *Oncorhynchus mykiss*. *Fish Shellfish Immunol*. (1996) 6:321–33. doi: 10.1006/fsim.1996.0033
21. Ohtani M, Villumsen KR, Koppang EO, Raida MK. Global 3D imaging of Yersinia ruckeri bacterin uptake in rainbow trout fry. *PLoS ONE* (2015) 10:e0117263. doi: 10.1371/journal.pone.0117263
22. Korbut R, Mehrdana F, Kania PW, Larsen MH, Frees D, Dalsgaard I, et al. Antigen uptake during different life stages of zebrafish (*Danio rerio*) using a gfp-tagged *Yersinia ruckeri*. *PLoS ONE* (2016) 11:e0158968. doi: 10.1371/journal.pone.0158968
23. Kato G, Takano T, Sakai T, Matsuyama T, Nakayasu C. Vibrio anguillarum bacterin uptake via the gills of Japanese flounder and subsequent immune responses. *Fish Shellfish Immunol*. (2013) 35:1591–7. doi: 10.1016/j.fsi.2013.09.007
24. Granja AG, Leal E, Pignatelli J, Castro R, Abós B, Kato G, et al. Identification of teleost skin CD8α+ dendritic-like cells, representing a potential common ancestor for mammalian cross-presenting dendritic cells. *J Immunol*. (2015) 195:1825–37. doi: 10.4049/jimmunol.1500322
25. Torroba M, Anderson DP, Dixon OW, Casares F, Varas A, Alonso L, et al. *In vitro* antigen trapping by gill cells of the rainbow trout: an immunohistochemical study. *Histol Histopathol*. (1993) 8:363–7.
26. Svendsen YS, Dalmo RA, Bøgwald J. Tissue localization of *Aeromonas salmonicida* in Atlantic salmon, *Salmo salar* L., following experimental challenge. *J Fish Dis*. (1999) 22:125–31. doi: 10.1046/j.1365-2761.1999.00153.x
27. Zapata AG, Torroba M, Alvarez F, Anderson DP, Dixon OW, Wisniewski M. Electron microscopic examination of antigen uptake by salmonid gill cells after bath immunization with a bacterin. *J Fish Biol*. (1987) 31:209–17. doi: 10.1111/j.1095-8649.1987.tb05315.x
28. Kiryu I, Ototake M, Nakanishi T, Wakabayashi H. The uptake of fluorescent microspheres into the skin, fins and gills of rainbow trout during immersion. *Fish Pathol*. (2000) 35:41–8. doi: 10.3147/jsfp.35.41
29. Terahara K, Yoshida M, Igarashi O, Nochi T, Pontes GS, Hase K, et al. Comprehensive gene expression profiling of Peyer's patch M cells, villous M-like cells, and intestinal epithelial cells. *J Immunol*. (2008) 180:7840–6. doi: 10.4049/jimmunol.180.12.7840
30. Verbrugghe P, Waelput W, Dieriks B, Waeytens A, Vandesompele J, Cuvelier CA. Murine M cells express annexin V specifically. *J Pathol*. (2006) 209:240–9. doi: 10.1002/path.1970
31. Nochi T, Yuki Y, Matsumura A, Mejima M, Terahara K, Kim DY, et al. A novel M cell-specific carbohydrate-targeted mucosal vaccine effectively induces antigen-specific immune responses. *J Exp Med*. (2007) 204:2789–96. doi: 10.1084/jem.20070607
32. Nagura H, Ohtani H, Masuda T, Kimura M, Nakamura S. HLA-DR expression on M cells overlying Peyer's patches is a common feature of human small intestine. *Acta Pathol Jpn*. (1991) 41:818–23. doi: 10.1111/j.1440-1827.1991.tb01624.x
33. Allan CH, Mendrick DL, Trier JS. Rat intestinal M cells contain acidic endosomal-lysosomal compartments and express class II major histocompatibility complex determinants. *Gastroenterology* (1993) 104:698–708. doi: 10.1016/0016-5085(93)91004-2
34. Owen RL, Apple RT, Bhalla DK. Morphometric and cytochemical analysis of lysosomes in rat Peyer's patch follicle epithelium: their reduction in volume fraction and acid phosphatase content in M cells compared to adjacent enterocytes. *Anat Rec*. (1986) 216:521–7. doi: 10.1002/ar.1092160409
35. Koppang EO, Hordvik I, Bjerkås I, Torvund J, Aune L, Thevarajan J, et al. Production of rabbit antisera against recombinant MHC class II β chain and identification of immunoreactive cells in Atlantic salmon (*Salmo salar*). *Fish Shellfish Immunol*. (2003) 14:115–32. doi: 10.1006/fsim.2002.0424
36. Kambayashi T, Laufer TM. Atypical MHC class II-expressing antigen-presenting cells: can anything replace a dendritic cell? *Nat Rev Immunol*. (2014) 14:719–30. doi: 10.1038/nri3754
37. Debbabi H, Ghosh S, Kamath AB, Alt J, Demello DE, Dunsmore S, et al. Primary type II alveolar epithelial cells present microbial antigens to antigen-specific $CD4^+$ T cells. *Am J Physiol Lung Cell Mol Physiol*. (2005) 289:L274–9. doi: 10.1152/ajplung.00004.2005

38. Black AP, Ardern-Jones MR, Kasprowicz V, Bowness P, Jones L, Bailey AS, et al. Human keratinocyte induction of rapid effector function in antigen-specific memory $CD4^+$ and $CD8^+$ T cells. *Eur J Immunol*. (2007) 37:1485–93. doi: 10.1002/eji.200636915
39. Mao P, Wu S, Li J, Fu W, He W, Liu X, et al. Human alveolar epithelial type II cells in primary culture. *Physiol Rep*. (2015) 3:e12288. doi: 10.14814/phy2.12288
40. Press CM, Evensen O, Reitan LJ, Landsverk T. Retention of furunculosis vaccine components in Atlantic salmon, Salmo salar L., following different routes of vaccine administration. *J Fish Dis*. (1996) 19:215–24. doi: 10.1111/j.1365-2761.1996.tb00128.x
41. Press CM, Evensen Ø. The morphology of the immune system in teleost fishes. *Fish Shellfish Immunol*. (1999) 9:309–18. doi: 10.1006/fsim.1998.0181
42. Vigliano FA, Bermúdez R, Quiroga MI, Nieto JM. Evidence for melano-macrophage centres of teleost as evolutionary precursors of germinal centres of higher vertebrates: an immunohistochemical study. *Fish Shellfish Immunol*. (2006) 21:467–71. doi: 10.1016/j.fsi.2005.12.012
43. Rességuier J, Delaune E, Coolen AL, Levraud JP, Boudinot P, Le Guellec D, et al. Specific and efficient uptake of surfactant-free poly (lactic acid) nanovaccine vehicles by mucosal dendritic cells in adult zebrafish after bath immersion. *Front Immunol*. (2017) 8:190. doi: 10.3389/fimmu.2017.00190
44. Palm RC, Landolt ML, Busch RA. Route of vaccine administration: effects on the specific humoral response in rainbow trout *Oncorhynchus mykiss*. *Dis Aquat Org*. (1998) 33:157–66. doi: 10.3354/dao033157
45. Lamichhane A, Azegami T, Kiyono H. The mucosal immune system for vaccine development. *Vaccine* (2014) 32:6711–23. doi: 10.1016/j.vaccine.2014.08.089
46. Xu Z, Takizawa F, Parra D, Gómez D, von Gersdorff Jørgensen L, LaPatra SE, et al. Mucosal immunoglobulins at respiratory surfaces mark an ancient association that predates the emergence of tetrapods. *Nat Commun*. (2017) 7:10728. doi: 10.1038/ncomms 10728
47. Kai YH, Wu YC, Chi SC. Immune gene expressions in grouper larvae (*Epinephelus coioides*) induced by bath and oral vaccinations with inactivated betanodavirus. *Fish Shellfish Immunol*. (2014) 40:563–9. doi: 10.1016/j.fsi.2014.08.005

Conflict of Interest Statement: The authors declare that the research was conducted in the absence of any commercial or financial relationships that could be construed as a potential conflict of interest.

Copyright © 2018 Kato, Miyazawa, Nakayama, Ikari, Kondo, Yamaguchi, Sano and Fischer. This is an open-access article distributed under the terms of the Creative Commons Attribution License (CC BY). The use, distribution or reproduction in other forums is permitted, provided the original author(s) and the copyright owner(s) are credited and that the original publication in this journal is cited, in accordance with accepted academic practice. No use, distribution or reproduction is permitted which does not comply with these terms.

frontiers in Immunology

ORIGINAL RESEARCH
published: 27 September 2018
doi: 10.3389/fimmu.2018.02115

Origin of Public Memory B Cell Clones in Fish After Antiviral Vaccination

Susana Magadan[1†], Luc Jouneau[1], Maximilian Puelma Touzel[2], Simon Marillet[1,3], Wahiba Chara[4], Adrien Six[4], Edwige Quillet[5], Thierry Mora[6], Aleksandra M. Walczak[2], Frédéric Cazals[3], Oriol Sunyer[7], Simon Fillatreau[8,9,10] and Pierre Boudinot[1*]*

[1] INRA, Virologie et Immunologie Moléculaires, Université Paris-Saclay, Jouy-en-Josas, France, [2] Laboratoire de Physique Théorique, CNRS, Sorbonne Université, and École Normale Supérieure (PSL), Paris, France, [3] Université Côte d'Azur and INRIA, Sophia Antipolis, France, [4] Sorbonne Université, INSERM, UMR S 959, Immunology-Immunopathology -Immunotherapy (I3), Paris, France, [5] INRA, Génétique Animale et Biologie Intégrative, Université Paris-Saclay, Jouy-en-Josas, France, [6] Laboratoire de Physique Statistique, CNRS, UPMC and Ecole Normale Supérieure, PSL, Paris, France, [7] Department of Pathobiology, School of Veterinary Medicine, University of Pennsylvania, Philadelphia, PA, United States, [8] INEM, INSERM U1151/CNRS UMR8253, Institut Necker-Enfants Malades, Faculté de Médecine Paris Descartes, Paris, France, [9] Faculté de Médecine, Université Paris Descartes, Sorbonne Paris Cité, Paris, France, [10] Assistance Publique – Hôpitaux de Paris (AP-HP), Hôpital Necker Enfants Malades, Paris, France

OPEN ACCESS

Edited by:
Roy Ambli Dalmo, UiT The Arctic University of Norway, Norway

Reviewed by:
Yuri B. Lebedev, Institute of Bioorganic Chemistry (RAS), Russia
Maria Forlenza, Wageningen University & Research, Netherlands

***Correspondence:**
Susana Magadan
smaga@uvigo.es
Pierre Boudinot
pierre.boudinot@inra.fr

†Present Address:
Susana Magadan, CINBIO, Immunología, Campus Lagoas Marcosende, Vigo, Spain

Specialty section:
This article was submitted to Comparative Immunology, a section of the journal Frontiers in Immunology

Received: *07 June 2018*
Accepted: *28 August 2018*
Published: *27 September 2018*

Citation:
Magadan S, Jouneau L, Puelma Touzel M, Marillet S, Chara W, Six A, Quillet E, Mora T, Walczak AM, Cazals F, Sunyer O, Fillatreau S and Boudinot P (2018) Origin of Public Memory B Cell Clones in Fish After Antiviral Vaccination. Front. Immunol. 9:2115. doi: 10.3389/fimmu.2018.02115

Vaccination induces "public" antibody clonotypes common to all individuals of a species, that may mediate universal protection against pathogens. Only few studies tried to trace back the origin of these public B-cell clones. Here we used Illumina sequencing and computational modeling to unveil the mechanisms shaping the structure of the fish memory antibody response against an attenuated Viral Hemorrhagic Septicemia rhabdovirus. After vaccination, a persistent memory response with a public VH5JH5 IgM component was composed of dominant antibodies shared among all individuals. The rearrangement model showed that these public junctions occurred with high probability indicating that they were already favored before vaccination due to the recombination process, as shown in mammals. In addition, these clonotypes were in the naïve repertoire associated with larger similarity classes, composed of junctions differing only at one or two positions by amino acids with comparable properties. The model showed that this property was due to selective processes exerted between the recombination and the naive repertoire. Finally, our results showed that public clonotypes greatly expanded after vaccination displayed several VDJ junctions differing only by one or two amino acids with similar properties, highlighting a convergent response. The fish public memory antibody response to a virus is therefore shaped at three levels: by recombination biases, by selection acting on the formation of the pre-vaccination repertoire, and by convergent selection of functionally similar clonotypes during the response. We also show that naive repertoires of IgM and IgT have different structures and sharing between individuals, due to selection biases. In sum, our comparative approach identifies three conserved features of the antibody repertoire associated with public memory responses. These features were already present in the last common ancestors of fish and mammals, while other characteristics may represent species-specific solutions.

Keywords: antibodies, repertoire, B cells, public response, comparative immunology, fish immunology, RepSeq

INTRODUCTION

The adaptive immune system provides vertebrates with a unique ability to generate antigen-specific memory cells associated with an increased protection against previously encountered pathogens. Such responses depend on the available immunological repertoire. The term "repertoire" refers here to the V(D)J rearrangements expressed by the lymphocytes of a particular tissue, at a given moment of the life of an individual, and not to the potential diversity of sequences that can be produced from the genomic resources of the organism (1). Immunological repertoires can now be accessed with unprecedented accuracy using high-throughput DNA sequencing (2–4).

The global characterization of the antibody (Ab) repertoires of unchallenged mammals and fish has highlighted the presence of highly frequent clonotypes shared between several individuals (5–9). This observation indicates that repertoires are not simply determined by equally likely random rearrangements of Ig gene segments (2, 10). Thus, certain receptors might be shared between unchallenged controls simply due to their high generation probability.

The sequencing of the IgH repertoires of humans vaccinated against influenza showed that clonotype expansions reflect secreted Ab responses (11, 12). In addition, a dominant set of convergent VDJ rearrangements specific to influenza and shared by the majority of exposed individuals was identified. Such responses made of clonotypes expanded in nearly all individuals are called public responses, and usually contain potent effector clones (13). Public responses are interesting because it is reasonable to assume that they are directed toward the eliciting antigen, while that assumption can generally not be made for individual-specific private responses. The well-studied case of anti-phosphorylcholine public T15 response exemplifies that public responses can play a major role in protection against the targeted pathogen (14, 15). Understanding how public memory clonotypes are selected from the naïve repertoire after an immune challenge might facilitate the development of better universal vaccines. Recently, a few studies have pointed the importance of a genetic pre-determination of the rearrangement probability as a mechanism affecting the establishment of public memory responses after an immune challenge (5, 16, 17).

Public Ab responses are observed in evolutionarily distant species since they are also found in fish, which evolved in parallel to tetrapods over the past 400 million years. We previously identified a public IgM effector response to an attenuated strain of the rhabdovirus Viral Hemorrhagic Septicemia Virus (VHSV) in isogenic rainbow trout (18). In fish, IgM^+ B cells are complemented by IgT^+ B cells (19), which constitute a distinct lineage since these two Ig are produced from alternative rearrangements, and B cells do not undergo isotype switch recombination. IgM acts primarily as a systemic Ig and is the major Ig class in the serum, while IgT is mainly — but not exclusively—specialized in mucosal immunity (20) and in the control of the gut microbiota (21). In spleen, 70–80% of B cells express IgM, and 20–30% IgT. IgM^+ B cells are the main source of circulating virus-neutralizing Abs following VHSV infection (18). However, a response was also detected for IgT after a prime/boost with VHSV, which did not show evidence of a public component (18).

In this work, starting with the characterization of the pre-vaccination repertoire, we found that IgM repertoires of naïve fish included highly abundant fish-specific clonotypes, as well as less abundant clonotypes with a higher degree of sharing between fish. By contrast, IgT repertoires were richer in shared clonotypes, and the most abundant ones were much less frequent than for IgM. Following vaccination, fish established persistent public IgM clonotype expansions in spleen for several months after the clearance of the virus. We sought to elucidate the properties of these clonotypes, to gain some insight into the selection processes associated with the establishment of public memory cells. We demonstrate that both the statistics of Ig gene rearrangement and selection processes prior to vaccination contribute to the generation of repertoires in unvaccinated fish that yield the public memory responses.

MATERIALS AND METHODS

Fish Vaccination and Ethical Statement

Rainbow trout were raised, vaccinated against VHSV and boosted in the fish facilities of INRA (Jouy en Josas, France). This study was carried out in accordance with the recommendations of the European Union guidelines for the handling of laboratory animals (http://ec.europa.eu/environment/chemicals/lab_animals/index_en.htm). All animal work at INRA was approved by the Direction of the Veterinary Services of Versailles (authorization 78-28) as well as fish facilities (authorization B78-720), and the experimental protocols were approved by the INRA institutional ethical committee "Comethea" (permit license number #15-60).

ELISPOT and Virus Neutralization Assay

VHSV specific IgM secreting cells were determined in head kidney using *ex vivo* ELISPOT (22) and **Supplementary Methods**. Virus neutralization assay with complement addition was performed in 12-well plates as previously described (18). The neutralizing titer was calculated as highest trout serum dilution causing a 50% reduction of the average number of plaques in control cultures inoculated with control trout serum, complement and virus.

CDR3 Length Spectratyping Analysis and Preparation of Illumina MiSeq Libraries

CDR3 length spectratyping analysis was performed as described in Castro et al. (18), and CDR3 length profiles were generated by GeneMapper (Applied). Libraries for Illumina deep sequencing were prepared as described in Vollmers et al. (11). For cDNA barcoding, the primers used for second strand cDNA contained 15 random nt (**Figure S1** and **Supplementary Methods**).

Sequencing and Data Analysis

Sequencing consisted in paired-end 2 × 300 pb runs, using a MiSeq instrument (Illumina) and the MiSeq Reagent Kit v3 (600 cycles) (Illumina). Sequencing analysis and annotation,

estimation of error rate, and normalization by subsampling, as well as validation of our barcoded IgH cDNA sequencing approach, are described in **Supplementary Methods**.

Sequence data were registered in the BioProject ncbi database with the SRA accession number: SRP128087.

Computational Model of IgH VDJ Rearrangements

We employed an existing computational tool suite, IGoR (23), to construct a generative probabilistic model of the IgH VDJ recombination process and generate corresponding synthetic receptor sequences. The parameters were inferred for each VHC combination sequenced in this work, from the corresponding sets of non-productive sequences. IGoR can then be used to generate synthetic nucleotide sequences, which can readily be translated into amino-acid sequences and compared between synthetic datasets (i.e., generated by the model). A detailed description of the model is provided in **Supplementary Methods**.

RESULTS

Vaccination With Attenuated VHSV Induces Persistent Public IgM Response in Spleen

Long-lasting humoral immune responses can be induced in fish after immunization (22, 24). Five months after vaccination with an attenuated VHSH strain (**Figure 1A**), rainbow trout had elevated serum neutralizing Ab titers (**Table S1A**), long after the elimination of the virus, which was not detectable by qPCR already 1 month post-injection. We analyzed the spleen B cell repertoire at 5 months post-vaccination to characterize the long-term persisting reactive B cells, which we called "memory" following A Radbruch's definition in Farber et al. (25). This was first performed with a global cost-effective CDR3 spectratyping of all expressed combinations of heavy chain variable (VH) and constant (C) genes, to identify the Ig gene segments implicated in the response and therefore relevant for further analysis by high-throughput sequencing (**Supplementary Methods**). In fish all VH segments can recombine with either μ or τ DJC units, while IgM and IgT have distinct repertoires of DH and JH genes (**Figure S1**). An isogenic trout clone was used to avoid genetic background heterogeneity (18).

The IgM repertoires of vaccinated fish had altered profiles for the VH1, VH4, and VH5 families (**Figure 1B**, **Figure S3**). The altered profile of VH5 was the only one found in all vaccinated individuals (**Figure 1B**), suggesting that it may contain a persisting public component, while the responses associated with VH1 and VH4 varied from fish to fish. Notably, the VH5 family was previously found to be implicated in the VHSV-specific public effector B cell response (18). The IgT repertoire was also modified 5 months after vaccination, with most individuals displaying skewed VH4Cτ profiles compared to unvaccinated controls, even though no common peak was identified (**Figure 1B**, **Figure S3**).

The implication of only a few VH families in the long-term B cell response is in contrast to the previous identification of broad Ig repertoire alterations affecting almost all VH families shortly after two infections at a 3-weeks interval with the same rhabdovirus (18). This suggests that the spectratype analysis performed 5 months after vaccination may have identified only a part of the memory compartment. To look for other rearrangements that were potentially implicated in the memory response, vaccinated fish were boosted at 5 months post-vaccination, and their repertoire was analyzed 1 month later (**Figure 1A**). The boost induced a >10-fold increase of the frequency of anti-VHSV IgM-secreting cells in pronephros, proving that a secondary response occurred (**Table S1B**), even though it did not lead to a significant increase of neutralizing Ab titers (**Table S1A**). Importantly, the response observed in the spleen after the boost remained restricted to the VH families that were already identified 5 months post-vaccination (**Figure 1B**, **Figure S3**).

We conclude from these results that the vaccination induced a long-lasting IgM memory response associated with only a few VH families, which persisted beyond the elimination of the virus.

Distinct Properties of the Most Abundant IgM and IgT Clonotypes in Unvaccinated Controls

Having validated that it was possible to identify a memory B cell response in fish, potentially comprising a public VH5Cμ response, we then examined the clonal structure of the VH5Cμ response using Illumina deep sequencing. We also investigated the private VH4Cμ and VH4Cτ responses, as well as some VHC combinations that did not obviously contribute to the response (VH8Cμ, VH5Cτ, and VH9Cτ) as controls. Sequencing was performed in unvaccinated control (Ctl), vaccinated (Vac), and boosted (Bst) fish with 4 individuals per group. We used a consensus read sequencing approach based on the incorporation of a unique random barcode serving as molecular identifier in each cDNA molecule, as described for human IgH (11) [see **Figures S1**, **S2** and **Supplementary Methods** about molecular identifiers (MID)]. We define a clonotype as a specific combination of C (μ or τ), VH, JH, and CDR3 amino acid sequence. We first describe results obtained for unvaccinated controls, which provide a benchmark for the analysis of the changes induced by the vaccination and the boost.

Individual fish datasets obtained for each VHC combination were normalized by random subsampling of 7,000 clonotypes without replacement to quantitatively compare all fish together despite varying sequencing depths, while preserving the clonotypes' relative frequencies. Ten subsamplings were performed, and the average results were analyzed (see Supporting methods for details). A comparison of the number of distinct IgM and IgT clonotypes in unvaccinated controls suggested that the repertoires were more diverse for IgT than for IgM for all VH (**Table S2A**). We counted the number of IgM and IgT clonotypes found in at least 3 individuals, which were labeled as "highly shared" (HS). The numbers of HS clonotypes were higher for VHCτ than for VHCμ sequences, except for VH5Cμ (**Table S2B**). These two observations suggested that the IgT repertoires were richer in shared clonotypes of small abundances, while IgM repertoires included

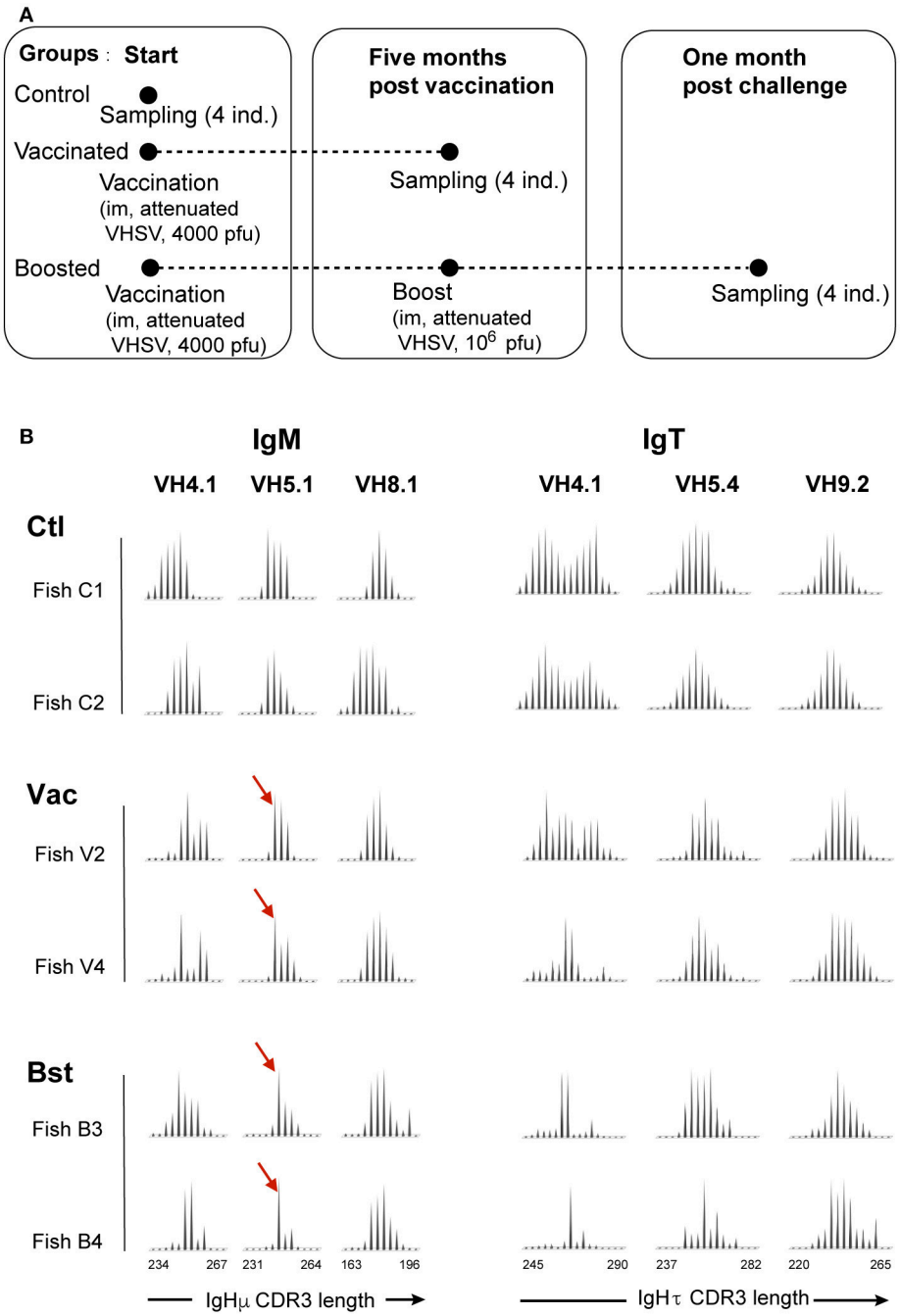


FIGURE 1 | Spectratyping analysis identifies persistent Ab memory responses to VHSV. **(A)** Time line of sampling, vaccination and boost experiments. Groups of six fish were constituted. **(B)** Typical CDR3 length profiles of μ and τ transcripts for selected VH in the spleen of controls ("Ctl"), vaccinated fish analyzed 5 months post-injection ("Vac"), and boosted fish analyzed month later ("Bst"). Profiles for other VH are shown in **Figure S3**. The red arrows denote the main peak of the putative public response. VH primers used are indicated at the top of the figure. Y-axis, fluorescence arbitrary units; X-axis, length of the run-off products; same scale for IgM and IgT.

clonotypes of large abundances that were fish-specific. This last statement was further supported by the abundance distribution of clonotypes present in 1, 2, 3 or all unvaccinated control fish (**Figure S4A**). It is nonetheless noteworthy that the VH5Cμ repertoire contained a higher number of HS clonotypes of small abundance compared to the other IgM repertoires.

We next focused on the most abundant clonotypes for each VHC combination in each fish. To this end, we considered the 50 or 100 most abundant clonotypes (called "Top50" and "Top100"

clonotypes thereafter). For each group (Ctl, Vac, and Bst), the 4 sets of "Top50" clonotypes from each of the 4 fish in the group were aggregated to obtain lists of non-redundant clonotypes called Top Clonotype Lists ($TCL)_{Ctl}$, $TCL_{Vac,}$ or TCL_{Bst}. The total number of clonotypes in a TCL was thus between 50 (if all were shared by the 4 fish of the group), and 200 (if none were shared) for the Top50 case. We then analyzed for each clonotype of a TCL in how many fish of a group (Ctl, Vac, or Bst) it was found. The distributions of TCL_{Ctl} clonotypes are represented in the left column in **Figure 2**, **Figure S5A**. Individual fish datasets, for each VHC combination, were normalized as described above. The clonotype sharing was also studied for the Top100 (**Figure S5B**), and for the whole set of subsampled sequences (**Figure S5C**).

In the unvaccinated control group, most of the VH4Cμ and VH8Cμ TCL_{Ctl} clonotypes were found in only one fish (**Figure S5A**,a,g, blue bars). These clonotypes were not found in any other fish of the vaccinated or boosted groups, indicating that they were private expansions found in a single fish. In contrast, 53 out of 190 VH5Cμ TCL_{Ctl} clonotypes were shared by two or more fish (**Figure S5A,**d, blue bars). The total number of clonotypes in the TCL_{Ctl} was lower for IgT rearrangements than for IgM (197 for VH4Cμ, 189 for VH5Cμ, 198 for VH8Cμ, vs. 146 for VH4Cτ, 110 for VH5Cτ, and 103 for VH9Cτ), indicating a higher degree of sharing of the most abundant IgT clonotypes between fish for IgT compared to IgM. A substantial fraction of the IgT TCL_{Ctl} were found in several fish, i.e., 70% for VH5Cτ, 66% for VH9Cτ, and 45% for VH4Cτ (**Figure S5A**,j,m,p, blue bars). As expected from this elevated degree of sharing, a significant fraction of the IgT TCL_{Ctl} were also found in the vaccinated (48% for VH4Cτ, 68% for VH5Cτ, and 68% for VH9Cτ), and boosted (56% for VH4Cτ, 75% for VH5Cτ, and 72% for VH9Cτ) fish (**Figure S5A**,j,m,p, red and green bars).

Top100 clonotypes were shared in a very similar manner (**Figure S5B**) as Top50 clonotypes, with close to double the number of shared clonotypes compared to the Top50 lists. In contrast, when all 7,000 subsampled clonotypes were taken into account (**Figure S5C**), only a small fraction were shared by two or more individuals, even for the VHC combinations that share a significant numbers of Top clonotypes, i.e., VH5Cμ (6%), VH4Cτ (2%), VH5Cτ (5%), and VH9Cτ (4%) This shared fraction therefore mostly involved the most abundant clonotypes (i.e., included in the Top 50 lists), in unvaccinated fish.

To assess the overall contribution of the Top50 clonotypes to the repertoire in unvaccinated controls, we analyzed the cumulative expression of these TCL_{Ctl} within each group. The cumulative counts of the Top50 clonotypes for the 4 naïve control fish were on average >10,000 for all VHCμ combinations, out of a total number of 28,000 sequences analyzed (4 fish × 7,000 MID subsampled per fish). Highly frequent clonotypes thus represent a large fraction of the IgM transcripts in the control group. In contrast, Top50 clonotypes did not represent a large part of the IgT repertoires, with averaged cumulative counts of about 1,000 (**Figure 2A**, left column, blue bars). Distributions of cumulative expression of Top100 clonotypes showed only a small increase compared to Top50 clonotypes (**Figure S6A**), indicating that Top50 clonotypes account for most of the cumulative counts (see also **Figure S6B** for all clonotypes).

In summary, in unvaccinated control fish, the most frequent clonotypes represent a considerable fraction of IgM transcripts and differ from fish to fish (except for VH5), while the most frequent IgT clonotypes account for only a small fraction of the expressed repertoire and are generally shared between individuals (**Figure S4B**). Our results thus reveal different degrees of sharing among IgM and IgT repertoires in the spleen of naïve unvaccinated control fish, and point to the peculiarity of the VH5Cμ repertoire.

Sharing of IgM and IgT Top50 Clonotypes in Unvaccinated Controls Is Determined by Selection Rather Than at the Rearrangement Level

These differences between IgM and IgT Top50 clonotypes, i.e., their contrasted degree of sharing between unvaccinated controls, may already exist in the clonotypes that emerge from the recombination process, before any selection. To assess this possibility, we constructed a model of the recombination machinery using the IGoR software (23). IGoR can be used to generate "synthetic" nucleotide sequences, which can readily be translated into amino-acid sequences and used for comparisons. It is based on the statistics of IgH VDJ rearrangements computed using the non-productive (either out-of-frame or with an in-frame premature stop codon) junctions of our dataset (see Supporting methods), which were not subjected to selection since they were not expressed at the protein level. The model was parametrized by the probabilities of the events that form a recombination event: the choice of VH, DH, and JH segments as well as the insertion and deletion profiles at the VD and DJ joints. DH and JH gene usage varied across VH family and Ig isotype, while insertion and deletion profiles were largely similar, with the exception of VH5Cμ for which insertions at the VD junction were smaller (**Figures S7A,B**).

To evaluate the degree to which the difference in IgM and IgT repertoire diversity was determined by the rearrangement process, we estimated IgM and IgT diversity from the distribution of clonotype generation probabilities (P_{gen}) obtained from the repertoires generated by IGoR. We quantified diversity using the entropy, S, a well-established diversity measure expressed in units of bits (26). The entropy estimates (27) varied by <15% across the various VHC combinations (**Table S2C**). This is consistent with the observation of similar deletion and insertion profiles at the VD and DJ joints across VHC combinations (**Figure S7B**), as previous work (10, 28) has shown that the diversity does not arise mainly from the variety of VDJ combinations but from the deletions and insertions.

Thus, the model predicts similar diversity for IgM and IgT. We infer from this result that the observed difference in diversity between IgT and IgM naive repertoires (**Table S2A**) is not pre-determined by rearrangements, but rather results from B cell selection.

We next used this model to address whether the different sharing patterns of TCL between IgM and IgT may be explained, at least partly, by the different probability of generation (P_{gen}) of the frequent clonotypes across VHC combinations. The model

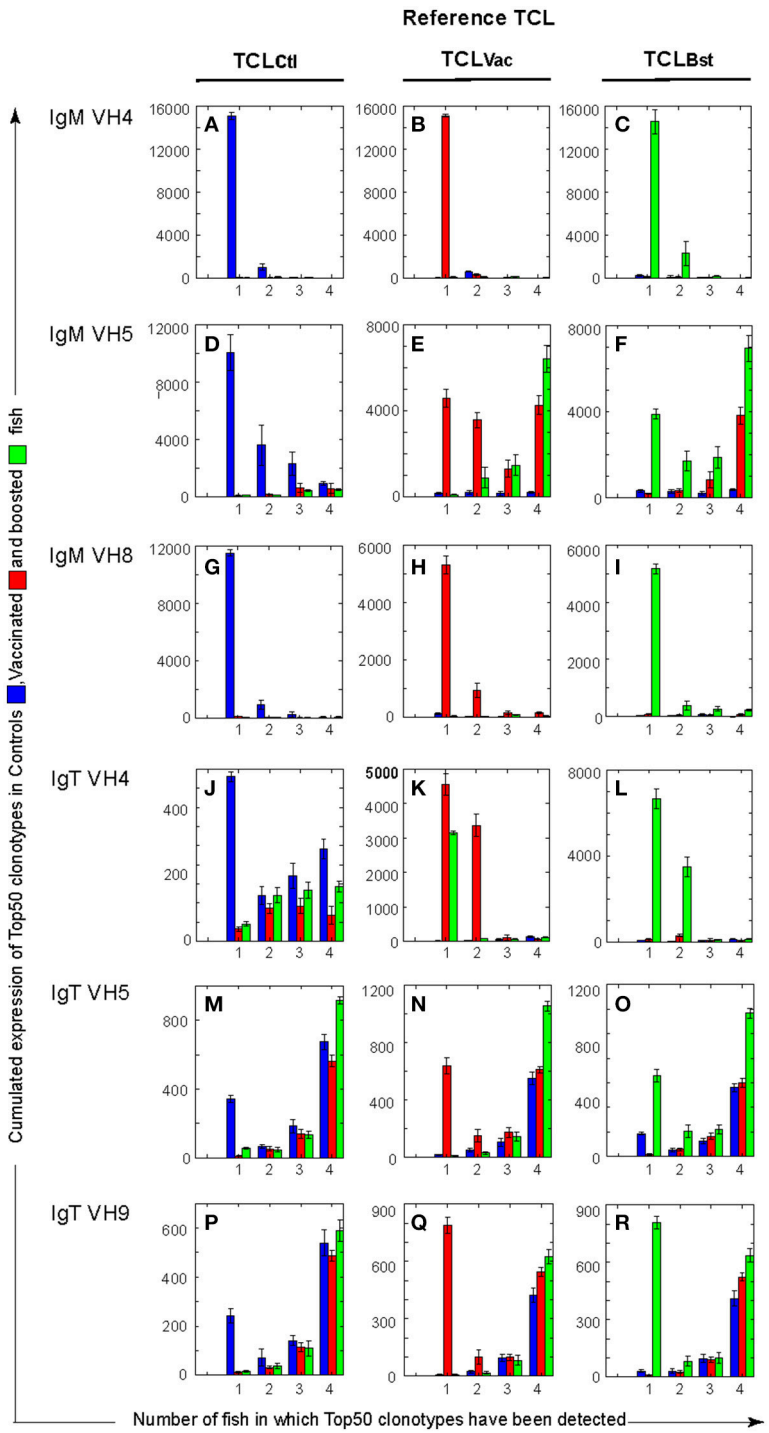


FIGURE 2 | Cumulative expression of Top50 clonotypes shared by *n* individuals within each group (Ctl, control; Vac, vaccinated; and Bst, Boosted) unveils differences between VH and isotypes. For each TCL (TCLCtl, (**A,D,G,J,M,P**); TCLVac, (**B,E,H,K,N,Q**); TCLBst, (**C,F,I,L,O,R**)), bar plots showing the cumulative expression of TCL clonotypes found in individual subsample(s) from *n* fish ($n = 1, 2, 3, 4$). For example, in **(A)** blue bars show the cumulative counts of TCLCtl clonotypes in fish from the control group, while red (respectively green) bars show TCLCtl cumulative expression in fish from the vaccinated (respectively boosted) group. Similarly, in **(B)** red bars show the cumulative counts of TCLVac clonotypes in vaccinated fish, while blue (respectively green) bars show TCLVac cumulative expression in control and boosted groups, respectively. Bars are computed from the average values corresponding to top clonotypes found in 1–4 fish, over 10 subsamplings of 7,000). The standard deviations are shown as error bars.

was therefore used to evaluate the P_{gen} of observed TCL_{Ctl} junctions. **Figure 3A** shows that for four VHC combinations, the Top50 clonotypes from controls (purple line) are more likely to be generated via the recombination process, compared to the P_{gen} distributions of all observed clonotypes from naive controls (black line), which are fairly similar across VHC combinations (**Figure S7C**). These P_{gen} distributions are in agreement with the model prediction for all possible junctions (green line in **Figure 3A**). It is however difficult to conclude that the rearrangement process favors Top50 clonotypes in general because such a bias in P_{gen} was not observed for VH4Cμ and VH4Cτ.

To investigate the possible effect of this VDJ rearrangement bias on the difference between IgM and IgT in clonotype sharing, we computed the amount of sharing expected for a simulated set of clonotypes from the synthetic repertoire, through the same procedure used to produce **Figure S5A**. In **Figure S7D**, we compare these results to the distributions in the experimental data from control fish. For IgM, both the empirical and predicted distributions show similar levels of sharing, except for VH5. In contrast, for IgT, the amount of sharing predicted by the model differs from the experimental data. Hence, comparing the model's and control group's number of clonotypes shared at the level of all 7,000-subsampled clonotypes, the model accounts neither for the high sharing of IgT clonotypes (dark vs. light red), nor for much of the sharing of VH5Cμ clonotypes (**Figure S7D**). The analysis of the level of sharing of Top50 clonotypes showed the same trend (**Figure 3B**).

We conclude that the difference in the sharing pattern between IgM and IgT for the Top50 clonotypes in unvaccinated controls is not pre-determined by biases of VDJ rearrangements, but rather reflects selection acting on cells of the B lineage before or at the primary B cell stage.

Impact of Vaccination and Boost on the Structure of Repertoires of Most Abundant IgM and IgT Clonotypes

We next analyzed whether the vaccination or the boost affected the composition of the Top50 IgM and IgT clonotypes.

The distribution of Top50 clonotypes in vaccinated fish (middle column in **Figure 2**, **Figure S5A**) was clearly altered in the VH5Cμ repertoire, with a strong increase in the cumulative counts of clonotypes shared by all fish of the vaccinated and boosted groups compared to unvaccinated controls (**Figures 2E,F**, red and green bars, respectively). A significant proportion of the TCL_{Vac} clonotypes were found in several vaccinated or boosted fish (**Figure S5A**,e, red and green bars). Interestingly, most of the VH5Cμ clonotypes found in both TCL_{Vac} and TCL_{Bst} (19/26) were not among the Top50 clonotypes from unvaccinated control fish (**Figure S5A**, Venn diagrams). The change in the VH5Cμ distribution is peculiar because, by contrast, the IgM VH4Cμ and VH8Cμ TCL_{Vac} displayed distributions of sharing similar to those observed in unvaccinated controls. They were mostly found in single vaccinated or boosted fish (**Figure S5A**,b,h). These results demonstrate that VH5Cμ rearrangements are involved in a public memory response.

The vaccination also altered the distribution of Top50 VH4Cτ clonotypes, that showed a clear increase in the cumulative number of counts for the most abundant clonotypes, from 500 to about 4,500 (**Figure 2**). However, these expansions were specific to each individual since the cumulative counts of clonotypes shared by several fish remained low (**Figure 2**). This supports the notion that some VH4Cτ rearrangements are implicated in a private manner in the response to vaccination. As expected, the VH5Cτ and VH9Cτ distributions found in vaccinated and boosted fish were reminiscent of those found in unvaccinated controls with no obvious evidence of vaccine-induced modifications (**Figure 2**, **Figure S5A**,n,q, red bars).

Comparison of the cumulative expression of Top50 and Top100 clonotypes (**Figure 2**, **Figure S6A**) showed that the increase of shared clonotypes in vaccinated and boosted groups is based on the expansion of the Top50 clonotypes. The particular level of sharing observed for VH5Cμ was very clear even when all 7,000-subsampled clonotypes were analyzed (**Figure S6B**).

Taken together, these data highlight the contribution of the VH5Cμ to the public response. The responding clonotypes become part of the Top50 clonotypes in the vaccinated and boosted fish, reaching high cumulative counts with a high degree of sharing. The clonotypes implicated in the response were not among the Top50 clonotypes in unvaccinated controls, indicating that the response was recruited from less abundant clonotypes. The analysis of the Top100 and 7,000-subsampled clonotypes supported these conclusions (**Figure S6A**), and showed that the highly shared clonotypes are mainly found among the most frequent clonotypes.

Public IgM Memory Clonotypes of Vaccinated Fish Are Frequent in Unvaccinated Controls, and Produced at High Frequency by the Rearrangement Process

In order to characterize the origin of the VH5Cμ clonotypes implicated in the public memory response to VHSV, we first identified the clonotypes that were (1) detected in at least three out of four fish of the vaccinated or boosted groups, (2) more expressed in vaccinated (or boosted) fish than in unvaccinated, and (3) consistently well-expressed across most fish of the vaccinated and/or boosted groups (i.e., found >10 times in ≥ 3 fish in Vac or Bst groups; See **Supplementary Methods**, **Table S3**). This led us to identify 8 IgM clonotypes. These clonotypes all had the VH5 and JH5 segments and had a common CDR3 length of 10 amino acids (AA), which coincides with the public peak in the spectratypes (**Figure 4**). Five among these 8 clonotypes had been identified among the most abundant shared clonotypes of the effector response in our previous study of the immediate response following immmunization (18), and differences with the other three sequences were substitutions by AA with similar properties. These 8 public clonotypes were also among the VH5Cμ Top50 clonotype lists from the vaccinated

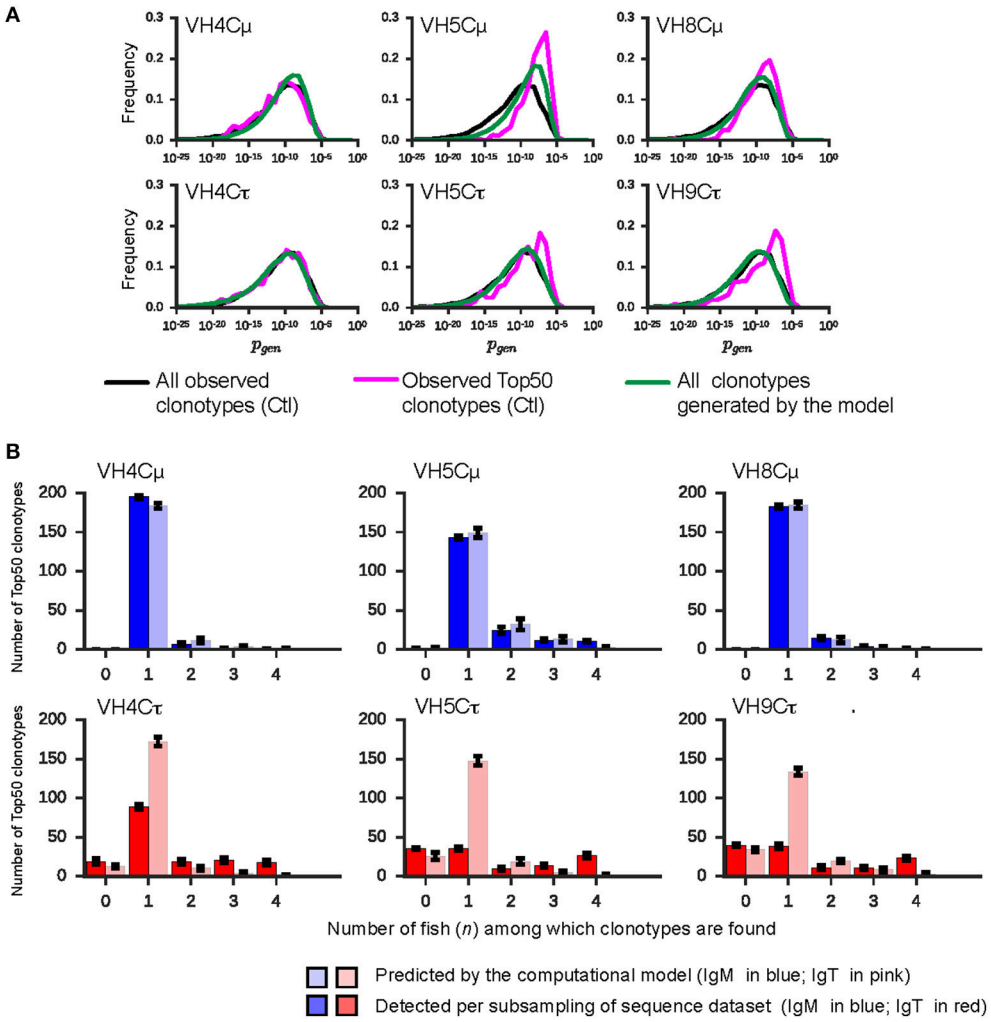


FIGURE 3 | The sharing of Top50 clonotypes between individuals is determined by selection. **(A)** Distribution of Pgen for all clonotypes from controls (black line), for Top50 clonotypes of controls (i.e., TCLCtl; pink line), and for all sequences generated by the computational model (green line). **(B)** Histograms of the sharing of TCLCtl clonotypes. Left (right) bars show the numbers of measured (respectively predicted) TCLCtl clonotypes shared among n individual measured (predicted) repertoires (n = 0, 1, 2, 3, 4) out of 4. IgM is colored in blue; IgT is colored in red. Error bars for the rearrangement model correspond to standard error values across sampled repertoires. Error bars for the sequencing data correspond to the standard deviations of 10 subsamplings of 7,000.

and boosted groups (TCL_{Vac} and TCL_{Bst}) (**Figures 5A,B**, **Figures S4C,D**).

Each of the these eight public VH5JH5Cμ clonotypes was encoded by 4–17 different nucleotide sequences in vaccinated and boosted fish; this diversity highlights a form of convergence, strongly suggesting that these clonotypes had been subjected to antigen-driven clonal selection during the response (**Table S4**). Additionally, these Ig sequences had overall very few N/P nucleotides especially at the V-D joint, in line with their increased probability of generation (**Figure 5D**).

We next examined unvaccinated controls to determine how frequent these clonotypes were, and their degree of sharing prior to vaccination. At least 2 and up to 6 of these clonotypes were detected per control fish in the various sub-samplings. Within the frequency distribution of all the clonotypes found in unvaccinated fish (**Figure 5C**), they were among the relatively frequent clonotypes.

We then used the computational model presented above to evaluate whether these clonotypes were favored by the VDJ recombination process. Indeed, the distribution of the generation probabilities P_{gen} of all the nucleotide sequences coding for the 8 public amino acid clonotypes was higher than for all VH5Cμ nucleotide sequences (**Figure 5D**). The set of VH5-JH5 rearrangements with a CDR3 length of 10 AA also had a higher probability of generation than the one estimated for all VH5Cμ (**Figure 5D**). Thus, the high probability of generation of these

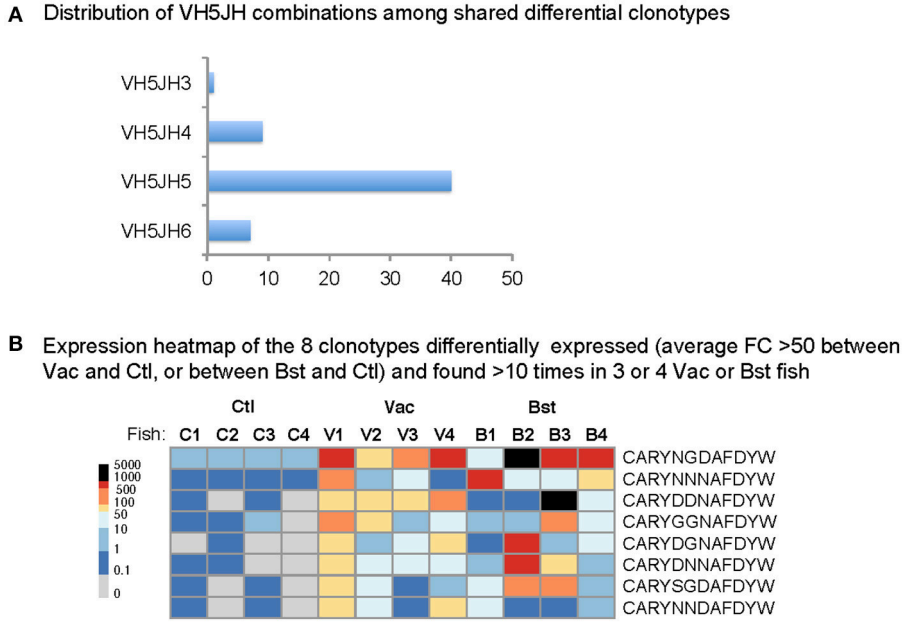


FIGURE 4 | Identification of eight clonotypes of the public response against VHSV. **(A)** The distribution of VH5JH IgM clonotypes shared within vaccinated and boosted groups (detected in ≥3 fish per group) and differentially expressed, compared to the naïve unvaccinated control (Ctl) groups (average FC >50) is shown. **(B)** Expression heatmap of the eight clonotypes detected >10 times in at least vaccinated (vac) or bosted (Bst) fish. All these clonotypes express the VH5JH5 combination. The bar on the left defines the color code of the heatmap, graduated in average MID numbers per subsample.

eight rearrangements is at least partially due to the length of the CDR3 and the usage of JH5.

Collectively, these data suggest that the IgM clonotypes implicated in the public memory response are already present at modestly elevated frequencies in all/most unvaccinated controls, consistently with the higher probability of rearrangement of these clonotypes.

Distinct VHC Combinations Differ by Their Production of Similar Clonotypes

So far we have considered the public response from the point of view of individual clonotypes taken separately. However, public responses generally involve a mixture of similar clonotypes differing only by one or two "conservative" mutations in their CDR3 i.e., by substitutions with amino acids that share similar properties and usually preserve the recognition of the same epitope (18, 29–31). Such clonotypes—hereafter refered to as "similar"—are often present at variable frequencies in different immunized individuals. Notably, the 8 VH5JH5 clonotypes identified in this study are similar to each other since they differ only by small changes in their CDR3 sequences (**Figure 4**). For any clonotype found in the public response, a class of "similar" clonotypes may also have responded. The size of these classes in unvaccinated controls is likely to influence the probability that they are shared between distinct individuals and their likelihood of being implicated in a public response. It is therefore important to take into account these classes of "similar" sequences when assessing the propensity of clonotypes to generate a public response.

We first assessed whether distinct VHC combinations differed in the amount of junction similarity exhibited between clonotypes from the same VHC combination. We thus counted pairs of "similar" sequences formed from any set of two individual repertoires among the 4 fish in a given group (i.e., 6 such sets of two repertoires per group), for each VHC combination. This procedure was applied to data obtained from each of the control, vaccinated and boosted conditions (see **Figure 6A**). We observed that these counts were much higher for VH5Cμ than for any other combination and progressively more in the vaccinated and boosted groups. This feature was present already before vaccination (**Figure 6A**, left panel). Thus, this higher level of convergence might confer to the VH5Cμ combination a higher probability of generating public responses than the other analyzed VHC combinations.

We then checked whether the computational model could predict this particular feature of the VH5Cμ repertoire. Using the same definition of clonotype similarity class, we assessed the propensity for convergence within repertoires predicted by the recombination model describe earlier, for each VHC combination (see **Supplementary Methods**), and compared it to the observed data for the unvaccinated controls (**Figure 6B**). We found that VH5Cμ (along with VH4Cμ) exhibited only slightly higher amounts of convergence than the rest of the combinations in the modeled data (**Figure 6B**), while it was much higher

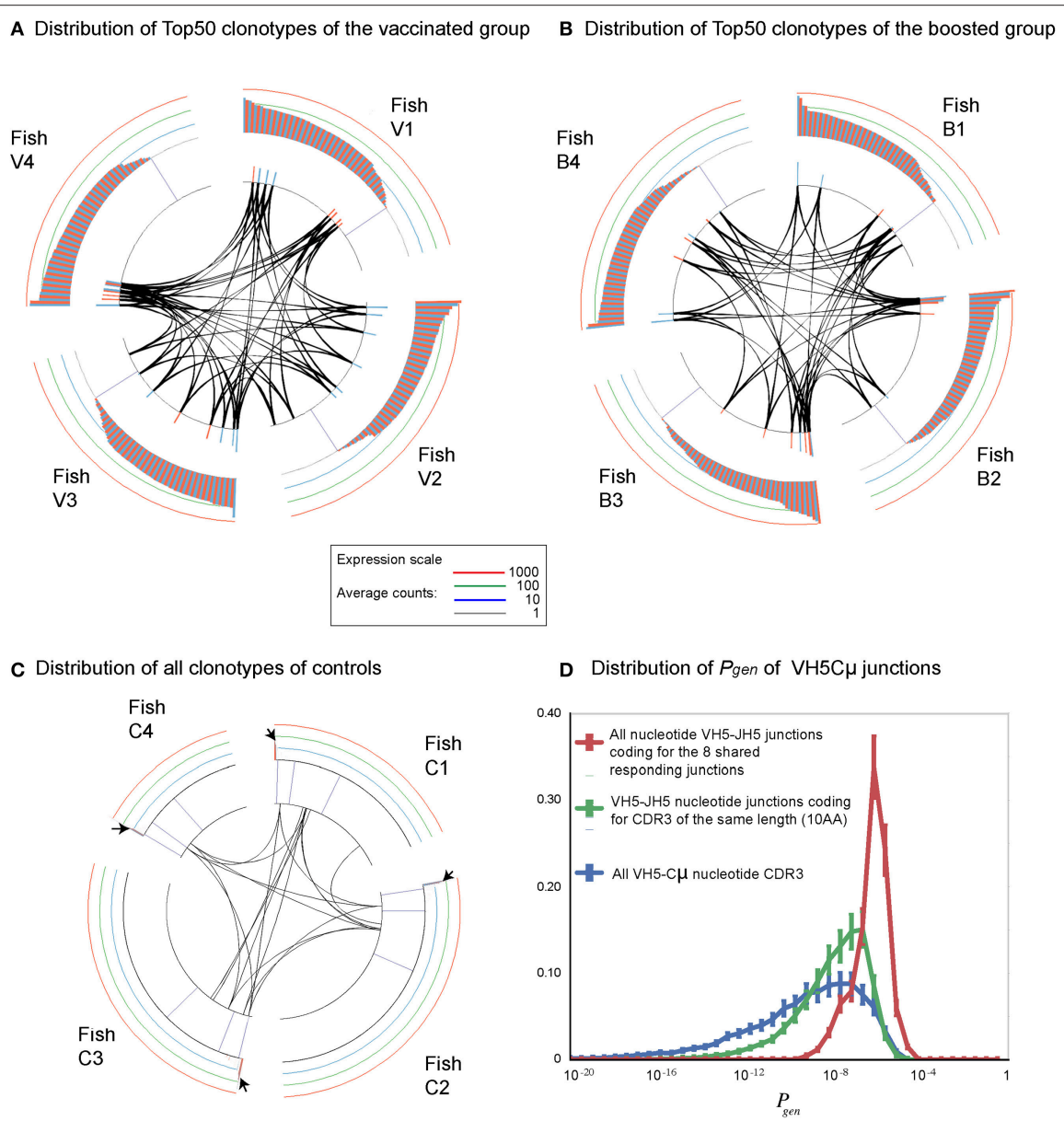


FIGURE 5 | Clonotypes implicated in the shared/public response are already frequent in naive unvaccinated fish. **(A,B)** the eight clonotypes of the VH5 public response are placed into the expression profile of the VH5 TCLvac (respectively TCLbst) of each fish. VH5Cμ Top50 clonotypes of each fish are plotted on circumference of the outer circle, by decreasing expression order, with the alternated red and blue bars representing their respective abundance at logarithmic scale. When detected within the Top50 lists of two individuals, clonotypes are connected with black lines. **(C)** Ranking of the VH5-JH5 "public" clonotypes detected within the whole distribution of VH5Cμ clonotypes in controls. Small arrows denote the most frequent clonotypes at the top side of the distribution **(D)** Distribution of generation probability of junctions coding for the 8 core responding clonotypes (in red), compared with the distribution computed for all VH5Cμ junctions (in blue), or for all VH5JH5 junctions of the same length (in green).

in the experimental data. The same difference of convergence between model and experimental data was observed when the analysis was restricted to the 8 public clonotypes (**Figure 6C**), confirming that selection before vaccination (i.e., within the naive repertoire or during the differentiation at earlier stages), rather than the rearrangement process alone, promoted the presence of large shared classes of "similar" clonotypes for the VH5Cμ rearrangement.

DISCUSSION

High-throughput sequencing has made the complexity of immunological repertoires accessible to experimental investigations (32). We used this approach to characterize the persistent public immune response induced upon vaccination in fish, and to examine its origin in the naïve pre-vaccination repertoire. The public Ab response after

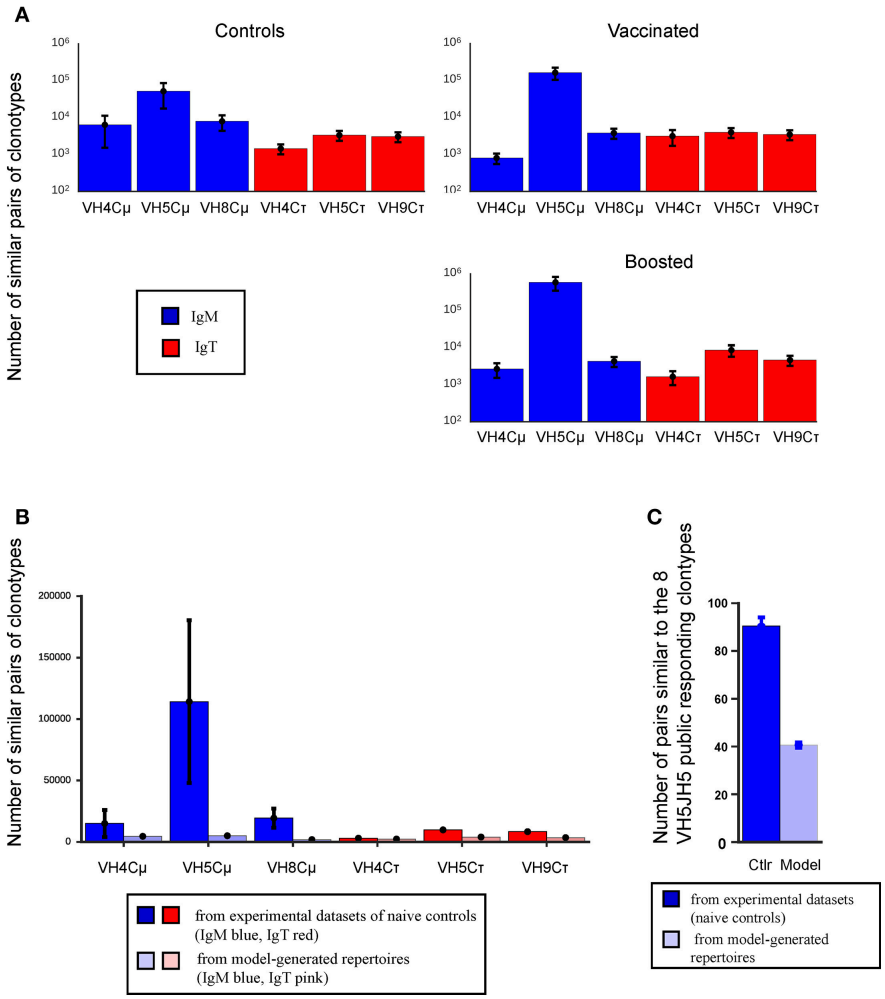


FIGURE 6 | VH5Cμ exhibits distinctly higher CDR3 similarity classes than other VHC, even in naive unvaccinated individuals, but not in the model prediction. Bars show the mean number of similar pairs of clonotypes, (i.e., those with a CDR3 differing by up to 2 AA substitutions within AA groups with similar properties). **(A)** Mean number of pairs of clonotypes deemed similar to each other for each VHC combination and across conditions. For a given condition, pairs of clonotypes were formed from any of the 6 distinct sets of two individual repertoires among the four individuals analyzed. Blue bars represent Cμ, while red bars represent Cτ. Means are calculated across the 6 possible distinct combinations and error bars show their standard error. Note the distinctly larger number of shared clonotype for VH5Cμ. **(B)** Number of similar pairs of clonotypes within the measured control (left) and predicted model (right) repertoires for each VHC combination. Means and standard errors calculated as in **(A)**. Note that the number for VH5Cμ is less distinct compared to **(A)**. **(C)** The number of VH5Cμ clonotypes similar to any of the eight VH5JH5 clonotypes of the public response for the measured control (left bar) and model predicted (right bar) repertoires for the model and three conditions. Means and standard errors are calculated across four individual repertoires.

vaccination against VHSV, a natural pathogen of rainbow trout, constituted a unique fish model for this approach, with isogenic genetic background available. Our study led us to identify three layers of organization of the IgM repertoire in naïve unvaccinated controls. The first layer comprises the most abundant clonotypes, of which we characterized the top 50 as being mostly present only in given individuals and arising from selection during Ag driven responses. The second layer contains clonotypes favored genetically by the rearrangement process, which are more abundant than if generated via an equally likely rearrangement process. Such clonotypes are more likely to be found in multiple fish, and some of them do give rise to the public response after vaccination, as shown here for the VH5JH5 clonotypes of the anti-VHSV public response. The third layer, which we did not characterize in detail, is made of less frequent clonotypes and encompasses the main fraction of the repertoire. Collectively, our findings identify two complementary processes of the naïve repertoire that are associated with the VH5 public memory response: (1) the high probability of rearrangements encoding public junctions, and (2) a high frequency of selection of classes of clonotypes with CDR3

similar to each other into the naive pre-vaccination VH5 IgM repertoire.

Importantly, while we have no biochemical evidence that the 8 public clonotypes encode Ab directed against the VHSV epitope, this specificity is strongly suggested by several lines of evidence: following our definition of "public," the set of 8 clonotypes was expanded in all immunized individuals, as in our previous study. These clonotypes or similar ones were not expanded in isogenic trout after vaccination against another virus, the Infectious Pancreatic Necrosis Virus (data not shown). Second, these expanded clonotypes were encoded by multiple nucleotide sequences, which is a good indication for Ag driven selection. Altogether, these observations indicate that the 8 public sequences are very different from clonotypes named "public" in other contexts. Indeed, another definition for public clonotypes that has recently been used by different authors is "shared by at least two individuals" (17, 33), or (3) for T cells.

Contrasted Structures of IgM and IgT Repertoires in Spleen Before Vaccination

For both IgM and IgT, most VDJ combinations were present at low frequency in unvaccinated controls. However, the normalized distributions of IgM and IgT clonotypes differed when considering the most abundant ones. The abundance of Top50 clonotypes was typically 10–20 times higher for IgM than for IgT. This pattern was not predicted by our computational model of rearrangements, indicating that it was due to post-recombination selective processes exerted on B cells before vaccination. The spleen IgM and IgT repertoires also differed in the degree of sharing of the most frequent clonotypes (**Figure 7**). Very few top IgM clonotypes, except for VH5, were shared by more than two individuals, while more than one third of the top IgT clonotypes were shared. A similar pattern was observed when considering all clonotypes. Hence, IgM most abundant clonotypes may reflect each individual's unique immunological

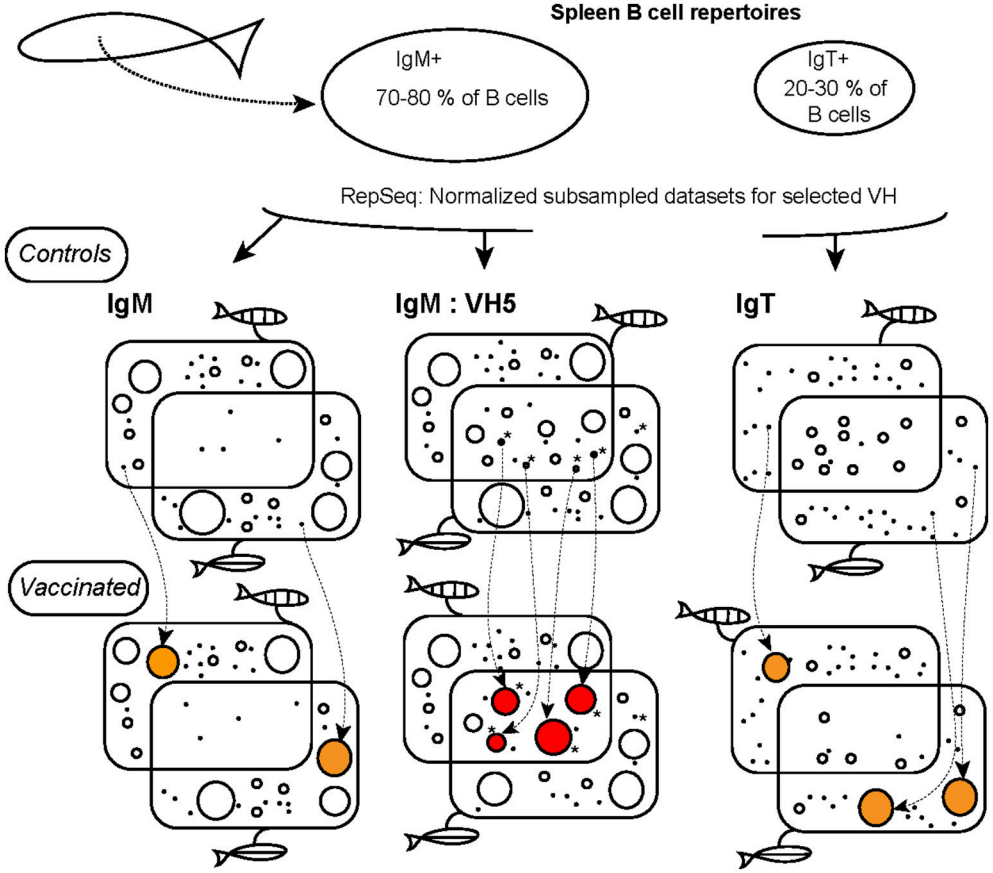


FIGURE 7 | Schematic model of trout IgM and IgT responses against the virus. The diameter of circles reflects the size of clonotypes. Two individual fish are identified by vertical or horizontal stripes. Naïve unvaccinated IgT repertoires contain shared clonotypes of small size, even the Top clonotypes, while IgM repertoires included clonotypes of large size that are mainly specific to individuals. Response to the virus comprises private IgM or IgT clonotypes (represented in orange), or public clonotypes (represented in red). Note that IgT private response reduces the level of sharing of top clonotypes, and leads to highly frequent clonotypes specific to the virus. The VH5 IgM public response is based on highly shared clonotypes already present in naïve unvaccinated controls. Sets of clonotypes similar (but not identical) to public anti VHSV clonotypes, are denoted by*. Such sets of similar clonotypes are very prominent in the VH5 IgM repertoire. The proportions of clonotypes of different sizes reflect the global structure of the repertoires, but does not exactly correspond to the average distribution of our datasets (see **Figure S4** for such a representation).

history, while the stereotyped IgT repertoire may be shaped by common components of the environment. Since IgT is the main isotype involved in mucosal immunity, this may reflect the effect of common components of the microbiota, in line with the key role of intestinal microbes in the generation of the IgA repertoire in human and mice (34). Additionally, differences of IgH mRNA expression level between (activated) IgM^+ and IgT^+ B cells may also affect clonotype sharing in sequence data. This remains difficult to take into account because these expression levels are poorly defined.

Fish Maintain IgM and IgT Components of the Response to Vaccination Over 5 Months in the Spleen

The B cell repertoire response signatures persisted in spleen for months after vaccination, involving public clonotypes previously found in fish infected twice at 3 weeks interval (18). Our previous data suggested that the most frequent clonotypes of the VH5Cμ public response after two infections in quick succession could represent up to 25–30% of the total VH5Cμ transcripts (18). In this dataset, they reached 10–15% at most, suggesting that the size of public VHSV-specific top clonotypes is smaller 5 months post-vaccination. This is consistent with the maintenance of a lower pool of "memory" clonotypes after the elimination of the attenuated virus. This result differs from immunizations with hapten-carrier conjugates (TNP-KLH), where the high-affinity Abs appeared only 3 months after trout immunization (35). In line with the notion that the vaccination induced the generation of memory cells, the boost was associated with a marked accumulation of virus-specific antibody-secreting cells in the pronephros, and an increased abundance of similar clonotypes shared by all fish in the spleen for the VH5Cμ rearrangement that contained the public response (**Figure 2**).

The VH Repertoire Involved in Public Memory Responses Has Distinctive Characteristics

Eight VH5JH5 clonotypes were expanded in most or all vaccinated fish, with CDR3 differing only by one or two "conservative" substitutions. Overall, this VH5JH5 IgM response can therefore be named truly "public" (36). These public clonotypes were among the most frequent in VH5Cμ, and were as frequent as the top clonotypes of the other responding VHC families (data not shown), indicating that public and private responses were of the same order of magnitude.

Public responses depend on clones that are relatively frequent before immunization (5, 16, 17, 37). It is more likely for such clones to be selected by their specific epitope early in the response in all individuals, and to outcompete other clones as was proposed for T-cell receptors (38). Most public VH5JH5Cμ clonotypes were detected in several unvaccinated controls, and ranked on the high side of the frequency distribution, although far below the Top50. Our computational model showed that these public rearrangements were more likely produced by the recombination machinery than other VH5-JH5 junctions. The IgM public response is therefore at least partly biased by recombination. In contrast, the clonotypes involved in the large private VH4Cτ expansions observed in infected fish were not detected in controls (data not shown). These findings should be put in the context of a growing evidence for repertoire biasing across vertebrates. In adult zebrafish, Weinstein et al. found that 250 clonotypes were shared much more often than predicted by a uniform random model (2). A strong bias in the recombination process was also reported for human (10) and mouse (17) B cell repertoires, and the effect of such bias on the sharing of repertoires has been extensively studied for T cell receptors (39–42).

In human and mice, public responses comprise multiple clonotypes with the same VH and JH, and CDR3 amino acid sequences of identical length differing by one or two AA (9, 26–28, 38, 39). To investigate the role of this property in our system, we first determined the fraction of the repertoire that consisted in classes of similar clonotypes differing from each other in such a way. We found that this fraction was higher for VH5Cμ than for any other VHC combination even in unvaccinated controls, suggesting a generic characteristic of the VH5Cμ combination independent of the public response to VHSV. Since our model of rearrangements did not predict this distinctive property of VH5Cμ (**Figure 6**), it must be mainly due to the selection processes shaping the naive pre-vaccination repertoire, possibly involving previous exposure to environmental microbes, as reported for mice (17). Thus, the junctions of the public clonotypes are not only favored by the rearrangement process, but also are found together with many other highly similar VH5DHJH5 junctions in unvaccinated controls that may bind related epitopes. A schematic representation of the IgM public response, compared to IgM and IgT private responses, is shown in **Figure 7**. VHSV being a natural pathogen of rainbow trout evolving as a viral quasi-species, our data may suggest that some properties of the VH5Cμ repertoire have been selected during trout/VHSV co-evolution. Further studies in different host/pathogens models across vertebrates will determine whether the degree of convergence of IgH CDR3 between different VH (before immunization) is correlated to their implication in public responses.

CONCLUSION

Our data provide novel insights into the generation of public memory responses in the context of vaccination with an attenuated virus in fish. This information could be useful practically: if public clonotype expansions are correlated to protective specific Ab responses against pathogens, they could constitute excellent biomarkers of the efficiency of vaccines in aquaculture. On the other hand, observations from fish have a further interest when compared to other vertebrates. Teleost fish are an old, basal lineage of vertebrates, which has evolved in parallel with tetrapods for more than 350 million years. Their immune system shares basic components with other vertebrates, but is nonetheless very divergent. Regarding B cells and Ab responses, lack of lymph nodes and germinal centers, slow kinetics of Abs responses, poor affinity maturation are important

differences compared to humans and mice. Hence, the fish B cell system is adapted to very different anatomical and physiological constraints (43). Therefore, features conserved with respect to the common ancestors of fish and mammals are likely to be essential, while other characteristics may represent fish-specific original solutions. The implication of clonotypes with a high probability of generation in public responses therefore appears to be one of the fundamental traits conserved across vertebrates, for B and T cells (39, 41). This mechanism could have been selected during evolution because it favored B cells mediating public responses against microbial epitopes. In contrast, the idea that for certain VH (VH5 in this study) large classes of "similar" clonotypes are positively selected before vaccination, guaranteeing the presence of relevant clonotypes targeting key epitopes, remains to be tested in other groups of vertebrates. Overal, our data show that the fish public memory antibody response to a virus is determined at three levels: by recombination biases, by selection acting on the formation of the pre-vaccination repertoire, and by convergent selection of functionally similar clonotypes during the response. Our data pave the way for a better definition of the features of public responses across vertebrates.

AUTHOR CONTRIBUTIONS

SuM, TM, AW, SF, and PB conceived the project. SuM, AS, OS, SF, and PB designed experiments. SuM and PB performed wet-lab experiments. MPT, AW,TM designed the computational model. SuM, LJ, MPT, SM, WC, AS, FC, AW, TM, and PB performed primary data analysis. AS and EQ provided resources. SuM, MPT, TM, AW, SF, and PB wrote the manuscript. All authors edited the manuscript.

FUNDING

This work was supported by the Institut National de la Recherche Agronomique (INRA), by the European Commission under the Work Programme 2012 of the 7th Framework Programme for Research and Technological Development of the European Union (Grant Agreements 311993 TARGETFISH, ERCStG n. 306312, and 600391 People Programme) and by the ANR-16-CE20-0002-01 (FishRNAVax). SM has been supported by an INRA-INRIA contract Young scientist. OS has been supported by NIH grant# R01-GM085207-08 and by NSF grant# IOS-1457282.

ACKNOWLEDGMENTS

We acknowledge L. du Pasquier, J. Hansen, Yan Jaszczyszyn, A. Krasnov, J. P. Levraud, and P. A. Cazenave for helpful discussions, and the INRA fish facilities (IERP). This work has benefited from the facilities and expertise of the Molecular Biology platform of TEFOR and I2BC.

SUPPLEMENTARY MATERIAL

The Supplementary Material for this article can be found online at: https://www.frontiersin.org/articles/10.3389/fimmu.2018.02115/full#supplementary-material

REFERENCES

1. Jerne N. What precedes clonal selection? ontogeny of acquiredimmunity. In: *Proceedings of the CIBA Foundation Symposium* (Amsterdam: CIBA) (1971).
2. Weinstein JA, Jiang N, White RA, Fisher DS, Quake SRS, White III R. High-throughput sequencing of the zebrafish antibody repertoire. *Science* (2009) 324:807–11. doi: 10.1126/science.1170020
3. Covacu R, Philip H, Jaronen M, Almeida J, Kenison JE, Darko S, et al. System-wide analysis of the T cell response. *Cell Rep.* (2016) 14:2733–44. doi: 10.1016/j.celrep.2016.02.056
4. Ma KY, He C, Wendel BS, Williams CM, Xiao J, Yang H, et al. Immune repertoire sequencing using molecular identifiers enables accurate clonality discovery and clone size quantification. *Front Immunol.* (2018) 9:33. doi: 10.3389/fimmu.2018.00033
5. Mora T, Walczak AM, Bialek W, Callan CG. Maximum entropy models for antibody diversity. *Proc Natl Acad Sci USA.* (2010) 107:5405–10. doi: 10.1073/pnas.1001705107
6. Galson JD, Truck J, Fowler A, Munz M, Cerundolo V, Pollard AJ, et al. In-depth assessment of within-individual and inter-individual variation in the B cell receptor repertoire. *Front Immunol.* (2015) 6:531. doi: 10.3389/fimmu.2015.00531
7. DeWitt WS, Lindau P, Snyder TM, Sherwood AM, Vignali M, Carlson CS, et al. A public database of memory and naive B-cell receptor sequences. *PLoS ONE* (2016) 11:e0160853. doi: 10.1371/journal.pone.0160853
8. Krasnov A, Jorgensen SM, Afanasyev S. Ig-seq: deep sequencing of the variable region of atlantic salmon IgM heavy chain transcripts. *Mol Immunol.* (2017) 88:99–105. doi: 10.1016/j.molimm.2017.06.022
9. Fu X, Sun J, Tan E, Shimizu K, Reza MS, Watabe S, et al. High-throughput sequencing of the expressed torafugu (*Takifugu rubripes*) antibody sequences distinguishes IgM and IgT repertoires and reveals evidence of convergent evolution. *Front Immunol.* (2018) 9:251. doi: 10.3389/fimmu.2018.00251
10. Elhanati Y, Sethna Z, Marcou, Q, Callan CGJr, Mora T, Walczak AM. Inferring processes underlying B-cell repertoire diversity. *Philos Trans R Soc Lond B Biol Sci.* (2015) 370:20140243. doi: 10.1098/rstb.2014.0243
11. Vollmers C, Sit RV, Weinstein JA, Dekker CL, Quake SR. Genetic measurement of memory B-cell recall using antibody repertoire sequencing. *Proc Natl Acad Sci USA.* (2013) 110:13463–8. doi: 10.1073/pnas.1312146110
12. Jackson KJ, Liu Y, Roskin KM, Glanville J, Hoh RA, Seo K, et al. Human responses to influenza vaccination show seroconversion signatures and convergent antibody rearrangements. *Cell Host Microbe* (2014) 16:105–14. doi: 10.1016/j.chom.2014.05.013
13. Acha-Orbea H, Mitchell DJ, Timmermann L, Wraith DC, Tausch GS, Waldor MK, et al. Limited heterogeneity of T cell receptors from lymphocytes mediating autoimmune encephalomyelitis allows specific immune intervention. *Cell* (1988) 54:263–73. doi: 10.1016/0092-8674(88)90558-2
14. Briles DE, Forman C, Hudak S, Claflin JL. Anti-phosphorylcholine antibodies of the T15 idiotype are optimally protective against *Streptococcus pneumoniae. J Exp Med.* (1982) 156:1177–85. doi: 10.1084/jem.156.4.1177
15. Mi QS, Zhou L, Schulze DH, Fischer RT, Lustig A, Rezanka LJ, et al. Highly reduced protection against *Streptococcus pneumoniae* after deletion of a single heavy chain gene in mouse. *Proc Natl Acad Sci USA.* (2000) 97:6031–6. doi: 10.1073/pnas.110039497
16. Wang C, Liu Y, Cavanagh MM, Le Saux S, Qi Q, Roskin KM, et al. B-cell repertoire responses to varicella-zoster vaccination in human identical twins. *Proc Natl Acad Sci USA.* (2015) 112:500–5. doi: 10.1073/pnas.1415875112
17. Greiff V, Menzel U, Miho E, Weber C, Riedel R, Cook S, et al. Systems analysis reveals high genetic and antigen-driven predetermination of antibody

repertoires throughout B cell development. *Cell Rep.* (2017) 19:1467–78. doi: 10.1016/j.celrep.2017.04.054
18. Castro R, Jouneau L, Pham HP, Bouchez O, Giudicelli V, Lefranc MP, et al. Teleost fish mount complex clonal IgM and IgT responses in spleen upon systemic viral infection. *PLoS Pathog.* (2013) 9:e1003098. doi: 10.1371/journal.ppat.1003098
19. Hansen J, Landis E, Phillips R. Discovery of a unique Ig heavy-chain isotype (IgT) in rainbow trout: implications for a distinctive B cell developmental pathway in teleost fish. *Proc Natl Acad Sci USA.* (2005) 102:6919–24. doi: 10.1073/pnas.0500027102
20. Salinas I, Zhang Y-A, Sunyer JO. Mucosal immunoglobulins and B cells of teleost fish. *Dev. Comp. Immunol.* (2011) 35:1346–65. doi: 10.1016/j.dci.2011.11.009
21. Zhang Y-A, Salinas I, Li J, Parra D, Bjork S, Xu Z, et al. IgT, a primitive immunoglobulin class specialized in mucosal immunity. *Nat. Immunol.* (2010) 11:827–35. doi: 10.1038/ni.1913
22. Bromage ES, Kaattari IM, Zwollo P, Kaattari SL. Plasmablast and plasma cell production and distribution in trout immune tissues. *J Immunol.* (2004) *173*:7317–23. doi: 10.4049/jimmunol.173.12.7317
23. Marcou Q, Mora T, Walczak AM. High-throughput immune repertoire analysis with IGoR. *Nat Commun.* (2018) 9:561–9. doi: 10.1038/s41467-018-02832-w
24. Ma C, Ye J, Kaattari SL. Differential compartmentalization of memory B cells versus plasma cells in salmonid fish. *Eur J Immunol.* (2013) 43:360–70. doi: 10.1002/eji.201242570
25. Farber DL, Netea MG, Radbruch A, Rajewsky K, Zinkernagel RM. Immunological memory: lessons from the past and a look to the future. *Nat Rev Immunol.* (2016) 16:124–8. doi: 10.1038/nri.2016.13
26. Cover TM, Thomas JA. *Elements of Information Theory.* Hoboken, NJ: Wiley (2006).
27. Mora T, Walczak AM. Renyi entropy, abundance distribution, and the equivalence of ensembles. *Phys Rev E* (2016) 93:052418. doi: 10.1103/PhysRevE.93.052418
28. Murugan A, Mora T, Walczak AM, Callan CG. Statistical inference of the generation probability of T-cell receptors from sequence repertoires. *Proc Natl Acad Sci USA.* (2012) 109:16161–6. doi: 10.1073/pnas.1212755109
29. Cibotti R, Cabaniols JP, Pannetier C, Delarbre C, Vergnon I, Kanellopoulos JM, et al. Public and private V beta T cell receptor repertoires against hen egg white lysozyme (HEL) in nontransgenic versus HEL transgenic mice. *J Exp Med.* (1994) 180:861–72. doi: 10.1084/jem.180.3.861
30. Bousso P, Casrouge A, Altman JD, Haury M, Kanellopoulos J, Abastado J-PP, et al. Individual variations in the murine T cell response to a specific peptide reflect variability in naive repertoires. *Immunity* (1998) 9:169–78. doi: 10.1016/S1074-7613(00)80599-3
31. Lin MY, Welsh RM. Stability and diversity of T cell receptor repertoire usage during lymphocytic choriomeningitis virus infection of mice. *J Exp Med.* (1998) 188:1993–2005. doi: 10.1084/jem.188.11.1993
32. Friedensohn S, Khan TA, Reddy ST. Advanced methodologies in high-throughput sequencing of immune repertoires. *Trends Biotechnol.* (2017) 35:203–14. doi: 10.1016/j.tibtech.2016.09.010
33. Greiff V, Weber CR, Palme J, Bodenhofer U, Miho E, Menzel U, et al. Learning the high-dimensional immunogenomic features that predict public and private antibody repertoires. *J Immunol.* (2017) 199:2985–97. doi: 10.4049/jimmunol.1700594
34. Macpherson AJ, Koller Y, McCoy KD. The bilateral responsiveness between intestinal microbes and IgA. *Trends Immunol.* (2015) 36:460–70. doi: 10.1016/j.it.2015.06.006
35. Ye J, Kaattari IM, Kaattari SL. The differential dynamics of antibody subpopulation expression during affinity maturation in a teleost. *Fish Shellfish Immunol.* (2011) 30:372–7. doi: 10.1016/j.fsi.2010.11.013
36. Castro R, Navelsaker S, Krasnov A, Du Pasquier L, Boudinot P. Describing the diversity of Ag specific receptors in vertebrates: contribution of repertoire deep sequencing. *Dev Comp Immunol.* (2017) 75:28–37. doi: 10.1016/j.dci.2017.02.018
37. Sigal NH, Gearhart PJ, Klinman NR. The frequency of phosphorylcholine-specific B cells in conventional and germfree BALB/C mice. *J Immunol.* (1975) 114:1354–8.
38. Bousso P, Levraud JP, Kourilsky P, Abastado JP. The composition of a primary T cell response is largely determined by the timing of recruitment of individual T cell clones. *J Exp Med.* (1999) 189:1591–600. doi: 10.1084/jem.189.10.1591
39. Venturi V, Kedzierska K, Price DA, Doherty PC, Douek DC, Turner SJ, et al. Sharing of T cell receptors in antigen-specific responses is driven by convergent recombination. *Proc Natl Acad Sci USA.* (2006) 103:18691–6. doi: 10.1073/pnas.0608907103
40. Elhanati Y, Murugan A, Callan CGJr, Mora T, Walczak AM. Quantifying selection in immune receptor repertoires. *Proc Natl Acad Sci USA.* (2014) 111:9875–80. doi: 10.1073/pnas.1409572111
41. Madi A, Shifrut E, Reich-Zeliger S, Gal H, Best K, Ndifon W, et al. T-cell receptor repertoires share a restricted set of public and abundant CDR3 sequences that are associated with self-related immunity. *Genome Res.* (2014) 24:1603–12. doi: 10.1101/gr.170753.113
42. Madi A, Poran A, Shifrut E, Reich-Zeliger S, Greenstein E, Zaretsky I, et al. T cell receptor repertoires of mice and humans are clustered in similarity networks around conserved public CDR3 sequences. *Elife* (2017) 6:e22057. doi: 10.7554/eLife.22057
43. Magadan S, Sunyer OJ, Boudinot P. Unique features of fish immune repertoires: particularities of adaptive immunity within the largest group of vertebrates. *Results Probl Cell Differ.* (2015) 57:235–64. doi: 10.1007/978-3-319-20819-0_10

Conflict of Interest Statement: The authors declare that the research was conducted in the absence of any commercial or financial relationships that could be construed as a potential conflict of interest.

The reviewer YL declared a past co-authorship with several of the authors (MT, TM, AW) to the handling Editor.

Copyright © 2018 Magadan, Jouneau, Puelma Touzel, Marillet, Chara, Six, Quillet, Mora, Walczak, Cazals, Sunyer, Fillatreau and Boudinot. This is an open-access article distributed under the terms of the Creative Commons Attribution License (CC BY). The use, distribution or reproduction in other forums is permitted, provided the original author(s) and the copyright owner(s) are credited and that the original publication in this journal is cited, in accordance with accepted academic practice. No use, distribution or reproduction is permitted which does not comply with these terms.

frontiers in Immunology

ORIGINAL RESEARCH
published: 09 January 2019
doi: 10.3389/fimmu.2018.03054

Studies on the Use of Flagellin as an Immunostimulant and Vaccine Adjuvant in Fish Aquaculture

Eakapol Wangkahart[1,2], *Christopher J. Secombes*[2*] *and Tiehui Wang*[2*]

[1] *Division of Fisheries, Department of Agricultural Technology, Faculty of Technology, Mahasarakham University, Mahasarakham, Thailand,* [2] *Scottish Fish Immunology Research Centre, School of Biological Sciences, University of Aberdeen, Aberdeen, United Kingdom*

Immunostimulants and vaccines are important for controlling infectious diseases in fish aquaculture. In this study we assess the potential of flagellin to be used for such purposes in rainbow trout (*Oncorhynchus mykiss*). A recombinant flagellin from the salmonid pathogen *Yersinia ruckeri* (YRF) has been produced previously by us and shown to be a potent activator of inflammatory cytokines, acute phase proteins and antimicrobial peptides *in vitro*. Here we show that YRF is the most potent inflammatory activator of three bacterial PAMPs (LPS, peptidoglycan and flagellin) tested. The host response to flagellin was next studied *in vivo*. The YRF modulated gene expression was examined in two systemic (spleen and liver) and two mucosa-associated (gills and skin) tissues. YRF injection initiated a transient systemic inflammatory response with key pro-inflammatory cytokines (IL-1β, TNFα, IL-6, and IL-11 etc.) and chemokines (CXCL_F4 and CXCL-8) induced rapidly (by 6 h) but subsiding quickly (by 24 h) in multiple tissues. Consequently, a variety of anti-microbial pathways were activated systemically with heightened expression of acute phase proteins, antimicrobial peptides and complement genes in multiple tissues, which was sustained to 24 h in the liver and mucosal tissues. The Th17 cytokine IL-17A/F1 was also induced in the spleen and liver, and Th2 cytokine IL-4/13 was induced in the liver. However, the anti-inflammatory IL-10 and the Th1 cytokine IFNγ were refractory. A secreted form of TLR5 (TLR5s) was induced by flagellin in all tissues examined whilst the membrane form was refractory, suggesting that TLR5s may function as a negative feedback regulator. Trout liver appeared to be an important organ responding to flagellin stimulation, with marked induction of IL-11, IL-23P19, IL-17C1, SAA, and cathelicidin-2. YRF induced a strong antibody response. These antibodies reacted against the middle domain of YRF and were able to decrease YRF bioactivity. Intact YRF was necessary for its bioactivity, as deletion of the N-terminal, C terminal or middle domain of YRF led to functional loss. This study suggests that flagellin could be a potent immunostimulant and vaccine adjuvant for fish aquaculture.

Keywords: flagellin, immunostimulant, vaccine adjuvant, salmonids, cytokine, antimicrobial peptides, gene expression, inflammatory response

OPEN ACCESS

Edited by:
Hetron Mweemba Munang'andu, Norwegian University of Life Sciences, Norway

Reviewed by:
Dimitar Borisov Iliev, UiT The Arctic University of Norway, Norway
Carlos Angulo, Centro de Investigación Biológica del Noreste (CIBNOR), Mexico

***Correspondence:**
Christopher J. Secombes
c.secombes@abdn.ac.uk
Tiehui Wang
t.h.wang@abdn.ac.uk

Specialty section:
This article was submitted to Comparative Immunology, a section of the journal Frontiers in Immunology

Received: *30 October 2018*
Accepted: *10 December 2018*
Published: *09 January 2019*

Citation:
Wangkahart E, Secombes CJ and Wang T (2019) Studies on the Use of Flagellin as an Immunostimulant and Vaccine Adjuvant in Fish Aquaculture. Front. Immunol. 9:3054. doi: 10.3389/fimmu.2018.03054

INTRODUCTION

Aquaculture accounts for more than half of the fish consumed worldwide and contributes greatly to the supply of affordable protein in developing countries (1). The farmed fish are kept at high population densities that increase the risk of disease outbreaks caused by infectious bacteria, viruses, parasites and fungi (2–4), hence infectious disease is one of the major limiting factors in aquaculture. Multiple measures must be taken to ensure the health of these fish and the use of immune-stimulants and vaccination represent two important strategies for controlling diseases in aquaculture (2, 3, 5–13).

Fish have a strong innate immune system that can cope with a large variety of infectious agents. However, many pathogens have developed evasion mechanisms to resist innate immune defenses, and in such cases the adaptive immune system, that evolved for the first time in early vertebrates, must come into play to fight these pathogens (8). The innate and adaptive immune systems are cross-linked, and the magnitude and specificity of the signals perceived by the innate immune cells following infection or vaccination shape subsequent adaptive immune responses (9).

Immune-stimulants are chemical compounds that activate leukocytes and hence may render animals more resistant to infections. The innate immune response is initiated upon recognition of pathogen-associated molecular patterns (PAMPs), such as double stranded RNA, flagellin, lipopolysaccharide (LPS) and β-glucans (9, 14), by pattern recognition receptors (PRRs) such as Toll-like receptors (TLR), C-type lectin receptors (CLRs), NOD-like receptors (NLR) and RIG-I-like receptors (RLR) (15). In the presence of PAMPs, the immune system will respond as if challenged by a pathogenic microbe. Hence, PAMPs, when administrated prior to an infection, may elevate defenses and function as immune stimulants. They can also function as adjuvants when formulated with vaccines, to elevate the specific adaptive immune response (11–13).

Bacterial flagellin is the major structural protein in the flagellum of Gram positive and negative bacteria (8, 16). Due to its presence in diverse bacterial species and high abundance in bacterial cells, flagellin is a potent PAMP and a major target of the host immune system. Monomeric flagellin (30–60 kDa, dependent upon the taxa of the bacterium) contains in general an N-terminal D0/D1, a middle D2/D3 and a C-terminal D1/D0 domain. The last ∼40 amino acids of each terminus of the flagellin molecule form the D0 domain. The D1 domain constitutes the next ∼100 residues from the N-terminus and 50 residues from the C-terminus. The D0 and D1 domains are key for assembly of the helical filamentous structure and hence are highly conserved across different species of bacteria, and contain primarily α-helical structures. In contrast the D2 and D3 domains have high sequence diversity and can be absent in some bacterial species, such as *B. cereus* (17–20). The hypervariable D2 and D3 domains are composed of β-sheets bearing adhesion-like properties and are essential for flagellin immunogenicity (16, 17).

In mammals, extracellular flagellin is recognized by TLR5 expressed by antigen-presenting cells and T cells (21, 22). Mammalian TLR5 is a plasma membrane-localized PRR (TLR5M) that possesses an extracellular domain with leucine-rich repeats (LRRs), a transmembrane region, and a cytoplasmic signaling domain termed the Toll/interleukin-1 receptor homology (TIR) domain. Crystal structure analysis showed that two flagellin molecules simultaneously bind two TLR5 receptors on the D1 domain, forming a 2:2 complex. In addition to the D1 domain, deletion mutant experiments revealed that the D0 domain is also required to produce maximum TLR5-mediated signaling (17–19). The activation of TLR5 mediates the production and secretion of pro-inflammatory cytokines, chemokines and other mediators for the development of an effective immune response (21, 23). In rainbow trout (*Oncorhynchus mykiss*) and other teleost species, two TLR5 genes are present in the genome (24–29). One (TLR5M) encodes for an extracellular LRR domain, a transmembrane region, and a cytoplasmic TIR domain as seen in mammalian TLR5. The second encodes only the LRR in the extracellular domain and hence is a soluble form of TLR5 (TLR5S). Trout TLR5M is widely expressed in all tissues whereas TLR5S is mainly expressed in liver (24, 25). Both the TLR5M and TLR5S recognize flagellin from *Vibrio anguillarum* a Gram-negative bacterium (24).

The evaluation of flagellin as a vaccine candidate, and as a vaccine adjuvant have been examined in fish recently (16, 30–35). Flagellin has also been shown to induce non-specific protection to a variety of bacterial pathogens *in vivo* in rainbow trout (36). However, the immune pathways elicited and the mechanisms responsible are largely unknown, with only few pro-inflammatory genes and tissues studied (14, 15, 37).

A recombinant flagellin from the fish pathogen *Yersinia ruckeri* (YRF) was produced in our lab and shown *in vitro* to upregulate the transcript level of a large number of pro-inflammatory cytokines, APPs, AMPs and members of the IL-12 cytokine family in the monocyte/macrophage-like cell line, RTS-11 (23). In the present study the immunomodulatory effects of flagellin were explored further *in vivo* in several major immune tissues, namely spleen, liver, gills and skin. In teleost fish the kidney, spleen and liver are major systemic lymphoid tissues containing many immune cell types that are vital components for initiating immune reactions within the immune system (38, 39). Mucosa-associated lymphoid tissues (gut, gills, nares and skin) are also important to prevent invasion of pathogens from the surrounding environment of the host (40–42). Hence two systemic and two mucosa-associated tissues were chosen for study of the immune-modulatory effects following YRF injection *in vivo*. Our results show that YRF activates a systemic inflammatory response and multiple antimicrobial pathways *in vivo*. To pave the way for the use of YRF as an immune stimulant or a vaccine adjuvant, we also investigated the antigenicity of full-length YRF and the bioactivity of YRF deletion mutants. The results showed that fish could produce high serum antibody titres against flagellin after vaccination, and that these antibodies recognize the middle D2/D3 domain of the flagellin and can decrease flagellin bioactivity. However, deletion of either the N-terminal, C terminal or the middle domain of YRF led to loss of the proinflammatory activity. The impact of these

results on the potential use of flagellin as an immune-stimulant or vaccine adjuvants in fish aquaculture is discussed.

MATERIALS AND METHODS

Experimental Fish

Healthy rainbow trout were bought from the Mill of Elrich Trout Fishery (Aberdeenshire, Scotland, United Kingdom) and kept in 1-m-diameter fiberglass tanks with recirculating freshwater at 14°C at the Scottish Fish Immunology Research Centre, University of Aberdeen, UK. Fish were fed twice daily with a commercial diet (EWOS) and were given at least 2 weeks to acclimate before use. Routine screening of head kidney swabs showed no bacterial presence (43).

Production of Recombinant *Y. ruckeri* Flagellin and Its Mutants

The construct pTri-YRF for expression of full-length recombinant *Y. ruckeri* flagellin (YRF) and the production of YRF was described previously (23). The mutant YRF constructs, YRF-N, YRF-C and YRF-NC, were prepared from pTRI-YRF by PCR using the Q5 high fidelity enzyme (New England Biolabs, United Kingdom) and re-ligation, using primer pairs GCCAGTTCCGCTCATCACCAC/GGAACGGAA GTTACCGTTAACCATC (YRF-N), GCCCATGGTATATCT CCTTTGATTGT/GATAACCGCACGGCAGCCA (YRF-C), and CAAGACTTTAATGCCGTTGAAATCGGT/GTTGAA GCCAAAGGTTTTGACGTATTGA (YRF-NC), respectively. Whilst the YRF-N and YRF-C have the C-terminal and N-terminal D0/D1 domains deleted, respectively, the YRF-NC has the middle D2/D3 removed and replaced with a GS linker [SGGGGSGGGGSGGGGS, (44)]. All the muteins have a his-tag (ASSAHHHHHHHHHH) at the C-terminus for purification. A multiple alignment of YRF and its muteins is provided in **Figure S1**. Following sequence confirmation, the transformation of BL21 Star (DE3) competent cells (Invitrogen), induction of recombinant protein production, purification under denaturing conditions, refolding, re-purification under native conditions, SDS-PAGE analysis of proteins and quantification of protein concentration were as described previously (23).

Stimulation of RTS-11 Cells

The monocyte/macrophage-like cell line, RTS-11, from rainbow trout spleen was cultured in Leibovitz (L-15) medium (Invitrogen, United Kingdom) plus 30% fetal calf serum (FCS; Labtech International, United Kingdom) and antibiotics (100 U/ml penicillin and 100 μg/ml streptomycin; Invitrogen, UK) at 20°C, and passaged as described previously (45). For experiments, cells were collected by centrifugation (200 × g, 5 min), re-suspended in L-15 containing 10% FCS to 1 x 10^6 cells/ml, and seeded into 12-well cell culture plates at 2 ml/well. Overnight cell cultures were stimulated with 100 ng/ml YRF, 5 μg/ml ultrapure lipopolysaccharide (LPS, Invivogen) from *E. coli* 0111:B4, and 5 μg/ml peptidoglycan (PGN, Invivogen) purified from the Gram-positive bacterium *Staphylococcus aureus*, for 1, 2, 4, 8, and 24 h. Subsequently the cells were stimulated with different concentrations of YRF and its muteins for 4 h. The stimulation was terminated by dissolving the cells in TRI reagent (Sigma, United Kingdom). The RNA preparation and cDNA synthesis was as described previously (23, 46).

Administration of YRF *in vivo* and Sampling

Twenty eight rainbow trout (∼210 g) were randomly divided into two groups. Fish were injected intraperitoneally (ip) with 200 μl of phosphate-buffered saline (PBS, pH 7.4) or PBS containing 10 μg of YRF per fish. The dose chosen was based on the finding that 50 ng/ml *in vitro* induces the highest gene expression changes in most of the genes examined (23), and equates to 50 ng/g body weight *in vivo*. Whilst this dose is at the low end of those used previously in salmon and trout (10–50 μg per fish) (16, 36), the results demonstrate it was highly effective. Seven fish per group were killed at 6 and 24 h post injection, and the gills, skin, spleen and liver were taken and homogenized in TRI reagent with 5 mm stainless steel beads using a TissueLyser II (Qiagen) as described previously (46).

Real-Time PCR Analysis of Gene Expression

Total RNA extraction, cDNA synthesis and real-time PCR analysis of gene expression were as described previously (47, 48). The expression of cytokines, antimicrobial peptides (AMPs), acute phase proteins (APPs), complement components, arginase genes, and suppressor of cytokine signaling (SOCS) genes as well as the house keeping gene elongation factor-1α (EF-1α), was examined. The primers for real-time PCR are given in **Table S1**, with at least one primer per pair designed to cross an intron to ensure genomic DNA could not be amplified under the PCR conditions used. The expression of each gene was initially normalized to that of EF-1α, and then shown as a fold change by calculating the average expression level of the treated samples divided by that of time-matched controls.

Immunization and Antiserum Preparation

Ten rainbow trout (∼200 g) were ip injected with 90 μg/fish of YRF mixed with 0.2 ml of complete Freund's adjuvant (CFA, Sigma, United Kingdom) (YRF+CFA). A control group of 10 fish was ip. injected with CFA alone. The fish were bled from the caudal vein 3 months post immunization. Blood samples were incubated at 4°C overnight and then centrifuged at 5,000 rpm for 10 min at 4°C. Serum was collected and stored at −80°C until use.

Enzyme-Linked Immunosorbent Assay (ELISA)

YRF-specific IgM antibody titres in serum samples were determined by ELISA using mouse anti-trout IgM (clone I-14) (49). Briefly, high binding capacity 96 well-plates (Thermo scientific) were coated with 1,000 ng/well of YRF in coating buffer (pH 9.0, 100 mM $NaHCO_3$, 12 mM Na_2CO_3) for 2 h at 37°C and washed 3 times with wash buffer (PBS containing 1% (w/v) skimmed milk and 0.05% (v/v) Tween 20) and then blocked for 2 h at 37°C with 5% (w/v) skimmed milk in wash buffer. Plates were washed 3 times with wash buffer before addition of serum samples. Individual fish serum was serially diluted 2-fold in 1%

milk in 1X PBS. Each dilution was added to YRF coated plates (50 μl/well) in duplicate and incubated at 4°C overnight. Plates were then washed 3 times with wash buffer and mouse anti-trout IgM added (50 μl/well) and incubated for 2 h at 37°C. After washing 3 times with wash buffer, the detection antibody (goat anti-mouse IgG labeled with horseradish peroxidase, Sigma, UK) diluted 1:3,000 in 1X PBS, 1% milk was added (50 μl/well) and incubated for 1 h at 37°C. The plates were again washed 3 times with wash buffer and developed by adding 50 μl/well of 3, 3′, 5,5′-Tetramethylbenzidine (TMB) Liquid Substrate, Supersensitive, for ELISA (Sigma, UK) to each well for 30 min. The reaction was stopped by adding 50 μl/well of 0.5 M sulphuric acid and the color reaction read at 450 nm in an ELISA plate reader (SoftMax Pr0 5.3). The antibody titres were determined as the reciprocal of the maximal serum dilution that exceeded double the reading of the negative control.

Neutralization Assay

The potential of antisera (see section Immunization and Antiserum Preparation) to neutralize YRF bioactivity was test in RTS-11 cells. Ten nanogram of YRF was mixed with 100 μl anti-YRF sera or control sera, or L-15 cell culture medium and incubated at room temperature for 1 h. The samples were then added (in quadruplicate) to each well of a 12-well plate containing RTS-11 cells prepared as above (section Stimulation of RTS-11 Cells). A matched serum or L-15 sample without YRF was also added to RTS-11 cells to function as additional controls. The incubation was terminated at 4 h by dissolving the cells in TRI reagent® (Sigma, United Kingdom). The expression of IL-1β1 and IL-1β2 was determined by RT-qPCR as described above.

Western Blot

The binding capacity of antisera from rainbow trout immunized with YRF/CFA to YRF and its muteins was examined by Western blot analysis. The preparation of full-length YRF and its deletion mutants YRF-N, YRF-C and YRF-NC was as described above (section Production of Recombinant *Y. ruckeri* Flagellin and Its Mutants). Four concentrations (1,000, 500, 250, and 125 ng) of YRF and mutated proteins (∼1,000 ng) were separated by SDS-PAGE. Another un-related recombinant flagellin (Flagellin-B) prepared in a similar way as YRF was also included as a control. Briefly, each sample was mixed with NuPAGE LDS Sample Buffer (Invitrogen, United Kingdom) and 0.5% of 2-ME, boiled at 95°C for 15 min, and loaded into the wells of a NuPAGE™ Novex™ 4–12% Bis-Tris Protein Gel (Invitrogen, United Kingdom), along with SeeBlue® Plus2 Pre-stained Protein marker (Invitrogen, United Kingdom). The gel was run in 1X NuPAGE® MES SDS Running Buffer, at 200 Volts for 30 min. The protein gel was either stained with Imperial protein stain (Thermo Scientific, UK), or transferred to Hybond®-P polyvinylidene difluoride (PVDF) membranes (Ambion) using a NuPAGE® Transfer Buffer system (Invitrogen) as recommended by the manufacturer.

The PVDF membrane was blocked with 5% skimmed milk in PBS (pH 7.2) containing 0.05% Tween 20 (PBST) for 1 h and washed 3 times with 1X PBST. The membrane was then incubated with the trout anti-YRF sera (diluted 1:1,000 in PBST) overnight at 4°C. After subsequent addition of mouse anti-trout IgM (I-14 diluted 1:1,000 in PBST) and goat anti-mouse IgG labeled with horseradish peroxidase (diluted 1:2,000, Sigma, UK), with three washes between treatments, the membrane was washed 5 times with 1X PBST and antibody binding detected with a SuperSignal™ West Pico Chemiluminescent Substrate kit (Thermo Scientific, United Kingdom).

Statistical Analysis

The data were statistically analyzed using the SPSS Statistics package 24 (SPSS Inc., Chicago, Illinois). The analysis of real-time PCR data was as described previously (47, 48). To improve the normality of data, real-time quantitative PCR measurements were scaled, with the lowest expression level in a data set defined as 1, and log2 transformed. One way-analysis of variance (ANOVA) and the Bonferroni *post-hoc* test were used to analyse the gene expression data, with $P < 0.05$ between treatment and control groups considered significant. Genes significantly modulated by YRF *in vivo* were selected and their fold changes were log2 transformed and subjected to hierarchical clustering analysis using the Morpheus program at https://software.broadinstitute.org/morpheus.

RESULTS

Yersinia ruckeri Flagellin (YRF) Is the Most Potent Bacterial Derived PAMP to Activate Pro-Inflammatory Genes in RTS-11 Cells

LPS, PGN and flagellins are bacterial derived PAMPs that can activate an inflammatory response in mammals and have the potential to be used as an immune stimulant or vaccine adjuvants in fish aquaculture. To compare the immune stimulatory potency of these PAMPs, a fish macrophage-like cell line (RTS-11) was incubated with an optimal dose (100 ng/ml, 23) of YRF, or 50-fold higher dose (5,000 ng/ml) of ultrapure LPS and PGN in a time course from 1 to 24 h. The expression of major proinflammatory cytokines, IL-1β1-2 (50), TNFα1-3 (51), and IL-6 (52) was examined. YRF rapidly activated all the proinflammatory cytokines from 1 h-24 h, with a peak already seen at 1 h for IL-1β2 and TNFα3, or at 4 h for other genes (**Figure 1**) as seen previously (23). PGN also activated all the inflammatory cytokines examined but at later time points, 4–24 h for TNFα3, 8–24 h for IL-1β2, IL-6 and TNFα2, and 24 h for IL-1β1 and TNFα1, and with less potency, eg IL-6 expression was increased over 1,000-fold by YRF but only 10-fold by PGN (**Figure 1**). Ultrapure LPS only slightly increased the expression of TNFα3 at 24 h post stimulation and had no effect on the other cytokines examined. The expression of proinflammatory cytokines in samples stimulated with YRF at each time point was higher than that with LPS from 1 to 24 h, and with PGN from 1 to 8 h. At 24 h, YRF stimulated samples expressed higher levels of IL-1β1, IL-1β2 and IL-6, similar level of TNFα1, but lower levels of TNFα2 and TNFα3, compared to PGN stimulated samples. These expression profiles suggest that flagellin (YRF) is the most potent PAMP tested *in vitro* to date in rainbow trout.

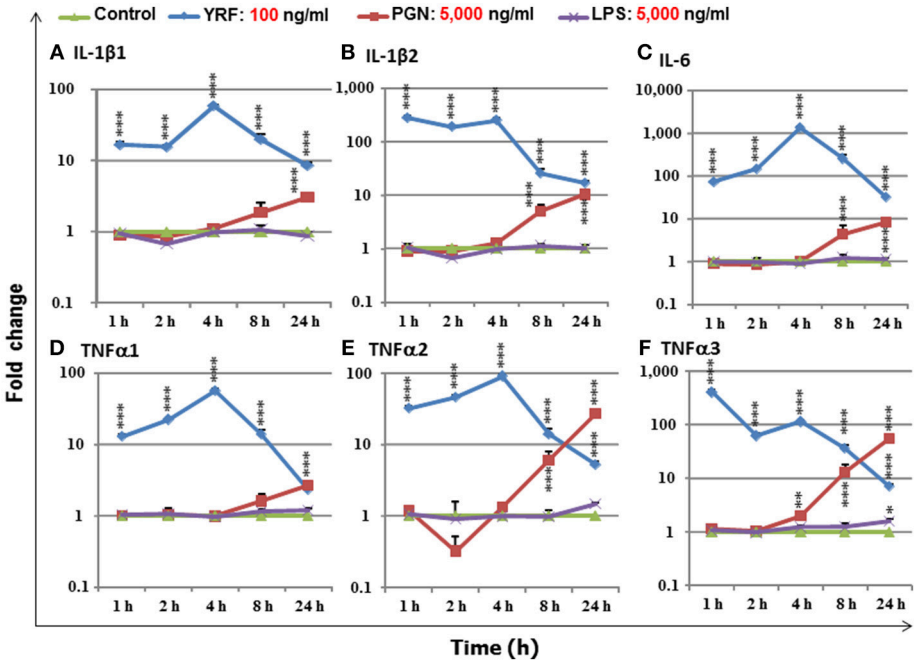


FIGURE 1 | The expression of IL-1β1 **(A)**, IL-1β2 **(B)**, IL-6 **(C)**, TNFα1 **(D)**, TNFα2 **(E)**, and TNFα3 **(F)**, in response to stimulation by YRF, LPS and PGN in RTS-11 cells. RTS-11 cells were stimulated with 100 ng/ml of YRF, 5,000 ng/ml of ultrapure LPS or 5,000 ng/ml of PGN for 1, 2, 4, 8, and 24 h. The expression levels were quantified by RT-qPCR and expressed as a fold change that was calculated as the average expression level of stimulated samples divided by that of the time-matched controls. The results are presented as the average + SEM from four wells of cells. Differences between stimulated samples and controls were tested by One way-ANOVA followed by the Bonferroni *post hoc* test. $^{*}p < 0.05$, $^{**}p < 0.01$, and $^{***}p < 0.001$.

Systematic Activation of Early Pro-Inflammatory Pathways *in vivo* by YRF

After injection with YRF the fish behaved normally and no side-effects were observed postmortem. The expression profiles of 120 trout genes were determined by RT-qPCR in spleen, liver, gills and skin, at 6 h and 24 h post injection (hpi). The genes analyzed included the known cytokines and SOCS genes in trout, and genes of the acute phase response and antimicrobial defense. The time points chosen were based on our previous study that showed YRF activates a rapid increase in proinflammatory genes *in vitro* (23). Thus the early response (at 6 hpi) and late response (at 24 hpi) were studied here. Detailed fold changes for each genes analyzed are provided in **Table S2**.

Expression of the Main Proinflammatory Cytokines

The activation of TLR5 by flagellin triggers an inflammatory response and activates the expression of fish immune relevant genes *in vitro* (23). Therefore, following injection of YRF the expression of major proinflammatory cytokines of the IL-1 family, IL-6 family and TNFα family was first examined. Five IL-1 family members, three IL-1β paralogues (50), IL-18 (53) and a novel IL-1 family member (nIL-1Fm) that antagonizes IL-1β activity (54) are present in rainbow trout. The expression of IL-1β1 and IL-1β2 was rapidly increased at 6 hpi in all tissues. This activation subsided to control levels at 24 hpi with the exception of IL-1β1 in the liver and IL-1β2 in the spleen where the expression remained higher than the control (**Figures 2A,B**). The expression of IL-1β3 was also rapidly induced but in a tissue specific way at 6 h. Thus IL-1β3 expression was only induced at 6 h in the gills and skin (**Figure 2C**). IL-18 expression was induced only in spleen at 6 h and in the liver at 24 h (**Table 1**).

The expression of TNFα paralogues was also rapidly activated. The expression profiles of both TNFα1 and TNFα2 were similar and both were induced at 6 h in all four tissues examined (**Figures 2D,E**). However, TNFα3 expression was only induced at 6 hpi in the liver and skin (**Figure 2F**). The expression had returned to control levels by 24 hpi for all genes.

IL-6 expression was rapidly and highly induced at 6 hpi in the spleen, liver, gills and skin of injected fish **(Figure 2G**). The heightened expression was retained in the spleen, liver and skin to 24 hpi, albeit at lower levels. Similarly, the expression level of IL-11 (55) was also significantly up-regulated in all the four tissues examined at both time points, with an exceptionally high induction of 1,776-fold at 6 hpi in the liver (**Figure 2G**). The expression of M17 (56) was also induced but with lower fold-induction. In contrast, CNTF (56) expression was refractory after YRF injection in all tissues examined (**Table 1**).

IL-34 is a ligand for macrophage colony-stimulating factor-1 receptor, promotes the differentiation, proliferation, and survival of monocytes, macrophages, and osteoclasts (57). Its expression was also rapidly activated in spleen, liver and skin but only at 6 hpi (**Table 1**).

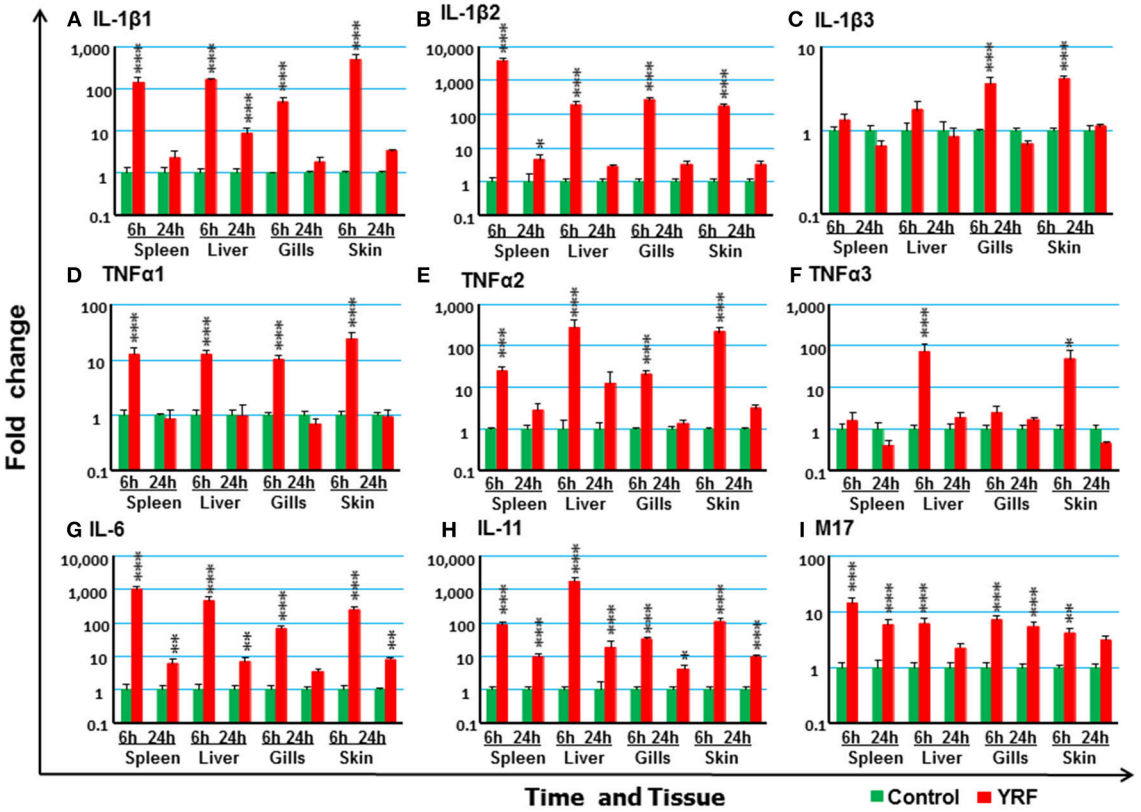


FIGURE 2 | The activation of major proinflammatory cytokines *in vivo* by YRF. Rainbow trout were ip injected with 10 μg YRF/fish in PBS or PBS only as control. The fish were killed, and spleen, liver, gills and skin samples were taken from each fish at 6 and 24 h post injection. The expression of IL-1β1 **(A)**, IL-1β2 **(B)**, IL-1β3 **(C)**, TNFα1 **(D)**, TNFα2 **(E)**, TNFα3 **(F)**, IL-6 **(G)**, IL-11 **(H)**, and M17 **(I)** in each tissue was examined by RT-qPCR. A fold change was calculated as the average expression level of YRF injected fish divided by that of time matched controls. The means + SEM of six fish are shown. Significant differences between injected fish and controls were tested by one way-ANOVA followed by the Bonferroni *post hoc* test and are shown over the bars as; $^{*}p < 0.05$, $^{**}p < 0.01$, and $^{***}p < 0.001$.

The Expression of CXC Chemokines

Chemokines are chemotactic cytokines that regulate cell trafficking during an immune response to recruit cells of the immune system to a site of infection. The expression of 12 known trout CXC chemokines (58) was examined. The proinflammatory CXCL8/IL-8 expression was rapidly up-regulated in the spleen, liver, gills and skin at 6 hpi, with up-regulation sustained in the spleen and liver to 24 h (**Figure 3B**). CXCL_F4 expression was also rapidly induced at 6 hpi and sustained to 24 hpi in all the four tissues examined (**Figure 3E**). A transient up-regulation of CXCL_F5 was seen in the spleen, liver and skin at the early time point (**Figure 3F**). However, CXCL13 expression was up-regulated at only the late time point in all tissues (**Figure 3D**). In contrast, CXCL_F1c expression was downregulated in gills at 24 hpi (**Figure 3A**). The expression of CXCL_F1a in the spleen was irregular and no significant difference was observed post YRF injection. The expression of other CXC chemokines, CXCL_F1b, CXCL_F2, CXCL11_L1/γIP, CXCL12, and CXCL14, was refractory (**Figure 3C** and **Table 1**).

The Expression of IL-12 Family

IL-12 family members are heterodimeric cytokines of α/β chains. Genes for 6 active α-chains (p19, p28A, p28B, p35A1, p35A2, and p35B) and 4 β-chains (p40B1, p40B2, p40C, and EBI3) have been cloned in rainbow trout recently (44, 46, 59, 60). P19 (59) expression was rapidly up-regulated at 6 hpi in the spleen, liver and skin, and this was sustained in liver to 24 hpi (**Figure 4A**). P35A1 (46) expression was only up-regulated in the liver at 6 h and 24 h and in the skin at 6 hpi (**Figure 4B**). A transient up-regulation was also seen with p35A2 in the spleen, liver, gills and skin, and with EBI3 (61) in spleen (**Figures 4C,D**). The expression of P28A (62), P28B and P40B1 was undetectable in control samples of some tissues thus a fold change could not be calculated. However, P40B1 expression was detected in the spleen and liver samples at 6 hpi. No significant change was observed in the expression of p28A, p28B, P40B2, and P40C (**Table 1**). These expression profiles suggest specific IL-12, IL-23 and IL-35 isoforms may be induced by *in vivo* YRF administration.

The Expression of Adaptive Cytokines

Next the expression of cytokines involved in adaptive immunity was examined, including IFNγ, IL-17 family, γ-chain cytokine family and IL-20/22 to investigate if they were modulated by YRF. Both IFNγ1 and IFNγ2 were refractory to YRF stimulation in all tissues (**Figures 5A,B**). IL-17A/F1a (63) expression was highly up-regulated in the spleen and liver at 6 hpi and 24 hpi, but

TABLE 1 | Fold change of transcript expression of selected genes in the spleen, liver, gills, and skin of fish injected ip with YRF.

Tissue	Spleen		Liver		Gills		Skin	
Time	**6 h**	**24 h**	**6 h**	**24 h**	**6 h**	**24 h**	**6 h**	**24 h**
IL-18	**2.7*** **	1.2	1.5	**4.9*** **	1.2	1.2	1.2	1.5
CNTF	0.5	0.9	0.8	0.6	1.0	0.6	1.0	0.6
P35B1	2.4	0.3	9.0	0.1	1.6	0.8	13.9	0.9
P28A	2.3	0.9	ND	ND	13.4	1.5	7.5	0.4
P28B	5.9	2.0	ND	ND	ND	ND	ND	ND
CXCL_F1a	22.2	103.0	1.5	1.0	0.6	0.7	1.6	0.8
CXCL_F1b	0.8	12.2	0.7	2.7	1.5	2.6	1.2	1.6
CXCL_F2	1.1	0.3	2.0	0.7	1.1	0.5	0.7	0.6
CXCL12a	0.9	0.4	1.8	0.4	0.8	1.6	0.9	1.5
CXCL12b	0.8	0.4	0.7	1.2	0.8	1.7	0.5	0.8
CXCL14	1.6	0.7	0.8	0.6	1.0	1.5	0.9	1.8
IFNγ1	1.3	0.7	1.0	3.8	0.3	0.9	0.2	0.4
IFNγ2	1.0	1.9	1.3	1.3	0.4	0.8	0.5	0.5
IL-17A/F1b	ND	17.5	ND	ND	1.2	0.6	0.3	0.6
IL-17A/F2a	0.6	0.7	1.9	**11.4*** **	0.4	0.5	0.2	0.4
IL-17A/F2b	0.8	1.1	2.0	2.2	0.9	1.0	0.5	0.9
IL-17A/F3	0.6	1.2	1.6	0.6	0.7	1.1	0.4	0.7
IL-17N	1.9	1.6	1.1	1.2	2.2	1.0	0.9	0.8
IL-17D	0.9	0.4	0.4	0.6	1.0	0.8	0.6	0.4
IL-2	1.1	0.7	1.2	1.1	1.0	0.6	1.0	1.1
IL-15	1.0	0.6	**2.7*** **	**8.4*** **	**2.4***	0.7	1.2	1.0
IL-20	6.5	1.2	2.0	2.1	1.0	1.8	1.0	1.1
IL-21	1.6	0.9	1.7	1.4	1.5	0.8	0.9	0.9
IL-34	**2.9*** **	1.0	**18.7*** **	0.7	1.7	1.1	**3.4*** **	1.5
CISHb1	1.9	2.5	1.4	0.8	1.2	0.6	1.2	0.8
CISHb2	2.8	2.1	0.9	1.0	1.4	1.0	1.8	1.0
SOCS1B	1.2	1.4	0.5	2.8	0.8	1.2	0.9	1.3
SOCS2A1	2.4	3.7	1.1	0.3	1.3	1.8	1.0	1.3
SOCS2A2	0.6	0.5	3.3	0.2	1.4	1.2	0.7	0.8
SOCS2B	1.0	0.2	2.5	0.4	1.2	0.3	1.1	0.3
SOCS3B1	1.5	1.5	1.7	3.8	1.0	2.5	2.2	3.4
SOCS4	1.3	0.3	0.3	0.5	1.8	1.7	0.8	1.3
SOCS5A1	1.2	1.5	0.1	2.3	1.2	1.8	0.8	2.4
SOCS5A2	0.6	1.3	0.1	0.9	0.9	1.6	1.0	1.6
SOCS5B1	1.0	1.0	0.4	1.1	1.0	1.4	1.4	1.3
SOCS5B2	1.4	1.1	0.7	1.4	2.8	1.7	2.8	2.4
SOCS6B1	1.0	1.0	0.4	0.8	1.2	1.4	0.5	0.9
SOCS7A1	1.4	1.0	0.6	1.2	1.7	1.3	1.6	1.3
SOCS7A2	0.9	0.6	1.5	0.9	1.6	1.0	0.9	1.2
SOCS7B1	3.0	2.0	1.5	1.6	1.8	2.5	0.7	1.4
SAP2	1.8	1.8	0.9	1.7	1.1	0.9	0.9	2.1
β-defensin 1	ND	0.0	ND	ND	1.8	0.3	0.9	1.2
β-defensin 2	3.1	5.4	1.5	0.8	0.8	0.7	0.3	1.2
β-defensin 3	4.4	1.3	0.9	1.8	7.6	3.3	3.0	1.3
LEAP2A	0.6	1.3	2.6	**0.04*** **	0.5	0.8	1.3	1.1
LEAP2B	0.8	0.2	1.2	**0.05*** **	1.3	0.6	0.7	0.6
Bf-2	1.9	1.9	1.7	1.4	1.4	0.9	0.2	0.5

(Continued)

TABLE 1 | Continued

Tissue	Spleen		Liver		Gills		Skin	
Time	**6 h**	**24 h**	**6 h**	**24 h**	**6 h**	**24 h**	**6 h**	**24 h**
C1 inhibitor	2.8	1.1	1.0	0.7	0.8	1.2	0.8	1.3
C4	0.8	0.9	1.2	0.9	1.2	1.9	0.6	3.2
C5	7.8	1.4	1.3	1.3	1.1	0.7	0.2	1.2
C7-2	1.2	0.7	0.9	0.8	0.9	1.2	1.3	0.7
C8α	5.4	1.5	0.9	0.8	1.3	0.3	0.6	0.7
C8β	1.9	1.0	1.3	0.6	1.2	0.9	0.7	0.8
C8γ	0.9	0.5	1.2	0.6	1.2	1.4	1.1	0.8
C9	1.0	1.0	1.5	1.8	0.6	0.9	0.6	0.5
C3-3	4.0	**3.7***	1.0	1.3	0.6	2.0	0.4	1.4
C3-4	**6.2***	2.0	1.1	0.5	1.8	0.9	0.9	0.6
C3aR	1.8	1.7	1.5	1.5	2.5	1.1	1.9	1.6

*The fold change was calculated as the average expression level of YRF injected fish divided by that of time-matched controls (N = 6). A number in bold with asterisks indicates significant differences between YRF injected fish and controls as follows; * $p < 0.05$, ** $p < 0.01$, and *** $p < 0.001$ (One-way-ANOVA with Bonferroni correction).*
ND, not determined due to low expression levels.
ND, detectable in YRF injected fish but not detectable in time-matched controls.*

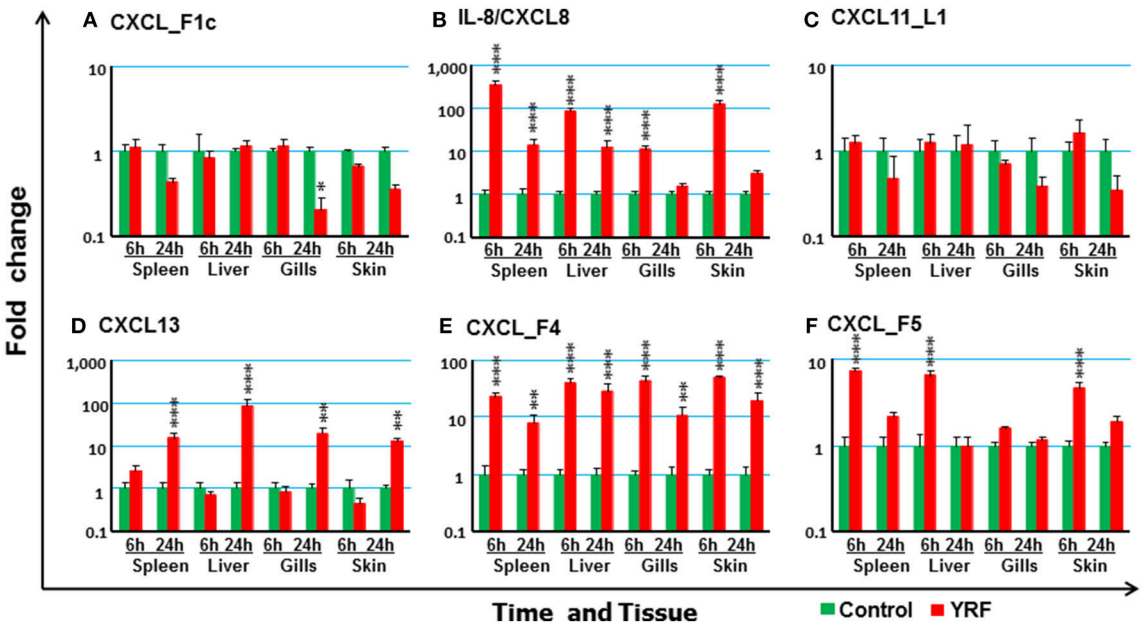


FIGURE 3 | The modulation of the expression of CXC chemokines *in vivo* by YRF. Rainbow trout were ip injected with YRF or PBS, sampled and analyzed as described in **Figure 2**. The expression of CXCL_F1c **(A)**, IL-8/CXCL8 **(B)**, CXCL11_L1/γIP **(C)**, CXCL13 **(D)**, CXCL_F4 **(E)**, and CXCL_F5 **(F)** was examined. A fold change was calculated as the average expression level of YRF injected fish divided by that of time matched controls. The means + SEM of six fish are shown. Significant differences between injected fish and controls were tested by one way-ANOVA followed by the Bonferroni *post hoc* test and are shown over the bars as; *$p < 0.05$, **$p < 0.01$, and ***$p < 0.001$.

not in the gills and skin at both time points post YRF injection (**Figure 5C**). IL-17A/F2a (64) expression was only upregulated in the liver at 24 hpi (**Table 1**). Interesting, IL-17C1 (65) was highly induced in the liver at 6 hpi and 24 hpi, and to a lesser extent in the gills and skin at 6 hpi (**Figure 5D**). Similarly, IL-17C2 expression was also induced in the liver at 6 hpi and 24 hpi and in the skin at 6 hpi (**Figure 5E**). The expression of IL-1A/F1b, IL-17A/F2b, IL-17A/F3, IL-17N, and IL-17D was refractory (**Table 1**). IL-22 (66) expression was rapidly induced in the spleen, liver, gills and skin at 6 hpi, and this was sustained in the liver to 24 hpi (**Figure 5F**). IL-20L (62) expression was refractory (**Table 1**).

Upregulation of Th2 cytokines (67) was seen only in the liver at 24 hpi, for IL-4/13A and IL-4/13B1 but not IL-4/13B2

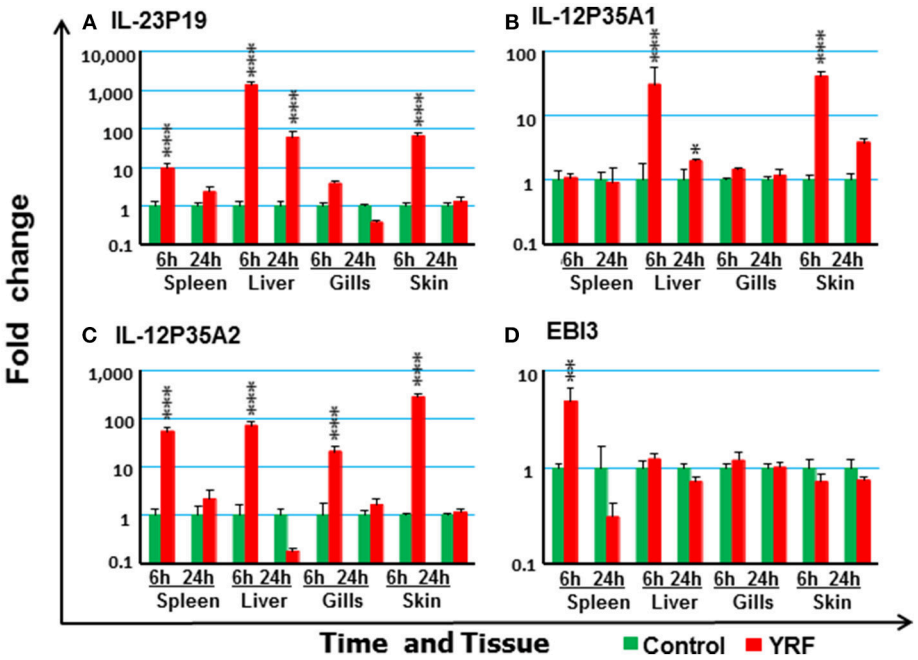


FIGURE 4 | The modulation of the expression of IL-12 family cytokines *in vivo* by YRF. Rainbow trout were ip injected with YRF or PBS, sampled and analyzed as described in **Figure 2**. The expression of IL-23P19 **(A)**, IL-12P35A1 **(B)**, IL-12P35A2 **(C)**, and EBI3 **(D)** was examined. A fold change was calculated as the average expression level of YRF injected fish divided by that of time matched controls. The means + SEM of six fish are shown. Significant differences between injected fish and controls were tested by one way-ANOVA followed by the Bonferroni *post hoc* test and are shown over the bars as; $*p < 0.05$, $**p < 0.01$, and $***p < 0.001$.

(**Figures 5G–I**). IL-15 (68) expression was also seen up-regulated in the liver at 6 and 24 hpi, and in the gills at 6 hpi (**Table 1**). The expression of other γ-chain cytokines, IL-2 (69) and IL-21 (47) was refractory in all tissues (**Table 1**).

The Expression of Anti-inflammatory Cytokines

The rapid but transient activation of major proinflammatory cytokine gene expression suggests some negative regulatory mechanisms must be activated by YRF. Thus, the expression of several anti-inflammatory cytokines known in rainbow trout was examined post YRF injection. The expression of both IL-10A and IL-10B (70) was refractory (**Figures 6A,B**). A small induction was seen in the liver at 24 hpi for TGFβ1A and at 6 hpi for TGFβ1B (71) (**Figures 6C,D**). In addition, the expression of nIL-1Fm was induced in the spleen, liver and skin at 6 hpi (**Figure 6E**).

The Expression of SOCS Genes

The SOCS family are key negative regulators of cytokine and growth factor signaling, with 26 SOCS genes expressed in rainbow trout [including an expressed pseudogene, (72)]. CISHa1 (73) was upregulated at 6 hpi but downregulated at 24 hpi in the liver (**Figure 7A**). CISHa2 was also up-regulated at 6 hpi and downregulated at 24 hpi in the liver, but in addition it was upregulated at 6 hpi in the spleen, gills and skin (**Figure 7B**). Both SOCS1 and SOCS3A were rapidly upregulated at 6 hpi, but this had subsided at 24 hpi in all four tissues examined with the exception of SOCS3A in the spleen (**Figures 7C,D**). SOCS3B2 expression was only increased in spleen at 6 hpi and in liver at 24 hpi (**Figure 7E**). The expression of both SOCS6A1, SOCS6A2, and SOCS6B2 decreased at 6 hpi in the liver (**Figures 7F–H** and **Table 1**). SOCS7B2 was increased in the liver at 6 and 24 hpi (**Figure 7I**). The expression of other SOCS genes, CISHb1-2, SOCS1B, SOCS2A1-2, SOCS2B, SOCS3B1, SOCS4, SOCS5A1-2/B1-2, SOCS6B1, and SOCS7A1-2, was refractory in all tissues (**Table 1**).

Systematic Activation of Anti-microbial Defense Pathways *in vivo* by YRF

To investigate potential antimicrobial pathways activated by YRF injection, the expression of several known APPs, AMPs and complement components was examined. SAA (74) expression was upregulated in the spleen, liver and skin at 6 hpi, and in the spleen, liver, gills and skin at 24 hpi (**Figure 8A**). SAP1 expression was upregulated only in the spleen at 6 hpi (**Figure 8B**), and SAP2 was refractory (**Table 1**).

A systemic activation of cathelicidins, hepcidin and β-defensin 4 was observed in multiple tissues after YRF administration (**Figures 8C–F**). CATH1 (75) expression was up-regulated in the spleen, liver and skin at 6 hpi, and this was sustained in the skin to 24 hpi (**Figure 8C**). The expression of CATH2 and hepcidin (76) was induced and sustained from 6 hpi to 24 hpi in all the four tissues examined (**Figures 8D–E**). It is noteworthy that the induction of CATH2 and hepcidin in the liver, gills and skin was higher at 24 hpi than that at 6 hpi. A small induction of β-defensin 4 (77) expression was observed in the spleen and liver but only at 24 hpi (**Figure 8F**), whilst the expression of β-defensin 1–3

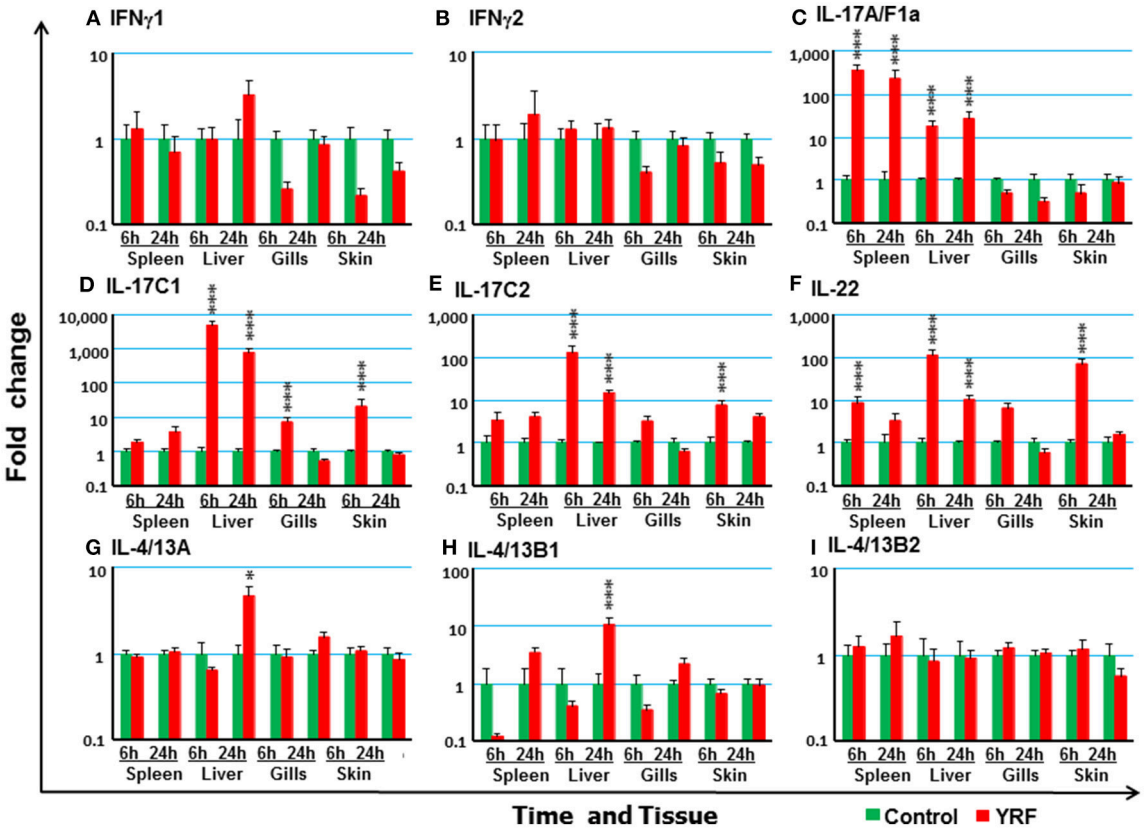


FIGURE 5 | The modulation of the expression of adaptive cytokines *in vivo* by YRF. Rainbow trout were ip injected with YRF or PBS, sampled and analyzed as described in **Figure 2**. The expression of IFNγ1 **(A)**, IFNγ2 **(B)**, IL-17A/F1a **(C)**, IL-17C1 **(D)**, IL-17C2 **(E)**, IL-22 **(F)**, IL-4/13A **(G)**, IL-4/13B1 **(H)**, and IL-4/13B2 (**I**), was examined. A fold change was calculated as the average expression level of YRF injected fish divided by that of time matched controls. The means + SEM of six fish are shown. Significant differences between injected fish and controls were tested by one way-ANOVA followed by the Bonferroni *post hoc* test and are shown over the bars as; $^{*}p < 0.05$ and $^{***}p < 0.001$.

was refractory (**Table 1**). The expression of both LEAP2A and LEAP2B was down-regulated in the liver at 24 hpi (**Table 1**).

The Expression of Complement Genes *in vivo* After YRF Injection

The expression of 18 trout genes in the complement system (78) was examined after YRF injection (**Figure 9**). C7-1 expression was activated and sustained from 6 to 24 hpi in all four tissues examined (**Figure 9C**). The expression of C1r and Bf-2 was increased in spleen at 6 hpi (**Figures 9A,D**). C6 expression was increased in the skin but only at 24 hpi (**Figure 9B**). Whilst the expression of complement receptor CR1-like gene was increased at 6 and 24 h hpi in both spleen and skin, it was only increased at 6 hpi in the gills and at 24 hpi in the liver (**Figure 9E**), C5aR expression was increased at 6 hpi in the spleen, and at 24 hpi in the liver and gills (**Figure 9F**). The expression of other complement genes tested was refractory (**Table 1**)

Modulation of the Expression of Arginase Genes and TLR5 *in vivo* by YRF

Macrophages are a first line of innate responders controlling and organizing host defenses against pathogens and are essential for maintaining homeostasis (79). They undergo specific activation into functionally distinct phenotypes, such as M1 and M2 (80). Arginase expression is an important marker of macrophage activation, with four genes present in rainbow trout (81). Whilst the expression of arginase 1a was upregulated at 6 and 24 hpi in the spleen, arginase 1b expression was refractory (**Figures 10A,B**). Arginase 2a expression was rapidly activated in the spleen, liver and skin at 6 hpi, and this was sustained in the liver to 24 hpi (**Figure 10C**). Arginase 2b expression was upregulated in both spleen and liver at 6 and 24 hpi (**Figure 10D**).

To further study the molecular mechanisms involved in the above induction of immune genes by flagellin, the two types of TLR5 genes (TLR5M and TLR5S, 24) present in trout were examined. The expression of TLR5M and TLR5S was detectable in all the tissues. However, there was no significant impact of YRF on the expression of TLR5M in any tissue (**Figure 10E**). Interestingly, TLR5S expression was significantly up-regulated in all tissues at 6 hpi and this was maintained to 24 hpi in liver, gills and skin (**Figure 10F**).

Clustering Analysis of Genes Modulated by YRF *in vivo*

The genes that showed significant changes after YRF injection were subjected to hierarchical clustering analysis that revealed a

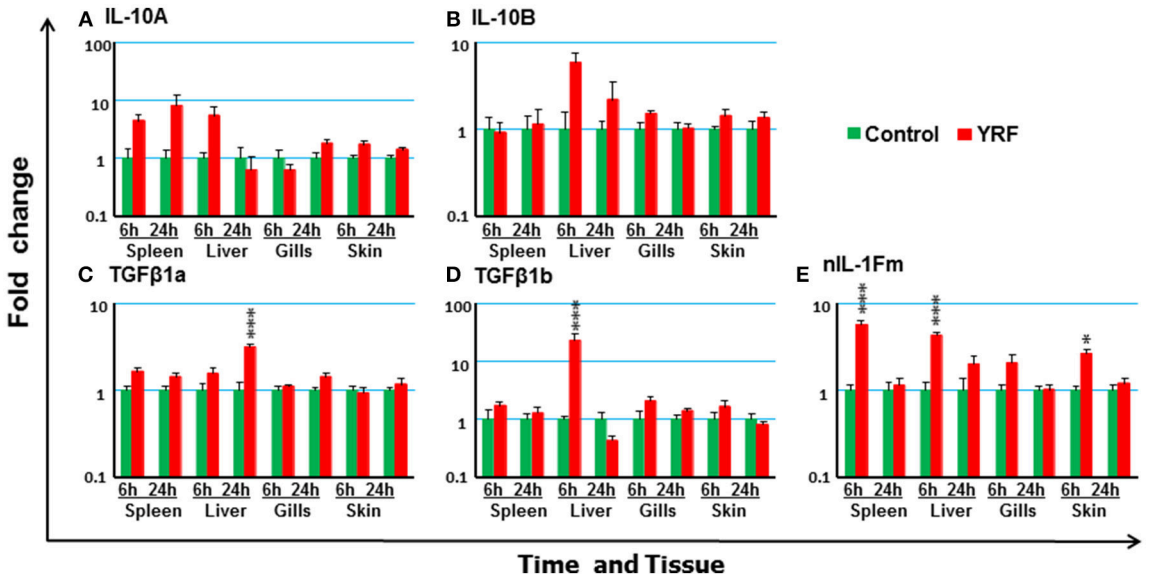


FIGURE 6 | The modulation of the expression of anti-inflammatory cytokines genes *in vivo* by YRF. Rainbow trout were ip injected with YRF or PBS, sampled and analyzed as described in **Figure 2**. The expression of IL-10A **(A)**, IL-10B **(B)**, TGFβ1a **(C)**, TGFβ1b **(D)**, and nIL-1Fm **(E)** was examined. A fold change was calculated as the average expression level of YRF injected fish divided by that of time matched controls. The means + SEM of six fish are shown. Significant differences between injected fish and controls were tested by one way-ANOVA followed by the Bonferroni *post hoc* test, and are shown over the bars as; $*p < 0.05$ and $***p < 0.001$.

time effect upon gene expression, with the gills and skin showing a similar response (**Figure 11**). Three major expression profiles (clusters A-C) of genes were observed after YRF injection. Cluster A included the major proinflammatory cytokines (IL-1β, TNFα, IL-6, IL-11, IL-17C, IL-12P35A, and IL-23P19), chemokines (CXCL8 and CXCL_F4-5), anti-inflammatory genes (TGFβ1B, CISHa, SOCS-1A, and SOCS3A) and TLR5S. These genes were rapidly induced at 6 hpi by YRF in all or most of the tissues but had decreased at 24 hpi (**Figures 2–7**, **10** for detail), suggesting rapid albeit transient activation. Cluster B, including IL-17A/F1a, EBI3, arginase-1 and several complement genes, was also rapidly induced but mainly in the spleen. Cluster C included the cytokines IL-4/13, IL-15, IL-17A/F2a, IL-18, and TGFβ1a, arginase-2, several complement genes and SOCS genes, APP and AMPs (**Figure 11**). This cluster of genes showed higher expression at 24 hpi, especially in the liver.

Antibody Response to YRF Vaccination in Rainbow Trout

Low titres (average of 6) of anti-YRF IgM antibodies were detected by ELISA in the sera 3 months-post injection with CFA (Control serum). The YRF-specific IgM antibody titres were markedly increased to 130,253 (average of 10 fish, $p < 0.001$) in fish immunized with YRF/CFA (Anti-serum) (**Figure 12A**). When 10 ng of YRF was incubated with cell culture medium (L-15), anti-serum or control serum for 1 h, it could still significantly activate the expression of IL-1β1 and IL-1β2. However, the fold change of the anti-serum treated YRF was lower than YRF incubated with L-15 or with control serum (**Figures 12B,C**). These results show that YRF-specific antibodies are induced by flagellin immunization, and that the antiserum can decrease flagellin bioactivity.

Anti YRF Antibody Reacts Against the Middle D2/D3 Domain

Full-length YRF contains N-terminal D0/D1 domains, middle unstructured D2/D3 domains and C terminal D0/D1 domains. To investigate the binding sites/domains of the anti-YRF antibodies produced in rainbow trout, three mutants were produced with the N-terminal deleted (YRF-C), middle domain deleted (YRF-NC) and the C-terminal deleted (YRF-N) (**Figure 13A**). The YRF and its mutants had expected sizes of 45.4, 33.6, 29.2 and 30.9 kDa for YRF, YRF-N, YRF-NC, and YRF-C, respectively, and were successfully produced as shown by SDS-PAGE after Imperial protein staining (**Figure 13B**). Western blot analysis revealed that the antibodies produced after YRF immunization reacted with full-length YRF, as well as the mutant proteins with the middle D2/D3 domain retained (ie YRF-N and YRF-C), but lost the reactivity against YRF-NC with the middle D2/D3 domains deleted. Furthermore, the antiserum did not react against an unrelated flagellin (flagellin-B) from an unrelated fish bacterial pathogen (**Figure 13C**). This data shows that the middle D2/D3 domain of YRF contains the major antigenic determinants recognized by the host (rainbow trout), and that the his-tag (ASSAHHHHHHHHHH) did not contribute significantly to YRF immunogenicity.

Mutation of YRF Abrogates YRF Proinflammatory Activity

To directly compare the proinflammatory activity of YRF and its mutants, a dose-response analysis on a molar basis was

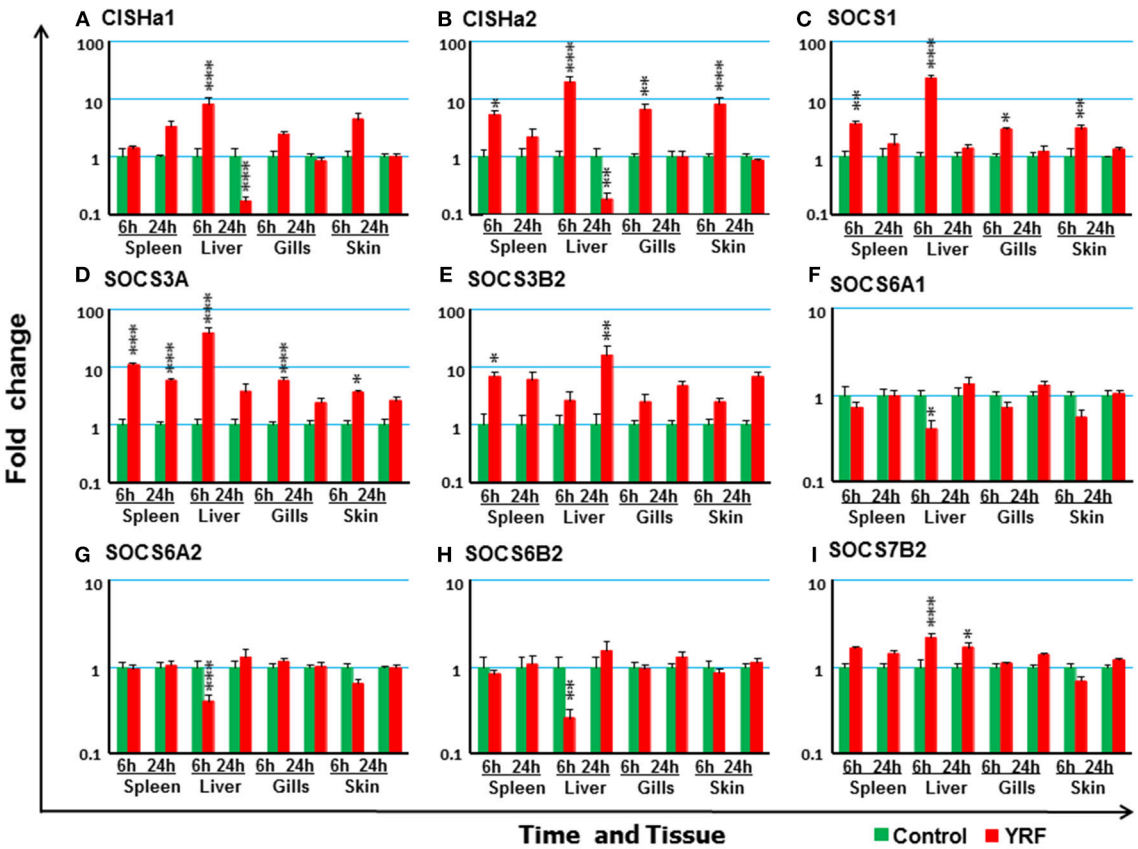


FIGURE 7 | The modulation of the expression of SOCS genes *in vivo* by YRF. Rainbow trout were ip injected with YRF or PBS, sampled and analyzed as described in **Figure 2**. The expression of CISHa1 **(A)**, CISHa2 **(B)**, SOCS1 **(C)**, SOCS3A **(D)**, SOCS3B2 **(E)**, SOCS6A1 **(F)** SOCS6A2 **(G)** SOCS6B2 **(H)** SOCS7B2 **(I)** was examined. A fold change was calculated as the average expression level of YRF injected fish divided by that of time matched controls. The means + SEM of six fish are shown. Significant differences between injected fish and controls were tested by one way-ANOVA followed by the Bonferroni *post hoc* test, and are shown over the bars as; $*p < 0.05$, $**p < 0.01$, and $***p < 0.001$.

undertaken, using RTS-11 cells stimulated for 4 h. An initial analysis revealed that the mutants lost their ability to induce inflammatory gene expression. Thus, different (increased) dose ranges were chosen, e.g,. 2–20,000 pM for YRF, 2,000–200,000 pM for YRF-N and YRF-C, and 200-200,000 pM for YRF-NC. As expected, YRF was able to upregulate the expression of all genes tested, including IL-1β2, IL-6, CXCL-8, TNFα3, and SAA at all doses tested (2–20,000 pM) (**Figure 14A**). However, all the YRF mutants lost the ability to upregulate the biomarker gene expression at all the doses tested (**Figures 14B–D**).

DISCUSSION

Using an *in vitro* fish macrophage model, we have demonstrated that, compared to LPS and peptidoglycan, flagellin is a particularly potent inflammatory trigger, in terms of activation of proinflammatory cytokine gene expression. Therefore, the immune stimulatory effects of flagellin were studied *in vivo* in an important model fish species, the rainbow trout. After ip injection with the recombinant flagellin YRF, from the fish pathogen *Yersinia ruckeri*, a transient systemic inflammation was activated, along with multiple antimicrobial pathways. Tissue-specificity of the response was also observed. High antibody titres could be induced by flagellin, and these antibodies were shown to react against the middle D2/D3 domains (demonstrated using a variety of muteins), and to neutralize the bioactivity of flagellin. Interestingly, the bioactivity was retained only with full-length YRF. These results are discussed in the context of innate host responses to flagellin, host/pathogen interactions, and the use of flagellin as an immune stimulant or vaccine adjuvant in fish aquaculture.

A Transient Systemic Activation of Inflammation

To use a PAMP, such as a flagellin, as an immunostimulant or a vaccine adjuvant in a fish species, it is necessary to first understand the early events of the host response, the activation of inflammatory responses and anti-microbial defense mechanisms. In this study we used a targeted approach to determine the impact of YRF on selected immune relevant genes as a means to gain in-depth information on these events in our model species, the rainbow trout.

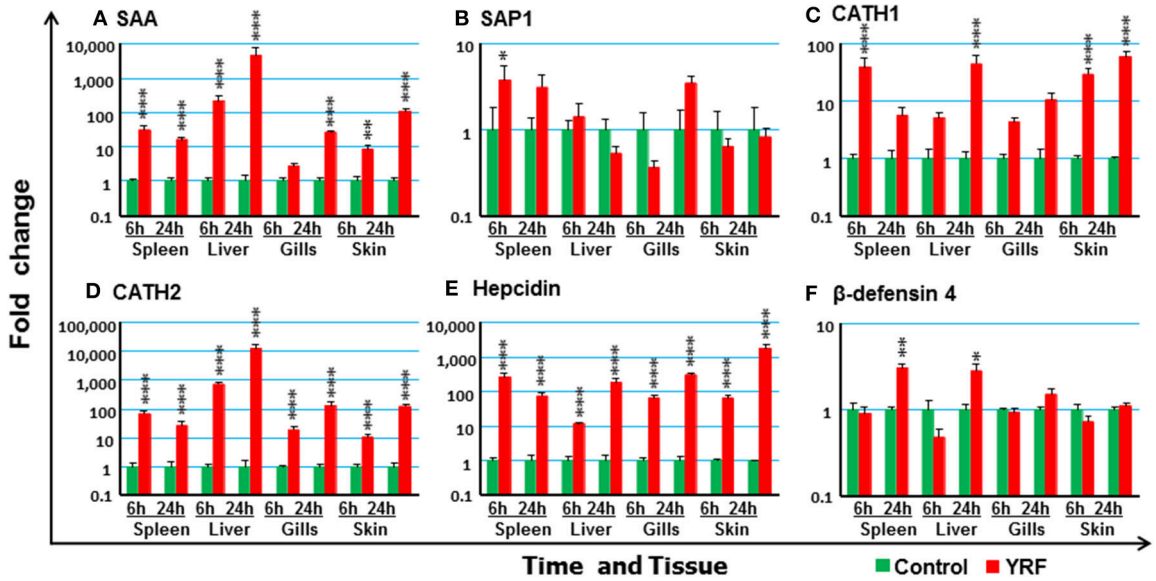


FIGURE 8 | The activation of APPs and AMPs *in vivo* by YRF. Rainbow trout were ip injected with YRF or PBS, sampled and analyzed as described in **Figure 2**. The expression of SAA **(A)**, SAP1 **(B)**, CATH1 **(C)**, CATH2 **(D)**, hepcidin **(E)**, and β-defensin-4 **(F)**, was examined. A fold change was calculated as the average expression level of YRF injected fish divided by that of time matched controls. The means + SEM of six fish are shown. Significant differences between injected fish and controls were tested by one way-ANOVA followed by the Bonferroni *post hoc* test, and are shown over the bars as; $*p < 0.05$, $**p < 0.01$, and $***p < 0.001$.

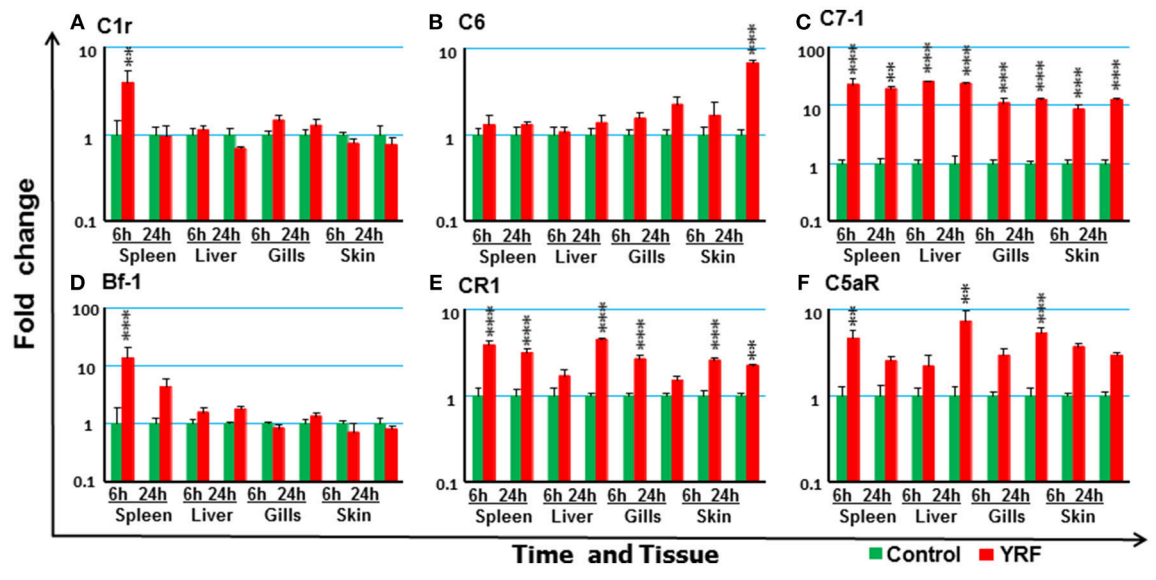


FIGURE 9 | The activation of complements *in vivo* by YRF. Rainbow trout were ip injected with YRF or PBS, sampled and analyzed as described in **Figure 2**. The expression of complement genes C1r **(A)**, C6 **(B)**, C7-1 **(C)**, Bf-1 **(D)**, CR1 like **(E)**, and C5aR **(F)** was examined. A fold change was calculated as the average expression level of YRF injected fish divided by that of time matched controls. The means + SEM of six fish are shown. Significant differences between injected fish and controls were tested by one way-ANOVA followed by the Bonferroni *post hoc* test, and are shown over the bars as; $**p < 0.01$ and $***p < 0.001$.

Following YRF administration multiple proinflammatory cytokines, including IL-1β, TNFα, IL-6, IL-11, M17, IL-17C, IL-12, IL-22, IL-23, and chemokines (CXCL8, and CXCL_F4-5) were induced by 6 hpi in all or most of the tissues examined but had decreased by 24 hpi. A similar response was also observed for several anti-inflammatory genes, including nIL-1Fm, IL-35 and the type II SOCS family genes (CISHa, SOCS1, and SOCS3A) that function intracellularly. However, the anti-inflammatory cytokines IL-10A and IL-10B were refractory, and TGFβ1 was only induced to a small extent in the liver although several proinflammatory cytokine genes were highly induced. These expression profiles suggest a rapid but transient

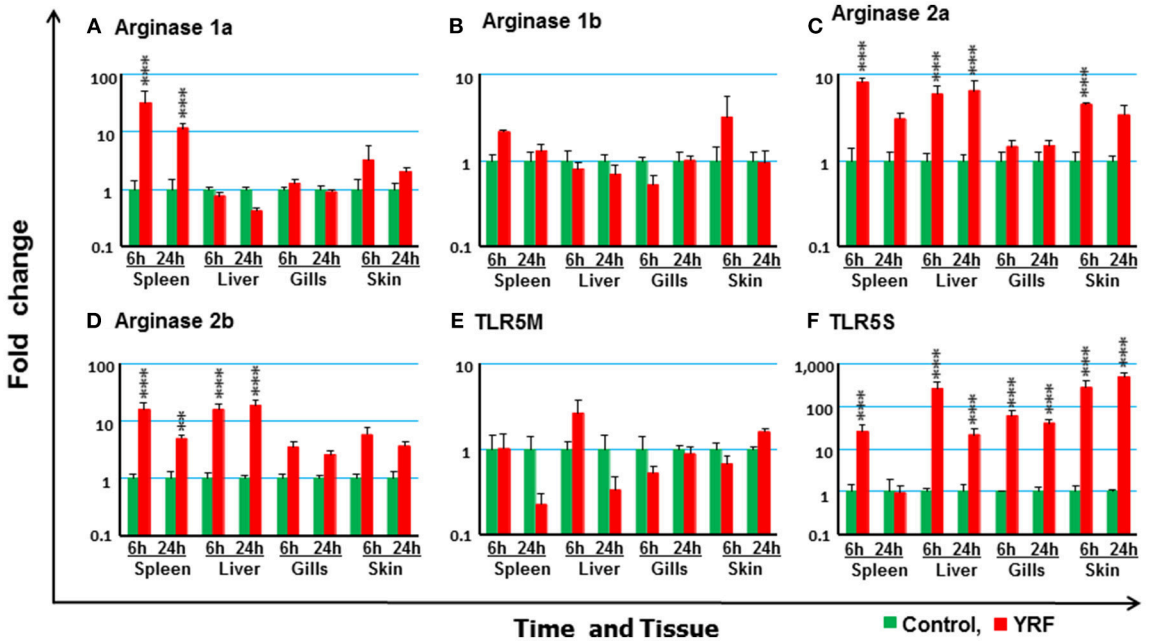


FIGURE 10 | The modulation of the expression of arginase genes and TLR5 *in vivo* by YRF. Rainbow trout were ip injected with YRF or PBS, sampled and analyzed as described in **Figure 2**. The expression of arginase 1a **(A)**, arginase 1b **(B)**, arginase 2a **(C)**, arginase 2b **(D)**, TLR5M **(E)**, and TLR5S **(F)** in each tissue was examined by RT-qPCR. A fold change was calculated as the average expression level of YRF injected fish divided by that of time matched controls. The means + SEM of six fish are shown. Significant differences between injected fish and controls were tested by one way-ANOVA followed by the Bonferroni *post hoc* test, and are shown over the bars as; $^{**}p < 0.01$ and $^{***}p < 0.001$.

systemic inflammatory host response is elicited after YRF injection.

The huge early induction (three orders of magnitude) of IL-1β2 and IL-6 in the spleen, and IL-11, IL-17C1, and IL-23P19 in liver is noteworthy. Trout IL-1β is known to induce the expression of itself and other inflammatory cytokines, eg TNF-α (51), IL-6 (52), IL-11 (55), IL-17C2 (65), IL-23P19 (61), IL-34 (57), and chemokines, eg CXCL8_L1 (IL-8), CXCL11_L1, CXCL_F4, and CXCL_F5 (58). Trout IL-6 has been shown to have effects on macrophages and B cells and promote the expression of AMP genes, eg, hepcidin, CATH2 and LEAP2, and complement genes (52), but has little effects on the expression of proinflammatory cytokines. Although there are no bioactivity studies reported for trout IL-11, IL-17C, and IL-23, it is possible to assume their function from other fish species (eg IL-17C) and mammals, although it should be noted that fish IL-17C genes may have arisen from an ancestral gene that gave rise to mammalian IL-17C and IL-17E/IL-25 (65). Hence, the expression of many of the proinflammatory cytokines and other immune genes may be attributed to the early induction of IL-1β or IL-6. However, the high level induction of IL-11, IL-17C1 and IL-23P19 expression is in the liver where IL-1β expression is moderate. Furthermore, IL-1β preferentially induces the expression of IL-17C2 but not IL-17C1 that is highly induced by YRF. These expression profiles may suggest multiple cells or signaling pathways are activated by YRF injection in different tissues.

The lack of response of Th1 pathway genes (82) in all tissues was surprising. This included IFNγ1, IFNγ2, and IFNγ inducible chemokine CXCL11_L (58), and the cytokines IL-2 and IL-21 that induce IFNγ expression (47, 69). However, the Th17 marker genes IL-17A/F1 and IL-17A/F2 (63) were induced in spleen and/or liver, whilst the Th2 cytokines IL-4/13A and IL-4/13B (67) and Treg pathway cytokine TGFβ1 were induced in liver only. The implications of these responses will be discussed later in terms of the potential adjuvant effects of flagellin.

Systemic Activation of Multiple Anti-microbial Defense Pathways by IP Injection of YRF

In response to flagellin injection, fish rapidly increase the expression of multiple APPs, AMPs and complement genes in addition to proinflammatory cytokines and chemokines. These molecules may play an important role in mediating protection against intruding pathogens. Cytokines such as IL-1β and IL-6 induce the expression of APPs, AMPs and complement genes, and may indirectly induce their upregulation following YRF injection.

APPs are involved in diverse defensive functions, such as induction of cytokine synthesis, leukocyte recruitment, activation of epithelial immunity, opsonisation and antiviral activity. Trout SAA is strongly induced in a wide variety of immune-relevant tissues by infection or challenge with PAMPs and can be detected in all primary defense barriers and in mononuclear cells of head kidney, spleen and liver, suggesting a role in local

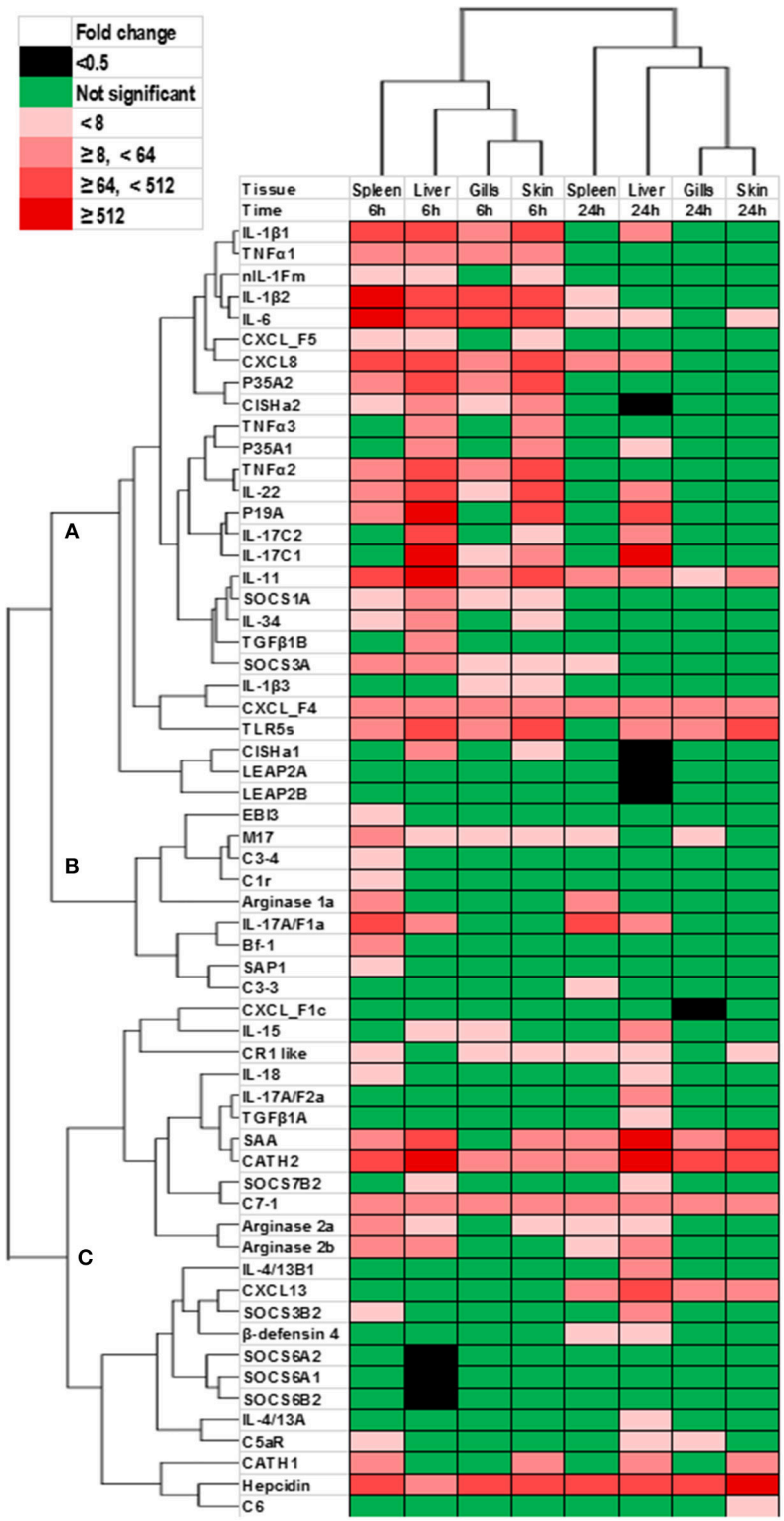


FIGURE 11 | Clustering analysis of genes modulated by YRF *in vivo*. Rainbow trout were ip injected with YRF or PBS, sampled and gene expression analyzed. Genes significantly modulated (at least onetime point/tissue) were selected for analysis. The fold changes were log2 transformed and subjected to hierarchical clustering using the Morpheus program. Three major expression profiles (clusters **A–C**) of genes are apparent.

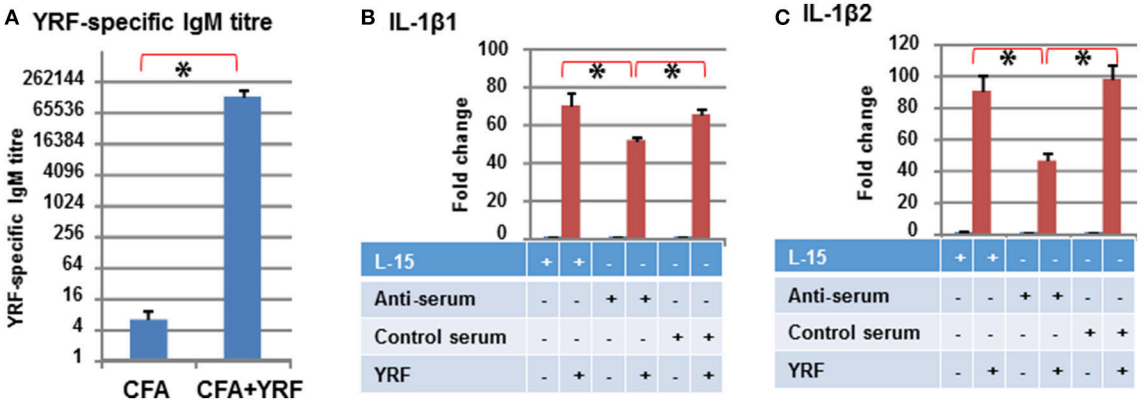


FIGURE 12 | Antibody response to YRF vaccination. **(A)** YRF-specific IgM antibody titer. Rainbow trout were immunized with CFA+YRF or CFA alone as control. YRF specific IgM antibody was detected by ELISA in sera collected 3 months post immunization. The mean+SEM of 10 fish from each group are shown. Neutralization of YRF activated IL-1β1 **(B)** and IL-1β2 **(C)** expression. YRF was incubated with sera from CFA+YRF immunized trout (Anti-serum), or sera from CFA immunized fish (Control serum), or cell culture medium (L-15) for 1 h before addition to RTS-11 cells. Matched serum or L-15 samples without YRF were also added to RTS-11 cells as controls. After 4 h the incubation was terminated and the expression of IL-1β1 and IL-1β2 determined by RT-qPCR as described above. The bridge and asterisk connected bars indicate a statistical difference ($P < 0.05$).

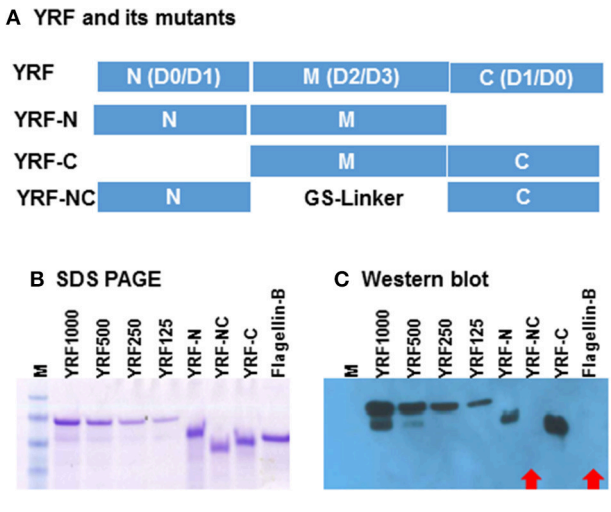


FIGURE 13 | (A) Schematic representation of YRF and its mutants. Full-length YRF contains the N-terminal D0/D1 domains, the middle unstructured D2/D3 domain and the C terminal D1/D0 domains. Three mutants with the N-terminal deleted (YRF-C), middle domain deleted (YRF-NC) and the C-terminal deleted (YRF-N) were produced. **(B)** SDS-PAGE and **(C)** Western blot analysis of YRF and its mutants. YRF1000, 500, 250, and 125 indicate amount (ng) of protein loaded. An unrelated flagellin protein (Flagellin-B) was also included as a control. The protein gel was stained with Imperial protein stain **(B)** or detected by Western blotting **(C)** using antisera from rainbow trout immunized with YRF + CFA. M = SeeBlue plus 2 protein marker. Red arrows indicate a negative signal.

defense (74). AMPs, such as hepcidins, cathelicidins and β-defensins play an important role in defense against microbial invasion (75–77). Although the primary mode of action of antimicrobial peptides has been described as lysis of pathogens, they have also been reported to exert a number of other effects such as immune modulation. For example, mammalian hepcidin regulates iron homeostasis, and cathelicidins have been implicated in wound healing, angiogenesis, and other innate immune mechanisms (52). The complement system plays a central role in early pathogen defense by opsonization of pathogens, release of anaphylatoxins, and formation of the membrane attack complex (78). Interestingly, the peak induction of APPs, AMPs and complement genes was delayed, with highest expression observed at 24 hpi in the liver, gills and skin. The expression modulation patterns suggest that YRF injection activates an early inflammation leading to activation of systemic antimicrobial defenses that may account for the non-specific protection seen in rainbow trout against different bacteria after YRF injection (36). Thus flagellin may have potential to be used as an immunostimulant in fish aquaculture.

Interestingly, arginase 1 was up-regulated in only spleen whilst arginase 2 was induced in the spleen, liver and skin. In mammals, macrophages have functionally distinct phenotypes defined by two activation states, M1 and M2, which represent two polar ends of a continuum exhibiting pro-inflammatory and tissue repair activities, respectively (80). Arginase is one of the key components driving the molecular mechanisms involved in macrophage polarization. Arginase 1 is induced by the Th2 cytokines IL-4 and IL-13, and is considered a M2 marker in mammals (80). However, arginase 2 may be a more relevant marker of M2 cells in teleost fish (81). In rainbow trout arginase 1 expression is highly modulated by PAMPs and pro-inflammatory cytokines whilst arginase 2 is induced by the fish specific Th2 cytokine IL-4/13 (81). Whether the increased expression of arginases is due to increased trafficking of arginase expressing macrophages, or is induced *in situ* directly by flagellin or by upregulated cytokines, or both, remains to be determined. The co-expression of arginase 2 and IL-4/13 in the liver may suggest the activation of a homeostatic tissue repair mechanism after an acute inflammatory event.

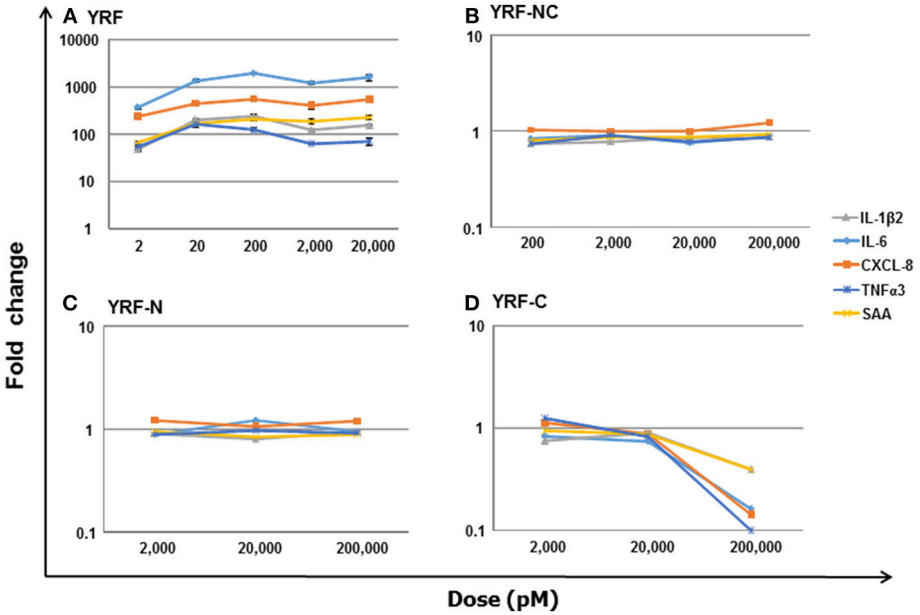


FIGURE 14 | Dose-response of biomarker gene expression in response to YRF and its mutants. RTS-11 cells was stimulated with different concentrations of YRF **(A)**, and its mutants YRF-NC **(B)**, YRF-N **(C)**, and YRF-C **(D)** for 4 h. The gene expression of IL-1β2, IL-6, CXCL-8, TNFα3, and SAA was determined by qPCR, and expressed as a fold change relative to the control samples. The means + SEM of four independent samples are shown. Note: the expression of all the genes was significantly different from controls in YRF stimulated samples only.

Tissue Specific Responses to IP Injection of YRF

The clustering analysis revealed a tissue specific gene expression profile, with the liver showing modulation of the largest number of immune genes, especially at 24 hpi. The liver is the central metabolic organ that must actively prevent the induction of immune responses to gut-derived antigens, and neo-antigens that are generated by the liver's metabolic and detoxification activities. In addition, gut-derived microbes and microbial products must be removed from the circulation to prevent systemic immune activation. Thus, the liver serves as an important barrier between the gut and the circulation. Both the maintenance of hepatic tolerance and the initiation of inflammation are mainly mediated by the liver-resident antigen-presenting cells (APCs) that are constantly exposed to gut-derived dietary and microbial antigens (83). These APCs include liver-resident dendritic cells, liver-resident macrophages, Kupffer cells and the liver sinusoidal endothelial cells, and semi-professional APCs, such as hepatocytes and hepatic stellate cells. These cells are instrumental for the downregulation of immune responses in the liver and the initiation of liver inflammation/ recruitment of leukocytes to the liver (83). An acute inflammatory response was clearly initiated in liver by YRF injection of trout, as shown by the up-regulation of many inflammatory genes. Interestingly, the major specific primary targets of TLR5 agonists (eg flagellin) in liver of rodents and primates are hepatocytes (84). The most inducible genes in trout liver were IL-11, IL-23P19 and IL-17C1 that were induced over 1,000 fold at 6 hpi, and remained elevated to 24 hpi. However, *in vitro* IL-11 was only moderately induced by YRF in the macrophage cell line RTS-11 and head kidney (HK) cells that contain macrophages (as well as other leucocytes), IL-23P19 was induced in RTS-11 but not HK cells and IL-17C1 was not induced in either RTS-11 or HK cells (23). This difference in immune gene induction may suggest different cells in liver are involved in the YRF response. Whether these cells are hepatocytes or other APCs remains to be determined in fish.

SAA (APP) and CATH2 (AMP) were massively induced by YRF in liver, especially at the late time point. Their later upregulation may suggest that these genes are affected by the cytokines (IL-11, IL-23, and IL-17C1) induced early by YRF, alone or in combination.

The best way for mass application of immunostimulants in aquaculture is their use as dietary additives (9). The activation of an inflammatory response and multiple defense pathways by YRF injection in liver suggests that flagellin could be delivered via the diet if formulated to protect its degradation in the gastric and intestinal tract of fish.

The Middle D2/D3 Domain Is the Main Target of the Host Immune Response

A strong IgM response was induced after YRF immunization in rainbow trout. The antiserum could decrease the bioactivity of YRF, and our results showed that these antibodies reacted against the middle D2/D3 domain. However, an antibody response is not desirable when flagellin is used as an immunostimulant or vaccine adjuvant, since the antibodies may affect the flagellin stimulatory effect on repeat exposure. Although there is no direct experimental evidence, the binding of antibodies may block

flagellin binding to its receptor, or opsonize the flagellin for its removal. A strong antibody response to flagellin may also adversely affect the specific response to the target antigen (s) when used as an vaccine adjuvant. To mitigate against these undesirable effects, a flagellin could be modified to remove the middle D2/D3 domain to eliminate or reduce the antibody response but retain the immunostimulatory effects (17, 20).

Full-Length YRF Is Necessary for Activation of Inflammation: An Evasion Mechanism of the Pathogen?

The immunological impact of flagellin stimulation has driven several bacterial pathogens to evolve mechanisms to escape TLR5-mediated host defense. For example, Listeria shuts off flagellin expression at the host temperature of 37°C, and in the major food-borne pathogen *Campylobacter jejuni* and the gastric pathogen *Helicobacter pylori*, flagellin structural changes lead to the evasion of TLR5 activation (85). The activation of TLR5 requires a specific structural conformation in flagellin that is mainly defined in the D1 domain although other domains may contribute. Thus, flagellin that has been modified by removing the middle D2/D3 domain can retain its TLR5 activation capacity (20). It is also worth noting that different host species may have different structural requirements for flagellin to activate TLR5 signaling, as shown in mammals and birds (85). Our results showed that only full-length YRF is bioactive; any changes at the N-terminal, the C-terminal or the middle D2/D3 domain led to loss of bioactivity *in vitro*. This data suggests that TLR5 signaling in rainbow trout requires a structural conformation maintained by full-length YRF.

YRF originates from *Yersinia ruckeri*, a flagellated Gram-negative enterobacterium that is the causative agent of enteric redmouth disease (ERM), a hemorrhagic septicemia that primarily affects farmed salmonid fish species (23). A bacterin vaccine against ERM prepared from motile serovar 1 *Y. ruckeri* strains was the first commercialized fish vaccine. This vaccine has been used worldwide for several decades and has proven an effective and economical means for the control of ERM. It appears that the flagellum is necessary for vaccine-mediated immunity and that the prolonged use of this vaccine has provided a selective force driving the emergence of nonmotile variants associated with disease outbreaks in previously vaccinated fish, independently in the USA and Europe (86). These cases suggest that flagellin is an important virulence factor of motile *Y. ruckeri* and an important immune determinant of the host immune response and vaccine mediated protection. The requirement of a full-length YRF for TLR5 activation in rainbow trout may benefit this motile pathogen to evade TLR5 activation. It is perceivable that the required structural conformation might be easily disturbed by protease cleavage after flagellin release, or by binding of other proteins or antibodies *in vivo* or at the mucosal surface of the fish host.

In contrast to the single membrane form of TLR5 in mammals, teleost fish (including salmonids) possess one membrane TLR5 and one secreted TLR5. Both TLR5M and TLR5S bind flagellin (24). The modulation of TLR5M and TLR5S expression by flagellin is controversial in fish. In rainbow trout, YRF did not induce the expression of TLR5M and TLR5S *in vitro* in either RTS-11 cells or in primary HK cells (23) and only up-regulated the expression of TLR5S *in vivo*, as shown in this study. A strong up-regulation of TLR5S has also been reported in Atlantic salmon after vaccination with *V. anguillarum* flagellin (16). In channel catfish, both TLR5M and TLR5S are upregulated by recombinant *Y. ruckeri* flagellins *in vitro* in primary HK macrophages and *in vivo* in HK (87). It is noteworthy that fish TLR5M and TLR5S can be upregulated by bacterial infection and by LPS (24, 87). Clearly the fish species-specific modulation of TLR5 expression in response to flagellin needs further research in different species using pure flagellins.

In the present study rainbow trout TLR5S expression was induced rapidly *in vivo* in all the tissues examined at 6 hpi and this was sustained in the liver, gills and intestine to 24 hpi when the expression of most proinflammatory cytokines activated by flagellin had subsided. The different expression patterns suggest that trout TLR5S may function as a negative feedback regulator of flagellin signaling, that is induced by flagellin and competes with TLR5M for flagellin binding. This notion is in contrast to the hypothesis that the inducible TLR5S amplifies membrane TLR5-mediated cellular responses in a positive feedback fashion (24), and warrants further investigation to understand how flagellin signaling is regulated in fish.

Using Flagellin as an Immunostimulant or Vaccine Adjuvant

Flagellin is a potent activator of innate immune responses *in vitro* in different fish species (23, 87). Our results in rainbow trout show that a transient systemic inflammation is activated following flagellin injection, leading to the activation of multiple antimicrobial pathways in both internal and mucosal tissues. Furthermore, non-specific protection against bacterial infections can be elicited in rainbow trout after flagellin injection (36). All these data suggest that flagellin can be used as a potent immunostimulant or a vaccine adjuvant in fish aquaculture.

The most convenient use of immunostimulants in aquaculture is as diet additives. Due to its protein nature, flagellin must be reformulated to avoid degradation in the gastric and intestinal tract, and should be modified by removing the antigenic D2/D3 domain. Although it is not possible to obtain functional mutants with YRF, research by others (85, 88) and by us suggests that some flagellins are malleable and functional mini-flagellins can be generated.

A vaccine-mediated immune response involves the integration of three distinct signals delivered in sequence. Signal 1 is antigen recognition; signal 2 is co-stimulation provided by APC; and signal 3 is the cytokine milieu that drives lymphocyte differentiation and expansion. Adjuvants can be distinguished between signal 1 facilitators and signal 2 facilitators. The signal 1 facilitators influence the fate of the vaccine antigen in time, place, and concentration, ultimately improving its immune-availability, while signal 2 facilitators provide the co-stimulatory signals during antigen recognition (8).

Flagellin can be a signal 1 facilitator as it can induce the expression of proinflammatory cytokines and chemokines eg CXCL8 and CXCL13, which promote the recruitment of T and B lymphocytes and APCs to the site of immunization, thus maximizing the chances of antigen-specific lymphocytes encountering their cognate antigens. It may also function as a signal 2 facilitator by activating APCs to express co-stimulatory receptors. Furthermore, flagellin in combination with other TLR agonists may function as a signal 3 facilitator by induction of cytokines for specific T helper cell subsets. For example, the induction of IL-4/13 expression by flagellin in rainbow trout may facilitate a Th2 type response, whilst IL-12 and IL-23 expression may drive Th1 and Th17 responses, respectively. It is widely accepted that as an adjuvant, flagellin can induce an enhanced antigen-specific immune response in different animals (31–35, 88).

In vaccine development for fish aquaculture, flagellin could be added to existing bacterin or inactivated viral vaccines by mixing or conjugating to enhance their immunogenicity. It could also be formulated in subunit vaccines as fusion proteins. The uniqueness of flagellin as an adjuvant is its ability to be easily incorporated into a DNA vaccine. DNA vaccines induce both early and late immune responses in fish and more than 20 different viral DNA vaccines have been developed experimentally for prophylactic use in fish. The rhabdoviridae DNA vaccines (eg VHSV and IHNV) have shown high levels of efficacy, athough with some viruses only moderate to low efficacies are seen (12). Thus, incorporation of adjuvants into these less effective vaccines may be needed to provide adequate protection. As a protein adjuvant, flagellin can be easily incorporated into a DNA vaccine as a DNA construct, or with the target antigen physically linked to the N- or C-terminal or replacing the D2/D3 domain. Thus, flagellin adjuvants have the potential to open new avenues for efficacious vaccine development for fish aquaculture.

CONCLUSION

Of three bacterial PAMPs (LPS, peptidoglycan and flagellin) tested in this study, flagellin (YRF) was the most potent activator of proinflammatory cytokine expression *in vitro*. YRF injection of trout initiated a transient systemic inflammatory response with key pro-inflammatory cytokines (IL-1β, TNFα, IL-6, and IL-11 etc.) and chemokines (CXCL_F4 and CXCL-8), induced rapidly (6 hpi) but subsiding quickly in multiple tissues. Consequently, several anti-microbial pathways were activated systemically with heightened expression of APPs (SAA), AMPs (cathelicidins and hepcidin) and complement genes in multiple tissues, which was sustained to 24 hpi in the liver and mucosal tissues. The Th17 cytokines IL-17A/F1a and IL-17A/F2a were also induced in the liver and spleen (IL-17A/F1a only), and Th2 cytokine IL-4/13 was induced in the liver. However, the anti-inflammatory IL-10 and Th1 cytokine IFNγ were refractory. The secreted TLR5S was induced by flagellin in all tissues examined whilst the membrane TLR5M was refractory, suggesting that TLR5S may function as a negative feedback regulator. Trout liver appeared to be an important organ responding to flagellin stimulation, with marked induction of IL-11, IL-23P19, IL-17C1, SAA and cathelicidin-2. YRF induced a strong antibody response, with the generated antibodies binding the middle domain of YRF and able to neutralize YRF bioactivity. Intact YRF is necessary for its bioactivity, with deletion of either the N-terminal, C terminal or middle domain of YRF leading to functional loss. This study adds to the growing literature suggesting that flagellin could be a potent immunostimulant and vaccine adjuvant for fish aquaculture.

ETHICS STATEMENT

All the experiments described comply with the Guidelines of the European Union Council (2010/63/EU) for the use of laboratory animals, and were carried out under UK Home Office project license PPL 60/4013, approved by the ethics committee at the University of Aberdeen.

AUTHOR CONTRIBUTIONS

TW conceived and planned the study, analyzed and interpreted the data, and wrote the first draft of the manuscript. EW performed experiments, analyzed the data, and wrote the paper. CS conceived and planned the study, analyzed and interpreted the data, and wrote the paper. All authors read and approved the final manuscript.

ACKNOWLEDGMENTS

EW was supported by a Ph.D. studentship from the Ministry of Science and Technology of Thailand and Mahasarakham University. TW received funding from the MASTS pooling initiative (The Marine Alliance for Science and Technology for Scotland), that is funded by the Scottish Funding Council (grant reference HR09011). This research was also funded by the European Commission under the 7th Framework Programme for Research and Technological Development (FP7) of the European Union (grant agreement No. 311993 TARGETFISH).

SUPPLEMENTARY MATERIAL

The Supplementary Material for this article can be found online at: https://www.frontiersin.org/articles/10.3389/fimmu.2018.03054/full#supplementary-material

REFERENCES

1. FAO. *The State of World Fisheries and Aquaculture 2016: Contributing to food security and nutrition for all*. Rome: FAO. p. 200 (2016). Available online at: http://www.fao.org/3/a-i5555e.pdf
2. Kibenge FS, Godoy MG, Fast M, Workenhe S, Kibenge MJ. Countermeasures against viral diseases of farmed fish. *Antiviral Res.* (2012) 95:257–81. doi: 10.1016/j.antiviral.2012.06.003
3. Lafferty KD, Harvell CD, Conrad JM, Friedman CS, Kent ML, Kuris AM, et al. Infectious diseases affect marine fisheries and aquaculture economics.

Ann Rev Mar Sci. (2015) 7:471–96. doi: 10.1146/annurev-marine-010814-015646
4. Santos L, Ramos F. Antimicrobial resistance in aquaculture: current knowledge and alternatives to tackle the problem. *Int J Antimicrob Agents* (2018) 52:135–143. doi: 10.1016/j.ijantimicag.2018.03.010
5. Assefa A, Abunna F. Maintenance of fish health in aquaculture: review of epidemiological approaches for prevention and control of infectious disease of fish. *Vet Med Int*. (2018) 2018:5432497. doi: 10.1155/2018/5432497
6. Pérez-Sánchez T, Mora-Sánchez B, Balcázar JL. Biological approaches for disease control in aquaculture: advantages, limitations and challenges. *Trends Microbiol*. (2018)26: 896–903. doi: 10.1016/j.tim.2018.05.002
7. Newaj-Fyzul A, Austin B. Probiotics, immunostimulants, plant products and oral vaccines, and their role as feed supplements in the control of bacterial fish diseases. *J Fish Dis*. (2015) 38:937–55. doi: 10.1111/jfd.12313
8. Tafalla C, Bøgwald J, Dalmo RA. Adjuvants and immunostimulants in fish vaccines: current knowledge and future perspectives. *Fish Shellfish Immunol*. (2013) 35:1740–50. doi: 10.1016/j.fsi.2013.02.029
9. Vallejos-Vidal E, Reyes-López F, Teles M, MacKenzie S. The response of fish to immunostimulant diets. *Fish Shellfish Immunol*. (2016) 56:34–69. doi: 10.1016/j.fsi.2016.06.028
10. Librán-Pérez M, Costa MM, Figueras A, Novoa B. β-glucan administration induces metabolic changes and differential survival rates after bacterial or viral infection in turbot (*Scophthalmus maximus*). *Fish Shellfish Immunol*. (2018) 82:173–182. doi: 10.1016/j.fsi.2018.08.005
11. Munang'andu HM. Intracellular bacterial infections: a challenge for developing cellular mediated immunity vaccines for farmed fish. *Microorganisms* (2018) 6:E33. doi: 10.3390/microorganisms6020033
12. Dalmo RA. DNA vaccines for fish: review and perspectives on correlates of protection. *J Fish Dis*. (2018) 41:1–9. doi: 10.1111/jfd.12727
13. Del Giudice G, Rappuoli R, Didierlaurent AM. Correlates of adjuvanticity: a review on adjuvants in licensed vaccines. *Semin Immunol.* (2018) 39:14–21. doi: 10.1016/j.smim.2018.05.001
14. Chettri JK, Raida MK, Holten-Andersen L, Kania PW, Buchmann K. PAMP induced expression of immune relevant genes in head kidney leukocytes of rainbow trout (*Oncorhynchus mykiss*). *Dev Comp Immunol*. (2011) 35: 476–82. doi: 10.1016/j.dci.2010.12.001
15. Kawai T, Akira S. The role of pattern-recognition receptors in innate immunity: update on Toll-like receptors. *Nature Immunol*. (2010) 11: 373–84. doi: 10.1038/ni.1863
16. Hynes NA, Furnes C, Fredriksen BN, Winther T, Bøgwald J, Larsen AN, Dalmo RA. Immune response of Atlantic salmon to recombinant flagellin. *Vaccine* (2011) 29:7678–87. doi: 10.1016/j.vaccine.2011.07.138
17. Yoon SI, Kurnasov O, Natarajan V, Hong M, Gudkov AV, Osterman AL, Wilson IA. Structural basis of TLR5-flagellin recognition and signalling. *Science* (2012) 335:859–64. doi: 10.1126/science.1215584
18. Akira S, Uematsu S, Takeuchi O. Pathogen recognition and innate immunity. *Cell* (2006) 124:783–801. doi: 10.1016/j.cell.2006.02.015
19. Zhao Y, Shao F. The NAIP-NLRC4 inflammasome in innate immune detection of bacterial flagellin and type III secretion apparatus. *Immunol Rev*. (2015) 265:85–102. doi: 10.1111/imr.12293
20. Il Kim M, Lee C, Park J, Jeon BY, Hong M. Crystal structure of *Bacillus cereus* flagellin and structure-guided fusion-protein designs. *Sci Rep*. (2018) 8:5814. doi: 10.1038/s41598-018-24254-w
21. Hayashi F, Smith KD, Ozinsky A, Hawn TR, Yi EC, Goodlett DR, et al. The innate immune response to bacterial flagellin is mediated by Toll-like receptor 5. *Nature* (2001) 410:1099–103. doi: 10.1038/35074106
22. Okugawa S, Yanagimoto S, Tsukada K, Kitazawa T, Koike K, Kimura S, et al. Bacterial flagellin inhibits T cell receptor-mediated activation of T cells by inducing suppressor of cytokine signalling-1 (SOCS-1). *Cell Microbiol*. (2006) 8:1571–80. doi: 10.1111/j.1462-5822.2006.00731.x
23. Wangkahart E, Scott C, Secombes CJ, Wang T. Re-examination of the rainbow trout (*Oncorhynchus mykiss*) immune response to flagellin: *Yersinia ruckeri* flagellin is a potent activator of acute phase proteins, anti-microbial peptides and pro-inflammatory cytokines *in vitro*. *Dev Comp Immunol.*(2016) 57:75–87. doi: 10.1016/j.dci.2015.12.017
24. Tsujita T, Tsukada H, Nakao M, Oshiumi H, Matsumoto M, Seya T. Sensing bacterial flagellin by membrane and soluble orthologs of Toll-like receptor 5 in rainbow trout (*Oncorhynchus mykiss*). *J Biol Chem*. (2004) 279:48588–97. doi: 10.1074/jbc.M407634200
25. Tsoi S, Park KC, Kay HH, O'Brien TJ, Podor E, Sun G, et al. Identification of a transcript encoding a soluble form of toll-like receptor 5 (TLR5) in Atlantic salmon during *Aeromonas salmonicida* infection. *Vet Immunol Immunopathol*. (2006) 109:183–7. doi: 10.1016/j.vetimm.2005.05.013
26. Baoprasertkul P, Xu P, Peatman E, Kucuktas H, Liu Z. Divergent Toll-like receptors in catfish (*Ictalurus punctatus*): TLR5S, TLR20, TLR21. *Fish Shellfish Immunol*. (2007) 23:1218–30. doi: 10.1016/j.fsi.2007.06.002
27. Hwang SD, Asahi T, Kondo H, Hirono I, Aoki T. Molecular cloning and expression study on Toll-like receptor 5 paralogs in Japanese flounder, *Paralichthys olivaceus*. *Fish Shellfish Immunol*. (2010) 29:630–8. doi: 10.1016/j.fsi.2010.06.011
28. Muñoz I, Sepulcre MP, Meseguer J, Mulero V. Molecular cloning, phylogenetic analysis and functional characterization of soluble Toll-like receptor 5 in gilthead seabream, *Sparus aurata*. *Fish Shellfish Immunol*. (2013) 35: 36–4. doi: 10.1016/j.fsi.2013.03.374
29. Bai JS, Li YW, Deng Y, Huang YQ, He SH, Dai J, et al. Molecular identification and expression analysis of TLR5M and TLR5S from orange-spotted grouper (*Epinepheluscoioides*). *Fish Shellfish Immunol*. (2017) 63:97–102. doi: 10.1016/j.fsi.2017.01.037
30. Zhang M, Wu H, Li X, Yang M, Chen T, Wang Q, et al. *Edwardsiella tarda* flagellar protein FlgD: a protective immunogen against *edwardsiellosis*. *Vaccine* (2012) 30:3849–56. doi: 10.1016/j.vaccine.2012.04.008
31. Jia PP, Hu YH, Chi H, Sun BG, Yu WG, Sun L. Comparative study of four flagellins of *Vibrio anguillarum*: vaccine potential and adjuvanticity. *Fish Shellfish Immunol*. (2013) 34:514–20. doi: 10.1016/j.fsi.2012.11.039
32. Liu X, Zhang H, Jiao C, Liu Q, Zhang Y, Xiao J. Flagellin enhances the immunoprotection of formalin-inactivated *Edwardsiella tarda* vaccine in turbot. *Vaccine* (2017) 35:369–74. doi: 10.1016/j.vaccine.2016.11.031
33. Xing J, Zhou X, Tang X, Sheng X, Zhan W. FlaC supplemented with VAA, OmpK or OmpR as bivalent subunit vaccine candidates induce immune responses against *Vibrio anguillarum* in flounder (*Paralichthys olivaceus*). *Vaccine* (2018) 36:1316–22 doi: 10.1016/j.vaccine.2017.11.074
34. Beck BR, Lee SH, Kim D, Park JH, Lee HK, Kwon SS, et al. A Lactococcus lactis BFE920 feed vaccine expressing a fusion protein composed of the OmpA and FlgD antigens from *Edwardsiella tarda* was significantly better at protecting olive flounder (*Paralichthys olivaceus*) from *edwardsiellosis* than single antigen vaccines. *Fish Shellfish Immunol*. (2017) 68:19–28. doi: 10.1016/j.fsi.2017.07.004
35. Liang HY, Wu ZH, Jian JC, Liu ZH. Construction of a fusion flagellin complex and evaluation of the protective immunity of it in red snapper (*Lutjanus sanguineus*). *Lett Appl Microbiol*. (2012) 55:115–21. doi: 10.1111/j.1472-765X.2012.03267.x
36. Scott CJW, Austin B, Austin DA, Morris PC. Non-adjuvanted flagellin elicits a non-specific protective immune response in rainbow trout (*Oncorhynchus mykiss*, Walbaum) towards bacterial infections. *Vaccine* (2013) 31:3262–7. doi: 10.1016/j.vaccine.2013.05.025
37. González-Stegmaie, R, Romero A, Estepa A, Montero J, Mulero V, Mercado L. Effects of recombinant flagellin B and its ND1 domain from *Vibrio anguillarum* on macrophages from gilthead seabream (*Sparus aurata* L.) and rainbow trout (*Oncorhynchus mykiss*, W.). *Fish Shellfish Immunol*. (2015) 42:144–52. doi: 10.1016/j.fsi.2014.10.034
38. Cesta MF. Normal structure, function, and histology of the spleen. *Toxicol Pathol.* (2006) 34:455–65. doi: 10.1080/01926230600867743
39. Awasthi A, Rathore G, Pradhan PK, Rebello SC, Khan MY, Lakra WS. Isolation and characterization of head kidney derived macrophages of *Labeo rohita*. *J Environ Biol.* (2014) 35:949.
40. Rombout JHWM, Taverne-Thiele AJ, Villena MI. The gut-associated lymphoid tissue (GALT) of carp (*Cyprinus carpio* L.): an immunocytochemical analysis. *Dev Comp Immunol*. (1993) 17:55–66. doi: 10.1016/0145-305X(93)90015-I
41. Xu Z, Parra D, Gómez D, Salinas I, Zhang YA, Jørgensen L von G, et al. Teleost skin, an ancient mucosal surface that elicits gut-like immune response. *Proc Natl Acad Sci USA*. (2013) 110:13097–102. doi: 10.1073/pnas.1304319110
42. Salinas I, Magadán S. Omics in fish mucosal immunity. *Dev Comp Immunol*. (2017) 75:99–108. doi: 10.1016/j.dci.2017.02.010

43. Wangkahart E, Secombes CJ, Wang T. Dissecting the immune pathways stimulated following injection vaccination of rainbow trout (*Oncorhynchus mykiss*) against enteric redmouth disease (ERM). *Fish Shellfish Immunol*. (2017) doi: 10.1016/j.fsi.2017.07.056. [Epub ahead of print].
44. Wang T, Husain M, Hong S, Holland JW. Differential expression, modulation and bioactivity of distinct fish IL-12 isoforms: implication towards the evolution of Th1-like immune responses. *Eur J Immunol*. (2014) 44:1541–51. doi: 10.1002/eji.201344273
45. Ganassin RC, Bols NC. Development of a monocyte/macrophage-like cell line, RTS11, from rainbow trout spleen. *Fish Shellfish Immunol*. (1998) 8:457–76. doi: 10.1006/fsim.1998.0153
46. Wang T, Husain M. The expanding repertoire of the IL-12 cytokine family in teleost fish: identification of three paralogues each of the p35 and p40 genes in salmonids, and comparative analysis of their expression and modulation in Atlantic salmon *Salmo salar*. *Dev Comp Immunol*. (2014) 46:194–207. doi: 10.1016/j.dci.2014.04.008
47. Wang T, Diaz-Rosales P, Costa MM, Campbell S, Snow M, Collet B, et al. Functional characterization of a nonmammalian IL-21: rainbow trout *Oncorhynchus mykiss* IL-21 upregulates the expression of the Th cell signature cytokines IFN-gamma, IL-10, and IL-22. *J Immunol*. (2011) 186:708–21. doi: 10.4049/jimmunol.1001203
48. Wang T, Huang W, Costa MM, Martin SA, Secombes CJ. Two copies of the genes encoding the subunits of putative interleukin (IL)-4/IL-13 receptors, IL-4Rα, IL-13Rα1 and IL-13Rα2, have been identified in rainbow trout (*Oncorhynchus mykiss*) and have complex patterns of expression and modulation. *Immunogenetics* (2011) 63:235–53. doi: 10.1007/s00251-010-0508-2
49. DeLuca D, Wilson M, Warr GW. Lymphocyte heterogeneity in the trout, *Salmo gairdneri*, defined with monoclonal antibodies to IgM. *Eur J Immunol*. (1983) 13:546–51. doi: 10.1002/eji.1830130706
50. Husain M, Bird S, van Zwieten R, Secombes CJ, Wang T. Cloning of the IL-1β3 gene and IL-1β4 pseudogene in salmonids uncovers a second type of IL-1β gene in teleost fish. *Dev Comp Immunol*. (2012) 38:431–46. doi: 10.1016/j.dci.2012.07.010
51. Hong S, Li R, Xu Q, Secombes CJ, Wang T. Two types of TNF-α exist in teleost fish: phylogeny, expression, and bioactivity analysis of type-II TNF-α3 in rainbow trout *Oncorhynchus mykiss*. *J Immunol*. (2013) 191:5959–72. doi: 10.4049/jimmunol.1301584
52. Costa MM, Maehr T, Diaz-Rosales P, Secombes CJ, WangT. Bioactivity studies of rainbow trout (*Oncorhynchus mykiss*) interleukin-6: effects on macrophage growth and antimicrobial peptide gene expression. *Mol Immunol*. (2011) 48:1903–16. doi: 10.1016/j.molimm.2011.05.027
53. Zou J, Bird S, Truckle J, Bols N, Horne M, Secombes CJ. Identification and expression analysis of an IL-18 homologue and its alternatively spliced form in rainbow trout (*Oncorhynchus mykiss*). *Eur J Biochem*. (2004) 271:1913–23. doi: 10.1111/j.1432-1033.2004.04101.x
54. Wang T, Bird S, Koussounadis A, Holland JW, Carrington A, Zou J, et al. Identification of a novel IL-1 cytokine family member in teleost fish. *J Immunol*. (2009) 183:962–74. doi: 10.4049/jimmunol.0802953
55. Wang T, Holland JW, Bols N, Secombes CJ. Cloning and expression of the first nonmammalian interleukin-11 gene in rainbow trout *Oncorhynchus mykiss*. *FEBS J*. (2005) 272:1136–47. doi: 10.1111/j.1742-4658.2005.04544.x
56. Wang T, Secombes CJ. Identification and expression analysis of two fish-specific IL-6 cytokine family members, the ciliary neurotrophic factor (CNTF)-like and M17 genes, in rainbow trout *Oncorhynchus mykiss*. *Mol Immunol*. (2009) 46:2290–8. doi: 10.1016/j.molimm.2009.04.003
57. Wang T, Kono T, Monte MM, Kuse H, Costa MM, Korenaga H, et al. Identification of IL-34 in teleost fish: differential expression of rainbow trout IL-34, MCSF1 and MCSF2, ligands of the MCSF receptor. *Mol Immunol*. (2013) 53:398–409. doi: 10.1016/j.molimm.2012.09.008
58. Chen J, Xu Q, Wang T, Collet B, Corripio-Miyar Y, Bird S, et al. Phylogenetic analysis of vertebrate CXC chemokines reveals novel lineage specific groups in teleost fish. *Dev Comp Immunol*. (2013) 41:137–52. doi: 10.1016/j.dci.2013.05.006
59. Jiang Y, Husain M, Qi Z, Bird S, Wang T. Identification and expression analysis of two interleukin-23α (p19) isoforms, in rainbow trout *Oncorhynchus mykiss* and Atlantic salmon Salmo salar. *Mol Immunol*. (2015) 66:216–28. doi: 10.1016/j.molimm.2015.03.014
60. Husain M, Martin SAM, Wang T. Identification and characterisation of the IL-27 p28 subunits in fish: cloning and comparative expression analysis of two p28 paralogues in Atlantic salmon *Salmo salar*. *Fish Shellfish Immunol*. (2014) 41:102–12. doi: 10.1016/j.fsi.2014.06.024
61. Secombes CJ, Wang T, Bird S. The interleukins of fish. *Dev Comp Immunol*. (2011) 35:1336–45. doi: 10.1016/j.dci.2011.05.001
62. Wang T, Díaz-Rosales P, Martin SA, Secombes CJ. Cloning of a novel interleukin (IL)-20-like gene in rainbow trout *Oncorhynchus mykiss* gives an insight into the evolution of the IL-10 family. *Dev Comp Immunol*. (2010) 34:158–67. doi: 10.1016/j.dci.2009.09.003
63. Wang T, Jiang Y, Wang A, Husain M, Xu Q, Secombes CJ. Identification of the salmonid IL-17A/F1a/b, IL-17A/F2b, IL-17A/F3 and IL-17N genes and analysis of their expression following in vitro stimulation and infection. *Immunogenetics* (2015) 67:395–412. doi: 10.1007/s00251-015-0838-1
64. Monte MM, Wang T, Holland JW, Zou J, Secombes CJ. Cloning and characterization of rainbow trout interleukin-17A/F2 (IL-17A/F2) and IL-17 receptor A: expression during infection and bioactivity of recombinant IL-17A/F2. *Infect Immun*. (2013) 81:340–53. doi: 10.1128/IAI.00599-12
65. Wang T, Martin SAM, Secombes CJ. Two interleukin-17C-like genes exist in rainbow trout *Oncorhynchus mykiss* that are differentially expressed and modulated. *Dev Comp Immunol*. (2010) 34: 491–500. doi: 10.1016/j.dci.2009.11.011
66. Monte MM, Zou J, Wang T, Carrington A, Secombes CJ. Cloning, expression analysis and bioactivity studies of rainbow trout (*Oncorhynchus mykiss*) interleukin-22. *Cytokine* (2011) 55:62–73. doi: 10.1016/j.cyto.2011.03.015
67. Wang T, Johansson P, Abós B, Holt A, Tafalla C, Jiang Y, et al. First in-depth analysis of the novel Th2-type cytokines in salmonid fish reveals distinct patterns of expression and modulation but overlapping bioactivities. *Oncotarget* (2016) 7:10917–46. doi: 10.18632/oncotarget.7295
68. Wang T, Holland JW, Carrington A, Zou J, Secombes CJ. Molecular and functional characterization of IL-15 in rainbow trout *Oncorhynchus mykiss*: a potent inducer of IFN-γ expression in spleen leukocytes. *J Immunol.* (2007) 179:1475–88. doi: 10.4049/jimmunol.179.3.1475
69. Wang T, Hu Y, Wangkahart E, Liu F, Wang A, Zahran E, et al. Interleukin (IL)-2 Is a Key Regulator of T Helper 1 and T Helper 2 Cytokine Expression in Fish: functional characterization of two divergent IL2 paralogs in salmonids. *Front Immunol*. (2018) 9:1683. doi: 10.3389/fimmu.2018.01683.
70. Harun NO, Costa MM, Secombes CJ, Wang T. Sequencing of a second interleukin-10 gene in rainbow trout *Oncorhynchus mykiss* and comparative investigation of the expression and modulation of the paralogues *in vitro* and *in vivo*. *Fish Shellfish Immunol*. (2011) 31:107–17. doi: 10.1016/j.fsi.2011.04.010
71. Maehr T, Costa MM, Vecino JLG, Wadsworth S, Martin SAM, Wang T, Secombes CJ. Transforming growth factor-β1b: a second TGF-β1 paralogue in the rainbow trout (*Oncorhynchus mykiss*) that has a lower constitutive expression but is more responsive to immune stimulation. *Fish Shellfish Immunol*. (2013) 34:420–32. doi: 10.1016/j.fsi.2012.11.011
72. Wang B, Wangkahart E, Secombes CJ, Wang T. Insights into the evolution of the suppressors of cytokine signalling (SOCS) gene family in vertebrates. *Mol Biol Evol*. (2018) doi: 10.1093/molbev/msy230. [Epub ahead of print].
73. Maehr T, Vecino JL, Wadsworth S, Wang T, Secombes CJ. Four CISH paralogues are present in rainbow trout *Oncorhynchus mykiss*: differential expression and modulation during immune responses and development. *Mol Immunol*. (2014) 62:186–98. doi: 10.1016/j.molimm.2014.06.021
74. Villarroel F, Casado A, Vásquez J, Matamala E, Araneda B, Amthauer R, et al. Serum amyloid A: a typical acute-phase reactant in rainbow trout? *Dev Comp Immunol*. (2008) 32: 1160–9. doi: 10.1016/j.dci.2008.03.004
75. Chang CI, Zhang, YA, Zou J, Nie P, Secombes. Two cathelicidin genes are present in both rainbow trout (*Oncorhynchus mykiss*) and Atlantic salmon (*Salmo salar*) Antimicrob. *Antimicrob Agents Chemother*. (2006) 50:185–95. doi: 10.1128/AAC.50.1.185-195.2006
76. Douglas SE, Gallant JW, Liebscher RS, Dacanay A, Tsoi SC. Identification and expression analysis of hepcidin-like antimicrobial peptides in bony fish. *Dev Comp Immunol*. (2003) 27:589–601. doi: 10.1016/S0145-305X(03)00036-3
77. Casadei E, Wang T, Zou J, González Vecino JL, Wadsworth S, Secombes CJ. Characterization of three novel beta-defensin antimicrobial peptides in rainbow trout (*Oncorhynchus mykiss*). *Mol Immunol*. (2009) 46:3358–66. doi: 10.1016/j.molimm.2009.07.018

78. Köbis JM, Rebl A, Kühn C, Korytár T, Köllner B, Goldammer T. Comprehensive and comparative transcription analyses of the complement pathway in rainbow trout. *Fish Shellfish Immunol*. (2015) 42:98–107. doi: 10.1016/j.fsi.2014.10.032
79. Grayfer L, Kerimoglu B, Yaparla A, Hodgkinson JW, Xie J, Belosevic M. Mechanisms of fish macrophage antimicrobial immunity. *Front Immunol*. (2018) 9:1105. doi: 10.3389/fimmu.2018.01105
80. Edholm ES, Rhoo KH, Robert J. Evolutionary aspects of macrophages polarization. *Results Probl Cell Differ*. (2017) 62:3–22. doi: 10.1007/978-3-319-54090-0_1
81. Benedicenti O, Wang T, Wangkahart E, Milne DJ, Holland JW, Collins C, Secombes CJ. Characterisation of arginase paralogues in salmonids and their modulation by immune stimulation/infection. *Fish Shellfish Immunol.* (2017) 61:138–151. doi: 10.1016/j.fsi.2016.12.024
82. Wang, T., Secombes, CJ. The cytokine networks of adaptive immunity in fish. *Fish Shellfish Immunol.* (2013) 35:1703–18. doi: 10.1016/j.fsi.2013.08.030
83. Carambia A, Herkel J. Dietary and metabolic modulators of hepatic immunity. *Semin Immunopathol*. (2018) 40:175–88. doi: 10.1007/s00281-017-0659-4
84. Burdelya LG, Brackett CM, Kojouharov B, Gitlin II, Leonova KI, Gleiberman AS, Aygun-Sunar S, et al. Central role of liver in anticancer and radioprotective activities of Toll-like receptor 5 agonist. *Proc Natl Acad Sci USA*. (2013) 110:E1857–66. doi: 10.1073/pnas.1222805110
85. de Zoete MR, Keestra AM, Wagenaar JA, van Putten JP. Reconstitution of a functional Toll-like receptor 5 binding site in *Campylobacter jejuni* flagellin. *J Biol Chem*. (2010) 285:12149–58 doi: 10.1074/jbc.M109.070227
86. Welch TJ, Verner-Jeffreys DW, Dalsgaard I, Wiklund T, Evenhuis JP, Garcia JA, et al. Independent emergence of *Yersinia ruckeri* biotype 2 in the United States and Europe. *Appl Env Micriobiol*. (2011)77: 3493–9. doi: 10.1128/AEM.02997-10
87. Jiang J, Zhao W, Xiong Q, Wang K, He Y, Wang J, et al. Immune responses of channel catfish following the stimulation of three recombinant flagellins of *Yersinia ruckeri in vitro* and *in vivo*. *Dev Comp Immunol*. (2017) 73:61–71. doi: 10.1016/j.dci.2017.02.015
88. Cui B, Liu X, Fang Y, Zhou P, Zhang Y, Wang Y. Flagellin as a vaccine adjuvant. *Expert Rev Vaccines* (2018) 17:335–49. doi: 10.1080/14760584.2018.1457443

Conflict of Interest Statement: The authors declare that the research was conducted in the absence of any commercial or financial relationships that could be construed as a potential conflict of interest.

Copyright © 2019 Wangkahart, Secombes and Wang. This is an open-access article distributed under the terms of the Creative Commons Attribution License (CC BY). The use, distribution or reproduction in other forums is permitted, provided the original author(s) and the copyright owner(s) are credited and that the original publication in this journal is cited, in accordance with accepted academic practice. No use, distribution or reproduction is permitted which does not comply with these terms.

frontiers in Immunology

REVIEW
published: 25 January 2019
doi: 10.3389/fimmu.2019.00042

Trained Innate Immunity of Fish Is a Viable Approach in Larval Aquaculture

Zuobing Zhang[1]*, *Heng Chi*[2,3]* and *Roy A. Dalmo*[3]*

[1] School of Life Science, Shanxi University, Taiyuan, China, [2] Key Laboratory of Experimental Marine Biology, Institute of Oceanology, Chinese Academy of Sciences, Qingdao, China, [3] Research Group Aquaculture and Environment, Norwegian College of Fishery Science, Faculty of Biosciences, Fisheries and Economy, University of Tromsø—The Arctic University of Norway, Tromsø, Norway

The general understanding has been that only adaptive immunity is capable of immunological memory, but this concept has been challenged in recent years by studies showing that innate immune systems can mount resistance to reinfection—as the innate immune system can adapt its function following an insult. Innate immune training offers an attractive approach in intensive fish larval rearing, especially since the adaptive immune system is not fully developed. Trained innate immunity will potentially favor robust fish in terms of resistance to viral and bacterial diseases. So-called immunostimulants such as ß-glucans have for decades been used both in laboratories and in intensive fish aquaculture. Treatment of fish by ß-glucans (and by other substances with pathogen-associated molecular patterns) often induces activation of non-specific/innate immune mechanisms and induces higher disease resistance. The reported effects of e.g., ß-glucans fit nicely into the concept "trained innate immunity," but the research on fish does not yet include analysis of epigenetic changes that may be a prerequisite for long-lasting trained innate immunity. In this "perspective," we will discuss how in practical terms and based on prior knowledge one can introduce innate immune training in brood stock fish, and their offspring, and whether innate immune training by ß-glucans is a viable approach in larval aquaculture.

Keywords: trained innate immunity, aquaculture, fish, beta-glucan, fish larvae

OPEN ACCESS

Edited by:
Brian Dixon,
University of Waterloo, Canada

Reviewed by:
Katherine Buckley,
Carnegie Mellon University, United States
Stephanie DeWitte-Orr,
Wilfrid Laurier University, Canada

***Correspondence:**
Zuobing Zhang
zbzhang@sxu.edu.cn
Heng Chi
chiheng@qdio.ac.cn;
heng.chi@uit.no
Roy A. Dalmo
roy.dalmo@uit.no

Specialty section:
This article was submitted to Comparative Immunology, a section of the journal Frontiers in Immunology

Received: *09 November 2018*
Accepted: *09 January 2019*
Published: *25 January 2019*

Citation:
Zhang Z, Chi H and Dalmo RA (2019) Trained Innate Immunity of Fish Is a Viable Approach in Larval Aquaculture. Front. Immunol. 10:42. doi: 10.3389/fimmu.2019.00042

INTRODUCTION

ß-glucans are naturally occurring polysaccharides consisting of glucose residues with ß-1, 3→ß1, 4 or/and ß-1, 6→D-glycosidic bonds with various degree of polymerization. They are major structural components of the cell walls of many organisms such as fungi, plants, mushrooms, bacteria, and yeasts. ß-glucans have been reported to possess anti-cancer, pro-inflammatory, and anti-fungal activities when administered to animals. Some reports have even indicated anti-parasitic effects. Stimulation of non-specific defense mechanisms has also been reported in fish (1–4). The terminology typically used to indicate any activation of immune mechanisms is either "priming," "immune induction" "immunostimulation" or "immunomodulation," explaining the outcome of a particular treatment (5). More recently the terminology has more or less shifted and is now called trained immunity, or better—trained innate immunity if the effects from the particular treatment induces non-specific/heterologous disease resistance, it is relatively long-lasting and it

induce epigenetic changes (5, 6). In this perspective, we will discuss how in practical terms and based on prior knowledge one can introduce innate immune training in brood stock fish, and their offspring, and whether innate immune training by ß-glucans is a viable approach in larval aquaculture.

TRAINED INNATE IMMUNITY: CONCEPT AND EXAMPLES

Trained innate immunity can be explained by innate immune defense stimulation that may in turn confer increased non-specific resistance to infection by homologous or heterologous pathogens. Examples have been retrieved from research on plants and invertebrates, where a certain kind of memory from previous insults exists (7). In vertebrate species, several approaches using ligands to pattern recognition receptors (e.g., ß-glucan, muramyl dipeptide, CpG containing oligodeoxynucleotides, flagellin) have suggested that priming of mice by some of these stimulants may facilitate protection against infection by heterologous pathogens (8). An illustrative example is where pretreatment of ß-glucan coated microbeads fully protect mice against an otherwise lethal *Escherichia coli* challenge in mice (9). Other examples are the prophylactic effects from a ß-glucan (laminaran) injection against *Vibrio salmonicida* infection in fish (10) and where Bacillus Calmette Guerin (BCG) vaccination induce T-cell independent non-specific disease protection against infections of e.g., *Candida albicans* and *Schistosoma mansoni* in mice (11, 12). Thus, the term trained innate immunity is a new wrapping of what has been observed and reported decades ago. However, a few more characteristics have since been added to the concept due to more research and the use of modern technologies. These are: T- and B-cell independent process, epigenetic changes together with altered metabolic profile (13). The mechanisms behind priming or training are acknowledged to be functional (re)programming of cells (monocytes, macrophages, NK cells) induced by activation of particular pattern recognition receptors, mainly MAP kinase dependent intracellular signaling, and resulting epigenetic changes (8, 14). It should be noted that there exist other venues where cross-protection occurs. Poly-specific lymphocytes, the Mackaness reaction (chronic infection), and microbiota-mediated protection may all be venues to protective mechanisms, reviewed by Muraille (15). It is commonly acknowledged that B-cell produced antibodies, including natural antibodies, are not involved in trained innate immunity (16). Sea water is extremely rich in microbes (phages, viruses, bacteria), containing molecules that may induce immune activation or tolerance. The fish gut microbiome has been reported to consist of many species of the proteobacterial phylum (17). These are gram-negative bacteria with bacterial lipopolysaccharide (LPS) in their outer membrane, which is known to induce substantial immune activation. An attractive research question is why continuous exposure of high amounts of environmental LPS does not induce hyperactivation of the immune system. This issue may be dependent on the dose, where sensitization occurs by a low-dose LPS, whereas priming with high-dose LPS induces prolonged inhibition of inflammatory cytokine release—dependent on the mTOR (mammalian target of rapamycin) and AMPK (AMP-activated kinase) signaling axes. Such inhibition can be translated as LPS tolerance (8, 18, 19). mTOR is involved in anabolic processes during cell activation, whereas the latter is central in tissue homeostasis and tolerogenic responses. It is not yet clear whether ß-glucans themselves induce tolerance that would be detrimental to their stimulating effects. Moreover, many fish species possess several splicing isoforms of e.g., PPRs where an activation of one of the spliced isoforms of a given pattern recognition receptor (12) might give another outcome (e.g., negative regulation) than expected (20–22).

ß-GLUCANS: NOT ALL ARE ALIKE

Since there are high level of heterogeneities (and impurities) among different commercial preparations of ß-glucans from various sources cautions must be made (23). One type of ß-glucan from one species can be very different with respect to solubility in e.g., PBS/saline and gelling characteristics, compared to another ß-glucan preparation. Zymosan (*Saccharomyces cerevisiae*), the most widely applied and investigated ß-glucan, is composed of ∼50% ß-glucan, 17% mannan, 14% protein, and other substances (24, 25). Zymosan (average 3 μm particles) is extremely aqueous insoluble, but the particles can be dispersed in solutions. Other well-studied biologically active ß-glucans includes laminarin, curdlan, lentinan, scleroglucan, and schizophyllan. In many cases their names are trivial describing their sources; Lentinan from *Lentinula edodes*, scleroglucan from *Sclerotium* sp., and schizophyllan from *Schizophyllum commune* (26). These microbial or fungal ß-glucans possess various degrees of polymerization that dictate, in some instances, a higher order of conformation—they are either linear and unbranched, or branched with single glucose residue—which in turns determines aqueous solubility, gelling characteristics, and often biological activities (27). Many ß-glucans have been reported to possess biological activities, such as induction of disease resistance, in both animals (vertebrates, invertebrates) and plants (4, 28–30).

WHICH ß-GLUCANS INDUCE TRAINED IMMUNITY?

It is suggested that in order to induce trained innate immunity by ß-glucans, several different receptors must be engaged, such as Dectin-1, and dimeric TLR2/6 (31). The simultaneous binding of ß-glucan to two or more different receptors in clusters normally gives a higher response, compared to a single receptor. It is acknowledged that, among ß-glucans, particulate ß-glucans may be the optimal preparation to induce innate immune training, whereas low molecular weight ß-glucans (e.g., laminarin) do not favor a high response (32).

HIGH DIVERSITY OF INNATE RECEPTORS FOR INNATE TRAINING

Teleost fish constitute a highly diverse group of animals, comprising of more than 23,000 different species. Twenty-one different Toll-like receptors (TLRs), together with additional splicing variants (subtypes/isotypes), have thus far been identified in teleost, reviewed by Chang et al. (22) and Nie et al. (33). The number of TLR variants far exceeds that found in mice and human (34). Furthermore, a recent analysis of the Atlantic cod genome and RNAseq analysis revealed that the cod TLR repertoire is extremely diversified, with 43 different TLRs ortologs and paralogs (35). Another example is that of the blue-spotted (*Periophthalmodon schlosseri*) and giant-fin (*Periophthalmus magnuspinnatus*) mudskipper genomes which contain 11 copies of TLR13 (36). Genome duplication events in fishes during evolution has been attributed to the diversity of TLRs, thus differences with respect to the number of TLR loci exist between mammalian species and many fish species (34). The number of TLRs added to other pattern recognition receptors (12) (including splice variants) such as different C-type lectin receptors, NOD-like (nucleotide-binding oligomerization domain-like) receptors (NLRs), RIG-1-like receptors, and scavenger receptors (37), suggests that fish may very well be equipped with innate receptors that may likely be targets for innate immune training. Especially NLRs has been found to be highly expanded as shown in zebrafish, where nearly 400 NLR proteins are encoded in the zebrafish genome (38). The TLRs and NLRs outnumbers RIG-1-like receptors (39) and scavenger receptors (40) in fish, but future genomic analysis may reveal whether there are more copies of the two latter receptor families. The NLRs may likely be involved in gut responses to microbiota, as NOD1/2 are expressed on gut (zebrafish) epithelial cells (41).

One may strongly assume that trained innate immunity also exists in fish, but no definite proof exists—especially with regards to both epigenetic and metabolic changes together with the possibility of rewiring the trained state. Suggestions that trained innate immunity indeed is present in fish are based on experiments using ß-glucans and other immunostimulants *in vitro* and *in vivo*, summarized by Petit and Wiegertjes (4) and Rojo-Cebreros et al. (42).

TRAINED INNATE IMMUNITY IN BROOD STOCK FISH AND FISH LARVAL REARING

Given that it is possible enhance the innate defense of fish through immune training—especially against pathogens—it opens up for several interesting approaches in fish larval rearing. Firstly, brood stock (female and male) fish may be stimulated with PAMP(s) at a low dose (16) inducing increased potential to, not only resist present pathogens, but to also transfer trained innate immunity to offspring (F1 generation). This is in line with a study by Beemelmanns and Roth that suggested the occurrence of maternal and paternal transfer of immune traits. In this study they found that pipefish (*Syngnathus typhle*) offspring expression patterns of immune genes and epigenetic regulation is correlated to parental gene expression patterns (43). Intergenerational (F0F1) transfer of trained innate immunity has been reported for other animal species such as Artemia, oyster, red flour beetle, and humans (44–47). Interestingly transgenerational immune priming beyond F1 generation (F0F2) has also been observed in fish (*S. typhle*) (48).

Besides direct innate immune training of brood stock fish and transfer to F1 (and maybe F2) generations, molecules that are known to induce trained innate immunity may be maternally transferred and taken up by developing oocytes during vitellogenesis (49)—potentially increasing the innate defense of developing embryo/larvae—while the fish embryo or larvae is still in the eggs. The latter do not represent heritable trained traits, merely a direct innate immune stimulation of offspring. In summary, by administering immunostimulants (e.g., certain PAMPs) to brood stock fish one may obtain: (1) Direct maternal and paternal immunostimulation/training, (2) consequently inherited trained innate immunity, and (3) direct

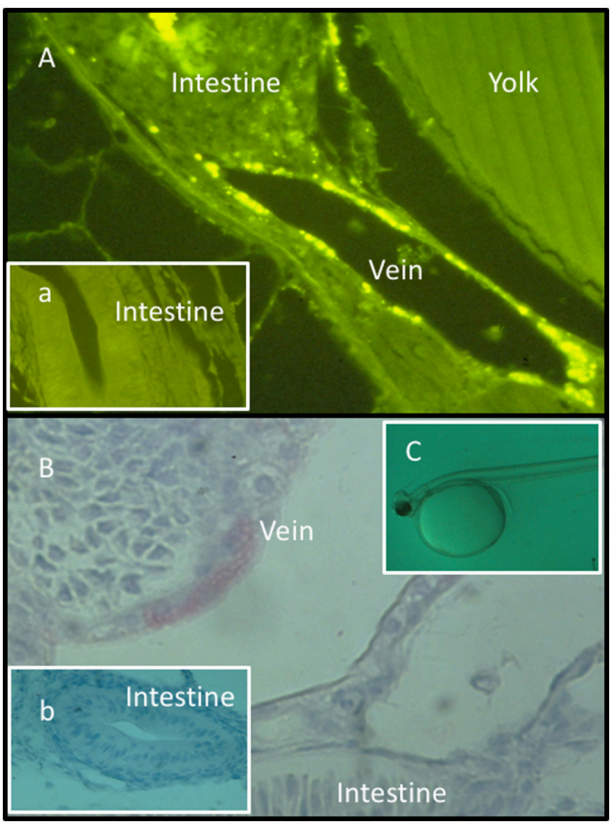


FIGURE 1 | Fluorescence **(A, a)** and light micrographs (immunohistochemistry) **(B, b)** of sections from Atlantic halibut yolk sac larvae **(C)** bath treated with FITC-labeled lipopolysaccharide (FITC-LPS). **(a,b)** Sections obtained from untreated larvae. FITC-LPS was found in endothelial cells in blood veins and in intestinal tissue documenting that yolk sac larvae cells have taken up FITC-LPS after bath treatment. Permission has been granted from Elsevier for **(A)**, where the rabbit anti *A. salmonicida* pabs was characterized and used (52).

immune stimulation and training of developing embryo/larvae (inside egg chorion).

Secondly, substances expected to induce trained innate immunity may be administered directly to newly hatched fragile fish larvae or alevins (before first feeding) simply by bath treatment (50–54) (**Figure 1**).

Thirdly, first feeding represents a milestone during development of fish. After the yolk has more or less been utilized, the fish start feeding on algae, zooplankton, other prey, or simply pelleted formulated fish feed [for overview see Davies (53)] (55). For those fish species that feed on particulate feed, immunostimulants may simply be added to the formulated fish feed—for the purpose to induce innate immune training or immunostimulation (42, 50, 53).

POTENTIAL NEGATIVE EFFECTS OF EARLY TRAINED INNATE IMMUNITY

If the initial stimulation, with purpose to induce innate immune training, otherwise induces hyperimmune responses in the mother/father or offspring it may give unwanted effects (56, 57)—especially in vulnerable offspring that have not fully developed regulatory mechanisms. This issue, or related issues where brood stock fish has been (over)stimulated, has not been addressed yet. An important step will be to optimize the dose and duration for full innate immune training in brood stock fish. Early trained innate immunity may, at a later time point, interfere with subsequent vaccination regime, e.g., in commercial salmonid aquaculture. The fish vaccines often contain different inactivated bacteria emulsified in mineral oil, containing many substances (58) that potentially have effect on innate defense mechanisms. Would the trained characteristics in non-vaccinated individuals be wiped out/rewired or further potentiated? One should also address whether innate trained immunity affects (later) antibody response from vaccination, especially since there is an interplay between innate pattern recognition receptors and acquired immunity (59).

CONCLUSION

Training of innate immunity offers an interesting and attractive approach to increase disease resistance of brood stock fish, newly hatched fish larvae, and first feeding fish. Several TLR receptor ligands may be used to study innate training, assessed by modern technologies such as transcriptomics, epigenetics, proteomics, and metabolomics. In addition, *in vivo* pathogen challenge would be necessary to analyze whether a trained innate immunity has occurred or not.

AUTHOR CONTRIBUTIONS

All authors listed have made a substantial, direct and intellectual contribution to the work, and approved it for publication.

FUNDING

The work was supported by grants from the Research Council of Norway (grants 237315 and 239140), University of Tromsø (UIT The Arctic University of Norway Open Access publication Fund) and Tromsø Research Foundation.

REFERENCES

1. Dalmo RA, Bogwald J. Beta-glucans as conductors of immune symphonies. *Fish Shellfish Immun.* (2008) 25:384–96. doi: 10.1016/j.fsi.2008.04.008
2. Meena DK, Das P, Kumar S, Mandal SC, Prusty AK, Singh SK, et al. Beta-glucan: an ideal immunostimulant in aquaculture (a review). *Fish Physiol Biochem.* (2013) 39:431–57. doi: 10.1007/s10695-012-9710-5
3. Vetvicka V, Vannucci L, Sima P. The effects of beta - glucan on fish immunity. *N Am J Med Sci.* (2013) 5:580–8. doi: 10.4103/1947-2714.120792
4. Petit J, Wiegertjes GF. Long-lived effects of administering beta-glucans: indications for trained immunity in fish. *Dev Comp Immunol.* (2016) 64:93–102. doi: 10.1016/j.dci.2016.03.003
5. Boraschi D, Italiani P. Innate immune memory: time for adopting a correct terminology. *Front Immunol.* (2018) 9:799. doi: 10.3389/fimmu.2018.00799
6. Netea MG, Quintin J, van der Meer JWM. Trained immunity: a memory for innate host defense. *Cell Host Microbe* (2011) 9:355–61. doi: 10.1016/j.chom.2011.04.006
7. Netea MG, van der Meer JWM. Trained immunity: an ancient way of remembering. *Cell Host Microbe* (2017) 21:297–300. doi: 10.1016/j.chom.2017.02.003
8. Ifrim DC, Quintin J, Joosten LAB, Jacobs C, Jansen T, Jacobs L, et al. Trained immunity or tolerance: opposing functional programs induced in human monocytes after engagement of various pattern recognition receptors. *Clin Vaccine Immunol.* (2014) 21:534–45. doi: 10.1128/CVI.00688-13
9. Seljelid R, Rasmussen LT, Larm O, Hoffman J. The protective effect of beta 1-3D-glucan-derivatized plastic beads against *Escherichia coli* infection in mice. *Scand J Immunol.* (1987) 25:55–60. doi: 10.1111/j.1365-3083.1987.tb01046.x
10. Dalmo RA, Martinsen B, Horsberg TE, Ramstad A, Syvertsen C, Seljelid R, et al. Prophylactic effect of beta(1,3)-D-glucan (laminaran) against experimental *Aeromonas salmonicida* and *Vibrio salmonicida* infections. *J Fish Dis.* (1998) 21:459–62. doi: 10.1046/j.1365-2761.1998.00120.x
11. van 't Wout JW, Poell R, van Furth R. The role of BCG/PPD-activated macrophages in resistance against systemic candidiasis in mice. *Scand J Immunol.* (1992) 36:713–9. doi: 10.1111/j.1365-3083.1992.tb03132.x
12. Tribouley J, Tribouley-Duret J, Appriou M. [Effect of Bacillus Callmette Guerin (BCG) on the receptivity of nude mice to *Schistosoma mansoni*]. Influence du bacille de Calmette et Guerin (BCG) sur la receptivite de la Souris nude vis-a-vis de *Schistosoma mansoni*. *C R Seances Soc Biol Fil.* (1978) 172:902–4.
13. Arts RJW, Joosten LAB, Netea MG. The potential role of trained immunity in autoimmune and autoinflammatory disorders. *Front Immunol.* (2018) 9:298. doi: 10.3389/fimmu.2018.00298
14. Lau CM, Adams NM, Geary CD, Weizman OE, Rapp M, Pritykin Y, et al. Epigenetic control of innate and adaptive immune memory. *Nat Immunol.* (2018) 19:963–72. doi: 10.1038/s41590-018-0176-1
15. Muraille E. The unspecific side of acquired immunity against infectious disease: causes and consequences. *Front Microbiol.* (2015) 6:1525. doi: 10.3389/fmicb.2015.01525
16. Rusek P, Wala M, Druszczynska M, Fol M. Infectious agents as stimuli of trained innate immunity. *Int J Mol Sci.* (2018) 19:e456. doi: 10.3390/ijms19020456
17. Egerton S, Culloty S, Whooley J, Stanton C, Ross RP. The gut microbiota of marine fish. *Front Microbiol.* (2018) 9:873. doi: 10.3389/fmicb.2018.00873
18. Bauer M, Weis S, Netea MG, Wetzker R. Remembering pathogen dose: long-term adaptation in innate immunity. *Trends Immunol.* (2018) 39:438–45. doi: 10.1016/j.it.2018.04.001
19. Butcher SK, O'Carroll CE, Wells CA, Carmody RJ. Toll-like receptors drive specific patterns of tolerance and training on restimulation of macrophages. *Front Immunol.* (2018) 9:933. doi: 10.3389/fimmu.2018.00933
20. Lee FFY, Chuang HC, Chen NY, Nagarajan G, Chiou PP. Toll-like receptor 9 alternatively spliced isoform negatively regulates tlr9 signaling in teleost fish. *PLoS ONE* (2015) 10:e0126388. doi: 10.1371/journal.pone.0126388

21. Candel S, Tyrkalska SD, Garcia-Moreno D, Meseguer J, Mulero V. Identification of evolutionarily conserved md1 splice variants that regulate innate immunity through differential induction of NF-?B. *J Immunol.* (2016) 197:1379–88. doi: 10.4049/jimmunol.1502052
22. Chang MX, Zhang J. Alternative Pre-mRNA splicing in mammals and teleost fish: a effective strategy for the regulation of immune responses against pathogen infection. *Int J Mol Sci.* (2017) 18:e1530. doi: 10.3390/ijms18071530
23. Camilli G, Tabouret G, Quintin J. The complexity of fungal beta-glucan in health and disease: effects on the mononuclear phagocyte system. *Front Immunol.* (2018) 9:673. doi: 10.3389/fimmu.2018.00673
24. Vetvicka V, Vetvickova J. Glucans and cancer: comparison of commercially available beta-glucans - Part IV. *Anticancer Res.* (2018) 38:1327–33. doi: 10.21873/anticanres.12355
25. Bacon JSD, Farmer VC, Jones D, Taylor IF. Glucan components of cell wall of bakers yeast (*Saccharomyces cerevisiae*) considered in relation to its ultrastructure. *Biochem J.* (1969) 114:557–67. doi: 10.1042/bj1140557
26. Synytsya A, Novak M. Structural analysis of glucans. *Ann Transl Med.* (2014) 2:17. doi: 10.3978/j.issn.2305-5839.2014.02.07
27. Wang Q, Sheng XJ, Shi AM, Hu H, Yang Y, Liu L, et al. beta-Glucans: relationships between modification, conformation and functional activities. *Molecules* (2017) 22:e257. doi: 10.3390/molecules22020257
28. Fesel PH, Zuccaro A. beta-glucan: Crucial component of the fungal cell wall and elusive MAMP in plants. *Fungal Genet Biol.* (2016) 90:53–60. doi: 10.1016/j.fgb.2015.12.004
29. Soltanian S, Stuyven E, Cox E, Sorgeloos P, Bossier P. Beta-glucans as immunostimulant in vertebrates and invertebrates. *Crit Rev Microbiol.* (2009) 35:109–38. doi: 10.1080/10408410902753746
30. Bashir KMI, Choi J-S. Clinical and physiological perspectives of beta-glucans: the past, present, and future. *Int J Mol Sci.* (2017) 18:e1906. doi: 10.3390/ijms18091906
31. Batbayar S, Lee DH, Kim HW. Immunomodulation of fungal beta-glucan in host defense signaling by dectin-1. *Biomol Ther.* (2012) 20:433–45. doi: 10.4062/biomolther.2012.20.5.433
32. Goodridge HS, Reyes CN, Becker CA, Katsumoto TR, Ma J, Wolf AJ, et al. Activation of the innate immune receptor Dectin-1 upon formation of a 'phagocytic synapse'. *Nature* (2011) 472:471–5. doi: 10.1038/nature10071
33. Nie L, Cai SY, Shao JZ, Chen J. Toll-Like receptors, associated biological roles, and signaling networks in non-mammals. *Front Immunol.* (2018) 9:1523. doi: 10.3389/fimmu.2018.01523
34. Palti Y. Toll-like receptors in bony fish: from genomics to function. *Dev Comp Immunol.* (2011) 35:1263–72. doi: 10.1016/j.dci.2011.03.006
35. Solbakken MH, Torresen OK, Nederbragt AJ, Seppola M, Gregers TF, Jakobsen KS, et al. Evolutionary redesign of the Atlantic cod (*Gadus morhua L.*) Toll-like receptor repertoire by gene losses and expansions. *Sci Rep.* (2016) 6:25211. doi: 10.1038/srep25211
36. You XX, Bian C, Zan QJ, Xu X, Liu X, Chen JM, et al. Mudskipper genomes provide insights into the terrestrial adaptation of amphibious fishes. *Nat Commun.* (2014) 5:5594. doi: 10.1038/ncomms6594
37. Brubaker SW, Bonham KS, Zanoni I, Kagan JC. Innate immune pattern recognition: a cell biological perspective. *Ann Rev Immunol.* (2015) 33:257–90. doi: 10.1146/annurev-immunol-032414-112240
38. Howe K, Schiffer PH, Zielinski J, Wiehe T, Laird GK, Marioni JC, et al. Structure and evolutionary history of a large family of NLR proteins in the zebrafish. *Open Biol.* (2016) 6:160009. doi: 10.1098/rsob.160009
39. Chen SN, Zou PF, Nie P. Retinoic acid-inducible gene I (RIG-I)-like receptors (RLRs) in fish: current knowledge and future perspectives. *Immunology* (2017) 151:16–25. doi: 10.1111/imm.12714
40. Yap NVL, Whelan FJ, Bowdish DME, Golding GB. The evolution of the scavenger receptor cysteine-rich domain of the class A scavenger receptors. *Front Immunol.* (2015) 6:342. doi: 10.3389/fimmu.2015.00342
41. Oehlers SH, Flores MV, Hall CJ, Swift S, Crosier KE, Crosier PS. The inflammatory bowel disease (IBD) susceptibility genes NOD1 and NOD2 have conserved anti-bacterial roles in zebrafish. *Dis Model Mech.* (2011) 4:832–41. doi: 10.1242/dmm.006122
42. Rojo-Cebreros AH, Ibarra-Castro L, Martinez-Brown JM. Immunostimulation and trained immunity in marine fish larvae. *Fish Shellfish Immun.* (2018) 80:15–21. doi: 10.1016/j.fsi.2018.05.044
43. Beemelmanns A, Roth O. Biparental immune priming in the pipefish *Syngnathus typhle*. *Zoology* (2016) 119:262–72. doi: 10.1016/j.zool.2016.06.002
44. Roth O, Joop G, Eggert H, Hilbert J, Daniel J, Schmid-Hempel P, et al. Paternally derived immune priming for offspring in the red flour beetle, Tribolium castaneum. *J Anim Ecol.* (2010) 79:403–13. doi: 10.1111/j.1365-2656.2009.01617.x
45. Hong M, Sandalova E, Low D, Gehring AJ, Fieni S, Amadei B, et al. Trained immunity in newborn infants of HBV-infected mothers. *Nat Commun.* (2015) 6:6588. doi: 10.1038/ncomms7588
46. Norouzitallab P, Baruah K, Biswas P, Vanrompay D, Bossier P. Probing the phenomenon of trained immunity in invertebrates during a transgenerational study, using brine shrimp Artemia as a model system. *Sci Rep.* (2016) 6:21166. doi: 10.1038/srep21166
47. Green TJ, Helbig K, Speck P, Raftos DA. Primed for success: oyster parents treated with poly(I:C) produce offspring with enhanced protection against Ostreid herpesvirus type I infection. *Mol Immunol.* (2016) 78:113–20. doi: 10.1016/j.molimm.2016.09.002
48. Beemelmanns A, Roth O. Grandparental immune priming in the pipefish *Syngnathus typhle*. *BMC Evol Biol.* (2017) 17:44. doi: 10.1186/s12862-017-0885-3
49. Hara A, Hiramatsu N, Fujita T. Vitellogenesis and choriogenesis in fishes. *Fish Sci.* (2016) 82:187–202. doi: 10.1007/s12562-015-0957-5
50. Bricknell I, Dalmo RA. The use of immunostimulants in fish larval aquaculture. *Fish Shellfish Immun.* (2005) 19:457–72. doi: 10.1016/j.fsi.2005.03.008
51. Zhang ZB, Swain T, Bogwald J, Dalmo RA, Kumari J. Bath immunostimulation of rainbow trout (*Oncorhynchus mykiss*) fry induces enhancement of inflammatory cytokine transcripts, while repeated bath induce no changes. *Fish Shellfish Immun.* (2009) 26:677–84. doi: 10.1016/j.fsi.2009.02.014
52. Dalmo RA, Kjerstad AA, Arnesen SM, Tobias PS, Bogwald J. Bath exposure of Atlantic halibut (*Hippoglossus hippoglossus* L.) yolk sac larvae to bacterial lipopolysaccharide (LPS): absorption and distribution of the LPS and effect on fish survival. *Fish Shellfish Immun.* (2000) 10:107–28. doi: 10.1006/fsim.1999.0231
53. Magnadottir B, Gudmundsdottir BK, Lange S, Steinarsson A, Oddgeirsson M, Bowden T, et al. Immunostimulation of larvae and juveniles of cod, *Gadus morhua* L. *J Fish Dis.* (2006) 29:147–55. doi: 10.1111/j.1365-2761.2006.00701.x
54. Oyarbide U, Rainieri S, Pardo MA. Zebrafish (*Danio rerio*) larvae as a system to test the efficacy of polysaccharides as immunostimulants. *Zebrafish* (2012) 9:74–84. doi: 10.1089/zeb.2011.0724
55. Davis DA. *Feed and Feeding Practices in Aquaculture*. Boston, MA: Elsevier (2015).
56. Levy O, Wynn JL. A prime time for trained immunity: innate immune memory in newborns and infants. *Neonatology* (2014) 105:136–41. doi: 10.1159/000356035
57. Morelli SS, Mandal M, Goldsmith LT, Kashani BN, Ponzio NM. The maternal immune system during pregnancy and its influence on fetal development. *Res Rep Biol.* (2015) 6:171–89. doi: 10.2147/RRB.S80652
58. Savva A, Roger T. Targeting toll-like receptors: promising therapeutic strategies for the management of sepsis-associated pathology and infectious diseases. *Front Immunol.* (2013) 4:387. doi: 10.3389/fimmu.2013.00387
59. Akira S, Takeda K, Kaisho T. Toll-like receptors: critical proteins linking innate and acquired immunity. *Nat Immunol.* (2001) 2:675–80. doi: 10.1038/90609

Conflict of Interest Statement: The authors declare that the research was conducted in the absence of any commercial or financial relationships that could be construed as a potential conflict of interest.

Copyright © 2019 Zhang, Chi and Dalmo. This is an open-access article distributed under the terms of the Creative Commons Attribution License (CC BY). The use, distribution or reproduction in other forums is permitted, provided the original author(s) and the copyright owner(s) are credited and that the original publication in this journal is cited, in accordance with accepted academic practice. No use, distribution or reproduction is permitted which does not comply with these terms.

frontiers in Immunology

ORIGINAL RESEARCH
published: 29 January 2019
doi: 10.3389/fimmu.2019.00037

Profiling the Atlantic Salmon IgM$^+$ B Cell Surface Proteome: Novel Information on Teleost Fish B Cell Protein Repertoire and Identification of Potential B Cell Markers

Ma. Michelle D. Peñaranda[1]*, *Ingvill Jensen*[1], *Linn G. Tollersrud*[1], *Jack-Ansgar Bruun*[2] *and Jorunn B. Jørgensen*[1]

[1] *The Norwegian College of Fishery Science, Faculty of Biosciences, Fisheries and Economics, UiT The Arctic University of Norway, Tromsø, Norway,* [2] *Tromsø University Proteomics Platform, Institute of Medical Biology, UiT The Arctic University of Norway, Tromsø, Norway*

OPEN ACCESS

Edited by:
Hetron Mweemba Munang'andu, Norwegian University of Life Sciences, Norway

Reviewed by:
Yong-An Zhang, Huazhong Agricultural University, China
Aleksei Krasnov, Nofima, Norway

***Correspondence:**
Ma. Michelle D. Peñaranda
michelle.penaranda@uit.no

Specialty section:
This article was submitted to Comparative Immunology, a section of the journal Frontiers in Immunology

Received: *31 October 2018*
Accepted: *08 January 2019*
Published: *29 January 2019*

Citation:
Peñaranda MMD, Jensen I, Tollersrud LG, Bruun J-A and Jørgensen JB (2019) Profiling the Atlantic Salmon IgM$^+$ B Cell Surface Proteome: Novel Information on Teleost Fish B Cell Protein Repertoire and Identification of Potential B Cell Markers. Front. Immunol. 10:37. doi: 10.3389/fimmu.2019.00037

Fish immunology research is at a pivotal point with the increasing availability of functional immunoassays and major advances in *omics* approaches. However, studies on fish B cells and their distinct subsets remain a challenge due to the limited availability of differentially expressed surface markers. To address this constraint, cell surface proteome of Atlantic salmon IgM$^+$ B cells were analyzed by mass spectrometry and compared to surface proteins detected from two adherent salmon head kidney cell lines, ASK and SSP-9. Out of 21 cluster of differentiation (CD) molecules identified on salmon IgM$^+$ B cells, CD22 and CD79A were shortlisted as potential markers based on the reported B cell-specific surface expression of their mammalian homologs. Subsequent RT-qPCR analyses of flow cytometry-sorted subpopulations from head kidney leukocytes confirmed that both *cd22* and *cd79a* genes were highly expressed in IgM$^+$ lymphoid cells but were observed in barely detectable levels in IgM$^-$ non-lymphoid suspension and adherent cells. Similarly, significantly high *cd22* and *cd79a* mRNA levels were observed in IgM$^+$ or IgT$^+$ lymphoid cells from the spleen and peritoneal cavity, but not in their corresponding IgM$^-$ IgT$^-$ non-lymphoid fractions. This suggests that the B cell restrictive expression of CD22 and CD79A extend down to the transcription level, which was consistent across different lymphoid compartments and immunoglobulin isotypes, thus strongly supporting the potential of CD22 and CD79A as pan-B cell markers for salmon. In addition, this study provides novel information on the salmon B cell surface protein repertoire, as well as insights on B cell evolution. Further investigation of the identified salmon CD molecules, including development of immunological tools for detection, will help advance our understanding of the dynamics of salmon B cell responses such as during infection, vaccination, or immunostimulation.

Keywords: B cells, cell surface markers, teleost fish, salmon, CD22, CD79A, IgM, proteomics

INTRODUCTION

The sustainability of aquaculture is constantly being challenged by the occurrence and re-occurrence of infectious diseases (1). Fish vaccination has become the main prophylactic strategy against these economically-devastating pathogens. However, unlike many bacterial vaccines that are highly protective, most of the available vaccines against viral pathogens in salmon only provide suboptimal protection (2). It is not clear why the elicited immune responses of fish virus vaccines are not efficient in providing protection against subsequent infection. Consequently, an important question is: What set of host responses constitute protective immunity in salmon? Critical to this host response are the B cells with diverse functional properties that encompass both the innate and adaptive arms of the immune system, including antigen presentation (3), phagocytosis (4), production of natural (5) and antigen-specific antibodies (Abs) (6, 7), and the generation of immunological memory [reviewed in (8)].

Different lineages and subsets of B cells exist, each exhibiting specific phenotypic characteristics that respond differentially to TLR ligands, pathogens, and/or immunogens. In mammals, four subsets that belong either to the B-1 or B-2 lineages have been clearly defined. B-2 cells consist of two subpopulations: the more conventional follicular (FO) B cells that constitute the major subset in the spleen and trigger the formation of germinal centers and the subsequent production of plasmablasts, plasma cells, and memory B cells with high affinity Ag-binding capacities upon activation of T cell dependent (TD) antigens [reviewed in (9)]; and the marginal zone (MZ) B cells that integrate classical innate and adaptive signaling pathways to mount rapid antibody responses, particularly to blood-borne pathogens [reviewed in (10)]. Similar to MZ B cells, B-1 cells, which can be subdivided further into B1a and B1b based on their CD5 surface expression, have important innate functions such as phagocytosis and production of polyreactive natural Abs in a T cell independent (TI) manner (11, 12). The B-1 cells are predominantly located in the peritoneal cavity (13), but are also present in the spleen and other lymphoid organs at very low levels. While initially thought to lack memory B cell generation, recent data have shown that these innate-like B cells also generate memory B cells during TI immune responses [reviewed in (14–16)].

As the first vertebrate group that possesses all elements of adaptive immunity, teleost fish are able to execute immune functions comparable to that of mammals. Although clear differences exist between the structure and organization of the teleost and mammalian immune systems, functional equivalent lymphoid compartments have been reported [reviewed in (17, 18)]. Analogous to the mammalian bone marrow (BM), the teleost head kidney (HK) serves as both the major hematopoietic tissue and reservoir for long-lived plasma cells (6). In the absence of lymph nodes, teleost spleen constitutes as the main secondary lymphoid organ, where the majority of naïve B cells mature and circulate for continuous immune surveillance. In addition to the systemic lymphoid compartments, teleost peritoneal cavity also houses B cells whose development and migration pathways remain largely unexplored (19). In contrast to mammals, however, teleosts lack follicular structures and do not form distinguishable germinal centers (20). Little is still also known about the characteristics of teleost memory B cells but it appears to have a relatively low proliferation potential (6). Moreover, their systemic Ab responses rely on unswitched low-affinity IgM responses (21).

Three classes of immunoglobulins (Igs) have been identified in teleosts: IgM, IgD, and IgT (or IgZ in some species), with IgM^+ being the predominant surface Ig isotype (22). IgD is usually co-expressed on the surface of teleost IgM^+ B cells, although single positive IgM^+ or IgD^+ B cells (23) also exist. IgT^+ only B cells comprise a separate lineage of fish B cells that appears to have a main role in mucosal immunity (24). Morphological and functional studies suggest that teleost B cells resemble mammalian B1 cells more than B2 cells (25, 26). In fact, it is hypothesized that mammalian innate-like B cells, characterized by high surface IgM expression (27), evolved from fish IgM^+ B cells (18), with the B2 lineage emerging later as a more efficient subset that gradually acquired a dominant role in the mammalian adaptive immunity. Fish B cells exhibit both innate and adaptive immune functions (6), but whether these functions are performed by distinct B cell subsets or not is unknown. Specifically, which B cell subpopulation/s and/or lineages play an important role in protection against infection and/or immunity following vaccination are still open questions in fish immunology.

Cluster of differentiation (CD) is a system used for identifying cell surface markers for various leukocyte subpopulations, including B cells. At present, at least 371 CD proteins have been reported in mammals (28)—making immunophenotyping a rather trivial task. In contrast to the mammalian system where different lineages and subtypes of B cells can be identified and sorted with greater clarity through commercially available marker Abs, studying the dynamics of fish B cell responses has been challenging due to lack of pan and subset-specific markers. For Atlantic salmon, in particular, B cells are currently sorted from the total leukocyte population using surface Igs as sole markers, typically via the predominant IgM isotype (22, 29). While this approach has been extremely useful, the binding of Abs to surface Igs could trigger unwanted activation of the BCR, which may interfere with downstream assays. In addition, since the status of surface Ig expression of salmon B cells at various stages of differentiation (i.e., putative naïve B cells, plasmablasts, plasma cells, or memory B cells) is largely unknown, some of these subsets may not be detected during sorting and hence, will be excluded from further analysis.

To address this current limitation, we aimed to identify CD molecules than can be potentially used as pan- or subset-specific B cell markers and, in turn, facilitate molecular, and functional investigations of the heterogeneous salmon B cell population. Additionally, we aimed to profile the salmon B cell surface proteome in order to have a better understanding of the phenotypic characteristics of teleost IgM^+ B cells.

MATERIALS AND METHODS

Experimental Fish

Healthy Atlantic salmon (*Salmo salar* L.) QTL fish strain Aquagen standard (Aquagen, Kyrksæterøra, Norway) were obtained from the Tromsø Aquaculture Research Station (Tromsø, Norway). Fish were kept at 10°C in tanks supplied with running filtered water, natural light and fed on commercial dry feeds (Skretting, Stavanger, Norway). Estimated weight of fish used for isolation of peripheral blood leukocytes (PBL) and subsequent sorting of IgM^+ B cells for proteomics analyses was 700–900 g. Head kidney leukocytes (HKL) were collected separately from the same batch of fish. Peritoneal cavity leukocytes (PeL) and splenocytes (SpL) were collected simultaneously from another batch of smaller fish (estimated mean weight: ∼60 g).

Cell Culture

Atlantic Salmon Kidney (ASK) cells (30) and *Salmo salar* pronephros 9 (SSP-9) cells (31), derived from the major hematopietic tissue of Atlantic salmon, were grown as monolayers at 20°C in Leibovitz (L-15) medium (Gibco, Life Technologies). ASK cell culture medium was supplemented with P/S (100 units/mL penicillin, 100 μg/mL streptomycin) and 12% fetal bovine serum (FBS), while SSP-9 cell culture medium was supplemented with 50 μg/mL gentamycin and 8% FBS. Five T-75 flasks were seeded with ASK or SSP-9 cells at a density of $\sim 2 \times 10^6$ cells per flask and collected after 72 h at 90% confluence for subsequent cell surface protein isolation.

Tissue Collection and Leukocyte Isolation

Blood was extracted from the caudal vein of Atlantic salmon using a vacutainer with 68 I.U. sodium heparin (Becton Dickinson) and immediately transferred into transport medium (L-15 with P/S, 2% FBS, and 20 IE/mL heparin). Spleen and HK were aseptically collected into transport medium after ensuring that all blood was drained from fish tissues. Cells from salmon peritoneal cavity were obtained by lavage and immediately stored in transport medium.

Leukocyte isolations (PBL, HKL, SpL, or PeL) were performed on Percoll gradients as described previously (32). Blood suspension was placed directly onto 54% Percoll (GE Healthcare) and centrifuged at 400 × g for 40 min at 4°C. Spleen and HK were homogenized on 100-μm cell strainers (Falcon), loaded onto 25/54% discontinuous Percoll gradients, and centrifuged as above. Similarly, peritoneal cavity cells were loaded onto 25/54% discontinuous Percoll gradient for PeL isolation. Leukocytes at the interface were collected and washed twice in L-15 with P/S before further use.

For stimulation with lipopolysaccharide (LPS), freshly isolated PBLs were seeded in two T25 flasks (Nunclon Delta Surface ThermoFisher Scientific, 6.25×10^6 cells/flask). One flask was treated with 50 μg/mL LPS (purified by Phenol extraction from *Escherichia coli* O111:B4, Sigma-Aldrich) diluted in Dulbecco's Phosphate Buffered Saline (DPBS; Sigma-Aldrich), while control group received only DPBS. Cells were incubated at 14°C for 72 h before staining, sorting, and surface protein isolation as detailed below.

Cell Staining and FACS Sorting

Total leukocytes were centrifuged at 500 × g, resuspended in PBS^+ (Dulbecco PBS with 1% BSA, filter-sterilized), and stained with anti-salmon IgM (IgF1-18) (1:200 dilution) and/or anti-trout IgT (2 μg/mL) monoclonal antibodies (mAbs) for 30 min. These mAbs were generously provided by Dr. Karsten Skjødt and Prof. Oriol Sunyer, respectively. Salmon anti-IgM have been shown to recognize both IgM-A and -B isotypes of Atlantic salmon (29), while trout α-IgT has been previously validated for cross-specificity with Atlantic salmon IgT (22). After two washing steps, leukocytes were incubated with isotype specific secondary Abs: IgG1-RPE (1:400 dilution) and IgG2a-APC (1:400 dilution), respectively, and viability dye FVD780 (1 μL/mL; eBioscience) in PBS^+ for 20 min. All staining and centrifugation steps were done at 4°C.

Stained leukocytes were resuspended in PBS^+ at 5.0×10^7 cells/mL for sorting using the BD FACS Aria III flow cytometer (BD Biosciences). Dead cells ($FVD780^+$) and doublets (SSC-A vs. SSC-H) were excluded from the population. Remaining cells were sorted on the basis of their forward scatter (FSC) and side scatter (SSC) profiles, and then on their IgM^+ (RPE fluorescence emission) and/or IgT^+ (APC fluorescence emission) surface expression. FSC^{low} SSC^{low} subpopulation that excludes granulocytes and myeloid cells was designated lymphoid gate. Cells outside this gate were considered "non-lymphoid" (nL). PBLs with surface IgM expression within the lymphoid gate (PBL L IgM^+, **Figure 1A**) were collected in cell culture media and used as samples for surface protein isolation by biotinylation enrichment method.

For the validation of B-cell restrictive expression of candidate pan-B cell markers at the mRNA level, sorted HKL, SpL, and PeL subpopulations were used for RT-qPCR assays. Leukocytes were collected in culture either as suspension (SC) and adherent (AC) cells and stained separately as described above, and then sorted by FACS based on their FSC/SSC gating profile: lymphoid (L) vs. non-lymphoid (cells outside the lymphoid gating, nL) and their IgM and/or IgT surface expression (IgM^+ vs. IgM^-, IgT^+ vs. IgT^-). For HKLs, 4 subpopulations were obtained: SC within the lymphoid gate that was either IgM^+ (HKL SC-L IgM^+) or IgM^- (HKL SC-L IgM^-); non-lymphoid SC that was IgM^- (HKL SC-nL IgM^-); and non-lymphoid AC that was IgM^- (HKL AC-nL IgM^-) (**Figure 2A**). SpLs, which were mostly suspension cells, were sorted as lymphoid cells with either IgM^+ (SpL L IgM^+); IgT^+ (SpL L IgT^+), or IgM^-IgT^- (SpL L IgM^-IgT^-) surface expression; and non-lymphoid cells without IgM and IgT surface expression (SpL nL IgM^-IgT^-) (**Figure 3A**). Finally, suspension cells from PeLs were sorted as lymphoid cells expressing either IgM (PeL L IgM^+) or IgT (PeL L IgT^+) on their surface; and non-lymphoid cells without IgM and IgT surface expression (PeL nL IgM^-IgT^-) (**Figure 4A**). These HKL, SpL, and PeL subsets were sorted directly on RNAProtect Cell Reagent (Qiagen) and stored at −80°C until RNA extraction.

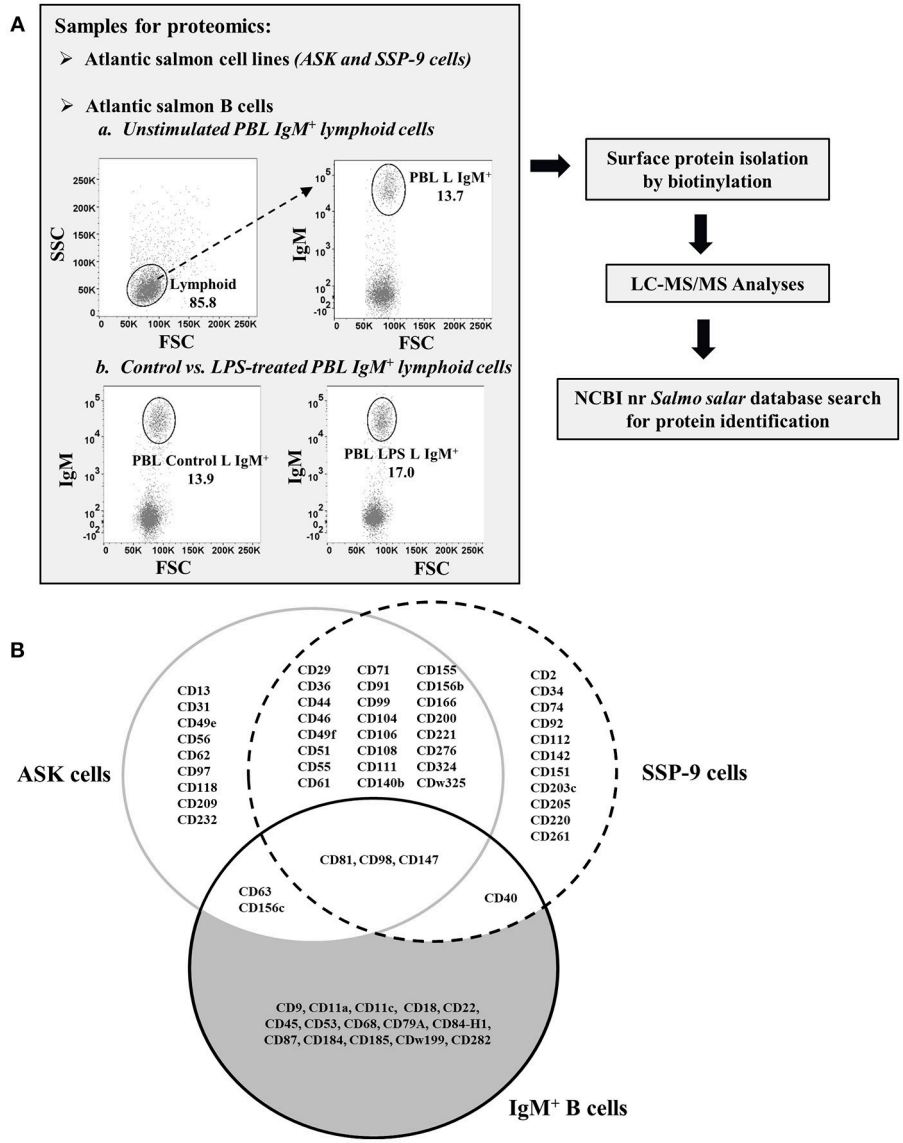


FIGURE 1 | Isolation and identification of CD molecules on surface of Atlantic salmon B cells and head kidney cell lines. **(A)** Schematic diagram of proteomics workflow performed in the study. **(B)** Venn diagram comparing the CD molecules detected on cell surface of sorted IgM$^+$ PBLs vs. head kidney cell lines, ASK and SSP-9, of Atlantic salmon.

Cell Surface Protein Isolation

Cell surface proteins from Atlantic salmon cell lines and IgM$^+$ PBLs were isolated using the Pierce® Cell Surface Protein Isolation Kit (Thermo Scientific) according to the manufacturer's protocol. ASK and SSP-9 monolayers ($\sim 4 \times 10^7$ cells) were quickly washed twice with ice-cold phosphate buffered saline (PBS) followed by incubation with 0.25 mg/mL Sulfo-NHS-SS-Biotin in ice-cold PBS (10 mL biotin solution per flask) on a rocking platform (100 rpm) for 30 min at 4°C. The biotinylation reaction was quenched by adding 500 μL of the provided Quenching Solution. Cells were harvested by gentle scraping, pooled, rinsed with Tris Buffered Saline (TBS), and lysed using the provided Lysis Buffer with Protease Inhibitor Cocktail (Halt™ ThermoFisher Scientific). Cells were sonicated on ice at low power using five 1 s bursts and then incubated for 30 min on ice with intermittent vortexing. The lysates were centrifuged at 10,000 × *g* for 2 min at 4°C to remove cell remnants and the resulting clarified supernatant was added to 500 μL of NeutrAvidin Agarose slurry. Biotinylated proteins were allowed to bind to the NeutrAvidin by incubating for 1 h at room temperature (RT) in the closed column with end-over-end mixing on an orbital rotator. Unbound proteins were removed by centrifugation of the column at 1,000 × *g* for 1 min followed by repetitive washing using the provided Wash Buffer with protease inhibitor. Finally, the captured surface proteins were eluted from the biotin-NeutrAvidin Agarose by incubation with

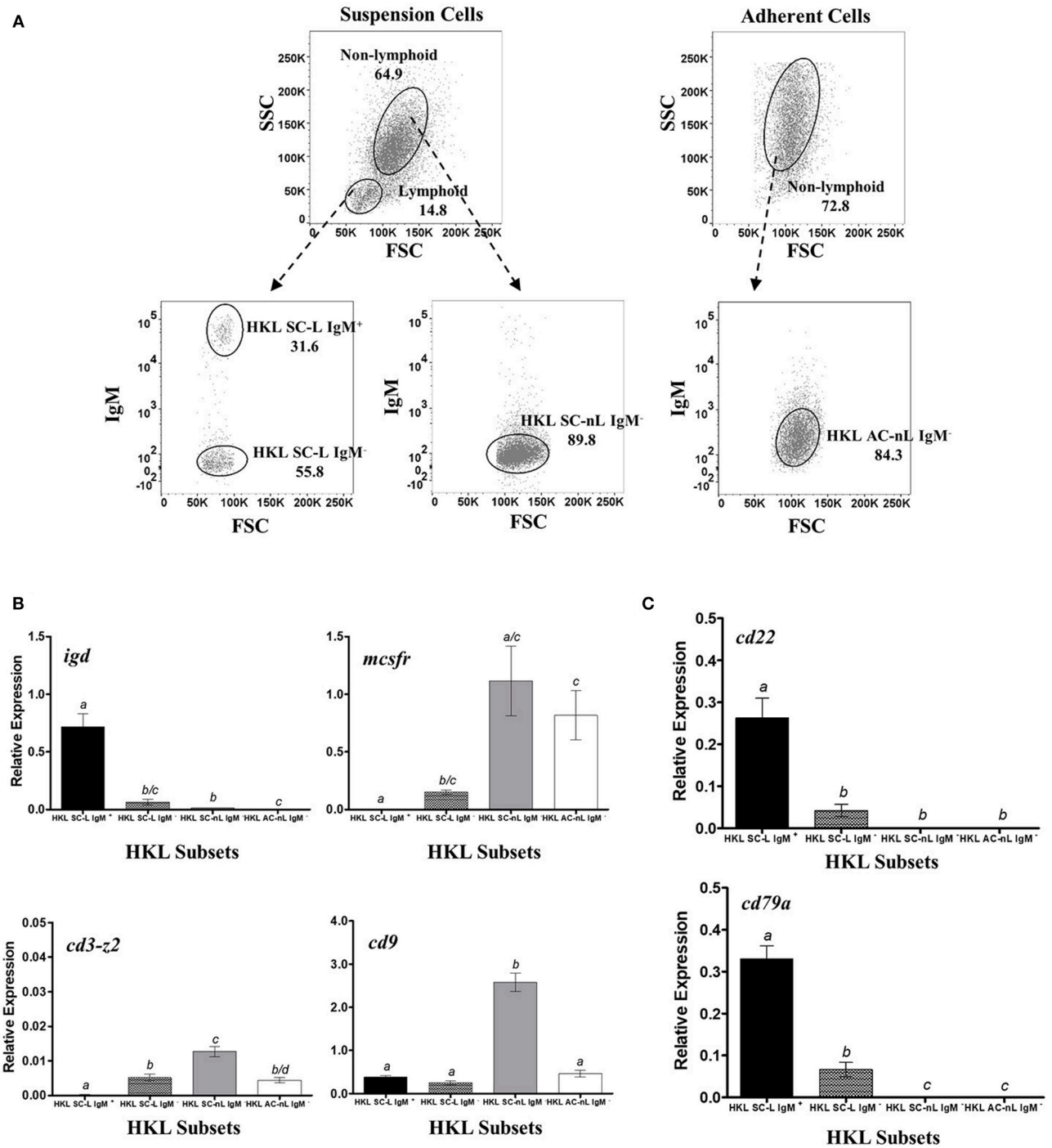


FIGURE 2 | Restrictive gene expression of candidate pan-B cell markers in leukocytes from head kidney, a primary lymphoid organ of salmon. Suspension and adherent head kidney leukocytes (HKLs) were collected separately after 72 h in culture and subsequently sorted by flow cytometry based on cell size and granularity (FSC vs. SSC) and then surface IgM expression. Representative dot plot of the HKL subpopulations are shown in **(A)** with mean percentage of each fraction indicated in the graph. To ensure purity and quality of the sorted HKL subpopulations, expression of several marker genes: *igd* (B cell subset), *mcsfr* (macrophage), *cd3-z2* (T cells), and *cd9* (broad expression) were examined by RT-qPCR assay **(B)**. Upon validation of sorting protocol, gene expression of *cd22* and *cd79a* genes were subsequently determined **(C)**. Each bar represents mean relative expression data from 3 to 4 fish ± SEM. Means with different letters are significantly different (two-tailed *t*-test with Welch's correction, $p < 0.05$).

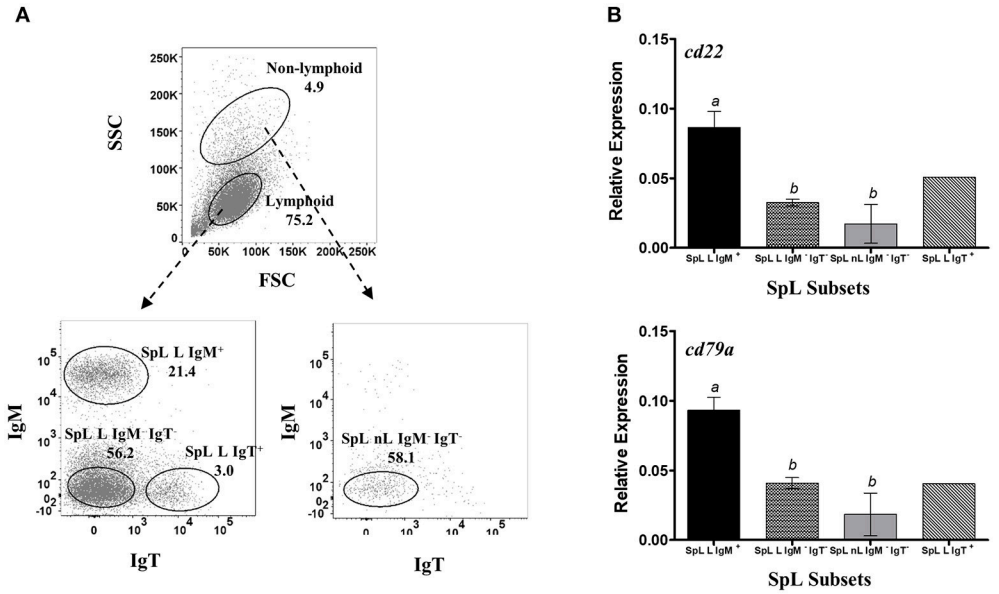


FIGURE 3 | Restrictive gene expression of candidate pan-B cell markers in leukocytes from spleen, a secondary lymphoid organ of salmon. Freshly isolated splenocytes were sorted based on size and granularity (FSC vs. SSC) and then surface expression of IgM or IgT. Representative dot plot of the SpL subpopulations are shown in **(A)** with mean percentage of each fraction indicated in the graph. Cells within the lymphoid gate were sorted into IgM^+, IgT^+, or IgM^- IgT^- subsets (SpL L IgM^+, SpL L IgT^+, and SpL L IgM^- IgT^-, respectively). IgM^- IgT^- cells outside the lymphocyte gate (SpL nL IgM^- IgT) was also collected. Expression of *cd22* and *cd79a* genes were subsequently determined in the different splenocyte subpopulations **(B)**. Each bar represents mean relative expression data from three pooled samples (five fish per pooled sample) ± SEM. Means with different letters are significantly different (two-tailed *t*-test with Welch's correction, $p < 0.05$). Due to very low cell frequency, sorted IgT data was obtained from a pool of 15 fish.

400 µL SDS-PAGE Sample Buffer (62.5 mM Tris-HCl pH 6.8, 1% SDS, 10% glycerol) containing 50 mM dithiothreitol (DTT) for 1 h at RT on an orbital rotator. The eluted proteins, representing the cell surface proteins, were collected by column centrifugation at 1,000 × *g* for 2 min.

For surface protein isolation in FACS-sorted IgM^+ PBLs, cell suspension was centrifuged at 500 × g for 5 min at 4°C, washed twice with 3 mL ice-cold PBS to remove residual FBS, and then resuspended in 0.5 mL ice-cold PBS prior to biotinylation (1×10^6 IgM^+ cells/mL biotin solution) as described above.

To maximize the quantity of surface proteins for subsequent mass-spectrometry analysis, eluted proteins were concentrated using the Pierce™ Protein Concentrator PES 3K MWCO (ThermoFisher Scientific) following the manufacturer's protocol.

Mass Spectrometry Analyses

Surface proteins isolated from the ASK and SSP-9 cell lines, naïve IgM^+ PBLs, and control vs. LPS-stimulated IgM^+ PBLs were subjected to proteomics analyses. Concentrated surface protein samples were directly lysed in 1× NuPAGE LDS sample buffer (ThermoFisher Scientific), heated at 70°C for 10 min, and then fractionated by SDS-PAGE for 5 min at 200 V followed by Coomassie blue staining (SimplyBlue SafeStain; Thermo Fisher Scientific). Protein bands were cut and subjected to in-gel trypsin digestion before analysis by liquid chromatography-tandem mass spectrometry (LC-MS/MS).

Gel slices were subjected to in-gel reduction, alkylation, and protease digestion with 6 ng/µl trypsin (V5111; Promega) (33). OMIX C18 tips (Varian, Inc., Palo Alto, CA, USA) were used for sample cleanup and concentration. Peptide mixtures containing 0.1% formic acid were loaded onto a Thermo Fisher Scientific EASY-nLC 1,000 system and EASY-spray column (C18; 2 µm; 100 Å; 50 µm; 50 cm). Peptides were fractionated using a 2–100% acetonitrile gradient in 0.1% formic acid over 50 min at a flow rate of 250 nl/min. The separated peptides were analyzed using a ThermoFisher Scientific Q-Exactive mass spectrometer.

Raw files from the QExactive were analyzed using the Proteome Discoverer 2.2 software (Thermo Fisher). The fragmentation spectra was searched against the NCBI non-redundant (nr) *Salmo salar* 2017_1 database using an in-house Mascot server (Matrix Sciences, UK). Peptide mass tolerances used in the search were 10 ppm, and fragment mass tolerance was 0.02 Da. Peptide ions were filtered using a false discovery rate (FDR) set to 5 % for peptide identifications.

Relative protein quantitations were done using precursor ion intensities in Proteome Discoverer 2.2. To determine the relative protein amount in each sample, Exponentially Modified Protein Abundance Index (emPAI) values were extracted from mascot search results.

RNA Isolation and cDNA Synthesis

Total RNA from sorted cells was extracted using either the RNeasy® Mini (≥500,000 cells) or Micro (< 500,000 cells) Kits (Qiagen), with in-column DNAse I treatment (Qiagen) according to the manufacturer's protocol. For sorted HKL, SpL,

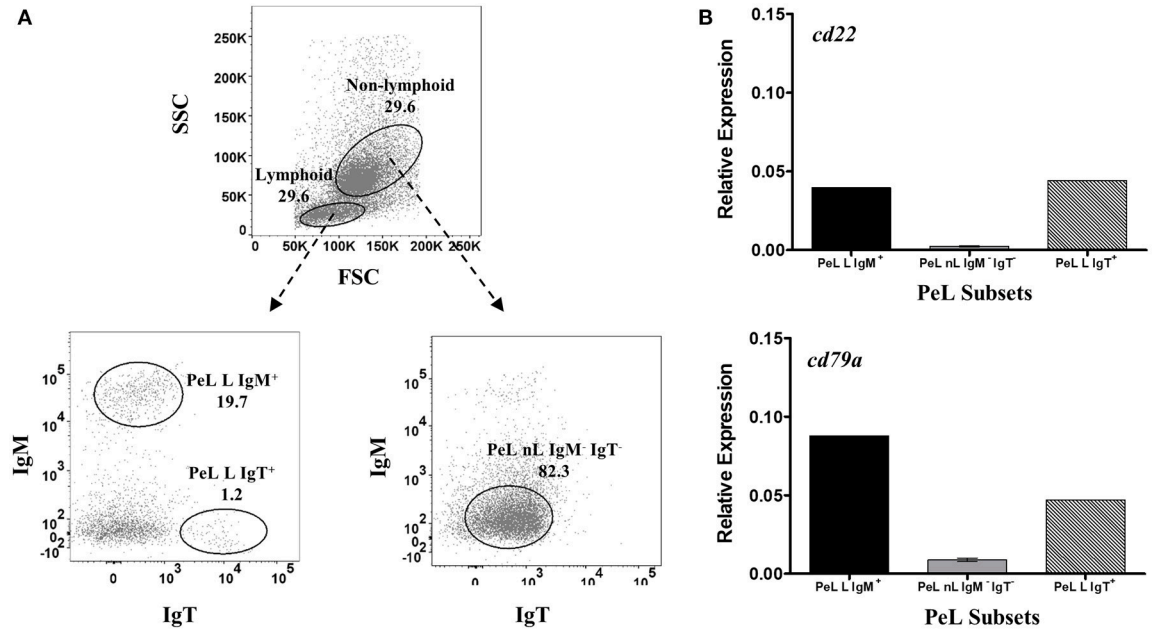


FIGURE 4 | Restrictive gene expression of candidate pan-B cell markers in peritoneal cavity leukocytes of salmon. Freshly isolated peritoneal leukocytes were sorted based on size and granularity (FSC vs. SSC) and then surface expression of IgM or IgT. Representative dot plot of the PeL subpopulations are shown in **(A)** with mean percentage of each fraction indicated in the graph. PeL subsets included IgM^+ or IgT^+ cells within the lymphoid gate (PeL L IgM^+ and PeL L IgT^+, respectively) and IgM^- IgT^- cells within the non-lymphoid gate (PeL nL IgM^- IgT^-). Expression of *cd22* and *cd79a* genes were investigated in peritoneal leukocyte subpopulations **(B)**. Due to low cell frequency, PeL L IgM^+ and PeL L IgT^+ bars represent the relative expression data from pooled samples of 15 fish. Relative expression data for PeL nL IgM^- IgT^- was obtained from the mean of 3 pooled samples (5 fish per pooled sample) ± SEM.

and PeL subsets, an extra centrifugation step at 5,000 × g for 10 min was performed to remove the RNAProtect Cell Reagent before proceeding to RNA extraction of the cell pellet. RNA yield and purity were determined using Nanodrop ND-1,000 Spectrophotometer (Nanodrop Tec. Wilmington, DA, USA) and stored at −80°C. Isolated RNA (75–150 ng) was reverse transcribed into cDNAs in 20 μl reaction volumes using the QuantiTect Reverse Transription Kit (Qiagen) following the manufacturer's protocol. Resulting cDNA was diluted 1:5 and stored at −20°C until further use.

Gene Expression Analyses

Expression levels of RNA transcripts of selected genes were analyzed by RT-qPCR on an ABI Prism 7500 FAST Cycler (Applied Biosystems). cDNAs from sorted HKL subpopulations (2.5 ng total cDNA input) was used per qPCR reaction (20 μL final volume) using the Fast SYBR® Green Master Mix (Applied Biosystems). For SpL and PeL subsets, total cDNA input was 1.5 ng. Information for all primers used is listed in **Table 1**. The efficiency of the amplification was determined for each primer pair using serial 2-fold dilutions of pooled cDNA, and only primer pairs with efficiencies between 1.90 and 2.10 were used. Each sample was measured in duplicate under the following conditions: 95°C for 20 s followed by 40 cycles of 95°C for 3 s and 60°C for 30 s.

The expression of individual genes was normalized to that of Atlantic salmon elongation factor 1αβ (EF1αβ) and presented as relative expression using the $2^{-\Delta Ct}$ method, where ΔCt is determined by subtracting the EF-1α value from the target Ct as described previously (35, 36). Negative controls with no template were included in all experiments. A melting curve for each PCR was determined by reading fluorescence every degree between 60 and 95°C to ensure only a single product had been amplified.

Statistical analyses of RT-qPCR data were performed in GraphPad Prism 5.04 using a two-tailed student *t*-test with Welch's correction when the *F* test indicated that the variances of both groups differed significantly. The differences between the mean values were considered significant when $p \leq 0.05$.

RESULTS

Our mass spectrometry approach was able to identify a combined dataset of 3,140 proteins from our surface protein-enriched salmon B cell and/or HK cell line samples (full list of identified proteins is available at https://doi.org/10.18710/JU3DWE), of which 21% were deemed to be membrane proteins by GO-annotation or transmembrane predictions. This percentage, however, may have been underestimated due to incomplete annotation in some Atlantic salmon proteins. We subsequently focused on surface protein orthologs that were previously reported as part of the CD molecules in mice and/or humans.

TABLE 1 | Primers used for SYBR green qPCR assays.

Genes	Accession no.	Oligo name	Sequence (5′-3′)	Product size (bp)	Efficiency
ef1αβ	NM_001123629.1	Fwd	CCCCTCCAGGACGTTTACAAA	57	1.97
		Rev	CACACGGCCCACAGGTACA		
igd	XM_014203123.1[a]	Fwd	CCAGGTCCGAGTGGGATCA	136	1.92
		Rev	TGGAGCAGGGTTGCTGTTG		
mcsfr	NM_001171807.1	Fwd	CACCAGTAACCCTAACCACTTC	97	2.00
		Rev	GACCTGCTTGTCCTGCATTA		
cd3-z2	NM_001123620.1	Fwd	ATTCTGGATGGCTTCCTCCT	144	2.03
		Rev	TATTCGCCCATAACCACCTC		
cd9	XM_014187224.1	Fwd	GAGGCCTTGAAGGAGACATTAC	115	2.00
		Rev	CCTCCAGTCCTTCCTTCTTTG		
cd22	XM_014165590.1	Fwd	GCCAGAGGACAAAGGTCATTA	106	2.04
		Rev	CTGAGTGTATCTTGGAACATAGGAA		
cd79a	XM_014187908.1	Fwd	TCTGAACGACTCAGGGTTGTA	105	2.02
		Rev	TTCACCATCGGCCTGTAGA		

[a] *Used qPCR primers previously designed by Tadiso et al. (34).*

CD Proteins Exclusively Identified From Atlantic Salmon HK Cell Lines

A total of 38 and 39 CD proteins were identified from ASK and SSP-9 cells, respectively (**Figure 1B**). Nine CD proteins were detected only in ASK cells, while 11 CD proteins were detected only in SSP-9 cells. Twenty-four CD proteins were shared between these two cell lines.

CD Proteins Common to Atlantic Salmon B Cells and HK Cell Lines

In agreement with the established broad expression of CD81 in mammals (37), this multifunctional tetraspanin protein was detected in high quantities in all proteomics samples (**Table 2**). Similarly, ubiquitously expressed transmembrane glycoproteins (38–40), CD98 and CD147 were detected in salmon ASK, SSP-9, and IgM^+ peripheral B cells. CD147 can bind directly to CD98, which associates with integrins, which is in turn involved in cell adhesion, fusion, proliferation, and growth (41). CD98 was more abundant in LPS-stimulated B cells than control (relative abundance > 2.00; **Table 2**).

The tetraspanin CD63 and transmembrane protein CD156c, also known to be expressed in many cell types (42, 43), were identified in both ASK and B cells. CD63 functions as a transport regulator implicated in intracellular protein trafficking (44). It has been shown to down-regulate CD184 (CXCR4) by serving as a molecular target of the transcriptional repressor Bcl6 (45). CD156c (ADAM10) functions as a molecular scissor that cleaves the extracellular regions of its transmembrane target proteins, which is an important mechanism for the regulation of leukocyte development and function (43).

The transmembrane protein receptor CD40 was detected in both SSP-9 and IgM^+ B cells. This member of the TNFR superfamily has been initially characterized on B cells and subsequently found to be expressed on antigen-presenting cells, and many other immune and non-immune cells (46). The binding of CD40 to its CD154 ligand (CD40L) regulates a wide spectrum of cellular processes, including the activation, proliferation, and differentiation of B cells (47). CD40 exhibited the highest increase in salmon B cell surface expression upon stimulation with a TI antigen, with relative abundance value of 8.60 in LPS-treated vs. control B cells (**Table 2**).

CD Proteins Exclusively Identified From Atlantic Salmon B Cells

Out of the 21 total CD molecules Identified from salmon IgM^+ PBLs, 15 were found to be present in these B cell samples only and were not detected in the two salmon hematopoietic organ-derived cell lines (**Figure 1B**). The receptor-like protein tyrosine phosphatase, CD45, reported to be one of the most abundant cell surface glycoproteins expressed on mammalian leukocytes (48), was the most abundant protein detected in the salmon B cell samples with a relative quantitation value of 1.79 as estimated by emPAI (**Table 2**) based on protein coverage by the peptide matches in the database search result (49).

B Cell-Restricted Proteins (CD22 and CD79A)

Two surface proteins (CD22 and CD79A) that previously have been used as B cell-exclusive markers in mammals were identified in the salmon B cell samples. CD22 is a transmembrane glycoprotein that belongs to the sialic acid-binding immunoglobulin-like lectins (SIGLEC) family that serves as a BCR co-receptor (50, 51). In mammals, its expression is predominantly exclusive to subsets of mature B cells, with surface expression appearing simultaneously with surface IgD and is subsequently lost on plasma cells (52–54). CD22 is a well-established regulator of innate and adaptive B cell responses in mammals [reviewed in (55)]. One of the main functions of CD22 is to down-regulate the activation threshold of BCR through its association with tyrosine phosphatases and other signaling molecules (51, 56). In addition to BCR signaling, several initial studies in mice have shown that CD22 also regulates TLR

TABLE 2 | CD molecules identified in Atlantic salmon IgM^+ B cell samples.

CD molecule	Protein name	Known expression of mammalian homolog	Function of mammalian homolog	Accession no.	Mascot score	Sequence coverage	No. of peptides	No. of PSMs	No. of unique peptides	emPAI in naïve B cells[a]	Relative abundance (LPS/Control)
CD9	Tetraspanin-29 (Tspan-29)	Leukocytes, epithelial and endothelial cells	Cell adhesion, migration, signal transduction	XP_014042699.1	395	29	4	12	4	0.52	1.17
CD11a	Integrin alpha-L-like (ITGAL)	Exclusive to leukocytes	Leukocyte-endothelial cell interactions, cell adhesion, differentiation/development	XP_013986946.1	292	7	6	9	6	–	1.17
CD11c	Integrin alpha-X-like (ITGAX)	Exclusive to leukocytes	Adhesion, cell migration, survival, and proliferation	XP_014014772.1	273	7	7	9	7	0.09	1.59
CD18	Integrin beta-2-like (ITGB2)	Exclusive to leukocytes	Signal transduction, adhesion	XP_014019758.1	2,358	34	20	85	20	1.33	1.19
CD22	SIGLEC-2	Exclusive to B cells	Immunoregulation, B cell adhesion, BCR co-receptor, signal transduction	XP_014021065.1	329	8	8	13	8	0.19	1.53
CD40	Tumor necrosis factor receptor superfamily member 5 (TNFRSF5)	B cells, monocytes, antigen-presenting cells, endothelial and epithelial cells	Cell adhesion, cell proliferation, and signal transduction	NP_001134708.1	64	9	3	4	3	–	8.60
CD45	Protein tyrosine phosphatase receptor type C (PTPRC)	All hematopoietic cells except erythrocytes and plasma cells; B220 isoform exclusive on murine B cells	Regulator of B- and T-cell antigen receptor signaling, cell growth and differentiation	XP_013979041.1	5,714	42	43	207	43	1.79	1.66
CD53	Tetraspanin-25 (Tspan-25)	Exclusive to hematopoietic cells	Cell adhesion, activation, and migration	NP_001134048.1	51	3	1	2	1	–	1.40
CD63	Tetraspanin-30 (Tspan-30)	Leukocytes, endothelial cells	Complexes with integrins, regulation of cell growth and motility	XP_013991669.1	192	9	2	8	2	–	0.98
CD68	Macrosialin	Hematopoietic and non-hematopoietic cell types	Phagocytosis, macrophage homing	NP_001158857.1	34	3	1	1	1	–	0.79
CD79A	B cell antigen receptor complex-associated protein alpha chain; MB-1 membrane glycoprotein	Almost exclusive to B cells	Part of the BCR complex, required in B cell signaling	XP_014041898.1 XP_014010819.1	84 72	12 13	3 3	4 5	1 1	0.30 0.13	1.71 1.22
CD81	Target of the Antiproliferative Antibody 1 (TAPA-1); Tetraspanin-28 (Tspan-28)	Broad expression	B cell activation, cell adhesion, stimulation, differentiation/development	XP_014031360.1	1,139	28	4	31	1	0.30	1.43

(Continued)

TABLE 2 | Continued

CD molecule	Protein name	Known expression of mammalian homolog	Function of mammalian homolog	Accession no.	Mascot score	Sequence coverage	No. of peptides	No. of PSMs	No. of unique peptides	emPAI in naïve B cells[a]	Relative abundance (LPS/Control)
CD84-H1	Signaling lymphocyte activation molecule 9 (SLAM-9)	Macrophages, monocytes, lymphocytes	Long-term humoral immune response	XP_014062779.1	50	3	1	2	1	0.09	0.01[b]
CD87	Urokinase plasminogen activator surface receptor-like	Monocytes and granulocytes, T lymphocytes, NK cells	Cell adhesion, migration, chemotaxis, proliferation, receptor/co-receptor	XP_014012019.1	1,255	54	7	32	5	1.01	1.10
CD98	4F2 cell-surface antigen heavy chain-like	Lymphocytes, NK cells, macrophages, granulocytes, endothelial and epithelial cells	Activation/costimulation, immunoregulation	XP_013984627.1 XP_014051944.1	1,664 1,397	40 40	12 13	44 30	10 11	– –	3.93 2.28
CD147	Basigin	Hematopoietic cells, epithelial and endothelial cells	Regulation of immune responses, lymphocyte activation, adhesion, cell recruitment	XP_014071798.1	296	19	4	10	4	–	1.36
CD156c	A disintegrin and metalloproteinase domain-containing protein 10 (ADAM-10)-like	Broad expression	"Molecular scissors" important in leukocyte regulation	XP_014025741.1	52	4	2	2	2	–	N/A[c]
CD184	C-X-C chemokine receptor type 4-like (CXCR4)	Broad expression	Receptor/coreceptor, chemotaxis	NP_001158765.1	121	2	1	4	1	–[d]	1.53
CD185	C-X-C chemokine receptor type 5-like (CXCR5)	Broad expression	Homing and cell movement and migration	XP_014071056.1	70	3	1	1	1	0.10	1.24
CDw199	C-C chemokine receptor type 9-like (CCR9)	Leukocytes	Important in B cell migration, maturation, and function	XP_014043995.1	78	3	2	4	2	–	1.15
CD282	Toll-like receptor 2 (TLR2)	Monocytes, granulocytes, B cells, resting T cells,	Recognition of bacterial lipopeptides and subsequent activation of innate immune responses	XP_014061839.1	29	2	1	1	1	–	0.88

PSM, peptide-spectrum match; emPAI, exponentially modified protein abundance index.

[a] *No emPAI value for proteins with weak positive hits.*

[b] *Below detection threshold in LPS-stimulated B cell sample.*

[c] *Below threshold level for relative abundance ratio.*

[d] *Detected in 1 of 2 naïve/control-stimulated B cell samples.*

signaling and the survival of B cells (55). However, it has been suggested that CD22 likely functions differently between innate-like B-1 and conventional B-2 cells since CD22 is differentially regulated after BCR-mediated and -independent activation in these B cell lineages (57).

CD79A, on the other hand, is an integral membrane protein belonging to the Ig gene superfamily that associates with membrane Ig on B cell surface and, together with CD79B, forms the signal transduction region of the B cell antigen receptor (BCR) complex (58, 59). Due to their importance in B cell development and induction of B cell activation, CD79 proteins are expressed in virtually all subsets of B cells (60), from the very early stages of B cell development to plasma cells (61–65).

Tetraspanins (CD9 and CD53)

Of the four tetraspanin proteins that were identified by proteomics, detectable quantities of CD9 and CD53 were only present in salmon B cells, despite the reported surface expression in different hematopoietic cell types (66, 67) and/or endothelial cells (68) of their mammalian homologs. This protein family consists of four-span transmembrane proteins that have been described as "master organizers" of the plasma membrane (69) and "molecular facilitators" (42) in a variety of biological processes.

β_2 Integrins (CD11a, CD11c, and CD18)

CD18 (ITGB2), CD11a (ITGAL), and CD11c (ITGAX) that were detected on salmon B cell surface belong to the β_2 integrin family of adhesion and signaling molecules. Integrin β chain subunit CD18 can pair with one of four alpha chain subunits (CD11a, CD11b, CD11c, or CD11d) to form the CD11/CD18 complex that play important roles in the recruitment of immune cells to sites of inflammation, cell–cell contact formation, and regulation of downstream effects on cellular signaling (70). In mammals, these β_2 integrin complexes are found exclusively on leukocytes, particularly myeloid cells and NK cells, and to a lower expression level, B and T lymphocytes.

Chemokine Receptors: CD184, CD185, and CDw199

Three chemokine receptors, CD184 (CXCR4), CD185 (CXCR5), and CDw199 (CCR9) were identified in Atlantic salmon B cells. These are G-protein coupled, seven-transmembrane receptors with CD184 and CD185 classified into the C-X-C (alpha) class and CDw199 into the CC (beta) class. CD184 and CD185 are known to have broad expression across many cell types, including lymphocytes, endothelial, epithelial and hematopoietic stem cells (71). Similarly, CDw199 is expressed in different leukocyte subpopulations such as macrophages, dendritic cells, T cells, and B cells (72–75). These chemokine receptors are important in the migration, maturation, and function of B cells (76–78).

Other Surface Proteins (CD68, CD84-H1, CD87, and CD282)

In addition to members of the protein families described above, several other surface proteins were found present on salmon B cells. These included CD68, CD84-H1, CD87, and CD282.

CD68, the human homolog of macrosialin, is a highly glycosylated type I transmembrane protein belonging to the lysosomal-associated membrane protein (LAMP) family of glycoproteins (79). While this protein was initially regarded as a macrophage marker (80), CD68 expression on other hematopoietic and non-hematopoietic cell types have been subsequently reported, including B cell lines (81–83).

CD84-H1 (a.k.a. CD2-F10 and SLAM9) belongs to the signaling lymphocyte activation molecule (SLAM) family of cell surface receptors within the immunoglobulin superfamily (84, 85). This protein has been shown to be widely expressed in many immune cells of humans, including B cells (84, 85). However, the exact function of CD84-H1 in B cells is still unclear. In general, SLAM proteins are said to contribute to the generation of long-term humoral immune response (86, 87).

CD87, also called urokinase plasminogen activator receptor (uPAR), is a surface glycoprotein that mediates a wide range of biological processes beyond plasminogen activation, including cellular adhesion, migration, chemotaxis, and proliferation [reviewed in (88, 89)]. In humans, CD87 is known to be highly expressed on monocytes and granulocytes, particularly on mature cells (90). As such, it is used as a surface marker for terminal granulocytic maturation (91). Resting B and T lymphocytes and cell lines of lymphoid lineage do not seem to express CD87 (90, 92), although surface expression has been reported on activated T cells and NK cells (90). Next to CD45 and CD18, salmon CD87 had the highest emPAI obtained in naïve B cells, with relative abundance comparable between control and LPS-activated B cell samples.

Another surface protein detected on salmon B cell surface was CD282, more commonly known as toll-like receptor 2 (TLR2), a membrane-bound protein that recognizes the evolutionarily conserved bacterial lipopeptides (93). In humans, surface expression of CD282 is found to be highest on innate cells such as monocytes and granulocytes (94). Detectable level of CD282 expression has also been observed on activated but not resting T cells (95, 96), as well as on surface of different B cell subpopulations, albeit mostly at low level (94, 97, 98).

B Cell-Restrictive Gene Expression of Candidate Salmon Pan-B Cell Markers

Given the known B cell-exclusive surface expression of their mammalian homologs, CD22 and CD79A were shortlisted as potential pan-B cell markers for salmon. In the absence of definitive Abs against these candidate markers, we resorted to qPCR assays for validating their B cell restrictive expression using leukocyte subsets from different lymphoid organs.

Sorted cells from HK (**Figure 2A**) were used as the main source of different leukocyte subpopulations for the RT-qPCR validation assays. As the major hematopoietic organ in teleost, HK consists of a heterogeneous mixture of leukocytes belonging to the lymphoid and myeloid lineages (99). HKL subsets were first examined for gene expression of known markers for B cells, macrophages, and T cells in order to confirm the nature of cells present in each subset, as well as to ensure that no cross-contamination of cell subsets occurred during FACS sorting.

As expected, only the lymphoid subsets had detectable *igd* expression, with transcript levels highest in the HK suspension cell IgM^+ lymphoid subset (HKL SC-L IgM^+, **Figure 2B**), in accordance with the reported dual IgM and IgD expression in majority of naïve mature peripheral B cells of mammals [reviewed in (100–102)] and trout (103). Significant albeit much lower *igd* expression was also observed in HK suspension cell IgM^- lymphoid subset (HKL SC-L IgM^-), which could suggest the presence of IgD^+ only B cells in naïve HKLs. By contrast, the suspension and adherent IgM^- non-lymphoid subsets (HKL SC-nL IgM^- and HKL AC-nL IgM^-, respectively), assumed to consist of myeloid cells (macrophages, monocytes, and/or granulocytes), had very low to non-existent *igd* expression.

The HK suspension cell IgM^+ lymphoid subset had no detectable transcription of the macrophage marker, *mcsfr*, which was expressed in high levels in the putative myeloid cell subsets, HKL SC-nL IgM^- and HKL AC-nL IgM^-. Detectable levels of *mcsfr* transcripts was present in the HK suspension cell IgM^- lymphoid subset, which could indicate the presence of contaminating macrophages in this leukocyte subpopulation. Similarly, no detectable *cd3-z2* gene expression was observed in the HK suspension cell IgM^+ lymphoid subset, while the remaining HKL subsets exhibited relatively low expression of this T cell marker.

Additionally, to ensure that any observed absence of detectable transcripts was not due to poor cDNA/RNA quality of our samples, the mRNA levels of the broadly expressed CD9 tetraspanin were also determined in the sorted HKL subpopulations. In general, relative expression of *cd9* was comparably high across all HKL subsets, with the HK suspension cell IgM^- non-lymphoid subset having the most expression.

The gene expression of our candidate B cell markers was subsequently investigated. HK suspension cell IgM^+ lymphoid subset with a putative B cell phenotype (i.e., significant gene expression of *igd* and *cd9*, but not *mcsfr* and *cd3-z2*) exhibited the highest *cd22* and *cd79a* expression (**Figure 2C**). By contrast, very low to non-existent mRNA levels were observed in both the suspension and adherent IgM^- non-lymphoid subsets (HKL SnL IgM^- and HKL AnLIgM$^-$, respectively), consisting mostly of cells from the myeloid lineage and some T lymphocytes as per *mcsfr* and *cd3z* gene expression profile. Low but detectable levels of *cd22* and *cd79a* were also observed in the HKL SL IgM^- subset, likely due to the presence of IgD^+ and IgT^+ B cells in this leukocyte subpopulation.

To check whether the apparent B cell restrictive expression of *cd22* and *cd79a* is consistent across different B cells from different lymphoid sources, we also performed the same gene expression assay in leukocyte subsets from spleen (**Figure 3A**) and peritoneal cavity (**Figure 4A**). IgT subpopulation was also added in the analysis to determine *cd22* and *cd79a* expression in a non-IgM B cell isotype. Similar to what was observed in HKLs, highest and lowest *cd22* and *cd79a* mRNA levels were obtained in the spleen IgM^+ lymphoid (SpL L IgM^+) and IgM^- non-lymphoid subsets (SpL nL IgM^-), respectively (**Figure 3B**). High mRNA expression for these candidate markers was also found in the spleen IgT^+ lymphoid subset (SpL L IgT^+) as well as in the IgM^- IgT^- lymphoid subset (SpL L IgM^- IgT^-), which could contain IgD only B cells.

For PeLs, comparable levels of *cd22* transcription were observed between IgM^+ (PeL L IgM^+) and IgT^+ (PeL L $IgT^{+)}$ lymphoid subsets, while very low *cd22* gene expression was obtained in the PeL IgM^- IgT^- non-lymphoid subset (PeL nL IgM^- IgT^-) (**Figure 4B**). Gene expression of *cd79a*, on the other hand, was higher in the IgM^+ than IgT^+ peritoneal lymphoid cells. Lowest *cd79a* expression was observed in the IgM^- IgT^- non-lymphoid subset of the peritoneal leukocytes (PeL nL IgM^- IgT^-).

DISCUSSION

To our knowledge, this is the first report on the profiling of salmon B cell surface protein repertoire. Although proteomics has been employed in some investigations of fish immune responses to various infections [reviewed in (104)], it is not commonly used to characterize the surface protein expression of specific immune-related cells in teleosts. A previous proteomics study on Atlantic salmon focused on profiling changes in fish serum proteins following infection with salmonid alphavirus (105). Our approach focused on B cells and was useful in the identification of 21 CD molecules from salmon IgM^+ B cells. The relatively limited number of CD proteins identified could be partially explained by the initial low number of B cells in the starting material (3×10^6 viable IgM^+ B cells after 72 h in culture) used in the surface protein isolation. In addition, despite being one of the popular choices for cell surface proteome profiling, the biotinylation technique employed for the enrichment of plasma membrane proteins may not be the most effective method for isolating glycosylated proteins (106). Since majority of cell surface proteins are glycosylated (107), many surface glycoproteins may not have been included in our mass spectrometry samples.

Peripheral blood was used as source of salmon B cells for proteomics due to higher total leukocyte yield [i.e., 15× and 4× more total leukocytes than the spleen and the HK, respectively (108)] and the abundance of IgM^+ B cells in this compartment (22). For comparison, surface proteins from two Atlantic salmon head kidney cell lines, ASK and SSP-9, were also identified. Although the exact cell composition of these hematopoietic-tissue derived cell lines is unknown, these seem to include cells from the myeloid lineage based on their respective proteomics profile. Given its epithelial-like morphology and previously reported gene expression profile (31), SSP-9 is likely comprised of macrophage-like cells. Specifically, majority of the identified SSP-9-exclusive surface proteins (CD2, CD34, CD74, CD151, CD205) are associated with expression on a macrophage subset with antigen-presenting capacity (109–113). Detection of CD203c, a known basophil and mast cell marker in humans (114), suggest that SSP-9 may contain granulocytes.

Salmon IgM^+ B Cell Surface Proteome

All the surface proteins identified from our salmon B cell samples have been previously detected on the surface of mammalian B

cells, except for CD87. In teleost, only a few of these B cell-associated proteins have been studied so far. Constitutive gene expression of tetraspanins *cd9* and *cd63* have been reported in sorted IgM^+ B cells of trout from different immune organs (115). Surface expression of CD22 has also been shown in PBLs of tongue sole (116).

In keeping with their established roles in B cell activation, CD40 (117) and CD98 (118) surface expression were significantly higher in LPS-stimulated IgM^+ B cell samples. Co-expression of CD40 and IgM^+ has been established on B cell surface of zebrafish, with significant up-regulation of CD40 similarly observed following LPS treatment (119). In addition, modest increase in CD40 transcripts has been reported for Atlantic salmon IgM^+ B cells in the presence of another TLR agonist, CpG oligodeoxynucleotides (22).

Surprisingly, CD87, which has been reported to be absent on surface of resting B lymphocytes and B cell lines of mammals (90, 92), was detected in our naïve salmon IgM^+ B cell samples. It should be noted that CD87 acts as a ligand for β_2 integrins such as CD18 and CD11a/c identified on salmon B cells, and thus usually found in close association with these protein complexes on leukocytes (120). CD87 has been demonstrated to mediate cell-cell adhesion by interaction with integrins on the same as well as apposing cells (121). Hence, the CD87 proteins detected in our proteomics experiment may be an artifact from a CD87-β_2 integrin complex formed by trans-interaction of salmon B cells with CD87-expressing monocytes or granulocytes. It is unlikely that the proteins were contributed directly by contaminating monocytes or granulocytes since the samples were checked for purity (>98% IgM^+ PBLs) before surface protein isolation. Alternatively, it is also possible that salmon, in contrast to mammals, express CD87 on their B cell surface.

Peripheral blood provides the means for cells to move systemically within the animal body; hence, one would expect a mixture of circulating B cell subsets in this compartment. Surface detection of chemokine receptors CXCR4, CXCR5, and CCR9 important in trafficking naïve B lymphocytes (76) seem to suggest that our peripheral IgM B cell population is comprised of a migrating population of B cells from different lymphoid compartments. In humans, the majority of peripheral B cells are of the conventional B-2 cell type bearing both membrane IgM and membrane IgD, which accounts for about 10% of total PBLs (122). Given the current technical constraints, it was not possible to further sort the largely undefined subsets of the salmon IgM^+ peripheral B cell subpopulation.

More recently, it has been shown that, contrary to the dogma that all plasma cells have permanently switched off expression of membrane-bound Ig molecules to produce their secreted version (antibodies), some mature plasma cells in mice retain their expression of surface IgM and functional BCR (123, 124). Thus, it is possible that our LPS-treated peripheral B cells contained some differentiating IgM^+ plasmablasts, plasma cells, or memory B cells. However, none of the known markers for these differentiated B cells [i.e., CD27 for memory B cells (125), CD138 for plasma cells (126)] was identified in the stimulated B cell samples. Based on previous studies in trout, this can be partially explained by the relatively short stimulation period (72 h incubation in culture) used in our study. In naïve trout PBLs, significant antibody secreting cell response is observed only after 4 days of LPS stimulation using 4 times higher dose, with peak responses occurring by Day 7 in culture (127). In addition, memory B cell responses to TI and TD antigens are observed only after 4–7 days of *in vitro* re-stimulation of PBLs from previously immunized trout (108).

It should be emphasized that several other mammalian pan-B cell and subset markers known to be encoded in the Atlantic salmon genome were not detected in our salmon IgM^+ B cell samples. Failure to detect a particular surface protein should be interpreted with caution due to previously indicated technical limitations of our experimental approach or their presence at low frequency in our heterogeneous pool of IgM^+ B cell subpopulations. Moreover, it should be noted that our shortlist of salmon CD proteins was based on their mammalian counterparts. Other surface proteins that were detected exclusively in the IgM^+ samples but without homologs or are not classified as CD molecules in mammals were not included in this list. Further investigation of the "non-CD" surface proteins is therefore needed in order to determine whether or not these can serve as unique B cell markers in salmon.

Identification of CD22 and CD79A as Potential Salmon B Cell Markers

Due to lack of access to antibodies against salmon IgD and myeloid markers, our analysis was constrained to leukocyte subpopulations sorted by cell size and granularity and subsequent positive selection for IgM^+ or IgT^+ cells, representing independent salmon B cell lineages. Despite this clear limitation, our current sorting protocol is still a valid useful tool in studying the different salmon leukocyte populations as evidenced by the results of our qPCR validation assays using different leukocyte markers.

In general, *cd22* vs. *cd79a* gene expression patterns of the different leukocyte subsets were comparable across different lymphoid organs. Highest relative expression were observed in all IgM^+ B cell subsets, while very low to below detectable level of expression were found in IgM^-/IgT^- non-lymphoid subset (likely consisting of myeloid cells). Relatively lower but significant level of expression was also found in non-IgM subsets within the lymphoid gate, which likely consist of either a mixed population of IgT^+ or IgD^+ only B cells (i.e., HKL SC-L IgM^-) or IgD^+ only B cells (i.e., SpL L IgM^- IgT^-). While generally regarded as B cell-exclusive proteins (52, 128), it is important to note that mammalian CD22 and CD79A have also been reported to be expressed on the surface of some non-B cell populations, including T cells (129) and various myeloid cells (130–133). However, this is likely not the case for Atlantic salmon given the negligible transcript levels of *cd22* and *cd79a* in all the myeloid-containing leukocyte subsets tested.

Although mRNA levels do not necessarily correlate directly with surface protein expression, gene expression profiles of salmon *cd22* and *cd79a* clearly showed that the B cell exclusivity of our candidate CD molecules extend down to the level of

transcription. This B cell-restrictive expression was consistent across different lymphoid compartments (peripheral blood, head kidney, spleen, peritoneal cavity) and different Ig isotypes (IgM and IgT), thus providing strong support to the potential of CD22 and CD79A as pan-B cell markers for salmon.

Extensive gene duplications in the Atlantic salmon genome (134, 135) should be taken into account in finding appropriate B cell markers. Specifically, Atlantic salmon encodes an unusually high number of CD22-like paralogs and isoforms (**Supplementary Table 1**) that could have different regulatory expression and conformation on B cells. Interestingly, peptide sequences specific to only one CD22 paralog was detected on the salmon B cell surface in our mass spectrometry analysis. Based on our qPCR assay, mRNA expression of this particular variant was also specific in salmon B cells. In humans, a CD22 molecule with a different conformation to that found on B cells has been detected on basophils (130). Whether other CD22 variants/isoforms are also expressed in other subpopulations of salmon leukocytes, or in specific subsets of salmon B cells, is still unknown, but is beyond the scope of this study. For simplicity, the particular CD22 paralog (XP_014021065.1) identified in this study was referred as CD22.

Other Potential B Cell Markers

CD45, the most abundant surface protein identified in our salmon B cell samples, exists in different alternative splicing isoforms, which are expressed in cell-type specific patterns on functional subsets of mammalian lymphocytes (48). In mice, a long isoform of CD45 called B220 (136) has been used as a pan B-cell marker due to its specific expression throughout stages of B cell development, including entry into the memory B cell pool (137). A similar long CD45 isoform (CD45RABC) has been identified in human B cells (96), which has been used as marker for certain human B cell subsets (138). This B-cell specific CD45 isoform in mammals consists of all 33 exons of the CD45 gene (139). Atlantic salmon genome encodes for seven CD45 transcript variants in Chromosome 10 (**Supplementary Table 1**), with alternate splicing of three exons (4, 5, 6) producing six CD45 isoforms [GenBank Assembly Accession No. GCA_000233375.4 (135)]. Given that all exons are present in the B cell-specific isoform, it was not possible to determine whether the long CD45 isoform was the only isoform detected on salmon B cell surface. Hence, further investigation for the presence of other CD45 isoforms in sorted salmon B cell subpopulations (i.e., qPCR assays using primers specific for the other splice variants) is still needed before its potential as another salmon pan-B cell marker can be fully appreciated.

Several other CD molecules identified on salmon B cell samples can be explored for their potential in discriminating specific B cell subsets despite their non-exclusive B cell surface expression. Murine CD9 is expressed on the surface of innate-like B cells and plasma cells, but not on naïve conventional B2 cells (140, 141). In our proteomics data, CD9 was detected in high abundance in all samples of salmon IgM^+ peripheral B cells but not in either of the two salmon head kidney cell lines. This implies that the salmon IgM^+ peripheral B cell subpopulation are comprised of cells with significantly high expression of this protein. In rainbow trout, *cd9* mRNA levels are similar in IgM^+ and IgM^- B cells from blood and HK (115). In agreement with this, comparable levels of *cd9* expression was also observed in the IgM^+ and IgM^- fractions of our sorted HKL lymphoid cells, but highest constitutive gene expression was still found in the myeloid fractions. Thus, while CD9 cannot be used as the sole and primary marker for salmon B cells, its potential for identifying specific B cell subsets should be explored further.

Other potential B cell subset markers are the CD11 β_2 integrins. In contrast to mammals wherein four β_2 integrins have been identified, Atlantic salmon genome encodes only two: CD11a and CD11c. Both of these proteins were detected in our salmon IgM^+ B cell samples, which could suggest their potential use as markers to functionally-equivalent B cell subsets in mammals. High surface CD11a expression has been associated with a new subpopulation of IFN-γ-secreting innate B cells (142). Expression of CD11c has also been recently used as marker for distinct B cell subsets in mice and humans (143, 144), including $CD11c^{low}$-expressing plasmablasts that predominantly secrete Ag-specific IgM antibodies in a T cell-independent manner (145) and $CD11c^+$ 'atypical memory B cells' (144).

Interestingly, CD11b, which is used as a marker to differentiate B1 cells that reside in the peritoneal cavity and those that recently migrated into the spleen (146), has not been detected until present. Among salmonids, only coho and Chinook salmon have CD11b-like protein recorded in the sequence database. However, the salmonid sequences of CD11c (ITGAX) is very similar to that of CD11b (70). In fact, Atlantic salmon CD11c (XP_014014772.1) has 70 and 90% homology with CD11c-like proteins of coho (XP_020308950.1) and Chinook (XP_024269535.1) salmon, respectively. Similarly, CD11d, which is only found in coho (XP_020334852.1), has 95% homology with Atlantic salmon CD11a (XP_014032228.1). At this point, it is unknown whether Atlantic salmon CD11c-like and CD11a-like proteins have overlapping functions with the mammalian CD11b and CD11d proteins, and whether expression patterns of these mammalian B cell subset markers are similar to their ancestral counterpart in teleosts.

Salmon IgM^+ B Cell Surface Phenotype Is Consistent With Innate-Like B Cells of Mammals

It is worthy to note that several of the surface proteins (CD9, CD11a, CD11c) identified on salmon IgM^+ B cells in high abundance are associated with innate-like B cells in mice and humans. CD22, one of the identified potential salmon B cell marker in this study, is also known to be expressed the highest in MZ B cell precursors out of any mammalian B cell subset (147). Additionally, detection of CD282 (TLR2), which has been previously shown to be expressed higher in naïve innate-like B cells than conventional B2 cells (97), implies a possible function of salmon IgM^+ peripheral B cells in TI-responses. Altogether, these are consistent with a salmon IgM^+ B cell phenotype closer to innate-like B cells (B1 and MZ B2) than conventional B2 cells in mammals. This supports the previously proposed B cell evolution hypothesis (18) which suggests that teleost IgM B cells are the ancestors of the innate-like B cells of mammals (25, 148). Whether these innate-like B cell-associated proteins detected

from our B cell samples are evenly expressed on the surface of all salmon IgM^+ B cells or only expressed at very high levels on certain sub-populations, is a question that warrants further investigations. This can be determined upon availability of the necessary immunological tools and antibodies to analyze the frequency and level of their surface expression.

Speculations regarding the possible characteristics of salmon IgM B cell populations based solely on pre-conceived notions of the surface phenotype, function, and anatomical distribution of their mammalian counterparts should come with a caveat. Indeed, the conservation of protein functions between mammals and teleosts for many of the B cell-associated CD molecules identified in this study has to be established. Therefore, subsets comprising the salmon IgM^+ B cells need to be better defined, in order to facilitate further functional studies of these individual surface proteins.

SUMMARY AND CONCLUSION

In summary, our salmon B cell proteomics approach provide novel information on the surface phenotype of salmon IgM B cells as well as some evolutionary insights in reference to their mammalian counterparts. While possible exclusion of several glycosylated and/or less abundant proteins cannot be discounted due to technical limitations of the protocols used, our detection of 21 CD molecules remains a significant advancement in profiling the salmon B cell surface proteome. In addition, identification of CD22 and CD79A as potential pan-B cell markers represents a considerable positive step toward salmon B cell marker development. Further investigation and evaluation of the salmon CD molecules identified in this study would improve our understanding of B cell dynamics in salmon in the presence of TI and TD antigens during immunostimulation, pathogen infection, or vaccination.

ETHICS STATEMENT

The authors confirm that the experimental protocols used for the live fish experiments were based on the Animal Welfare Act (https://www.regjeringen.no/en/dokumenter/animal-welfare-act/id571188/) and performed in accordance with relevant guidelines and regulations given by the Norwegian Animal Research Authority.

AUTHOR CONTRIBUTIONS

MP performed most of the experimental work (leukocyte isolation, FACS sorting, surface protein isolation, qPCR analyses) and wrote the manuscript. J-AB was responsible for the mass spectrometry analyses. LT performed RNA extraction and cDNA syntheses. IJ and JJ collaborated in obtaining funding, helped designed the experiments, and reviewed the manuscript.

FUNDING

This work was supported by the Aquaculture program of The Research Council of Norway (Grant No. 254892): Multiple routes to B cell memory in Atlantic salmon and UiT The Arctic University of Norway. The publication charges for this article have been funded by a grant from the publication fund of UiT The Arctic University of Norway.

ACKNOWLEDGMENTS

The authors wish to thank Dr. Karsten Skjødt and Prof. Oriol Sunyer for generously providing the mAbs for sorting IgM and IgT B cells. Toril Anne Grønset, Shiferaw Jenberie, Guro Strandskog, Mikael Fjeld Wold, and Morten Bay Styrvold are also acknowledged for their excellent technical assistance (processing of mass spectrometry samples, cell isolation).

SUPPLEMENTARY MATERIAL

The Supplementary Material for this article can be found online at: https://www.frontiersin.org/articles/10.3389/fimmu.2019.00037/full#supplementary-material

REFERENCES

1. Thorarinsson R, Powell DB. Effects of disease risk, vaccine efficacy, and market price on the economics of fish vaccination. *Aquaculture* (2006) 256:42–9. doi: 10.1016/j.aquaculture.2006.01.033
2. Holvold LB, Myhr AI, Dalmo RA. Strategies and hurdles using DNA vaccines to fish. *Vet Res,* (2014) 45:21. doi: 10.1186/1297-9716-45-21
3. Zhu LY, Lin AF, Shao T, Nie L, Dong WR, Xiang LX., et al. B cells in teleost fish act as pivotal initiating APCs in priming adaptive immunity: an evolutionary perspective on the origin of the B-1 cell subset and B7 molecules. *J Immunol.* (2014) 192:2699–714. doi: 10.4049/jimmunol.1301312
4. Li J, Barreda DR, Zhang YA, Boshra H, Gelman AE, Lapatra S., et al. B lymphocytes from early vertebrates have potent phagocytic and microbicidal abilities. *Nat Immunol.* (2006) 7:1116–24. doi: 10.1038/ni1389
5. Sinyakov MS, Dror M, Zhevelev HM, Margel S, Avtalion RR. Natural antibodies and their significance in active immunization and protection against a defined pathogen in fish. *Vaccine* (2002). 20:3668–3674. doi: 10.1016/S0264-410X(02)00379-1
6. Ye J, Kaattari IM, Ma C, Kaattari S. The teleost humoral immune response. *Fish Shellfish Immunol.* (2013) 35:1719–28. doi: 10.1016/j.fsi.2013.10.015
7. Zwollo P. The humoral immune system of anadromous fish. *Dev Comp Immunol.* (2018) 80:24–33. doi: 10.1016/j.dci.2016.12.008
8. Yamaguchi T, Quillet E, Boudinot P, Fischer U. What could be the mechanisms of immunological memory in fish? *Fish Shellfish Immunol.* (2019) 85:3–8. doi: 10.1016/j.fsi.2018.01.035
9. Vale AM, Kearney JF, Nobrega A, Schroeder HW. Chapter 7–Development and function of B cell subsets. In: Alt FW, Honjo T, Radbruch A, Reth M, editors. *Molecular Biology of B Cells*, 2nd ed. London: Academic Press (2015). p. 99–119. doi: 10.1016/B978-0-12-397933-9.00007-2
10. Cerutti A, Cols M, Puga I. Marginal zone B cells: virtues of innate-like antibody-producing lymphocytes. *Nat Rev Immunol.* (2013) 13:118–32. doi: 10.1038/nri3383
11. Haas KM, Poe JC, Steeber DA, Tedder TF. B-1a and B-1b cells exhibit distinct developmental requirements and have unique functional roles in

innate and adaptive immunity to *S. pneumoniae*. *Immunity* (2005) 23:7–18. doi: 10.1016/j.immuni.2005.04.011
12. Baumgarth N. B-1 Cell heterogeneity and the regulation of natural and antigen-induced IgM production. *Front Immunol.* (2016) 7:324. doi: 10.3389/fimmu.2016.00324
13. Baumgarth N. Innate-like B cells and their rules of engagement. *Adv Exp Med Biol.* (2013) 785:57–66. doi: 10.1007/978-1-4614-6217-0_7
14. Yang Y, Ghosn EE, Cole LE, Obukhanych TV, Sadate-Ngatchou P, Vogel SN., et al. Antigen-specific memory in B-1a and its relationship to natural immunity. *Proc Natl Acad Sci USA.* (2012) 109:5388–93. doi: 10.1073/pnas.1121627109
15. Yang Y, Ghosn EE, Cole LE, Obukhanych TV, Sadate-Ngatchou P, Vogel SN., et al. Antigen-specific antibody responses in B-1a and their relationship to natural immunity. *Proc Natl Acad Sci USA.* (2012) 109:5382–7. doi: 10.1073/pnas.1121631109
16. Kurosaki T, Kometani K, Ise W. Memory B cells. *Nat Rev Immunol.* (2015) 15:149. doi: 10.1038/nri3802
17. Sunyer JO. Fishing for mammalian paradigms in the teleost immune system. *Nat Immunol.* (2013) 14:320–6. doi: 10.1038/ni.2549
18. Sunyer JO. Evolutionary and functional relationships of B cells from fish and mammals: insights into their novel roles in phagocytosis and presentation of particulate antigen. *Infect Disord Drug Targets* (2012) 12:200–12. doi: 10.2174/187152612800564419
19. Korytár T, Jaros J, Verleih M, Rebl A, Kotterba G, Kühn C., et al. Novel insights into the peritoneal inflammation of rainbow trout (*Oncorhynchus mykiss*). *Fish Shellfish Immunol.* (2013) 35:1192–9. doi: 10.1016/j.fsi.2013.07.032
20. Zapata AG, Torroba M, Vicente A, Varas A, Sacedón R, Jiménez E. The relevance of cell microenvironments for the appearance of lympho-haemopoietic tissues in primitive vertebrates. *Histol Histopathol.* (1995) 10:761–78.
21. Cain KD, Jones DR, Raison RL. Antibody-antigen kinetics following immunization of rainbow trout (Oncorhynchus mykiss) with a T-cell dependent antigen. *Dev Comp Immunol.* (2002) 26:181–90. doi: 10.1016/S0145-305X(01)00063-5
22. Jenberie S, Thim HL, Sunyer JO, Skjødt K, Jensen I, Jørgensen JB, et al. Profiling Atlantic salmon B cell populations: CpG-mediated TLR-ligation enhances IgM secretion and modulates immune gene expression. *Sci Rep.* (2018) 8:3565. doi: 10.1038/s41598-018-21895-9
23. Edholm ES, Bengtén E, Stafford JL, Sahoo M, Taylor EB, Miller NW., et al. Identification of two IgD+ B cell populations in channel catfish, *Ictalurus punctatus*. *J Immunol.* (2010) 185:4082–94. doi: 10.4049/jimmunol.1000631
24. Zhang YA, Salinas I, Li J, Parra D, Bjork S, Xu Z., et al. IgT, a primitive immunoglobulin class specialized in mucosal immunity. *Nat Immunol.* (2010) 11:827–35. doi: 10.1038/ni.1913
25. Abós B, Bird S, Granja AG, Morel E, More Bayona JA, Barreda DR., et al. Identification of the first teleost CD5 molecule: additional evidence on phenotypical and functional similarities between Fish IgM(+) B cells and mammalian B1 cells. *J Immunol.* (2018) 201:465–480. doi: 10.4049/jimmunol.1701546
26. Gonzalez R, Matsiota P, Torchy C, De Kinkelin P, Avrameas S. Natural anti-TNP antibodies from rainbow trout interfere with viral infection *in vitro*. *Res Immunol.* (1989) 140:675–84. doi: 10.1016/0923-2494(89)90021-7
27. Chumley MJ, Dal Porto JM, Cambier JC. The unique antigen receptor signaling phenotype of B-1 cells is influenced by locale but induced by antigen. *J Immunol.* (2002) 169:1735–43. doi: 10.4049/jimmunol.169.4.1735
28. Clark G, Stockinger H, Balderas R, van Zelm MC, Zola H, Hart D., et al. Nomenclature of CD molecules from the tenth human leucocyte differentiation antigen workshop. *Clin Transl Immunol.* (2016) 5:e57. doi: 10.1038/cti.2015.38
29. Hedfors IA, Bakke H, Skjødt K, Grimholt U. Antibodies recognizing both IgM isotypes in Atlantic salmon. *Fish Shellfish Immunol.* (2012) 33:1199–206. doi: 10.1016/j.fsi.2012.09.009
30. Devold M, Krossøy B, Aspehaug V, Nylund A. Use of RT-PCR for diagnosis of infectious salmon anaemia virus (ISAV) in carrier sea trout Salmo trutta after experimental infection. *Dis Aquat Organ.* (2000) 40:9–18. doi: 10.3354/dao040009
31. Rodriguez Saint-Jean S, González C, Monrás M, Romero A, Ballesteros N, Enríquez R., et al. Establishment and characterization of a new cell line (SSP-9) derived from Atlantic salmon Salmo salar that expresses type I ifn. *J Fish Biol.* (2014) 85:1526–45. doi: 10.1111/jfb.12503
32. Jørgensen JB, Johansen A, Stenersen B, Sommer AI. CpG oligodeoxynucleotides and plasmid DNA stimulate Atlantic salmon (Salmo salar L.) leucocytes to produce supernatants with antiviral activity. *Dev Comp Immunol.* (2001) 25:313–21. doi: 10.1016/S0145-305X(00)00068-9
33. Shevchenko A, Wilm M, Vorm O, Mann M. Mass spectrometric sequencing of proteins silver-stained polyacrylamide gels. *Anal Chem.* (1996) 68:850-8. doi: 10.1021/ac950914h
34. Tadiso Lie KK, Hordvik I. Molecular cloning of IgT from Atlantic salmon, and analysis of the relative expression of τ, μ and δ in different tissues. *Vet Immunol Immunopathol.* (2011) 139:17–26. doi: 10.1016/j.vetimm.2010.07.024
35. Cuesta A, Meseguer J, Esteban MA. The antimicrobial peptide hepcidin exerts an important role in the innate immunity against bacteria in the bony fish gilthead seabream. *Mol Immunol.* (2008) 45:2333–42. doi: 10.1016/j.molimm.2007.11.007
36. Wang T, Bird S, Koussounadis A, Holland JW, Carrington A, Zou J., et al. Identification of a novel IL-1 cytokine family member in teleost fish. *J Immunol.* (2009) 183:962–74. doi: 10.4049/jimmunol.0802953
37. Levy S, Todd SC, Maecker HT. CD81 (TAPA-1): a molecule involved in signal transduction and cell adhesion in the immune system. *Annu Rev Immunol.* (1998) 16:89–109. doi: 10.1146/annurev.immunol.16.1.89
38. Haynes BF, Hemler ME, Mann DL, Eisenbarth GS, Shelhamer J, Mostowski HS., et al. Characterization of a monoclonal antibody (4F2) that binds to human monocytes and to a subset of activated lymphocytes. *J Immunol.* (1981) 126:1409–14.
39. Moretta A, Mingari MC, Haynes BF, Sekaly RP, Moretta L, Fauci AS. Phenotypic characterization of human cytolytic T lymphocytes in mixed lymphocyte culture. *J Exp Med.* (1981) 153:213–8. doi: 10.1084/jem.153.1.213
40. Attia M, Huet E, Delbé J, Ledoux D, Menashi S, Martelly I. Extracellular matrix metalloproteinase inducer (EMMPRIN/CD147) as a novel regulator of myogenic cell differentiation. *J Cell Physiol.* (2011) 226:141–9. doi: 10.1002/jcp.22315
41. Nguyen HT, Merlin D. Homeostatic and innate immune responses: role of the transmembrane glycoprotein CD98. *Cell Mol Life Sci.* (2012) 69:3015–26. doi: 10.1007/s00018-012-0963-z
42. Maecker HT, Todd SC, Levy S. The tetraspanin superfamily: molecular facilitators. *Faseb J.* (1997) 11:428–42. doi: 10.1096/fasebj.11.6.9194523
43. Matthews AL, Koo CZ, Szyroka J, Harrison N, Kanhere A, Tomlinson MG. Regulation of leukocytes by tspanC8 tetraspanins and the "Molecular Scissor" ADAM10. *Front Immunol.* (2018) 9:1451. doi: 10.3389/fimmu.2018.01451
44. Pols MS, Klumperman J. Trafficking and function of the tetraspanin CD63. *Exp Cell Res.* (2009) 315:1584–92. doi: 10.1016/j.yexcr.2008.09.020
45. Yoshida N, Kitayama D, Arima M, Sakamoto A, Inamine A, Watanabe-Takano H., et al. CXCR4 expression on activated B cells is downregulated by CD63 and IL-21. *J Immunol.* (2011) 186:2800–8. doi: 10.4049/jimmunol.1003401
46. van Kooten C, Banchereau J. Functions of CD40 on B cells, dendritic cells and other cells. *Curr Opin Immunol.* (1997) 9:330–7.
47. Durie FH, Foy TM, Masters SR, Laman JD, Noelle RJ. The role of CD40 in the regulation of humoral and cell-mediated immunity. *Immunol Today.* (1994) 15:406–11. doi: 10.1016/0167-5699(94)90269-0
48. Trowbridge IS, Thomas ML. CD45: an emerging role as a protein tyrosine phosphatase required for lymphocyte activation and development. *Annu Rev Immunol.* (1994) 12:85–116.
49. Ishihama Y, Oda Y, Tabata T, Sato T, Nagasu T, Rappsilber J., et al. Exponentially modified protein abundance index (emPAI) for estimation of absolute protein amount in proteomics by the number of sequenced peptides per protein. *Mol Cell Proteomic* (2005) 4:1265–72. doi: 10.1074/mcp.M500061-MCP200
50. Nitschke L. CD22 and Siglec-G: B-cell inhibitory receptors with distinct functions. *Immunol Rev.* (2009) 230:128–43. doi: 10.1111/j.1600-065X.2009.00801.x

51. Nitschke L. CD22 and Siglec-G regulate inhibition of B-cell signaling by sialic acid ligand binding and control B-cell tolerance. *Glycobiology* (2014) 24:807–17. doi: 10.1093/glycob/cwu066
52. Clark EA. CD22, a B cell-specific receptor, mediates adhesion and signal transduction. *J Immunol.* (1993) 150:4715–8.
53. Erickson LD1 TL, Bhatia SK, Grabstein KH, Waldschmidt TJ. Differential expression of CD22 (Lyb8) on murine B cells. *Int Immunol.* (1996) 8:1121–9. doi: 10.1093/intimm/8.7.1121
54. Moyron-Quiroz JE, Partida-Sánchez S, Donís-Hernández R, Sandoval-Montes C, Santos-Argumedo L. Expression and function of CD22, a B-cell restricted molecule. *Scand J Immunol.* (2002) 55:343–51. doi:10.1046/j.1365-3083.2002.01063.x
55. Clark EA, Giltiay NV. CD22: a regulator of innate and adaptive b cell responses and autoimmunity. *Front Immunol.* (2018) 9:2235. doi: 10.3389/fimmu.2018.02235
56. Nitschke L, Carsetti R, Ocker B, Köhler G, Lamers MC. CD22 is a negative regulator of B-cell receptor signalling. *Curr Biol.* (1997) 7:133–43.
57. Lajaunias F, Nitschke L, Moll T, Martinez-Soria E, Semac I, Chicheportiche Y., et al. Differentially regulated expression and function of CD22 in activated B-1 and B-2 lymphocytes. *J Immunol.* (2002) 168:6078–83. doi: 10.4049/jimmunol.168.12.6078
58. Wienands J. The B-cell antigen receptor: formation of signaling complexes and the function of adaptor proteins. *Curr Top Microbiol Immunol.* (2000) 245:53–76. doi: 10.1007/978-3-642-57066-7_2
59. van Noesel CJ, van Lier RA, Cordell JL, Tse AG, van Schijndel GM, de Vries EF., et al. The membrane IgM-associated heterodimer on human B cells is a newly defined B cell antigen that contains the protein product of the mb-1 gene. *J Immunol.* (1991) 146:3881–8.
60. Chu PG, Arber DA. CD79: a review. *Appl Immunohistochem Mol Morphol.* (2001) 9:97–106.
61. Patterson HC, Kraus M, Wang D, Shahsafaei A, Henderson JM, Seagal J., et al. Cytoplasmic Ig alpha serine/threonines fine-tune Ig alpha tyrosine phosphorylation and limit bone marrow plasma cell formation. *J Immunol.* (2011) 187:2853–8. doi: 10.4049/jimmunol.1101143
62. Leduc I, Preud'homme JL, Cogne M. Structure and expression of the mb-1 transcript in human lymphoid cells. *Clin Exp Immunol.* (1992) 90:141–6. doi: 10.1111/j.1365-2249.1992.tb05846.x
63. Mason D, Cordell JL, Tse AG, van Dongen JJ, van Noesel CJ, Micklem K, et al. The IgM-associated protein mb-1 as a marker of normal and neoplastic B cells. *J Immunol.* (1991) 147:2474–2482.
64. Dworzak MN, Fritsch G, Fröschl G, Printz D, Gadner H. Four-color flow cytometric investigation of terminal deoxynucleotidyl transferase-positive lymphoid precursors in pediatric bone marrow: CD79a expression precedes CD19 in early B-cell ontogeny. *Blood* (1998) 92:3203–9.
65. Tanaka T, Ichimura K, Sato Y, Takata K, Morito T, Tamura M., et al. Frequent downregulation or loss of CD79a expression in plasma cell myelomas: potential clue for diagnosis. *Pathol Int.* (2009) 59:804–8. doi: 10.1111/j.1440-1827.2009.02448.x
66. Horejsi V, Vlcek C. Novel structurally distinct family of leucocyte surface glycoproteins including CD9, CD37, CD53 and CD63. *FEBS Lett.* (1991) 288:1–4.
67. Tohami T, Drucker L, Radnay J, Shapira H, Lishner M. Expression of tetraspanins in peripheral blood leukocytes: a comparison between normal and infectious conditions. *Tissue Antigens.* (2004) 64:235–42. doi: 10.1111/j.1399-0039.2004.00271.x
68. Gutierrez-Lopez MD, Ovalle S, Yanez-Mo M, Sanchez-Sanchez N, Rubinstein E, Olmo N., et al. A functionally relevant conformational epitope on the CD9 tetraspanin depends on the association with activated beta1 integrin. *J Biol Chem.* (2003) 278:208–18. doi: 10.1074/jbc.M207805200
69. Florin L, Lang T. Tetraspanin assemblies in virus infection. *Front Immunol.* (2018) 9:1140. doi: 10.3389/fimmu.2018.01140
70. Schittenhelm L, Hilkens CM, Morrison VL. Beta2 integrins as regulators of dendritic cell, monocyte, and macrophage function. *Front Immunol.* (2017) 8:1866. doi: 10.3389/fimmu.2017.01866
71. Rossi D, Zlotnik A. The biology of chemokines and their receptors. *Ann Rev Immunol.* (2000) 18:217–42. doi: 10.1146/annurev.immunol.18.1.217
72. Demberg T, Mohanram V, Venzon D, Robert-Guroff M. Phenotypes and distribution of mucosal memory B-cell populations in the SIV/SHIV rhesus macaque model. *Clin Immunol.* (2014) 153:264–76. doi: 10.1016/j.clim.2014.04.017
73. Lee HS, Kim HR, Lee EH, Jang MH, Kim SB, Park JW., et al. Characterization of CCR9 expression and thymus-expressed chemokine responsiveness of the murine thymus, spleen and mesenteric lymph node. *Immunobiology* (2012) 217:402–11. doi: 10.1016/j.imbio.2011.10.014
74. Amiya T, Nakamoto N, Chu PS, Teratani T, Nakajima H, Fukuchi Y., et al. Bone marrow-derived macrophages distinct from tissue-resident macrophages play a pivotal role in concanavalin a-induced murine liver injury via CCR9 axis. *Sci Rep.* (2016) 6:35146. doi: 10.1038/srep35146
75. Mizuno S, Kanai T, Mikami Y, Sujino T, Ono Y, Hayashi A., et al. CCR9+ plasmacytoid dendritic cells in the small intestine suppress development of intestinal inflammation in mice. *Immunol Lett.* (2012) 146:64–9. doi: 10.1016/j.imlet.2012.05.001
76. Stein JV, Nombela-Arrieta C. Chemokine control of lymphocyte trafficking: a general overview. *Immunology* (2005) 116:1–12. doi: 10.1111/j.1365-2567.2005.02183.x
77. Wurbel MA, Malissen M, Guy-Grand D, Meffre E, Nussenzweig MC, Richelme M., et al. Mice lacking the CCR9 CC-chemokine receptor show a mild impairment of early T- and B-cell development and a reduction in T-cell receptor gammadelta(+) gut intraepithelial lymphocytes. *Blood* (2001) 98:2626–32. doi: 10.1182/blood.V98.9.2626
78. Mora JR, von Andrian UH. Differentiation and homing of IgA-secreting cells. *Mucosal Immunol.* (2008) 1:96–109. doi: 10.1038/mi.2007.14
79. Holness CL, da Silva RP, Fawcett J, Gordon S, Simmons DL. Macrosialin, a mouse macrophage-restricted glycoprotein, is a member of the lamp/lgp family. *J Biol Chem.* (1993) 268:9661–6.
80. Gordon S. Macrophage-restricted molecules: role in differentiation and activation. *Immunol Lett.* (1999) 65:5–8. doi: 10.1016/S0165-2478(98)00116-3
81. Gottfried E, Kunz-Schughart LA, Weber A, Rehli M, Peuker A, Müller A., et al. Expression of CD68 in non-myeloid cell types. *Scand J Immunol.* (2008) 67:453–63. doi: 10.1111/j.1365-3083.2008.02091.x
82. Kunisch E, Fuhrmann R, Roth A, Winter R, Lungershausen W, Kinne RW. Macrophage specificity of three anti-CD68 monoclonal antibodies (KP1, EBM11, and PGM1) widely used for immunohistochemistry and flow cytometry. *Ann Rheum Dis.* (2004) 63:774–84. doi: 10.1136/ard.2003.013029
83. O'Reilly D, Greaves DR. Cell-type-specific expression of the human CD68 gene is associated with changes in Pol II phosphorylation and short-range intrachromosomal gene looping. *Genomics* (2007) 90:407–15. doi: 10.1016/j.ygeno.2007.04.010
84. Fennelly JA, Tiwari B, Davis SJ, Evans EJ. CD2F-10: a new member of the CD2 subset of the immunoglobulin superfamily. *Immunogenetics* (2001) 53:599–602. doi: 10.1007/s002510100364
85. Zhang W, Wan T, Li N, Yuan Z, He L, Zhu X., et al. Genetic approach to insight into the immunobiology of human dendritic cells and identification of CD84-H1, a novel CD84 homologue. *Clin Cancer Res.* (2001) 7(Suppl. 3):822–9s.
86. De Salort J, Sintes J, Llinàs L, Matesanz-Isabel J, Engel P. Expression of SLAM (CD150) cell-surface receptors on human B-cell subsets: from pro-B to plasma cells. *Immunol Lett.* (2011) 134:129–36. doi: 10.1016/j.imlet.2010.09.021
87. Schwartzberg PL, Mueller KL, Qi H, Cannons JL. SLAM receptors and SAP influence lymphocyte interactions, development and function. *Nat Rev Immunol.* (2009) 9:39. doi: 10.1038/nri2456
88. Reuning U, Magdolen V, Hapke S, Schmitt M. Molecular and functional interdependence of the urokinase-type plasminogen activator system with integrins. *Biol Chem.* (2003) 384:1119–31. doi: 10.1515/BC.2003.125
89. Ge Y, Elghetany MT. Urokinase plasminogen activator receptor (CD87): something old, something new. *Lab Hematol.* (2003) 9:67–71.
90. Plesner T, Behrendt N, Ploug M. Structure, function and expression on blood and bone marrow cells of the urokinase-type plasminogen activator receptor. *uPA*Stem Cells *R* (1997) 15:398–408. doi: 10.1002/stem.150398
91. Elghetany MT, Patel J, Martinez J, Schwab H. CD87 as a marker for terminal granulocytic maturation: assessment of its expression during granulopoiesis. *Cytometry B Clin Cytom.* (2003) 51:9–13. doi: 10.1002/cyto.b.10008

92. Jardí M, Inglés-Esteve J, Burgal M, Azqueta C, Velasco F, López-Pedrera C., et al. Distinct patterns of urokinase receptor (uPAR) expression by leukemic cells and peripheral blood cells. *Thromb Haemost*. (1996) 76:1009–19.
93. Schwandner R, Dziarski R, Wesche H, Rothe M, Kirschning CJ. Peptidoglycan- and lipoteichoic acid-induced cell activation is mediated by toll-like receptor 2. *J Biol Chem*. (1999) 274:17406–9. doi: 10.1074/jbc.274.25.17406
94. Flo TH, Halaas O, Torp S, Ryan L, Lien E, Dybdahl B., et al. Differential expression of Toll-like receptor 2 in human cells. *J Leukoc Biol*. (2001) 69:474–81. doi: 10.1189/jlb.69.3.474
95. Lee SM, Joo YD, Seo SK. Expression and Function of TLR2 on CD4 Versus CD8 T Cells. *Immune Netw*. (2009) 9:127–32. doi: 10.4110/in.2009.9.4.127
96. Bleesing JJ, Fleisher TA. Human B cells express a CD45 isoform that is similar to murine B220 and is downregulated with acquisition of the memory B-cell marker CD27. *Cytometry B Clin Cytom*. (2003) 51:1–8. doi: 10.1002/cyto.b.10007
97. Dasari P, Nicholson IC, Hodge G, Dandie GW, Zola H. Expression of toll-like receptors on B lymphocytes. *Cell Immunol*. (2005) 236:140–5. doi: 10.1016/j.cellimm.2005.08.020
98. Booth J, Wilson H, Jimbo S, Mutwiri G. Modulation of B cell responses by Toll-like receptors. *Cell Tissue Res*. (2011) 343:131–40. doi: 10.1007/s00441-010-1031-3
99. Kobayashi I, Katakura F, Moritomo T. Isolation and characterization of hematopoietic stem cells in teleost fish. *Dev Comp Immunol*. (2016) 58:86–94. doi: 10.1016/j.dci.2016.01.003
100. Geisberger R, Lamers M, Achatz G. The riddle of the dual expression of IgM and IgD. *Immunology* (2006) 118:429–37. doi: 10.1111/j.1365-2567.2006.02386.x
101. Edholm ES, Bengten E, Wilson M. Insights into the function of IgD. *Dev Comp Immunol*. (2011) 35:1309–16. doi: 10.1016/j.dci.2011.03.002
102. Gutzeit C, Chen K, Cerutti A. The enigmatic function of IgD: some answers at last. *Eur J Immunol*. (2018) 48:1101–13. doi: 10.1002/eji.201646547
103. Ramirez-Gomez F, Greene W, Rego K, Hansen JD, Costa G, Kataria P., et al. Discovery and characterization of secretory IgD in rainbow trout: secretory IgD is produced through a novel splicing mechanism. *J Immunol*. (2012) 188:1341–9. doi: 10.4049/jimmunol.1101938
104. Ye H, Lin Q, Luo H. Applications of transcriptomics and proteomics in understanding fish immunity. *Fish Shellfish Immunol*. (2018) 77:319–27. doi: 10.1016/j.fsi.2018.03.046
105. Braceland M, Bickerdike R, Tinsley J, Cockerill D, Mcloughlin MF, Graham DA., et al. The serum proteome of Atlantic salmon, Salmo salar, during pancreas disease (PD) following infection with salmonid alphavirus subtype 3 (SAV3). *J Proteomics* (2013) 94:423–36. doi: 10.1016/j.jprot.2013.10.016
106. Elschenbroich S, Kim Y, Medin JA, Kislinger T. Isolation of cell surface proteins for mass spectrometry-based proteomics. *Expert Rev Proteomics* (2010) 7:141–54. doi: 10.1586/epr.09.97
107. Schiess R, Mueller LN, Schmidt A, Mueller M, Wollscheid B, Aebersold R. Analysis of cell surface proteome changes via label-free, quantitative mass spectrometry. *Mol Cell Proteomics* (2009) 8:624–38. doi: 10.1074/mcp.M800172-MCP200
108. Ma C, Ye J, Kaattari SL. Differential compartmentalization of memory B cells versus plasma cells in salmonid fish. *Eur J Immunol*. (2013) 43:360–70. doi: 10.1002/eji.201242570
109. Crawford K, Gabuzda D, Pantazopoulos V, Xu J, Clement C, Reinherz E., et al. Circulating CD2+ monocytes are dendritic cells. *J Immunol*. (1999) 163:5920–8.
110. Eto H, Ishimine H, Kinoshita K, Watanabe-Susaki K, Kato H, Doi K., et al. Characterization of human adipose tissue-resident hematopoietic cell populations reveals a novel macrophage subpopulation with CD34 expression and mesenchymal multipotency. *Stem Cells Dev*. (2013) 22:985–97. doi: 10.1089/scd.2012.0442
111. Stumptner-Cuvelette P, Benaroch P. Multiple roles of the invariant chain in MHC class II function. *Biochim Biophys Acta* (2002) 1542:1–13. doi: 10.1016/S0167-4889(01)00166-5
112. Champion TC, Partridge LJ, Ong SM, Malleret B, Wong SC, Monk PN. Monocyte subsets have distinct patterns of tetraspanin expression and different capacities to form multinucleate giant cells. *Front Immunol*. (2018) 9:1247. doi: 10.3389/fimmu.2018.01247
113. Bonifaz L, Bonnyay D, Mahnke K, Rivera M, Nussenzweig MC, Steinman RM. Efficient targeting of protein antigen to the dendritic cell receptor DEC-205 in the steady state leads to antigen presentation on major histocompatibility complex class I products and peripheral CD8+ T cell tolerance. *J Exp Med*. (2002) 196:1627–38. doi: 10.1084/jem.20021598
114. Bühring HJ, Simmons PJ, Pudney M, Müller R, Jarrossay D, van Agthoven A., et al. The monoclonal antibody 97A6 defines a novel surface antigen expressed on human basophils and their multipotent and unipotent progenitors. *Blood* (1999) 94:2343–56.
115. Castro R, Abós B, González L, Aquilino C, Pignatelli J, Tafalla C. Molecular characterization of CD9 and CD63, two tetraspanin family members expressed in trout B lymphocytes. *Dev Comp Immunol*. (2015) 51:116–25. doi: 10.1016/j.dci.2015.03.002
116. Li Y-Q, Zhang J, Li J, Sun L. First characterization of fish CD22: An inhibitory role in the activation of peripheral blood leukocytes. *Vet Immunol Immunopathol*. (2017) 190:39–44. doi: 10.1016/j.vetimm.2017.07.006
117. Xu H, Liew LN, Kuo IC, Huang CH, Goh DL, Chua KY. The modulatory effects of lipopolysaccharide-stimulated B cells on differential T-cell polarization. *Immunology* (2008) 125:218–28. doi: 10.1111/j.1365-2567.2008.02832.x
118. Kehrl JH, Fauci AS. Identification, purification, and characterization of antigen-activated and antigen-specific human B lymphocytes. *Trans Assoc Am Physicians* (1983) 96:182–7.
119. Gong YF, Xiang LX, Shao JZ. CD154-CD40 interactions are essential for thymus-dependent antibody production in zebrafish: insights into the origin of costimulatory pathway in helper T cell-regulated adaptive immunity in early vertebrates. *J Immunol*. (2009) 182:7749–62. doi: 10.4049/jimmunol.0804370
120. Chapman HA, Wei Y, Simon DI, Waltz DA. Role of urokinase receptor and caveolin in regulation of integrin signaling. *Thromb Haemost*. (1999) 82:291–7.
121. Tarui T, Mazar AP, Cines DB, Takada Y. Urokinase-type plasminogen activator receptor (CD87) is a ligand for integrins and mediates cell-cell interaction. *J Biol Chem*. (2001) 276:3983–90. doi: 10.1074/jbc.M008220200
122. Vuillier F, Scott-Algara D, Dighiero G. Extensive analysis of lymphocyte subsets in normal subjects by three-color immunofluorescence. *Nouv Rev Fr Hematol*. (1991) 33:31–8.
123. Blanc P, Moro-Sibilot L, Barthly L, Jagot F, This S, de Bernard S., et al. Mature IgM-expressing plasma cells sense antigen and develop competence for cytokine production upon antigenic challenge. *Nat Commun*. (2016) 7:13600. doi: 10.1038/ncomms13600
124. Racine R, McLaughlin M, Jones DD, Wittmer ST, MacNamara KC, Woodland DL., et al. IgM production by bone marrow plasmablasts contributes to long-term protection against intracellular bacterial infection. *J Immunol*. (2011) 186:1011–21. doi: 10.4049/jimmunol.1002836
125. Agematsu K. Memory B cells and CD27. *Histol Histopathol*. (2000) 15:573–6. doi: 10.14670/HH-15.573
126. Chilosi M, Adami F, Lestani M, Montagna L, Cimarosto L, Semenzato G., et al. CD138/syndecan-1: a useful immunohistochemical marker of normal and neoplastic plasma cells on routine trephine bone marrow biopsies. *Mod Pathol*. (1999) 12:1101–6.
127. Bromage ES, Kaattari IM, Zwollo P, Kaattari SL. Plasmablast and plasma cell production and distribution in trout immune tissues. *J Immunol*. (2004) 173:7317–23. doi: 10.4049/jimmunol.173.12.7317
128. Herren B, Burrows PD. B cell-restricted human mb-1 gene: expression, function, and lineage infidelity. *Immunol Res*. (2002) 26:35–43. doi: 10.1385/IR:26:1-3:035
129. Sathish JG, Walters J, Luo JC, Johnson KG, Leroy FG, Brennan P., et al. CD22 is a functional ligand for SH2 domain-containing protein-tyrosine phosphatase-1 in primary T cells. *J Biol Chem*. (2004) 279:47783–91. doi: 10.1074/jbc.M402354200
130. Toba K, Hanawa H, Fuse I, Sakaue M, Watanabe K, Uesugi Y., et al. Difference in CD22 molecules in human B cells and *basophils. Exp Hematol*. (2002) 30:205–11. doi: 10.1016/S0301-472X(01)00791-3
131. Wen T, Mingler MK, Blanchard C, Wahl B, Pabst O, Rothenberg ME. The pan-B cell marker CD22 is expressed on gastrointestinal eosinophils and

negatively regulates tissue eosinophilia. *J Immunol.* (2012) 188:1075–82. doi: 10.4049/jimmunol.1102222
132. Luger D, Yang YA, Raviv A, Weinberg D, Banerjee S, Lee MJ., et al. Expression of the B-cell receptor component CD79a on immature myeloid cells contributes to their tumor promoting effects. *PLoS ONE* (2013) 8:e76115. doi: 10.1371/journal.pone.0076115
133. Bhargava P, Kallakury BV, Ross JS, Azumi N, Bagg A. CD79a is heterogeneously expressed in neoplastic and normal myeloid precursors and megakaryocytes in an antibody clone-dependent manner. *Am J Clin Pathol.* (2007) 128:306–13. doi: 10.1309/UXCDG9PWN7G89Y54
134. Warren IA, Ciborowski KL, Casadei E, Hazlerigg DG, Martin S, Jordan WC., et al. Extensive local gene duplication and functional divergence among paralogs in Atlantic salmon. *Genome Biol Evol.* (2014) 6:1790–1805. doi: 10.1093/gbe/evu131
135. Lien S, Koop BF, Sandve SR, Miller JR, Kent MP, Nome T., et al. The Atlantic salmon genome provides insights into rediploidization. *Nature* (2016) 533:200. doi: 10.1038/nature17164
136. Coffman RL, Weissman IL. B220: a B cell-specific member of the T200 glycoprotein family. *Nature* (1981) 289:681. doi: 10.1038/289681a0
137. Hardy RR, Hayakawa K. B Cell Development Pathways. *Ann Rev Immunol.* (2001) 19:595–621. doi: 10.1146/annurev.immunol.19.1.595
138. Rodig SJ, Shahsafaei A, Li B, Dorfman DM. The CD45 isoform B220 identifies select subsets of human B cells and B-cell lymphoproliferative disorders. *Hum Pathol.* (2005) 36:51–7. doi: 10.1016/j.humpath.2004.10.016
139. Zikherman J, Weiss A. Alternative splicing of CD45: the tip of the iceberg. *Immunity* (2008) 29:839–41. doi: 10.1016/j.immuni.2008.12.005
140. Yoon SO, Zhang X, Lee IY, Spencer N, Vo P, Choi YS. CD9 is a novel marker for plasma cell precursors in human germinal centers. *Biochem Biophys Res Commun.* (2013) 431:41–6. doi: 10.1016/j.bbrc.2012.12.102
141. Won WJ, Kearney JF. CD9 is a unique marker for marginal zone B cells, B1 cells, and plasma cells in mice. *J Immunol.* (2002) 168:5605–11. doi: 10.4049/jimmunol.168.11.5605
142. Bao Y, Liu X, Han C, Xu S, Xie B, Zhang Q., et al. Identification of IFN-gamma-producing innate B cells. *Cell Res.* (2014) 24:161–76. doi: 10.1038/cr.2013.155
143. Winslow GM, Papillion Am, Kenderes KJ, Levack RC. CD11c+ T-bet+ memory B cells: Immune maintenance during chronic infection and inflammation? *Cell Immunol.* (2017) 321:8–17. doi: 10.1016/j.cellimm.2017.07.006
144. Karnell JL, Kumar V, Wang J, Wang S, Voynova E, Ettinger R. Role of CD11c(+) T-bet(+) B cells in human health and disease. *Cell Immunol.* (2017) 321:40–45. doi: 10.1016/j.cellimm.2017.05.008
145. Racine R, Chatterjee M, Winslow GM. CD11c expression identifies a population of extrafollicular antigen-specific splenic plasmablasts responsible for CD4 T-independent antibody responses during intracellular bacterial infection. *J Immunol.* (2008) 181:1375–85. doi: 10.4049/jimmunol.181.2.1375
146. Ghosn EE, Yang Y, Tung J, Herzenberg LA, Herzenberg LA. CD11b expression distinguishes sequential stages of peritoneal B-1 development. *Proc Natl Acad Sci USA.* (2008) 105:5195–200. doi: 10.1073/pnas.0712350105
147. Santos L, Draves KE, Boton M, Grewal PK, Marth JD, Clark EA. Dendritic cell-dependent inhibition of B cell proliferation requires CD22. *J Immunol.* (2008) 180:4561–9. doi: 10.4049/jimmunol.180.7.4561
148. Scapigliati G, Fausto AM, Picchietti S. Fish lymphocytes: an evolutionary equivalent of mammalian innate-like lymphocytes? *Front Immunol.* (2018) 9:971. doi: 10.3389/fimmu.2018.00971

Conflict of Interest Statement: The authors declare that the research was conducted in the absence of any commercial or financial relationships that could be construed as a potential conflict of interest.

Copyright © 2019 Peñaranda, Jensen, Tollersrud, Bruun and Jørgensen. This is an open-access article distributed under the terms of the Creative Commons Attribution License (CC BY). The use, distribution or reproduction in other forums is permitted, provided the original author(s) and the copyright owner(s) are credited and that the original publication in this journal is cited, in accordance with accepted academic practice. No use, distribution or reproduction is permitted which does not comply with these terms.

frontiers in Immunology

REVIEW
published: 05 February 2019
doi: 10.3389/fimmu.2019.00153

Comparative Study of Immune Reaction Against Bacterial Infection From Transcriptome Analysis

Shun Maekawa[1], *Pei-Chi Wang*[1,2*] *and Shih-Chu Chen*[1,2,3,4*]

[1] *Department of Veterinary Medicine, College of Veterinary Medicine, National Pingtung University of Science and Technology, Pingtung, Taiwan,* [2] *Southern Taiwan Fish Disease Centre, College of Veterinary Medicine, National Pingtung University of Science and Technology, Pingtung, Taiwan,* [3] *International Degree Program of Ornamental Fish Technology and Aquatic Animal Health, International College, National Pingtung University of Science and Technology, Pingtung, Taiwan,* [4] *Research Center for Animal Biologics, National Pingtung University of Science and Technology, Pingtung, Taiwan*

OPEN ACCESS

Edited by:
Hetron Mweemba Munang'andu, Norwegian University of Life Sciences, Norway

Reviewed by:
Ming-Wei Lu, National Taiwan Ocean University, Taiwan
Syarul Nataqain Baharum, National University of Malaysia, Malaysia

***Correspondence:**
Pei-Chi Wang
pc921003@gmail.com
Shih-Chu Chen
scchen@mail.npust.edu.tw

Specialty section:
This article was submitted to Comparative Immunology, a section of the journal Frontiers in Immunology

Received: *29 October 2018*
Accepted: *17 January 2019*
Published: *05 February 2019*

Citation:
Maekawa S, Wang P-C and Chen S-C (2019) Comparative Study of Immune Reaction Against Bacterial Infection From Transcriptome Analysis. Front. Immunol. 10:153. doi: 10.3389/fimmu.2019.00153

Transcriptome analysis is a powerful tool that enables a deep understanding of complicated physiological pathways, including immune responses. RNA sequencing (RNA-Seq)-based transcriptome analysis and various bioinformatics tools have also been used to study non-model animals, including aquaculture species for which reference genomes are not available. Rapid developments in these techniques have not only accelerated investigations into the process of pathogenic infection and defense strategies in fish, but also used to identify immunity-related genes in fish. These findings will contribute to fish immunotherapy for the prevention and treatment of bacterial infections through the design of more specific and effective immune stimulants, adjuvants, and vaccines. Until now, there has been little information regarding the universality and diversity of immune reactions against pathogenic infection in fish. Therefore, one of the aims of this paper is to introduce the RNA-Seq technique for examination of immune responses in pathogen-infected fish. This review also aims to highlight comparative studies of immune responses against bacteria, based on our previous findings in largemouth bass (*Micropterus salmoides*) against *Nocardia seriolae,* gray mullet (*Mugil cephalus*) against *Lactococcus garvieae,* orange-spotted grouper (*Epinephelus coioides*) against *Vibrio harveyi*, and koi carp (*Cyprinus carpio*) against *Aeromonas sobria*, using RNA-seq techniques. We demonstrated that only 39 differentially expressed genes (DEGs) were present in all species. However, the number of specific DEGs in each species was relatively higher than that of common DEGs; 493 DEGs in largemouth bass against *N. seriolae*, 819 DEGs in mullets against *L. garvieae*, 909 in groupers against *V. harveyi*, and 1471 in carps against *A. sobria.* The DEGs in different fish species were also representative of specific immune-related pathways. The results of this study will enhance our understanding of the immune responses of fish, and will aid in the development of effective vaccines, therapies, and disease-resistant strains.

Keywords: transcriptome, RNA-Seq, immune response, fish disease, bacteria

INTRODUCTION

Transcriptome analysis is used to study principal pathways of development, cellular fate, physiology, activity, and disease progression. RNA sequencing (RNA-Seq) is a modern technology for transcriptome profiling that uses next-generation sequencing (NGS). Advancements in bioinformatics has significantly supported RNA-Seq technology to accelerate the knowledge on transcriptomes (1).

In the aquaculture field, there is wide utility for RNA-Seq in various applications, such as understanding the development of embryo and larvae, toxicology, environmental stress, effect of dietary conditions, and discovery of novel transcripts (2–4). In addition, RNA-Seq has been used in many studies of fish immunology (5, 6). Pathogenic infection is a major concern for maintaining economic sustainability in natural and farmed fish; it results in high mortality and economical loss in aquaculture. An innate immunity is a front line of host defense, producing effectors that directly to the pathogen and attack it. An adaptive immune system is also present in teleost, including humoral and cellular mechanisms. To reduce disease outbreaks, it is essential to understand the immune mechanisms in fish during pathogenic infections. This knowledge will support the development of effective vaccines and adjuvants against pathogens. However, it has not been reported that the universality and diversity of immune reactions against pathogenic infection in fish.

In this paper, we firstly introduce the RNA-Seq technique and current knowledge for investigations of immune responses in pathogen-infected fish. This review also aims to highlight comparative studies of fish immune responses against bacteria based on our previous studies that we demonstrated the transcriptome of bacteria infected fish, largemouth bass (*Micropterus salmoides*) against *Nocardia seriolae,* gray mullet (*Mugil cephalus*) against *Lactococcus garvieae,* orange-spotted grouper (*Epinephelus coioides*) against *Vibrio harveyi*, and koi carp (*Cyprinus carpio*) against *Aeromonas sobria*.

ADVANTAGE OF RNA-seq ANALYSIS IN FISH AQUACULTURE

Since the 2000s, hybridization-based microarray has been used to examine fish immunology in aquacultures; some early examples included Japanese flounder (*Paralichthys olivaceus*) (7), rainbow trout (*Oncorhynchus mykiss*) (8), and Atlantic salmon (*Salmo salar*) (9). Although species-specific probes should be designed, microarray technology could provide us with high throughput gene expression data. For transcriptome analysis, series analysis of gene expression (SAGE) and cap analysis gene expression (CAGE) have also been utilized. SAGE and CAGE, which are tag-based technology, are more precise; however, the number of genes that can be analyzed at one time is lower as compared with that of microarrays. Recently, the number of reports that uses RNA-Seq in aquaculture studies has rapidly increased. For the complete detail of RNA-Seq methodology, please refer the nicely reviews focused on aquaculture field (3, 6). The advantage of RNA-Seq is that it could determine expression levels of low-level transcripts as well as each splice variant isoforms. Current focus in aquaculture fish research is to examine organisms that do not process reference gene sequences; unigenes are obtained via *de novo* assembly using Trinity or similar programs without requiring reference gene sequences (10). RNA-Seq could provide novel transcript sequences, thereby expanding our current list of known transcripts in fish.

ANNOTATION, ENRICHMENT ANALYSIS, AND PATHWAY ANALYSIS USING *DE NOVO* ASSEMBLY DATA

Although RNA-Seq technology could be applied to non-model animals, there are problems associated with the functional annotation and enrichment analysis of transcripts data. Transcripts sequences following assembly are usually searched via several databases, such as NCBI nucleotide sequences (NT), NCBI non-redundant protein (NR), Clusters of Orthologous Groups (COGs) (11), Kyoto Encyclopedia of Genes and Genomes (KEGG) (12, 13), gene ontology (GO) (14), and InterPro annotation (15). In our previous study on orange-spotted grouper (*Epinephelus coioides*), a total of 79,128 unigenes were identified and aligned with each database; 58,926 (74.47%) in NT, 43,576 (55.07%) in NR, 14,750 (18.64%) in COG, 34711 (43.87%) in KEGG, and 4232 (5.35%) in GO (16). The number of genes aligned with existing genes in the database was the highest in NT, while gene alignment was the lowest in GO. Differences in the number of aligned genes between the databases were similar to those found in other aquaculture studies (17–19). Although the GO database could provide enrichment analysis and pathway analysis, due to low gene alignment, results may be limited to generalized conclusions. There are programs that can convert gene IDs from one database to those of another database. For example, DAVID and ID Converter Systems are able to change gene IDs from NT to that of GO. However, these systems are not very useful in genes of aquaculture species. Currently, the KEGG database shows a relatively high number of aligned genes, which allows for enrichment analysis of aquaculture species. To obtain generalized conclusions using transcriptome data, it is essential that systems are developed to describe non-model organisms. There are databases now under construction that contain transcriptome information of aquaculture species. In the European common carp (*Cyprinus carpio*), a wide range of data on tissue-specific gene expression and translation (20) has been presented. These datasets will allow us to investigate immune responses in aquaculture species via transcriptome analysis.

IMMUNE RESPONSES AGAINST PATHOGENS IN TELEOST USING RNA-seq

Although fish are constantly exposed to risk of microorganism pathogens, fish could keep in shape to act immune mechanisms against pathogens. In a first line of immune response, fish are protected by non-specific humoral factors including growth inhibiting substances (transferrin and antiproteases), lysins

(lysozyme, C-reactive protein, and bactericidal peptides), and making a link with non-specific phagocyte responses. Second, fish produce antibody constitutes for a specific humoral defense inhibiting bacterial adherence and invasion of non-phagocytic host cells and counteracting toxins from bacterial (21). After developing the technology of molecular biology, the immune-related gene functions and responses against pathogens have been one of the major topic in fish immunology field. To investigate the expression pattern of immune-associated genes, real-time PCR is usually performed. However, this method is expensive and not recommended for a genome-wide survey of gene expression. As RNA-Seq could provide us with quantitative data on transcript expression levels, this technique has been commonly used to identify genes that respond to pathogenic conditions during exogenous challenge. **Table 1** lists transcriptome analysis studies that examined immune regulations in teleost. In this review, we will also focus on studies that investigated immune responses to pathogen or their mimic molecules, using RNA-Seq analysis.

Aeromonus hydrophila is a Gram-negative bacterium, and causes a wide spectrum of diseases in vertebrates (69, 70). It is a major pathogen in aquaculture farms, and leads to high mortalities and economic losses worldwide (71, 72). In blunt snout bream (*Megalobrama amblycephala*), RNA-Seq analysis was conducted with RNA from several tissues, and 238 differentially expressed unigenes were identified in infected fish (22). In grass carp (*Ctenopharygodon idella*), 2121 DEGs were identified in spleens of *A. hydrophila* (6 hpi)-infected fish, some of which were involved in phagocytosis, the complement system, and cytokine production (25). Using transcriptome analysis, another study showed that *A. hydrophila* infected grass carp exhibited 2992 DEGs in the spleen, which were associated with the complement and coagulation cascades (26). In golden mahseer (*Tor putitora*), DEGs in *A. hydrophila*-infected livers were mainly associated with Th1/2 cell differentiation pathways, as well as in pathogen recognition and complement system (24).

Flavobacterium columnare is a Gram-negative bacterium, and causes columnaris in freshwater fish (73). This disease induces pathological changes, and damages epidermal tissues, gills, and the skin (74). In channel catfish (*Ictalurus punctatus*), the transcript profile of *F. columnare*-infected gills was examined using RNA-Seq to investigate differences in susceptibility to *F. columnare* (34). In resistant fish, the expression level of innate immune-associated genes (iNOS2b, lysozyme C, IL-8, and TNFα) was found to be elevated. In susceptible fish, the expression of secreted mucin forms, mucosal immune factors (CD103 and IL-17a), and rhamnose-binding lectin (34) was upregulated. The transcriptomic profiles of *F. columnare*-infected and non-infected mandarin fish (*Siniperca chuatsi*) have been reported using the head kidney *F. columnare*-infected and non-infected group (35). The results indicated that 1019 genes were differentially expressed between the two groups, of which 27 were immune-related (35). A similar study using the head kidney *F. columnare*-infected topmouth culter (*Culter alburnus*) (36) was also conducted. A total of 4037 DEGs (1217 upregulated and 2820 downregulated genes) were identified, and were found to be involved in phagosome formation, carbohydrate metabolism, amino acid metabolism, and lipid metabolism (36).

Streptococcus agalactiae, a Gram-positive round bacterium, is a harmful aquaculture pathogen that leads to enormous economic losses in various teleost (75–78). Transcriptome analysis of hybrid tilapia (*Oreochromis* spp.) after *S. agalactiae* infection was conducted, and results indicated that DEGs are mainly involved in immune-related pathways, especially Toll-like receptor signaling and leukocyte transendothelial migration (49). Moreover, time-course expression profile of genes suggested that induction of the NADPH oxidase complex and piscidin is mediated by Toll-like receptor pathways (49). Another research group conducted RNA-Seq analysis in tilapia (*Oreochromis niloticus*) spleens following *S. agalactiae* infections (51). A total of 2822 DEGs were detected, many of which were involved in pathogen attachment and recognition, antioxidant/apoptosis, cytoskeletal rearrangement, and immune activation (51). Wang et al. (50) focused on the relation between temperature and bacterial infection. They showed that temperature influences mRNA profiles of the spleen in tilapia during *S. agalactiae* infections. In addition, it was suggested that DEGs are involved in immune responses and oxygen related metabolisms (50).

Vibrio alginolyticus is a halophilic Gram-negative bacterium that causes septicemias, ulcers, exophthalmia, and corneal opaqueness in marine fish worldwide (79, 80). Transcriptome analysis in larvae of orange-spotted grouper (*Epinephelus coioides*) revealed that the expression of genes involved in the complement pathway and antimicrobial peptides is enhanced upon *V. alginolyticus* infection (39). In addition, transcriptome profiles of giant grouper (*Epinephelus lanceolatus*) larvae infected with *Vibrio alginolyticus* suggested that TLR5 signaling induces secretion of several cytokines (IL-1β and IL-8) (40).

DIVERSITY OF IMMUNE RESPONSES AMONG SPECIES AND PATHOGENS

In the previous section, we introduced various RNA-seq analyses conducted in fish with bacterial infections. We have also previously published **four** research papers that conducted transcriptome analysis on infected fish, namely largemouth bass (*Micropterus salmoides*) against *Nocardia seriolae* (17), gray mullet (*Mugil cephalus*) against *Lactococcus garvieae* (18), orange-spotted grouper (*Epinephelus coioides*) against *Vibrio harveyi* (16), and koi carp (*Cyprinus carpio*) against *Aeromonas sobria* (19). Based on the transcriptome data from these reports, we gained a deeper understanding of immune responses to bacterial infections. However, there is little information regarding the universality and diversity of immune reactions of fish against pathogenic infections. Here, we investigated specific genes and pathways that are involved in each bacterial infection in various fish species. In this study, we used DEGs (transcripts from spleen at 1 dpi with $\log2 > 1$ or < -1 between infected and control group) with KEGG-annotations. We **first** identified overlapping and specific genes that were up- or down- regulated in each species. Venn diagrams (**Figure 1**) showed that only 39 DEGs (25 up-regulated and 14 down regulated) were involved in all species. The number of specific DEGs in each species was

TABLE 1 | List of Transcriptome report in immune systems of teleost.

Pathogen or stimulator	Fish	Target tissue or cell	Responding genes and pathways	References
GRAM-NEGATIVE BACTERIA				
Aeromonas hydrophila	Blunt snout bream (*Megalobrama amblycephala*)	Mixture of RNA sample form tissues	Toll-like receptor signaling, complement cascade.	(22)
Aeromonas hydrophila	Darkbarbel catfish (*Pelteobagrus vachellii*)	Spleen	Complement and coagulation cascades, pattern recognition pathways, Nk cell mediated cytotoxicity, Fcγ receptor-mediated phagocytosis, B cell and T cell receptor signaling pathway.	(23)
Aeromonas hydrophila	Golden mahseer (*Tor putitora*)	Liver	Th1 and 2 cell differentiation, pathogen recognition, complement cascade pathways.	(24)
Aeromonas hydrophila	Grass carp (*Ctenopharygodon idella*)	Spleen	Antigen processing and presentation, Phagocytosis, Complement system, Cytokines	(25)
Aeromonas hydrophila	Grass carp (*Ctenopharyngodon idella*)	Spleen	Complement and coagulation cascades pathway.	(26)
Aeromonas salmonicida	Rainbow trout (*Oncorhynchus mykiss*)	Spleen	Hematopoietic cell lineage and complement and coagulation cascades.	(27)
Aeromonas sobria	Koi Carp (*Cyprinus carpio*)	Muscle, spleen	Toll-like receptor signaling and complement cascade pathway.	(19)
Edwardsiella ictaluri	Yellow catfish (*Pelteobagrus fulvidraco*)	Spleen	DEGs linked to several innate and adaptive immune related pathways.	(28)
Edwardsiella tarda	Japanese flounder (*Paralichthys olivaceus*)	Blood	A total of 30 immune related DEGs were extracted based on protein–protein interaction networks.	(29)
Edwardsiella tarda	Japanese flounder (*Paralichthys olivaceus*)	Gill	Based on protein–protein interaction networks, 24 genes were found as key regulators in immune responses.	(30)
Edwardsiella tarda	Japanese flounder (*Paralichthys olivaceus*)	Kidney	PI3K family, antigen processing and presentation.	(31)
Edwardsiella tarda (mutant with low virulence)	Zebrafish (*Danio rerio*)	Liver	Complement activation, antigen processing and presentation pathway.	(32)
Escherichia coli (Heat-killed)	Black rockcod (*Notothenia coriiceps*)	Liver	MHC class I and II antigen-processing moleules.	(33)
Flavobacterium columnare	Channel catfish (*Ictalurus punctatus*)	Gill	Innate immune genes (iNOS2b, lysozyme C, IL-8, and TNF-α) and mucosal immuen factors (CD103 and IL-17)	(34)
Flavobacterium columnare	Mandarin fish (*Siniperca chuatsi*)	Head kidney	Upregulated cytokine genes (IL-1β, IL-8, CXCL14, CCK3, CCL25, Angpt1, Thpo, MMP-9)	(35)
Flavobacterium columnare	Topmouth culter (*Culter alburnus*)	Head kidney	Phagosome pathway, complement activation	(36)
Piscirickettsia salmonis	Atlantic salmon (*Salmo salar*)	Brain, head kidney, spleen	Endocytosis, Phagosome, Heme metabolism	(37)
Pseudomonas fluorescens	Whitefish (*Coregnous palaea*)	Embryo	Ion binding, aminoacyl-tRNA-biosynthesis, complement cascade, MHC class I and II, TNF-α, T-cell differentiation.	(38)
Vibrio alginolyticus	Orange-spotted grouper (*Epinephelus coioides*)	Whole body of larvae	Complementation cascades, phagosome activity, antigen processing, antigen presentation pathway.	(39)
Vibrio alginolyticus	Giant grouper (*Epinephelus lanceolatus*)	Whole body of larvae	Inductions of TLR5, IL-1β, IL-8, hepcidin genes	(40)

(Continued)

TABLE 1 | Continued

Pathogen or stimulator	Fish	Target tissue or cell	Responding genes and pathways	References
Vibrio anguillarum	Half-smooth tongue sole (*Cynoglossus semilaevis*)	Mixture of RNA sample form tissues	Complement cascades, antigen processing and presentation, toll-like receptor signaling, NOD-like receptor signaling	(41)
Vibrio anguillarum	Japanese seabass (*Lateolabrax japonicas*)	Head kidney, liver, spleen	Toll-like receptor signaling, NOD-like receptor signaling, RIG-I-like receptor signaling, T cell receptor signaling	(42)
Vibrio anguillarum	Miiuy croaker (*Miichthys miiuy*)	Spleen	Phagosome pathway, NF-κB signaling pathway, hematopoietic cell lineage, cytokine–cytokine receptor interaction.	(43)
Vibrio anguillarum	Southern flounder (*Paralichthys lethostigma*)	Liver	Upregulated hematopoiesis related genes, β-hemoglobin and erythropoiten.	(44)
Vibrio anguillarum	Turbot (*Scophthalmus maximus*)	Intestine	Pathogen attachment and recognition, antioxidant/apoptosis, mucus barrier modification, immune activation/inflammation	(45)
Vibrio harveyi	Orange-spotted grouper (*Epinephelus coioides*)	Head kidney, spleen	NOD-like receptor signaling, toll-like receptor signaling, NF-κB signaling, Jak-STAT signaling	(16)
Vibrio parahaemolyticus	Brown-marbled grouper (*Epinephelus fuscoguttatus)*	Spleen	Cell killing, antioxidant activity	(46)
Vibrio parahaemolyticus	Zebrafish (*Danio rerio*)	Whole body of larvae	Complement cascades, chemokine, TNF signaling, NF-κB signaling, JAK-STAT signaling	(47)
Yersinia ruckeri	Amur sturgeon (*Acipenser schrencki*)	Spleen	Antigen processing and presentation, complement cascades, T cell receptor signaling, B and T cell receptor signaling.	(48)
GRAM-POSITIVE BACTERIA				
Lactococcus garvieae	Gray mullet (*Mugil cephalus*)	Head kidney, spleen	Complement and coagulation cascades, toll-like receptor signaling, antigen processing and presentation	(18)
Nocardia seriolae	Largemouth bass (*Micropterus salmoides*)	Spleen	Cytokines, toll-like receptor signaling, T cell receptor signaling, NF-κB signaling, JAK-STAT signaling	(17)
Streptococcus agalactiae	Hybrid tilapia (*Oreochromis* spp.)	Whole body of larvae	Toll-like receptor signaling, leukocyte transendothelial migration, TNF signaling, PI3K-Akt signaling, Jak-STAT signaling MAPK signaling	(49)
Streptococcus agalactiae	Mozambique tilapia (*Oreochromis mossambicus*)	Spleen	Toll-like receptor signaling, chemokine signaling, antigen processing and presentation, NF-κB signaling, TNF signaling, cytokines	(50)
Streptococcus agalactiae	Nile tilapia (*Oreochromis niloticus*)	Spleen	Pathogen attachment and recognition, antioxidant/apoptosis, cytoskeletal dynamics regulation, immune activation	(51)
Streptococcus dysgalactiae	Soiny mullet (*Liza haematocheila*)	Spleen	Complemen cascades, toll-like receptor signaling, chemokine signaling pathway, B snd T cell receptor signaling, antigen processing and presentation, natural killer cell mediated cytotoxicity	(52)
VIRUS				
Carassius auratus herpesvirus	Gibel carp (*Carassius gibelio*)	Head kidney	Chemokine signaling, toll-like receptor signaling, type I IFN, IL-6 etc.	(53)
Grass carp reovirus	Grass carp (*Ctenopharyngodon idella*)	Gill, intestine, liver, spleen	Complemen cascades, antigen presentation, Nk cell mediated cytotoxicity, proteasome, lysosome, peroxisome, phagosome	(54)
Grass carp reovirus	Grass carp (*Ctenopharyngodon idella*)	Spleen	Complement cascades, hematopoietic cell lineage, phagosome, cytokine-cytokine receptor interaction	(55)
Grass carp reovirus	Grass carp (*Ctenopharyngodon idellus*)	Kidney	Complement and coagulation cascades, Glycolysis/gluconeogenesis	(56)

(Continued)

TABLE 1 | Continued

Pathogen or stimulator	Fish	Target tissue or cell	Responding genes and pathways	References
Grass carp reovirus	Grass Carp (*Ctenopharyngodon idella*)	Kidney cell line	Focal adhesion, ECM–receptor interactions in early stage of infection, phagosome, lysosome in the midle stage	(57)
Lymphocystis disease virus	Japanese flounder (*Paralichthys olivaceus*)	Gill	Cell cycle, DNA replication, proteasome, p53 signaling, TNF signaling	(58)
Nervous necrosis virus	Grouper (*Epinephelus spp*)	Kidney cell line	Endoplasmic reticulum stress response	(59)
Nervous necrosis virus	Asian seabass (*Lates calcarifer*)	Epithelial cell line	Upregulation of pro-inflammatory cytokines, type I interferon, chemokines	(60)
Salmon anemia virus	Atlantic salmon (*Salmo salar*)	Spleen	Protein translation; protein processing in endoplasmic reticulum, proteasome, phagosome, lysosome, antigen processing and presentation	(61)
Spring viraemia of carp virus	Fathead minnow (*Pimephales promelas*)	Epithelioma papulosum cyprinid (EPC) cell line	Oxidative stress, apoptosis, cytoskeleton, interferon system	(62)
Spring viraemia of carp virus	Zebrafish (*Danio rerio*)	Brain, spleen	Influenza A pathway, herpes simplex infection pathway, tuberculosis and toxoplasmosis pathways	(63)
MIMIC MOLECULES				
Lipopolysaccharide	Zebrafish (*Danio rerio*)	Whole body of larvae	Chemokines and G protein-coupled receptor signaling. (mild dose treatment). Down-modulated proinflammatory genes after sublethal dose treatment.	(64)
Lipopolysaccharide	Yellow catfish (*Pelteobagrus fulvidraco*)	Liver	Up-regulated expressions of CXCL2-like chemokine, goose-type lysozyme, and cathepsin K	(65)
Poly(I:C)	Large yellow croaker (*Pseudosciaena crocea*)	Spleen	Toll-like receptor signaling, RIG-I-like receptors signaling, JAK-STAT signaling, and T-cell receptor signaling	(66)
Poly(I:C)	Miiuy croaker (*Miichthys miiuy*)	Spleen	Cytokine–cytokine receptor interaction, complement cascades, NF-κB signaling, toll-like receptor signaling	(67)
Poly(I:C)	Black rockcod (*Notothenia coriiceps*)	Liver	Upregulation of TNFα and TNF2 expressions	(33)
Poly(I:C)	*Schizothorax prenanti*	Spleen	MDA5 and JAK mediated signaling pathways	(68)

relatively higher than that of common DEGs; 493 DEGs (167 up-regulated and 326 down regulated) were found in largemouth bass against *N. seriolae*, 819 DEGs (291 up-regulated and 528 down regulated) were found in mullets against *L. garvieae*, 909 DEGs (601 up-regulated and 308 down regulated) were found in groupers (*Epinephelus coioides*) against *V. harveyi*, and 1471 DEGs (1,001 up-regulated and 470 down regulated) were found in carps against *A. sobria* (**Figure 1**).

Of the common DEGs, we found several immune-related genes that were upregulated, including C4 (complement component 4), CCL19 (C-C motif chemokine 19), and SOCS1 (suppressor of cytokine signaling 1) (**Table S1**). The complement system is an important innate immune system that functions to detect pathogenic infections in both vertebrates and invertebrates. C4 is an important part of the classical and lectin pathways, which form enzymes C3 and C5 convertases (81, 82). CCL19, a CC chemokine that is expressed in lymphoid organs, manages the migration of antigen presenting cells and lymphocytes (83). In teleost, there are also various reports that investigated potential chemokine genes and their chemotactic activity (84–86). SOCS1 is a regulator of JAK/STAT signaling, and is induced by type I interferon (IFN) and IFN-γ via binding and blocking of JAK2 activation (87). It has been reported that SOCS1 acts as an inhibitor of IFN-mediated signaling in Atlantic salmon (*Salmo salar*) (88). From other reports of the transcriptome analysis (**Table 1**), complement system, JAK/STAT signaling and chemokine systems are also commonly appeared in responding pathways to bacterial infections. Therefore, it is suggested that these genes contribute to early immune responses following bacterial infections (within 24 h).

Nocardia seriolae is a filamentous Gram-positive bacterium that causes nocardiosis with high mortality in many fish species in Japan, Taiwan and Japan. The infected fish showed a lethal granulomatous disease of the skin, muscle, spleen, kidney, and liver tissues (89). Unlike other bacterial species from our previous studies, *N. seriolae* is an intercellular bacteria. To determine specific DEGs elicited by *N. seriolae* infections, we performed functional enrichment of the KEGG pathway for specific up-regulated genes in largemouth bass. As shown in **Table S2**, specific upregulated genes were assigned to 11 KEGG pathways; based on the enrichment analysis. From the enrichment analysis, Notch signaling pathway was focused and illustrated using expression levels of RNA-seq data from all four fish species (**Figure 2A**). Results indicated that Notch1 and HES1 (hairy and enhancer of split 1) were specifically upregulated in largemouth bass against *N. seriolae*. The Notch and HES1 axis present in hematopoietic cells and stroma of the thymus plays an important role in T cell development (90, 91). Additionally, in the "cytokine-cytokine receptor interaction" pathway, IL12RB1 (interleukin 12 receptor β-1) and IL12RB2 (interleukin 12 receptor β2) in largemouth bass against *N. seriolae* were upregulated. IL12B is a ligand of IL12RBs, and is highly, but not specifically expressed, in largemouth bass (**Figure 2B**). IL-12, a heterodimetric cytokine consisting of p35 and p40 subunits, is a key regulator of T helper 1 development (Th1), which promotes cellular immunity against intracellular pathogens. In Amberjack (*Seriola dumerili*), administrated recombinant IL-12 and formalin-killed *N. seriolae* showed the higher survival rates after challenged with *N. seriolae,* compared to vehicle and FKC only groups (92). These pathways promote immune reactions against *N. seriola*e during early stages of the infection, and are candidates for infection prevention and adjuvants in fish.

Aeromonas sobria is a Gram-negative, motile, rod-shaped bacterium that has been isolated from many diseased fish (93–95). In the spleen and head kidney of disease fish, necrotized spleen cells and hemorrhagic pulps were observed (93). From the extracted data of specific up-regulated genes (1001 genes) in koi carp against *A sobria* (**Figure 1**), we performed functional enrichment of the KEGG pathway for specific up-regulated genes. As shown in **Table S3**, specific upregulated genes of koi carp against *A. sobria* are associated with 45 KEGG pathways. As shown in **Figure S1**, regulation of the actin cytoskeleton was activated during *A. sobria* infection. In addition, CXCL12 (C-X-C motif chemokine 12) and CXCR4 (C-X-C motif chemokine receptor 4) in were also up-regulated in koi carps during *A sobria* infections (**Figure S1**). The CXCL12-CXCR4 axis modulates various immune functions, such as induction of hematopoiesis and accumulation of immune cells in inflamed tissues (96). Therefore, the CXCL12-CXCR4 axis may function in reorganization of hematopoiesis in injured tissues during *A. sobria* infections.

Vibrio harveyi is one of the major photogenes of a luminescent Gram-negative bacterium, which impacts to wide range of aquaculture species (97–99). The 601 specific upregulated genes in orange-spotted grouper against *Vibrio harveyi* (**Figure 1**) were assigned to 8 KEGG pathways (**Table S4**). We focused on the ErbB signaling pathway, and found that expression of TGFα (transforming growth factor α) and its receptor, ERBB1 (epidermal growth factor receptor), were upregulated (**Figure S2**). Previous studies have shown that TGFα promotes the expression and activity of TLR5 and TLR9 in skin keratinocytes (100). In our previous study, expressions of TRL5 and its downstream genes in the spleen were found to be enhanced 2 days following *V. harveyi* infections (16). While the immunological function of TGFα in the spleen of fish is unclear, we hypothesize that TGFα is a key regulator for prevention of *V. harveyi* infection in fish.

Lactococcus garvieae is a Gram-positive, facultative anaerobic, non-motile bacterium, and affects freshwater and marine cultured fish species worldwide (101, 102). Functional enrichment analysis of the KEGG pathway was performed to determine specific upregulated genes (291 genes) in gray mullets against *L. garvieae* (**Figure 1**). Specific upregulated genes were mapped to 10 KEGG pathways during *L. garvieae* infection in gray mullets (**Table S5**). Results indicated that the IL-17 signaling pathway is clearly enhanced during the infection, as illustrated by **Figure S3**. IL-17 is composed of six ligands (IL-17A to F), and plays critical roles in inflammatory responses and host defenses during invasion by extracellular pathogens. Binding of IL-17s to its five perspective receptors (IL-17Rs; IL-17RA to E), induces inflammatory and immune responses (103). In *vitro* study, exogenous IL-17A induced bacterial clearance in F. tularensis LVS- live vaccine strain infected cells (104). Additionally, in mice model, it has been reported that *in vivo*

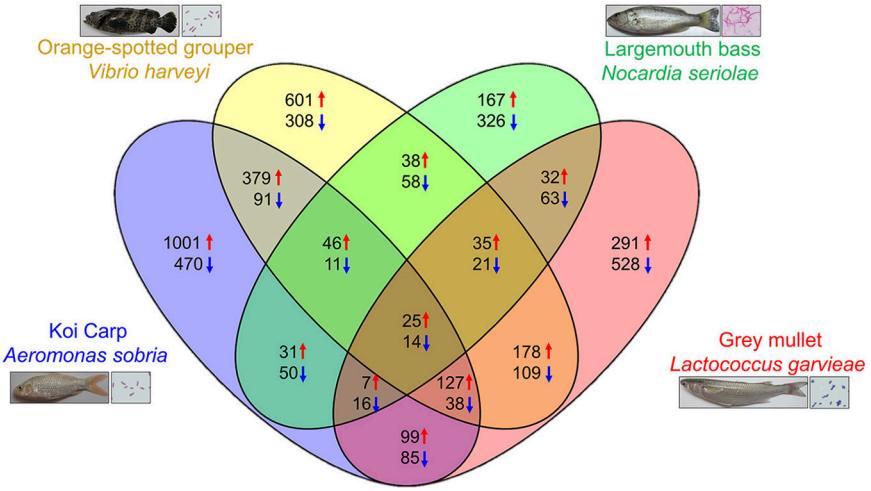


FIGURE 1 | Venn diagrams showing overlaps of up and down regulated genes among each fish with bacterial challenge. The numbers indicate up (red arrow) and down (blue arrow) regulated genes in each categories.

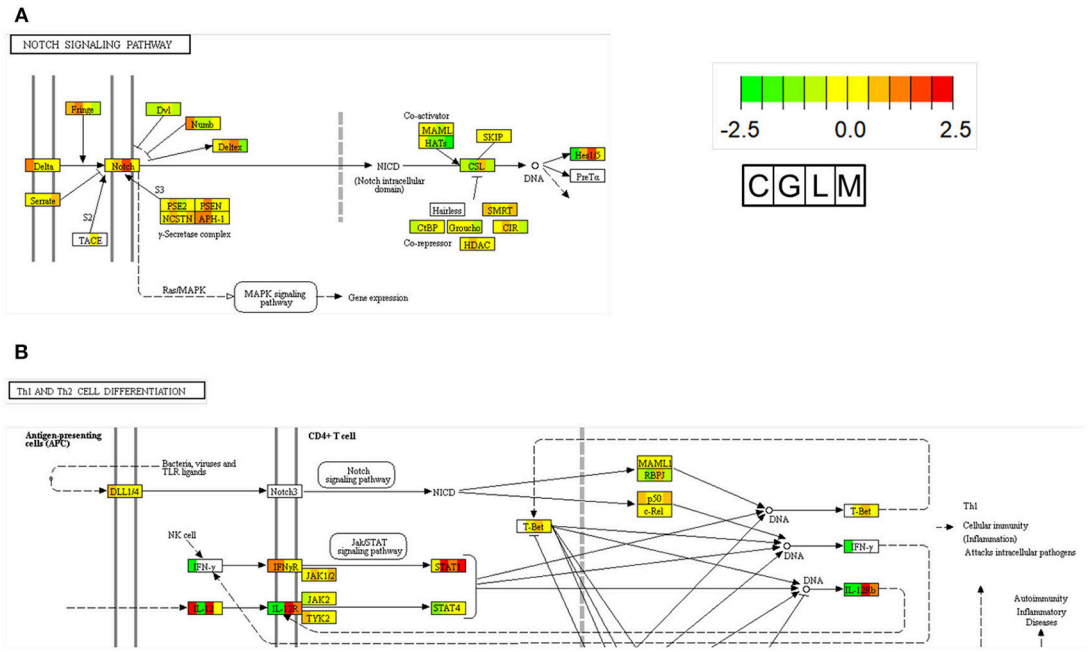


FIGURE 2 | Pathway map of Notch signaling **(A)** and Th1 differentiation **(B)** in KEGG. In each gene boxes, the gene expression levels are shown in 4 fish (C, Carp; G, Grouper; L, Largemouth bass; M, Mullet) spleen 1 day after infection with *A. sobria*, *V. harveyi*, *N. seriolae,* and *L. garvieae*, respectively, when compared to the control group. The lower expression levels of genes are shown in green, and the higher expression levels of genes are shown in red. Undetected genes are shown by white coloring (see color legend in figure).

administration of IL-17A moderately delays time of death from lethal infection of *Francisella tularensis* live vaccine strain (105). While we did not detect expression of IL-17 ligands in this study, we found that expressions of IL-17RB, IL17RC, and IL-17RE were up-regulated in gray mullets infected with *L. garvieae*. There are studies that aimed to identify and characterize IL-17 and IL17Rs in fish (106, 107). However, functional differentiations of teleost IL-17s and these receptors remain elusive. Our findings on the expression pattern of IL17Rs will provide useful models that can be used to investigate immune functions of IL17s in teleost.

A. sobria and *V. harveyi* are classified to Gram-negative bacteria. Therefore, we approached to find the immune-related genes and pathways using commonly DEG (379 upregulated genes and 91 downregulated genes) of koi carp against *A. sobria* and orange-spotted grouper against *V. harveyi* (**Figure 1**).

However, any immune-related pathways were not assigned by KEGG enrichments analysis. TLR4, which is the pathogen recognized receptor for the Gram-negative bacteria specific lipopolysaccharide, is not highly expression in the spleen of koi carp against *A. sobria* and orange-spotted grouper against *V. harveyi*. While, we could find the up-regulated immune-related gene of these two species, such as pattern recognition receptors (TLR6 and TLR5), cytokines and chemokines (CSF3 and CCL21), lysosome related genes (LYPLA3 and SLC11A1) and caspase recruitment domain-containing protein (Card) 9 (**Table S6**). *N. seriolae* and *L. garvieae* are classified to Gram-positive bacteria. Therefore, we investigated to commonly immune-related genes and pathways in Gram-positive bacteria using commonly DEGs (32 upregulated genes and 63 downregulated genes) of largemouth bass against *N. seriolae* and gray mullet against *L. garvieae* (**Figure 1**). Up-regulated immune-related genes of these two species were identified, such as IL-6, TNF Receptor Superfamily Member 11b (TNFRSF11B), interferon regulatory factors (IRF4 and IRF8) and CD83 (**Table S7**). Although it is unclear the pathways to induce these up-regulated genes, these immune related genes may become the marker and immune factors in Gram-negative or positive bacterial infection.

CONCLUSION AND FUTURE PERSPECTIVES

In this review, we first introduced applications of the RNA-Seq technology in aquaculture studies. The RNA-Seq technology has allowed us to identify many novel genes, and to investigate the expression patterns at various conditions in non-model teleost. Therefore, findings based on this technology have accelerated research in the aquaculture field. Additionally, high throughput quantification by RNA-seq could be used to identify pathogen, and to evaluate the efficacy of vaccines and adjuvants against pathogen *in vivo*. We also summarized current knowledge on immune responses to pathogenic challenges via RNA-Seq in teleost. In this study, we could identify the specific pathway in each fish against bacteria species, Noth1 signaling and IL-12 signaling pathway in largemouth bass against *N. seriolae*, CXCL12 and CXCR4 signaling pathway in koi carp against *A. sobria*, TGFα signaling pathway in orange-spotted grouper against *V. harveyi*, and IL-17 signaling pathway in gray mullet against *L. garvieae*. These types of studies are increasing, and have enormously aided in our understanding of pathogenic strategies and immune defense systems in aquaculture fish. However, there remains certain limitations of RNA-Seq analysis in aquaculture species. Additionally, the RNA-seq technology could be used to expand existing datasets on splicing variants in mRNA and SNP. Currently, differences in immune response against different pathogens are not well-described. In this study, we attempted to investigate both species-specific and common immune related genes that are up-regulated during bacterial infections based on our previous RNA-seq data. Secondary use of RNA-seq datasets may be essential for preparation of future RNA-seq studies in aquaculture species, which can further deepen our understanding of specific immune functions against pathogens. In aquaculture field, these deep and particular understanding of immune response against each pathogens will provide us to more accurate diagnosis of disease and develop a more effective vaccine and adjuvant of each pathogens.

AUTHOR CONTRIBUTIONS

SM analyzed transcriptome data and wrote the paper. P-CW and S-CC reviewed the paper.

FUNDING

This research was funded by National Science Council, Taiwan, grant number NSC 104-2622-B-020-002-CC1 and MOST 107-2313-B-020−012 -MY3.

ACKNOWLEDGMENTS

We thank Genomics Bioscience Technology Co. Ltd. (Taipei, Taiwan) for assistance with transcriptome analysis.

SUPPLEMENTARY MATERIAL

The Supplementary Material for this article can be found online at: https://www.frontiersin.org/articles/10.3389/fimmu.2019.00153/full#supplementary-material

Figure S1 | Pathway map of Regulation of actin cytoskeleton in KEGG. In each gene boxes, the gene expression levels are shown in 4 fish (C, Carp; G, Grouper; L, Largemouth bass; M, Mullet) spleen 1 day after infection with *A. sobria*, *V. harveyi*, *N. seriolae,* and *L. garvieae*, respectively, when compared to the control group. The lower expression levels of genes are shown in green, and the higher expression levels of genes are shown in red. Undetected genes are shown by white coloring (see color legend in figure).

Figure S2 | Pathway map of ErbB signaling pathway in KEGG. In each gene boxes, the gene expression levels are shown in 4 fish (C, Carp; G, Grouper; L, Largemouth bass; M, Mullet) spleen 1 day after infection with *A. sobria*, *V. harveyi*, *N. seriolae,* and *L. garvieae*, respectively, when compared to the control group. The lower expression levels of genes are shown in green, and the higher expression levels of genes are shown in red. Undetected genes are shown by white coloring (see color legend in figure).

Figure S3 | Pathway map of Il-17 signaling pathway in KEGG. In each gene boxes, the gene expression levels are shown in 4 fish (C, Carp; G, Grouper; L, Largemouth bass; M, Mullet) spleen 1 day after infection with *A. sobria*, *V. harveyi*, *N. seriolae,* and *L. garvieae*, respectively, when compared to the control group. The lower expression levels of genes are shown in green, and the higher expression levels of genes are shown in red. Undetected genes are shown by white coloring (see color legend in figure).

Table S1 | Expression levels of commonly up or down regulated genes among 4 fish infected with bacteria. Each expression data indicated fold-change (log2) of bacterial infection/control groups.

Table S2 | Functional enrichment KEGG pathway for specific up-regulated genes of largemouth bass against *N. seriolae*.

Table S3 | Functional enrichment KEGG pathway for specific up-regulated genes of koi carp against *A. sobria*.

Table S4 | Functional enrichment KEGG pathway for specific up-regulated genes of orange-spotted grouper against *V. harveyi*.

Table S5 | Functional enrichment KEGG pathway for specific up-regulated genes of gray mullet against *Lactococcus garvieae*.

Table S6 | Expression levels of commonly up regulated immune-related genes among koi carp against *A. sobria* and orange-spotted grouper against *V. harveyi*. Each expression data indicated fold-change (log2) of bacterial infection/control groups.

Table S7 | Expression levels of commonly up regulated immune-related genes among largemouth bass against *N. seriolae* and gray mullet against *L. garvieae*. Each expression data indicated fold-change (log2) of bacterial infection/control groups.

REFERENCES

1. Wang Z, Gerstein M, Snyder M. RNA-Seq: a revolutionary tool for transcriptomics. *Nat Rev Genet.* (2009) 10:57–63. doi: 10.1038/nrg2484
2. Qian X, Ba Y, Zhuang Q, Zhong G. RNA-Seq technology and its application in fish transcriptomics. *OMICS* (2014) 18:98–110. doi: 10.1089/omi.2013.0110
3. Martin SA, Dehler CE, Krol E. Transcriptomic responses in the fish intestine. *Dev Comp Immunol.* (2016) 64:103–17. doi: 10.1016/j.dci.2016.03.014
4. Jacobson G, Muncaster S, Mensink K, Forlenza M, Elliot N, Broomfield G, et al. Omics and cytokine discovery in fish: presenting the Yellowtail kingfish (*Seriola lalandi*) as a case study. *Dev Comp Immunol.* (2017) 75:63–76. doi: 10.1016/j.dci.2017.04.001
5. Petit J, David L, Dirks R, Wiegertjes GF. Genomic and transcriptomic approaches to study immunology in cyprinids: what is next? *Dev Comp Immunol.* (2017) 75:48–62. doi: 10.1016/j.dci.2017.02.022
6. Sudhagar A, Kumar G, El-Matbouli M. Transcriptome analysis based on RNA-Seq in understanding pathogenic mechanisms of diseases and the immune system of fish: a comprehensive review. *Int J Mol Sci.* (2018) 19:245. doi: 10.3390/ijms19010245
7. Byon JY, Ohira T, Hirono I, Aoki T. Use of a cDNA microarray to study immunity against viral hemorrhagic septicemia (VHS) in Japanese flounder (*Paralichthys olivaceus*) following DNA vaccination. *Fish Shellfish Immunol.* (2005) 18:135–47. doi: 10.1016/j.fsi.2004.06.008
8. MacKenzie S, Iliev D, Liarte C, Koskinen H, Planas JV, Goetz FW, et al. Transcriptional analysis of LPS-stimulated activation of trout (*Oncorhynchus mykiss*) monocyte/macrophage cells in primary culture treated with cortisol. *Mol Immunol.* (2006) 43:1340–8. doi: 10.1016/j.molimm.2005.09.005
9. Martin SA, Blaney SC, Houlihan DF, Secombes CJ. Transcriptome response following administration of a live bacterial vaccine in Atlantic salmon (*Salmo salar*). *Mol Immunol.* (2006) 43:1900–11. doi: 10.1016/j.molimm.2005.10.007
10. Grabherr MG, Haas BJ, Yassour M, Levin JZ, Thompson DA, Amit I, et al. Full-length transcriptome assembly from RNA-Seq data without a reference genome. *Nat Biotechnol.* (2011) 29:644–52. doi: 10.1038/nbt.1883
11. Altschul SF, Gish W, Miller W, Myers EW, Lipman DJ. Basic local alignment search tool. *J Mol Biol.* (1990) 215:403–10. doi: 10.1016/S0022-2836(05)80360-2
12. Ogata H, Goto S, Sato K, Fujibuchi W, Bono H, Kanehisa M. KEGG: Kyoto Encyclopedia of Genes and Genomes. *Nucleic Acids Res.* (1999) 27:29–34. doi: 10.1093/nar/27.1.29
13. Kanehisa M, Sato Y, Kawashima M, Furumichi M, Tanabe M. KEGG as a reference resource for gene and protein annotation. *Nucleic Acids Res.* (2016) 44:D457–62. doi: 10.1093/nar/gkv1070
14. Conesa A, Gotz S, Garcia-Gomez JM, Terol J, Talon M, Robles M. Blast2GO: a universal tool for annotation, visualization and analysis in functional genomics research. *Bioinformatics* (2005) 21:3674–6. doi: 10.1093/bioinformatics/bti610
15. Quevillon E, Silventoinen V, Pillai S, Harte N, Mulder N, Apweiler R, et al. InterProScan: protein domains identifier. *Nucleic Acids Res.* (2005) 33:W116–20. doi: 10.1093/nar/gki442
16. Maekawa S, Byadgi O, Chen YC, Aoki T, Takeyama H, Yoshida T, et al. Transcriptome analysis of immune response against *Vibrio harveyi* infection in orange-spotted grouper (*Epinephelus coioides*). *Fish Shellfish Immunol.* (2017) 70:628–37. doi: 10.1016/j.fsi.2017.09.052
17. Byadgi O, Chen CW, Wang PC, Tsai MA, Chen SC. *De novo* transcriptome analysis of differential functional gene expression in largemouth bass (*Micropterus salmoides*) after challenge with *Nocardia seriolae*. *Int J Mol Sci.* (2016) 17:1315. doi: 10.3390/ijms17081315
18. Byadgi O, Chen YC, Barnes AC, Tsai MA, Wang PC, Chen SC. Transcriptome analysis of grey mullet (*Mugil cephalus*) after challenge with *Lactococcus garvieae*. *Fish Shellfish Immunol.* (2016) 58:593–603. doi: 10.1016/j.fsi.2016.10.006
19. Byadgi O, Chen YC, Maekawa S, Wang PC, Chen SC. Immune-Related functional differential gene expression in Koi carp (*Cyprinus carpio*) after Challenge with *Aeromonas sobria*. *Int J Mol Sci.* (2018) 19:2107. doi: 10.3390/ijms19072107
20. Kolder IC, van der Plas-Duivesteijn SJ, Tan G, Wiegertjes GF, Forlenza M, Guler AT, et al. A full-body transcriptome and proteome resource for the European common carp. *BMC Genomics* (2016) 17:701. doi: 10.1186/s12864-016-3038-y
21. Ellis AE. Immunity to bacteria in fish. *Fish Shellfish Immunol.* (1999) 9:291–308. doi: 10.1006/fsim.1998.0192
22. Tran NT, Gao ZX, Zhao HH, Yi SK, Chen BX, Zhao YH, et al. Transcriptome analysis and microsatellite discovery in the blunt snout bream (*Megalobrama amblycephala*) after challenge with *Aeromonas hydrophila*. *Fish Shellfish Immunol.* (2015) 45:72–82. doi: 10.1016/j.fsi.2015.01.034
23. Qin C, Gong Q, Wen Z, Yuan D, Shao T, Wang J, et al. Transcriptome analysis of the spleen of the darkbarbel catfish *Pelteobagrus vachellii* in response to *Aeromonas hydrophila* infection. *Fish Shellfish Immunol.* (2017) 70:498–506. doi: 10.1016/j.fsi.2017.09.042
24. Kumar R, Sahoo PK, Barat A. Transcriptome profiling and expression analysis of immune responsive genes in the liver of Golden mahseer (*Tor putitora*) challenged with *Aeromonas hydrophila*. *Fish Shellfish Immunol.* (2017) 67:655–66. doi: 10.1016/j.fsi.2017.06.053
25. Yang Y, Yu H, Li H, Wang A. Transcriptome profiling of grass carp (*Ctenopharyngodon idellus*) infected with *Aeromonas hydrophila*. *Fish Shellfish Immunol.* (2016) 51:329–36. doi: 10.1016/j.fsi.2016.02.035
26. Dang Y, Xu X, Shen Y, Hu M, Zhang M, Li L, et al. Transcriptome analysis of the innate immunity-related complement system in spleen tissue of *Ctenopharyngodon idella* Infected with *Aeromonas hydrophila*. *PLoS ONE* (2016) 11:e0157413. doi: 10.1371/journal.pone.0157413
27. Long M, Zhao J, Li T, Tafalla C, Zhang Q, Wang X, et al. Transcriptomic and proteomic analyses of splenic immune mechanisms of rainbow trout (*Oncorhynchus mykiss*) infected by *Aeromonas salmonicida* subsp. salmonicida. *J Proteomics* (2015) 122:41–54. doi: 10.1016/j.jprot.2015.03.031
28. Zhu R, Liu XX, Lv X, Li SY, Li YD, Yu XJ, et al. Deciphering transcriptome profile of the yellow catfish (*Pelteobagrus fulvidraco*) in response to *Edwardsiella ictaluri*. *Fish Shellfish Immunol.* (2017) 70:593–608. doi: 10.1016/j.fsi.2017.08.040
29. Li Z, Liu X, Liu J, Zhang K, Yu H, He Y, et al. Transcriptome profiling based on protein-protein interaction networks provides a core set of genes for understanding blood immune response mechanisms against *Edwardsiella tarda* infection in Japanese flounder (*Paralichthys olivaceus*). *Dev Comp Immunol.* (2018) 78:100–13. doi: 10.1016/j.dci.2017.09.013
30. Li Z, Liu X, Cheng J, He Y, Wang X, Wang Z, et al. Transcriptome profiling provides gene resources for understanding gill immune responses in Japanese flounder (*Paralichthys olivaceus*) challenged with *Edwardsiella tarda*. *Fish Shellfish Immunol.* (2018) 72:593–603. doi: 10.1016/j.fsi.2017.11.041
31. Liu X, Li Z, Wu W, Liu Y, Liu J, He Y, et al. Sequencing-based network analysis provides a core set of gene resource for understanding kidney immune response against *Edwardsiella tarda* infection in Japanese flounder. *Fish Shellfish Immunol.* (2017) 67:643–54. doi: 10.1016/j.fsi.2017.06.051
32. Yang D, Liu Q, Yang M, Wu H, Wang Q, Xiao J, et al. RNA-seq liver transcriptome analysis reveals an activated MHC-I pathway and an inhibited MHC-II pathway at the early stage of vaccine immunization in zebrafish. *BMC Genomics* (2012) 13:319. doi: 10.1186/1471-2164-13-319
33. Ahn DH, Kang S, Park H. Transcriptome analysis of immune response genes induced by pathogen agonists in the Antarctic bullhead notothen

Notothenia coriiceps. *Fish Shellfish Immunol.* (2016) 55:315–22. doi: 10.1016/j.fsi.2016.06.004
34. Peatman E, Li C, Peterson BC, Straus DL, Farmer BD, Beck BH. Basal polarization of the mucosal compartment in *Flavobacterium columnare* susceptible and resistant channel catfish (*Ictalurus punctatus*). *Mol Immunol.* (2013) 56:317–27. doi: 10.1016/j.molimm.2013.04.014
35. Zhou W, Zhang Y, Wen Y, Ji W, Zhou Y, Ji Y, et al. Analysis of the transcriptomic profilings of Mandarin fish (*Siniperca chuatsi*) infected with *Flavobacterium columnare* with an emphasis on immune responses. *Fish Shellfish Immunol.* (2015) 43:111–9. doi: 10.1016/j.fsi.2014.12.006
36. Zhao L, Tu J, Zhang Y, Wang J, Yang L, Wang W, et al. Transcriptomic analysis of the head kidney of Topmouth culter (*Culter alburnus*) infected with *Flavobacterium columnare* with an emphasis on phagosome pathway. *Fish Shellfish Immunol.* (2016) 57:413–8. doi: 10.1016/j.fsi.2016.09.001
37. Valenzuela-Miranda D, Gallardo-Escarate C. Novel insights into the response of Atlantic salmon (*Salmo salar*) to *Piscirickettsia salmonis*: interplay of coding genes and lncRNAs during bacterial infection. *Fish Shellfish Immunol.* (2016) 59:427–38. doi: 10.1016/j.fsi.2016.11.001
38. Wilkins LG, Clark ES, Farinelli L, Wedekind C, Fumagalli L. Embryonic gene expression of *Coregonus palaea* (whitefish) under pathogen stress as analyzed by high-throughput RNA-sequencing. *Fish Shellfish Immunol.* (2015) 47:130–40. doi: 10.1016/j.fsi.2015.08.035
39. Wang YD, Huang SJ, Chou HN, Liao WL, Gong HY, Chen JY. Transcriptome analysis of the effect of *Vibrio alginolyticus* infection on the innate immunity-related complement pathway in *Epinephelus coioides*. *BMC Genomics* (2014) 15:1102. doi: 10.1186/1471-2164-15-1102
40. Wang YD, Wang YH, Hui CF, Chen JY. Transcriptome analysis of the effect of *Vibrio alginolyticus* infection on the innate immunity-related TLR5-mediated induction of cytokines in *Epinephelus lanceolatus*. *Fish Shellfish Immunol.* (2016) 52:31–43. doi: 10.1016/j.fsi.2016.03.013
41. Zhang X, Wang S, Chen S, Chen Y, Liu Y, Shao C, et al. Transcriptome analysis revealed changes of multiple genes involved in immunity in *Cynoglossus semilaevis* during *Vibrio anguillarum* infection. *Fish Shellfish Immunol.* (2015) 43:209–18. doi: 10.1016/j.fsi.2014.11.018
42. Zhao C, Fu M, Wang C, Jiao Z, Qiu L. RNA-Seq analysis of immune-relevant genes in *Lateolabrax japonicus* during *Vibrio anguillarum* infection. *Fish Shellfish Immunol.* (2016) 52:57–64. doi: 10.1016/j.fsi.2016.02.032
43. Chu Q, Song W, Cui J, Xu T. Genome-guided transcriptome analysis of miiuy croaker provides insights into pattern recognition receptors and cytokines in response to *Vibrio anguillarum*. *Dev Comp Immunol.* (2017) 73:72–8. doi: 10.1016/j.dci.2017.03.009
44. Bayha KM, Ortell N, Ryan CN, Griffitt KJ, Krasnec M, Sena J, et al. Crude oil impairs immune function and increases susceptibility to pathogenic bacteria in southern flounder. *PLoS ONE* (2017) 12:e0176559. doi: 10.1371/journal.pone.0176559
45. Gao C, Fu Q, Su B, Zhou S, Liu F, Song L, et al. Transcriptomic profiling revealed the signatures of intestinal barrier alteration and pathogen entry in turbot (*Scophthalmus maximus*) following *Vibrio anguillarum* challenge. *Dev Comp Immunol.* (2016) 65:159–68. doi: 10.1016/j.dci.2016.07.007
46. Low CF, Mariana NS, Maha A, Chee HY, Fatimah MY. Identification of immune response-related genes and signalling pathways in spleen of *Vibrio parahaemolyticus*-infected *Epinephelus fuscoguttatus* (Forskal) by next-generation sequencing. *J Fish Dis.* (2016) 39:389–94. doi: 10.1111/jfd.12359
47. Zhang Q, Ji C, Ren J, Dong X, Zu Y, Jia L, et al. Differential transcriptome analysis of zebrafish (*Danio rerio*) larvae challenged by *Vibrio parahaemolyticus*. *J Fish Dis.* (2018) 41:1049–62. doi: 10.1111/jfd.12796
48. Li S, Zhang Y, Cao Y, Wang D, Liu H, Lu T. Trancriptome profiles of Amur sturgeon spleen in response to *Yersinia ruckeri* infection. *Fish Shellfish Immunol.* (2017) 70:451–60. doi: 10.1016/j.fsi.2017.09.033
49. Ken CF, Chen CN, Ting CH, Pan CY, Chen JY. Transcriptome analysis of hybrid tilapia (*Oreochromis* spp.) with *Streptococcus agalactiae* infection identifies Toll-like receptor pathway-mediated induction of NADPH oxidase complex and piscidins as primary immune-related responses. *Fish Shellfish Immunol.* (2017) 70**:**106–20. doi: 10.1016/j.fsi.2017.08.041
50. Wang L, Liu P, Wan ZY, Huang SQ, Wen YF, Lin G, et al. RNA-Seq revealed the impairment of immune defence of tilapia against the infection of *Streptococcus agalactiae* with simulated climate warming. *Fish Shellfish Immunol.* (2016) 55:679–89. doi: 10.1016/j.fsi.2016.06.058
51. Zhu J, Fu Q, Ao Q, Tan Y, Luo Y, Jiang H, et al. Transcriptomic profiling analysis of tilapia (*Oreochromis niloticus*) following *Streptococcus agalactiae* challenge. *Fish Shellfish Immunol.* (2017) 62:202–12. doi: 10.1016/j.fsi.2017.01.023
52. Qi Z, Wu P, Zhang Q, Wei Y, Wang Z, Qiu M, et al. Transcriptome analysis of soiny mullet (*Liza haematocheila*) spleen in response to *Streptococcus dysgalactiae*. *Fish Shellfish Immunol.* (2016) 49:194–204. doi: 10.1016/j.fsi.2015.12.029
53. Gao FX, Wang Y, Zhang QY, Mou CY, Li Z, Deng YS, et al. Distinct herpesvirus resistances and immune responses of three gynogenetic clones of gibel carp revealed by comprehensive transcriptomes. *BMC Genomics* (2017) 18:561. doi: 10.1186/s12864-017-3945-6
54. Shi M, Huang R, Du F, Pei Y, Liao L, Zhu Z, et al. RNA-seq profiles from grass carp tissues after reovirus (GCRV) infection based on singular and modular enrichment analyses. *Mol Immunol.* (2014) 61:44–53. doi: 10.1016/j.molimm.2014.05.004
55. Xu BH, Zhong L, Liu QL, Xiao TY, Su JM, Chen KJ, et al. Characterization of grass carp spleen transcriptome during GCRV infection. *Genet Mol Res.* (2016) 15. doi: 10.4238/gmr.15026650
56. He L, Zhang A, Pei Y, Chu P, Li Y, Huang R, et al. Differences in responses of grass carp to different types of grass carp reovirus (GCRV) and the mechanism of hemorrhage revealed by transcriptome sequencing. *BMC Genomics* (2017) 18:452. doi: 10.1186/s12864-017-3824-1
57. Chen G, He L, Luo L, Huang R, Liao L, Li Y, et al. Transcriptomics sequencing provides insights into understanding the mechanism of grass carp reovirus infection. *Int J Mol Sci.* (2018) 19:488. doi: 10.3390/ijms19020488
58. Wu R, Sheng X, Tang X, Xing J, Zhan W. Transcriptome analysis of flounder (*Paralichthys olivaceus*) gill in response to Lymphocystis Disease Virus (LCDV) infection: novel insights into fish defense mechanisms. *Int J Mol Sci.* (2018) 19:160. doi: 10.3390/ijms19010160
59. Lu MW, Ngou FH, Chao YM, Lai YS, Chen NY, Lee FY, et al. Transcriptome characterization and gene expression of *Epinephelus* spp in endoplasmic reticulum stress-related pathway during betanodavirus infection *in vitro*. *BMC Genomics* (2012) 13:651. doi: 10.1186/1471-2164-13-651
60. Liu P, Wang L, Kwang J, Yue GH, Wong SM. Transcriptome analysis of genes responding to NNV infection in Asian seabass epithelial cells. *Fish Shellfish Immunol.* (2016) 54:342–52. doi: 10.1016/j.fsi.2016.04.029
61. Dettleff P, Moen T, Santi N, Martinez V. Transcriptomic analysis of spleen infected with infectious salmon anemia virus reveals distinct pattern of viral replication on resistant and susceptible Atlantic salmon (*Salmo salar*). *Fish Shellfish Immunol.* (2017) 61:187–93. doi: 10.1016/j.fsi.2017.01.005
62. Yuan J, Yang Y, Nie H, Li L, Gu W, Lin L, et al. Transcriptome analysis of epithelioma papulosum cyprini cells after SVCV infection. *BMC Genomics* (2014) 15:935. doi: 10.1186/1471-2164-15-935
63. Wang Y, Zhang H, Lu Y, Wang F, Liu L, Liu J, et al. Comparative transcriptome analysis of zebrafish (*Danio rerio*) brain and spleen infected with spring viremia of carp virus (SVCV). *Fish Shellfish Immunol.* (2017) 69:35–45. doi: 10.1016/j.fsi.2017.07.055
64. Dios S, Balseiro P, Costa MM, Romero A, Boltana S, Roher N, et al. The involvement of cholesterol in sepsis and tolerance to lipopolysaccharide highlighted by the transcriptome analysis of zebrafish (*Danio rerio*). *Zebrafish* (2014) 11:421–33. doi: 10.1089/zeb.2014.0995
65. Liu QN, Xin ZZ, Liu Y, Zhang DZ, Jiang SH, Chai XY, et al. *De novo* transcriptome assembly and analysis of differential gene expression following lipopolysaccharide challenge in *Pelteobagrus fulvidraco*. *Fish Shellfish Immunol* (2018) 73:84–91. doi: 10.1016/j.fsi.2017.11.045
66. Mu Y, Li M, Ding F, Ding Y, Ao J, Hu S, et al. *De novo* characterization of the spleen transcriptome of the large yellow croaker (*Pseudosciaena crocea*) and analysis of the immune relevant genes and pathways involved in the antiviral response. *PLoS ONE* (2014) 9:e97471. doi: 10.1371/journal.pone.0097471
67. Chu Q, Gao Y, Xu G, Wu C, Xu T. Transcriptome comparative analysis revealed poly(I:C) activated RIG-I/MDA5-mediated signaling pathway in miiuy croaker. *Fish Shellfish Immunol.* (2015) 47:168–74. doi: 10.1016/j.fsi.2015.08.032
68. Du X, Li Y, Li D, Lian F, Yang S, Wu J, et al. Transcriptome profiling of spleen provides insights into the antiviral mechanism in *Schizothorax prenanti* after poly (I: C) challenge. *Fish Shellfish Immunol.* (2017) 62:13–23. doi: 10.1016/j.fsi.2017.01.004

69. Cascon A, Yugueros J, Temprano A, Sanchez M, Hernanz C, Luengo JM, et al. A major secreted elastase is essential for pathogenicity of *Aeromonas hydrophila*. *Infect Immun.* (2000) 68:3233–41. doi: 10.1128/IAI.68.6.3233-3241.2000
70. Gong YX, Zhu B, Liu GL, Liu L, Ling F, Wang GX, et al. Single-walled carbon nanotubes as delivery vehicles enhance the immunoprotective effects of a recombinant vaccine against *Aeromonas hydrophila*. *Fish Shellfish Immunol.* (2015) 42:213–20. doi: 10.1016/j.fsi.2014.11.004
71. Kozinska A. Dominant pathogenic species of mesophilic aeromonads isolated from diseased and healthy fish cultured in Poland. *J Fish Dis.* (2007) 30:293–301. doi: 10.1111/j.1365-2761.2007.00813.x
72. Hossain MJ, Sun D, McGarey DJ, Wrenn S, Alexander LM, Martino ME, et al. An Asian origin of virulent *Aeromonas hydrophila* responsible for disease epidemics in United States-farmed catfish. *MBio* (2014) 5:e00848–00814. doi: 10.1128/mBio.00848-14
73. Decostere A. *Flavobacterium columnare* infections in fish: the agent and its adhesion to the gill tissue. *Verh K Acad Geneeskd Belg.* (2002) 64:421–30.
74. Wakabayashi H. Effect of environmental conditions on the infectivity of Flexibacter columnaris to fish. *J Fish Dis.* (1991) 14:279–90. doi: 10.1111/j.1365-2761.1991.tb00825.x
75. Duremdez R, Al-Marzouk A, Qasem JA, Al-Harbi A, Gharabally H. Isolation of *Streptococcus agalactiae* from cultured silver pomfret, *Pampus argenteus* (Euphrasen), in Kuwait. *J Fish Dis.* (2004) 27:307–10. doi: 10.1111/j.1365-2761.2004.00538.x
76. Jafar QA, Sameer AZ, Salwa AM, Samee AA, Ahmed AM, Al-Sharifi F. Molecular investigation of *Streptococcus agalactiae* isolates from environmental samples and fish specimens during a massive fish kill in Kuwait Bay. *Pak J Biol Sci.* (2008) 11:2500–4. doi: 10.3923/pjbs.2008.2500.2504
77. Amal MN, Zamri-Saad M, Iftikhar AR, Siti-Zahrah A, Aziel S, Fahmi S. An outbreak of *Streptococcus agalactiae* infection in cage-cultured golden pompano, *Trachinotus blochii* (Lacepede), in Malaysia. *J Fish Dis.* (2012) 35:849–52. doi: 10.1111/j.1365-2761.2012.01443.x
78. Bowater RO, Forbes-Faulkner J, Anderson IG, Condon K, Robinson B, Kong F, et al. Natural outbreak of *Streptococcus agalactiae* (GBS) infection in wild giant Queensland grouper, *Epinephelus lanceolatus* (Bloch), and other wild fish in northern Queensland, Australia. *J Fish Dis.* (2012) 35:173–86. doi: 10.1111/j.1365-2761.2011.01332.x
79. Cai SH, Wu ZH, Jian JC, Lu YS. Cloning and expression of the gene encoding an extracellular alkaline serine protease from *Vibrio alginolyticus* strain HY9901, the causative agent of vibriosis in *Lutjanus erythopterus* (Bloch). *J Fish Dis.* (2007) 30:493–500. doi: 10.1111/j.1365-2761.2007.00835.x
80. Liang HY, Wu ZH, Jian JC, Huang YC. Protection of red snapper (*Lutjanus sanguineus*) against *Vibrio alginolyticus* with a DNA vaccine containing flagellin flaA gene. *Lett Appl Microbiol.* (2011) 52:156–61. doi: 10.1111/j.1472-765X.2010.02981.x
81. Muller-Eberhard HJ. Molecular organization and function of the complement system. *Annu Rev Biochem.* (1988) 57:321–47. doi: 10.1146/annurev.bi.57.070188.001541
82. Boshra H, Gelman AE, Sunyer JO. Structural and functional characterization of complement C4 and C1s-like molecules in teleost fish: insights into the evolution of classical and alternative pathways. *J Immunol.* (2004) 173:349–59. doi: 10.4049/jimmunol.173.1.349
83. Takamura K, Fukuyama S, Nagatake T, Kim DY, Kawamura A, Kawauchi H, et al. Regulatory role of lymphoid chemokine CCL19 and CCL21 in the control of allergic rhinitis. *J Immunol.* (2007) 179:5897–906. doi: 10.4049/jimmunol.179.9.5897
84. Khattiya R, Ohira T, Hirono I, Aoki T. Identification of a novel Japanese flounder (*Paralichthys olivaceus*) CC chemokine gene and an analysis of its function. *Immunogenetics* (2004) 55:763–9. doi: 10.1007/s00251-003-0638-x
85. Li YX, Sun JS, Sun L. An inflammatory CC chemokine of Cynoglossus semilaevis is involved in immune defense against bacterial infection. *Fish Shellfish Immunol.* (2011) 31:446–52. doi: 10.1016/j.fsi.2011.06.017
86. Chen C, Hu YH, Xiao ZZ, Sun L. SmCCL19, a CC chemokine of turbot *Scophthalmus maximus*, induces leukocyte trafficking and promotes anti-viral and anti-bacterial defense. *Fish Shellfish Immunol.* (2013) 35:1677–82. doi: 10.1016/j.fsi.2013.08.020
87. Yasukawa H, Misawa H, Sakamoto H, Masuhara M, Sasaki A, Wakioka T, et al. The JAK-binding protein JAB inhibits Janus tyrosine kinase activity through binding in the activation loop. *EMBO J.* (1999) 18:1309–20. doi: 10.1093/emboj/18.5.1309
88. Sobhkhez M, Joensen LL, Tollersrud LG, Strandskog G, Thim HL, Jorgensen JB. A conserved inhibitory role of suppressor of cytokine signaling 1 (SOCS1) in salmon antiviral immunity. *Dev Comp Immunol.* (2017) 67:66–76. doi: 10.1016/j.dci.2016.11.001
89. Maekawa S, Yoshida T, Wang PC, Chen SC. Current knowledge of nocardiosis in teleost fish. *J Fish Dis.* (2018) 41:413–9. doi: 10.1111/jfd.12782
90. Wong GW, Knowles GC, Mak TW, Ferrando AA, Zuniga-Pflucker JC. HES1 opposes a PTEN-dependent check on survival, differentiation, and proliferation of TCRbeta-selected mouse thymocytes. *Blood* (2012) 120:1439–48. doi: 10.1182/blood-2011-12-395319
91. Rani A, Greenlaw R, Smith RA, Galustian C. HES1 in immunity and cancer. *Cytokine Growth Factor Rev.* (2016) 30:113–7. doi: 10.1016/j.cytogfr.2016.03.010
92. Matsumoto M, Araki K, Hayashi K, Takeuchi Y, Shiozaki K, Suetake H, et al. Adjuvant effect of recombinant interleukin-12 in the Nocardiosis formalin-killed vaccine of the amberjack *Seriola dumerili*. *Fish Shellfish Immunol.* (2017) 67:263–9. doi: 10.1016/j.fsi.2017.06.025
93. Yu J, Koo BH, Kim DH, Kim DW, Park SW. *Aeromonas sobria* infection in farmed mud loach (*Misgurnus mizolepis*) in Korea, a bacteriological survey. *Iran J Vet Res.* (2015) 16:194–201.
94. Dar GH, Dar SA, Kamili AN, Chishti MZ, Ahmad F. Detection and characterization of potentially pathogenic *Aeromonas sobria* isolated from fish *Hypophthalmichthys molitrix* (*Cypriniformes*: *Cyprinidae*). *Microb Pathog.* (2016) 91:136–40. doi: 10.1016/j.micpath.2015.10.017
95. Zhu M, Wang XR, Li J, Li GY, Liu ZP, Mo ZL. Identification and virulence properties of *Aeromonas veronii* bv. sobria isolates causing an ulcerative syndrome of loach Misgurnus anguillicaudatus. *J Fish Dis* (2016) 39:777–81. doi: 10.1111/jfd.12413
96. Kucia M, Jankowski K, Reca R, Wysoczynski M, Bandura L, Allendorf DJ, et al. CXCR4-SDF-1 signalling, locomotion, chemotaxis and adhesion. *J Mol Histol.* (2004) 35:233–45. doi: 10.1023/B:HIJO.0000032355.66152.b8
97. Zhang X, Austin B. Pathogenicity of *Vibrio harveyi* to salmonids. *J Fish Dis.* (2000) 23:93–102. doi: 10.1046/j.1365-2761.2000.00214.x
98. Lee K, Liu P, Chuang W. Pathogenesis of gastroenteritis caused by Vibrio carchariae in cultured marine fish. *Marine Biotechnology* (2002) 4:267–77. doi: 10.1007/s10126-002-0018-9
99. Pujalte M, Sitjà-Bobadilla A, Macián M, Belloch C, Alvarez-Pellitero P, Pérez-Sánchez J, et al. Virulence and molecular typing of *Vibrio harveyi* strains isolated from cultured dentex, gilthead sea bream and European sea bass. *Syst Appl Microbiol.* (2003) 26:284–92. doi: 10.1078/072320203322346146
100. Miller LS, Sorensen OE, Liu PT, Jalian HR, Eshtiaghpour D, Behmanesh BE, et al. TGF-alpha regulates TLR expression and function on epidermal keratinocytes. *J Immunol.* (2005) 174:6137–43. doi: 10.4049/jimmunol.174.10.6137
101. Vendrell D, Balcazar JL, Ruiz-Zarzuela I, de Blas I, Girones O, Muzquiz JL. Lactococcus garvieae in fish: a review. *Comp Immunol Microbiol Infect Dis.* (2006) 29:177–98. doi: 10.1016/j.cimid.2006.06.003
102. Meyburgh CM, Bragg RR, Boucher CE. *Lactococcus garvieae*: an emerging bacterial pathogen of fish. *Dis Aquat Org.* (2017) 123:67–79. doi: 10.3354/dao03083
103. Moseley TA, Haudenschild DR, Rose L, Reddi AH. Interleukin-17 family and IL-17 receptors. *Cytokine Growth Factor Rev.* (2003) 14:155–74. doi: 10.1016/S1359-6101(03)00002-9
104. Lin Y, Ritchea S, Logar A, Slight S, Messmer M, Rangel-Moreno J, et al. Interleukin-17 is required for T helper 1 cell immunity and host resistance to the intracellular pathogen *Francisella tularensis*. *Immunity* (2009) 31:799–810. doi: 10.1016/j.immuni.2009.08.025

105. Markel G, Bar-Haim E, Zahavy E, Cohen H, Cohen O, Shafferman A, et al. The involvement of IL-17A in the murine response to sub-lethal inhalational infection with *Francisella tularensis*. *PLoS ONE* (2010) 5:e11176. doi: 10.1371/journal.pone.0011176
106. Kono T, Korenaga H, Sakai M. Genomics of fish IL-17 ligand and receptors: a review. *Fish Shellfish Immunol.* (2011) 31:635–43. doi: 10.1016/j.fsi.2010.11.028
107. Ding Y, Ai C, Mu Y, Ao J, Chen X. Molecular characterization and evolution analysis of five interleukin-17 receptor genes in large yellow croaker *Larimichthys crocea*. *Fish Shellfish Immunol.* (2016) 58:332–9. doi: 10.1016/j.fsi.2016.09.017

Conflict of Interest Statement: The authors declare that the research was conducted in the absence of any commercial or financial relationships that could be construed as a potential conflict of interest.

Copyright © 2019 Maekawa, Wang and Chen. This is an open-access article distributed under the terms of the Creative Commons Attribution License (CC BY). The use, distribution or reproduction in other forums is permitted, provided the original author(s) and the copyright owner(s) are credited and that the original publication in this journal is cited, in accordance with accepted academic practice. No use, distribution or reproduction is permitted which does not comply with these terms.

frontiers in Immunology

ORIGINAL RESEARCH
published: 06 February 2019
doi: 10.3389/fimmu.2019.00152

Rainbow Trout (*Oncorhynchus Mykiss*) Intestinal Epithelial Cells as a Model for Studying Gut Immune Function and Effects of Functional Feed Ingredients

Jie Wang[1], *Peng Lei*[2], *Amr Ahmed Abdelrahim Gamil*[1], *Leidy Lagos*[2], *Yang Yue*[1], *Kristin Schirmer*[3,4,5], *Liv Torunn Mydland*[2], *Margareth Øverland*[2], *Åshild Krogdahl*[1] *and Trond M. Kortner*[1]*

[1] *Department of Basic Sciences and Aquatic Medicine, Faculty of Veterinary Medicine, Norwegian University of Life Sciences (NMBU), Oslo, Norway,* [2] *Department of Animal and Aquacultural Sciences, Faculty of Biosciences, Norwegian University of Life Sciences (NMBU), Oslo, Norway,* [3] *Eawag, Swiss Federal Institute of Aquatic Science and Technology, Dübendorf, Switzerland,* [4] *EPF Lausanne, School of Architecture, Civil and Environmental Engineering, Lausanne, Switzerland,* [5] *ETH Zürich, Institute of Biogeochemistry and Pollutant Dynamics, Zurich, Switzerland*

OPEN ACCESS

Edited by:
Roy Ambli Dalmo, UiT The Arctic University of Norway, Norway

Reviewed by:
Caterina Faggio, Università degli Studi di Messina, Italy
Laura M. Langan, Plymouth University, United Kingdom

***Correspondence:**
Trond M. Kortner
trond.kortner@nmbu.no

Specialty section:
This article was submitted to Comparative Immunology, a section of the journal Frontiers in Immunology

Received: *31 October 2018*
Accepted: *17 January 2019*
Published: *06 February 2019*

Citation:
Wang J, Lei P, Gamil AAA, Lagos L, Yue Y, Schirmer K, Mydland LT, Øverland M, Krogdahl Å and Kortner TM (2019) Rainbow Trout (Oncorhynchus Mykiss) Intestinal Epithelial Cells as a Model for Studying Gut Immune Function and Effects of Functional Feed Ingredients. Front. Immunol. 10:152. doi: 10.3389/fimmu.2019.00152

The objective of this study was to evaluate the suitability of the rainbow trout intestinal epithelial cell line (RTgutGC) as an *in vitro* model for studies of gut immune function and effects of functional feed ingredients. Effects of lipopolysaccharide (LPS) and three functional feed ingredients [nucleotides, mannanoligosaccharides (MOS), and beta-glucans] were evaluated in RTgutGC cells grown on conventional culture plates and transwell membranes. Permeation of fluorescently-labeled albumin, transepithelial electrical resistance (TEER), and tight junction protein expression confirmed the barrier function of the cells. Brush border membrane enzyme activities [leucine aminopeptidase (LAP) and maltase] were detected in the RTgutGC cells but activity levels were not modulated by any of the exposures. Immune related genes were expressed at comparable relative basal levels as these in rainbow trout distal intestine. LPS produced markedly elevated gene expression levels of the pro-inflammatory cytokines *il1b*, *il6*, *il8*, and *tnfa* but had no effect on ROS production. Immunostaining demonstrated increased F-actin contents after LPS exposure. Among the functional feed ingredients, MOS seemed to be the most potent modulator of RTgutGC immune and barrier function. MOS significantly increased albumin permeation and *il1b*, *il6*, *il8*, *tnfa*, and *tgfb* expression, but suppressed ROS production, cell proliferation and *myd88* expression. Induced levels of *il1b* and *il8* were also observed after treatment with nucleotides and beta-glucans. For barrier function related genes, all treatments up-regulated the expression of *cldn3* and suppressed *cdh1* levels. Beta-glucans increased TEER levels and F-actin content. Collectively, the present study has provided new information on how functional ingredients commonly applied in aquafeeds can affect intestinal epithelial function in fish. Our findings

suggest that RTgutGC cells possess characteristic features of functional intestinal epithelial cells indicating a potential for use as an efficient *in vitro* model to evaluate effects of bioactive feed ingredients on gut immune and barrier functions and their underlying cellular mechanisms.

Keywords: RTgutGC, *in vitro* model, lipopolysaccharide, functional feed ingredients, mucosal immune responses, gut barrier

INTRODUCTION

The fish intestine is a multifunctional organ responsible for key physiological processes such as digestion, absorption of nutrients, and osmoregulation (1). Furthermore, the intestine has an important immunological role and constitutes a physical barrier against pathogens (1). In order to secure optimal gut health and function in farmed fish, there is now particular focus on various feed additives including functional feed ingredients that are branded not only in terms of their nutritional value, but also based on their health promoting and disease preventing properties. These functional feed ingredients could include intact microbes (e.g., probiotic organisms), mixed or purified extracts from microbial or plant structural components [e.g., mannanoligosaccarides (MOS), beta-glucans], metabolites (e.g., nucleotides) or even conventional nutrients, if their dietary inclusion is higher than the animal's requirement. Functional feeds are typically applied during predicted stressful events or challenging farming conditions, such as grading, sea water transfer, vaccination, and during critical life stages to help the animal ward off pathogens and secure good health (2). Functional feed ingredients are generally believed to exert their main actions locally within the gut, and may have direct modulatory effects on gut microbiota (3), gut barrier, immune, and/or metabolic functions (4–7). For example, nucleotides are of crucial importance for a whole range of normal intestinal functions, such as growth, nutrient metabolism, immune system, tissue repair, and development (8). Beta-glucans can increase cellular and humoral immune responses in immune cells and epithelial tissues of fish (9–11). MOS as an immune modulator has a close relation to pathogen colonization blocking and immune system regulation, as well as improving intestinal morphology and the epithelial brush border (10, 12, 13).

Current knowledge regarding mechanisms underlying effects of functional feed ingredients on fish gut health and function is, however, limited largely due to a lack of targeted research tools. The use of *in vitro* approaches, such as appropriate cell lines, would facilitate further research on basic functions of the digestive tract and effects of functional feed ingredients on host intestinal immune, barrier and digestive function. It would also reduce the current dependence on large-scale feeding trials, thus contributing to a shift toward 3R studies within fish nutrition research. In mammalian research, intestinal cell lines have proven to be valuable tools for exploration of basic mechanisms of gut function and health and interactions with dietary components. For example, nucleotide supplements in human Caco-2 and rat IEC-6 cell lines have been observed to strengthen intestinal maturation and growth (14). Beta-glucans and plant flavonoids can suppress nuclear factor-kB transactivation, regulate immune response, and strengthen intestinal epithelial barrier function in human Caco-2 cells (15–17).

Until recently, no relevant intestinal cell lines from fish have been available, but promising cultures have been established based on the rainbow trout (*Oncorhynchus mykiss*) intestinal derived cell line RTgutGC (18). Since their initial isolation, RTgutGC cells have been relatively well-characterized and are now routinely grown as monolayers on permeable supports, leading to a two-compartment intestinal barrier model consisting of a polarized epithelium. The system is divided into an upper (apical) and a lower (basolateral) compartment, thereby mimicking the intestinal lumen and the portal blood, respectively. Reported structural and functional features of the RTgutGC cells include tight junction and desmosome formation between adjacent cells, development of transepithelial resistance and polarization over time to exhibit epithelial and brush border characteristics (18–20). The cell line has, as such, been proposed as a physiologically adequate fish intestinal epithelial model, equivalent to the Caco-2 cell line for human intestinal epithelium (20, 21), and has been used recently in studies on fish intestinal immune and barrier function (18, 22, 23).

The objective of this study was to evaluate the suitability of the RTgutGC cells as an *in vitro* model for studies of gut immune function and effects of functional feed ingredients. Effects of a prototype pathogen-associated molecular pattern (PAMP), lipopolysaccharide (LPS), and three functional ingredients commonly applied in commercial fish feeds (nucleotides, MOS, and beta-glucans) were evaluated by diverse analyses, including cell viability measurements and proliferation, brush border digestive enzyme activity, barrier function, ROS production, morphology, and relevant gene and protein expression.

MATERIALS AND METHODS

RTgutGC Cell Culture

Routine RTgutGC cell cultivation was based on the description by Kawano et al. (18). Briefly, RTgutGC cells were cultured in 75-cm^2 flasks (TPP, Trasadingen, Switzerland). L-15 complete medium (L-15/C), i.e., Leibovitz's L-15 medium without Phenolred (21083, Gibco Invitrogen, Basel, Switzerland) supplemented with 10% bovine serum (F7524, Sigma Aldrich, Buchs, Switzerland) and gentamicin (15710-049, Invitrogen, Basel, Switzerland) with a final concentration of 100 μg/mL, was used to culture cells in a 20°C incubator under normal atmosphere. Cells were split in a 1:2 ratio using trypsin (0.25% in PBS w/o Ca^{2+},

Mg^{2+}; L0910; Biowest; Nuaillé, France) after reaching confluency.

For cells grown on conventional culture plates without inserts, 1 mL or 3.5 mL cell suspensions (1.5×10^5 cells/mL, 78,947 cells per cm^2 for 24-well plates and 54,688 cells per cm^2 for 6-well plates) were seeded in 24-well (No.662160, Greiner-Bio-one, Frickenhausen, Germany) or 6-well plates (No. 657960, Greiner-Bio-one, Frickenhausen, Germany), respectively, and were cultured to reach at least 80 % confluency before use (3–4 days).

For the two-compartment intestinal barrier model, RTgutGC cells were cultured as described previously (19, 20). Briefly, 24-well plates with 33.6 mm^2 transwell inserts (No. 662 630, Greiner-Bio-one, Frickenhausen, Germany) and 6-well plates with 425.4 mm^2 transwell inserts (No. 657 630, Greiner-Bio-one, Frickenhausen, Germany) with pore sizes of 3 μm were used to simulate gut lumen (apical /upper chamber) and portal blood (basolateral /lower chamber). Cells were seeded adding 300 μL or 3.5 mL cell suspension (8×10^4 cells/mL, 71,429 cells per cm^2 for 24-well plates and 65,820 cells per cm^2 for 6-well plates) in the apical chamber of 24-well or 6-well plates, respectively. Then, 1 or 3.5 mL of L-15/C were added into the basolateral chamber of 24-well or 6-well plates, respectively. The apical and basolateral medium was changed once per week for a total of 28 days.

Exposure Design

Stock solutions were prepared for LPS and the functional ingredients. LPS (L2630, Sigma, Norway) stock solution was prepared to 1 mg/mL in L15/ex medium. The L15/ex medium contains only the inorganic salts, galactose, and pyruvate concentrations of L-15 (24). Nucleotides (T25-1KT, Sigma, Norway) stock solution was prepared to 10 mg/mL using milliQ water. MOS (Active MOS extracted from yeast, Biorigin, São Paulo, Brazil) stock solution was prepared to 20 mg/mL using sterile PBS, and then sonicated in a water bath (30 s/3 times) and centrifuged (500 × g/ 5 min). The supernatant was subsequently transferred into new vials and stored at −20°C according to previous descriptions (13). Beta-glucans (G5011, Sigma, Norway) stock solution was prepared to 2 mg/mL in sterile PBS according to previous reports (23).

For all exposure tests performed with the two-compartment intestinal barrier model, the stock solutions of LPS and the functional ingredients were diluted in mucosal saline, prepared according to Genz et al. (25) (**Supplementary Table 1**), and added to the apical chamber in order to mimic intestinal lumen conditions. Before performing the exposure tests with LPS and the functional ingredients, L-15/C and mucosal saline acted as exposure medium for RTgutGC cells to evaluate whether the mucosal saline affected cell viability. For exposure tests performed with conventional plates, working solutions were prepared by diluting in mucosal saline or L15 medium, depending on the analytical assay as specified below. To select final working concentrations for further analysis, LPS and the functional ingredients were tested at a range of different concentrations in 6 h exposures in 24-well-conventional plates without inserts (**Supplementary Table 2**).

Assessment of Cell Viability

Alamar Blue (AB, DAL1025, Invitrogen, Basel, Switzerland) and 5-carboxyfluorescein diacetate acetoxymethyl ester (CFDA-AM, C1345, Invitrogen, Basel, Switzerland) were used to measure cell viability (24, 26). AB was used to measure cell metabolic activity, whereas CFDA-AM was used to measure cell membrane integrity. After 6 h of incubation, stimulant working solutions were discarded, cells were washed twice using 1 mL PBS and subsequently, a volume of 400 μL of fresh AB and CFDA-AM were added to each well. The plates were then incubated at 20°C for 30 min in the dark before measurement. The Cytation 3 plate reader (Bio Tek Instruments, Winooski, USA) was used to measure the fluorescence of AB ($\lambda ex = 530$ nm; $\lambda ex = 595$ nm) and CFDA-AM ($\lambda ex = 493$ nm; $\lambda ex = 541$ nm).

Measurement of Transepithelial Electrical Resistance (TEER)

As a quality measure of monolayer formation, TEER was measured in RTgutGC cells grown in 24-well-culture plates with membrane inserts at day 1, 7, 14, and 28. Additionally, TEER was measured in RTgutGC cells exposed to LPS and the functional ingredients for 6 h after 28 days of culture on transwell membrane inserts in 6-well plates. TEER levels were measured using an EVOM Voltohmmeter with STX2 electrode and Endohm-6 electrode (World Precision Instruments, Berlin, Germany) as described by Geppert et al. (19). TEER was calculated by subtracting the values without cells from the values with cells. TEER values were given as $\Omega \times cm^2$.

Brush Border Membrane Enzyme Activity

After 3–4 days of culture on conventional 24-well plates, RTgutGC cells were exposed to LPS and the functional ingredients for 6 h. After discarding the mucosal saline with LPS or functional ingredients, cells were harvested by trypsination and centrifugation. Cell pellets were reconstituted in 1 mL ice-cold 2 mM Tris/50 mM mannitol pH 7.1, containing phenyl-methyl-sulphonyl fluoride (P-7626, Sigma, Norway) as serine protease inhibitor. Brush border membrane enzyme activities, i.e., leucine amino peptidase (LAP) and maltase, were subsequently measured. LAP activity was analyzed colorimetrically with a commercial kit (NO. 251, Sigma, Norway) using L-leucine-β-naphthylamide as substrate according to the methods described by Krogdahl et al. (27). Maltase activity was measured using maltose as substrate according to the description of Dahlquist (28). Total protein concentrations were determined using a Bio-Rad Protein Assay (Bio-Rad Laboratories, Munich, Germany). Enzyme activities were expressed as mol substrate hydrolysed per hour per mg protein.

Albumin Translocation Assay

After 28 days of culture on transwell-membrane inserts in 6-well plates, RTgutGC cells with an initial seeding density of 8×10^4 cells/mL (65,820 cells per cm^2) were exposed to LPS and the functional ingredients for 6 h. The permeation of fluorescent-labeled albumin was then used to evaluate the barrier potential of the cells. 20 μL albumin (Alexa FluorTM 488 Bovine Serum Albumin, Thermo Fisher Scientific, USA) was added into the

apical chamber of each well, and 250 μL of culture medium was collected from the basolateral chamber at the following intervals: 10, 30, 45, 60, and 90 min and temporary stored in the dark at 20 °C. After collecting all the samples, 100 μL of each sample was added to a 96- well black plate (M5061-40EA, Sigma, Norway) in duplicate, and fluorescence was measured using a Cytation 3 plate reader (Bio Tek Instruments, Winooski, USA) equipped with a 490 excitation and 525 emission filter.

Quantitative Real Time PCR (qPCR)

After 28 days of culture on transwell membrane inserts in 6-well plates, RTgutGC cells were exposed to LPS and the functional ingredients for 6 h, and subsequently harvested for gene expression profiling. After discarding the mucosal saline with LPS or functional ingredients, 1 mL of TRIzol (Invitrogen, Thermo Fisher Scientific, USA) was added to each apical chamber. Cells were collected by scarping and flushing the membrane inserts 10 times with the TRIzol solution. The cell homogenate was transferred into a 1.5 mL Eppendorf tube, snap frozen in liquid N_2 and subsequently stored at −80 °C until RNA extraction. Gene expression levels in RTgutGC cells were compared with those of rainbow trout tissues by using total RNA samples from liver, pyloric, mid and distal intestine obtained from a fresh-water stage female rainbow trout as previously described (29). RNA was subsequently purified using a PureLink RNA mini Kit (Invitrogen, Thermo Fisher Scientific, USA). RNA purity and concentration were measured using an Epoch Microplate Spectrophotometer (BioTeK Instruments, Winooski, USA). The RNA integrity was verified using a 2100 Bioanalyzer in combination with RNA Nano Chip (Agilent Technologies, Santa Clara, USA). First-strand complementary DNA was synthesized from 1.0 μg total RNA from all samples using SuperScript IV VILO Master Mix (Invitrogen™, ThermoFisher Scientific). Negative controls were performed in parallel by omitting RNA or enzyme.

Twelve target genes with important functions related to immunity, barrier function and metabolism were profiled. The qPCR primers were designed using Primer3web software version 4.0.0 (http://primer3.ut.ee/) or obtained from the literature. Primer details are shown in **Supplementary Table 3**. All primer pairs were first used in gradient reactions in order to determine optimal annealing temperatures. To confirm amplification specificity, the PCR products from each primer pair were subjected to melting curve analysis and visual inspection of the PCR products by agarose gel electrophoresis. PCR efficiency for each gene assay was determined using 2-fold serial dilutions of randomly pooled complementary DNA. The expressions of individual gene targets were analyzed using the LightCycler 96 (Roche Diagnostics, Basel, Switzerland). Each 10 μl DNA amplification reaction contained 2 μl PCR grade water, 2 μl of 1:10 diluted complementary DNA template, 5 μl LightCycler 480 SYBR Green I Master (Roche Diagnostics) and 0.5 μl (10 mM) of each forward and reverse primer. Each sample was assayed in duplicate, including a no-template control. The three-step qPCR run included an enzyme activation step at 95°C (5 min), forty to forty-five cycles at 95°C (10 s), 60°C (10 s), and 72°C (15 s) and a melting curve step. Target gene expression was normalized to the geometric average of beta-actin (*actb*) and ribosomal protein s20 (*rps20*) after confirming reference gene intra- and interspecific stability (30). Mean normalized expression of the target genes was calculated from raw Cq values by relative quantification (31).

Cell Proliferation Assay

The ability of RTgutGC cells to close a gap during exposure to LPS, MOS and beta-glucans was investigated in a cell proliferation assay by using 2-well-culture inserts (80241, Ibidi GmbH, Martinsried, Germany). The inserts were placed on a conventional cell culture surface, i.e., a μ-Dish 35 mm (81156, Ibidi GmbH, Martinsried, Germany) creating two wells, which were separated by a rubber partition. Approximately 10,000 cells in 70 μL L-15/C were seeded into each well. The cultures were incubated at 20 °C for 2 days until confluence. Then, the rubber partition was removed to create a 500 μm gap between the cells. Immediately, LPS (50 μg/mL), MOS (4 mg/mL), beta-glucans (100 μg/mL) and PBS (control), all dissolved in L-15 medium, were added to the cultures and phase contrast pictures were captured at day 0, 1, 2, and 4 (or until the gap was closed) using a ZEISS Axio microscope (with Axiocam 105 color). The image were processed using ImageJ (32). In brief, all images were first adjusted using Adjust tool for achieving a clear contrast between the cell-free area and area covered by cells. Subsequently, the cell-free area was measured using Analyze particles tool. The cell proliferation rate was calculated by dividing the cell-free area at each time point with the cell-free area at day 0.

Oxidative Stress Detection and Substrate Uptake Assay

After 3–4 days of culture on conventional 6-well plates, RTgutGC cells were exposed to LPS and the functional ingredients for 6 h. After discarding the mucosal saline with LPS or functional ingredients, cells were harvested by trypsination and centrifugation. Cell pellets were reconstituted in 5% FBS in PBS for ROS generation measurement. CellROX® (C10444, Thermo Fisher, Waltham, USA) reagent was added to the cell suspensions at a final concentration of 5 mM, followed by incubation at room temperature for 30 min. After the incubation, cells were washed three times with ice-cold phosphate buffered saline (PBS) and ROS generation was analyzed by flow cytometry (Beckman Coulter Gallios). At least 10,000 events were collected for each sample. Data were analyzed using Kaluza software v.2.1 (Beckman Coulter) and gated using Side scatter (SSC) (granularity) and Forward scatter (FSC) (size) parameters. Discrimination of aggregates from single cells was performed using side scatter-W (SSC-W) vs. side scatter (SSC). ROS was measured at 650/675 nm (FL3).

Fluorescence conjugated Zymosan (Z23373, Thermo Fisher Scientific, USA) and albumin (Alexa FluorTM 488 Bovine Serum Albumin, Thermo Fisher Scientific, USA) were added into culture media at 20 and 12.5 μg/ml, respectively for cells growing in 6-well-conventional plates. Cells were trypsinized and centrifuged after 1, 1.5, and 3 h after adding substrates, respectively. Cell pellets were reconstituted in 5% FBS in PBS before flow cytometry (Beckman Coulter Gallios) was performed to analyze the cells with or without fluorescence at 495/519 nm.

Immunocytochemistry of F-actin Content

For morphological characterization, confocal laser microscopy was used for imaging. RTgutGC cells in L-15/C were seeded in an 8 chamber tissue cultured treated glass Falcon CultureSlide® (Corning, New York, USA) at a density of 150,000 cells per chamber. When reaching 80% confluence, cells were washed with Dulbecco's Phosphate-Buffered Saline (DPBS) and treated with LPS (50 μg/mL), MOS (4 mg/mL), beta-glucans (100 μg/mL), and PBS (control), all dissolved in L-15 medium. After 6 h, cells were washed with DPBS and fixed with 3% paraformaldehyde (Sigma-Aldrich) for 20 min at 4°C. Following fixation, the cells were permeabilized with 0.1% Triton X-100 (Sigma-Aldrich, St. Louis, USA) for 10 min at room temperature. Cells were then incubated in blocking buffer (BB) (10% goat serum, 3% bovine serum albumin, and 0.1% Triton X-100 in DPBS) for 1 h at room temperature. Afterwards, cells were incubated with phalloidin (R425, Thermo Fisher) for F-acin staining according to the manufacturer's instruction. After staining, cells were washed three times for 3 min with DBPS and left to air dry. Once dry, plastic chambers were removed from the slides. Three drops of mounting medium, Fluoroshield (Sigma-Aldrich), containing DAPI were added to the slides, followed by covering with coverslip. The image was analyzed by ImageJ software to investigate the morphology change of the cells under different treatments. Three random pictures were taken from cells under respective treatments. Individual cell numbers were counted based on DAPI-stained nuclear numbers manually. F-actin contents were subsequently calculated by the total fluorescence intensity of phalloidin divided by number of the cells.

Protein Expression of E-cadherin, Aquaporin 8, and Hsp70 by Western Blot Analysis

RTgutGC cells were seeded on 6-well plates and grown until confluence before 6 h exposure to LPS (50 μg/mL), MOS (4 mg/mL), beta-glucans (100 μg/mL), and PBS (control), all dissolved in L-15 medium. Cells were harvested by trypsinization and centrifugation and protein was extracted using PARIS Kit (AM 1921, Thermo Fisher) according to the manual. Protein concentrations were measured using Bradford protein assay kit (Bio-Rad, Hercules, California, United States) and 10 or 20 μg of the protein were loaded on SDS page gels. After 40 min electrophoresis at 100 voltage, proteins were transferred to PVDF membranes, blocked with 5% dry milk for 1 h at room temperature, and incubated consecutively with E-cadherin monoclonal antibody (#701134, Thermo Fisher), Heat shock protein 70 (Hsp70) monoclonal antibody (MA3-008, Thermo Fisher), or Aquaporin 8 (Aqp8) polyclonal antibody (kindly provided by Prof. Steffen S. Madsen, Institute of Biology, University of Southern Denmark). After 3 times washing in PBS and incubation of HRP conjugated secondary antibody, the signal was visualized with Bio-Rad Gel Doc system after adding ECL detection reagents (GERPN2209, Sigma-Aldrich) to the membrane. Due to the potential influence of treatments on candidate reference protein expression, the total membrane protein content was visualized with Ponceau S (P3504, Sigma) and used as a qualitative loading control.

Statistical Analysis

All data were tested for normality and variance homogeneity using histogram and "residual by predicted" plot, respectively, using JMP Pro 13.0.0 (SAS Institute, United States). When necessary, the data were transformed to achieve normal distribution. Further statistical analyses and graphics were made using GraphPad Prism 7 (GraphPad Software, La Jolla, California, United States). The flow cytometry figures were made by Kaluza (Beckman Coulter). Data of albumin translocation and cell proliferation rate were analyzed using two-way ANOVA using time and treatment as class variables followed by Dunnett multiple comparisons tests. Other data were analyzed using one-way ANOVA followed by Dunnett multiple comparisons tests. Data were calculated as mean ± SEM of two or three independent experiments with 3 or 4 technical well or insert replicates (depending on analytical assays, see specifications in figure legends). Asterisks denote the level of statistical significance ($^{*}P < 0.05$, $^{**}P < 0.01$, $^{***}P < 0.001$).

RESULTS

Key Features of RTgutGC Cells Exposed in Mucosal Saline in Conventional Culture Plates and Transwell Membranes

Compared with RTgutGC cells cultivated in L-15/C medium, cells cultivated in mucosal saline maintained above 80% cell viability after 12 h exposure (**Figure 1A**). When RTgutGC cells were grown on transwell membrane inserts in 24-well plates, TEER levels increased steadily and reached about 26 Ω × cm^2 after 4 weeks of culture (**Figure 1B**). After addition of fluorescent albumin to mucosal saline solution in the apical chamber, basolateral fluorescence levels increased steadily with time when no cells were seeded on the membrane whereas with cells, low fluorescence was observed over the 90 min observation period, demonstrating that the RTgutGC cells formed a barrier and strongly attenuated albumin translocation from the apical to the basolateral chamber (**Figure 1C**). Confocal fluorescence microscopy images of RTgutGC cells grown on conventional culture plates illustrated presence of the tight junction protein Claudin 3 (red) and the nuclei (blue) (**Figure 1D**).We also investigated the uptake of albumin and zymozan in RTgutGC cells, grown on conventional support, as a character of functional enterocytes. During a time course of 3 h, albumin uptake into RTgutGC cells increased (**Figure 1E**). However, RTgutGC cells did not take up zymosan as shown in **Figure 1F**.

Effects of LPS and Functional Ingredients

Cell Viability

Using a cell viability cut-off level of 80% compared to control cells, 6 h of exposure to 50 μg/mL LPS (**Figure 2A**), 75 μg/mL nucleotides (**Figure 2B**), 4 mg/mL MOS (**Figure 2C**) and 100 μg/mL beta-glucans (**Figure 2D**) were selected as final working concentration for further analysis.

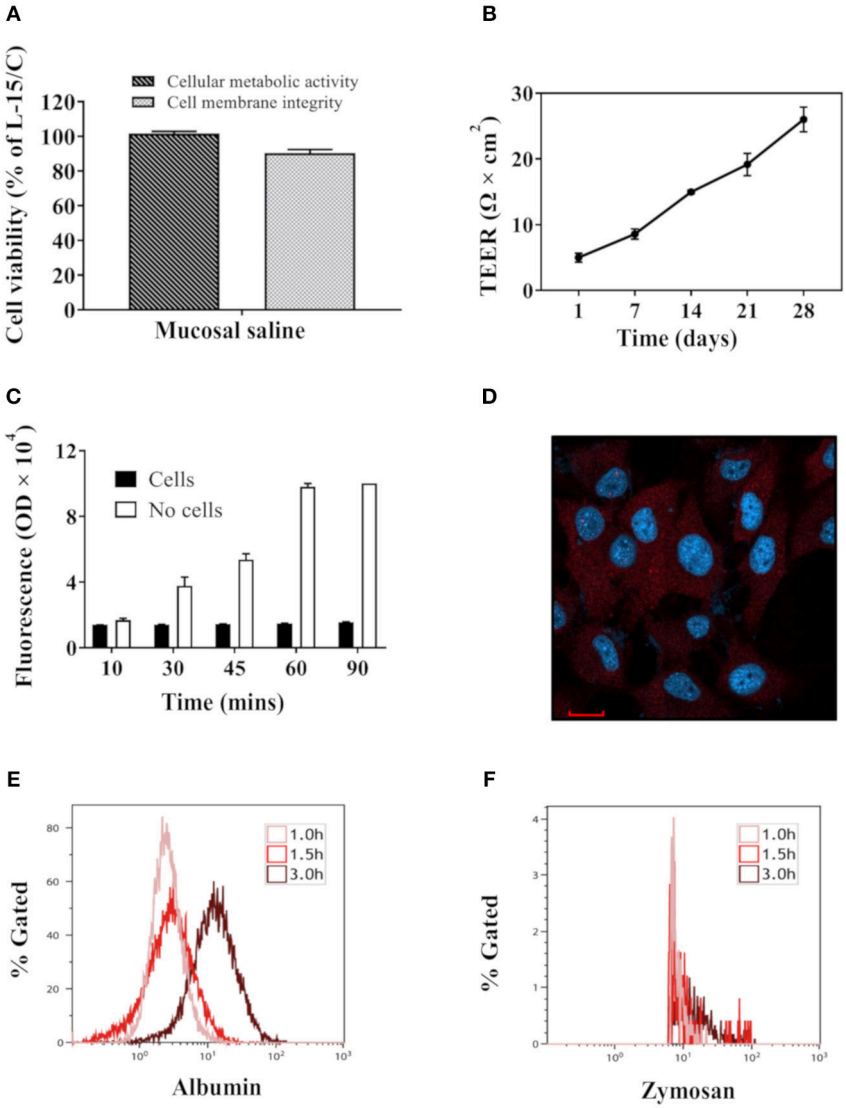


FIGURE 1 | Key features of RTgutGC cells grown on conventional culture plates or transwell membranes. **(A)** Viability of RTgutGC cells in 24-well-culture plates with 1.5×10^5 cells/mL (78,947 cells per cm^2) exposed to mucosal saline for 12 h. **(B)** TEER of RTgutGC cells grown up to 4 weeks in 24-well-culture plates with membrane inserts at initial density of 8×10^4 cells/mL (71,429 cells per cm^2). **(C)** Fluorescent levels in basolateral media after fluorescent albumin exposure into apical chamber in 24-well-transwell membrane plates with or without RTgutGC cells. **(D)** Confocal fluorescence microscopy images of the tight junction protein claudin 3 (red) and the nuclei (blue) in RTgutGC cells grown on conventional culture plates. **(E,F)** Uptake of albumin **(E)** and zymosan **(F)** during the 3 h exposure time with cells cultured in conventional 6-well plates. For both panels **(E,F)**, X axis shows the fluorescence signal from albumin or zymosan in cells. Y axis shows the percentage of albumin/zymosan positive cells out of total live cell population. Data represent mean ± SEM of two independent experiments with 3–4 technical replicates each (wells or inserts). Scale bar = 100 μm.

TEER and Albumin Translocation

After 6 h of exposure to beta-glucans, TEER levels increased significantly compared to control (**Figure 3**, $P < 0.05$). Other treatments had no effect on TEER levels (**Figure 3**, original TEER values seen in **Supplemental Figure 1**).

After 6 h of exposure to MOS increases in basolateral albumin fluorescent levels were observed compared to control cells, significantly at 30 and 60 min time points ($P < 0.05$). No significant effects on the fluorescent level were observed for other treatments (**Figure 4**, $P > 0.05$).

Brush Border Membrane Enzymatic Activity

Brush border membrane enzyme activities (LAP and maltase) were detected in the RTgutGC cells. There were no significant effects of LPS or any of the functional ingredients on LAP (**Figure 5A**) or maltase (**Figure 5B**) activities ($P > 0.05$).

Gene Expression

LPS exposure resulted in markedly increased mRNA levels of several pro-inflammatory cytokines, including interleukin 1β (*il1b*), interleukin 6 (*il6*), interleukin 8 (*il8*), and tumor

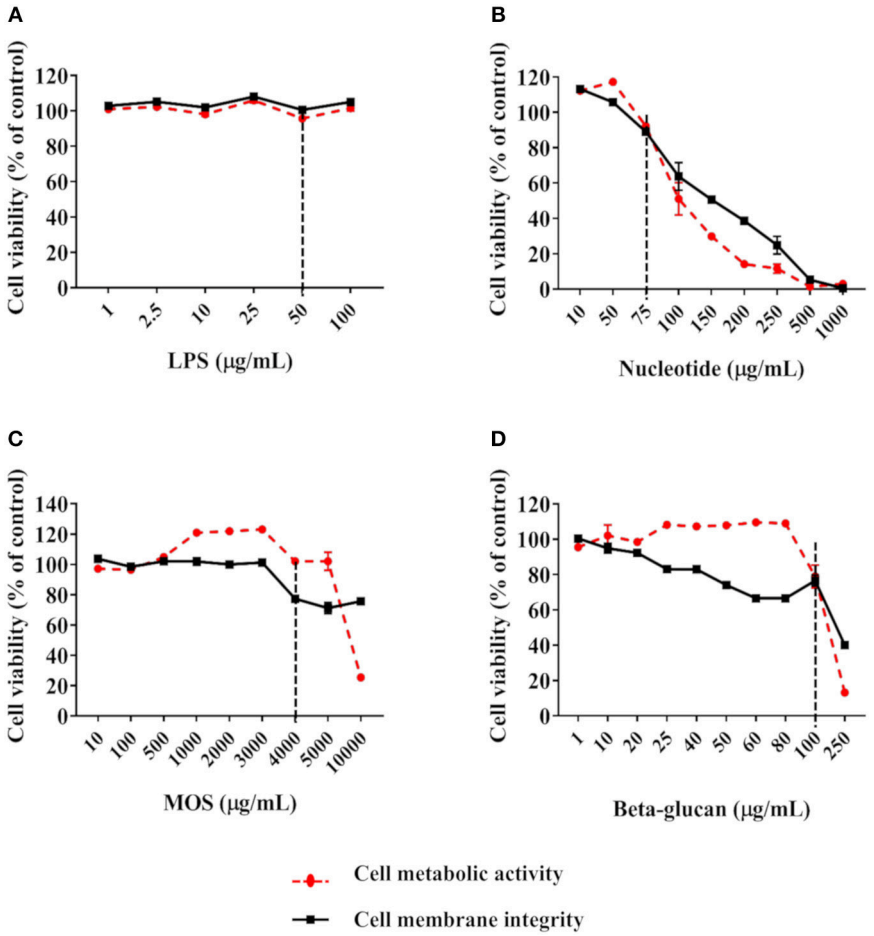


FIGURE 2 | Viability of RTgutGC cells exposed to LPS **(A)**, nucleotides **(B)**, MOS **(C)**, and beta-glucan **(D)**. Breaking lines indicate cut-off level of about 80% cell viability compared to control cells. For LPS, data represent mean ± SEM of two independent experiments with 3 technical well-replicates. For nucleotides, MOS and beta-glucan, two independent experiments with 3 technical well-replicates each and concentrations as shown in **Supplementary Table 1** were conducted. For concentrations evaluated in both experiments, data represent mean ± SEM of the two experiments. For concentrations only evaluated in one of the experiments, single mean values are plotted.

necrosis factor alpha (*tnfa*). Furthermore, LPS up-regulated the expression of the tight junction gene Claudin 3 (*cldn3*, $P < 0.001$), but suppressed the intestinal alkaline phosphatase (*ialp)* expression (**Figure 6**, $P < 0.05$).

Pro-inflammatory cytokine genes (*il1b* and *il8*) were significantly increased after exposing cells to functional ingredients, especially MOS ($P < 0.01$). MOS also produced a significant up-regulation of transforming growth factor beta (*tgfb*) following 6 h of exposure ($P < 0.05$) while expression of myeloid differentiation factor 88 (*myd88*) and proliferating cell nuclear antigen (*pcna*) were significantly decreased (**Figure 6**, $P < 0.01$).

Compared to control, MOS and beta-glucans up-regulated the expression of *cldn3* ($P < 0.01$) while the expression of *ialp* and Na/K-ATPase (*nkaα1b*) decreased significantly following exposure to MOS (**Figure 6**, $P < 0.05$). There was also a significant decrease in the expression of E-cadherin (*cdh1*) after exposure to the different functional ingredients ($P < 0.05$). Gene expression levels of the bile acid transporter solute carrier family 10 member 2 (*slc10a2*) in RTgutGC cells increased significantly after exposure to nucleotides and MOS ($P < 0.05$).

In general, immune genes were expressed at comparable relative basal levels in RTgutGC cells as in rainbow trout distal intestinal tissue, whereas most genes related to barrier function and metabolism showed lower relative expression (**Supplementary Table 3**). Overall, nucleotides produced little or no effect on analytical endpoints related to barrier function and gene expression. In order to reduce costs, we therefore chose to omit nucleotide exposures in the additional analyses outlined below.

Cell Proliferation

In control cells, the gap area of the culture wells was fully closed by day 4 (**Figure 7**). When treated with LPS or beta-glucans, cells were able to close the gap in a similar pace as in the control cells.

In contrast, MOS treatment reduced the cell proliferation and consequently the gap closure rate to <50% at day 4 as shown in **Figure 7**.

ROS Generation

As shown in **Figures 8A–C**, viable cell numbers were not affected by treatments, while MOS diminished ROS positive cells markedly (96% decreased, $P < 0.001$). Moreover, mean fluorescence intensity of ROS in cells were significantly smaller than in other groups ($P < 0.001$).

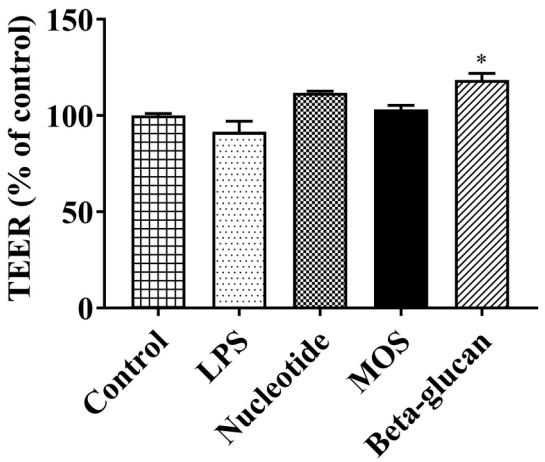


FIGURE 3 | TEER levels of RTgutGC cultures exposed to LPS and functional ingredients in 6-well-transwell membrane inserts for 6 h. Data are expressed as percent of control cells and represent mean + SEM of two independent experiments with 3 technical insert replicates each. Asterisks denote treatment groups statistically different to the control (*$P < 0.05$).

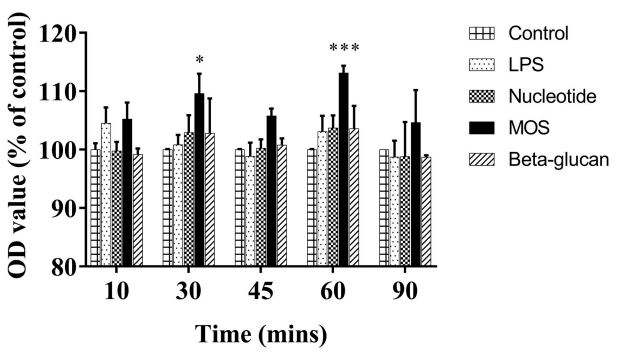


FIGURE 4 | Fluorescent levels in basolateral media after fluorescent albumin exposure into apical chamber in 24-well transwell membrane with RTgutGC cells exposed to LPS and functional ingredients for 6 h. Data are expressed as percent of control cells and represent mean + SEM of two independent experiments with 3 technical insert replicates each. Asterisks denote treatment groups statistically different to the control at the same time point (*$P < 0.05$, ***$P < 0.001$).

F-actin Content and E-cadherin, Aquaporin 8, and Hsp70 Protein Expression

As shown in **Figures 9A,B**, intracellular F-actin contents were significantly increased in LPS and beta-glucan groups ($P < 0.01$), while MOS treated cells remained at control levels. Western blot analyses demonstrated that expressions levels of Aqp8 and Hsp70 were not influenced by any of the treatments. E-cadherin expression was increased in cells treated with LPS, but decreased in beta-glucan and MOS treated groups ($P < 0.01$) (**Figure 10**).

DISCUSSION

Well-characterized *in vitro* model systems offer many benefits for screening purposes, given their simplicity and relative inexpensiveness compared to experiments using live animals. They could also serve as essential tools to increase the knowledge of cellular and molecular mechanisms underlying effects observed in animal trials. In the present work, we have continued the ongoing characterization of the first established intestinal epithelial cell line from fish, RTgutGC (18) and evaluated its suitability as an *in vitro* model for studies of effects of LPS and functional feed ingredients.

Functional Characterization of RTgutGC Cells

Based on previously established RTgutGC cell features (18–23, 33), we first confirmed the viability and barrier function of the RTgutGC cells when grown on transwell membranes. Barrier formation was assessed by TEER measurements and fluorescent albumin translocation from the apical to basolateral cell chamber. TEER levels in the present study were comparable to those reported previously (19, 20). We also observed a strong and time-dependent increase in basolateral fluorescence of albumin in wells without cells, whereas low and stable values were observed for wells with cells. Thus, our observations confirmed earlier reports (20, 33) demonstrating that RTgutGC cells grown on permeable inserts strongly attenuate fluorescent model molecules' translocation from apical to basolateral chamber. RTgutGC barrier function was further supported by related gene and protein expression (*cldn3*, *cdh1*, Claudin 3) as previously demonstrated (19, 20, 22). We also confirmed the findings by Minghetti and co-workers (20) by demonstrating the viability of the RTgutGC cells when exposed to a buffer designed to mimic the intestinal lumen (25), i.e., mucosal saline. Another indication that the RTgutGC cells function as enterocytes is the presence of brush border membrane enzymatic activity. Previous studies have demonstrated that RTgutGC cells possess alkaline phosphatase activity (18). In the current work, we continued to explore RTgutGC brush border features by measuring activity levels of two important brush border digestive enzymes, i.e., LAP and maltase. Activity of both these enzymes were detected in the RTgutGC cells. Higher LAP activity, but very low maltase activity, were found compared to the results of *in vivo* tests (34). Altogether, the current re-establishment of key barrier and brush border features demonstrates the robustness

of the RTgutGC transwell system and shows that RTgutGC cells develop certain intestinal functions similar to the *in vivo* situation.

Effects of LPS Exposure on RTgutGC

We continued to explore RTgutGC cell immune function by detailed exposures to a prototype PAMP, i.e., LPS. LPS showing no effect on cell viability at concentrations up to 100 μg/mL is in line with previous reports suggesting that fish cells without TLR4/CD14 signaling system may be less responsive to LPS compared to mammalian cells (18, 35, 36). The LPS used in the present study was derived from *E. coli*, and it is possible that LPS isolated from a fish pathogen could be more potent in RTgutGC cells. Anyhow, the final working concentration (50 μg/mL LPS) was clearly sufficient to induce immune-related gene expression responses and influence cell proliferation and F-actin contents of RTgutGC cells in this study.

The epithelial cells of the intestinal tract are in direct contact with the external environment of the gut lumen and must be prepared to mount an immune response against antigens and infections agents of dietary origin. It is well-known that intestinal epithelial cells of teleost fish produce several innate immune defense factors, and they can over-express pro-inflammatory cytokines following a bacterial infection (23). In the present study, LPS produced markedly elevated levels of pro-inflammatory cytokine gene expression (*il1b*, *il6*, *il8,* and *tnfa*). The data point toward RTgutGC immunocompetence, and demonstrate that RTgutGC cells possess the ability and transcriptional apparatus to mount an innate immune response against LPS, a common model PAMP. There are, to our knowledge, no published studies on spatial immune gene expression patterns along the rainbow trout intestinal tract. Given that the RTgutGC cell line was initially isolated from the distal intestine (18), which is believed to be a specific intestinal region for certain mucosal immune functions (29), it is interesting to note that RTgutGC relative immune gene expression were found at comparable levels as in the distal intestine of rainbow trout (**Supplementary Table 3**). Induced immune transcriptional responses to pathogen infection have previously been observed in human intestinal epithelial cells (37). In fish, similar effects of LPS on innate immune related gene expression have been observed also in head kidney leukocytes of rainbow trout (9). Moreover, LPS has been reported to up-regulate *tnfa* gene expression in RTgutGC cells grown on conventional culture plates (18). Intestinal alkaline phosphatase (Ialp) is an important apical brush border enzyme, which has been found to lower the expression of pro-inflammatory cytokines by inhibiting the activation and translocation of their master transcription factor NF-κB (38). LPS is a reported substrate for Ialp (38), and in the current work, LPS suppressed *ialp* expression. This response could reflect the interplay between LPS, Ialp and pro-inflammatory cytokine signaling.

Effects of Functional Feed Ingredients on RTgutGC

Our strategy for determining the final exposure concentrations of the functional ingredients was based on measurements of cell viability. When applied at high concentration, all functional ingredients significantly reduced cell viability in RTgutGC cells. We chose our final exposure concentrations at levels that maintained 80% cell viability as compared to control cells, with the underlying assumption that these cells were in a healthy state and could exert true physiological responses to the functional ingredients. It should be noted that the cell viability assays were performed with cells grown on conventional plates, and we therefore assume similar responses to the stimulants in cell grown on membrane inserts.

In two-compartment epithelial cell *in vitro* systems, increased TEER levels are interpreted as an increase in epithelial barrier tightness. In the present study, beta-glucans increased TEER values, whereas no significant effects were observed for nucleotides or MOS exposure. In contrast, MOS treatment increased albumin translocation across the RTgutGC monolayer, indicative of a reduced barrier function that could be attributed

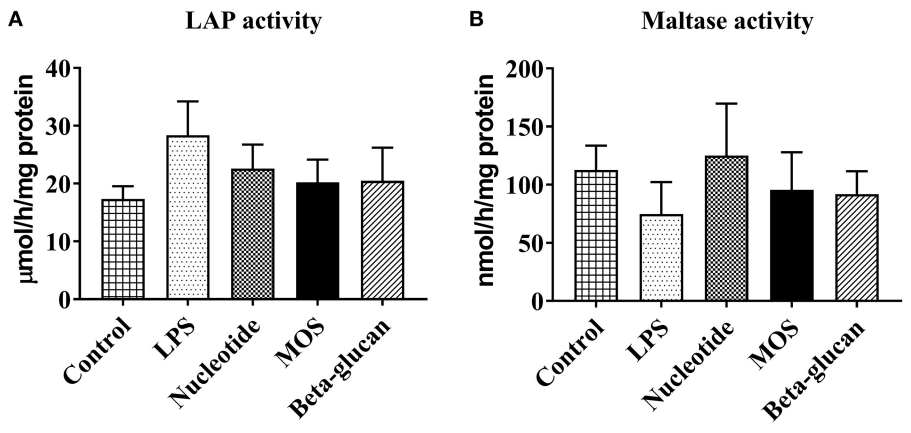


FIGURE 5 | Brush border membrane leucine aminopeptidase (LAP, **A**) and maltase **(B)** activity of RTgutGC cells grown on 24-well-conventional culture plates exposed to LPS and functional ingredients. Data represent mean + SEM of two independent experiments with 3 technical well replicates each.

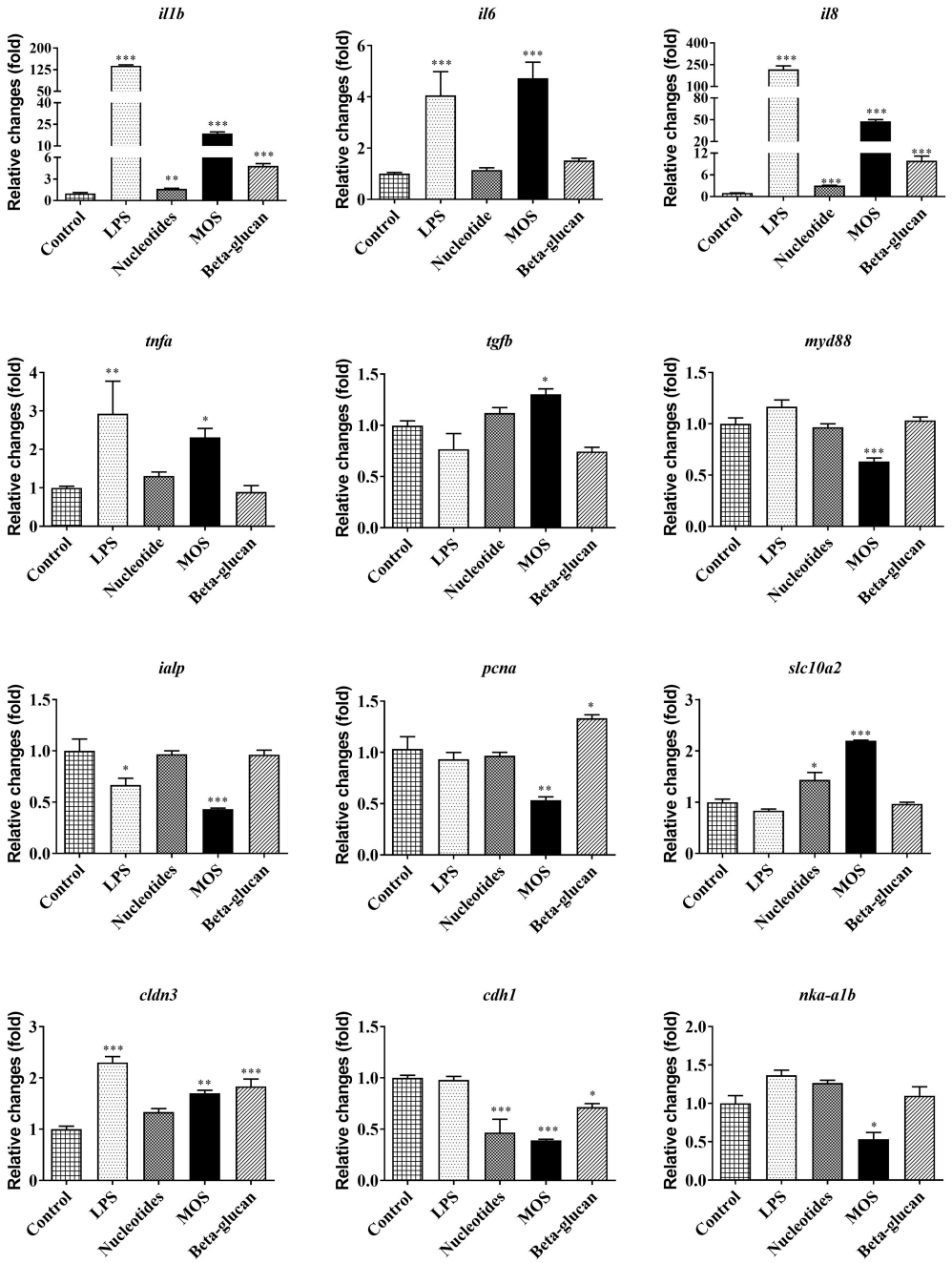


FIGURE 6 | Immune, barrier, and metabolic gene expression in RTgutGC cells grown on 6-well transwell membranes exposed to LPS and functional ingredients. Data are expressed relative to control cell levels and represent mean + SEM of two independent experiments with 3 technical insert replicates each. Asterisks denote treatment groups statistically different to the control (*$P < 0.05$, **$P < 0.01$, ***$P < 0.001$).

to alterations in both transcellular and paracellular routes. The relative proportion of trans- and paracellular translocation of albumin remains unknown, and should be explored in future studies, for example by detailed studies of albumin uptake kinetics into RTgutGC cells grown on permeable supports. Of note, we demonstrated that albumin was indeed taken up by the RTgutGC cells when grown on conventional supports, whereas no uptake of the larger molecule zymosan was detected. For junction barrier related gene expression, all functional ingredients suppressed *cdh1* levels and all ingredients except nucleotides increased *cldn3*. The suppressed *cdh1* levels in cells treated with MOS and beta-glucan were also mirrored by decreases at the protein expression level. In Caco-2 cells, decreases in *cldn3* mRNA levels were observed

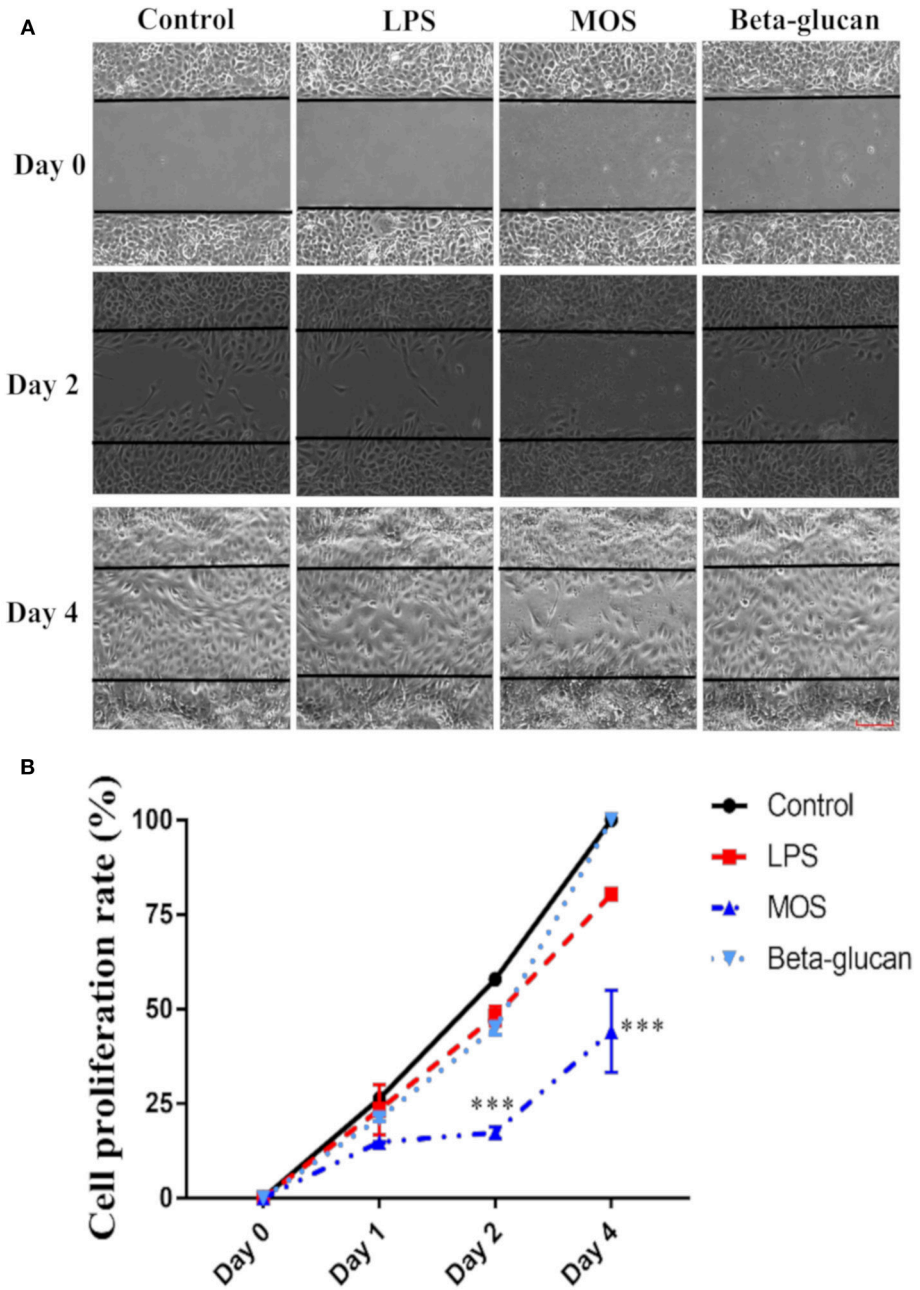


FIGURE 7 | Cell proliferation assay of RTgutGC cells. **(A)** Cells treated with LPS, MOS and beta-glucan at day 0, 2, and 4 after removal of the gap insert. Representative images of three independent experiments are shown. **(B)** Quantification of cell proliferation rate at different time points during treatment. Data represent mean ± SEM of three independent experiments with 3 technical well-replicates each. Asterisks denote treatment groups statistically significant different to the control at the same time point (***$P < 0.001$). Scale bar = 100 μm.

in concert with increase in paracellular permeability and a reduction in TEER (39). Similarly, the observed decreases in adherence junction-related *cdh1* expression would be expected to loosen the junction barrier and increase paracellular permeability. *In vivo*, MOS supplementation to fish has in several independent studies been found to improve microvilli integrity in terms of microvilli density (12) and length (12, 40, 41). In European seabass, MOS treatment enlarged intestinal fold height and reduced gut bacterial translocation, demonstrative of MOS effects on epithelial barrier function (42). Furthermore, beneficial physiological effects on epithelial cells of fish fed MOS could be a result of increasing mucus secretion (43), viscoelasticity of the mucus (44) or induced tight junction closure (ZO-1, occluding or E-cadherin) (45).

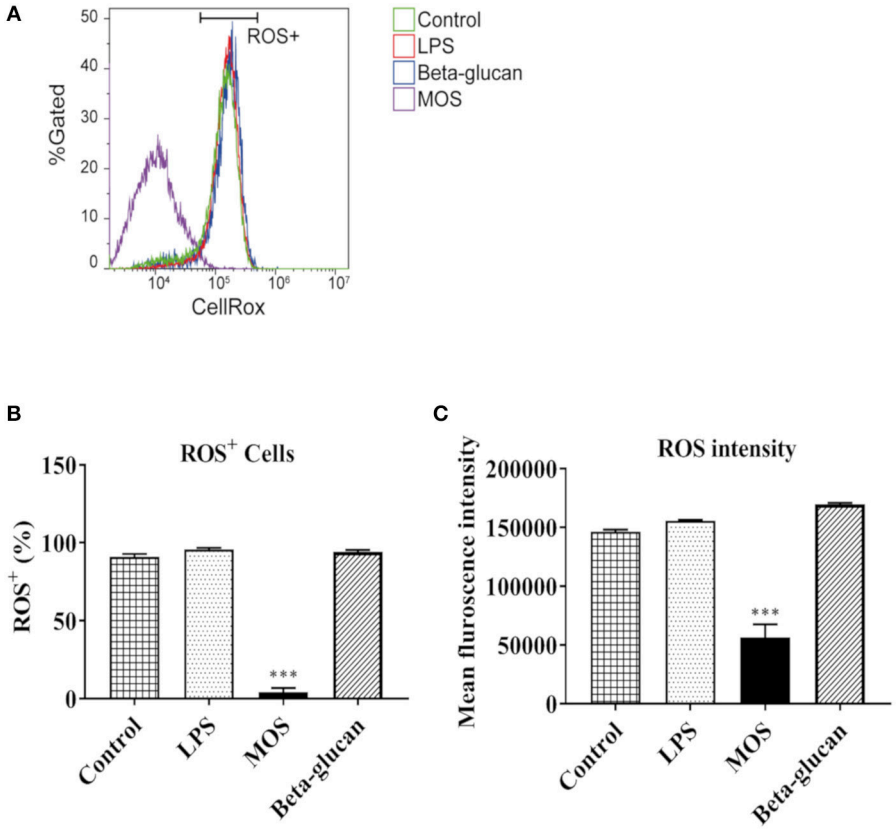


FIGURE 8 | Flow cytometry analysis of reactive oxygen species (ROS) production in RTgutGC cells grown on 6-well conventional plates and exposed to LPS, MOS and beta-glucan for 6 h. **(A)** Representative histograms of ROS dye fluorescence intensity. X axis shows the CellRox fluorescence signal in cells. Y axis shows the percentage of total live cell population. Horizontal bar indicate ROS positive (ROS^+) cells. **(B)** Statistical analysis of ROS^+ cell number under different treatments **(C)** Mean Fluorescent Intensities of ROS dye in cells under different treatments. Data represent mean + SEM of two independent experiments with 3 technical well-replicates each. Asterisks denote treatment groups statistically significant different to the control (***$P < 0.001$).

To our knowledge, there are no published studies of effects of MOS on gut epithelial barrier or tight junction function in rainbow trout. The findings of TEER, albumin translocation, and junction barrier related gene and protein expression in the present study may point to how MOS can act as homeostatic balancer of barrier function *in vivo* and *in vitro* (46).

RTgutGC cell proliferation was assessed by a previously established cell proliferation assay (22). RTgutGC cells had the ability to close the cell free gap in 4 days in this study, which was faster than in a previous report, possibly due to different culture conditions (22). During the 4-day period, MOS strongly reduced the cell proliferation speed compared to control. In addition, MOS significantly suppressed ROS production compared with control cells. ROS plays important roles in homeostasis and cell signaling, and ROS levels typically increase during periods of environmental stress and may cause significant damage to cell structures (47). Whether the MOS-induced decrease in RTgutGC proliferation ability could be a result of reduction in stress fibers and suppressed ROS production as previously reported (48, 49) warrants further investigation. Pcna plays an important role in cell proliferation (50). MOS also down-regulated *pcna* gene expression in the present study, confirming the cell proliferation assay results indicating that MOS inhibited cell proliferation (50).

Functional ingredients are expected to exert immune-modulatory effects in the intestine by regulating the expression of cytokines (2, 7, 10, 51). Among the functional ingredients evaluated in the present work, MOS seemed to be the most potent modulator of RTgutGC immune responses. Specifically, MOS treatment induced levels of pro-inflammatory (*il1b*, *il6*, *il8*, and *tnfa*) and *tgfb* cytokine transcripts, but suppressed *myd88* expression. In particular, the alterations of pro-inflammatory cytokine gene expression and the suppression of *ialp* mirrored the effect of LPS. *In vivo*, dietary MOS in European sea bass can provide protection against *Vibrio alginolyticus* infection (52) and counteract the side effects of soybean meal oil by increasing the mucus cell density and area in the distal intestine and regulating GALT-related genes (i.e. *il6*, *il10*, and *tgfb*) (46). MOS supplementation to rainbow trout was also found

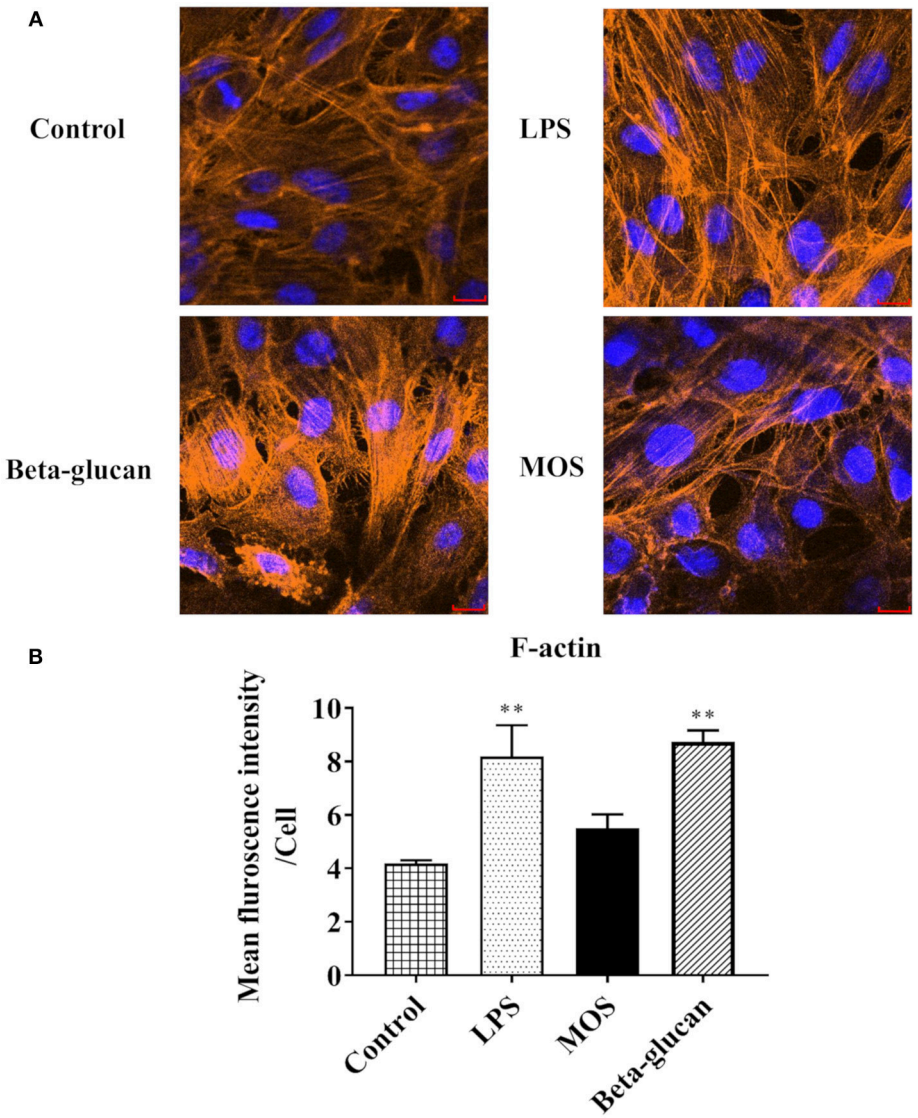


FIGURE 9 | RTgutGC cell morphology after treatments with LPS, MOS, and beta-glucan. **(A)** Staining of cell nuclei (blue) and skeleton (orange) after 6 h exposure to stimulants. **(B)** Mean Fluorescent Intensities (MFI) of RTgutGC skeleton (F-actin). Data represent mean + SEM of three independent experiments, with 3 technical replicates each. Asterisks denote treatment groups statistically significant different to the control (**$P < 0.01$). Scale bar = 100 μm.

to improve lysozyme concentration, classical pathway of complement (APCA and CPCA) (53), microvilli structure and absorptive surface area (12). Whether the immune-modulatory effects induced by MOS in the present study having any relation to the increase in epithelial permeability is a question that clearly warrants attention in future studies. Possibly, the increased permeability could lead to an increased antigen influx that would trigger mucosal immune responses, including modulation of cytokine expression.

Beta-glucan is one of the potent and promising immunostimulants in aquaculture which could be beneficial for growth, disease resistance and immune response of a range of fish species including rainbow trout (54–56). *In vitro*, beta-glucans were found to have positive effects on neutrophil degranulation of fathead minnows (57) and respiratory burst activity of Atlantic salmon (58). In the present study, beta-glucan treatment also produced increased mRNA levels of pro-inflammatory cytokine genes (*il1b* and *il8*). This observation is in agreement with previous studies demonstrating that beta-glucans up-regulated pro-inflammatory cytokine expression in head kidney cells of rainbow trout (9) and increased *il1b* expression in Atlantic cod after challenged with *Vibrio anguillarum* (10). A previous report also found that *il1b* production was induced by cathelicidin-2 variants and *il1b* expression upregulation was elicited by a synergic effect of zymosan and cathelicidin-2 variants in

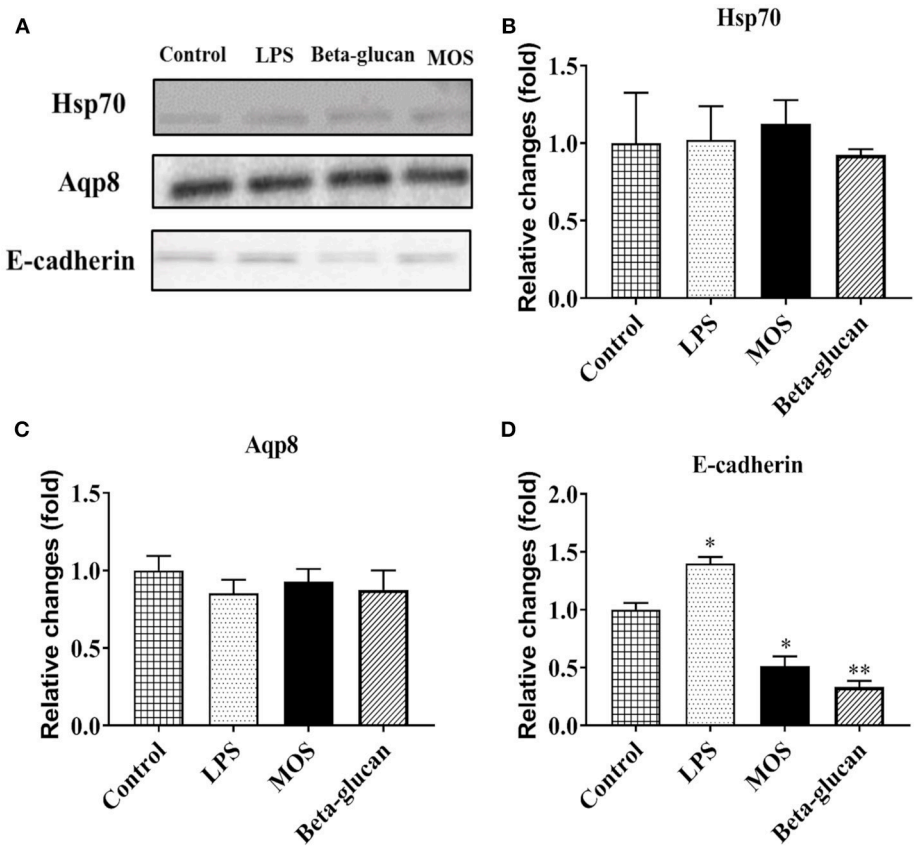


FIGURE 10 | (A) Representative Western blot pictures for target proteins. Statistical analysis of protein expression levels of heat shock protein 70 (hsp70, **B**), aquaporin 8 (Aqp8, **C**), and e-cadherin **(D)**. Data represent mean + SEM from two or three independent experiments with 3 technical replicates each. Asterisks denote treatment groups statistically significant different to the control (*$P < 0.05$, **$P < 0.01$). Full scans of the entire original blots are shown in **Supplementary Figure 2**.

RTgutGC cells (23). Beta-glucan lowered transactivation of NF-κB to stimulate immune response was also found in Caco-2 cells (15). Whether the expression of *il1b* and *il8* is affected by the cathelicidin-2 variants or the activation of NF-κB in RTgutGC still needs to be explored in future studies. *In vivo*, the expression of *il8* was not affected significantly in the distal intestine of Atlantic cod fed beta-glucans (10), which is different from our findings. Available literature suggests that beta-glucans may regulate inflammatory effects in an inconsistent pattern, possibly depending on the differences of composition, dosage, quality, route, and exposure time (11, 23, 54, 59). Nucleotides also produced elevated levels of *il1b* and *il8*, but the degree of response was minor compared to the other functional ingredients evaluated in the current study. Previous *in vivo* tests have found that dietary nucleotides might improve growth, disease resistance against *S. iniae* and pancreatic necrosis, serum alternative complement activity, serum lysozyme activity and crowding stress of rainbow trout (60–62) and influence macrophage activity, respiratory burst activity and expression of *il1b*, *il8,* and *tnfa* in turbot (63). However, the mechanism of growth and immune promotion by nucleotides still need to be identified *in vitro* or *in vivo* tests.

CONCLUSION

An increasing body of literature demonstrates that functional feed ingredients can support intestinal health and reduce disease susceptibility via multiple mechanisms, including direct effects on a variety of intestinal functions, e.g., barrier function, nutrient transport and immune responses (7, 23, 64–66). In fish, knowledge about basic mechanisms of functional ingredients and their interactions with the intestinal tissue is weak and fragmentary. The present study has provided new information on how functional ingredients commonly applied in aquafeeds can affect intestinal epithelial function in fish. Additionally, our study demonstrates the suitability of the RTgutGC transwell system as an alternative to fish feeding experiments for prediction of health effects of functional feeds.

AUTHOR CONTRIBUTIONS

JW, PL, AG, YY, ÅK, and TK: experiment design; JW, PL, AG, LL, YY, and TK: analyses; KS, LM, MØ, ÅK, and TK: supervision; JW and TK: writing, original draft; JW, PL, AG,

LL, YY, KS, LM, MØ, ÅK, and TK: writing, review, and editing.

FUNDING

JW was funded by China Scholarship Council (CSC). YY was funded by a Post-Doctoral fellowship issued by the Norwegian University of Life Sciences. The work was also funded by Foods of Norway, a Center for Research-based Innovation by the Research Council of Norway: grant no. 237841/030.

ACKNOWLEDGMENTS

We wish to thank Ellen Hage and Kirsti Præsteng for technical assistance in enzyme activity measurements.

SUPPLEMENTARY MATERIAL

The Supplementary Material for this article can be found online at: https://www.frontiersin.org/articles/10.3389/fimmu.2019.00152/full#supplementary-material

REFERENCES

1. Grosell M, Farrell AP, Brauner CJ. *Fish Physiology: The Multifunctional Gut of Fish*: London: Academic Press (2010).
2. Kiron V. Fish immune system and its nutritional modulation for preventive health care. *Anim Feed Sci Tech*. (2012) 173:111–33. doi: 10.1016/j.anifeedsci.2011.12.015
3. Ringø E, Zhou Z, Vecino JLG, Wadsworth S, Romero J, Krogdahl Å, et al. Effect of dietary components on the gut microbiota of aquatic animals. A never-ending story? *Aquacul Nutr*. (2016) 22:219–82. doi: 10.1111/anu.12346
4. Torrecillas S, Montero D, Izquierdo M. Improved health and growth of fish fed mannan oligosaccharides: potential mode of action. *Fish Shellfish Immunol*. (2014) 36:525–44. doi: 10.1016/j.fsi.2013.12.029
5. Carbone D, Faggio C. Importance of prebiotics in aquaculture as immunostimulants. Effects on immune system of *Sparus aurata* and *Dicentrarchus labrax*. *Fish Shellfish Immunol*. (2016) 54:172-8. doi: 10.1016/j.fsi.2016.04.011
6. Merrifield DL, Dimitroglou A, Foey A, Davies SJ, Baker RTM, Bøgwald J, et al. The current status and future focus of probiotic and prebiotic applications for salmonids. *Aquaculture* (2010) 302:1–18. doi: 10.1016/j.aquaculture.2010.02.007
7. Tacchi L, Bickerdike R, Douglas A, Secombes CJ, Martin SA. Transcriptomic responses to functional feeds in Atlantic salmon (*Salmo salar*). *Fish Shellfish Immunol*. (2011) 31:704–15. doi: 10.1016/j.fsi.2011.02.023
8. Gil A. Modulation of the immune response mediated by dietary nucleotides. *Eur J Clin Nutr*. (2002) 56:S1–4. doi: 10.1038/sj.ejcn.1601475
9. Chettri JK, Raida MK, Holten-Andersen L, Kania PW, Buchmann K. PAMP induced expression of immune relevant genes in head kidney leukocytes of rainbow trout (*Oncorhynchus mykiss*). *Dev Comp Immunol*. (2011) 35:476–82. doi: 10.1016/j.dci.2010.12.001
10. Lokesh J, Fernandes JM, Korsnes K, Bergh O, Brinchmann MF, Kiron V. Transcriptional regulation of cytokines in the intestine of Atlantic cod fed yeast derived mannan oligosaccharide or beta-glucan and challenged with *Vibrio anguillarum*. *Fish Shellfish Immunol*. (2012) 33:626–31. doi: 10.1016/j.fsi.2012.06.017
11. Skov J, Kania PW, Holten-Andersen L, Fouz B, Buchmann K. Immunomodulatory effects of dietary beta-1,3-glucan from Euglena gracilis in rainbow trout (*Oncorhynchus mykiss*) immersion vaccinated against *Yersinia ruckeri*. *Fish Shellfish Immunol*. (2012) 33:111–20. doi: 10.1016/j.fsi.2012.04.009
12. Dimitroglou A, Merrifield DL, Moate R, Davies SJ, Spring P, Sweetman J, et al. Dietary mannan oligosaccharide supplementation modulates intestinal microbial ecology and improves gut morphology of rainbow trout, *Oncorhynchus mykiss* (Walbaum). *J Anim Sci*. (2009) 87:3226–34. doi: 10.2527/jas.2008-1428
13. Hermes RG, Manzanilla EG, Martin-Orue SM, Perez JF, Klasing KC. Influence of dietary ingredients on *in vitro* inflammatory response of intestinal porcine epithelial cells challenged by an enterotoxigenic *Escherichia coli* (K88). *Comp Immunol Microbiol Infect Dis*. (2011) 34:479–88. doi: 10.1016/j.cimid.2011.08.006
14. He Y, Chu SH, Walker WA. Nucleotide supplements alter proliferation and differentiation of cultured human (Caco-2) and rat (IEC-6) intestinal epithelial cells. *J Nutr*. (1993) 123:1017–27. doi: 10.1093/jn/123.6.1017
15. Volman JJ, Helsper JP, Wei S, Baars JJ, van Griensven LJ, Sonnenberg AS, et al. Effects of mushroom-derived beta-glucan-rich polysaccharide extracts on nitric oxide production by bone marrow-derived macrophages and nuclear factor-kappaB transactivation in Caco-2 reporter cells: can effects be explained by structure? *Mol Nutr Food Res*. (2010) 54:268–76. doi:10.1002/mnfr.200900009
16. Amasheh M, Salah S, Amasheh S, Joachim M, Zeitz, M, Fromm M. Quercetin enhances epithelial barrier function and increases claudin-4 expression in Caco-2 cells. *J Nutr*. (2008) 138:1067–73. doi: 10.1093/jn/138.6.1067
17. Amasheh M, Andres S, Amasheh S, Fromm M, Schulzke JD. Barrier effects of nutritional factors. *Ann NY Acad Sci*. (2009) 1165:267–73. doi: 10.1111/j.1749-6632.2009.04063.x
18. Kawano A, Haiduk C, Schirmer K, Hanner R, Lee LEJ, Dixon B, et al. Development of a rainbow trout intestinal epithelial cell line and its response to lipopolysaccharide. *Aquacul Nutr*. (2011) 17:e241–e52. doi: 10.1111/j.1365-2095.2010.00757.x
19. Geppert M, Sigg L, Schirmer K. A novel two-compartment barrier model for investigating nanoparticle transport in fish intestinal epithelial cells. *Environ Sci Nano* (2016) 3:388–95. doi: 10.1039/c5en00226e
20. Minghetti M, Drieschner C, Bramaz N, Schug H, Schirmer K. A fish intestinal epithelial barrier model established from the rainbow trout (*Oncorhynchus mykiss*) cell line, RTgutGC. *Cell Biol Toxicol*. (2017) 33:539–55. doi: 10.1007/s10565-017-9385-x
21. Kawano A. (2009) *Developing and Characterizing a Salmonid Intestinal Epithelial Cell Line for Use in Studies of Inflammation in the Fish Gastrointestinal Tract*. Master's thesis. University of Waterloo.
22. Pumputis PG. (2017) *Development of RTgutGC as a Tool for Fish Feed Development*. Master's thesis. University of Waterloo.
23. Schmitt P, Wacyk J, Morales-Lange B, Rojas V, Guzman F, Dixon B, et al. Immunomodulatory effect of cathelicidins in response to a beta-glucan in intestinal epithelial cells from rainbow trout. *Dev Comp Immunol*. (2015) 51:160–9. doi: 10.1016/j.dci.2015.03.007
24. Schirmer K, Chan A, Greenberg B, Dixon D, Bols N. Methodology for demonstrating and measuring the photocytotoxicity of fluoranthene to fish cells in culture. *Toxi in vitro* (1997) 11:107–19.
25. Genz J, Esbaugh AJ, Grosell M. Intestinal transport following transfer to increased salinity in an anadromous fish (*Oncorhynchus mykiss*). *Comp Biochem Physiol A Mol Integr Physiol*. (2011) 159:150–8. doi: 10.1016/j.cbpa.2011.02.011
26. Schirmer K, Dixon D, Greenberg B, Bols N. Ability of 16 priority PAHs to be directly cytotoxic to a cell line from the rainbow trout gill. *Toxicology* (1998) 127:129–41.
27. Krogdahl A, Bakke-McKellep AM, Baeverfjord G. Effects of graded levels of standard soybean meal on intestinal structure, mucosal enzyme activities, and pancreatic response in Atlantic salmon (*Salmo salar L.*). *Aquaculture Nutr*. (2003) 9:361–71. doi: 10.1046/j.1365-2095.2003.00264.x
28. Dahlqvist A. Assay of intestinal disaccharidases. *Enzymol Biol Clin*. (1970) 11:52–66.
29. Venold FF, Penn MH, Krogdahl A, Overturf K. Severity of soybean meal induced distal intestinal inflammation, enterocyte proliferation rate, and fatty acid binding protein (Fabp2) level differ between strains of rainbow trout (*Oncorhynchus mykiss*). *Aquaculture* (2012) 364:281–92. doi: 10.1016/j.aquaculture.2012.08.035

30. Kortner TM, Valen EC, Kortner H, Marjara IS, Krogdahl A, Bakke AM. Candidate reference genes for quantitative real-time PCR (qPCR) assays during development of a diet-related enteropathy in Atlantic salmon (*Salmo salar L.*) and the potential pitfalls of uncritical use of normalization software tools. *Aquaculture* (2011) 318: 355–63. doi: 10.1016/j.aquaculture.2011.05.038
31. Muller PY, Janovjak H, Miserez AR, Dobbie Z. Processing of gene expression data generated by quantitative real-time RT-PCR. *Biotechniques* (2002) 32:1372–4.
32. Schneider CA, Rasband WS, Eliceiri KW. NIH Image to ImageJ: 25 years of image analysis. *Nat Methods* (2012) 9:671–5. doi: 10.1038/nmeth.2089
33. Drieschner C, Minghetti M, Wu SM, Renaud P, Schirmer K. Ultrathin alumina membranes as scaffold for epithelial cell culture from the intestine of rainbow trout. *ACS Appl Mater Inter*. (2017) 9: 9496–505. doi: 10.1021/acsami.7b00705
34. Krogdahl Å, Sundby A, Olli JJ. Atlantic salmon (*Salmo salar*) and rainbow trout (*Oncorhynchus mykiss*) digest and metabolize nutrients differently. Effects of water salinity and dietary starch level. *Aquaculture* (2004) 229:335–60. doi: 10.1016/s0044-8486(03)00396-x
35. Iliev DB, Roach JC, Mackenzie S, Planas JV, Goetz FW. Endotoxin recognition: in fish or not in fish? *FEBS Lett*. (2005) 579:6519–28. doi: 10.1016/j.febslet.2005.10.061
36. Chin AC, Flynn AN, Fedwick JP, Buret AG. The role of caspase-3 in lipopolysaccharide-mediated disruption of intestinal epithelial tight junctions. *Can J Physiol Pharmacol*. (2006) 84:1043–50. doi: 10.1139/y06-056
37. Baldwin DN, Vanchinathan V, Brown PO, Theriot JA. A gene-expression program reflecting the innate immune response of cultured intestinal epithelial cells to infection by *Listeria monocytogenes*. *Genome Biol*. (2002) 4:R2. doi: 10.1186/gb-2002-4-1-r2
38. Fawley J, Gourlay DM. Intestinal alkaline phosphatase: a summary of its role in clinical disease. *J Surg Res*. (2016) 202: 225–34. doi: 10.1016/j.jss.2015.12.008
39. McLaughlin J, Padfield PJ, Burt JPH, O'Neill CA. Ochratoxin A increases permeability through tight junctions by removal of specific claudin isoforms. *Am J Physiol-Cell Physiol*. (2004) 287:C1412–C7. doi: 10.1152/ajpcell.00007
40. Yilmaz E, Genc MA, Genc E. Effects of dietary mannan oligosaccharides on growth, body composition, and intestine and liver histology of rainbow trout, *Oncorhynchus mykiss*. *Isr J Aqua–Bam*. (2007) 59:182.e8.
41. Salze G, McLean E, Schwarz M, Craig S. Dietary mannan oligosaccharide enhances salinity tolerance and gut development of larval cobia. *Aquaculture* (2008) 274:148–52. doi: 10.1016/j.aquaculture.2007.11.008
42. Torrecillas S, Makol A, Benitez-Santana T, Caballero MJ, Montero D, Sweetman J, et al. Reduced gut bacterial translocation in European sea bass (*Dicentrarchus labrax*) fed mannan oligosaccharides (MOS). *Fish Shellfish Immunol*. (2011) 30:674–81. doi: 10.1016/j.fsi.2010.12.020
43. Torrecillas S, Makol A, Caballero MJ, Montero D, GinÉS R, Sweetman J, et al. Improved feed utilization, intestinal mucus production and immune parameters in sea bass (*Dicentrarchus labrax*) fed mannan oligosaccharides (MOS). *Aquaculture Nutr*. (2011) 17:223–33. doi: 10.1111/j.1365-2095.2009.00730.x
44. Schroers V, van der Marel M, Neuhaus H, Steinhagen D. Changes of intestinal mucus glycoproteins after peroral application of Aeromonas hydrophila to common carp (*Cyprinus carpio*). *Aquaculture* (2009) 288:184–9. doi: 10.1016/j.aquaculture.2008.12.013
45. Torrecillas S, Makol A, Betancor MB, Montero D, Caballero MJ, Sweetman J, et al. Enhanced intestinal epithelial barrier health status on European sea bass (*Dicentrarchus labrax*) fed mannan oligosaccharides. *Fish Shellfish Immunol*. (2013) 34:1485–95. doi: 10.1016/j.fsi.2013.03.351
46. Torrecillas S, Montero D, Caballero MJ, Pittman KA, Custodio M, Campo A, et al. Dietary mannan oligosaccharides: counteracting the side effects of soybean meal oil inclusion on european sea bass (*Dicentrarchus labrax*) gut health and skin mucosa mucus production? *Front Immunol*. (2015) 6:397. doi: 10.3389/fimmu.2015.00397
47. Faggio C, Pagano M, Alampi R, Vazzana I, Felice MR. Cytotoxicity, haemolymphatic parameters, and oxidative stress following exposure to sub-lethal concentrations of quaternium-15 in *Mytilus galloprovincialis*. *Aquat Toxical*. (2016) 180:258–65. doi: 10.1016/j.aquatox.2016.10.010
48. Vallenius T. Actin stress fibre subtypes in mesenchymal-migrating cells. *Open Biol*. (2013) 3:130001. doi: 10.1098/rsob.130001
49. Zimmerman NP, Kumar SN, Turner JR, Dwinell MB. Cyclic AMP dysregulates intestinal epithelial cell restitution through PKA and RhoA. *Inflamm Bowel Dis*. (2012) 18:1081–91. doi: 10.1002/ibd.21898
50. Dezfuli BS, Giari L, Lui A, Squerzanti S, Castaldelli G, Shinn AP, et al. Proliferative cell nuclear antigen (PCNA) expression in the intestine of *Salmo trutta trutta* naturally infected with an acanthocephalan. *Parasit Vectors* (2012) 5:198. doi: 10.1186/1756-3305-5-198.
51. Iswarya A, Vaseeharan B, Anjugam M, Gobi N, Divya M, Faggio C. beta-1, 3 glucan binding protein based selenium nanowire enhances the immune status of *Cyprinus carpio* and protection against *Aeromonas hydrophila* infection. *Fish Shellfish Immunol*. (2018) 83:61–75. doi: 10.1016/j.fsi.2018.08.057
52. Torrecillas S, Makol A, Caballero MJ, Montero D, Dhanasiri AK, Sweetman J, et al. Effects on mortality and stress response in European sea bass, *Dicentrarchus labrax* (L.), fed mannan oligosaccharides (MOS) after *Vibrio anguillarum* exposure. *J Fish Dis*. (2012) 35:591–602. doi: 10.1111/j.1365-2761.2012.01384.x
53. Staykov Y, Spring P, Denev S, Sweetman J. Effect of a mannan oligosaccharide on the growth performance and immune status of rainbow trout (*Oncorhynchus mykiss*). *Aquaculture Inter*. (2007) 15:153–61. doi: 10.1007/s10499-007-9096-z
54. Meena DK, Das P, Kumar S, Mandal SC, Prusty AK, Singh SK, et al. Beta-glucan: an ideal immunostimulant in aquaculture (a review). *Fish Physiol Biochem*. (2013) 39:431–57. doi: 10.1007/s10695-012-9710-5
55. Verlhac V, Gabaudan J, Obach A, Schuep W, Hole R. Influence of dietary glucan and vitamin C on non-specific and specific immune responses of rainbow trout (*Oncorhynchus mykiss*). *Aquaculture* (1996) 143:123–33. doi: 10.1016/0044-8486(95)01238-9
56. Sealey WM, Barrows FT, Hang A, Johansen KA, Overturf K, LaPatra SE, et al. Evaluation of the ability of barley genotypes containing different amounts of beta-glucan to alter growth and disease resistance of rainbow trout *Oncorhynchus mykiss*. *Anim Feed Sci Tec*. (2008) 141:115–28. doi: 10.1016/j.anifeedsci.2007.05.022
57. Palic D, Andreasen CB, Herolt DM, Menzel BW, Roth JA. Immunomodulatory effects of beta-glucan on neutrophil function in fathead minnows (*Pimephales promelas Rafinesque*, 1820). *Dev Comp Immunol*. (2006) 30:817–30. doi: 10.1016/j.dci.2005.11.004
58. Bridle A, Carter C, Morrison R, Nowak B. The effect of β-glucan administration on macrophage respiratory burst activity and Atlantic salmon, *Salmo salar L.*, challenged with amoebic gill disease–evidence of inherent resistance. *J Fish Dis*. (2005) 28:347–56. doi: 10.1111/j.1365-2761.2005.00636.x
59. Ringø E, Erik Olsen R, Gonzalez Vecino JL, Wadsworth S. Use of Immunostimulants and nucleotides in aquaculture: a review. *J Marine Sci Res Dev*. (2012) 2:104. doi: 10.4172/2155-9910.1000104
60. Tahmasebi-Kohyani A, Keyvanshokooh S, Nematollahi A, Mahmoudi N, Pasha-Zanoosi H. Dietary administration of nucleotides to enhance growth, humoral immune responses, and disease resistance of the rainbow trout (*Oncorhynchus mykiss*) fingerlings. *Fish Shellfish Immunol*. (2011) 30:189–93. doi: 10.1016/j.fsi.2010.10.005
61. Leonardi M, Sandino AM, Klempau A. Effect of a nucleotide-enriched diet on the immune system, plasma cortisol levels and resistance to infectious pancreatic necrosis (IPN) in juvenile rainbow trout (*Oncorhynchus mykiss*). *Bull Eur Assoc Fish Pathol*. (2003) 23:52–9.
62. Tahmasebi-Kohyani A, Keyvanshokooh S, Nematollahi A, Mahmoudi N, Pasha-Zanoosi H. Effects of dietary nucleotides supplementation on rainbow trout (*Oncorhynchus mykiss*) performance and acute stress response. *Fish Physiol Biochem*. (2012) 38:431–40. doi: 10.1007/s10695-011-9524-x
63. Low C, Wadsworth S, Burrells C, Secombes CJ. Expression of immune genes in turbot (*Scophthalmus maximus*) fed a nucleotide-supplemented diet. *Aquaculture* (2003) 221:23–40. doi: 10.1016/S0044-8486(03)00022-X

64. Wismar R, Brix S, Frokiaer H, Laerke HN. Dietary fibers as immunoregulatory compounds in health and disease. *Ann NY Acad Sci*. (2010) 1190:70–85. doi: 10.1111/j.1749-6632.2009.05256.x
65. Volman JJ, Ramakers JD, Plat J. Dietary modulation of immune function by beta-glucans. *Phys Behav*. (2008) 94:276–84. doi: 10.1016/j.physbeh.2007.11.045
66. Trischitta F, Faggio C. Effect of the flavonol quercetin on ion transport in the isolated intestine of the eel, *Anguilla anguilla*. *Comp Biochem Physiol C Toxicol Pharmacol*. (2006) 143:17–22. doi: 10.1016/j.cbpc.2005.11.012

Conflict of Interest Statement: The authors declare that the research was conducted in the absence of any commercial or financial relationships that could be construed as a potential conflict of interest.

Copyright © 2019 Wang, Lei, Gamil, Lagos, Yue, Schirmer, Mydland, Øverland, Krogdahl and Kortner. This is an open-access article distributed under the terms of the Creative Commons Attribution License (CC BY). The use, distribution or reproduction in other forums is permitted, provided the original author(s) and the copyright owner(s) are credited and that the original publication in this journal is cited, in accordance with accepted academic practice. No use, distribution or reproduction is permitted which does not comply with these terms.

frontiers in Immunology

REVIEW
published: 08 February 2019
doi: 10.3389/fimmu.2019.00179

Immunostimulatory Activities of CpG-Oligodeoxynucleotides in Teleosts: Toll-Like Receptors 9 and 21

Chao-Yang Lai[1], *Guann-Yi Yu*[2], *Yunping Luo*[3,4], *Rong Xiang*[5,6] *and Tsung-Hsien Chuang*[1,7]*

[1] *Immunology Research Center, National Health Research Institutes, Zhunan, Taiwan,* [2] *National Institute of Infectious Diseases and Vaccinology, National Health Research Institutes, Zhunan, Taiwan,* [3] *Deptartment of Immunology, Chinese Academy of Medical Science, School of Basic Medicine, Peking Union Medical College, Institute of Basic Medical Science, Beijing, China,* [4] *Collaborative Innovation Center for Biotherapy, School of Basic Medical Science, Chinese Academy of Medical Science and Peking Union Medical College, Beijing, China,* [5] *Department of Immunology, School of Medicine, Nankai University, Tianjin, China,* [6] *International Joint Center for Biomedical Research of the Ministry of Education, Tianjin, China,* [7] *Program in Environmental and Occupational Medicine, Kaohsiung Medical University, Kaohsiung, Taiwan*

OPEN ACCESS

Edited by:
Irene Salinas,
University of New Mexico, United States

Reviewed by:
Kevin R. Maisey,
Universidad de Santiago de Chile, Chile
Mark D. Fast,
University of Prince Edward Island, Canada

***Correspondence:**
Tsung-Hsien Chuang
thchuang@nhri.org.tw

Specialty section:
This article was submitted to Comparative Immunology, a section of the journal Frontiers in Immunology

Received: *30 October 2018*
Accepted: *21 January 2019*
Published: *08 February 2019*

Citation:
Lai C-Y, Yu G-Y, Luo Y, Xiang R and Chuang T-H (2019) Immunostimulatory Activities of CpG-Oligodeoxynucleotides in Teleosts: Toll-Like Receptors 9 and 21. Front. Immunol. 10:179. doi: 10.3389/fimmu.2019.00179

Toll-like receptors (TLRs) are pattern-recognition receptors that detect a wide variety of microbial pathogens for the initiation of host defense immunological responses. Thirteen TLRs have been identified in mammals, and teleosts contain 22 mammalian or non-mammalian TLRs. Of these, TLR9 and TLR21 are the cytosine-phosphate-guanosine-oligodeoxynucleotides (CpG-ODNs) recognition TLRs in teleosts. TLR9 is a mammalian TLR expressed in teleost but not in the avian species. TLR21 is a non-mammalian TLR expressed in both teleost and the avian species. Synthetic CpG-ODNs are potent immunostimulants that are being studied for their application against tumors, allergies, and infectious diseases, and as a vaccine adjuvant in humans. The immunostimulatory effects of CpG-ODNs as vaccine adjuvants and their antimicrobial function in domestic animals and teleosts are also being investigated. Most of our current knowledge about the molecular basis for the immunostimulatory activity of CpG-ODNs comes from earlier studies of the interaction between CpG-ODN and TLR9. More recent studies indicate that in addition to TLR9, TLR21 is another receptor for CpG-ODN recognition in teleosts to initiate immune responses. Whether these two receptors have differential functions in mediating the immunostimulatory activity of CpG-ODN in teleost has not been well-studied. Nevertheless, the existence of two recognition TLRs suggests that the molecular basis for the immunostimulatory activity of CpG-ODN in teleosts is different and more complex than in mammals. This article reviews the current knowledge of TLR9 and TLR21 activation by CpG-ODNs. The key points that need to be considered for CpG-ODNs as immunostimulants with maximum effectiveness in activation of immune responses in teleosts are discussed. This includes the structure/activity relationship of CpG-ODN activities for TLR9 and TLR21, the structure/functional relationship of these two TLRs, and differential expression levels and tissue distributions for these two TLRs.

Keywords: adjuvant, CpG-ODN, immune modulator, innate immunity, toll-like receptor

INTRODUCTION

Toll was originally identified in *Drosophila* as a type I transmembrane receptor involved in embryo development, and it plays an important role in innate immune responses to microbial infection in the adult fly (1–3). Thirteen toll-like receptors (TLRs), TLR1 to TLR13 were subsequently identified across all mammalian species, and humans contain ten of them, TLR1 to TLR10 (4–12). Human TLRs are well-investigated. These receptors can be divided into three subfamilies and play an essential role in innate immunity by recognizing a wide variety of pathogen-associated molecular patterns (PAMPs) from microbes (9–12). Phylogenetically, TLR1, TLR2, TLR6, and TLR10 are most closely related. TLR2 recognizes a broad range of microbial components, including lipoproteins, peptidoglycan, lipoteichoic acids, lipoarabinomannan, and zymosan (13–19). TLR2 and TLR6 form a complex that is more specific to triacyl lipopeptides; whereas, a heterodimer composed of TLR2 and TLR1 selectively recognizes triacyl lipopeptides (20–22). Ligand recognition of TLR10 has not been well-investigated; however, a recent paper showed that this TLR is a receptor for double-stranded RNA (dsRNA) (23). TLR4 is closely related to TLR5, with the former being responsible for recognizing lipopolysaccharides on the outer membrane of gram-negative bacteria and the latter recognizing flagellin, which is a component of bacterial flagella (24, 25). TLR3, TLR7, TLR8, and TLR9 comprise a TLR subfamily. These TLRs recognize nucleic acid-derived microbial PAMPs. TLR3 is activated by dsRNA generated during viral replication in infected cells (26). TLR7 and TLR8 recognize single-stranded (ss)RNA from viruses (27, 28). TLR9 is a receptor for microbial unmethylated cytosine-phosphate-guanosine (CpG) DNA (29, 30).

TLRs contain an extracellular domain (ectodomain) comprising multiple leucine-rich repeats (LLRs), a cysteine-rich motif followed by a transmembrane region, and a highly conserved cytoplasmic toll/interleukin (IL)-1 receptor (TIR) domain. The TLR ectodomain is the location of ligand binding, while the cytoplasmic TIR domain provides a key site for intracellular signaling (31, 32). Upon activation by ligand ligation, TLR monomers become dimerized. Their cytosolic domains subsequently recruit adaptor proteins from the myeloid differentiation primary response 88 (MyD88) family. These include MyD88, TIR-domain-containing adapter-inducing interferon-β (TRIF)/TIR domain-containing adapter molecule 1 (TICAM1), TIR domain-containing adapter protein (TIRAP)/MyD88 adapter-like (Mal), toll/interleukin-1 receptor protein (TIRP)/toll-like receptor adaptor molecule (TRAM), and SRAM; thereby, initiating downstream signaling pathways (31). All TLRs, except for TLR3, signal via a MyD88-dependent pathway. TLR3 and TLR4 utilize a TRIF-dependent pathway for signaling. In the MyD88-dependent pathway, a MyD88/IL-1R-associated kinase 1 (IRAK1)/IRAK4/TNFR-associated factor 6 (TRAF6) complex activates transforming growth factor beta-activated kinase 1 (TAK1), which in turn promotes the activation of several transcription factors, including factor kappa-light-chain-enhancer of activated B cells (NF-κB) and activator protein 1 (AP-1). In the TRIF-dependent pathway, the TLR recruits TRIF to activate NF-κB, AP-1, and interferon response factors (IRFs). Activation of NF-κB and AP-1 is mediated by TRAF6 and receptor-interacting protein (RIP), and IRF3/7 activation involves a TBK1-IKKε/IKKi complex (33–35). These transcription factors are key regulators of the expression of adhesion and co-stimulatory molecules and the production of various inflammatory cytokines required for triggering of innate immune responses. This subsequently leads to the activation of adaptive immune responses (36–38).

The immunostimulatory properties of microbial DNA were first discovered in a DNA fraction of bacillus Calmette–Guerin (39, 40). Additional studies have revealed that the immune stimulatory activity is present only when the DNA contains unmethylated CpG deoxynucleotides (41, 42). Synthetic phosphorothioate-modified CpG-ODNs mimic the functions of microbial CpG-deoxynucleotides containing DNA (CpG-DNA). In mammals, CpG-ODNs induce a wide variety of immune responses. Antigen presentation is promoted in dendritic cells because of the increased antigen processing and upregulated expression of costimulatory molecules. Production of inflammatory cytokines from dendritic cells, monocytes, and macrophages are increased. B-lymphocytes are activated, resulting in an increased proliferation and immunoglobulin (Ig) secretion. Natural killer (NK) cells are activated to produce IFN-γ. T-lymphocytes are also affected, resulting in initiation of T-helper (Th)1 responses. Moreover, the generation of cytotoxic T lymphocytes is increased (43–45).

By *in vivo* studies with gene knockout mice and *in vitro* studies with cell-based TLR9 activation assay, TLR9 was identified to be the cellular receptor for CpG-ODN (29, 30, 46). In mammals, TLR9 is mainly expressed in dendritic cells, monocytes/macrophages, and B cells (47–49). Activation of TLR9 by CpG-ODN results in several immunological effects, including activation of dendritic cells, monocytes, macrophages, and NK cells leading to antigen presentation and the production of cytokines. In addition, induction of TLR9 activates B cells and increases B-cell proliferation. TLR9 activation upregulates Th1 polarized cytokine productions. Cytokines including TNF-α, IL-6, IL-12, interferons, and chemokines promote T cell activation. These immunologic responses resulted by TLR9 activation replicate the *in vivo* function of CpG-ODNs further confirmed that TLR9 is the major cellular receptor for CpG-ODN in mammals (45, 50).

Because of these immunostimulatory activities, CpG-ODNs are being investigated for their properties against tumors, allergies, and infectious diseases for humans (50). In the last quarter of 2017, CpG-ODN was approved for the first time for application in humans. Heplisav-B, a hepatitis B vaccine containing CpG-ODN as an adjuvant, was approved by the United States Food and Drug Administration. Two doses of the new vaccine were satisfactory for immunization compared with three doses of the current hepatitis B vaccines that contain aluminum hydroxide as an adjuvant (51, 52). In addition to their application in humans, CpG-ODNs are being investigated for their adjuvant and antimicrobial activities in other species, including domestic animals and teleosts (53–56). These studies

reveal the potential usages of CpG-ODNs in human health, agriculture, and aquaculture.

TLR9 AND TLR21 MEDIATE THE IMMUNOSTIMULATORY ACTIVITY OF CPG-ODN

Other than the mammalian TLRs, several non-mammalian TLRs have also been identified in other vertebrate lineages (57, 58). For example, ten TLRs have been identified in avian genomes. Analysis of genomic DNA of two distantly related avian species, chicken and zebra finch, have identified: TLR1La, TLR1Lb, TLR2a, TLR2b, TLR3, TLR4, TLR5, TLR7, TLR15, and TLR21. The avian TLR1La, TLR1Lb, TLR2a, TLR2b, TLR3, TLR4, TLR5, and TLR7 are orthologs to the TLR found in mammals. The TLR1La and TLR1Lb result from duplication of TLR1-like genes, and TLR2a and TLR2b result from the duplication of TLR2 genes in avian evolution (59–63). Mammalian TLR7 and TLR8 have higher homology to each other than other TLRs, which could be due to a duplication of the same gene in some evolutionary duplication event (8). The avian genome contains TLR7 but does not contain TLR8. The mammalian TLR9 and TLR10 are also missing from the avian genomes. TLR15 and TLR21 found in the avian genome do not exist in genomes of mammalian species. TLR15 is phylogenetically related to the TLR2 family and appears to be unique to the avian species. In contrast, the avian TLR21 could be an ortholog to teleost and amphibian TLR21 (57–59). Interestingly, the avian species do not contain TLR9; however, like their actions in mammalian species, CpG-ODNs also activate marked immune responses and provide protection from microbial infections in chickens (50, 55, 64–67). Further studies have revealed that chicken TLR21 is a functional homolog to mammalian TLR9 in terms of responding to CpG-ODN stimulation (68, 69). The chicken TLR21 conferred cellular responses to CpG-ODN stimulation when it was over-expressed in human embryonic kidney (HEK) 293 cells. Knockdown of this receptor by shRNA significantly reduced the CpG-ODN-induced production of IL-1, IL-6, and iNOS from chicken DH11 cells (68, 69).

In teleosts, at least 22 different TLRs have been identified, including both mammalian (TLR1–TLR4, TLR5M, TLR5S, and TLR7–TLR9) and non-mammalian TLRs (TLR13, TLR14, TLR18–TLR28). In addition, orthologs of the mammalian signaling molecules and transcription factors for TLR functions have been identified (57, 58, 70–76). These TLRs are divided into six major subfamilies: TLR1, TLR3, TLR4, TLR5, TLR7, and TLR11 (57, 58).

The structure and ligand recognition properties of fish TLR1-3, 5, and 7–9 are similar to those of their mammalian counterparts. TLR2, a member of the TLR1 family, recognizes peptidoglycan, lipoteichoic acid, and lipopeptides. TLR3 detects dsRNAs. TLR5 recognizes bacterial flagellin. Teleost TLRs 7 and 8 respond to dsRNA, as well as to ssRNA, which is also recognized by mammalian TLR7 and TLR8 (57, 58). In contrast to mammalian TLR4, fish TLR4 does not recognize lipopolysaccharides (LPSs) despite its structural conservation with the former (77). Among non-mammalian TLRs, teleost TLR19 and TLR22 recognize dsRNAs (78–83). The recognition of dsRNAs by TLR19 results in the activation of IFN and NF-κB pathways and the protection of cells from infection by the grass carp reovirus (84). TLR22 recognizes dsRNAs to induce IFN production and protect cells from birnaviruses (83). In addition, a recent study showed that in fish, TLR22 functions as an equalizer for inflammation through the selective suppression of NF-κB and the activation of the MAPK pathway (85).

The immunologic effects of CpG-ODNs have been investigated in numerous teleost species. In these teleosts, much as in mammalian and avian species, CpG-ODNs upregulate the activation of macrophages, induce the proliferation of leukocytes, stimulate cytokine expression, and protect against bacterial, viral, and parasitic infections. Thus, CpG-ODNs have been studied for their application as antimicrobial agents and vaccine adjuvants in teleosts (53, 55). There is interest in the ligand recognition and functional properties of TLR9 and TLR21 in teleosts since these two TLRs have been shown to be the cellular receptors for CpG-ODN in mammals and chickens, respectively. TLR9 and TLR21 from zebrafish (*Danio rerio*) were comparatively investigated (86). Direct evidence to demonstrate that these two TLRs are the functional cellular receptors for CpG-ODN came from an experiment with cell-based activation assay in which the overexpression of both zebrafish (zeb)TLR9 and zebTLR21 in HEK293 cells conferred cellular responses to CpG-ODN stimulation (86). ZebTLR9 and zebTLR21 have different recognition profiles for CpG-ODNs with different nucleotide sequences. ZebTLR9 broadly recognizes CpG-ODN sequences that have higher activity for human cells and sequences that contain higher activity for mouse cells. In contrast, zebTLR21 prefers the CpG-ODNs that have higher activity for human cells (86). The biological functions of these two TLRs were investigated further in that study. CpG-ODNs that activate both zebTLR9 and zebTLR21 are more potent than others in the activation of cytokine productions in zebrafish and are more effective in protecting teleosts from the lethal effects of bacterial infection (86). These suggest that TLR9 and TLR21 cooperatively mediate the immunostimulatory effect of CpG-ODN in zebrafish. Beside these, the functions of TLR9 and TLR21 in other teleosts have not yet comparatively investigated.

STRUCTURAL FEATURES FOR THE IMMUNOSTIMULATORY PROPERTIES OF CPG-ODN

Natural CpG-DNA in microbial genomes contains a phosphodiester backbone that is quickly degraded by nucleases *in vivo*. Thus, the phosphorothioate backbone was developed to create synthetic CpG-ODNs by replacing oxygen with sulfur in the phosphate group of the nucleic acid to make them more resistant to nucleases (87–89). Other than this, the immunostimulatory activity of CpG-ODN is also dependent on its nucleotide sequence and structure, and it may involve different strengths of activity in different species, known as "species-specific activity." (90–92). Most of our knowledge

about the structure-dependent activity and species-specific activity of CpG-ODNs come from studies of the interaction between CpG-ODNs and mammalian TLR9 (29, 30, 46, 90–92). Because previous studies used human and mouse cells which have TLR9 only, in addition the mammalian TLR9 was identified for investigation earlier than the non-mammalian TLR21 was.

Based on their structural features, CpG-ODNs are divided mainly into four classes. Class A (also known as type D) CpG-ODNs contain a central phosphodiester palindromic region with one or more CpG-motifs in the palindrome and consist of poly (G) sequences with a phosphorothioate backbone attached to the 5′ and 3′ ends. Class B (type K) CpG-ODNs contain a phosphorothiolate backbone throughout the entire sequence with several CpG-motifs. Class C CpG-ODNs contain phosphorothioate backbone with one or two CpG-motifs and a palindromic sequence at the 3′ end. The CpG-ODNs of class P contain two palindromic sequences with phosphodiester cytosines in the palindrome (90, 93–96). **Table 1** shows the structures for the four classes of CpG-ODN. Different classes of CpG-ODNs have different immunostimulatory effects. Class A CpG-ODNs stimulate the production of large amounts of IFN-α and induce the maturation of plasmacytoid dendritic cells (pDCs) but have little effect on B-cell activation. Class B CpG-ODNs strongly induce B-cell proliferation, pDC and monocyte maturation, NK cell activation, and cytokine production. They also stimulate the production of IFN-α, but to a lesser extent than class A CpG-ODNs. The extent of the capability of class C CpG-ODNs to induce B-cell proliferation and IFN-α production is between that of class A and B CpG-ODNs. The immunological activities of class P CpG-ODNs are characterized by their high capability for inducing IFN-α production and NF-κB activation. Nearly all CpG-ODNs investigated in clinical trials have been class B CpG-ODNs (90, 93–96).

Another of the major structural features of CpG-ODNs is they include one or more copies of CpG-deoxynucleotide containing hexamer (CpG-hexamer) motifs. The immunostimulatory activity of these CpG-ODNs depends on the number, position, spacing, and surrounding bases of these CpG-hexamer motifs. Their species-specific activity is determined by the nucleotide context of these CpG-hexamer motifs (90–92). For example, CpG-1826, which contains two copies of the GACGTT-hexamer motif in 20 nucleotides, is more effective in activating murine cells than CpG-2007, which contains three copies of the GTCGTT-hexamer motif in 22 nucleotides; however, CpG-2007 is more potent in activating human cells than CpG-1826 (46, 90–92, 97). In addition, the nucleotide length of CpG-ODN plays a significant role in determining its immunostimulatory activity. In rabbit cells, CpG-C46 and CpG-C4609, which each contain 12 nucleotides and have a GACGTT- and AACGTT-hexamer motif, respectively, generate stronger immune responses than CpG-1826 and CpG-2007 (98).

TABLE 1 | Structural features of CpG-oligodeoxynucleotides (ODNs) in each of the four major classes.

Class	Name	Sequence
A	CpG-2336	5′- G*G*G*G-A-C-G-A-C-G-T-C-G-T-G-G*G*G*G*G*G–3′
B	CpG-2007	5′- T*C*G*T*C*G*T*T*G*T*C*G*T*T*T*T*G*T*C*G*T*T-3′
C	CpG-2395	5′-T*C*G*T*C*G*T*T*T*T*C*G*G*C*G*C*G*C*G*C*C*G-3′
P	CpG-21798	5-T*C-G*T*C-G*A*C-G*A*T*C-G*G*C*G*C-G*C*G*C*C*G-3

Hyphens indicate phosphodiester and asterisks stand for phosphorothioate bonds. Red color shows CpG-hexamer and underlining indicates palindromic sequence.

SEQUENCE OF CPG-ODN FOR TLR9 AND TLR21 ACTIVATION IN TELEOSTS

Several CpG-ODNs have been investigated in teleosts for their immunostimulatory activity and antimicrobial functions. There are well-written reviews for these properties of CpG-ODN in earlier works (53, 55). **Table 2** summarizes the more recent work. Most of the CpG-ODNs used in these studies are class B. Like in mammals, CpG-ODN nucleotide length determines its immunostimulatory activity in teleosts. In Atlantic salmon (*Salmo salar*), CpG-ODNs that are 16–17 nucleotides long show less immunostimulatory effects that those that are 20–22 nucleotides long. CpG-ODNs shorter than 13 nucleotides lose their immunostimulatory properties. In addition, CpG-ODNs that are more than 30 nucleotides long have rarely been investigated for their immunologic activity in teleosts (53, 55, 120).

Compared to what is known about the critical role of CpG-hexamer motif in the activity of CpG-ODN in mammalian species, a conclusion has not been reached on what type of CpG-hexamer motif is best for generating a strong immune response in teleosts. CpG-1668, which contains one copy of the GACGTT-hexamer motif in 20 nucleotides, is reported to have immunostimulatory activity, adjuvant effects, and antimicrobial properties in different teleosts, including rock bream (*Oplegnathus fasciatus*), olive flounder (*Paralichthys olivaceus*), orange-spotted grouper (*Epinephelus coioides*), Asian sea bass (*Lates calcarifer*), and Pacific red snapper (*Lutjanus peru*) (100–104, 115). Moreover, when fed to Atlantic salmon (*Salmo salar*), CpG1668 induced the expression of cytokines, such as IL-1β and IL-12β, to protect this teleost fish from infection by sea lice (*Lepeophtheirus salmonis*), which are the most important ectoparasites that affect the farming of Atlantic salmon (106, 107). When administered to rock bream, CpG-1668 activates stronger protective effects against viral infection than other CpG-ODNs with GTCGTT-hexamer or with the same GACGTT-hexamer motif but with different nucleotide lengths (100). CpG-2006 and CpG2007, which contain three copies of the GTCGTT-hexamer motifs in 24 and 22 nucleotides, respectively, have been shown to induce immune responses in yellowtail (*Seriola quinqueradiata*), olive flounder, large yellow croaker (*Larimichthys crocea*), grass carp (*Ctenopharyngodon idella*), Nile tilapia (*Oreochromis niloticus*), and Atlantic salmon (108, 109, 112, 113, 116, 121). In olive flounder, CpG-2007 has better protection against *Edwardsiella tarda* infection than CpG-1668 (112). In grass carp, CpG-1670A, which contains three copies of the AACGTT-hexamer motif in 25 nucleotides, displays a greater

TABLE 2 | Summary of CpG oligonucleotides used in teleost.

CpG-ODN	Sequence (5′->3′)	Action	Fish
2722	GTTGTCGTTTTTTGTCGTT	Induce NF-κB activation and cytokine expressions via TLR21 (99)	Grouper
2727	GTTGTCGTTTTTTGTGCTT	Induce NF-κB activation and cytokine expressions via TLR21 (99)	Grouper
1668	TCCATGACGTTCCTGATGCT	Activate innate and adaptive immune responses, and offer protection from bream iridovirus infection (100, 101)	Rock bream
		Used as an adjuvant for vaccines against V. harveyi infection (102)	Grouper
		Activate innate immune response and upregulate TLR9 and IgM-mediated immune response (103)	Pacific red snapper
		Increase protection against P. dicentrarchi infection (104)	Oliver flounder
		Stimulate upregulation of TLR9, IL-1and chemokine CC (105)	Cobia
		Decrease sea lice infection in CpG-1668 fed group via induction of inflammatory gene expression (106, 107)	Atlantic salmon
2006	TCGTCGTTTTGTCGTTTTGTCGTT	Induce IgM and antimicrobial peptide gene expression (108)	Yellowtail
		Stimulate IL-1 and IL-6 production and NF-κB activation in head kidney cells (109)	Yellow croaker
		Elicit better protection against E. tarda through activation of both TLR9 and TLR21 (86)	Zebrafish
		Stimulate upregulation of IgM, TLR9, IL-1 and chemokine CC (105)	Cobia
		Promote IgM secretion and upregulation of cd83, cd40, ifna1 and ifnb (110)	Atlantic salmon
		Induce MAPK-activated protein kinase 2 activation in phagocytes (111)	Atlantic salmon
2007	TCGTCGTTGTCGTTTTGTCGTT	Increase survival rates following challenge with E. tarda (112)	Olive flounder
		Activate IL-1, IL-6 production and NF-κB activation in head kidney cells (109)	Yellow croaker
		Induce protective effect against S. iniae infection (113)	Nile tilapia
		Elicit better protection against E. tarda through activation of both TLR9 and TLR21 (86)	Zebrafish
2395	TCGTCGTTTTCGGCGCGCGCCG	Induce expression of antiviral Mx gene in spleen and liver (105)	Cobia
		Upregulation of TLR21 expression (114)	Turbot
1013	CTCACTATCGTTCTTGATT	Increase WBC counts, peroxidase activity and oxidative radicals in head kidney, upregulate immune-related genes and enhance protection against S. iniae infection (115)	Asia sea bass
1670A	TCGAACGTTTTAACGTTTTAACGTT	Induce protective antiviral responses against grass carp reovirus (116)	Grass carp
1826	TCCATGACGTTCCTGACGTT	Activate IL-1, IL-6 production and NF-κB activation in head kidney cells (109)	Yellow croaker
C7	GGCGCGCGTCGCGCGCTA	Inhibite viral replication, promote proliferation of leukocytes, and enhance activation of head kidney phagocytes (117)	Olive flounder
205	GATCGCGTGCGTGCGTCTAT	Induce macrophage activation, leukocyte proliferation and protect against lethal E. tarda challenge (118)	Turbot
D	ACCGATAACGTTGCCAACGTTGGT	Upregulate leucocyte gene expressions including TNF-α, IL-1, TLR9, IRF-1, Mx, MHCIIa, IgM_H and CSF-1R (119)	Gilthead seabream

capacity to protect teleosts against viral infection than CpG-1668 and CpG-2006 (116).

The ability of teleost TLR9 and TLR21 to uniquely distinguish different types of CpG-hexamer motifs in teleosts may account for the different CpG-ODN sequences that have been reported to participate in the induction of immune responses in different teleost species. The zebTLR9 has been shown to broadly recognize different CpG-hexamer motifs; however, it more strongly recognizes CpG-ODN with the GACGTT- or AACGTT-hexamer motif than CpG-ODN with the GTCGTT-hexamer motif. In contrast, zebTLR21 responds more to CpG-ODN with the GTCGTT-hexamer motif. Further study suggests that CpG-ODNs with an optimized sequence for activating these two TLRs can generate the strongest immunostimulatory activity in this species (86). CpG-ODNs with the GTCGTT-hexamer motif, such as the CpG-2722 and CpG-2727, have strong effects on the TLR21 group like that required for the activation of zebTLR21; in contrast, CpG-1826 with the GACGTT-hexamer motif does not activate this TLR (99). CpG-2006, CpG-2007, and CpG-1826 are reportedly able to activate TLR21 in large yellow croakers (109). The optimized sequence for CpG-ODN to strongly activateTLR9s or TLR21s from other teleosts has not been investigated. Given the large diversity in teleost species, there is not expected to be a universal CpG-ODN sequence for strong activation of TLR9 or TLR21 from different teleost species. This means that the interaction of CpG-ODN with TLR9 or TLR21 from different teleost species must be investigated individually to generate conclusions about how to design a sequence for CpG-ODN with a strong immunostimulatory activity in the teleost species.

FUNCTIONAL ACTIVITY OF TELEOST TLR9 AND TLR21 IN RESPONSE TO CPG-ODN STIMULATION: SUGGESTIONS MADE BY THEIR STRUCTURE

Along with the requirement of an optimized nucleotide sequence for CpG-ODN to strongly activate TLR9 and TLR21, whether CpG-ODN can generate a strong immune response in a teleost

species is also determined by the intrinsic functional activity of TLR9 and TLR21 in that teleost. Furthermore, although both TLR9 and TLR21 in zebrafish are active in response to CpG-ODN stimulation (86), it is still unclear whether both are functional in other teleost species. Nevertheless, some suggestions can be made from the protein sequences analysis of these two TLRs from different teleost species and the study of the structure/functional activity relationship of mammalian TLR8.

In mammals, TLR7, TLR8, and TLR9 are phylogenetically closely related and are a subfamily of TLRs (5, 8). These three TLRs have an ectodomain in a horseshoe-like shape that consists of 25 copies of LRRs and a unique undefined region (also called a Z-loop) between LRR14 and LRR15 (122, 123), as shown in **Figures 1A,B** for the ectodomains of TLR9s. This unique undefined region plays an important role in ligand activation of members of this TLR subfamily (124–126). Previous studies have shown that TLR8s from several non-rodent species, including cat, horse, sheep, and bovine, are activated by their agonists; whereas, TLR8s from the mouse and rat, two rodent species, do not respond to ligand stimulation (127). Another study revealed that rabbit TLR8 (also a rodent TLR8) has very little activity after ligand stimulation compared to that of humans (128). Inspection of the ectodomains of these TLR8s reveals that the lengths of amino acid residues within the undefined regions varies between TLR8s from the non-rodent group and those from the rodent group. Compared to non-rodent TLR8s, the undefined regions of mouse and rat TLR8s are shorter by five amino acid residues; whereas, the undefined region of rabbit TLR8 is longer by 34 amino acid residues. Although the structural base is still unclear, it has been suggested that the lesser functional activity of these rodent TLR8s is a result of the varied lengths of their undefined regions (127, 128). Distinct from TLR8, non-functional TLR7 and TLR9 have not been reported in mammalian species. Consistently, the length of the undefined regions in mammalian TLR7s and TLR9s are more conserved than that in the TLR8s (127, 128).

Like mammalian TLR9s, teleost TLR9s also contain an undefined region in their ectodomain, which results in an extruded loop in the horseshoe-shaped ectodomain of these TLRs (**Figures 1A,B**). Interestingly, there are large variations in the length of undefined regions in teleost TLR9s. The regions in teleost TLR9s are longer than in mammalian TLR9s (**Figure 1B**). Moreover, the length of these undefined regions is more consistent in the more phylogenetically-related teleost TLR9s than in the more distantly-related teleost TLR9s. For example, TLR9s of zebrafish, grass carp, common carp (*Cyprinus carpio*), Mexican tetra (*Astyanax mexicanus*), and channel catfish (*Ictalurus punctatus*) are more closely phylogenetically related, and the lengths of their undefined regions are more consistent than in the TLR9s of the Atlantic salmon and orange-spotted grouper, which are more distantly related (**Figures 1B,C**). Given that the undefined regions play a role in the functional activity of TLR8, this structural analysis of undefined regions within TLR9s from different teleosts suggests that there is a large difference in the intrinsic functional activities of TLR9s from different teleost species. Furthermore, because the more phylogenetically-related teleost TLR9s contain more conserved undefined regions, it also suggests that there are more similar functional activities for the more closely related teleost TLR9s.

In contrast, although TLR21 is functionally related to TLR9 in response to CpG-ODN stimulation, TLR21 is more phylogenetically related to members of the TLR11 subfamily and is an ortholog closer to the TLR13 subfamily (129, 130). Analysis of chicken TLR21 revealed that it does not have an undefined region, as in TLR9. In addition, a study of TLR21 proteins from different species shows that these TLR21s are highly homologous (130). The same is true for teleost TLR21s. As **Figure 2** illustrates, undefined regions are not found in teleost TLR21s whether the TLR21s are closely related or distantly related to each other; therefore, the highly-diversified ectodomains of TLR9s from different teleost are not observed in teleost TLR21s. In general, the teleost TLR9s contain more than 1,000 amino acid residues, and the teleost TLR21s have <1,000. A lack of the undefined region in these teleost TLR21s is the main reason why teleost TLR9s contain more amino acid residues than TLR21s (**Figures 1C**, **2C**). The more conserved ectodomains of teleost TLR21s suggest a more stable functional activity of TLR21s within different teleost species. Nevertheless, these suggestions made by structural analyses of the teleost TLR9s and TLR21s are waiting for confirmation by experimental investigation.

EXPRESSION AND TISSUE DISTRIBUTION OF TLR9 AND TLR21 IN TELEOSTS

In addition to their functional activity, the differential expression levels and tissue distributions of TLR9 and TLR21 are likely to be another level of determinant of CpG-ODN efficacy in teleosts. The expression profile of TLR9 has been investigated in several different species of teleost and has been shown to be broadly expressed in different tissue types and development stages (131–135). In gilthead sea bream (*Sparus aurata*), the expression levels of TLR9 transcripts are detected in the gill, head kidney, and spleen (119). In channel catfish, TLR9 is expressed in the skin, gill, head kidney, and spleen (135). In addition, TLR9 expression is inducible by responding to different stimuli and microbial infections (105, 135). For example, TLR9 is broadly expressed in larval, juvenile, and adult stages of cobia (*Rachycentron canadum*) in all analyzed tissues, including the gill, intestine, head kidney, liver, skin, and spleen. Cobia challenged with *Photobacterium damselae* subsp. *piscicida* results in increased TLR9 expression in these tissues with different dynamic profiles (105). TLR9 expression in the skin and gills of channel catfish is induced by infection with *Ichthyophthirius multifiliis* (135).

TLR21 has an expression profile like that of TLR9. In yellow catfish, the TLR21 gene is detected in fertilized eggs and in the young up to 30 days after hatching. In adult fish, this gene is detected in the muscles, stomach, skin, swim bladder, midgut, brain, spleen, trunk kidney, skin mucus, head kidney, liver, heart, gill, and blood, with the highest expression in the spleen. TLR21 mRNA expression levels in the spleen, head kidney, trunk kidney, liver, and blood of yellow catfish are upregulated after challenging the fish with killed *Aeromonas hydrophila* (136). In turbot (*Scophthalmus maximus*), TLR21 transcripts are broadly

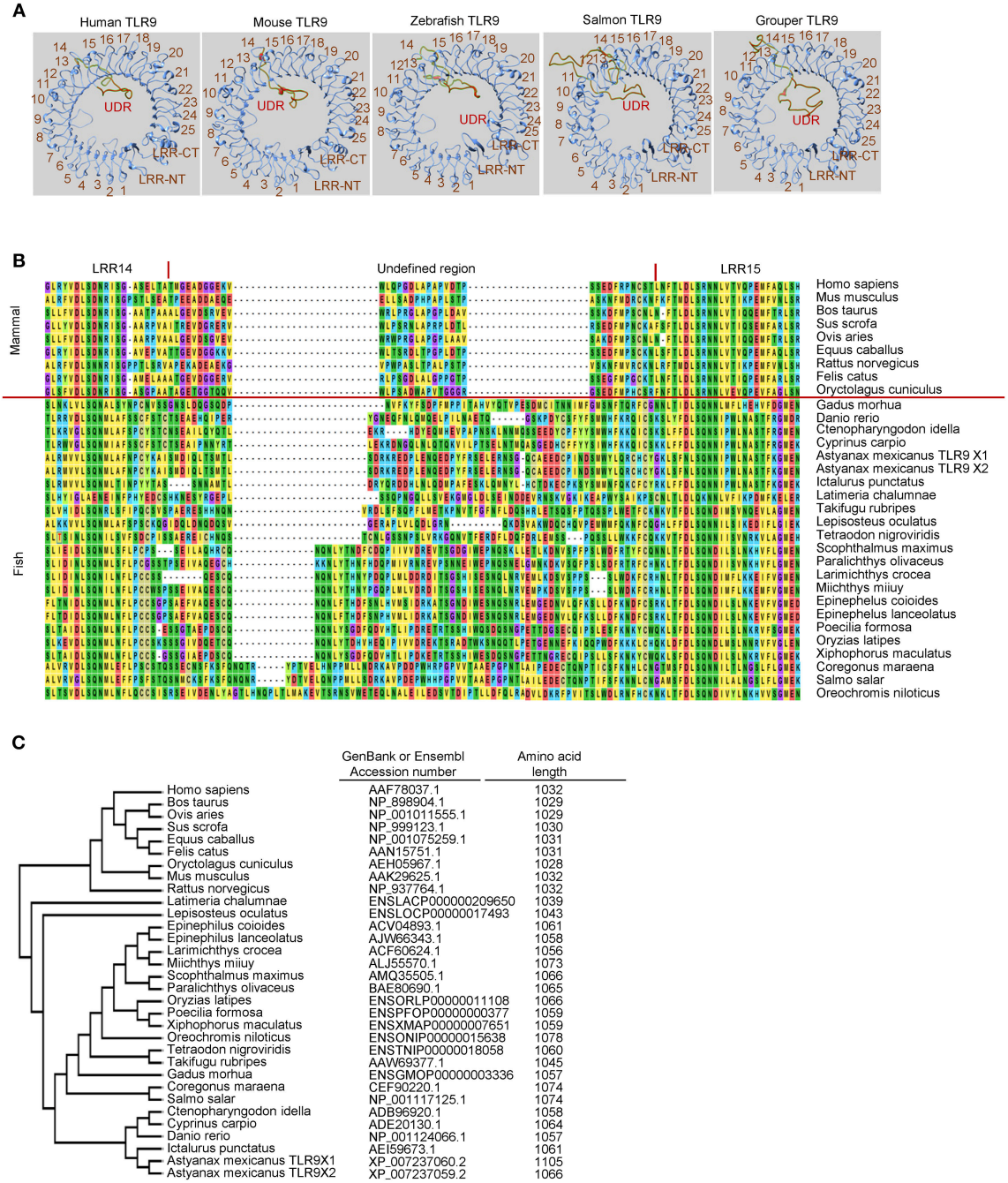


FIGURE 1 | Undefined region of toll-like receptor 9 (TLR9) from different teleost species. **(A)** Computational modeling of the ectodomain protein structures of TLR9 from different species as indicated. These structural models were predicted with SWISS MODEL (www.swissmodel.expasy.org). **(B)** Alignment of protein sequences for the undefined regions between leucine-reach repeat (LRR)14 and LRR15 in the ectodomain of TLR9 from different species. Multiple alignments of the amino acid sequences of TLR21s were performed using ClustalW2 (www.ebi.ac.uk/Tools/msa/clustalw2). **(C)** Phylogenetic analysis of TLR9s from different species. The GenBank accession numbers of these TLR9 protein sequences are listed in the left column. Numbers in the right column are the amino acid lengths of these TLR9s.

expressed in different tissues, with the highest expression in the spleen followed by the head kidney and liver. In addition, after infection with turbot reddish body iridovirus or stimulation with polyinosinic:polycytidylic acid and CpG-2395, which contain a GTCGTT-hexamer motif within 22 nucleotides, the expression of the turbot TLR21 transcript is upregulated in the gills, head kidney, spleen, and muscle (114). In large yellow croakers, TLR21 is expressed in all tested tissues, with higher levels in immune-related tissues such as the spleen, head kidney, and gills (109). In rock bream, TLR21 transcripts are ubiquitously expressed in

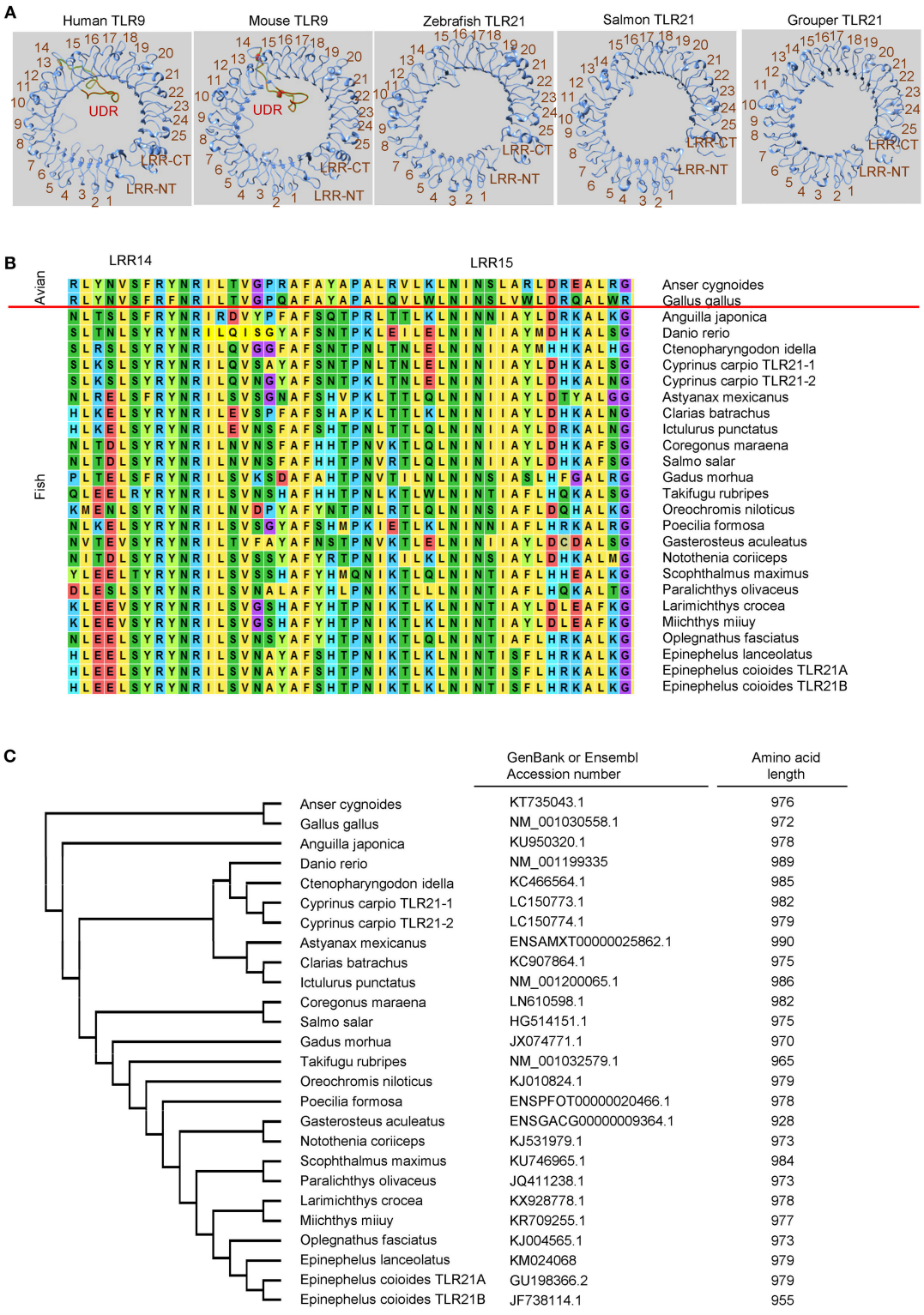


FIGURE 2 | Toll-like receptor 21 (TLR21) from different teleost species does not contain an undefined region. **(A)** Computational modeling of the ectodomain protein structures of TLR21 from different species as indicated. These structural models were predicted with SWISS MODEL (www.swissmodel.expasy.org). **(B)** Alignment of protein sequences for the regions from leucine-reach repeat (LRR)14 to LRR15 in the ectodomain of TLR21 from different species. ClustalW2 (www.ebi.ac.uk/Tools/msa/clustalw2) was used to perform multiple alignments of the amino acid sequences of TLR21s. **(C)** Phylogenetic analysis of TLR21 from different species. The GenBank accession numbers of these TLR21 protein sequences are listed in the left column. Numbers in the right column are the amino acid lengths of these TLR21s.

different tissues, with higher expression in the spleen followed by the liver and blood. In contrast, the kidney, heart, gill, head kidney, and skin have lower expression levels of these transcripts. In addition, mRNA of the rock bream TLR21 is significantly upregulated in the spleen after stimulation with *Streptococcus iniae*, rock bream iridovirus, and *Edwardsiella tarda* (137).

Interestingly, the induction of gene expression in different tissues of cobia by CpG-ODNs is reported to be CpG-ODN-sequence dependent. CpG-1668 and CpG-2006 induce high expression levels of TLR9 in the spleen; whereas, CpG-1668 is more potent in the induction of TLR9 expression in the liver. In the liver and spleen, CpG-1668 and CpG-2006 induce higher expressions of IL-1β and CC chemokines than CpG-2395 and the control CpG-2137; however, in these tissues, CpG-2006 induces high levels of immunoglobulin M (IgM), and CpG-2395 induces high expression levels of Mx (105). The underlying reason for this CpG-ODN sequence- and tissue type-dependent induction of gene expressions is unclear. However, it may reflect that the different expression levels of TLR9 and TLR21 in a tissue type and the ability of TLR9 and TLR21 to differentially recognize different type of CpG-ODN are the main causes for the different activity levels of a CpG-ODN in different tissues.

CONCLUSION AND PERSPECTIVES

Most of the knowledge on how to design a nucleotide sequence for CpG-ODN to achieve strong *in vivo* immunostimulatory activity has come from early studies on mammalian species that express TLR9 only and not TLR21. The discovery of TLR21 as another CpG-ODN receptor in teleosts may explain why previous experience on the activities of various CpG-ODNs in mammals cannot be replicated in teleosts. This also suggests that more understanding of both TLR9 and TLR21 is required for design of CpG-ODN sequence to have strong activity in teleosts. Given that the functional activity of TLR9 and TLR21 may vary among different teleosts, further investigations with cell-based TLR9 and TLR21 activation assays are required to determine whether both TLRs in a teleost are functional or if only one of the two TLRs has the dominant functional activity.

Aquaculture is one of the fastest growing areas of agriculture. The production of farmed teleosts has exceeded that of captured teleosts. Farmed teleosts are susceptible to viral, bacterial, and parasitic infections. Thus, effective immune modulators, including vaccines, and vaccine adjuvants, are required for the aquaculture of farmed teleosts (138–140). CpG-ODN has proven to be an effective adjuvant and antimicrobial agent in teleost (53, 55). The approval of its usage as a vaccine adjuvant in humans (51, 52) further supports its effectiveness and safety as an immunostimulant in agricultural areas, including aquaculture, for food production.

AUTHOR CONTRIBUTIONS

C-YL, G-YY, YL, RX, and T-HC the review results from the opinions and concepts of all authors listed. The review was written by C-YL and T-HC with the help of G-YY, YL, and RX.

FUNDING

This work was supported by grants from the National Health Research Institutes, Taiwan (IM-107-PP-02, NHRI-EX107-10630SI), and Ministry of Science and Technology of Taiwan (MOST 105-2314-B-400-006, and MOST 105-2320-B-400-013-MY3).

REFERENCES

1. Lemaitre B, Nicolas E, Michaut L, Reichhart JM, Hoffmann JA. The dorsoventral regulatory gene cassette spatzle/Toll/cactus controls the potent antifungal response in Drosophila adults. *Cell* (1996) 86:973–83. doi: 10.1016/S0092-8674(00)80172-5
2. Imler JL, Hoffmann JA. Toll receptors in Drosophila: a family of molecules regulating development and immunity. *Curr Top Microbiol Immunol.* (2002) 270:63–79. doi: 10.1007/978-3-642-59430-4_4
3. Valanne S, Wang JH, Ramet M. The Drosophila Toll signaling pathway. *J Immunol.* (2011) 186:649–56. doi: 10.4049/jimmunol.1002302
4. Rock FL, Hardiman G, Timans JC, Kastelein RA, Bazan JF. A family of human receptors structurally related to Drosophila Toll. *Proc Natl Acad Sci USA*. (1998) 95:588–93. doi: 10.1073/pnas.95.2.588
5. Chuang TH, Ulevitch RJ. Cloning and characterization of a sub-family of human toll-like receptors: hTLR7, hTLR8 and hTLR9. *Eur Cytokine Netw*. (2000) 11:372–8.
6. Takeuchi O, Kawai T, Sanjo H, Copeland NG, Gilbert DJ, Jenkins NA, et al. TLR6: a novel member of an expanding toll-like receptor family. *Gene* (1999) 231:59–65. doi: 10.1016/S0378-1119(99)00098-0
7. Du X, Poltorak A, Wei Y, Beutler B. Three novel mammalian toll-like receptors: gene structure, expression, and evolution. *Eur Cytokine Netw*. (2000) 11:362–71.
8. Chuang TH, Ulevitch RJ. Identification of hTLR10: a novel human Toll-like receptor preferentially expressed in immune cells. *Biochim Biophys Acta* (2001) 1518:157–61. doi: 10.1016/S0167-4781(00)00289-X
9. Medzhitov R, Preston-Hurlburt P, Janeway CA, Jr. A human homologue of the Drosophila Toll protein signals activation of adaptive immunity. *Nature* (1997) 388:394–7. doi: 10.1038/41131
10. Beutler B. Innate immune responses to microbial poisons: discovery and function of the Toll-like receptors. *Annu Rev Pharmacol Toxicol.* (2003) 43:609–28. doi: 10.1146/annurev.pharmtox.43.100901.135729
11. Kawai T, Akira S. The role of pattern-recognition receptors in innate immunity: update on Toll-like receptors. *Nat Immunol.* (2010) 11:373–84. doi: 10.1038/ni.1863
12. O'Neill LA, Golenbock D, Bowie AG. The history of Toll-like receptors - redefining innate immunity. *Nat Rev Immunol.* (2013) 13:453–60. doi: 10.1038/nri3446
13. Aliprantis AO, Yang RB, Mark MR, Suggett S, Devaux B, Radolf JD, et al. Cell activation and apoptosis by bacterial lipoproteins through toll-like receptor-2. *Science* (1999) 285:736–9. doi: 10.1126/science.285.5428.736
14. Coelho PS, Klein A, Talvani A, Coutinho SF, Takeuchi O, Akira S, et al. Glycosylphosphatidylinositol-anchored mucin-like glycoproteins isolated from *Trypanosoma cruzi* trypomastigotes induce *in vivo* leukocyte recruitment dependent on MCP-1 production by IFN-gamma-primed-macrophages. *J Leukoc Biol.* (2002) 71:837–44. doi: 10.1189/jlb.71.5.837
15. Janeway CA, Jr., Medzhitov R. Innate immune recognition. *Annu Rev Immunol.* (2002) 20:197–216. doi: 10.1146/annurev.immunol.20.083001.084359
16. Massari P, Henneke P, Ho Y, Latz E, Golenbock DT, Wetzler LM. Cutting edge: immune stimulation by neisserial porins is toll-like

receptor 2 and MyD88 dependent. *J Immunol.* (2002) 168:1533–7. doi: 10.4049/jimmunol.168.4.1533
17. Means TK, Wang S, Lien E, Yoshimura A, Golenbock DT, Fenton MJ. Human toll-like receptors mediate cellular activation by *Mycobacterium tuberculosis*. *J Immunol.* (1999) 163:3920–7.
18. Schwandner R, Dziarski R, Wesche H, Rothe M, Kirschning CJ. Peptidoglycan- and lipoteichoic acid-induced cell activation is mediated by toll-like receptor 2. *J Biol Chem.* (1999) 274:17406–9. doi: 10.1074/jbc.274.25.17406
19. Underhill DM, Ozinsky A, Hajjar AM, Stevens A, Wilson CB, Bassetti M, et al. The Toll-like receptor 2 is recruited to macrophage phagosomes and discriminates between pathogens. *Nature* (1999) 401:811–5. doi: 10.1038/44605
20. Ozinsky A, Underhill DM, Fontenot JD, Hajjar AM, Smith KD, Wilson CB, et al. The repertoire for pattern recognition of pathogens by the innate immune system is defined by cooperation between toll-like receptors. *Proc Natl Acad Sci USA*. (2000) 97:13766–71. doi: 10.1073/pnas.250476497
21. Takeuchi O, Kawai T, Muhlradt PF, Morr M, Radolf JD, Zychlinsky A, et al. Discrimination of bacterial lipoproteins by Toll-like receptor 6. *Int Immunol.* (2001) 13:933–40. doi: 10.1093/intimm/13.7.933
22. Takeuchi O, Sato S, Horiuchi T, Hoshino K, Takeda K, Dong Z, et al. Cutting edge: role of Toll-like receptor 1 in mediating immune response to microbial lipoproteins. *J Immunol.* (2002) 169:10–4. doi: 10.4049/jimmunol.169.1.10
23. Lee SM, Yip TF, Yan S, Jin DY, Wei HL, Guo RT, et al. Recognition of double-stranded RNA and regulation of interferon pathway by toll-like receptor 10. *Front Immunol.* (2018) 9:516. doi: 10.3389/fimmu.2018.00516
24. Poltorak A, He X, Smirnova I, Liu MY, Van Huffel C, Du X, et al. Defective LPS signaling in C3H/HeJ and C57BL/10ScCr mice: mutations in Tlr4 gene. *Science* (1998) 282:2085–8. doi: 10.1126/science.282.5396.2085
25. Hayashi F, Smith KD, Ozinsky A, Hawn TR, Yi EC, Goodlett DR, et al. The innate immune response to bacterial flagellin is mediated by Toll-like receptor 5. *Nature* (2001) 410:1099–103. doi: 10.1038/35074106
26. Alexopoulou L, Holt AC, Medzhitov R, Flavell RA. Recognition of double-stranded RNA and activation of NF-kappaB by Toll-like receptor 3. *Nature* (2001) 413:732–8. doi: 10.1038/35099560
27. Diebold SS, Kaisho T, Hemmi H, Akira S, Reis e Sousa C. Innate antiviral responses by means of TLR7-mediated recognition of single-stranded RNA. *Science* (2004) 303:1529–31. doi: 10.1126/science.1093616
28. Heil F, Hemmi H, Hochrein H, Ampenberger F, Kirschning C, Akira S, et al. Species-specific recognition of single-stranded RNA via toll-like receptor 7 and 8. *Science* (2004) 303:1526–9. doi: 10.1126/science.1093620
29. Bauer S, Kirschning CJ, Hacker H, Redecke V, Hausmann S, Akira S, et al. Human TLR9 confers responsiveness to bacterial DNA via species-specific CpG motif recognition. *Proc Natl Acad Sci USA*. (2001) 98:9237–42. doi: 10.1073/pnas.161293498
30. Hemmi H, Takeuchi O, Kawai T, Kaisho T, Sato S, Sanjo H, et al. A Toll-like receptor recognizes bacterial DNA. *Nature* (2000) 408:740–5. doi: 10.1038/35047123
31. O'Neill LA, Bowie AG. The family of five: TIR-domain-containing adaptors in Toll-like receptor signalling. *Nat Rev Immunol.* (2007) 7:353–64. doi: 10.1038/nri2079
32. Jin MS, Lee JO. Structures of the toll-like receptor family and its ligand complexes. *Immunity* (2008) 29:182–91. doi: 10.1016/j.immuni.2008.07.007
33. Moynagh PN. TLR signalling and activation of IRFs: revisiting old friends from the NF-kappaB pathway. *Trends Immunol.* (2005) 26:469–76. doi: 10.1016/j.it.2005.06.009
34. Fitzgerald KA, Rowe DC, Barnes BJ, Caffrey DR, Visintin A, Latz E, et al. LPS-TLR4 signaling to IRF-3/7 and NF-kappaB involves the toll adapters TRAM and TRIF. *J Exp Med.* (2003) 198:1043–55. doi: 10.1084/jem.20031023
35. Meylan E, Burns K, Hofmann K, Blancheteau V, Martinon F, Kelliher M, et al. RIP1 is an essential mediator of Toll-like receptor 3-induced NF-kappa B activation. *Nat Immunol.* (2004) 5:503–7. doi: 10.1038/ni1061
36. West AP, Koblansky AA, Ghosh S. Recognition and signaling by toll-like receptors. *Annu Rev Cell Dev Biol.* (2006) 22:409–37. doi: 10.1146/annurev.cellbio.21.122303.115827
37. Kawai T, Akira S. TLR signaling. *Semin Immunol.* (2007) 19:24–32. doi: 10.1016/j.smim.2006.12.004
38. Lee MS, Kim YJ. Signaling pathways downstream of pattern-recognition receptors and their cross talk. *Annu Rev Biochem.* (2007) 76:447–80. doi: 10.1146/annurev.biochem.76.060605.122847
39. Tokunaga T, Yamamoto H, Shimada S, Abe H, Fukuda T, Fujisawa Y, et al. Antitumor activity of deoxyribonucleic acid fraction from *Mycobacterium bovis* BCG. I. Isolation, physicochemical characterization, and antitumor activity. *J Natl Cancer Inst.* (1984) 72:955–62.
40. Shimada S, Yano O, Inoue H, Kuramoto E, Fukuda T, Yamamoto H, et al. Antitumor activity of the DNA fraction from *Mycobacterium bovis* BCG. II. Effects on various syngeneic mouse tumors. *J Natl Cancer Inst.* (1985) 74:681–8.
41. Krieg AM, Yi AK, Matson S, Waldschmidt TJ, Bishop GA, Teasdale R, et al. CpG motifs in bacterial DNA trigger direct B-cell activation. *Nature* (1995) 374:546–9. doi: 10.1038/374546a0
42. Roman M, Martin-Orozco E, Goodman JS, Nguyen MD, Sato Y, Ronaghy A, et al. Immunostimulatory DNA sequences function as T helper-1-promoting adjuvants. *Nat Med.* (1997) 3:849–54. doi: 10.1038/nm0897-849
43. Ballas ZK, Rasmussen WL, Krieg AM. Induction of NK activity in murine and human cells by CpG motifs in oligodeoxynucleotides and bacterial DNA. *J Immunol.* (1996) 157:1840–5.
44. Chu RS, Targoni OS, Krieg AM, Lehmann PV, Harding CV. CpG oligodeoxynucleotides act as adjuvants that switch on T helper 1 (Th1) immunity. *J Exp Med.* (1997) 186:1623–31. doi: 10.1084/jem.186.10.1623
45. Klinman DM, Yi AK, Beaucage SL, Conover J, Krieg AM. CpG motifs present in bacteria DNA rapidly induce lymphocytes to secrete interleukin 6, interleukin 12, and interferon gamma. *Proc Natl Acad Sci USA*. (1996) 93:2879–83. doi: 10.1073/pnas.93.7.2879
46. Chuang TH, Lee J, Kline L, Mathison JC, Ulevitch RJ. Toll-like receptor 9 mediates CpG-DNA signaling. *J Leukoc Biol.* (2002) 71:538–44. doi: 10.1189/jlb.71.3.538
47. Hornung V, Rothenfusser S, Britsch S, Krug A, Jahrsdorfer B, Giese T, et al. Quantitative expression of toll-like receptor 1–10 mRNA in cellular subsets of human peripheral blood mononuclear cells and sensitivity to CpG oligodeoxynucleotides. *J Immunol.* (2002) 168:4531–7. doi: 10.4049/jimmunol.168.9.4531
48. Jarrossay D, Napolitani G, Colonna M, Sallusto F, Lanzavecchia A. Specialization and complementarity in microbial molecule recognition by human myeloid and plasmacytoid dendritic cells. *Eur J Immunol.* (2001) 31:3388–93. doi: 10.1002/1521-4141(200111)31:11<3388::AID-IMMU3388>3.0.CO;2-Q
49. Kadowaki N, Ho S, Antonenko S, Malefyt RW, Kastelein RA, Bazan F, et al. Subsets of human dendritic cell precursors express different toll-like receptors and respond to different microbial antigens. *J Exp Med.* (2001) 194:863–9. doi: 10.1084/jem.194.6.863
50. Vollmer J, Krieg AM. Immunotherapeutic applications of CpG oligodeoxynucleotide TLR9 agonists. *Adv Drug Deliv Rev.* (2009) 61:195–204. doi: 10.1016/j.addr.2008.12.008
51. A Two-Dose Hepatitis B Vaccine for Adults (Heplisav-B). *JAMA* (2018) 319:822–823. doi: 10.1001/jama.2018.1097
52. Jackson S, Lentino J, Kopp J, Murray L, Ellison W, Rhee M, et al. Immunogenicity of a two-dose investigational hepatitis B vaccine, HBsAg-1018, using a toll-like receptor 9 agonist adjuvant compared with a licensed hepatitis B vaccine in adults. *Vaccine* (2018) 36:668–674. doi: 10.1016/j.vaccine.2017.12.038
53. Carrington AC, Secombes CJ. A review of CpGs and their relevance to aquaculture. *Vet Immunol Immunopathol.* (2006) 112:87–101. doi: 10.1016/j.vetimm.2006.03.015
54. Bode C, Zhao G, Steinhagen F, Kinjo T, Klinman DM. CpG DNA as a vaccine adjuvant. *Expert Rev Vaccines* (2011) 10:499–511. doi: 10.1586/erv.10.174
55. Chaung HC. CpG oligodeoxynucleotides as DNA adjuvants in vertebrates and their applications in immunotherapy. *Int Immunopharmacol.* (2006) 6:1586–96. doi: 10.1016/j.intimp.2006.06.001
56. Mutwiri G, Pontarollo R, Babiuk S, Griebel P, van Drunen Littel-van den Hurk S, Mena A, et al. Biological activity of immunostimulatory CpG DNA motifs in domestic animals. *Vet Immunol Immunopathol.* (2003) 91:89–103. doi: 10.1016/S0165-2427(02)00246-5

57. Nie L, Cai SY, Shao JZ, Chen J. Toll-like receptors, associated biological roles, and signaling networks in non-mammals. *Front Immunol*. (2018) 9:1523. doi: 10.3389/fimmu.2018.01523
58. Zhang J, Kong X, Zhou C, Li L, Nie G, Li X. Toll-like receptor recognition of bacteria in fish: ligand specificity and signal pathways. *Fish Shellfish Immunol*. (2014) 41:380–8. doi: 10.1016/j.fsi.2014.09.022
59. Brownlie R, Allan B. Avian toll-like receptors. *Cell Tissue Res*. (2011) 343:121–30. doi: 10.1007/s00441-010-1026-0
60. Smith J, Speed D, Law AS, Glass EJ, Burt DW. *In-silico* identification of chicken immune-related genes. *Immunogenetics* (2004) 56:122–33. doi: 10.1007/s00251-004-0669-y
61. Yilmaz A, Shen S, Adelson DL, Xavier S, Zhu JJ. Identification and sequence analysis of chicken Toll-like receptors. *Immunogenetics* (2005) 56:743–53. doi: 10.1007/s00251-004-0740-8
62. Boyd A, Philbin VJ, Smith AL. Conserved and distinct aspects of the avian Toll-like receptor (TLR) system: implications for transmission and control of bird-borne zoonoses. *Biochem Soc Trans*. (2007) 35:1504–7. doi: 10.1042/BST0351504
63. Temperley ND, Berlin S, Paton IR, Griffin DK, Burt DW. Evolution of the chicken Toll-like receptor gene family: a story of gene gain and gene loss. *BMC Genomics* (2008) 9:62. doi: 10.1186/1471-2164-9-62
64. Gupta SK, Deb R, Dey S, Chellappa MM. Toll-like receptor-based adjuvants: enhancing the immune response to vaccines against infectious diseases of chicken. *Expert Rev Vaccines* (2014) 13:909–25. doi: 10.1586/14760584.2014.920236
65. Gomis S, Babiuk L, Allan B, Willson P, Waters E, Ambrose N, et al. Protection of neonatal chicks against a lethal challenge of Escherichia coli using DNA containing cytosine-phosphodiester-guanine motifs. *Avian Dis*. (2004) 48:813–22. doi: 10.1637/7194-041204R
66. Patel BA, Gomis S, Dar A, Willson PJ, Babiuk LA, Potter A, et al. Oligodeoxynucleotides containing CpG motifs (CpG-ODN) predominantly induce Th1-type immune response in neonatal chicks. *Dev Comp Immunol*. (2008) 32:1041–9. doi: 10.1016/j.dci.2008.02.007
67. Haygreen L, Davison F, Kaiser P. DNA vaccines for poultry: the jump from theory to practice. *Expert Rev Vaccines* (2005) 4:51–62. doi: 10.1586/14760584.4.1.51
68. Brownlie R, Zhu J, Allan B, Mutwiri GK, Babiuk LA, Potter A, et al. Chicken TLR21 acts as a functional homologue to mammalian TLR9 in the recognition of CpG oligodeoxynucleotides. *Mol Immunol*. (2009) 46:3163–70. doi: 10.1016/j.molimm.2009.06.002
69. Keestra AM, de Zoete MR, Bouwman LI, van Putten JP. Chicken TLR21 is an innate CpG DNA receptor distinct from mammalian TLR9. *J Immunol*. (2010) 185:460–7. doi: 10.4049/jimmunol.0901921
70. Sullivan C, Kim CH. Zebrafish as a model for infectious disease and immune function. *Fish Shellfish Immunol*. (2008) 25:341–50. doi: 10.1016/j.fsi.2008.05.005
71. Meijer AH, Spaink HP. Host-pathogen interactions made transparent with the zebrafish model. *Curr Drug Targets* (2011) 12:1000–17. doi: 10.2174/138945011795677809
72. Meijer AH, Gabby Krens SF, Medina Rodriguez IA, He S, Bitter W, Ewa Snaar-Jagalska B, et al. Expression analysis of the Toll-like receptor and TIR domain adaptor families of zebrafish. *Mol Immunol*. (2004) 40:773–83. doi: 10.1016/j.molimm.2003.10.003
73. Phelan PE, Mellon MT, Kim CH. Functional characterization of full-length TLR3, IRAK-4, and TRAF6 in zebrafish (*Danio rerio*). *Mol Immunol*. (2005) 42:1057–71. doi: 10.1016/j.molimm.2004.11.005
74. Wang J, Zhang Z, Liu J, Li F, Chang F, Fu H, et al. Structural characterization and evolutionary analysis of fish-specific TLR27. *Fish Shellfish Immunol*. (2015) 45:940–5. doi: 10.1016/j.fsi.2015.06.017
75. Wang Y, Li J, Han J, Shu C, Xu T. Identification and characteristic analysis of TLR28: a novel member of the TLR1 family in teleost. *Dev Comp Immunol*. (2016) 62:102–7. doi: 10.1016/j.dci.2016.05.001
76. van der Vaart M, Spaink HP, Meijer AH. Pathogen recognition and activation of the innate immune response in zebrafish. *Adv Hematol*. (2012) 2012:159807. doi: 10.1155/2012/159807
77. Sepulcre MP, Alcaraz-Perez F, Lopez-Munoz A, Roca FJ, Meseguer J, Cayuela ML, et al. Evolution of lipopolysaccharide (LPS) recognition and signaling: fish TLR4 does not recognize LPS and negatively regulates NF-kappaB activation. *J Immunol*. (2009) 182:1836–45. doi: 10.4049/jimmunol.0801755
78. Quiniou SM, Boudinot P, Bengten E. Comprehensive survey and genomic characterization of Toll-like receptors (TLRs) in channel catfish, *Ictalurus punctatus*: identification of novel fish TLRs. *Immunogenetics* (2013) 65:511–30. doi: 10.1007/s00251-013-0694-9
79. Munoz I, Sepulcre MP, Meseguer J, Mulero V. Toll-like receptor 22 of gilthead seabream, *Sparus aurata*: molecular cloning, expression profiles and post-transcriptional regulation. *Dev Comp Immunol*. (2014) 44:173–9. doi: 10.1016/j.dci.2013.12.003
80. Ding X, Lu DQ, Hou QH, Li SS, Liu XC, Zhang Y, et al. Orange-spotted grouper (*Epinephelus coioides*) toll-like receptor 22: molecular characterization, expression pattern and pertinent signaling pathways. *Fish Shellfish Immunol*. (2012) 33:494–503. doi: 10.1016/j.fsi.2012.05.034
81. Lv J, Huang R, Li H, Luo D, Liao L, Zhu Z, et al. Cloning and characterization of the grass carp (*Ctenopharyngodon idella*) Toll-like receptor 22 gene, a fish-specific gene. *Fish Shellfish Immunol*. (2012) 32:1022–31. doi: 10.1016/j.fsi.2012.02.024
82. Sundaram AY, Consuegra S, Kiron V, Fernandes JM. Positive selection pressure within teleost Toll-like receptors tlr21 and tlr22 subfamilies and their response to temperature stress and microbial components in zebrafish. *Mol Biol Rep*. (2012) 39:8965–75. doi: 10.1007/s11033-012-1765-y
83. Matsuo A, Oshiumi H, Tsujita T, Mitani H, Kasai H, Yoshimizu M, et al. Teleost TLR22 recognizes RNA duplex to induce IFN and protect cells from birnaviruses. *J Immunol*. (2008) 181:3474–85. doi: 10.4049/jimmunol.181.5.3474
84. Ji J, Rao Y, Wan Q, Liao Z, Su J. Teleost-Specific TLR19 Localizes to endosome, recognizes dsRNA, recruits TRIF, triggers both IFN and NF-kappaB pathways, and protects cells from grass carp reovirus infection. *J Immunol*. (2018) 200:573–85. doi: 10.4049/jimmunol.1701149
85. Ding X, Liang Y, Peng W, Li R, Lin H, Zhang Y, et al. Intracellular TLR22 acts as an inflammation equalizer via suppression of NF-kappaB and selective activation of MAPK pathway in fish. *Fish Shellfish Immunol*. (2018) 72:646–57. doi: 10.1016/j.fsi.2017.11.042
86. Yeh DW, Liu YL, Lo YC, Yuh CH, Yu GY, Lo JF, et al. Toll-like receptor 9 and 21 have different ligand recognition profiles and cooperatively mediate activity of CpG-oligodeoxynucleotides in zebrafish. *Proc Natl Acad Sci USA*. (2013) 110:20711–6. doi: 10.1073/pnas.1305273110
87. Shaw JP, Kent K, Bird J, Fishback J, Froehler B. Modified deoxyoligonucleotides stable To exonuclease degradation in serum. *Nucleic Acids Res*. (1991) 19:747–50.
88. Stein CA, Subasinghe C, Shinozuka K, Cohen JS. Physicochemical properties of phosphorothioate oligodeoxynucleotides. *Nucleic Acids Res*. (1988) 16:3209–21. doi: 10.1093/nar/16.8.3209
89. Mutwiri GK, Nichani AK, Babiuk S, Babiuk LA. Strategies for enhancing the immunostimulatory effects of CpG oligodeoxynucleotides. *J Control Release* (2004) 97:1–17. doi: 10.1016/j.jconrel.2004.02.022
90. Krieg AM. CpG motifs in bacterial DNA and their immune effects. *Annu Rev Immunol*. (2002) 20:709–60. doi: 10.1146/annurev.immunol.20.100301.064842
91. Pisetsky DS. Mechanisms of immune stimulation by bacterial DNA. *Springer Semin Immunopathol*. (2000) 22:21–33. doi: 10.1007/s002810000021
92. Yamamoto S, Yamamoto T, Tokunaga T. The discovery of immunostimulatory DNA sequence. *Springer Semin Immunopathol*. (2000) 22:11–9. doi: 10.1007/s002810000019
93. Gursel M, Verthelyi D, Gursel I, Ishii KJ, Klinman DM. Differential and competitive activation of human immune cells by distinct classes of CpG oligodeoxynucleotide. *J Leukoc Biol*. (2002) 71:813–20. doi: 10.1189/jlb.71.5.813
94. Vollmer J, Weeratna R, Payette P, Jurk M, Schetter C, Laucht M, et al. Characterization of three CpG oligodeoxynucleotide classes with distinct immunostimulatory activities. *Eur J Immunol*. (2004) 34:251–62. doi: 10.1002/eji.200324032
95. Samulowitz U, Weber M, Weeratna R, Uhlmann E, Noll B, Krieg AM, et al. A novel class of immune-stimulatory CpG oligodeoxynucleotides unifies high potency in type I interferon induction with preferred structural properties. *Oligonucleotides* (2010) 20:93–101. doi: 10.1089/oli.2009.0210

96. Hanagata N. Structure-dependent immunostimulatory effect of CpG-oligodeoxynucleotides and their delivery system. *Int J Nanomed.* (2012) 7:2181–95. doi: 10.2147/IJN.S30197
97. Rankin R, Pontarollo R, Ioannou X, Krieg AM, Hecker R, Babiuk LA, et al. CpG motif identification for veterinary and laboratory species demonstrates that sequence recognition is highly conserved. *Antisense Nucleic Acid Drug Dev*. (2001) 11:333–40. doi: 10.1089/108729001753231713
98. Chuang TH, Lai CY, Tseng PH, Yuan CJ, Hsu LC. Development of CpG-oligodeoxynucleotides for effective activation of rabbit TLR9 mediated immune responses. *PLoS ONE* (2014) 9:e108808. doi: 10.1371/journal.pone.0108808
99. Yeh DW, Lai CY, Liu YL, Lu CH, Tseng PH, Yuh CH, et al. CpG-oligodeoxynucleotides developed for grouper toll-like receptor (TLR) 21s effectively activate mouse and human TLR9s mediated immune responses. *Sci Rep*. (2017) 7:17297. doi: 10.1038/s41598-017-17609-2
100. Jung MH, Jung SJ. CpG ODN 1668 induce innate and adaptive immune responses in rock bream. *Fish Shellfish Immunol.* (2017) 69:247–57. doi: 10.1016/j.fsi.2017.08.030
101. Jung MH, Lee J, Ortega-Villaizan M, Perez L, Jung SJ. Protective immunity against Megalocytivirus infection in rock bream (*Oplegnathus fasciatus*) following CpG ODN administration. *Vaccine* (2017) 35:3691–9. doi: 10.1016/j.vaccine.2017.05.073
102. Nguyen HT, Nguyen T TT, Wang YT, Wang PC, Chen SC. Effectiveness of formalin-killed vaccines containing CpG oligodeoxynucleotide 1668 adjuvants against Vibrio harveyi in orange-spotted grouper. *Fish Shellfish Immunol*. (2017) 68:124–31. doi: 10.1016/j.fsi.2017.07.018
103. Cardenas-Reyna T, Angulo C, Hori-Oshima S, Velazquez-Lizarraga E, Reyes-Becerril M. B-cell activating CpG ODN 1668 enhance the immune response of Pacific red snapper (*Lutjanus peru*) exposed to Vibrio parahaemolitycus. *Dev Comp Immunol*. (2016) 62:72–81. doi: 10.1016/j.dci.2016.04.022
104. Lee EH, Kim KH. CpG-ODN increases resistance of olive flounder (*Paralichthys olivaceus*) against Philasterides dicentrarchi (*Ciliophora: Scuticociliatia*) infection. *Fish Shellfish Immunol*. (2009) 26:29–32. doi: 10.1016/j.fsi.2008.10.001
105. Byadgi O, Puteri D, Lee YH, Lee JW, Cheng TC. Identification and expression analysis of cobia (*Rachycentron canadum*) Toll-like receptor 9 gene. *Fish Shellfish Immunol.* (2014) 36:417–27. doi: 10.1016/j.fsi.2013.12.017
106. Purcell SL, Friend SE, Covello J M, Donkin A, Groman DB, Poley J, et al. CpG inclusion in feed reduces sea lice, *Lepeophtheirus salmonis*, numbers following re-infection. *J Fish Dis.* (2013) 36:229–40. doi: 10.1111/jfd.12024
107. Covello JM, Friend SE, Purcell SL, Burka JF, Markham R JF, Donkin AW, et al. Effects of orally administered immunostimulants on inflammatory gene expression and sea lice (*Lepeophtheirus salmonis*) burdens on Atlantic salmon (*Salmo salar*) *Aquaculture* (2012) 366–367. doi: 10.1016/j.aquaculture.2012.08.051
108. Angulo C, Alamillo E, Hirono I, Kondo H, Jirapongpairoj W, Perez-Urbiola JC, et al. Class B CpG-ODN2006 is highly associated with IgM and antimicrobial peptide gene expression through TLR9 pathway in yellowtail *Seriola lalandi*. *Fish Shellfish Immunol.* (2018) 77:71–82. doi: 10.1016/j.fsi.2018.03.025
109. Sun M, Mu Y, Ding Y, Ao J, Chen X. Molecular and functional characterization of Toll-like receptor 21 in large yellow croaker (*Larimichthys crocea*). *Fish Shellfish Immunol.* (2016) 59:179–88. doi: 10.1016/j.fsi.2016.10.024
110. Jenberie S, Thim HL, Sunyer JO, Skjodt K, Jensen I, Jorgensen JB. Profiling Atlantic salmon B cell populations: CpG-mediated TLR-ligation enhances IgM secretion and modulates immune gene expression. *Sci Rep*. (2018) 8:3565. doi: 10.1038/s41598-018-21895-9
111. Iliev DB, Hansen T, Jorgensen SM, Krasnov A, Jorgensen JB. CpG- and LPS-activated MAPK signaling in *in vitro* cultured salmon (*Salmo salar*) mononuclear phagocytes. *Fish Shellfish Immunol.* (2013) 35:1079–85. doi: 10.1016/j.fsi.2013.07.014
112. Cha YJ, Lee CR, Kwon JY, Kang YJ. Protective effects of CpG-ODN 2007 administration against *Edwardsiella tarda* infection in olive flounder (*Paralichthys olivaceus*). *Fish Shellfish Immunol.* (2017) 68:327–31. doi: 10.1016/j.fsi.2017.07.037
113. Pridgeon JW, Klesius PH, Mu X, Yancey RJ, Kievit MS, Dominowski PJ. Efficacy of QCDCR formulated CpG ODN 2007 in Nile tilapia against *Streptococcus iniae* and identification of upregulated genes. *Vet Immunol Immunopathol*. (2012) 145:179–90. doi: 10.1016/j.vetimm.2011.11.001
114. Li S, Wang G, Liu D, Liu Q, Hu G. Cloning and expression analysis of a Toll-like receptor 21 (TLR21) gene from turbot, *Scophthalmus maximus*. *Dev Comp Immunol.* (2017) 73:163–8. doi: 10.1016/j.dci.2017.03.021
115. K UT, Chirapongsatonkul N, Itami T, Tantikitti C. CpG ODN mimicking CpG rich region of myxosporean Myxobolus supamattayai stimulates innate immunity in Asian sea bass (*Lates calcarifer*) and defense against *Streptococcus iniae*. *Fish Shellfish Immunol.* (2016) 58:116–24. doi: 10.1016/j.fsi.2016.09.005
116. Su H, Yuan G, Su J. A specific CpG oligodeoxynucleotide induces protective antiviral responses against grass carp reovirus in grass carp *Ctenopharyngodon idella*. *Dev Comp Immunol.* (2016) 60:218–27. doi: 10.1016/j.dci.2016.03.007
117. Zhou ZX, Zhang J, Sun L. C7: a CpG oligodeoxynucleotide that induces protective immune response against megalocytivirus in Japanese flounder (*Paralichthys olivaceus*) via Toll-like receptor 9-mediated signaling pathway. *Dev Comp Immunol.* (2014) 44:124–32. doi: 10.1016/j.dci.2013.12.002
118. Liu CS, Sun Y, Hu YH, Sun L. Identification and analysis of a CpG motif that protects turbot (*Scophthalmus maximus*) against bacterial challenge and enhances vaccine-induced specific immunity. *Vaccine* (2010) 28:4153–61. doi: 10.1016/j.vaccine.2010.04.016
119. Cuesta A, Esteban MA, Meseguer J. The expression profile of TLR9 mRNA and CpG ODNs immunostimulatory actions in the teleost gilthead seabream points to a major role of lymphocytes. *Cell Mol Life Sci.* (2008) 65:2091–104. doi: 10.1007/s00018-008-8146-7
120. Jorgensen JB, Johansen LH, Steiro K, Johansen A. CpG DNA induces protective antiviral ;immune responses in Atlantic salmon (*Salmo salar* L.). *J Virol*. (2003) 77:11471–9. doi: 10.1128/JVI.77.21.11471-11479.2003
121. Strandskog G, Ellingsen T, Jorgensen JB. Characterization of three distinct CpG oligonucleotide classes which differ in ability to induce IFN alpha/beta activity and cell proliferation in Atlantic salmon (*Salmo salar* L.) leukocytes. *Dev Comp Immunol*. (2007) 31:39–51. doi: 10.1016/j.dci.2006.05.004
122. Bell JK, Mullen GE, Leifer CA, Mazzoni A, Davies DR, Segal DM. Leucine-rich repeats and pathogen recognition in Toll-like receptors. *Trends Immunol.* (2003) 24:528–33. doi: 10.1016/S1471-4906(03)00242-4
123. Werling D, Jann OC, Offord V, Glass EJ, Coffey TJ. Variation matters: TLR structure and species-specific pathogen recognition. *Trends Immunol.* (2009) 30:124–30. doi: 10.1016/j.it.2008.12.001
124. Zhang Z, Ohto U, Shimizu T. Toward a structural understanding of nucleic acid-sensing Toll-like receptors in the innate immune system. *FEBS Lett*. (2017) 591:3167–81. doi: 10.1002/1873-3468.12749
125. Shimizu T. Structural insights into ligand recognition and regulation of nucleic acid-sensing Toll-like receptors. *Curr Opin Struct Biol*. (2017) 47:52–9. doi: 10.1016/j.sbi.2017.05.010
126. Maeda K, Akira S. TLR7 Structure: Cut in Z-Loop. *Immunity* (2016) 45:705–7. doi: 10.1016/j.immuni.2016.10.003
127. Liu J, Xu C, Hsu LC, Luo Y, Xiang R, Chuang TH. A five-amino-acid motif in the undefined region of the TLR8 ectodomain is required for species-specific ligand recognition. *Mol Immunol*. (2010) 47:1083–90. doi: 10.1016/j.molimm.2009.11.003
128. Lai CY, Liu YL, Yu GY, Maa MC, Leu TH, Xu C, et al. TLR7/8 agonists activate a mild immune response in rabbits through TLR8 but not TLR7. *Vaccine* (2014) 32:5593–9. doi: 10.1016/j.vaccine.2014.07.104
129. Matsushima N, Tanaka T, Enkhbayar P, Mikami T, Taga M, Yamada K, et al. Comparative sequence analysis of leucine-rich repeats (LRRs) within vertebrate toll-like receptors. *BMC Genomics* (2007) 8:124. doi: 10.1186/1471-2164-8-124
130. Wu H, Wang H, Jiang W, Lian Z. The evolutionary characteristics and structural biology of Gallus toll-like receptor 21. *J Mol Recognit*. (2018) 6:e2696. doi: 10.1002/jmr.2696
131. Jault C, Pichon L, Chluba J. Toll-like receptor gene family and TIR-domain adapters in *Danio rerio*. *Mol Immunol.* (2004) 40:759–71. doi: 10.1016/j.molimm.2003.10.001
132. Skjaeveland I, Iliev DB, Zou J, Jorgensen T, Jorgensen JB. A TLR9 homolog that is up-regulated by IFN-gamma in Atlantic salmon (*Salmo*

salar). *Dev Comp Immunol.* (2008) 32:603–7. doi: 10.1016/j.dci.2007.10.011

133. Yu Y, Zhong Q, Li C, Jiang L, Yan F, Wang Z, et al. Isolation and characterization of Toll-like receptor 9 in half-smooth tongue sole *Cynoglossus semilaevis*. *Fish Shellfish Immunol.* (2009) 26:492–9. doi: 10.1016/j.fsi.2009.02.005
134. Ortega-Villaizan M, Chico V, Falco A, Perez L, Coll JM, Estepa A. The rainbow trout TLR9 gene and its role in the immune responses elicited by a plasmid encoding the glycoprotein G of the viral haemorrhagic *septicaemia rhabdovirus* (VHSV). *Mol Immunol.* (2009) 46:1710–7. doi: 10.1016/j.molimm.2009.02.006
135. Zhao F, Li YW, Pan HJ, Shi CB, Luo XC, Li AX, et al. Expression profiles of toll-like receptors in channel catfish (*Ictalurus punctatus*) after infection with *Ichthyophthirius multifiliis*. *Fish Shellfish Immunol.* (2013) 35:993–7. doi: 10.1016/j.fsi.2013.05.023
136. Wang KL, Ji W, Zhang GR, Wei KJ, Shi ZC, Zhang XT, et al. Molecular characterization and expression analysis of three TLR genes in yellow catfish (*Pelteobagrus fulvidraco*): responses to stimulation of *Aeromonas hydrophila* and TLR ligands. *Fish Shellfish Immunol.* (2017) 66:466–79. doi: 10.1016/j.fsi.2017.05.056
137. Priyathilaka TT, Elvitigala DA, Whang I, Lim BS, Jeong HB, Yeo SY, et al. Molecular characterization and transcriptional analysis of non-mammalian type Toll like receptor (TLR21) from rock bream (*Oplegnathus fasciatus*). *Gene* (2014) 553:105–16. doi: 10.1016/j.gene.2014.10.008
138. Tafalla C, Bøgwald J, Dalmo RA. Adjuvants and immunostimulants in fish vaccines: current knowledge and future perspectives. *Fish Shellfish Immunol.* (2013) 35:1740–50. doi: 10.1016/j.fsi.2013.02.029
139. Dhar AK, Manna SK, Thomas Allnutt FC. Viral vaccines for farmed finfish. *Virus Dis.* (2014) 25:1–17. doi: 10.1007/s13337-013-0186-4
140. Brudeseth BE, Wiulsrød R, Fredriksen BN, Lindmo K, Løkling KE, Bordevik M, et al. Status and future perspectives of vaccines for industrialised fin-fish farming. *Fish Shellfish Immunol.* (2013) 35:1759–68. doi: 10.1016/j.fsi.2013.05.029

Conflict of Interest Statement: The authors declare that the research was conducted in the absence of any commercial or financial relationships that could be construed as a potential conflict of interest.

Copyright © 2019 Lai, Yu, Luo, Xiang and Chuang. This is an open-access article distributed under the terms of the Creative Commons Attribution License (CC BY). The use, distribution or reproduction in other forums is permitted, provided the original author(s) and the copyright owner(s) are credited and that the original publication in this journal is cited, in accordance with accepted academic practice. No use, distribution or reproduction is permitted which does not comply with these terms.

frontiers in Immunology

ORIGINAL RESEARCH
published: 18 February 2019
doi: 10.3389/fimmu.2019.00256

Comparative Extracellular Proteomics of *Aeromonas hydrophila* Reveals Iron-Regulated Secreted Proteins as Potential Vaccine Candidates

Yuqian Wang[1†], *Xiaoyun Wang*[1,2†], *Farman Ali*[1,2], *Zeqi Li*[1,2], *Yuying Fu*[1,2], *Xiaojun Yang*[1,2], *Wenxiong Lin*[1,2] *and Xiangmin Lin*[1,2*]

[1] Fujian Provincial Key Laboratory of Agroecological Processing and Safety Monitoring, College of Life Sciences, Fujian Agriculture and Forestry University, Fuzhou, China, [2] Key Laboratory of Crop Ecology and Molecular Physiology, Fujian Agriculture and Forestry University, Fujian Province University, Fuzhou, China

OPEN ACCESS

Edited by:
Carolina Tafalla,
Instituto Nacional de Investigación y Tecnología Agraria y Alimentaria (INIA), Spain

Reviewed by:
Ikuo Hirono,
Tokyo University of Marine Science and Technology, Japan
Alcia Gibello,
Universidad Complutense de Madrid, Spain

***Correspondence:**
Xiangmin Lin
xiangmin@fafu.edu.cn

[†]These authors have contributed equally to this work

Specialty section:
This article was submitted to Comparative Immunology, a section of the journal Frontiers in Immunology

Received: 03 September 2018
Accepted: 29 January 2019
Published: 18 February 2019

Citation:
Wang Y, Wang X, Ali F, Li Z, Fu Y, Yang X, Lin W and Lin X (2019) Comparative Extracellular Proteomics of Aeromonas hydrophila Reveals Iron-Regulated Secreted Proteins as Potential Vaccine Candidates. Front. Immunol. 10:256. doi: 10.3389/fimmu.2019.00256

In our previous study, several iron-related outer membrane proteins in *Aeromonas hydrophila*, a serious pathogen of farmed fish, conferred high immunoprotectivity to fish, and were proposed as potential vaccine candidates. However, the protective efficacy of these extracellular proteins against *A. hydrophila* remains largely unknown. Here, we identified secreted proteins that were differentially expressed in *A. hydrophila* LP-2 in response to iron starvation using an iTRAQ-based quantitative proteomics method. We identified 341 proteins, of which 9 were upregulated in response to iron starvation and 24 were downregulated. Many of the differently expressed proteins were associated with protease activity. We confirmed our proteomics results with Western blotting and qPCR. We constructed three mutants by knocking out three genes encoding differentially expressed proteins (Δ*orf01830*, Δ*orf01609,* and Δ*orf03641*). The physiological characteristics of these mutants were investigated. In all these mutant strains, protease activity decreased, and Δ*orf01609,* and Δ*orf01830* were less virulent in zebrafish. This indicated that the proteins encoded by these genes may play important roles in bacterial infection. We next evaluated the immune response provoked by the six iron-related recombinant proteins (ORF01609, ORF01830, ORF01839, ORF02943, ORF03355, and ORF03641) in zebrafish as well as the immunization efficacy of these proteins. Immunization with these proteins significantly increased the zebrafish immune response. In addition, the relative percent survival (RPS) of the immunized zebrafish was 50–80% when challenged with three virulent *A. hydrophila* strains, respectively. Thus, these extracellular secreted proteins might be effective vaccine candidates against *A. hydrophila* infection in fish.

Keywords: *Aeromonas hydrophila*, extracellular proteomics, iTRAQ, iron starvation, vaccine candidate

INTRODUCTION

The bacterial species *Aeromonas hydrophila* is an important pathogen of freshwater fish, causing major disease outbreaks and resulting in severe economic losses for the aquaculture industry every year (1). A antibiotics help to control this pathogen and prevent fish disease, but the frequent use of antibiotics might contaminate freshwater ecosystems and increase the spread of antibiotic-resistant bacterial strains (2). It is therefore critical to develop effective immunoprotective vaccines against *A. hydrophila.* It has been suggested that, in carp, mice, and channel catfish, effective vaccine candidates against *A. hydrophila* include DNA and Lipopolysaccharide (LPS) as well as outer membrane, extracellular, and S-layer proteins (3). Much recent research has focused on the immuoprotective properties of extracellular proteins, as these typically affect bacterial virulence (4). For example, in *A. hydrophila,* haemolysin and aerolysin are extracellular proteins that are well-known virulence factors (5). The immunization of catfish with these recombinant proteins significantly increased the relative percent survival (RPS), as compared to unimmunized catfish (6). In addition, two recombinant extracellular proteases (epr2 and epr3) of the *A. hydrophila* strain J-1 conferred significant protection against infection to *Parabramis pekinensis* (7). Therefore, the extracellular proteins of *A. hydrophila* might be good potential candidates for vaccine development.

As high-throughput technology has advanced, proteomics have been frequently used to identify novel antigens for the development of new vaccines (8–10). However, the immuoprotective properties of only a few extracellular or secreted proteins have been characterized to date. This may be in part because many secreted proteins are rare under normal culture conditions (11). This rarity represents a bottleneck for proteome research, despite the current development of highly sensitive mass spectrometry (MS). Thus, it is important to understand the proteomics profiles of the proteins secreted by *A. hydrophila,* which are closer to the natural state of host-pathogen interaction.

Elemental iron is abundant on earth, but ferrous iron, which is necessary for living things, is scarce because of Earth's oxygen-rich atmosphere. Host organisms may limit the ferrous iron concentration in the microenvironment using ferritin, so as to inhibit bacterial growth (12). However, bacteria respond to iron starvation by increasing the iron uptake of their outer membrane proteins (OMPs) or by secreting extracellular proteins to increase virulence and invasion speed (13). Previously, we compared the differential expression of OMPs in response to iron starvation, and identified several OMPs as potential vaccine candidates (14). However, the proteomics profiles of extracellular proteins under iron starvation, and their potential utility in vaccine development, remain largely unclear.

In this study, we compared the expression of extracellular proteins in *A. hydrophila* grown in iron-starved and normal conditions to identify secreted proteins associated with iron-limited environments. After validating the expression of several selected proteins with qPCR and Western blotting, we vaccinated zebrafish with the recombinant candidate proteins, and observed the immune response provoked and the protective efficacy of these proteins. The virulence of several candidate proteins was evaluated by knocking out the encoding genes. Using these techniques, we identified several novel extracellular proteins that may be virulence effectors with a high protective efficacy, making these proteins potential candidates for vaccine development against *A. hydrophila* infection.

METHODS AND MATERIALS

Bacterial Strains and Sample Preparation

The bacterial strain used in this study, *A. hydrophila* LP-2, is a virulent strain that was isolated from a diseased silver carp and was maintained in our laboratory. *A. hydrophila* YT-1 and LP-3 were isolated from diseased *European eel* (*Anguilla anguilla*), which were kindly provided by Prof. Hui Gong from Fujian Academy of Agricultural Sciences (Fuzhou, China) and Dr. Huanying Pang from Guangdong Ocean University (Zhanjiang, China), respectively. *A. hydrophila* ATCC 7966, *Vibrio alginolyticus* ATCC 33787*, Edwardsiella trada* ATCC 15947*Vibrio parahaemolyticus* ATCC 17802*, Vibrio fluvialis* VL 5125*and Edwardsiella trada* EIB202 were kept in our laboratory. The 50% lethal dose (LD50) of *A. hydrophila* LP-2, LP-3 and YT-1 in zebrafish were 8.1×10^3, 6.5×10^6, and 1.2×10^7 cells, respectively, suggesting that these strains are virulent.

To isolate extracellular proteins, *A. hydrophila* LP-2 was streaked for isolation on Luria-Bertani (LB) agar medium and incubated overnight at 30°C, as previously described (15). One colony was transferred to 5 mL fresh LB medium overnight, and then diluted 1:100 in 100 mL LB with or without 150 μM 2,2′-dipyridyl (DIP). The resulting mixtures were incubated at 30°C with shaking at 200 rpm for about 5 h (until OD at 600 nm was ∼1.5). Samples were collected by centrifugation at 4500 × g for 20 min at 4°C, and each supernatant was passed through a 0.45-μm filter membrane and then a 0.22-μm filter membrane to remove all of the bacterial cells. We then added 8% (v/v) ice-cold trichloroacetic acid to all of the filtered supernatants and incubated the resulting mixtures at 4°C overnight. After centrifugation at 11,000 × g for 40 min at 4°C, the resultant pellet was washed with pre-cooled acetone three times. Pellets were dissolved in 8 M urea, and protein concentrations were determined by the Bradford method. Dissolved pellets were stored at −80°C.

Protein Identification Using iTRAQ Labeling and LC-MS/MS

Protein digestion and iTRAQ labeling were performed as previously described (16). The iTRAQ labeling scheme was as follows: the two untreated biological repeats (controls) were labeled 113 and 117, and the two biological repeats treated with 150 μM DIP were labeled 114 and 118. Labeled peptides were quantified with an AB Sciex TripleTOF 5,600 mass spectrometer (AB SCIEX; Concord, ON, Canada) equipped with a NanoAcquity UPLC system (Waters, Milford, MA, USA). All of the settings were as previously described (17), except that we used the LP-2 genome re-sequencing database produced in our laboratory (unpublished data).Proteins matching at least two

unique peptides, with a false discovery rate (FDR) < 1%, were considered for further analysis. To quantify protein expression, we compared the degree of change in the iTRAQ ratio of the samples treated with DIP to that of the untreated controls. If the fold change as compared to the controls was >1.5 or <0.667 (a fold change of ±1.5), and the $p < 0.05$ for both biological replicates, these proteins were deemed significantly differentially expressed.

Bioinformatics Analysis

We investigated the gene ontology (GO) and Kyoto Encyclopedia of Genes and Genomes (KEGG) of the differentially expressed proteins using the online omicsbean resource (http://www.omicsbean.cn/) (18). The generated histogram and volcano plots were analyzed in R software version 3.4.0.

Purification of Recombinant Proteins

Six genes (*orf01609, orf01830, orf01839, orf02943, orf03355,* and *orf03641*) were cloned into the pET-32a plasmid and transformed into *Escherichia coli* BL21(DE3), using the primer sequences listed in **Supplementary Table 1**. The recombinant proteins were purified as previously described (19). Briefly, the recombinant strain was incubated in 5 mL LB medium overnight at 37°C 200 rpm, transferred to 200 mL LB medium supplemented 1:100 with 100 μg/mL ampicillin (Amp) for 2–3 h. Next, 0.5 mM Isopropyl -β-D-thiogalactopyranoside (IPTG) was added to the ice-cold culture for protein induction at 16°C for about 6–8 h. After washing with phosphate-buffered saline (PBS) three times, bacterial pellets were resuspended in binding buffer (25 mM $Na_2HPO_4 \cdot 12H_2O$, 10 mM $NaH_2PO_4 \cdot 2H_2O$, 500 mM NaCl, and 5 mM imidazole). The suspension was sonicated on ice for 30 min, and centrifuged to remove cellular debris. Finally, the supernatants containing the fusion proteins were purified using affinity chromatography on a HisTrap Sepharose nickel column (GE Healthcare, Uppsala, Sweden).

qPCR Assay

To measure the expression of genes associated with immune response in vaccinated fish, we collected tissue samples from zebrafish haslets (four fish per group). Tissue samples were frozen in liquid nitrogen and then ground. RNA was extracted from each tissue sample using RNAiso Plus reagent (TaKaRa Bio, Tokyo, Japan) as previously described (20). Briefly, RNA quality was first evaluated with a NanoDrop One (Thermo Scientific, USA), and then 1 μg RNA from each tissue sample was reverse-transcribed into cDNA using a PrimeScript RT reagent Kit (Takara Shuzo, Otsu, Japan). Real-time PCR was performed with the CFX96 Touch Deep Well Real-Time PCR Detection System (Bio-Rad, USA) using SYBR Premix Ex Taq II Kits (Takara Shuzo, Otsu, Japan), following the manufacturer's instructions. The β-actin gene was used as the internal control.

To validate gene expression under iron-limited conditions, total RNA was extracted from *A. hydrophila* LP-2 cells grown with and without 150 μM DIP. qPCR assays were performed as above, using the *16S rRNA* gene as the internal control. All the qPCR primers used in this study are listed in **Supplementary Table 2**. Three independent biological repeats were performed for DIP each experiment.

Western Blotting

The recombinant proteins were purified, and injected into mice to produce specific polyclonal antibodies. Western blotting was then performed as previously described (21). Briefly, a 12% SDS-PAGE was performed to separate the extracellular proteins grown with or without 150 mM DIP. After electrophoresis, proteins were transferred to polyvinylidene fluoride (PVDF) membranes in transfer buffer with a Trans-Blot Turbo Transfer System (Bio-Rad, Hercules, CA, USA). Membranes were blocked with PBST containing 5% (w/v) non-fat milk for 1 h, and then incubated with diluted mouse antiserum as the primary antibody. After being washed three times with PBST, membranes were incubated with horseradish peroxidase conjugated goat anti-mouse antibody (1:4,000) as the secondary antibody. The immune-stained proteins were detected using Clarity Western ECL Substrate (Bio-Rad) and visualized with Image Lab software (Bio-Rad) on the ChemiDoc MP imaging system (Bio-Rad, Hercules, CA). Finally, PVDF membranes were stained with Coomassie R-350 to verify that the loading amounts were equal.

Construction of Deletion Mutants

We constructed deletion mutants by deleting three of the six genes of interest (*orf01609, orf01830,* and *orf03641*) as previously described (22). Briefly, we amplified the sequence fragments (∼500 base pairs (bp) length) flanking each target gene ORF in *A. hydrophila* LP-2, using the primers listed in **Supplementary Table 3**. The resulting PCR products were ligated into the suicide vector pRE112 (Cm^r). The reconstruction plasmids were transformed into *E. coli* MC1061 λ*pir* competent cells and screened on LB agar containing 30 μg/ml chloramphenicol (Cm). Positive plasmids were transformed into *E. coli* S17-1 λpir competent cells and introduced into *A. hydrophila* LP-2 via bacterial conjugation. Single crossover mutants were screened on LB agar containing 100 μg/ml ampicillin and 30 μg/ml Cm for the first homologous recombination. Positive colonies were transferred into 1 ml fresh LB incubated overnight and then cultured on 20% sucrose LB ager plates for the second homologous recombination. Finally, deletion mutants were verified using PCR and sequencing using primers P7 and P8 (**Supplementary Table 1**).

Characterization of Mutant Strains

The phenotypes of the mutant strains were characterized by hemolytic activity, extracellular protease (ECPase) activity, and biofilm formation. Hemolytic and ECPase activity were assayed as previously described (23, 24). Biofilm formation was measured using crystal violet staining (25).

Bacterial Challenge of Mutant Strains

Zebrafish were purchased from the Fuzhou Flower, Bird & Fish Market (Fuzhou, China) and challenged by widetype and mutant strains of *A. hydrophila* as previously described (26). Briefly, sixteen zebrafish per treatment group were injected intraperitoneally with 10 μL *A. hydrophila* LP-2 (WT) or with

10 μL *A. hydrophila* mutants at a density of 10^3-10^5 CFU/ml PBS. Negative control zebrafish were injected with 10 μL sterile PBS. Challenged fish were monitored for 14 days, and LD50 values were calculated using the statistical approach of Reed and Muench (27). For the livability investigation of mutant strains, the zebrafish were intraperitoneally injected with 10 μl 2.0×10^4 cfu/ml mutants, and observed for 14 days as previously described with modification (26). The kidneys of dead fish were collected and were homogenized in 1 ml PBS. The homogenates were serially diluted and plated onto RS plates (Hope Bio Co.,Ltd., Qingdao, China) and incubated at 30°C for 16 h. Finally, the positive colonies were verified by PCR and sequencing.

Vaccination

Zebrafish were randomly divided into 7 groups with 20 fish per group, as previously described with some modifications (28). In brief, about 3 μg purified fusion protein emulsified with incomplete Freund's adjuvant (IFA) was administered to each fish via intraperitoneal injection. Negative control fish were injected with an equal amount of bovine serum albumin (BSA) which emulsified with IFA. After 28 days injection, fish in each group were challenged with 1.6×10^5 CFU/ml *A. hydrophila* LP-2 in 10 μL sterile PBS, delivered via intraperitoneal injection. This dose was 20-fold greater than the LD50 of *A. hydrophila* LP-2. All of the fish were observed for 14 days, and cumulative mortality and clinical signs were recorded daily. The experiment was repeated three times independently.

RESULTS

Identification of Differentially Expressed Proteins in Response to Iron Starvation Using iTRAQ Technology Coupled With MS

Extracellular proteins differentially expressed in *A. hydrophila* LP-2 grown with or without DIP treatment were isolated and separated using SDS-PAGE (**Figure 1A**). We observed that the different treatments resulted in different bands, which indicated that the extracellular proteins might be involved in iron homeostasis. However, the specific proteins could not be identified due to the low resolution of SDS-PAGE. Thus, we used iTRAQ labeling coupled with MS proteomics to quantify the differences in extracellular protein expression. We identified 341 differentially expressed proteins (**Supplementary Table 4**), with a substantial conservative threshold (confidence level ≥ 95%). Most of the ratios of these comparison were normally distributed ($\log_2$ scale range: ±1) across both biological duplicates **(Figure 1B)**. Under iron-limited conditions, nine proteins were significantly upregulated and 24 proteins were significantly downregulated ($p < 0.05$), with a minimum ± 1.5-fold change in expression as compared to controls (**Table 1** and **Figure 1C**). Subcellular localization prediction indicated that most of the 341 differentially expressed proteins were located in the cytoplasm, the inner membrane, and the periplasm (**Figure 1D**). Moreover, we found the extracellular proteins proportion increased almost 3-folds from 11.5 to 29.2% in 33 altered proteins than total identified proteins components, which suggest the important role of secreted protein in iron starvation condition.

Functional Classification and Annotation of Differentially Expressed Proteins

To investigate the functional characteristics of the proteins differentially expressed in *A. hydrophila* LP-2 starved of iron, we clustered these proteins by GO using the homologous *A. hydrophila* ATCC 7966 genome database. Most proteins were enriched in biological processes, molecular functions, and KEGG pathways (**Figure 2**). In general, under iron-starvation, upregulated proteins were enriched in fewer GO clusters than downregulated proteins. Proteolysis, regulation of nucleic acid-template transcription, and RNA biosynthesis regulation were the three biological process most enriched in upregulated proteins, while carbohydrate metabolism, amino sugar metabolic processes, and macromolecule catabolic processes were the biological processes most enriched in downregulated proteins (**Figures 2A,B**)**.** The molecular function analysis indicated that the upregulated proteins were related to the activity of several different proteases, including aldehydelyase, peptidase, S-methyltransferase, and ATPase coupled molybdate. In contrast, the downregulated proteins were involved in processes including carbohydrate binding, hydrolase activity, and chitinase activity (**Figures 2C,D**). The KEGG pathways most enriched in upregulated proteins included the pentose phosphate pathway and the ATP-binding cassette (ABC) transporters, while the KEGG pathways most enriched in downregulated proteins included metabolic pathways, glyceroloid metabolism, and D-alanine metabolism (**Figures 2E,F**).

Predicted Protein-Protein Interactions (PPIs) Among Extracellular Proteins in Response to Iron Starvation

We analyzed the PPIs of the proteins differentially expressed in response to iron starvation in *A. hydrophila* LP-2 based on the homologous *A. hydrophila* ATCC 7966 genomic database. The PPI network we constructed included nine genes encoding down-regulated proteins (*orf03029, orf02395, orf03889, orf02296, orf03869, orf04406, orf03984, orf03511,* and *orf03513*) and two genes encoding up-regulated proteins (*orf01609* and *orf03641*) (**Figure 3**). Interestingly, *orf03984* and *orf03641* were important nodes (hubs): *orf03984* interacted with seven other differentially expressed protein, and *orf03641* interacted with eight other differentially expressed proteins. Some periplasmic and outer cell membrane proteins were also included in our PPI network: two upregulated (*orf04443*(*hgpB)* and *orf01839*) and four downregulated [*orf02720, orf01386, orf00322,* and *orf01538(ppiB)*]. Our results suggested that secreted proteins have many biological functions and are involved in complex protein-protein interactions during iron homeostasis.

Validation of the Proteomics Results in Protein Level

We validated our proteomics data at the protein level using western blots. First, we cloned six genes (*orf01609, orf01830,*

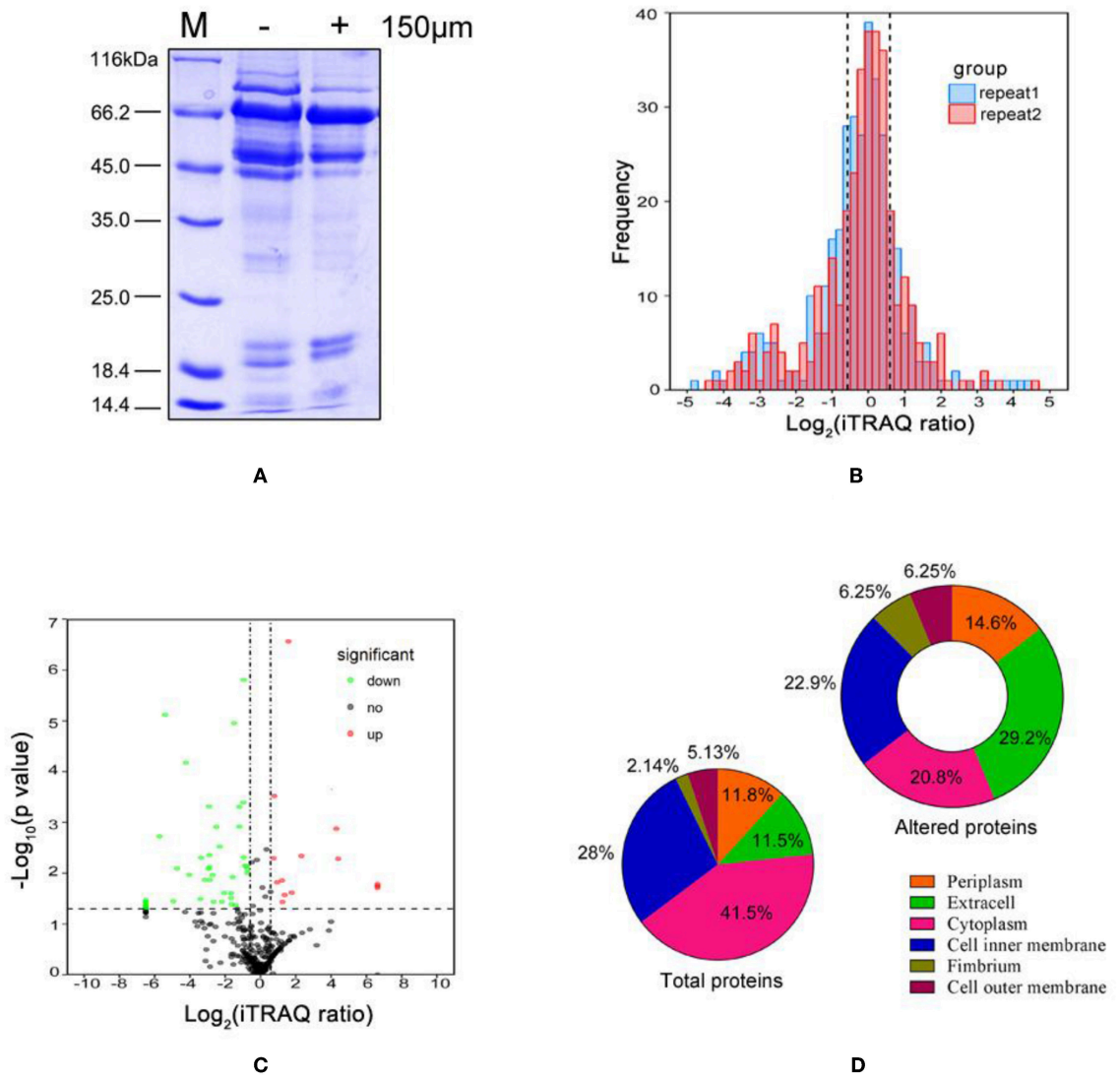


FIGURE 1 | Characteristics of *Aeromonas hydrophila* LP-2 grown in iron-limited conditions. **(A)** Coomassie brilliant blue(CBB) stained SDS-PAGE of extracelluar protein fractions from *A. hydrophila* treated with 150 μM DIP. Lane M, molecular mass standards. **(B)** The frequency distribution of protein iTRAQ $\log_2$ ratios between the two biological replicates. **(C)** Volcano plot comparing the extracellular proteomics of *A. hydrophila* grown in iron-limited conditions and *A. hydrophila* grown in normal conditions. Solid lines indicate statistically significant differences in protein expression (iTRAQ ratio >1.5 or <0.66 and $p < 0.05$ for both biological replicates). Upregulated proteins are indicated by red circles; downregulated proteins are indicated by green circles; and unaltered proteins are indicated by black circles. **(D)** Subcellular locations predicted for all identified proteins and for all differentially expressed proteins.

orf01839, orf02943, orf03355, and *orf03641*), all of which encode proteins that were upregulated under iron limiting conditions based on our proteomics analysis. These genes were overexpressed to produce purified recombinant proteins (**Figures 4A,B**). Recombinant plasmids were further validated using restriction enzymes (**Figure 4C**), to ensure that the correct recombinations had been constructed.

Mice were immunized with the purified recombinant proteins via subcutaneous injection to obtain specific polyclone antibodies. Western blotting was performed to validate our proteomics analysis. The six selected proteins were significantly upregulated in groups treated with DIP as compared to the control group (**Figure 5A**), especially ORF01830, ORF01839, and ORF02943. These three proteins were undetectable in the control group, but sharply upregulated under iron limited conditions. These results indicated that our proteomics results were reliable. Our results also suggested that these iron-related extracellular proteins might play a role in bacterial virulence, and might be potential vaccine candidates.

Validation of the Proteomics Results at the mRNA Level

To further confirm our proteomics results, we used qPCR to measure the expression levels of selected genes indicated

TABLE 1 | Selected identification of differentially proteins of *A. hydrophila* LP-2 in iron starvation conditions by iTRAQ labeling analysis.

Accession	Protein description	Peptide matched	%Coverage	iTRAQ ratio (Repeat1)	*P*-Value (Repeat1)	iTRAQ ratio (Repeat2)	*P*-Value (Repeat2)	Homologous to ATCC7966
ORF02943	Hypothetical protein	12	25.94	21.28	5.24E-03	58.08	4.31E-04	AHA_1448
ORF01839	Periplasmic iron-binding protein FecB	19	40.13	19.59	1.32E-03	41.30	1.31E-02	AHA_1964
ORF01830	FIG00919923: hypothetical protein	93	56.61	10.19	5.96E-12	9.82	3.70E-03	AHA_2481
ORF01609	Putative extracellular serine protease	3866	97.6	2.99	2.73E-07	4.06	3.79E-08	AHA_2687
ORF02793	Periplasmic molybdenum-binding protein ModA	18	43.8	2.33	1.40E-02	3.66	6.64E-03	modA
ORF04443	Outer membrane vitamin B12 receptor BtuB	21	40.74	2.58	2.69E-02	2.36	1.93E-02	hgpB
ORF00614	FIG003551: hypothetical protein	16	53.96	2.36	3.68E-02	1.84	2.88E-02	AHA_3660
ORF03355	FIG00545237: hypothetical protein	40	69.86	1.66	5.06E-03	1.98	3.45E-04	AHA_1098
ORF03641	Extracellular zinc protease	232	64.69	1.71	3.04E-04	1.91	3.43E-06	AHA_0851
ORF04406	Putative lipase	99	46.77	0.54	7.20E-03	0.52	3.82E-02	AHA_0104
ORF03115	Sialidase	174	74.79	0.51	4.07E-04	0.52	2.73E-02	nanH*
ORF03984	Microbial collagenase, secreted	185	68.09	0.36	1.10E-05	0.58	3.44E-03	AHA_0517
ORF02720	Substrate binding periplasmic protein MalE	63	66.16	0.43	4.95E-04	0.34	2.03E-02	AHA_1667
ORF03869	Type II secretory pathway, pullulanase	118	58.08	0.20	3.02E-03	0.49	7.19E-03	AHA_0628
ORF01696	Alanine racemase	11	33.09	0.13	8.19E-03	0.44	2.38E-02	alr-3
ORF02315	6-phosphofructokinase	9	29.1	0.10	4.93E-03	0.45	2.16E-02	pfkA
ORF04420	Porphobilinogen synthase	15	42.18	0.24	2.45E-02	0.24	3.19E-02	hemB
ORF00636	tolB protein precursor	6	22.9	0.22	3.64E-02	0.18	3.05E-02	tolB
ORF03513	Chitinase	204	60.07	0.18	1.23E-03	0.20	2.21E-05	AHA_0977
ORF04186	SSU ribosomal protein S13p	5	37.29	0.14	7.62E-03	0.20	1.18E-02	rpsM
ORF00322	FIG00362058: hypothetical protein	21	61.02	0.14	1.35E-02	0.18	2.27E-02	AHA_3948
ORF02209	FabA	6	42.47	0.15	1.10E-02	0.15	1.90E-02	fabA
ORF03511	Chitinase	187	72.97	0.13	4.82E-04	0.16	2.88E-04	AHA_0979
ORF03029	hypothetical protein	37	30.65	0.11	1.33E-02	0.14	2.99E-02	AHA_1406
ORF02740	Glycerol kinase	5	14.15	0.06	1.07E-02	0.09	1.85E-02	glpK
ORF03889	Chitin binding protein	360	78.69	0.05	6.62E-05	0.09	1.04E-04	AHA_0610
ORF01532	Cytochrome c4	29	46.23	0.03	3.55E-02	0.06	4.50E-02	AHA_2763
ORF02296	Chitinase	218	80.29	0.02	7.62E-06	0.05	3.47E-06	AHA_2363
ORF01386	Cold shock protein CspE	5	50	0.02	1.88E-03	0.03	8.51E-03	AHA_2864
ORF04175	CopG protein	2	12.59	0.01	4.48E-02	0.01	4.30E-02	AHA_0347
ORF02395	T1SS secreted agglutinin RTX	5	9.742	0.01	4.51E-02	0.01	4.39E-02	AHA_2463
ORF01538	Peptidyl-prolyl cis-trans isomerase PpiB	6	39.39	0.01	3.72E-02	0.01	3.70E-02	ppiB
ORF01093	Peptidyl-tRNA hydrolase	2	32.83	0.01	4.84E-02	0.01	4.83E-02	pth

**homologous to A. hydrophila strain ATCC 39315.*

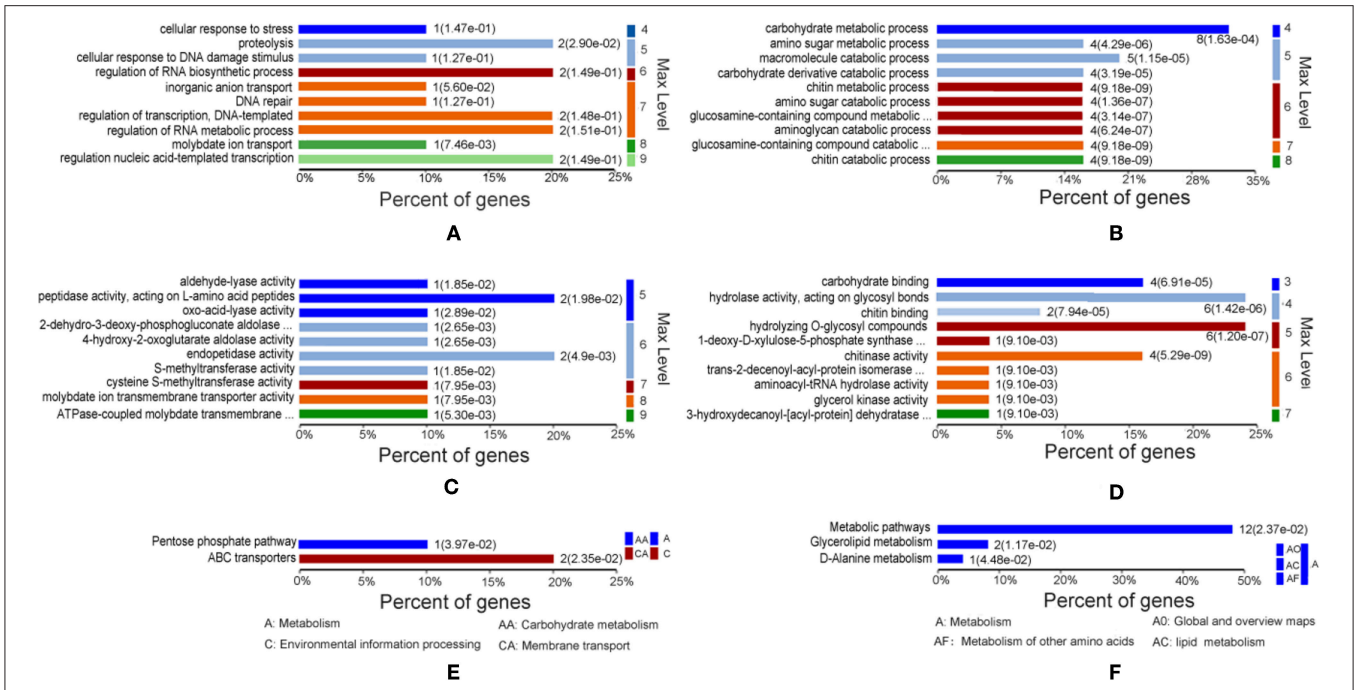


FIGURE 2 | Gene Ontology (GO) of differentially expressed proteins under iron starvation. **(A,C,E)** Upregulated proteins associated with biological processes, molecular functions, and KEGG pathways, respectively. **(B,D,F)** Downregulated proteins associated with biological processes, molecular functions, and KEGG pathways, respectively. The *p*-value cutoff was set at < 0.05. Different colors represent different GO levels, from 3 to 9.

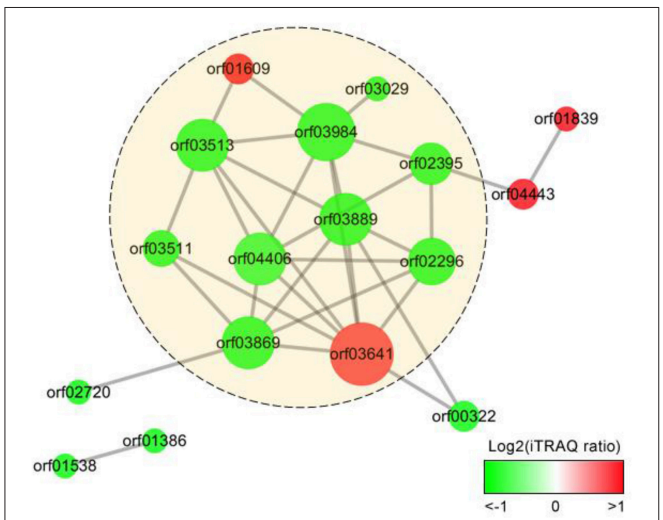


FIGURE 3 | Protein-protein interaction (PPI) networks of the extracellular proteins differentially expressed in *A. hydrophila* under iron starvation condition. The gradient color indicates iTRAQ protein ratio (on a $\log_2$ scale), and size represents protein interaction frequency. Predicted extracellular proteins are displayed in yellow circles.

to encode differentially expressed proteins by our proteomics analysis. There was a high correlation ($r^2 = 0.717$) between mRNA and proteomics across 12 genes of interest (**Figure 5B**). Except for *orf00614*, *orf03641,* and *orf02793*, the mRNA expression levels of the selected genes were consistent with our proteomics results. Although the intrinsic mechanism of the discrepancy between transcription and protein level remains largely unknown because of complicated regulative networks, the difference in temporal dimensions, time regulation delay, and protein post-translational modifications may contribute to the difference in both levels (29). Those results indicate that the combination of validation between protein and mRNA level will provide clearer clues for bacterial behaviors in iron starvation.

Deletion of Genes Encoding Extracellular Proteins and Characterization of Physiological Function

We next investigated the biological functions of the target proteins. Three of the six selected genes (*orf01609*, *orf01830*, and *orf03641*) were successfully knocked out using traceless methods (**Figure 6**). The physiological functions of these genes included biofilm formation, protease activity, and hemolysis. The LD50s of these knockout strains were compared with wildtype *A. hydrophila* LP-2 in zebrafish (**Table 2**). Although biofilm formations of mutants were unaffected, their protease activities were significantly decreased. The hemolysis activity had no difference in Δ*orf01609* and Δ*orf01830* when compared to WT control, while significantly increased in Δ*orf03641*. Meanwhile, to better understand the role of targeted genes in the virulence of *A. hydrophila* LP-2, zebrafish were injected intraperitoneally with WT and mutant strains. Mortality was recorded regularly for 14 days following infection. We found

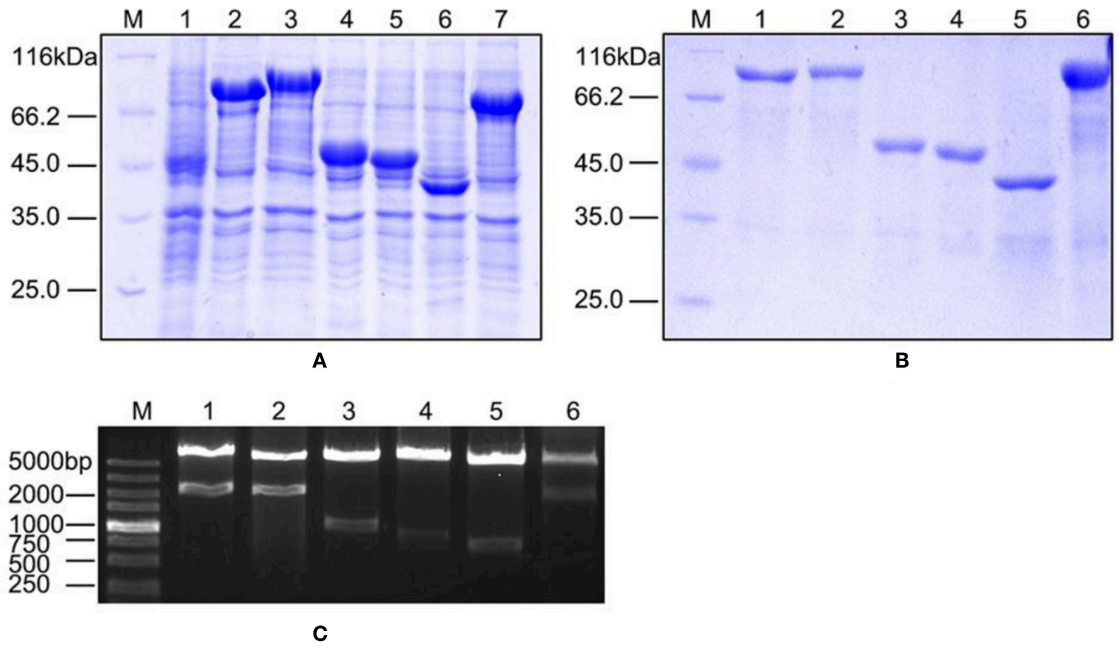


FIGURE 4 | The characteristics of overexpressed and purified recombinant proteins. **(A)** SDS-PAGE of overexpressed proteins in the BL21 strain. Lane 1: negative control; Lanes 2–7: ORF01609, ORF01830, ORF01839, ORF02943, ORF03355, and ORF03641, respectively. **(B)** SDS-PAGE of purified proteins. Lanes 1–6: purified ORF01609, ORF01830, ORF01839, ORF02943, ORF03355, and ORF03641, respectively. **(C)** Restriction enzyme identification of recombinant extracellular protein plasmids carried by the pET-32a vector. M: DL5000 marker; Lanes 1–6: ORF01609, ORF01830, ORF01839, ORF02943, ORF03355, and ORF03641, respectively.

that the LD50s of the Δ*orf01609* (3.30 x 10^4 CFU/ml) and Δ*orf01830* (2.90 × 10^4 CFU/ml) mutants were about 4- and 2-fold greater, respectively, than that of *A. hydrophila* LP-2 (0.81 × 10^4 CFU/ml), indicating a substantial reduction in virulence. However, the LD50 of Δ*orf03641* (1.35 × 10^4 CFU/ml) was similar to that of *A. hydrophila* LP-2. Our results therefore indicated that *orf01609* and *orf01830* may be novel virulent effectors, and might play important roles in bacterial invasions.

mRNA Expression of Immune-Related Genes in Response to Recombinant Proteins, as Measured by qPCR

The six iron-related recombinant proteins were injected into zebrafish. The immune response of the zebrafish was then evaluated using qPCR based on the transcription of eight immune-related genes (Lyz, MHC I, MHC II, IL-1β, IL8, IL10 IL15, and TNF-α) with BSA immunization as negative control. After ORF02943 and ORF01609 immunization, MHC II expression decreased slightly. And IL-1β expression was not significantly different after ORF02943 immunization (**Figure 7**), However, the expression levels of most of the immune-related genes increased significantly (≥1.5-fold) after immunization with the recombinant proteins. Therefore, these recombinant proteins could stimulate the immune response in fish, and might be good candidates for an *A. hydrophila* vaccine.

Protective Efficacy of Iron-Related Recombinant Proteins

To better understand the immunoprotective efficacy of proteins that were upregulated during iron starvation, zebrafish were immunized with related recombinant proteins (or with BSA, as the control) over 28 days. Immunized zebrafish were then challenged with the virulent *A. hydrophila* strain LP-2, LP-3, and YT-1, respectively. The overall survival rates of zebrafish immunized with BSA (control), ORF01609, ORF01830, ORF01839, ORF02943, ORF03355, and ORF03641 were 16.7, 68.8, 62.5, 83.3, 77.1, 66,7, and 70.8%, respectively, when challenged with *A. hydrophila* LP-2 (**Figure 8A**). The overall survival rates of zebrafish immunized with recombinant proteins as previously described order were 16.7, 64.6, 60.4, 75.0, 72.9, 58.3, and 66.7%, respectively, when challenged with *A. hydrophila* LP-3 (**Figure 8B**). And the overall survival rates of zebrafish were 12.5, 60.4, 58.3, 79.2, 72.9, 70.8, and 64.6%, respectively, when challenged with *A. hydrophila* YT-1 (**Figure 8C**).The RPS of the fish injected with 3 μg of each recombinant protein (ORF01609, ORF01830, ORF01839, ORF02943, ORF03355, and ORF03641) were 63.0 ± 6.3, 55.6 ± 6.1, 80.2 ± 4.1, 73.0 ± 7.5, 60.6 ± 14.6, and 65.2 ± 5.4% in *A. hydrophila* LP-2 challenging for 14 days, respectively, as compared to the unimmunized control. The RPS of the fish injected with recombinant proteins as previously described order were 57.3 ± 6.0, 52.6 ± 2.2, 70.1 ± 6.4, 67.5 ± 8.2, 50.1 ± 6.3, and 60.0 ± 5.4% in *A. hydrophila* LP-3 challenging for 7 days, respectively. The RPS of the fish injected with recombinant proteins were 53.7 ± 3.6, 51.3 ± 7.4, 74.2 ±

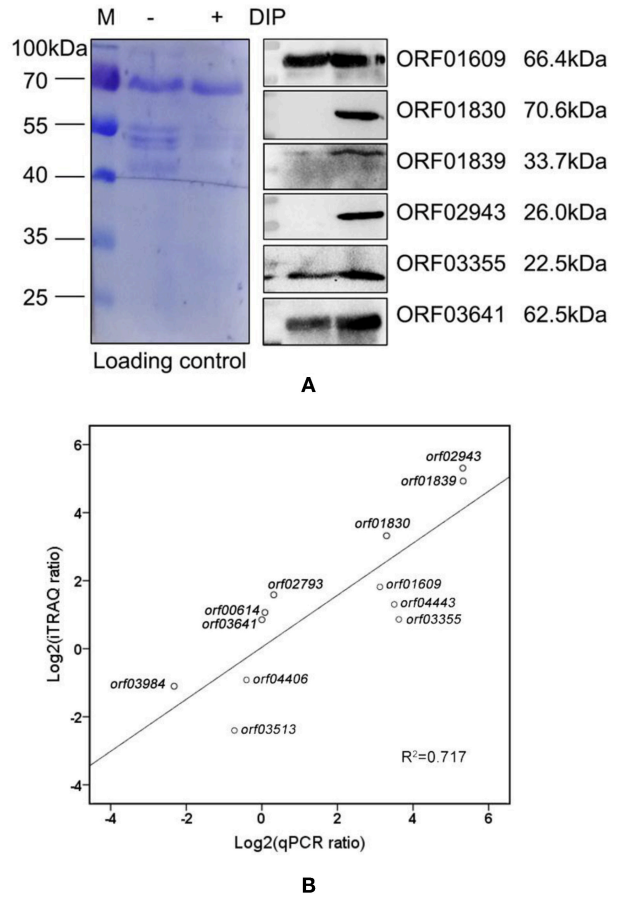


FIGURE 5 | Correlations between selected genes and proteins. **(A)** Western blot of differentially expressed extracellular proteins in *A. hydrophila* LP-2 with and without DIP treatment. Coomassie R-350 stained on PVDF membrane was used as the loading control. **(B)** The correlation between mRNA expression and proteomics in nine upregulated genes *(orf00614, orf01609, orf01830, orf01839, orf02793, orf02943, orf03355, orf03641,* and *orf04443*), and three downregulated genes (*orf03513, orf03984,* and *orf04406*).

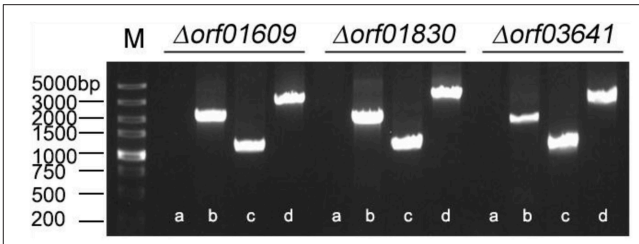


FIGURE 6 | Confirmation of the knockout mutant strains Δ*orf01609*, Δ*orf01830,* and Δ*orf03641*. M: DL5000 marker; a: The fragment of genomic deletion mutant DNA amplified using cloning primers. b: The fragment of genomic wild-type (LP-2) DNA amplified using cloning primers. c: The fragment of genomic deletion mutant DNA amplified using the primer pair P7/P8. d: The fragment of genomic wild-type (LP-2) DNA amplified using the primer pair P7/P8.

3.9, 69.3 ± 6.7, 65.7 ± 5.1, and 58.4 ± 5.4% in *A. hydrophila* YT-1 challenging for 7 days, respectively. Thus, RPS across all of the groups injected with recombinant proteins was >50%, indicating that these proteins, especially ORF01839 and ORF02943, may be promising candidates for *A. hydrophila* vaccine development.

DISCUSSION

Secreted proteins play important roles in bacterial virulence during host infection, and have been previously proposed as potential vaccine candidates (30, 31). However, the biological functions and protective efficacies of these proteins remain largely unknown. In addition, iron availability is an important environmental factor for bacterial reproduction, which is always trace available ferrous iron in the natural environment or in the host, may form part of an effective bacteriostatic strategy (32). Thus, iron-regulated proteins may contribute to bacterial virulence, and have been shown to be effective vaccine candidates against pathogenic infection (33). Meanwhile, component vaccines are highly specific and effective in protecting the immune system, but often fail to protect the host well when pathogenic microorganisms mutate (34). Moreover, due to the large number of pathogenic bacteria components, a lot of manpower, and resources are needed to develop new vaccines. Thus, the protein vaccine approach is more prefer for developing and researching new vaccines from a proteomic perspective (35).

To better understand secreted protein behavior in *A. hydrophila* LP-2 in response to iron starvation; to investigate the immune response that these proteins provoked in fish; and to test the efficacy of these proteins as a vaccine, we isolated the extracellular protein fraction in an iron-limited medium (i.e., treated with DIP) and in an untreated LB medium with the trichloroacetic acid (TCA) precipitation method (36–38). The extracellular proteins differentially expressed between groups were compared using iTRAQ label-based quantitative proteomics in combination with high resolution mass spectrometry. The proteomics analysis identified 341 proteins, 9 of which were upregulated in response to iron starvation, and 24 of which were downregulated.

Our proteomics results also indicated that only 10–30% of all differentially expressed proteins were extracellular proteins. However, unavoidable contamination from highly abundant cytoplasmic proteins might have affected the quality of the extracellular fraction. In addition, some proteins are predicted to be in multiple subcellular locations and might be secreted to extracellular space. One such protein was exodeoxyribonuclease III ORF01296, which was predicted to be located in both the extracellular space and in the cytoplasm. Indeed, it is unknown whether cytoplasmic proteins originate from cell lysis or are exported by a so-far unknown mechanism (39). In bacteria, some cytosolic proteins, such as glyceraldehyde-3-phosphate dehydrogenase (GAPDH), ornithine carbamoyltransferase, and α-enolase, have been reported to be secreted proteins, which was consistent with our proteomics results (40–42). Beside these, the secretion of bacterial outer membrane vesicles (OMVs) may also contribute components to the extracellular fraction, which include diverse proteins from different cellular locations (43). Thus, it is complicated to determine the exact components

TABLE 2 | Characteristics of the mutant strains.

Characteristics	*A. hydrophila* LP-2	Δ*ORF01609*	Δ*ORF01830*	Δ*ORF03641*
Biofilm formation[a]	0.84 ± 0.06	0.84 ± 0.12	0.83 ± 0.07	0.80 ± 0.12
Activity of ECPase (A_{442})[b]	0.34 ± 0.01	0.27 ± 0.01**	0.30 ± 0.02*	0.26 ± 0.01**
Hemolysis (%)[c]	4.27 ± 0.11	4.76 ± 0.19	4.01 ± 0.32	12.87 ± 0.18**
LD50 (cfu/mL)[d]	0.81 × 10^4	3.30 × 10^4**	2.90 × 10^4**	1.35 × 10^4

*Values are the mean ± standard deviation of three independent trials. Significant differences between A. hydrophila LP-2 and each mutant strain are indicated by asterisks. *P < 0.05; **P < 0.01.*

[a] *96-well-polypropylene plates incubated with bacteria for 48 h at 30°C and was measured using crystal violet staining method.*

[b] *bacteria were cultured on 1.5% LB agar plates and incubated for 18 h at 30°C, then collected using PBS. And use azocasein assay for extracellular protease.*

[c] *extracellular protease hemolytic activity was measured using defibrinated sheep blood. Culture supernatant was incubated with blood in PBS for 1 h at room temperature.*

[d] *LD50s were evaluated in healthy zebrafish with the weight of 0.32 ± 0.06 g.*

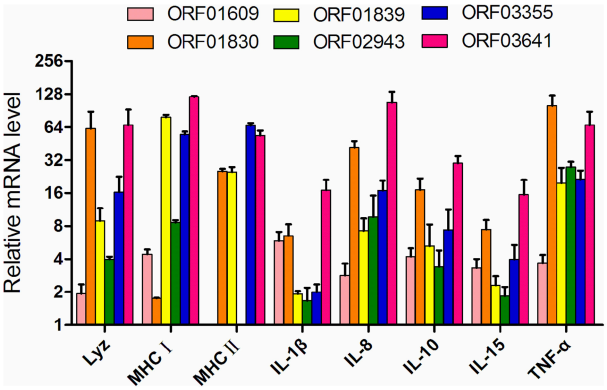


FIGURE 7 | Expression of immune-related genes in zebrafish immunized with recombinant proteins as compared to controls treated with BSA, as quantified by qPCR. Internal organs were collected before the *A. hydrophila* LP-2 challenge.

of excreted proteins. We therefore focused on the biological functions and immunoprotective efficacies of the iron-related proteins in the extracellular fraction.

We found that various biological processes, including carbohydrate metabolism, amino sugar metabolism, catabolic metabolism, and chitin metabolic processes, were enriched in the proteins downregulated in response to iron starvation. The downregulation of these proteins might reduce iron consumption, as these proteins use iron as a cofactor (44, 45). We also found that some extracellular proteins associated with chitinase metabolism, including ORF03511, ORF03513, ORF02296, and ORF03889 (homologous to AHA_0979, AHA_0977, AHA_2363, and AHA_0610 (chitin binding protein), respectively, in *A. hydrophila* ATCC 7966) were downregulated in response to iron starvation. Since chitin is a polymer of N-acetylglucosamine and glucosamine residues, and because it forms complexes with transition metal ions including ferric iron, this observed decrease in chitinase metabolism in response to iron starvation is reasonable (46). Proteins related to peptidase activity, the cellular response to stress, and the ABC transport processes were upregulated; these may improve bacterial survival in iron-limited environments by increasing bacterial virulence or adaptability (47).

We validated our proteomics results with Western blotting and qPCR. Six selected genes encoding proteins differentially expressed in response to *A. hydrophila* LP-2 iron starvation (*orf01609*, *orf01830*, *orf01839*, *orf02943*, *orf03355*, and *orf03641*) were cloned, overexpressed, and purified. Polyclonal antibodies specific to each gene were produced by immunizing mice. Western blots showed that these proteins were upregulated in response to iron starvation, which is consistent with our proteomics results. This indicated that our proteomics results were reliable. Moreover, we analyzed the homologies of these six proteins among twelve *A. hydrophila* strain genomes and found that most of them have considerable high identities (>80%), although the identities of ORF02943 in several strains are slightly low (>30%, **Figure S1**). We also compared the cross-immunogen reaction of these antigens among *A. hydrophila* LP-2, *A. hydrophila* ATCC 7966, and other popular fish pathogens such as *V. alginolyticus*, *E. tarda*, *V. parahaemolyticus*, and *V. fluvialis* by western blotting (**Figure S2**). Our results showed that many of antibodies against candidate proteins in *A. hydrophila* LP-2 cross-reacted with *A. hydrophila* ATCC 7966 except for ORF02943 and ORF03355, which indicate these specific antibodies plays role in the cross-immune protection among *A. hydrophila* strains. Besides these, some antibodies against antigens such as ORF01609, ORF01830, ORF01839, and ORF03641 have cross-reaction with other fish pathogens. The immunogenicity and immunoprotection properties of these candidate proteins against *A. hydrophila* spp. and other fish pathogens should be further investigated. qPCR analyses also indicated that most of selected genes were upregulated, suggesting a high correlation between mRNA expression and protein expression. These results indicated that the upregulated iron-related proteins might be involved in iron homeostasis or bacterial virulence, and that they had potential immuoprotective properties.

Some of the selected proteins (or their homologs) have been suggested as potential vaccine candidates or virulent effectors. ORF01839 (highly homologous to FecB in *A. hydrophila* ATCC 7966) is a periplasmic iron-binding protein that may affect the iron (III) dicitrate transport system by mediating iron uptake during invasive infections (48). The upregulation of this protein in response to iron starvation, as observed here, might increase the likelihood of bacterial survival by increasing

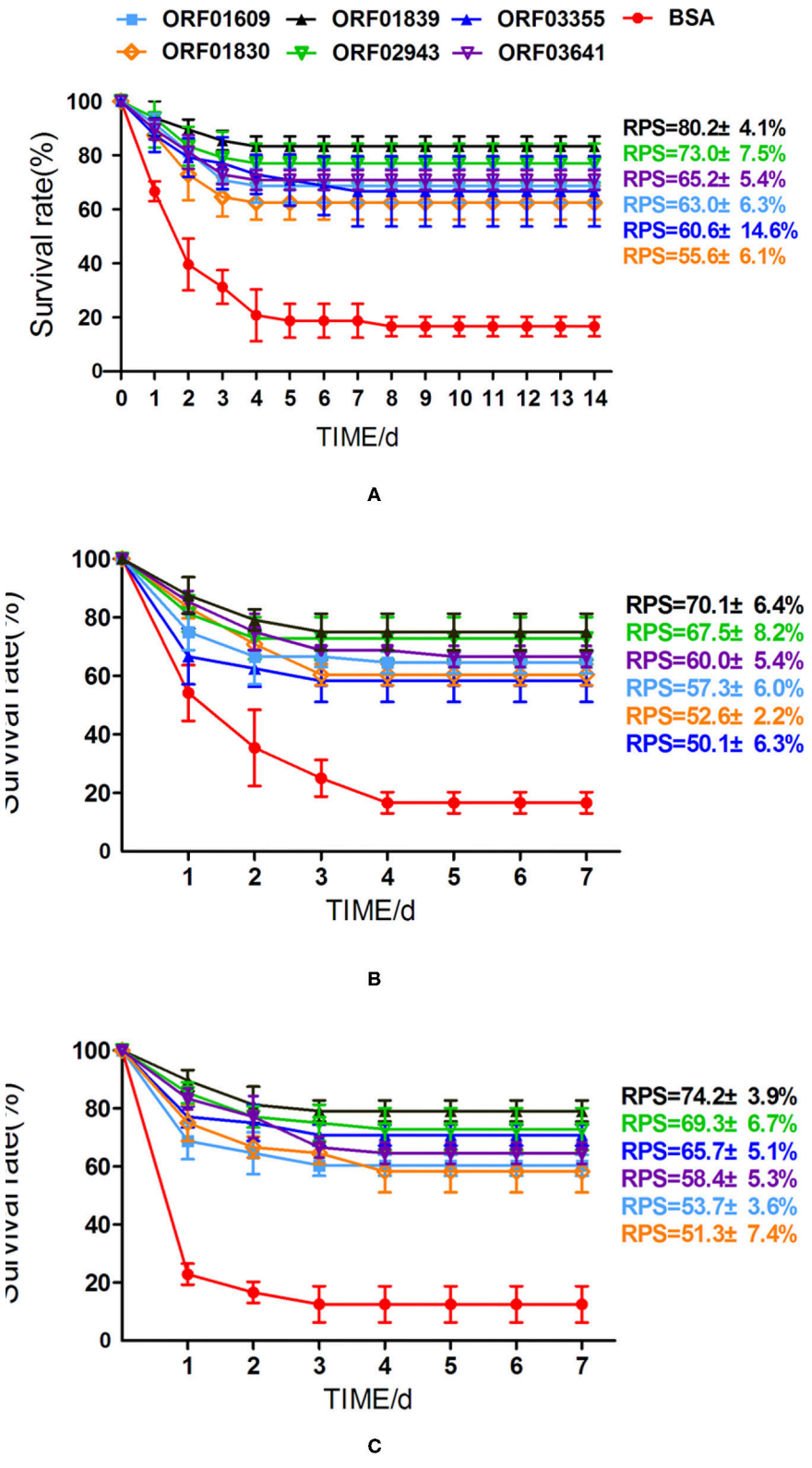


FIGURE 8 | Cumulative survival rates of zebrafish after challenge with *A. hydrophila*. **(A)** Zebrafish vaccinated with six iron-related extracellular proteins (ORF01609, ORF01830, ORF01839, ORF02943, ORF03355, and ORF03641) and a control treated with BSA were challenged with *A. hydrophila* LP-2 for 14 days. **(B,C)** Zebrafish vaccinated with six recombinant proteins and a control treated with BSA were challenged with *A. hydrophila* LP-3 and YT-1 for 7 days, respectively. Mortalities were recorded for 14 days. Data represent the mean ± SEM of $n \geq$ two independent replicates.

iron uptake. ORF01839 is also homologous to the siderophore-binding protein FhuD in *Staphylococcus aureus*, which belongs to iron regulated lipoproteins (IRLPs) and was reported to involve in the uptake of iron through siderophore (49). IRLPs may be the dominant immunobiologically active compounds in *S.aureus* and induce cytokine by Toll-like receptors (TLRs) (50). Moreover, it was reported that FuhD2 vaccination could evoke protective immunity against clinical *S. aureus* in infection mice by producing functional antibodies to mediate opsonophagocytosis, and has recently been described as a promising vaccine candidate (51, 52). ORF01609 is a serine protease (homologous to Ahe2), and was reported to be a type III secretion system virulence effector in both *A. hydrophila* J-1 and in *A. salmonicida* (53, 54). This protein is a multifunctional enzyme and a key factor of physiological and pathological inflammation which usually involved in the production of pro-inflammatory cytokines and the activation of immune cells such as macrophages (55, 56). Here, the deletion of *orf01609* significantly reduced the virulence of *A. hydrophila* LP-2 in zebrafish, suggesting that this protein is also an important virulence effector in *A. hydrophila*. Additionally, previous researches reported that extracellular serine protease Esp inhibits biofilm formation of *S. aureus* by cleaving autolysin (Atl)-derived murein hydrolases (57). However, the deletion of *orf01609* showed not difference in biofilm formation in this study, which suggest this protein may play more role on the invasion and that would helpful for the bacterial iron uptake from host.

ORF03641 is a hemagglutinin/elastase, which acts as an extracellular zinc-containing metalloendopeptidase. Unlikely extracellular zinc protease in *V. cholerae* participates in biofilm development, this protein may play an important role in bacterial infection by degrading various plasma proteins in the host, including Fe-containing proteins such as immunoglobulin and lactoferrin, thereby increasing the iron resources available to the pathogen (58–60). It was reported that neutrophil elastase can subvert the immune response by cleaving Toll-like receptors and cytokines in pneumococcal pneumonia, which indicate ORF03641 may play similar role on the host immune response (61). Moreover, previous research showed that immunization with elastase peptide reduced experimental lung infections caused by *Pseudomonas aeruginosa* and *Burkholderia cepacia*, indicating that this protein has immunogenic properties (62).

ORF03355 is an outer membrane autotransporter that contains a β-barrel structure according to the humongous analysis. Autotransporters have been shown to have immunoprotective effects against diverse pathogenic bacteria, including *Bordetella pertussis*, *Haemophilus ducreyi,* and *Edwardsiella tarda* (63–65). Previous research also showed that an outer membrane autotransporter regulates a component of the host inflammatory response, so that *Helicobacter pylori* can fine-tune the host immune response according to the expression of the outer membrane protein (66). That indicates ORF03355 may also play important role on the host immune response. ORF02943 and ORF01830 are hypothetical proteins predicted to be located either on the outer membrane or in the extracellular space. Here, the *orf01830* mutant affected the virulence of *A. hydrophila* LP-2, suggesting that the encoded protein plays a role in bacterial invasion. However, the immuoprotective characteristics of the proteins upregulated in *A. hydrophila* in response to iron starvation remain poorly understood.

To investigate the potential utility of these selected proteins as vaccine candidates, we evaluated the immune response that these proteins provoked in fish as well as their immunoprotective properties. Although immunization with ORF02943 slightly decreased MHCII expression in zebrafish, immunization with the recombinant proteins largely upregulated the six immune-related genes in zebrafish, as compared to the unimmunized control. ORF03641 immunization was particularly effective, increasing the expression of the selected immune-related genes by 16- to 120-fold. In current years, several researches have reported that outer membrane proteins (OMPs) such as OmpA1, OmpC, and Tdr in *A. hydrophila* affect the immune responses and protective efficacies in fish (14, 67, 68). For example, the rOmpF-immunized *Labeo rohita* showed an up-regulated expression of a proinflammatory cytokine IL-1β and phagocytes activation factor INF-α on day 28 challenge (69). rOmpR in *Aeromonas hydrophila*, for another example, was reported to elicit immune response genes such as lysozyme G, T cell response factors (MHC I, MHC II), and IL-1β in *L. rohita* at early time points post-immunization (70). Similar with the immune response of OMPs, immunization with targeted proteins increased the expression levels of several proinflammatory molecules, such as IL-1β, TNF-α, and IL-8 as well as cytokines IL-10 in this study. Likely outer membrane proteins, these extracellular proteins may be recognized by the pattern recognition receptors on the host cells (69), substantially increased the fish immune response, and their immunoprotective characters should be further explored.

Generally, oral, injection and immersion immunization are the three most popular immunization methods. Despite of the disadvantages of labor-intensive and be more likely to cause damage to fish, intraperitoneal injection immunization is more efficient, effective, and stable. It is by far the most effective method and is widely used in injection model for fish challenge (26, 71). Thus, the vaccine efficacy of these recombinant proteins was evaluated by challenging zebrafish with virulent *A. hydrophila*, after intraperitoneal injection immunization in this study. Our results showed that these proteins may be promising vaccine candidates, as RPS ranged from 55 to 80%. ORF02943 and ORF01839 increased RPS substantially, to 73.0 ± 7.5 and 80.2 ± 4.1% in *A. hydrophila* LP-2 challenging, respectively.

We further investigated whether these recombinant proteins eliciting high immune protection against other *A. hydrophila* pathogen infection could protect zebrafish. Therefore, recombinant proteins were used to immunize zebrafish and then challenged with virulent *A. hydrophila* YT-1 and LP-3 for 7 days. Our results showed that all proteins showed significant protection against *A. hydrophila* infection with considerable RPSs in the range from 50.1 ± 6.3 to 74.2 ± 3.9%, especially for ORF01839 and ORF02943 which RPSs were higher 65%. That indicates these proteins have the potential cross-protective abilities in *A. hydrophila* infection. In general, our results compared the differentially expression of extracellular proteins in iron starvation condition using proteomics method and

provided an effective strategy for the discovery of recombinant protein vaccine candidates. Additionally, based on the facts that many described proteins of *A. hydrophila*, especially for OMPs and extracellular proteins, have considerable protective effects in fish, which share similar effect with the results in this study, the current candidate proteins can be combined with them as an effective vaccine against the bacterial pathogen *A. hydrophila* in the future.

ETHICS STATEMENT

This study was approved by Fujian Agriculture and Forestry University Animal Care and Use Committee (Certification Number: CNFJAC0027).

AUTHOR CONTRIBUTIONS

XW and YW performed most of the experiments. ZL performed data analyses. YF and XY helped for gene clone. WL and XL designed all experiments. XL and FA wrote the manuscript.

FUNDING

This work was sponsored by grants from NSFC projects (Nos. 31670129 and 31470238), Program for Innovative Research Team in Fujian Agricultural and Forestry University (No.712018009), and the Fujian-Taiwan Joint Innovative Center for Germplasm Resources and Cultivation of Crop (FJ 2011 Program, No.2015-75, China). We would like to thank LetPub (www.letpub.com) for providing linguistic assistance during the preparation of this manuscript.

SUPPLEMENTARY MATERIAL

The Supplementary Material for this article can be found online at: https://www.frontiersin.org/articles/10.3389/fimmu.2019.00256/full#supplementary-material

Supplementary Figure 1 | Homology comparison of target proteins in different *A. hydrophila* stains. The protein homology of different bacteria is expressed as identity from 0 to 100%, and the corresponding color changes from blue to red.

Supplementary Figure 2 | Western blot for cross-immunogen reaction among seven species of bacteria with and without DIP treatment. The protein samples were separated with SDS-PAGE and the Western blotting was performed with anti-ORF01609, anti-ORF01830, anti-ORF01839, anti-ORF02943, anti-ORF03355, and ORF03641, respectively.

Supplementary Table 1 | Cloning primers sequences in this study.

Supplementary Table 2 | qPCR primers sequences in this study.

Supplementary Table 3 | Mutant construction primers sequences in this study.

Supplementary Table 4 | Identification of extracellular proteins in *A. hydrophila* LP-2 with DIP treatment by iTRAQ labeling analysis.

REFERENCES

1. Janda JM, Abbott SL. The genus *Aeromonas*: taxonomy, pathogenicity, and infection. *Clin Microbiol Rev.* (2010) 23:35–73. doi: 10.1128/CMR.00039-09
2. Zhu FJ, Yang ZY, Zhang Yl, Hu K, Fang WH. Transcriptome differences between enrofloxacin-resistant and enrofloxacin-susceptible strains of *Aeromonas hydrophila*. *PLoS ONE* (2017) 12:e0179549. doi: 10.1371/journal.pone.0179549
3. Guo Z, Lin YX, Wang XY, Fu YY, Lin WX, Lin XM. The protective efficacy of four iron-related recombinant proteins and their single-walled carbon nanotube encapsulated counterparts against *Aeromonas hydrophila* infection in zebrafish. *Fish Shellfish Immunol.* (2018) 82:50–9. doi: 10.1016/j.fsi.2018.08.009
4. Zhang D, Pridgeon JW, Klesius PH. Vaccination of channel catfish with extracellular products of *Aeromonas hydrophila* provides protection against infection by the pathogen. *Fish Shellfish Immunol.* (2014) 36:270–5. doi: 10.1016/j.fsi.2013.11.015
5. Rodriguez LA, Ellis AE, Nieto TP. Purification and characterisation of an extracellular metalloprotease, serine protease and haemolysin of *Aeromonas hydrophila* strain B_{32}: all are lethal for fish. *Microb Pathog.* (1992) 13:17–24. doi:10.1016/0882-4010(92)90028-M
6. Zhang D, Xu DH, Shoemaker CA. Immunization with recombinant aerolysin and haemolysin protected channel catfish against virulent *Aeromonas hydrophila*. *Aquacult Res.* (2017) 48:2–4. doi: 10.1111/are.12931
7. Wu L, Jiang YN, Tang Q, Lin HX, Lu CP, Yao HC. Development of an *Aeromonas hydrophila* recombinant extracellular protease vaccine. *Microb Pathog.* (2012) 53:183–8. doi: 10.1016/j.micpath.2012.07.007
8. Ni XD, Wang N, Liu YJ, Lu CP. Immunoproteomics of extracellular proteins of the *Aeromonas hydrophila* China vaccine strain J-1 reveal a highly immunoreactive outer membrane protein. *FEMS Immunol Med Microbiol.* (2010) 58:363–73. doi: 10.1111/j.1574-695X.2009.00646.x
9. Naz A, Awan FM, Obaid A, Muhammad SA, Paracha RZ, Ahmad J, et al. Identification of putative vaccine candidates against *Helicobacter pylori* exploiting exoproteome and secretome: a reverse vaccinology based approach. *Infect Genet Evol.* (2015) 32:280–91. doi: 10.1016/j.meegid.2015.03.027
10. Pang HY, Chen LM, Hoare R, Huang YC, Wu ZH, Jian JC. Identification of DLD, by immunoproteomic analysis and evaluation as a potential vaccine antigen against three Vibrio species in *Epinephelus coioides*. *Vaccine* (2016) 34:1225–31. doi: 10.1016/j.vaccine.2015.11.001
11. Fiester SE, Actis LA. Stress responses in the opportunistic pathogen *Acinetobacter baumannii*. *Future Microbiol.* (2013) 8:353–65. doi: 10.2217/fmb.12.150
12. Long A, Fehringer TR, Swain MA, LaFrentz BR, Call DR, Cain KD. Enhanced efficacy of an attenuated *Flavobacterium psychrophilum* strain cultured under iron-limited conditions. *Fish Shellfish Immunol.* (2013) 35:1477–82. doi: 10.1016/j.fsi.2013.08.009
13. Mittal R, Sharma S, Chhibber S, Harjai K. Iron dictates the virulence of *Pseudomonas aeruginosa* in urinary tract infections. *J Biomed Sci.* (2008) 15:731–41. doi: 10.1007/s11373-008-9274-7
14. Wang YQ, Chen HR, Guo Z, Sun LN, Fu YY, Li T, et al. Quantitative proteomic analysis of iron-regulated outer membrane proteins in *Aeromonas hydrophila* as potential vaccine candidates. *Fish Shellfish Immunol.* (2017) 68:1–9. doi: 10.1016/j.fsi.2017.07.002
15. Yu HB, Kaur R, Lim S, Wang XH, Leung KY. Characterization of extracellular proteins produced by *Aeromonas hydrophila* AH-1. *Proteomics* (2007) 7:436–49. doi: 10.1002/pmic.200600396
16. Cheng ZX, Yang MJ, Peng B, Peng XX, Lin XM, Li H. The depressed central carbon and energy metabolisms is associated to the acquisition of levofloxacin resistance in *Vibrio alginolyticus*. *J Proteomics* (2018) 181:83–91. doi: 10.1016/j.jprot.2018.04.002
17. Lin XM, Lin L, Yao ZJ, Li WX, Sun LN, Zhang DF, et al. An integrated quantitative and targeted proteomics reveals fitness mechanisms of *Aeromonas hydrophila* under oxytetracycline stress. *J Proteome Res.* (2015) 14:1515–25. doi: 10.1021/pr501188g
18. Li W, Yao ZJ, Zhang XY, Huang F, Lin WX, Lin XM. Global protein expression profile response of planktonic *Aeromonas hydrophila* exposed to

chlortetracycline. *World J Microbiol Biotechnol.* (2017) 33:68. doi: 10.1007/s11274-017-2204-y
19. Liu X, Yang MJ, Wang SN, Xu D, Li H, Peng XX. Differential antibody responses to outer membrane proteins contribute to differential immune protections between live and inactivated *Vibrio parahemolyticus*. *J Proteome Res.* (2018) 17:2987–94. doi: 10.1021/acs.jproteome.8b00176
20. Yang J, Zeng ZH, Yang MJ, Cheng ZX, Peng XX, Li H. NaCl promotes antibiotic resistance by reducing redox states in *Vibrio alginolyticus*. *Environ Microbiol.* (2018) 20:4022–36. doi: 10.1111/1462-2920.14443
21. Su YB, Peng B, Li H, Cheng ZX, Zhang TT, Zhu JX, et al. Pyruvate cycle increases aminoglycoside efficacy and provides respiratory energy in bacteria. *Proc Natl Acad Sci USA.* (2018) 115:E1578–87. doi: 10.1073/pnas.1714645115
22. Li WX, Ali F, Cai QL, Yao ZJ, Sun LN, Lin WX, et al. Reprint of: Quantitative proteomic analysis reveals that chemotaxis is involved in chlortetracycline resistance of *Aeromonas hydrophila*. *J Proteomics* (2018) 180:138–46. doi: 10.1016/j.jprot.2018.03.020
23. Zhu WH, Zhou YL, Sun DJ, Li ZW. An uPA cleavable conjugate of a recombinant αvβ3 targeting toxin and its bioactivity. *World J Microbiol Biotechnol.* (2011) 27:563–9. doi: 10.1007/s11274-010-0491-7
24. Varina M, Denkin SM, Staroscik AM, Nelson DR. Identification and characterization of Epp, the secreted processing protease for the *Vibrio anguillarum* EmpA metalloprotease. *J Bacteriol.* (2008) 190:6589–97. doi: 10.1128/JB.00535-08
25. Martinez-Granero F, Navazo A, Barahona E, Redondo-Nieto M, Gonzalez de Heredia E, Baena I, et al. Identification of *flgZ* as a flagellar gene encoding a PilZ domain protein that regulates swimming motility and biofilm formation in *Pseudomonas*. *PLoS ONE* (2014) 9:e87608. doi: 10.1371/journal.pone.0087608
26. Pang H, Qiu M, Zhao J, Hoare R, Monaghan SJ, Song D, et al. Construction of a *Vibrio alginolyticus hopPmaJ* (*hop*) mutant and evaluation of its potential as a live attenuated vaccine in orange-spotted grouper (*Epinephelus coioides*). *Fish Shellfish Immunol.* (2018) 76:93–100. doi: 10.1016/j.fsi.2018.02.012
27. Reed LJ, Muench H. A simple method of estimating fifty per cent endpoint. *Am J Epidemiol.* (1938) 27:493–7. doi: 10.1093/oxfordjournals.aje.a118408
28. Peng B, Lin XP, Wang SN, Yang MJ, Peng XX, Li H. Polyvalent protective immunogens identified from outer membrane proteins of *Vibrio parahaemolyticus* and their induced innate immune response. *Fish Shellfish Immunol.* (2018) 72:104–10. doi: 10.1016/j.fsi.2017.10.046
29. Muers M. Gene expression: transcriptome to proteome and back to genome. *Nat Rev Genet.* (2011) 12:518. doi: 10.1038/nrg3037
30. Goud GN, Zhan B, Ghosh K, Loukas A, Hawdon J, Dobardzic A, et al. Cloning, yeast expression, isolation, and vaccine testing of recombinant Ancylostoma-secreted protein (ASP)-1 and ASP-2 from *Ancylostoma ceylanicum*. *J Infect Dis.* (2004) 189:919–29. doi: 10.1086/381901
31. Li M, Song S, Yang D, Li C, Li G. Identification of secreted proteins as novel antigenic vaccine candidates of *Haemophilus parasuis* serovar 5. *Vaccine* (2015) 33:1695–701. doi: 10.1016/j.vaccine.2015.02.023
32. Ganz T. Correction to: iron and infection. *Int J Hematol.* (2018) 107:122. doi: 10.1007/s12185-017-2385-z
33. Alvarez Hayes J, Oviedo JM, Valdez H, Laborde JM, Maschi F, Ayala M, et al. A recombinant iron transport protein from *Bordetella pertussis* confers protection against *Bordetella parapertussis*. *Microbiol Immunol.* (2017) 61:407–15. doi: 10.1111/1348-0421.12532
34. Blake DP, Pastor-Fernandez I, Nolan MJ, Tomley FM. Recombinant anticoccidial vaccines - a cup half full? *Infect Genet Evol.* (2017) 55:358–65. doi: 10.1016/j.meegid.2017.10.009
35. Sommerset I, Krossoy B, Biering E, Frost P. Vaccines for fish in aquaculture. *Expert Rev Vaccines* (2005) 4:89–101. doi: 10.1586/14760584.4.1.89
36. Rajalingam D, Loftis C, Xu JJ, Kumar TK. Trichloroacetic acid-induced protein precipitation involves the reversible association of a stable partially structured intermediate. *Protein Sci.* (2009) 18:980–93. doi: 10.1002/pro.108
37. Chevallet M, Diemer H, Van Dorssealer A, Villiers C, Rabilloud T. Toward a better analysis of secreted proteins: the example of the myeloid cells secretome. *Proteomics* (2007) 7:1757–70. doi: 10.1002/pmic.200601024
38. Ji C, Juárez-Hernández RE, Miller MJ. Exploiting bacterial iron acquisition: siderophore conjugates. *Future Med Chem.* (2012) 4:297–313. doi: 10.4155/fmc.11.191
39. Götz F, Yu W, Dube L, Prax M, Ebner P. Excretion of cytosolic proteins (ECP) in bacteria. *Int J Med Microbiol.* (2015) 305:230–7. doi: 10.1016/j.ijmm.2014.12.021
40. Pancholi V, Fischetti VA. A major surface protein on group A streptococci is a glyceraldehyde-3-phosphate-dehydrogenase with multiple binding activity. *J Exp Med.* (1992) 176:415–26. doi: 10.1084/jem.176.2.415
41. Hughes MJ, Moore JC, Lane JD, Wilson R, Pribul PK, Younes ZN, et al. Identification of major outer surface proteins of *Streptococcus agalactiae*. *Infect Immun.* (2002) 70:1254–9. doi: 10.1128/IAI.70.3.1254-1259.2002
42. Pancholi V, Fischetti VA. Alpha-enolase, a novel strong plasmin(ogen) binding protein on the surface of pathogenic streptococci. *J Biol Chem.* (1998) 273:14503–15. doi: 10.1074/jbc.273.23.14503
43. Kulp A, Kuehn MJ. Biological functions and biogenesis of secreted bacterial outer membrane vesicles. *Annu Rev Microbiol.* (2010) 64:163–84. doi: 10.1146/annurev.micro.091208.073413
44. Meibom KL, Li XB, Nielsen AT, Wu CY, Roseman S, Schoolnik GK. The *Vibrio cholerae* chitin utilization program. *Proc Natl Acad Sci USA.* (2004) 101:2524–9. doi: 10.1073/pnas.0308707101
45. Vigani G, Morandini P, Murgia I. Searching iron sensors in plants by exploring the link among 2'-OG-dependent dioxygenases, the iron deficiency response and metabolic adjustments occurring under iron deficiency. *Front Plant Sci.* (2013) 4:169. doi: 10.3389/fpls.2013.00169
46. Karthikeyan G, Andal NM, Anbalagan K. Adsorption studies of iron (III) on chitin. *J Chem Sci.* (2005) 117:663–72. doi: 10.1007/BF02708296
47. Clarke SC, Dumesic PA, Homer CM, O'Donoghue AJ, La Greca F, Pallova L, et al. Integrated activity and genetic profiling of secreted peptidases in *Cryptococcus neoformans* reveals an aspartyl peptidase required for low pH survival and virulence. *PLoS Pathog.* (2016) 12:e1006051. doi: 10.1371/journal.ppat.1006051
48. Banerjee S, Paul S, Nguyen LT, Chu BC, Vogel HJ. FecB, a periplasmic ferric-citrate transporter from *E. coli*, can bind different forms of ferric-citrate as well as a wide variety of metal-free and metal-loaded tricarboxylic acids. *Metallomics* (2016) 8:125–33. doi: 10.1039/c5mt00218d
49. Sheldon JR, Heinrichs DE. The iron-regulated staphylococcal lipoproteins. *Front Cell Infect Microbiol.* (2012) 2:41. doi: 10.3389/fcimb.2012.00041
50. Hashimoto M, Tawaratsumida K, Kariya H, Kiyohara A, Suda Y, Krikae F, et al. Not lipoteichoic acid but lipoproteins appear to be the dominant immunobiologically active compounds in *Staphylococcus aureus*. *J Immunol.* (2006) 177:3162–9. doi: 10.4049/jimmunol.177.5.3162
51. Mariotti P, Malito E, Biancucci M, Lo Surdo P, Mishra RP, Nardi-Dei V, et al. Structural and functional characterization of the *Staphylococcus aureus* virulence factor and vaccine candidate FhuD2. *Biochem J.* (2013) 449:683–93. doi: 10.1042/BJ20121426
52. Mishra RP, Mariotti P, Fiaschi L, Nosari S, Maccari S, Liberatori S, et al. Staphylococcus aureus FhuD2 is involved in the early phase of staphylococcal dissemination and generates protective immunity in mice. *J Infect Dis.* (2012) 206:1041–9. doi: 10.1093/infdis/jis463
53. Li J, Zhang XL, Liu YJ, Lu CP. Development of an *Aeromonas hydrophila* infection model using the protozoan *Tetrahymena thermophila*. *FEMS Microbiol Lett.* (2011) 316:160–8. doi: 10.1111/j.1574-6968.2010.02208.x
54. Vanden Bergh P, Heller M, Braga-Lagache S, Frey J. The *Aeromonas salmonicida* subsp. *salmonicida* exoproteome: determination of the complete repertoire of type-three secretion system effectors and identification of other virulence factors. *Proteome Sci.* (2013) 11:42. doi: 10.1186/1477-5956-11-42
55. Soualmia F, El Amri C. Serine protease inhibitors to treat inflammation: a patent review (2011–2016). *Expert Opin Ther Pat.* (2018) 28:93–110. doi: 10.1080/13543776.2018.1406478
56. Rocha-Ramirez LM, Hernandez-Chinas U, Banos-Rojas D, Xicohtencatl-Cortes J, Chavez-Berrocal ME, Rico-Rosillo G, et al. Pet serine protease from enteroaggregative *Escherichia coli* stimulates the inflammatory response activating human macrophages. *BMC Microbiol.* (2016) 16:158. doi: 10.1186/s12866-016-0775-7
57. Chen C, Krishnan V, Macon K, Manne K, Narayana SV, Schneewind O. Secreted proteases control autolysin-mediated biofilm growth of *Staphylococcus aureus*. *J Biol Chem.* (2013) 288:29440–52. doi: 10.1074/jbc.M113.502039

58. Wretlind B, Pavlovskis OR. *Pseudomonas aeruginosa* elastase and its role in pseudomonas infections. *Rev Infect Dis.* (1983) 5(Suppl. 5):S998–1004. doi: 10.1093/clinids/5.Supplement_5.S998
59. Hase CC, Finkelstein RA. Comparison of the *Vibrio cholerae* hemagglutinin/protease and the *Pseudomonas aeruginosa* elastase. *Infect Immun.* (1990) 58:4011–5.
60. Benitez JA, Silva AJ. *Vibrio cholerae* hemagglutinin(HA)/protease: an extracellular metalloprotease with multiple pathogenic activities. *Toxicon* (2016) 115:55–62. doi: 10.1016/j.toxicon.2016.03.003
61. Domon H, Nagai K, Maekawa T, Oda M, Yonezawa D, Takeda W, et al. Neutrophil elastase subverts the immune response by cleaving Toll-like receptors and cytokines in *Pneumococcal Pneumonia*. *Front Immunol.* (2018) 9:732. doi: 10.3389/fimmu.2018.00732
62. Sokol PA, Kooi C, Hodges RS, Cachia P, Woods DE. Immunization with a *Pseudomonas aeruginosa* elastase peptide reduces severity of experimental lung infections due to *P. aeruginosa* or *Burkholderia cepacia*. *J Infect Dis.* (2000) 181:1682–92. doi: 10.1086/315470
63. Suzuki K, Shinzawa N, Ishigaki K, Nakamura K, Abe H, Fukui-Miyazaki A, et al. Protective effects of *in vivo*-expressed autotransporters against *Bordetella pertussis* infection. *Microbiol Immunol.* (2017) 61:371–9. doi: 10.1111/1348-0421.12504
64. Fusco WG, Choudhary NR, Stewart SM, Alam SM, Sempowski GD, Elkins C, et al. Defining potential vaccine targets of *Haemophilus ducreyi* trimeric autotransporter adhesin DsrA. *Monoclon Antib Immunodiagn Immunother.* (2015) 34:73–82. doi: 10.1089/mab.2014.0054
65. Hu YH, Zhou HZ, Jin QW, Zhang J. The serine protease autotransporter Tsh contributes to the virulence of *Edwardsiella tarda*. *Vet Microbiol.* (2016) 189:68–74. doi: 10.1016/j.vetmic.2016.04.021
66. Sause WE, Castillo AR, Ottemann KM. The *Helicobacter pylori* autotransporter ImaA (HP0289) modulates the immune response and contributes to host colonization. *Infect Immun.* (2012) 80:2286–96. doi: 10.1128/IAI.00312-12
67. Abdelhamed H, Ibrahim I, Nho SW, Banes MM, Wills RW, Karsi A, et al. Evaluation of three recombinant outer membrane proteins, OmpA1, Tdr, and TbpA, as potential vaccine antigens against virulent *Aeromonas hydrophila* infection in channel catfish (*Ictalurus punctatus*). *Fish Shellfish Immunol.* (2017) 66:480–6. doi: 10.1016/j.fsi.2017.05.043
68. Yadav SK, Meena JK, Sharma M, Dixit A. Recombinant outer membrane protein C of *Aeromonas hydrophila* elicits mixed immune response and generates agglutinating antibodies. *Immunol Res.* (2016) 64:1087–99. doi: 10.1007/s12026-016-8807-9
69. Yadav SK, Dash P, Sahoo PK, Garg LC, Dixit A. Modulation of immune response and protective efficacy of recombinant outer-membrane protein F (rOmpF) of *Aeromonas hydrophila* in *Labeo rohita*. *Fish Shellfish Immunol.* (2018) 80:563–72. doi: 10.1016/j.fsi.2018.06.041
70. Dash P, Sahoo PK, Gupta PK, Garg LC, Dixit A. Immune responses and protective efficacy of recombinant outer membrane protein R (rOmpR)-based vaccine of *Aeromonas hydrophila* with a modified adjuvant formulation in rohu (*Labeo rohita*). *Fish Shellfish Immunol.* (2014) 39:512–23. doi: 10.1016/j.fsi.2014.06.007
71. Gudding R, Van Muiswinkel WB. A history of fish vaccination: science-based disease prevention in aquaculture. *Fish Shellfish Immunol.* (2013) 35:1683–8. doi: 10.1016/j.fsi.2013.09.031

Conflict of Interest Statement: The authors declare that the research was conducted in the absence of any commercial or financial relationships that could be construed as a potential conflict of interest.

Copyright © 2019 Wang, Wang, Ali, Li, Fu, Yang, Lin and Lin. This is an open-access article distributed under the terms of the Creative Commons Attribution License (CC BY). The use, distribution or reproduction in other forums is permitted, provided the original author(s) and the copyright owner(s) are credited and that the original publication in this journal is cited, in accordance with accepted academic practice. No use, distribution or reproduction is permitted which does not comply with these terms.

frontiers in Immunology

ORIGINAL RESEARCH
published: 06 March 2019
doi: 10.3389/fimmu.2019.00392

Assessment of the Live Attenuated and Wild-Type *Edwardsiella ictaluri*-Induced Immune Gene Expression and Langerhans-Like Cell Profiles in the Immune-Related Organs of Catfish

*Adef O. Kordon[1], Hossam Abdelhamed[1], Hamada Ahmed[1,2], Wes Baumgartner[3], Attila Karsi[1] and Lesya M. Pinchuk[1]**

[1] Department of Basic Sciences, College of Veterinary Medicine, Mississippi State University, Mississippi State, MS, United States, [2] Department of Nutrition and Veterinary Clinical Nutrition, Faculty of Veterinary Medicine, Damanhour University, Damanhour, Egypt, [3] Department of Pathobiology and Population Medicine, College of Veterinary Medicine, Mississippi State University, Mississippi State, MS, United States

OPEN ACCESS

Edited by:
Roy Ambli Dalmo,
UiT The Arctic University of Norway, Norway

Reviewed by:
Eva-Stina Isabella Edholm,
UiT The Arctic University of Norway, Norway
Satoshi Tasumi,
Kagoshima University, Japan

***Correspondence:**
Lesya M. Pinchuk
pinchuk@cvm.msstate.edu

Specialty section:
This article was submitted to Comparative Immunology, a section of the journal Frontiers in Immunology

Received: 26 October 2018
Accepted: 14 February 2019
Published: 06 March 2019

Citation:
Kordon AO, Abdelhamed H, Ahmed H, Baumgartner W, Karsi A and Pinchuk LM (2019) Assessment of the Live Attenuated and Wild-Type Edwardsiella ictaluri-Induced Immune Gene Expression and Langerhans-Like Cell Profiles in the Immune-Related Organs of Catfish. Front. Immunol. 10:392. doi: 10.3389/fimmu.2019.00392

Edwardsiella ictaluri is a Gram-negative intracellular pathogen that causes enteric septicemia of catfish (ESC). Successful vaccination against intracellular pathogens requires T cell priming by antigen presenting cells (APCs) that bridge innate and adaptive immunity. However, the evidence on immunological mechanisms that underscore *E. ictaluri* pathogenesis and the protective role of live attenuated vaccines (LAVs) is scarce. We assessed the expression of immune genes related to antigen presentation by real-time PCR and the distribution patterns of Langerhans-like (L/CD207$^+$) cells by immunohistochemistry in the immune-related tissues of channel catfish challenged with two novel *E. ictaluri* LAVs, *Ei*Δ*evpB,* and ESC-NDKL1 and wild type (WT) strain. Our results indicated significantly elevated expression of IFN-γ gene in the anterior kidney (AK) and spleen of vaccinated catfish at the early stages of exposure, which correlated with increased numbers of L/CD207$^+$ cells. In general, the ESC-NDKL1-induced IFN-γ gene expression patterns in the AK resembled that of the patterns induced by *Ei*Δ*evpB*. However the MHCII gene expression patterns differed between the strains with significant increases at 6 h post-challenge (pc) with the *Ei*Δ*evpB* and at 7 d pc with the ESC-NDKL1 strains, respectively. Significant increases in activity of T helper type polarization genes such as IFN-γ and T cell co-receptors after exposure to ESC-NDKL1, in combination with elevated numbers of L/CD207$^+$ cells at 7 d pc with both LAVs compared to uninfected and the WT-exposed counterparts, were documented in the spleen. The dominant pro-inflammatory environment with dramatically overexpressed inflammatory genes in the AK and 7 d pc in the spleen in response to *E. ictaluri* was found in exposed catfish. In general, the pro-inflammatory gene expression profiles in the ESC-NDKL1 pc showed more similarities to the WT strain-induced gene profiles compared to the *Ei*Δ*evpB* counterpart. In addition, *E. ictaluri* WT significantly decreased the numbers of

Langerhans-like L/CD207$^+$ cells in the AK and spleen at 3 and 7 days pc. In conclusion, we report the differential framework of initiation of innate and adaptive immune responses between *E. ictaluri* strains with both LAVs having a potential of satisfying the stringent requirements for successful vaccines.

Keywords: Langerhans cells, channel catfish, *Edwardsiella ictaluri,* live attenuated vaccines, cytokines/chemokines, antigen presentation

INTRODUCTION

Edwardsiella ictaluri (*E. ictaluri*) is a Gram-negative facultative intracellular pathogen that causes enteric septicemia of channel catfish (ESC), one of the most devastating diseases in the US catfish industry (1–4). A live *E. ictaluri* vaccine (Aquavac-ESC) against ESC was developed by Klesius and Shoemaker, and this vaccine can provide efficient protection to juvenile catfish (5). Then, immersion studies demonstrated that Aquavac-ESC stimulated the protective immunity in catfish fry, fingerlings, and eyed catfish eggs (6–9). Recently, avirulent *E. ictaluri* isolate (S97-773) was developed by Wise et al. and oral vaccination with this live attenuated isolate protected fingerlings from *E. ictaluri* infection (10). *Edwardsiella ictaluri* can survive and replicate in channel catfish macrophages, and *E. ictaluri* live attenuated vaccines (LAVs) induced cell-mediated immunity to protect catfish against ESC (11–13). Also, catfish vaccinated with LAVs triggered humoral immune responses which augmented the bacterial killing activity of macrophages (12, 14).

Our research group has developed two novel *E. ictaluri* LAV strains (*Ei*Δ*evpB* and ESC-NDKL1), which provided significant protection against ESC in both catfish fry and fingerlings (15, 16). *Ei*Δ*evpB* was constructed by in-frame deletion of the *evpB* gene, one of the main components of type six secretion system (T6SS) (15). ESC-NDKL1 (Δ*gcvP*Δ*sdhC*Δ*frdA*) was constructed by in-frame deletion of three genes in the tricarboxylic acid cycle (*sdhC* and *frdA*) and one-carbon metabolism (*gcvP*) (16). Although we know the genetic differences among the strains, their phenotypes have not been characterized. Laboratory and field challenge study demonstrated that *Ei*Δ*evpB* and ESC-NDKL1 are safe in catfish fingerlings and provide significant protection from disease. In 7–14 days old fry, *Ei*Δ*evpB* was found to be completely attenuated while ESC-NDKL1 showed 3–4% mortality (16). Recently, we demonstrated the phagocytic and killing properties of catfish peritoneal macrophages that are induced by LAVs. However, the intensity of *Ei*Δ*evpB* phagocytic uptake was significantly higher compared to the ESC-NDKL1 uptake in catfish peritoneal macrophages (14).

Fish anterior kidney (AK) possesses hemopoietic tissue responsible for production of all blood elements (17–20). Several studies demonstrated that the AK is the target organ at the early time of *E. ictaluri* infection. Leukocytes containing *E. ictaluri* were detected in the AK of channel catfish at 48 h post-challenge (pc), and *E. ictaluri* was detected in the posterior kidney at 15 min pc (21). In addition, the dispersion of bioluminescent *E. ictaluri* was observed in the AK of catfish fingerlings at 15 min after intraperitoneal injection (22).

The spleen in mammals is one of the secondary lymphoid organs in which antigen presentation occurs, and adaptive immune responses are activated (23). Similar to mammals, the spleen serves as a secondary lymphoid tissue in teleost fish (24). In the immersion-exposed channel catfish, bioluminescent *E. ictaluri* was detected in the abdominal area at 60–72 h pc (22). It was demonstrated that as *E. ictaluri* loads increased, disease and mortalities progressed more rapidly. For instance, at high doses (2.5×10^7-2.5×10^8 CFU) fish died in about 2 days, but at low doses (2.5×10^2-2.5×10^3 CFU) fish died in about 6 days. Dissection of catfish organs revealed that the AK and spleen had high *E. ictaluri* load, while *E. ictaluri* presence was also detected in the gills (22). In the tissue persistence study, both mutant and WT *E. ictaluri* strains demonstrated similar trends over time. However, the overall mean CFU per gram of AK of *E. ictaluri* WT from all time points was significantly higher than that of the mutant strain. Similar results have been obtained in the tissue persistence study with *Ei*Δ*evpB* and ESC-NDKL1 in catfish fry (unpublished observation).

Dendritic cells (DCs) are the most potent antigen-presenting cells (APCs) and are critical players in bridging and shaping all innate and adaptive immune responses in vertebrates (25). Recently, DCs have been characterized in several teleost fish based on their morphology and function. For example, DC-like cells with mammalian DC morphology and T-cell stimulatory capability have been described in zebrafish (26, 27). DCs have also been identified in rainbow trout, barramundi, and medaka based on their morphology, motility, phagocytic ability, and T-cell activation properties (28–30). A previous study reported the presence of the major co-stimulatory molecules (e.g., CD80/CD86, and CD83) in zebrafish (31). Furthermore, similarly to mammals, a recent study showed that the surface molecules of zebrafish DCs (CD80/86/83/CD209$^+$) could promote CD4$^+$ naïve T-cell stimulation (32). Dendritic cells in mammals have multiple subsets, and Langerhans cells (LCs) are the distinct subset of DCs. Langerhans cells are present in the epidermis, and this unique location provides LCs with early recognition of pathogens, foreign chemicals, and self-antigens (33). Langerhans cells can engulf antigens and migrate to the secondary lymphoid tissues to present the antigen to naïve T-cells, thus initiating adaptive immune responses (34). Langerhans cells are uniquely characterized by Birbeck granules, which are rod-shaped organelles consisting of a superimposed and zippered membrane (35). Langerin is a type II transmembrane C-type lectin, which is a specific marker for LCs and associated with the formation of Birbeck granules (36, 37). The antigen capture function of Langerin triggers the induction of Birbeck

granules by allowing routing antigens into Birbeck granules, thus providing non-classical antigen processing pathway and cross-presentation (37, 38). Several studies have identified cells with mammalian LC morphology in teleost fish. In particular, Langerin/CD207$^+$ (L/CD207$^+$) cells have been described in the AK and spleen of Atlantic salmon and rainbow trout. Also, the same research group has observed DC-like cells containing Birbeck -like granules in the gills of Chinook salmon during *Loma salmonae* infection (39). Recently, our group identified L/CD207$^+$ cells in the channel catfish AK, spleen, and gills by immunohistochemistry (IHC), and described cells that resembled mammalian LC DCs containing Birbeck-like granules in the spleen, anterior and posterior kidneys, and gills of channel catfish by transmission electron microscopy (40).

It was demonstrated that the transcriptional regulator of the Zinc finger family DC-SCRIPT is expressed in all subsets of DCs in humans and mice (41, 42). Due to the lack of DC-specific markers in fish, DC-SCRIPT was considered as one of the markers for the barramundi fish DCs (30). A recent study showed that DC-SCRIPT in combination with MHCII expression was significantly upregulated in the AK of barramundi at both, 6 h and 1 d post-injection with peptidoglycan (PTG) and lipopolysaccharide (LPS), but relative expression of DC-SCRIPT was low at 3 d and 7 d (30). Also, another study reported that TLR ligands, such as LPS and Pam3CSK4, activated hematopoietic progenitor cells and induced their differentiation into myeloid cells, such as macrophages and DCs, in the bone marrow and spleen of mammals (43).

The effects of efficacious *E. ictaluri* LAVs on innate and adaptive immune responses, and, specifically, on innate antigen presentation are still unexplored. Therefore, we aimed to evaluate the immune gene and L/CD207$^+$ LC-like cells distribution patterns in the AK, spleen, and gills of catfish challenged with two LAV and WT strains of *E. ictaluri.*

MATERIALS AND METHODS

Bacterial Strains

Wild-type (WT) *E. ictaluri* strain 93–146, *Ei*Δ*evpB*, and ESC-NDKL1 were cultured in brain heart infusion (BHI) agar or broth (Difco, Sparks, MD) at 30°C. When required, media were supplemented with colistin (Col: 12.5 mg/ml, Sigma-Aldrich, Saint Louis, MN).

Catfish Vaccination and Tissue Collection

Two hundred specific-pathogen-free (SPF) channel catfish fingerlings (6-month old) were obtained from the College of Veterinary Medicine's fish hatchery at Mississippi State University, and all fish experiments were conducted according to the protocol approved by the Institutional Animal Care and Use Committee. Catfish were stocked into four 40-L tanks (25 fingerlings per tank) supplied with flow-through water and continuous aeration. Catfish were maintained at 25–28°C and fed twice daily with a floating catfish feed. After a week of acclimation, catfish were exposed to vaccine strains *Ei*Δ*evpB* and ESC-NDKL1, *E. ictaluri* WT (positive control), and BHI (sham-control) as previously described (44). Exposure dose was approximately 3.67×10^7 CFU/ml of water, which was calculated by serial dilutions of bacterial cultures. At 6 h, 1, 3, and 7 pc, five catfish from each group were euthanatized by 300 mg/L tricaine methanesulfonate (Sigma, St. Louis, MO) and placed in 10% neutral buffered formalin for 48 h (formalin was replaced after 24 h with a fresh batch). For immunohistochemistry (IHC) analysis, anterior kidney (AK), spleen, and gill tissues were isolated, dehydrated with a graded series of ethanol, and embedded in paraffin wax. Finally, tissue sections were cut as described previously (45). For gene expression analysis, six more fish were euthanatized from each group at 6 h, 1, 3, 7, 14, and 21 d, and spleen and AK were collected and placed immediately into RNase-free tubes (ThermoFisher Scientific) that contained 10 volumes of RNA*later* (Ambion, Austin, TX).

Immunohistochemistry (IHC)

To evaluate the numbers of L/CD207$^+$ cells during *E. ictaluri* infection, immunohistochemical staining of catfish AK, spleen, and gill tissue was performed with polyclonal antibodies (pAbs) specific to human CD207 (R&D Systems, Inc.) as described previously (40). Briefly, for antigen retrieval, tissue sections were incubated in target retrieval solution (DAKO) for 40 min at 100°C. Then, tissue sections were allowed to cool at room temperature and were washed in 1X phosphate-buffered saline (PBS) for 10 min. Following washing, tissue sections were incubated in protein block (DAKO) for 1 h. After that, they were incubated with primary antibodies (0.2 mg/ml, 1:500 dilution). Normal goat IgG were used as negative controls at the same concentrations as primary antibodies. Primary and control antibodies were incubated in a humid chamber overnight, followed by the addition of streptavidin/biotin for 15 min and incubation with secondary antibodies (1:200 dilution, Biotinylated Anti-Goat IgG (H+L), Vector Laboratories) for 1 h. Following secondary antibody incubation, samples were incubated in Streptavidin-HRP (Vector Laboratories) for 1 h. Tissue sections were stained in a solution of 3,3′-diaminobenzidine tetrahydrochloride (DAB) for 10 min, and then washed twice with water for 10 min and dehydrated through a graded series of ethanol to xylene. Slides were analyzed at 40x magnification with an Olympus BX60 microscope (Olympus U-TV1 X) and photographed with Infinity analyze software (Lumenera corporation). The number of L/CD207$^+$ cells in the AK, spleen, and gills of five catfish from each group was determined per each time point by using a "numbered indexed square grid" eyepiece graticule (1.00 mm^2 IN DEX SQU, PYSER-SGILTD) (46). The L/CD207$^+$ cell numbers were counted in 10 mm^2 per field, and a total of 10 fields and 100 mm^2 were counted for each organ. The mean value of L/CD207$^+$ cells was calculated for further statistical analysis. The presence of the LC-like cells in the lymphoid organs and gills of catfish at different time points of pc is shown in **Figure 1** and **Supplementary Figures 1–3**. In the following chapters, we provide detailed quantitative assessment of the numbers of L/CD207$^+$ cells at 6 h, 1, 3, and 7 d post challenge that correlated with the kinetics of initiation of innate and adaptive immune responses in the immune-competent organs of catfish fingerlings.

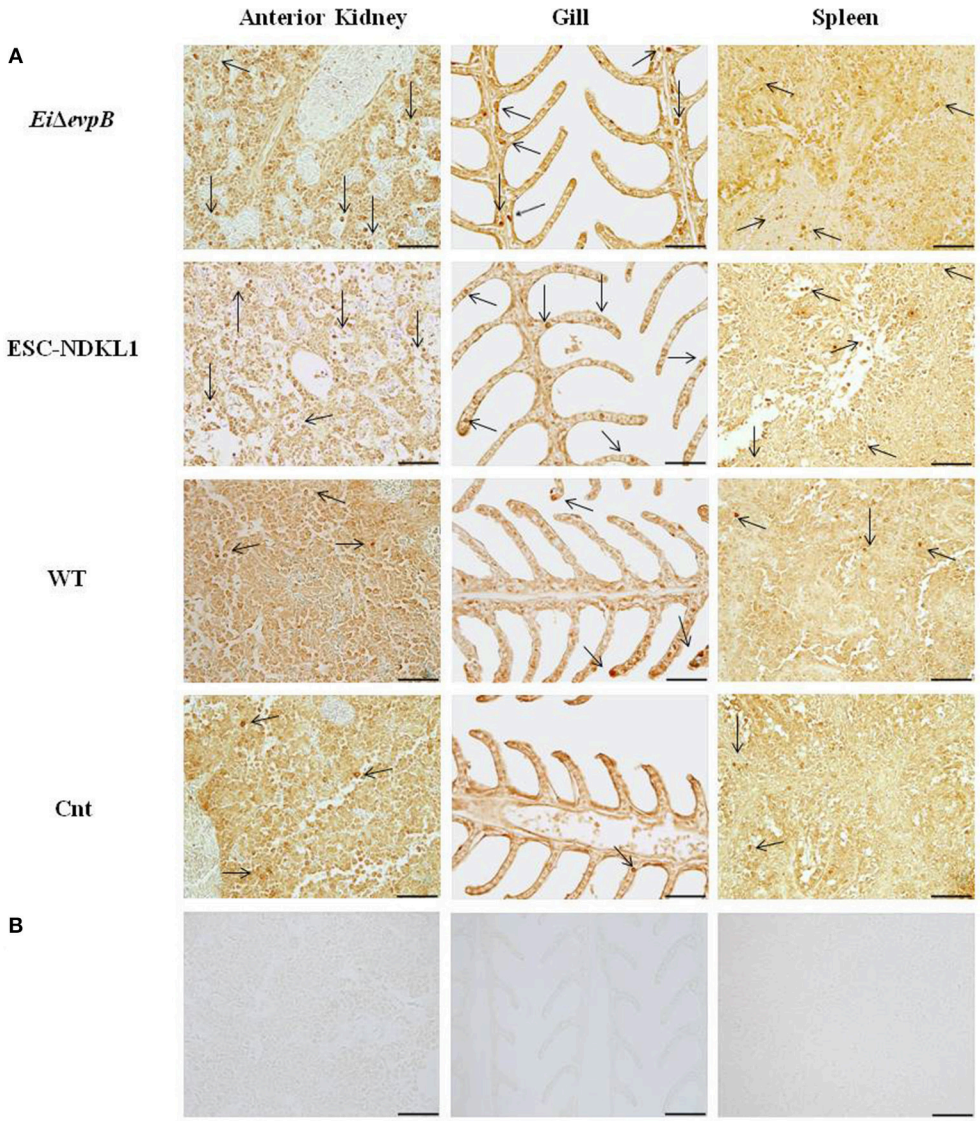


FIGURE 1 | Identification of L/CD207$^+$ cells by IHC in the lymphoid organs (AK, spleen) and gills of channel catfish challenged with *E. ictaluri* LAV and WT strains. The left column shows the L/CD207$^+$ specific **(A)** and background staining **(B)** in AK of catfish in all groups at 3 d pc. Middle column indicates the L/CD207$^+$ specific **(A)** and background staining **(B)** in the gill at 3 d pc. The right column shows the L/CD207$^+$ specific **(A)** and background **(B)** staining in the spleen at 7 d pc. The arrows indicate L/CD207$^+$ cells in the immune-related organs. Photomicrographs (400 x magnification, scale bar 50 mm).

RNA Extraction and cDNA Synthesis

To isolate total RNA from the tissues, the FastRNA^{TM} SPIN Kit for Microbes and the FastPrep-24^{TM}Instrument (MP Biomedicals, Santa Ana, CA) were used according to the manufacturer's instructions. DNase treatment with RNase-Free DNase Set (QIAGEN, Hilden, Germany) was used to eliminate any catfish gDNA contamination. The quantity and quality of total RNA were checked by using a NanoDrop ND-1000 spectrophotometer (Thermo Scientific, USA) and agarose gel.

We used Maxima First Strand cDNA Synthesis Kit for RT-qPCR (Thermo Scientific, USA) to convert total RNAs into cDNA according to the manufacturer's instructions. The cDNA was synthesized in a 20 μl reaction containing 2.5 ng of total RNA, 4 μl of 5X reaction mix, 2 μl of maximum enzyme mix, and nuclease-free water. The reactions were incubated at 25°C for 10 min, then at 50°C for 15–30 min and at 85°C for 5 min. After that, reactions were stored at −80°C.

Quantitative Real-Time PCR and Data Analysis

Immune genes and primers used in this study are listed in **Table 1**. Primers were designed by Primer 3 software (http://bioinfo.ut.ee/primer3-0.4.0/), and the 3′ end of one primer was placed on intron/exon junction to eliminate any potential non-cDNA amplifications. Primers were synthesized commercially (MWG Eurofins Genomics), and real-time PCR was run using FastStart Universal SYBR Green Master Kit (ROX; Roche, Basal,

TABLE 1 | Gene names, GenBank accession numbers, and primers used in this study.

Genes	Accession nos.	Primers	References
18S ribosomal RNA	AF021880	F-GAGAAACGGCTACCACATCC R-GATACGCTCATTCCGATTACAG	(47)
CD4-1	DQ435305	F-GATGTCATCATTGTAGATCTCG R-GAGGTAGCTGGCATTTCACTCC	This study
CD4-2	DQ435304	F-CTGTATGTTGTATCAGCCTCTG R-CAGTCACCTCCTTACTTTGGCTA	This study
CD8-α	HQ446239	F-CTACGCGGAGAGACAGTCCCAA R-CTCACAACCCAAAAGCACATC	This study
CD8-β	HQ446240	F-CCATCAGGCCTGGAGAAAGCA R-TCACCACCAGGAGTAGGACA	This study
IL-1β	DQ157743	F-TGATCCTTTGGCCATGAGCGGC R-AGACATTGAAAAGCTCCTGGTC	This study
IL-8	AY145142	F-CAATACTTTGTGAATTTCTGC R-TGTCCTTGGTTTCCTTCTGG	This study
INFγ	NC_030434	F-TTGGGCAAAGTAGAGGACACC R-TGTTTCCACACTGCCTGTTCG	This study
MHC class II	AF103002	F-GACACCAGGACATGGGAGGTG R-CGAGGAAGAAAGTTCCGGTAG	This study
TNFα	AJ417565	F-GCACAACAAACCAGACGAGA R-TCGTTGTCCTCCAGTTTCAA	This study

Switzerland). Each qPCR reaction was 20 μl and included 10 μl FastStart Universal SYBR Green Master (ROX), 0.6 μl primers, 6.8 μl nuclease-free water, and 2 μl of cDNA. The 7,500 Real-Time PCR System (Applied Biosystems) was used to perform qPCR reactions for this study. Thermal cycler was programmed with 45 cycles of 95°C for 10 s, 95°C for 15 s, 57°C for 30 s, and 72°C for 15 s. Each sample was run triplicate.

For normalization, the cycle threshold (Ct) of the 18 rRNA gene was subtracted from the Ct value of the gene of interest as described in the formula: ΔCt = Ct (target gene)—Ct (reference gene) (47). Then, the ΔCt value of the control was subtracted from the ΔCt value of the treatments to calculate the ΔΔCt value for each target as described in a formula: ΔΔCt target = ΔCt target treated—ΔCt target control. Fold changes were calculated for each gene using $2^{-\Delta\Delta Ct}$, and used for statistical analysis to determine significant differences between treatments *Ei*Δ*evpB*, ESC-NDKL1, and *E. ictaluri* WT.

Statistical Analyses

One-way and two-way ANOVA procedures of SAS (v 9.4, SAS Institute, Inc., Cary, NC) were used to evaluate differences in means of L/CD207$^+$ cells. The level of significance for all tests was set at $P < 0.05$.

RESULTS

Assessment of Immune Gene Expression and L/CD207$^+$ Cell Numbers in the AK of Catfish Challenged With *E. ictaluri* LAVs and WT

A significant increase in the IFN-γ gene expression was evident at 6 h, followed by a gradual decline at 7 d pc with both LAVs and the WT strain (**Figure 2A**). However, the IFN-γ gene expression was significantly upregulated at 7 d pc with WT only (**Figure 2A**). The MHC class II gene expression patterns differed between the strains with significant increases at 6 h pc with *Ei*Δ*evpB* and WT strains, followed by rapid declines at 1 and 3 d, then partial recovery after 7 d post-exposure to the ESC-NDKL1 strain (**Figure 2B**). In contrast, steady declines in the MHC class II gene expression were evident until a significant increase at 7 d post-exposure to the WT strain compared to the LAV-treated counterparts (**Figure 2B**). Importantly, ESC-NDKL1 induced significantly higher MHC class II gene expression levels compared to its LAV counterpart at 7 d pc (**Figure 2B**). In general, the T cell co-receptors gene expression patterns in the AK of LAVs and WT-challenged fish resembled the patterns for the MHC class II gene expression (**Figures 2C–F**). Pro-inflammatory chemokine and cytokine IL-8, IL-1β, and TNF-α genes were upregulated significantly in the AK at 6 h pc with *Ei*Δ*evpB* showing significant increases in IL-8 and IL-1β gene expression at 1 d pc compared to the control groups (**Figures 2G–I**). In contrast, IL-8 and IL-1β genes were upregulated significantly in the catfish AK at 1 d pc with ESC-NDKL1 only (**Figures 2G–I**). Changes in the cytokine/chemokine and lymphocyte-specific gene expression induced by WT *E. ictaluri* were evident at 6 h post-exposure, resulting in significant upregulation of most of the genes evaluated in the AK of catfish that survived infection (**Figures 2A–I**). However, genes that increased their expression the most were the Th1 type cytokine gene IFN-γ and pro-inflammatory cytokine/chemokine genes IL-1β, IL8, and TNF-α (**Figures 2A,G–I**).

The numbers of the L/CD207$^+$ cells in the AK of catfish challenged with two LAV and WT strains significantly increased at 6 h pc compared to control catfish (**Figure 3**). Interestingly, the L/CD207$^+$ cell numbers were significantly higher in the AK of

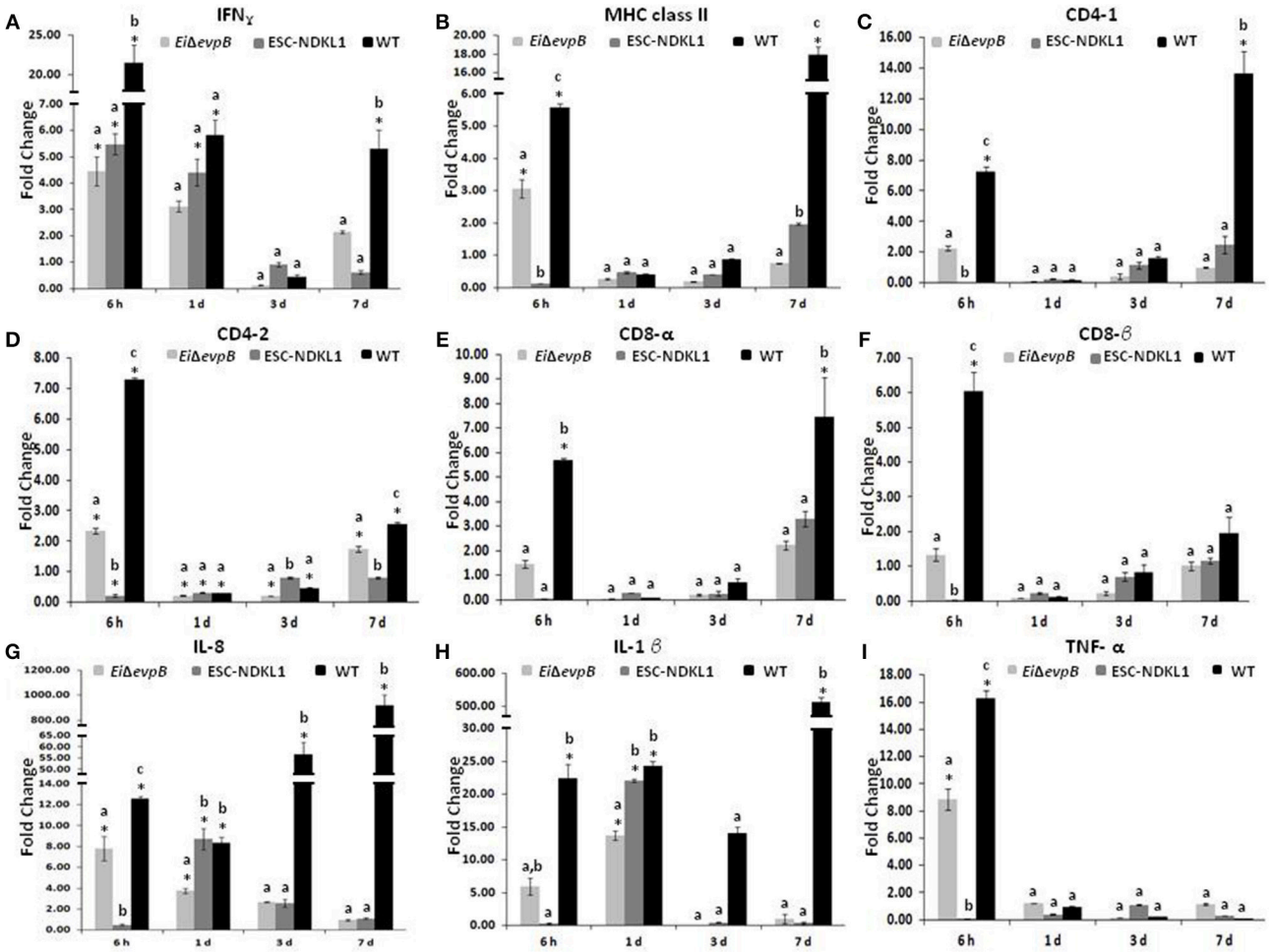


FIGURE 2 | Changes in the expression of IFN-γ **(A)**, MHC class II **(B)**, CD4-1 **(C)**, CD4-2 **(D)**, CD8-α **(E)**, CD8-β **(F)**, IL-8 **(G)**, IL-1β **(H)**, and TNF-α **(I)** genes in the anterior kidney of catfish challenged with *E. ictaluri* LAV and WT strains. Data are presented as fold difference of gene expression compared with values obtained for control uninfected cells. Samples were analyzed in triplicates from a pull of AK of six fish and presented as mean ± SD. $P < 0.05$. *Indicates significant differences compared to uninfected control ($p < 0.05$). ^{abc} Indicates differences within each time point ($P < 0.05$).

catfish challenged with the LAVs compared to their counterparts challenged with the WT strain at this time point. However, there was no significant difference in the numbers of L/CD207$^+$ cells between the LAVs (**Figure 3**).

Similar to 6 h pc, the numbers of L/CD207$^+$ cells in the AK of the WT- challenged catfish were significantly higher compared to non-treated controls at 1 d pc (**Figure 3**). Furthermore, the numbers of L/CD207$^+$ cells were significantly higher in the AK of catfish challenged with ESC-NDKL1 compared to the AK of catfish challenged with the WT strain. However, there was no significant difference between the two LAV strains (**Figure 3**). Interestingly, the numbers of L/CD207$^+$ cells at 3 d challenge were significantly decreased in the AK of catfish challenged with the WT strain and did not differ from the uninfected control group (**Figure 3**). In contrast, the numbers of L/CD207$^+$ cells in the AK declined compared to the 1 d challenge but were still significantly elevated in the groups challenged with both LAVs compared to their WT-treated and control counterparts (**Figure 3**). After 7 d post challenge, the groups exposed to LAVs showed significant decreases in the numbers of L/CD207$^+$ cells compared to 3 d numbers, which did not differ in the controls (**Figure 3**). Overall, we documented significant declines in the numbers of LC-like cells in the AK of catfish at 3 and 7 d pc with both LAVs following similar patterns (**Figure 3**).

Assessment of Immune Gene Expression and L/CD207$^+$ Cell Numbers in the Spleen of Catfish Challenged With *E. ictaluri* LAVs and WT

Significant increases in the IFN-γ gene expression in the spleen were documented at 6 h pc with ESC-NDKL1 LAV (**Figure 4A**). Furthermore, significant increases in IFN-γ gene expression in the spleen were evident at 1 d and 7 d pc with *EiΔevpB* and the WT strain, and with the ESC-NDKL1 strain, respectively, compared to uninfected controls (**Figure 4A**).

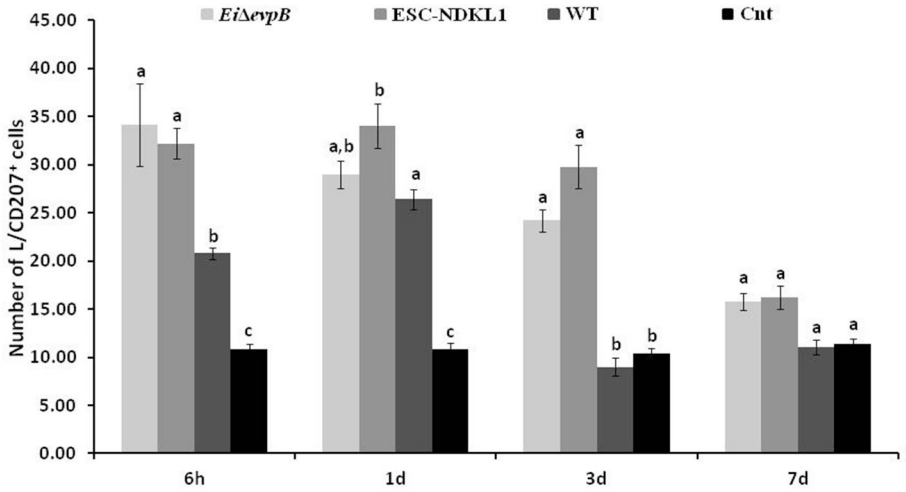


FIGURE 3 | The kinetics of L/CD207$^+$ cells numbers in the anterior kidney of catfish challenged with *E. ictaluri* LAV and WT strains. The (a, b, c) letters on top of bars indicate statistical group differences in L/CD207$^+$ cell numbers at each time point ($P < 0.05$). The data represent the mean of cell numbers from five AKs ± SD.

Significant increases in MHC class II gene expression at 7 d were evident in the spleen after exposure to the WT strain compared to the LAVs-exposed spleen and uninfected controls (**Figure 4B**). No significant changes were documented in CD4-1 gene expression following the LAVs challenge in the spleen. However, *E. ictaluri* WT induced strong upregulation of the CD4-1 T cell co-receptor gene (**Figure 4C**). The CD4-2 co-receptor gene was upregulated at 3 d with the WT strain only and at 7 d pc with both ESC-NDKL1 and the WT strain (**Figure 4D**). CD8-α gene expression levels were significantly increased in the spleen at 7 d pc with *E. ictaluri* WT (**Figure 4E**). However, the CD8-β gene expression patterns resembled the expression of the CD4-1 gene in both LAVs and WT treatments, with significant increases at 7 d ESC-NDKL1 and WT pcs (**Figure 4F**). Pro-inflammatory cytokine/chemokine IL-8 gene was significantly upregulated at 7 d pc with WT compared to the LAV-treated and untreated controls (**Figure 4G**). The TNF-α gene expression was significantly increased at 6 h pc with *Ei*Δ*evpB* and at 7 d pc with ESC-NDKL1, respectively (**Figure 4I**). No changes were found in the expression levels of IL-1β in the LAVs-challenged spleens compared to their untreated counterparts (**Figure 4H**). We documented significant changes in the pro-inflammatory cytokine/chemokine gene expression induced by WT *E. ictaluri* in the spleen of catfish at 3 and 7 d pc. Day 3 pc was characterized by significant increases in the TNF-α gene compared to the control and the LAVs-treated groups (**Figure 4I**). By day 7 of WT strain post-treatment, the gene expression pattern showed predominantly increased pro-inflammatory mediators IL-8 and IL-1β genes (**Figures 4G,H**).

We evaluated the L/CD207$^+$ cell numbers in the spleen of catfish challenged with *E. ictaluri* LAV and WT strains (**Figure 5**). The L/CD207$^+$ cell numbers in the spleen at 6 h showed significant treatment-related differences but were comparable to the LC-like cell numbers at 1 d pc (**Figure 5**). Namely, L/CD207$^+$ cell numbers significantly increased in the spleen of catfish challenged with two LAVs and WT strains compared to non-vaccinated catfish, whereas there was no significant difference between *Ei*Δ*evpB* and ESC-NDKL1 strains (**Figure 5**).

As expected, the numbers of L/CD207$^+$ cells in the spleen dramatically decreased in all groups at 3 d pc with no significant differences between treated and control fish (**Figure 5**). However, both LAV strains followed a similar pattern in the L/CD207$^+$ cell numbers, which was different from the WT-treated and control groups showing a significant increase in the L/CD207$^+$ cell numbers at 7 d pc (**Figure 5**). Overall, we showed that the kinetics of the L/CD207$^+$ cell numbers in the *Ei*Δ*evpB*-treated groups were similar to the kinetics of their ESC-NDKL1-treated counterparts. Furthermore, significant drops in the LC-like numbers occurred at 3 d pc in LAV and WT strain-challenged spleen followed by dramatic increases in LAVs-treated groups at 7 d post-exposure.

Assessment of L/CD207$^+$ Cell Numbers in the Gills of Catfish Challenged With *E. ictaluri* LAVs and WT

In this study, we evaluated L/CD207$^+$ cell numbers in the gills of catfish challenged with *E. ictaluri* LAVs and the WT strain at different time points (**Figure 6**). After 6 h pc infection, L/CD207$^+$ cell numbers significantly increased in the gills of catfish vaccinated with both the LAV and WT strains compared to non-vaccinated fish, and there was no significant difference in L/CD207$^+$ cell numbers between LAVs and WT strains (**Figure 6**). The numbers of L/CD207$^+$ cells in the gills of all treatment groups continued to increase at 1 d of pc, and there was a significant difference between *Ei*Δ*evpB* and ESC-NDKL1 strains but not compared to the WT strain (**Figure 6**). No significant shifts were documented in L/CD207$^+$ cell numbers in the gills of catfish vaccinated with both LAVs at 3 d pc. However, L/CD207$^+$ cell numbers dramatically decreased in the gills of fish

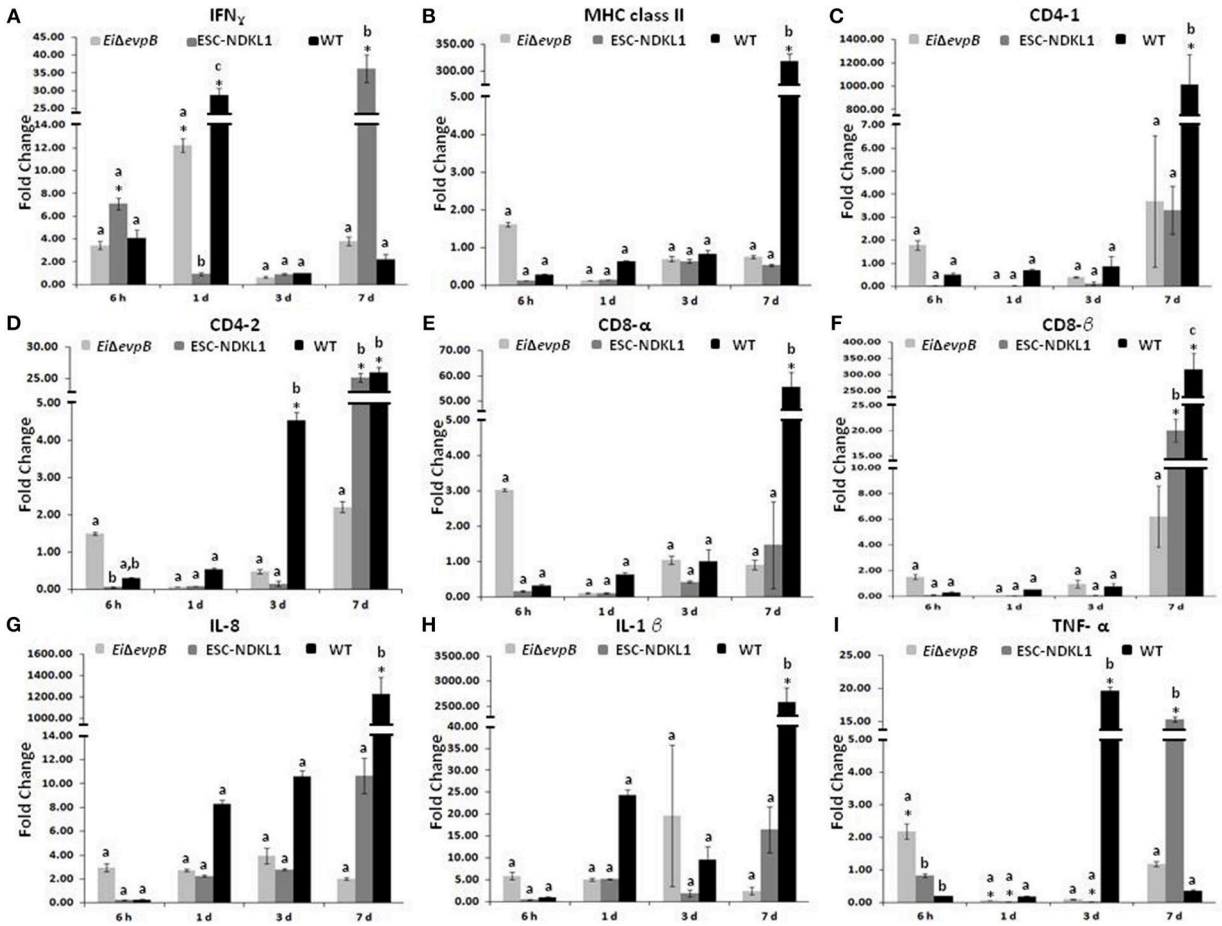


FIGURE 4 | Changes in the expression of IFN-γ **(A)**, MHC class II **(B)**, CD4-1 **(C)**, CD4-2 **(D)**, CD8-α **(E)**, CD8-β **(F)**, IL-8 **(G)**, IL-1β **(H)**, and TNF-α **(I)** genes in the spleen of catfish challenged with *E. ictaluri* LAV and WT strains. Data are presented as fold difference of gene expression compared with values obtained for control uninfected cells. Samples were analyzed in triplicates from a pull of spleen of six fish and presented as mean ± SD. *Indicates significant differences compared to uninfected control ($p < 0.05$). ^{abc} Indicates differences within each time point ($P < 0.05$).

challenged with WT but were still significantly higher than in non-challenged fish. On the other hand, after 7 d pc, L/CD207$^+$ cell numbers significantly decreased in the gills of fish vaccinated with both LAVs and were not different from non-vaccinated fish control group (**Figure 6**). The numbers of L/CD207$^+$ cells were significantly higher in catfish vaccinated with the WT strain compared to LAVs-treated and control groups (**Figure 6**). In summary, the most dramatic changes in the numbers of LC-like cells in the gills were evident as increases at 3 d pc and decreases at 7 d pc with LAVs compared to the WT strain treated and control groups, respectively (**Figure 6**).

DISCUSSION

The critical function of DCs is to bridge innate antigen recognition and adaptive immune responses. Recent studies showed that DCs in teleost fish have similar morphology and function as mammalian DCs (26, 28). Previously, our group showed the presence of DCs with remarkable similarities to human LCs in the spleen, anterior and posterior kidneys, and gills of channel catfish (40).

Due to the lack of information available on the mechanisms of immune responses to efficacious *E. ictaluri* LAVs, we assessed expression of the genes related to innate and specific antigen presentation and the genes that promote inflammation in the persistently infected immunocompetent tissues of catfish. Due to the lack of information available on the morphological and functional markers of catfish DCs, we applied the IHC approach described previously (40) to evaluate the LC-like expression patterns in the immune-related tissues of catfish challenged with two LAVs and WT *E. ictaluri* strains to underscore their immune effector mechanisms.

Our data suggest that rapid bacterial colonization in the AK of channel catfish challenged with *E. ictaluri* LAVs and WT at the early stage is combined with elevated IFN-γ gene and increased numbers of L/CD207$^+$ cells. This observation can be explained by the development of innate immune responses at the

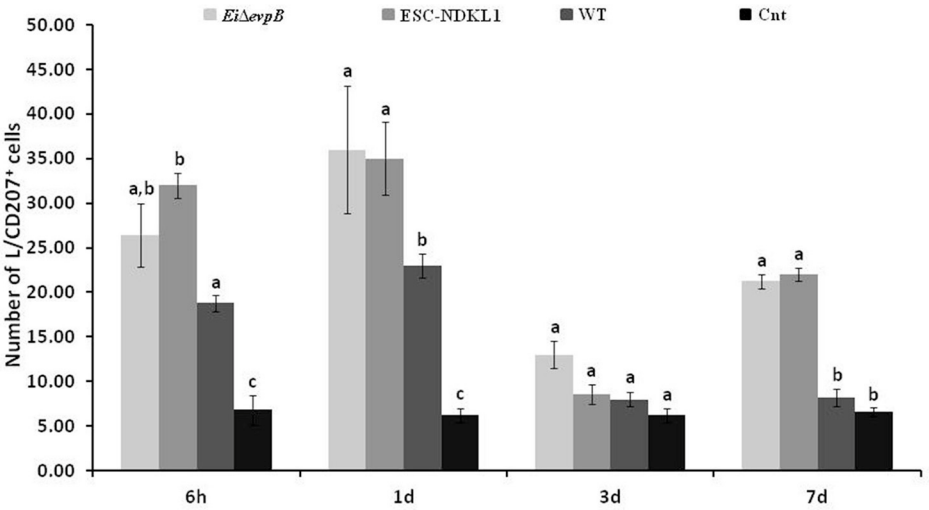


FIGURE 5 | The kinetics of L/CD207$^+$ cells numbers in the spleen of catfish challenged with *E. ictaluri* LAV and WT strains. The letters (a, b, c) show the significant differences between groups at each time point ($P < 0.05$). The data represented the mean of five fish ± SD.

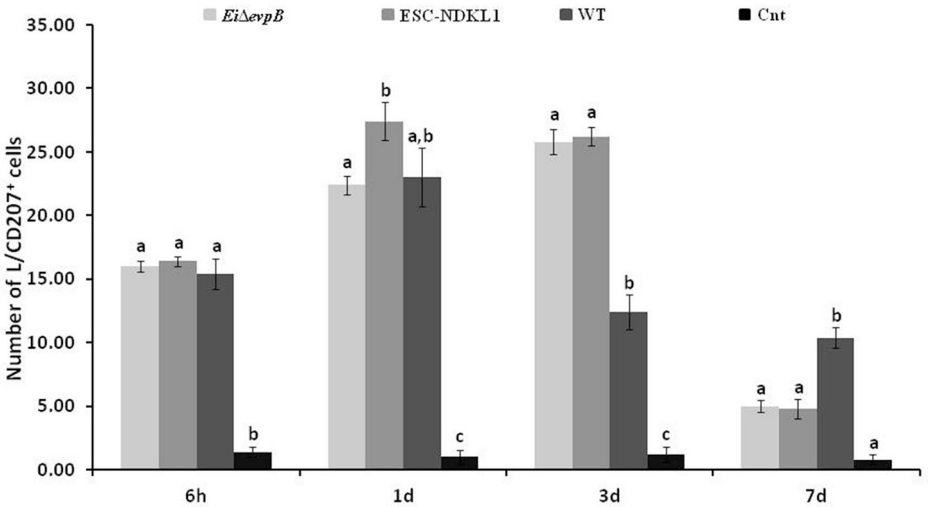


FIGURE 6 | The kinetics of L/CD207$^+$ cells numbers in the gills of catfish challenged with *E. ictaluri* LAV and WT strains. Different letters (a, b, and c) show the significant differences between groups at each time point ($P < 0.05$). The data represent the mean of cell numbers in five fish gills ± SD.

site of infection, and two LAVs were more efficient at inducing DC numbers compared to their WT counterpart. Importantly, the increased numbers of L/CD207$^+$ cells in combination with elevated IFN-γ gene expression at the early stages of exposure, followed by significant decreases in the DC-like cell numbers and relatively low expressed IFN-γ gene at 7 d post-exposure in catfish vaccinated with both LAVs, suggest the involvement of LC in the initiation of innate immune responses and their migration/maturation from the AK to the site of infection, the gills, after 3 day pc.

The ESC-NDKL1-induced IFN-γ gene expression patterns in general resembled the patterns induced by the *EiΔevpB* strain in the AK of catfish. However, differences regarding the MHC class II and T cell-related co-receptor gene expression patterns between two LAVs and the WT strain could be due to a different framework of initiation of innate and adaptive immune responses by *EiΔevpB* compared to the ESC-NDKL1 strain, in particular, earlier onset of innate immune mechanisms. Our previous reports showed vaccine strain-dependent differences in fish mortality rates, humoral immune responses, uptake, and bacterial killing properties of peritoneal macrophages (14, 16). In contrast to both LAVs, the WT strain significantly increased the immune gene expression levels of MHC class II, CD4-1, and CD8α in the AK of catfish fingerlings, which could be explained by the overall significantly higher bacterial load of *E. ictaluri* WT compared to the mutant strains, including both

LAVs (48), Ibrahim et al., unpublished observation. Although we documented increases in the activity of the genes encoding pro-inflammatory cytokines/chemokines in the AK of catfish vaccinated with both LAVs, they were not as dramatic and consistent as their counterparts in the WT *E. ictaluri*- infected fish that caused high mortality rates in fish (15, 16). In addition, our data on significant increases in the numbers of L/CD207$^+$ cells at 6 h and 1 d pc with *E. ictaluri* strains in the AK of catfish agree with and contribute to the previous report that DC-SCRIPT, a barramundi fish DC specific marker, in combination with MHCII expression, was significantly upregulated in the AK of barramundi at both 6 h and 1 d post-injection with peptidoglycan (PTG) and lipopolysaccharide (LPS), but relative expression of DC-SCRIPT was low at 3 and 7 d (30).

Importantly, significant increases in the expression of Th1 type polarization-related genes of adaptive immune responses were documented in the spleen at 7 d post-treatment with ESC-NDKL1 only. Namely, the IFN-γ gene was upregulated after exposure to the ESC-NDKL1 strain at 7 d post-exposure. Also, significant increases in the gene expression of T cell co-receptors, CD4-2 and CD8-β were evident in the spleen at 7 d post-exposure to the ESC-NDKL1 strain. Although as bacterial loads decreased (22), the dominant environment in the spleen of catfish survivors was inflammatory with dramatically overexpressed IL-1β and IL-8 mediators of inflammation at 7 d post-exposure to *E. ictaluri* WT. Interestingly, catfish fingerlings that survived the WT strain challenge 7 d pc showed significantly increased multiple adaptive immunity-related genes such as CD4 and CD8 T cell co-receptors and MHC class II, suggesting initiation of antibacterial immune responses under inflammatory conditions. Significantly elevated ESC-NDKL1-induced TNF-α gene expression levels in the spleen of catfish at 7 d pc could explain the higher mortality rates in catfish fingerlings challenged with the ESC-NDKL1 strain compared to its LAV counterpart (16).

Our data on dramatic increases in the numbers of L/CD207$^+$ cells in the spleen at 6 h pc, possibly via cytokine signaling cascades involving DCs, are due to the two LAVs being more efficient at inducing innate immune responses compared to their WT counterpart. The significant drops in the numbers of L/CD207$^+$ cells in the spleen at 3 d pc suggest possible migration of these cells from the spleen to the site of infection followed by remarkable increases in LC-like numbers in the spleens of the vaccinated catfish after 7 d of the treatment. The LAVs induced increases in the spleen but not in the AK after 7 days of challenge, suggesting the migration of LC-like cells back to the spleen to present the pathogen-derived antigen to specific T cells, thus initiating adaptive immune responses. Similarly to our findings, the study with barramundi reported that the expression of DC-SCRIPT was higher in the spleen at 6 h post-injection of LPS and PTG, but its expression level decreased in the spleen after 1 d, and DC-SCRIPT expression was again elevated at 7 d (30). The MHC class II gene expression patterns did not always correlate with the kinetics of the L/CD207$^+$ cell numbers. However, in the spleen, their significant increases were evident at 3 and 7 d compared to their counterparts at 6 h and 1 d post-treatment with both LAVs. The MHC class II molecules, unlike the DC-SCRIPT assessed in barramundi, are not limited to the pan-DC populations only but also expressed in other professional APCs, B cells and monocytes/macrophages (49–52).

Gills are one of the potential routes of entry for *E. ictaluri* into the channel catfish host (53). Our data on the significant spikes in the numbers of L/CD207$^+$ cells in the gills in all fish at 6 h, 1 and 3 d pc followed by decreases after 7 days could be interpreted as possible antigen recognition and capture by immature DCs. Our data support the previous observation that DC-like cells have been described in the gills of Chinook salmon heavily infected with *L. salmonae* (39). We expanded this earlier report by showing the kinetics of L/CD207$^+$ cells expression patterns in catfish gills at different time points of exposure to the LAVs and WT *E. ictaluri* strains. Our data suggest that L/CD207$^+$ cells in the gills may recognize and capture antigens at 6 h, 1 d, and 3 d pc, and after 7 d, L/CD207$^+$ cells in the gills of catfish vaccinated with two LAV strains have migrated to the secondary lymphoid tissue in the spleen for antigen presentation. However, the APC function of L/CD207$^+$ cells and, in particular, their migration to the spleen in the gills of catfish infected with WT strain was impaired.

In conclusion, followed by our previous observations on the vaccine strain-dependent differences in bacterial tissue persistence, fish mortality rates, humoral immune responses, uptake, and bacterial killing properties of macrophages (14, 16) here we report the differential framework of the initiation of innate and adaptive immune responses between two LAV and WT strains.

AUTHOR CONTRIBUTIONS

LP and AK conceived and designed the experiments. LP and AK provided the original idea of the study. AOK, HoA, and HaA performed the experiments. LP, AK, and WB contributed reagents, materials, tools. AOK wrote the first draft of the manuscript and was involved in all aspects of the study. All authors were involved in critical interpretation of the data, manuscript revision, and final version approval.

FUNDING

The funding for this research was provided by Agriculture and Food Research Initiative competitive grant no. 2016-67015-24909 from the USDA National Institute of Food and Agriculture.

ACKNOWLEDGMENTS

All the tissue slides have been prepared in the College of Veterinary Medicine Histology Laboratory. We acknowledge the assistance of Sinan Kordon in preparation of the IHC figures. We also thank Iman Ibrahim for her suggestion in cell counting. We acknowledge the editorial assistance of Maryana Pinchuk.

SUPPLEMENTARY MATERIAL

The Supplementary Material for this article can be found online at: https://www.frontiersin.org/articles/10.3389/fimmu.2019.00392/full#supplementary-material

REFERENCES

1. Hawke JPM, McWhorteralm AC, Steigerwalt AG, Brenner DJ. *Edwardsiella ictaluri* sp. nov., the causative agent of enteric septicemia of catfish. *Int J Syst Evol Microbiol*. (1981) 31:396–400.
2. Zhang Y, Arias CR. Identification and characterization of an intervening sequence within the 23S ribosomal RNA genes of *Edwardsiella ictaluri*. *Syst Appl Microbiol*. (2007) 30:93–101. doi: 10.1016/j.syapm.2006.04.004
3. Wagner BA, Wise DJ, Khoo LH, Terhune JS. The epidemiology of bacterial diseases in food-size channel catfish. *J Aquat Anim Health*. (2006) 18:263–72. doi: 10.1577/1548-8667(2002)014<0263:TEOBDI>2.0.CO;2
4. Miyazaki T, Plumb JA. Histopathology of *Edwardsiella ictalur*i in channel catfish, *Ictalurus punctatus* (Rafinesque). *J Fish Dis*. (1985) 8:389–92.
5. Klesius PH, Shoemaker CA. Development and use of modified live *Edwardsiella ictaluri* vaccine against enteric septicemia of catfish. *Adv. Vet. Med*. (1999) 41:523–37.
6. Shoemaker CA, Klesius PH, Bricker JM. Efficacy of a modified live *Edwardsiella ictaluri* vaccine in channel catfish as young as seven days post hatch. *Aquaculture*. (1999) 176:189–93. doi: 10.1016/S0044-8486(99)00116-7
7. Wise DJ, Klesius PH, Shoemaker CA, Wolters WR. Vaccination of mixed and full-sib families of channel catfish *Ictalurus punctatus* against enteric septicemia of catfish with a live attenuated *Edwardsiella ictaluri* Isolate (RE-33). *J World Aquacult Soc*. (2000) 31:206–12. doi: 10.1111/j.1749-7345.2000.tb00354.x
8. Shoemaker CA, Klesius PH, Evans JJ. In ovo methods for utilizing the modified live *Edwardsiella ictaluri* vaccine against enteric septicemia in channel catfish. *Aquaculture*. (2002) 203:221–7. doi: 10.1016/S0044-8486(01)00631-7
9. Shoemaker CA, Klesius PH, Evans JJ. Immunization of eyed channel catfish, *Ictalurus punctatus*, eggs with monovalent *Flavobacterium columnare* vaccine and bivalent *F. columnare* and *Edwardsiella ictaluri* vaccine. *Vaccine*. (2007) 25:1126–31. doi: 10.1016/j.vaccine.2006.09.055
10. Wise DJ, Greenway TE, Byars TS, Griffin MJ, Khoo LH. Oral vaccination of channel catfish against enteric septicemia of catfish using a live attenuated *Edwardsiella ictaluri* isolate. *J Aquat Anim Health*. (2015) 27:135–43. doi: 10.1080/08997659.2015.1032440
11. Ellis AE. Immunity to bacteria in fish. *Fish Shellfish Immunol*. (1999) 9:291–308. doi: 10.1006/fsim.1998.0192
12. Shoemaker CA, Klesius PH. Protective immunity against enteric septicaemia in channel catfish, *Ictalurus punctatus* (Rafinesque), following controlled exposure to *Edwardsiella ictaluri*. *J Fish Dis*. (1997) 20:361–8. doi: 10.1046/j.1365-2761.1997.00310.x
13. Booth NJ, Elkamel A, Thune RL. Intracellular replication of *Edwardsiella ictaluri* in channel catfish macrophages. *J Aquat Anim Health*. (2006) 18:101–8. doi: 10.1577/H05-025.1
14. Kordon AO, Abdelhamed H, Ahmed H, Park JY, Karsi A, Pinchuk LM. Phagocytic and bactericidal properties of channel catfish peritoneal macrophages exposed to *Edwardsiella ictaluri* live attenuated vaccine and wild-typestrains. *Front. Microbiol*. (2018) 8:2638. doi: 10.3389/fmicb.2017.02638
15. Abdelhamed H, Lawrence ML, Karsi A. Development and characterization of a novel live attenuated vaccine against enteric septicemia of catfish. *Front. Microbiol*. (2018) 9:1819. doi: 10.3389/fmicb.2018.01819
16. Nho SW, Abdelhamed H, Karsi A, Lawrence ML. Improving safety of a live attenuated *Edwardsiella ictaluri* vaccine against enteric septicemia of catfish and evaluation of efficacy. *Vet Microbiol*. (2017) 210:83–90. doi: 10.1016/j.vetmic.2017.09.004
17. Zapata A, Diez B, Cejalvo T, Gutiérrez-de Frías C, Cortés A. Ontogeny of the immune system of fish. *Fish Shellfish Immunol*. (2006) 20:126–36. doi: 10.1016/j.fsi.2004.09.005
18. Rombout JHWM, Huttenhuis HBT, Picchietti S, Scapigliati G. Phylogeny and ontogeny of fish leucocytes. *Fish Shellfish Immunol*. (2005) 19:441–55. doi: 10.1016/j.fsi.2005.03.007
19. Abdel-Aziz E-SH, Abdu SBS, Ali TE-S, Fouad HF. Haemopoiesis in the head kidney of tilapia, *Oreochromis niloticus* (Teleostei: Cichlidae): a morphological (optical and ultrastructural) study. *Fish Physiol Biochem*. (2010) 36:323–36. doi: 10.1007/s10695-008-9297-z
20. Abdelhamed H, Ibrahim I, Baumgartner W, Lawrence ML, Karsi A. Characterization of histopathological and ultrastructural changes in channel catfish experimentally infected with virulent *Aeromonas hydrophila*. *Front. Microbiol*. (2017) 8:1519. doi: 10.3389/fmicb.2017.01519
21. Baldwin TJ, Newton JC. Pathogenesis of enteric septicemia of channel catfish, caused by *Edwardsiella ictaluri*: bacteriologic and light and electron microscopic findings. *J Aquat Anim Health*. (1993) 5:189–98. doi: 10.1577/1548-8667(1993)005<0189:POESOC>2.3.CO;2
22. Karsi A, Menanteau-Ledouble S, Lawrence ML. Development of bioluminescent *Edwardsiella ictaluri* for noninvasive disease monitoring. *FEMS Microbiol Lett*. (2006) 260:216–23. doi: 10.1111/j.1574-6968.2006.00310.x
23. Ruddle NH, Akirav EM. Secondary lymphoid organs: responding to genetic and environmental cues in ontogeny and the immune response. *J Immunol*. (2009) 183:2205–12. doi: 10.4049/jimmunol.0804324
24. Koppang EO, Fischer U, Moore L, Tranulis MA, Dijkstra JM, Köllner B, et al. Salmonid T cells assemble in the thymus, spleen and in novel interbranchial lymphoid tissue. *J Anatomy*. (2010) 217:728–39. doi: 10.1111/j.1469-7580.2010.01305.x
25. Mildner A, Jung S. Development and function of Dendritic cell subsets. *Immunity*. (2014) 40:642–56. doi: 10.1016/j.immuni.2014.04.016
26. Lugo-Villarino G, Balla KM, Stachura DL, Bañuelos K, Werneck MBF, Traver D. Identification of dendritic antigen-presenting cells in the zebrafish. *Proc Natl Acad Sci USA*. (2010) 107:15850–5. doi: 10.1073/pnas.1000494107
27. Wittamer V, Bertrand JY, Gutschow PW, Traver D. Characterization of the mononuclear phagocyte system in zebrafish. *Blood*. (2011) 117:7126–35. doi: 10.1182/blood-2010-11-321448
28. Bassity E, Clark TG. Functional identification of dendritic cells in the teleost model, rainbow trout (*Oncorhynchus mykiss*). *PLoS ONE*. (2012) 7:e33196. doi: 10.1371/journal.pone.0033196
29. Aghaallaei N, Bajoghli B, Schwarz H, Schorpp M, Boehm T. Characterization of mononuclear phagocytic cells in medaka fish transgenic for a cxcr3a:gfp reporter. *Proc Natl Acad Sci USA*. (2010) 107:18079–84. doi: 10.1073/pnas.1000467107
30. Zoccola E, Delamare-Debouteville J, Barnes AC. Identification of Barramundi (*Lates calcarifer*) DC-SCRIPT, a specific molecular marker for Dendritic cells in Fish. *PLoS ONE*. (2015) 10:e0132687. doi: 10.1371/journal.pone.0132687
31. Lin A-F, Xiang L-X, Wang Q-L, Dong W-R, Gong Y-F, Shao J-Z. The DC-SIGN of zebrafish: insights into the existence of a CD209 homologue in a lower vertebrate and its involvement in adaptive immunity. *J Immunol*. (2009) 183:7398–410. doi: 10.4049/jimmunol.0803955
32. Shao T, Zhu L-Y, Nie L, Shi W, Dong W-R, Xiang L-X, et al. Characterization of surface phenotypic molecules of teleost dendritic cells. *Dev Comparative Immunol*. (2015) 49:38–43. doi: 10.1016/j.dci.2014.11.010
33. Igyártó BZ, Kaplan DH. Antigen presentation by Langerhans cells. *Curr Opin Immunol*. (2013) 25:115–9. doi: 10.1016/j.coi.2012.11.007
34. Sugita K, Kabashima K, Atarashi K, Shimauchi T, Kobayashi M, Tokura Y. Innate immunity mediated by epidermal keratinocytes promotes acquired immunity involving Langerhans cells and T cells in the skin. *Clin Exp Immunol*. (2007) 147:176–183. doi: 10.1111/j.1365-2249.2006.03258.x
35. McDermott R, Ziylan U, Spehner D, Bausinger H, Lipsker D, Mommaas M, et al. Birbeck granules are subdomains of endosomal recycling compartment in human epidermal Langerhans cells, which form where Langerin accumulates. *Mol Biol Cell*. (2002) 13:317–35. doi: 10.1091/mbc.01-06-0300
36. Lau SK, Chu PG, Weiss LM. Immunohistochemical expression of Langerin in Langerhans cell histiocytosis and Non-Langerhans cell histiocyticdisorders. *Am J Surg Pathol*. (2008) 32:615–9. doi: 10.1097/PAS.0b013e31815b212b
37. Valladeau J, Ravel O, Dezutter-Dambuyant C, Moore K, Kleijmeer M, Liu Y, et al. Langerin, a novel C-Type lectin specific to Langerhans cells, is an endocytic receptor that induces the formation of Birbeck granules. *Immunity*. (2000) 12:71–81. doi: 10.1016/S1074-7613(00)80160-0
38. Fehres CM, Bruijns SCM, Sotthewes BN, Kalay H, Schaffer L, Head SR, et al. Phenotypic and functional properties of human steady state $CD14^+$ and $CD1a^+$ antigen presenting cells and epidermal Langerhans cells. *PLoS ONE*. (2015) 10:e0143519. doi: 10.1371/journal.pone.0143519

39. Lovy J, Wright GM, Speare DJ. Morphological presentation of a dendritic-like cell within the gills of chinook salmon infected with *Loma salmonae*. *Dev Compar Immunol*. (2006) 30:259–63. doi: 10.1016/j.dci.2005.06.003
40. Kordon AO, Scott MA, Ibrahim I, Abdelhamed H, Ahmed H, Baumgartner W, et al. Identification of Langerhans-like cells in the immunocompetent tissues of channel catfish, *Ictalurus punctatus*. *Fish Shellfish Immunol*. (2016) 58:253–8. doi: 10.1016/j.fsi.2016.09.033
41. Triantis V, Trancikova DE, Looman MWG, Hartgers FC, Janssen RAJ, Adema GJ. Identification and characterization of DC-SCRIPT, a novel Dendritic cell-expressed member of the zinc finger family of transcriptional regulators. *J Immunol*. (2006) 176:1081–9. doi: 10.4049/jimmunol.176.2.1081
42. Triantis V, Moulin V, Looman MWG, Hartgers FC, Janssen RAJ, Adema GJ. Molecular characterization of the murine homologue of the DC-derived protein DC-SCRIPT. *J Leukocyte Biol*. (2006) 79:1083–91. doi: 10.1189/jlb.1005588
43. Nagai Y, Garrett KP, Ohta S, Bahrun U, Kouro T, Akira S, et al. Toll-Like receptors on hematopoietic progenitor cells stimulate innate immune system replenishment. *Immunity*. (2006) 24:801–12. doi: 10.1016/j.immuni.2006.04.008
44. Abdelhamed H, Lu J, Shaheen A, Abbass A, Lawrence ML, Karsi A. Construction and evaluation of an *Edwardsiella ictaluri* fhuC mutant. *Vet Microbiol*. (2013) 162:858–65. doi: 10.1016/j.vetmic.2012.11.006
45. Lovy J, Wright GM, Speare DJ. Comparative cellular morphology suggesting the existence of resident Dendritic cells within immune organs of salmonids. *The Anatomical Record*. (2008) 291:456–62. doi: 10.1002/ar.20674
46. Allen JE, Henshaw DL. An *in situ* study of $CD34^+$ cells in human fetal bone marrow. *Br J Haematol*. (2001) 114:201–10. doi: 10.1046/j.1365-2141.2001.02898.x
47. Karsi A, Waldbieser GC, Small BC, Liu Z, Wolters WR. Molecular cloning of proopiomelanocortin cDNA and multi-tissue mRNA expression in channel catfish. *Gen Compar Endocrinol*. (2004) 137:312–21. doi: 10.1016/j.ygcen.2004.03.012
48. Lawrence ML, Banes MM. Tissue persistence and vaccine efficacy of an O polysaccharide mutant strain of *Edwardsiella ictaluri*. *J Aquat Anim Health*. (2005) 17:228–32. doi: 10.1577/H04-049.1
49. Lipski DA, Dewispelaere R, Foucart V, Caspers LE, Defrance M, Bruyns C, et al. MHC class II expression and potential antigen-presenting cells in the retina during experimental autoimmune uveitis. *J Neuroinflamm*. (2017) 14:136. doi: 10.1186/s12974-017-0915-5
50. Hansen TH. Which lymphoid cells express MHC class II antigens; are TCRs encoded within the MHC? *J Immunol*. (2011) 187:2043–4. doi: 10.4049/jimmunol.1101982
51. Ma JK, Platt MY, Eastham-Anderson J, Shin J-S, Mellman I. MHC class II distribution in dendritic cells and B cells is determined by ubiquitin chain length. *Proc Natl Acad Sci USA*. (2012) 109:8820–7. doi: 10.1073/pnas.1202977109
52. Lee J, Tam H, Adler L, Ilstad-Minnihan A, Macaubas C, Mellins ED. The MHC class II antigen presentation pathway in human monocytes differs by subset and is regulated by cytokines. *PLoS ONE*. (2017) 12:e0183594. doi: 10.1371/journal.pone.0183594
53. Nusbaum KE, Morrison EE. Communications: entry of 35S-Labeled *Edwardsiella ictaluri* into Channel Catfish. *J Aquat Anim Health*. (1996) 8:146–9. doi: 10.1577/1548-8667(1996)008<0146:CEOSLE>2.3.CO;2

Conflict of Interest Statement: The authors declare that the research was conducted in the absence of any commercial or financial relationships that could be construed as a potential conflict of interest.

Copyright © 2019 Kordon, Abdelhamed, Ahmed, Baumgartner, Karsi and Pinchuk. This is an open-access article distributed under the terms of the Creative Commons Attribution License (CC BY). The use, distribution or reproduction in other forums is permitted, provided the original author(s) and the copyright owner(s) are credited and that the original publication in this journal is cited, in accordance with accepted academic practice. No use, distribution or reproduction is permitted which does not comply with these terms.

frontiers in Immunology

ORIGINAL RESEARCH
published: 13 March 2019
doi: 10.3389/fimmu.2019.00378

CpGs Induce Differentiation of Atlantic Salmon Mononuclear Phagocytes Into Cells With Dendritic Morphology and a Proinflammatory Transcriptional Profile but an Exhausted Allostimulatory Activity

Dimitar B. Iliev[1,2]*, *Leidy Lagos*[1], *Hanna L. Thim*[1†], *Sven M. Jørgensen*[3], *Aleksei Krasnov*[3] *and Jorunn B. Jørgensen*[1]*

[1] The Norwegian College of Fishery Science, UiT The Arctic University of Norway, Tromsø, Norway, [2] Department of Gene Regulation, Institute of Molecular Biology 'Roumen Tsanev', Bulgarian Academy of Sciences, Sofia, Bulgaria, [3] Nofima Marin AS, Oslo, Norway

Due to their ability to present foreign antigens and prime naïve T cells, macrophages, and dendritic cells (DCs) are referred to as professional antigen-presenting cells (APCs). Although activated macrophages may function as APCs, these cells are particularly effective at directly engaging pathogens through phagocytosis, and production of antimicrobial compounds. On the other hand, DCs possess superb antigen-presenting and costimulatory capacity and they are essential for commencement and regulation of adaptive immune responses. In *in vitro* models, development of mature mammalian DCs from monocytes requires sequential exposure to growth factors (including GM-CSF and IL-4) and proinflammatory stimuli such as toll-like receptor (TLR) ligands. Currently, except for IL-4/13, neither orthologs nor functional analogs of the growth factors which are essential for the differentiation of mammalian DCs (including GM-CSF and FLT3) have been identified in teleosts and data about differentiation of piscine APCs is scant. In the present study, primary salmon mononuclear phagocytes (MPs) stimulated *in vitro* for 5–7 days with a B-class CpG oligodeoxynucleotides (ODN 2006PS) underwent morphological differentiation and developed "dendritic" morphology, characterized by long, branching pseudopodia. Transcriptional profiling showed that these cells expressed high levels of proinflammatory mediators characteristic for M1 polarized MPs. However, the cells treated with CpGs for 7 days downregulated their surface MHCII molecules as well as their capacity to endocytose ovalbumin and exhibited attenuated allostimulatory activity. This concurred with transcriptional downregulation of costimulatory *CD80/86* and upregulation of inhibitory *CD274 (B7-H1)* genes. Despite their exhausted allostimulatory activity, these cells were still responsive to re-stimulation with gardiquimod (a TLR7/8 ligand) and further upregulated a wide array of immune genes including proinflammatory mediators such as *intereukin-1 beta* and *tumor necrosis factor*. Overall, the presented data highlight the disparate effects TLR ligands may have on the

OPEN ACCESS

Edited by:
Carolina Tafalla, Instituto Nacional de Investigación y Tecnología Agraria y Alimentaria (INIA), Spain

Reviewed by:
Uwe Fischer, Friedrich Loeffler Institut, Germany
Mark D. Fast, University of Prince Edward Island, Canada

***Correspondence:**
Dimitar B. Iliev
dimitar.iliev@uit.no;
diliev@bio21.bas.bg
Jorunn B. Jørgensen
jorunn.jorgensen@uit.no

†Present Address:
Hanna L. Thim, Vaxxinova Norway AS, Bergen, Norway

Specialty section:
This article was submitted to Comparative Immunology, a section of the journal Frontiers in Immunology

Received: *26 November 2018*
Accepted: *14 February 2019*
Published: *13 March 2019*

Citation:
Iliev DB, Lagos L, Thim HL, Jørgensen SM, Krasnov A and Jørgensen JB (2019) CpGs Induce Differentiation of Atlantic Salmon Mononuclear Phagocytes Into Cells With Dendritic Morphology and a Proinflammatory Transcriptional Profile but an Exhausted Allostimulatory Activity. Front. Immunol. 10:378. doi: 10.3389/fimmu.2019.00378

proinflammatory status of APCs, on one side, and their antigen-presenting/costimulatory functions, on the other. These findings also indicate that despite the poor phylogenetic conservation of the growth factors involved in the differentiation of DCs, some of the processes that orchestrate the development and the differentiation of professional APCs are conserved between teleosts in mammals.

Keywords: mononuclear phagocytes, antigen-presenting cells, dendritic cells, CpG oligodeoxynucleotides, Atlantic salmon, teleosts

INTRODUCTION

The mononuclear phagocyte (MP) system comprises circulating monocytes, tissue resident macrophages, and monocyte-derived DCs. The most important unifying properties of MPs are their common myeloid origin and their potential to serve as professional APCs. These professional APCs are innate immune cells; however they are very important for the commencement of the adaptive immune response (1, 2). More specifically, they are indispensable for the activation of naïve T cells by protein antigens and are essential for the maintenance of tolerance to self-antigens. The MP system is phylogenetically conserved and cells resembling mammalian monocytes, macrophages, and DCs have been identified across different vertebrate classes (3–5).

Although macrophages are mainly engaged in direct elimination of pathogens through endocytosis and production of antibacterial agents, they are also capable of presenting foreign antigens and priming naïve T cells (6). These cells have been studied extensively in fishes and the specifics of their development and functional diversity (including development of M1 and M2 functional phenotypes) within teleosts have recently been covered in review articles (7, 8).

DCs were initially "baptized" by Ralf Steinman based on their morphology characterized by long, branching pseudopodia (9). A unifying characteristic of DCs is their superior capability to activate naïve T cells through presentation of MHCI and II-associated foreign antigens and costimulatory molecules on their surface (2, 10). Studies on mammalian DCs have been facilitated by development of protocols for *in vitro* generation of large numbers of DCs (11–14). Myeloid DCs can be generated *in vitro* following incubation of monocytes with GM-CSF and IL-4 for up to 5 days. This results in development of a relatively homogeneous population of immature DCs which require further activation with microbial products such as lipopolysaccharide, bacterial DNA, and double stranded RNA or cytokines such as TNF-α in order to achieve a mature state (15). The maturation of DCs is hallmarked with increased expression of MHCII and costimulatory molecules (e.g., CD80, CD86) on their plasma membrane and decreased ability to endocytose soluble antigens.

Piscine DC-like cells have been described *in vivo* in different teleost species including salmonids, zebrafish, and medaka (16–21); however, lack of protocols and tools for large-scale production of mature fish DCs *in vitro* has hampered further characterization of these cells. Homologs of most of the major cytokines and growth factors involved in activation and differentiation of various leukocyte types have been identified and isolated in fish. However, the essential growth factors—GM-CSF and FMS-like tyrosine kinase three ligand (FLT3L) used to differentiate mammalian DCs *in vitro* (11, 22) have not been identified in any fish species suggesting that orthologs of these genes may be absent below the level of tetrapods.

We have previously reported that 24 h *in vitro* stimulation of salmon mononuclear phagocytes with class B CpGs, a ligand for TLR9 and TLR21 (23, 24) upregulates a number of immune genes some of which are highly expressed in mature DCs (25). However, data about the effects of TLR ligands on antigen-presenting functions of piscine APCs are still scarce. In the current study, we have investigated the effects of long-term *in vitro* stimulation with TLR ligands, including CpG-B (2006PS) and polyI:C (a TLR3/22 ligand), on primary salmon MPs. The propensity of the CpG stimulation to induce differentiation of MPs as shown by appearance of cells with "dendritic" morphology prompted us to investigate the phenotypical and the functional characteristics of these APCs. We further discuss the capacity of the CpG stimulation to induce a proinflammatory, M1 transcriptional profile but an exhausted allostimulatory activity of salmon APCs.

MATERIALS AND METHODS

Fish

Atlantic salmon (*Salmo salar*) strain Aquagen standard (Aquagen, Kyrksæterøra, Norway) was obtained from the Tromsø Aquaculture Research Station (Tromsø, Norway). The fish were kept at about 10°C in tanks supplied with running filtered water and were fed on commercial, dry food (Skretting, Stavanger, Norway). All experiments were approved by the national committee for animal experimentation (Norwegian Animal Research Authority) and performed according to its guidelines.

Reagents

Phosphorothioate-modified CpG-B (5′-TCGTCGTTTTGTCGT TTTGTCGTT-3′) were purchased from Thermo Scientific and polyI:C from InvivoGen. Cy5-conjugated CpG-B was obtained from Eurogentech. The antibodies against the β-chain of salmon MHCII and TLR9 have been previously described (25, 26). The antibody against actin was purchased from Sigma Aldrich (A2066). CellTrace™ Violet, CellTrace™ CFSE, AlexaFluor546, and Ova-Alexa488, were purchased from Life technologies.

Isolation of Leukocytes From Atlantic Salmon

HK and spleen leukocytes were isolated as described (27). The density of the leukocyte suspensions was adjusted to 7×10^6 cells/ml and the cells were incubated in 6-well plates (21×10^6 of cells/well) in L-15, supplemented with 0.1% fetal bovine serum (FBS) for 24 h before washing. In addition to displaying classical MP morphology, the adherent HK leukocytes were able to phagocytose large amounts of yeast cell wall particles (data not shown), endocytosed, and processed large amounts of ovalbumin (27) and expressed high levels of markers for MPs including the macrophage colony stimulator factor receptor (CSF-1R) and the macrophage scavenger receptor MARCO mRNAs (28). Adherent HK MPs (stimulators) and non-adherent spleen lymphocytes (responders) were washed and incubated in L-15 supplemented with 5% FBS, penicillin (10 U/ml), streptomycin (10 mg/ml) as described below.

Mixed Leukocyte Reactions (MLRs)

The adherent HK MPs were either left non-stimulated or treated with 2 μM CpG-B for 24 h or 7 days and were harvested on ice using Ca/Mg-free PBS/100 mM EDTA. Stimulators and responders were stained with CellTrace™ CFSE and CellTrace™ Violet, respectively. Staining of stimulators with CFSE was used to distinguish them from proliferating responders with reduced CellTrace™ Violet staining. The cells were washed with PBS and stained with 2 μM dye at 10^6cells/mL density for 10 min at room temperature. After staining, the cells were washed three times with L-15, 5% FBS using a 15 min interval between each washing. Responders were mixed with both non-stimulated and CpG-treated stimulators from the same or other individuals in duplicates at 2:1 ratio ($1 \times 10^5/0.5 \times 10^5$ cells) in 96-well round-bottom plates and incubated for 3, 5, 7, and 14 days before flow cytometry analysis. Fifty per cent of the medium was refreshed at 3-day intervals.

Flow Cytometry

To investigate the surface expression of MHCII together with the Ova and CpGs uptake capacity, non-stimulated and CpG-stimulated (2 μM, 7 days) MPs were incubated with 10 μg/ml of Ova-Alexa488, or 2 μM CpG-Cy5 conjugates for 1 h. The cells were harvested on ice using Ca/Mg-free PBS/100 mM EDTA. The samples were washed with ice-cold PBS and incubated with a polyclonal salmon MHCIIβ antibody (1,000-fold dilution) for 1 h in PBS, 5% FBS on ice. The secondary Alexa546 goat anti-rabbit antibody was diluted to 1 μg/ml in PBS, 5% FBS and the cells were incubated for 30 min on ice prior to washing, and flow cytometry. Samples from the MLRs (described in the previous paragraph) were harvested and analyzed directly without staining. The cells were analyzed using FACSAria (Becton Dickinson). Statistical analysis was performed with Student's *t*-test.

Confocal Microscopy

MPs cultured on 15 mm coverslips in 24-well plates cell culture plates (Falcon) were either left non-stimulated or treated with 2 μM CpGs for 7 days. The cells were then incubated with 2 μM CpG-Cy5 for 1 h, stained and analyzed as previously described (24).

Microarray Analysis

MPs were stimulated with 2 μM CpGs and 20 μg/ml of polyI:C and sampled after 24 h and 7 days. Control cells were left non-stimulated. On day 6, Gardiquimod (1 μg/ml) was added to restimulate the cells and RNA samples were harvested from the restimulated and the non-restimulated cells on day 7. Cells from three individuals were stimulated in parallel. Gene expression was analyzed using the salmonid oligonucleotide microarray (SIQ2.0, NCBI GEO platform GPL10679) (29) consisting of 21 K features printed in duplicates on 4 × 44 K chips produced by Agilent Technologies (CA, USA). Two-color hybridizations were applied, where test samples labeled with Cy5 dye were competitively hybridized against control samples labeled with Cy3 dye per array. Concentration of total RNA was measured with NanoDrop 1,000 Spectrometer (Thermo Scientific, Waltham, MA, USA) and quality was assessed using Agilent 2100 Bioanalyzer with RNA Nano kits (Agilent Technologies). Samples with RNA integrity number (RIN) of eight or higher were accepted for microarray analyses. RNA from cells obtained from two individuals was pooled and used for the analysis. Unless specified otherwise, all reagents and equipment used for microarray analyses were from Agilent Technologies. RNA amplification and labeling were performed using Quick Amp Labeling Kits, Two-Color, and RNA Spike-In Kits, Two-Color following the manufacturer's protocol for 4 × 44 K microarrays; each reaction used 500 ng of total RNA. Gene Expression Hybridization Kit was used for fragmentation of labeled RNA. Hybridizations to microarrays were performed in hybridization oven (Agilent Technologies) at 65°C and rotation speed of 10 rpm. Arrays were washed with Gene Expression Wash Buffers 1 and 2 and scanned with a GenePix 4,100A (Molecular Devices, Sunnyvale, CA, USA). GenePix software was used for spot-grid alignment, feature extraction, and quantification. Assessment of spot quality was done with aid of GenePix flags. After filtration of low quality spots, Lowess normalization of log2-expression ratios was performed. The replicates showed close concordance of gene expression profiles (Pearson $r = 0.93 \pm 0.01$). Features with >2-fold change in both samples per treatment were selected as differentially expressed.

Cell Surface Protein Isolation and Mass Spectrometry Analysis

Twenty ml of HK leukocyte suspensions (7×10^6/ml) were seeded in T75 flasks (BD Biosciences) and allowed to adhere overnight. Following washing, adherent MPs were further incubated without stimulation or treated with 2 μM CpGs for 7 days. Cells from two individuals with confluence of 80–90% were selected for isolation of cell surface proteins using Pierce® Cell Surface Protein Isolation Kit (Thermo Scientific) and following manufacturer's instructions. Briefly, the cells were rinsed with ice-cold PBS and cell surface proteins were labeled with 10 ml of Sulfo-NHS-SS-Biotin solution for 30 min at 4°C. Following a quenching reaction, the cells were collected with a scraper, washed with TBS, lysed with 500 μL of Lysis Buffer and subjected

to low power sonication on ice. Biotinylated proteins in clarified supernatants were captured using NeutrAvidin Agarose at RT for 1 h. The proteins were eluted from the agarose beads using SDS sample buffer, 50 mM DTT at RT for 1 h and subjected to SDS PAGE and Coomassie staining. Gel bands of interest were excised and subjected to in-gel reduction, alkylation, and tryptic digestion using 6 ng/μl trypsin (V511A, Promega). Peptide mixtures containing 1% formic acid were loaded onto a nanoAcquityTMUltra Performance LC (Waters), containing a 3-μm Symmetry® C18 Trap column (180 μm × 22 mm) (Waters) in front of a 3-μm AtlantisTM C18 analytical column (100 μm × 100 mm)(Waters). Peptides were separated with a gradient of 5–90% acetonitrile, 0.1% formic acid, with a flow of 0.4 μl/min eluted to a Q-TOF Ultima Global mass spectrometer (Micromass/Waters), and subjected to data-dependent tandem mass spectrometry analysis. Peak lists were generated by the ProteinLynx Global server software (version 2.1), and the resulting pkl files were searched against the NCBInr 20090214 protein sequence database using MASCOT search engine (http://www.matrixscience.com/). Peptide mass tolerances used in the search were 100 ppm, and fragment mass tolerance was 0.1 Da.

Western Blot Analysis (WB)

The flow-through lysates which contain proteins that did not bind to Neutravidin and LDS eluates, enriched in biotinylated proteins were analyzed as previously described (25). Briefly, samples dissolved in 4 X LDS were run on NuPAGE Novex Bis-Tris 4–12% gels (Invitrogen) in MOPS running buffer. The proteins were transferred to PVDF membranes, blocked (Tris-buffered saline, 5% BSA, 0.1% Tween-20) for 1 h, and incubated overnight with primary Abs (1: 1000 dilution for MHCII and 1:100 for the actin antibody) followed by 1 h of incubation with the secondary HRP-conjugated antibodies (1: 10 000 dilution). The blots were developed with SuperSignal West Pico substrate (Pierce, Rockford, IL, USA).

RESULTS

Prolonged *in vitro* Stimulation With CpGs Leads to Morphological Differentiation of Salmon MPs and Development of Cells With "Dendritic" Morphology

When adherent salmon head kidney (HK) MPs were stimulated *in vitro* for >5 days with CpGs (2 μM) many of the cells developed relatively long, branching pseudopodia, a morphological feature manifested by DCs (9) and, in some cases, M1 macrophages (30) (**Figure 1A**). This was not observed when cells were stimulated in parallel with polyI:C (20 μg/ml). After 7 days of treatment with CpGs, cells that had the original macrophage-like morphology were also present. A time lapse imaging showed that while many of the cells retained their dendritic-like morphology, the shape of some of the CpG-stimulated cells was dynamic as they could transition between dendritic-like to macrophage-like and vice versa morphology within a time span of 90 min (**Figure 1B**).

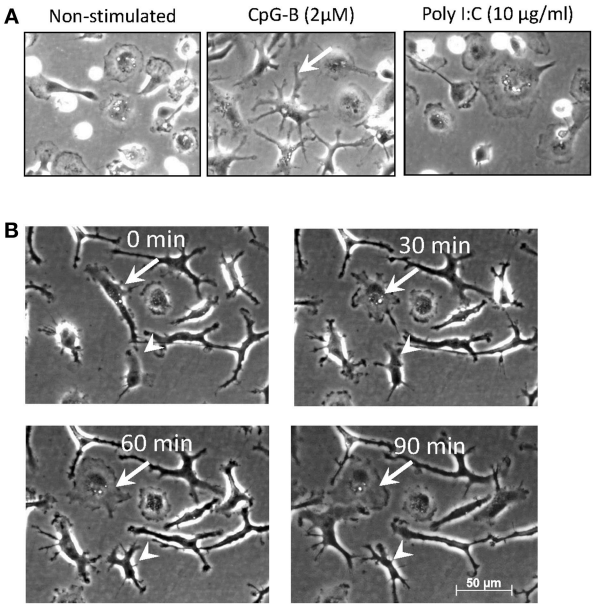


FIGURE 1 | Salmon MPs develop dendritic morphology following prolonged treatment with CpGs. **(A)** Images of non-stimulated MPs and cells stimulated for 7 days with 2 μM CpGs and 20 μg/ml of polyI:C. The arrow indicates a typical DC-like cell observed in the CpG-treated samples. **(B)** Dynamic reorganization of the morphology of CpG-treated MPs. Cells were stimulated as in panel A and images were taken at 30 min intervals over a period of 90 min. The arrow points at elongated DC-like cell which changes morphology into a more rounded macrophage-like cell. The arrowhead indicates a cell which undergoes the opposite changes. Images were taken at X200 magnification.

CpGs Upregulate Allostimulatory Activity and Surface MHCII Expression in Salmon MPs After a Short but Not After a Prolonged Treatment

In order to estimate the allostimulatory capacity of non-stimulated MPs and cells stimulated with CpGs for 24 h and 7 days we performed MLRs with spleen lymphocytes from different individuals. The experimental conditions were chosen based on preliminary experiments using responders from spleen, HK, and blood (results not shown). Spleen lymphocytes depleted of adherent cells showed the highest response and were further used in the study. Using a CellTrace™ Violet Cell Proliferation Kit we found that unlike autologous MPs, stimulators from other individuals incubated with responder spleen lymphocytes for 2 weeks induced modest spleen cell proliferation of the total population as indicated by the increased percentage of responders with reduced amount of dye. No significant response was observed in MLRs incubated for 3, 5, and 7 days (data not shown). The analysis setup of the flow cytometry data is shown in **Figure 2A**—proliferating responders are located in the lower left quadrant of the dot plots due to reduced CTV staining while CFSE staining was used to gate out stimulators. Incubation of splenocytes with stimulators from other individuals that had been stimulated with CpGs for 24 h induced significant proliferation response ($p < 0.05$), whereas autologous stimulators

and MPs stimulated with CpGs for 7 days prior to MLRs did not induce significant splenocyte proliferation (**Figure 2B**). CpG-B have been previously shown to be a potent mitogen for salmon splenocytes (31) and in the current study direct stimulation of responders with CpGs for 2 weeks was used as a positive control for the proliferation assay (**Figure 2C**). The CpG-induced proliferation of salmon leukocytes requires relatively high concentrations of CpGs (>0.5 μM) (31). This, as well as the fact that autologous stimulators treated with CpGs for 24 h and MPs stimulated for 7 days prior to MLRs did not induce significant splenocyte proliferation, indicates that the observed MLR response was not due to carryover of residual CpGs. In all of the experiments, the responders were cultured *in vitro* for the same period (15 days).

Using flow cytometry, the surface expression of MHCII and the level of Ova uptake were measured and compared between CpG-stimulated and non-treated HK-derived MPs. The representative results shown in **Figure 3** demonstrate that there was a slight increase of MHCII expression 1 day after the cells were exposed to CpGs, while on day 7 the surface expression on MHCII was substantially reduced. The uptake of fluorescent Ova was reduced on day 1 and was even lower on day 7.

In contrast to Ova endocytosis, the uptake of CpG ODNs was not affected in cells pre-treated with CpGs for 7 days. In the experiment presented in **Figure 4** cells were treated with CpGs for 7 days and then incubated with fluorescent CpG-Cy5 ODNs for 1 h prior to flow cytometry (**Figure 4A**) and immunostaining/confocal microscopy (**Figure 4B**). The results demonstrate that neither the level of uptake of CpGs ODNs nor the ability to accumulate the ODNs within TLR9-positive intracellular compartments was affected in the CpG-treated cells.

Transcriptional Response to Long-Term CpG and PolyI:C Stimulation. CpG-Pretreated Salmon MPs Retain Ability to Upregulate Proinflammatory Genes Upon Restimulation With Gardiquimod

The differentiation and maturation of APCs is a complex process in which the cells undergo a thorough transcriptomic reprogramming (32). Here, using a microarray platform we have analyzed the transcriptional response of salmon MPs to the long-term stimulation with CpGs and polyI:C. The latter, unlike CpGs, did not induce similar morphological differentiation of salmon MPs although it had a superior capacity to induce upregulation of IFN-stimulated genes (*ISGs*) after 24 h of stimulation (**Figure S1**). The results from the microarray analysis demonstrated that, after 7 days of stimulation, CpGs both up- and downregulated larger number of genes as compared to the polyI:C treatment (**Figure 5**). Unlike polyI:C, the CpG treatment upregulated proinflammatory cytokines (*IL-1β, TNF2/3*), genes associated with inflammation (including *SAA* and *MMP9*) and secreted TNF receptor superfamily (*TNFRSF*) members—*TNFRSF11B* and *TNFRSF6B* (**Figure 6**, **Figure S2**).

Among genes known to be implicated in the antigen-presenting functions of APCs, the CpG stimulation upregulated *CD83,* and the inhibitory *B7-H1* (*PDL1, CD274*) molecule while it downregulated the expression of *MHCII*, *CD80/86,* and *CCR9* homologs (**Figure 6**, **Figure S2**).

Interestingly, although, as mentioned above, after 24 h of stimulation, polyI:C upregulated ISGs to a much higher extent as compared to CpGs, after 7 days of stimulation, the opposite was observed for many key ISGs such as *CXCL10* (*IP-10*), *Vig1*, *Mx*, *SOCS1*, *STAT1,* and *RIG-I* as well as type II *IFN* homologs (**Figure 6**, **Figure S2**).

After 6 days of stimulation, the cells were restimulated with Gardiquimod (a TLR7/8 ligand) in order to investigate if the CpG- and polyI:C-treated cells retained their potential to respond to stimulation with TLR ligands. Compared to non-pretreated cells, Gardiquimod restimulation up- and downregulated fewer genes in CpG and polyI:C pretreated cells (**Figure 5**) indicating that the pretreatment modulated but did not completely suppress the potential of the cells to respond to secondary stimulations with TLR ligands. **Figure 6** shows the expression of selected groups of immune genes including cytokines and other immune mediators, receptors, and cell markers and ISGs. Upregulation of many of the selected genes was suppressed by the CpG and, to a lower extent, by the polyI:C pretreatments. Some of the genes whose upregulation was not repressed and was further upregulated in CpG- pretreated cells included proinflammatory cytokines (*IL-1β*, *IL-22,* and *TNF2*), and secreted TNF receptor family members (*TNFRSF11B* and *TNFRSF6B*). Interestingly, many ISGs were among the genes whose upregulation was suppressed by the pretreatment including *RIG-I, IFN-inducible Gig1, IRF3, STAT1,* as well as *IFN-γ*. Many of the genes listed in **Figure 6** can be assigned to more than one of the three categories. Therefore, it should be mentioned that the expression of immune receptors and cell markers, including CD64, CD83, CD40, and the M-CSF receptor, is known to be regulated by IFNs (33–36) and their gardiquimod-induced upregulation was also suppressed in CpG-pretreated cells.

The microarray data was validated using real-time PCR analysis in which samples from three individuals were analyzed separately. As demonstrated in **Figure S2**, except for the lower values, a commonly observed phenomenon caused by the lower dynamic range of the microarray analysis as compared to that of the real-time PCR, the two types of analysis produced similar results. The sequences of the primers used in the real-time PCR analysis are shown in **Table S1**.

Identification of Differentially Expressed Cell Surface Proteins on Non-stimulated and CpG-Treated Salmon MPs

To further define features that are characteristic for CpG-treated MPs, expression of surface proteins upon CpG-treatment were examined by mass spectrometry and compared to non-treated cells. Samples acquired using the cell surface protein isolation kit were analyzed with WB in order to estimate the efficiency of the protein purification. Compared to the flow-through lysates the pull-down samples are expected to be depleted of proteins which are not directly associated with the plasma membrane. The results shown in **Figure 7A** demonstrate that compared to the flow-through samples, the pull-down samples contained more

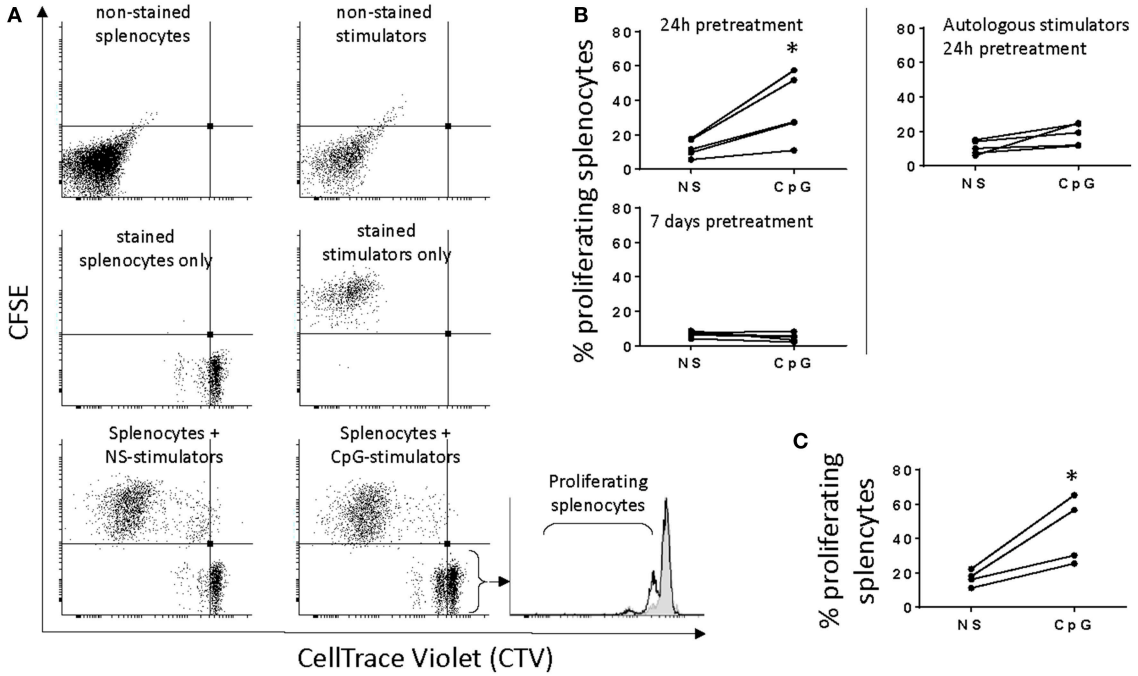


FIGURE 2 | Short, but not prolonged treatment of salmon MPs with CpGs upregulates their allostimulatory activity. **(A)**, adherent HK MPs were stained with CFSE upon 24 h of stimulation with 2 μM CpGs. Splenocytes stained with CellTrace Violet (CTV) were used as responders. The dot plots show that a significant number of stimulators take up CTV which necessitates their staining with CFSE in order to distinguish them from proliferating responders with reduced CTV staining. The CFSE-negative events were gated and displayed in histograms to quantify the percentage of proliferating splenocytes with reduced CTV staining. In the representative histogram (bottom right), responders were cultured with non-stimulated (NS) MPs from another individual (filled gray area), and stimulators pretreated with CpGs for 24 h (black contour). **(B)**, Stimulators pretreated with CpGs for 24 h but not 7 days show increased allostimulatory capacity ($n = 5$). Autologous stimulators did not significantly activate splenocyte proliferation even after pretreatment with CpGs for 24 h (*$p < 0.05$). **(C)**, Direct CpG stimulation of responders was included as a positive control for cell proliferation ($n = 4$). In all of the experiments, the responders were cultured *in vitro* for 15 days.

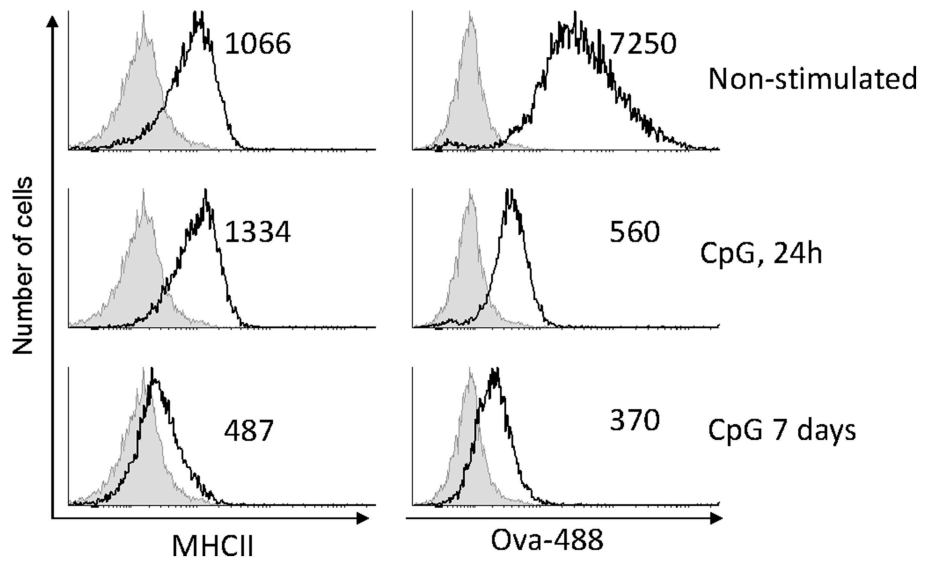


FIGURE 3 | CpG stimulation reduces antigen uptake capacity of MPs and, after a prolonged treatment, downregulates surface MHCII expression. MPs were either left untreated or stimulated with 2μM CpGs for 1 and 7 days, as indicated. The cells were incubated with 10 μg/ml of Ova conjugated with AlexaFluor-488 for 1 h prior to harvesting and analysis using flow cytometry. The numbers in the individual histograms show the mean fluorescence intensities of the stained samples (black contours). The non-stained samples are represented with filled gray contours. Representative results from two experiments with cells from different individuals are shown.

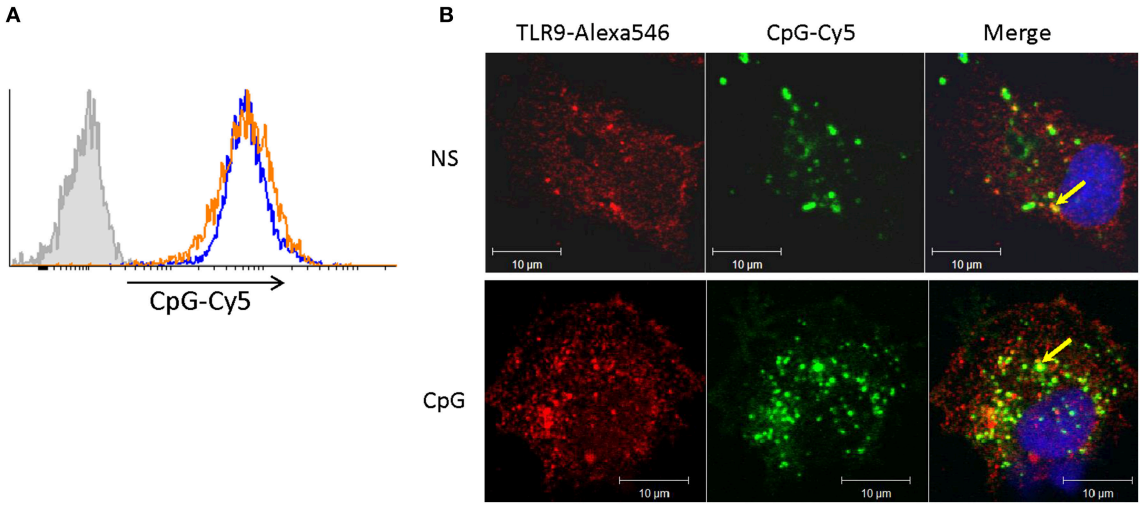


FIGURE 4 | Cells stimulated with CpGs for 7 days retain capacity to take up CpG ODNs and to translocate them into TLR9-positive endocytic compartments. **(A)** MPs were either left non-stimulated (blue contour) or were treated with 2 µM CpGs for 7 days (orange contour) prior to incubation with fluorescent (CpG-Cy5) ODNs for 1 h and flow cytometry analysis. The filled gray contour represents cells incubated without fluorescent CpGs. **(B)** Non-stimulated cells (NS) and cells pretreated with CpGs for 7 days were incubated with CpG-Cy5 for 1 h prior to fixation, permeabilization, and staining of intracellular TLR9. The endocytosed CpGs were visualized in the far-red channel and are shown in green pseudocolor. The nuclei were stained with SYTOX Green (blue pseudocolor). The colocalization between TLR9 and CpG-positive vesicles (yellow color) is indicated with arrows in the merged images.

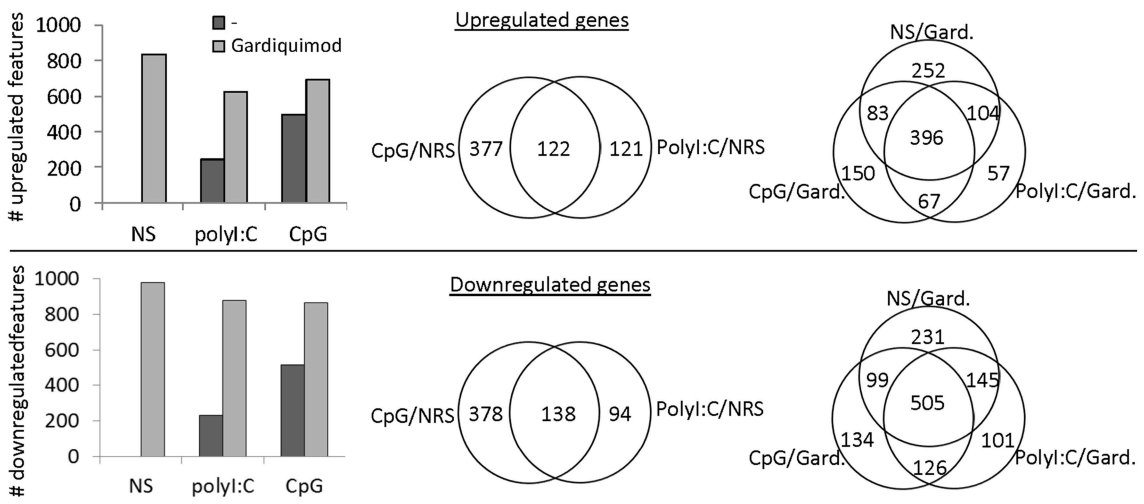
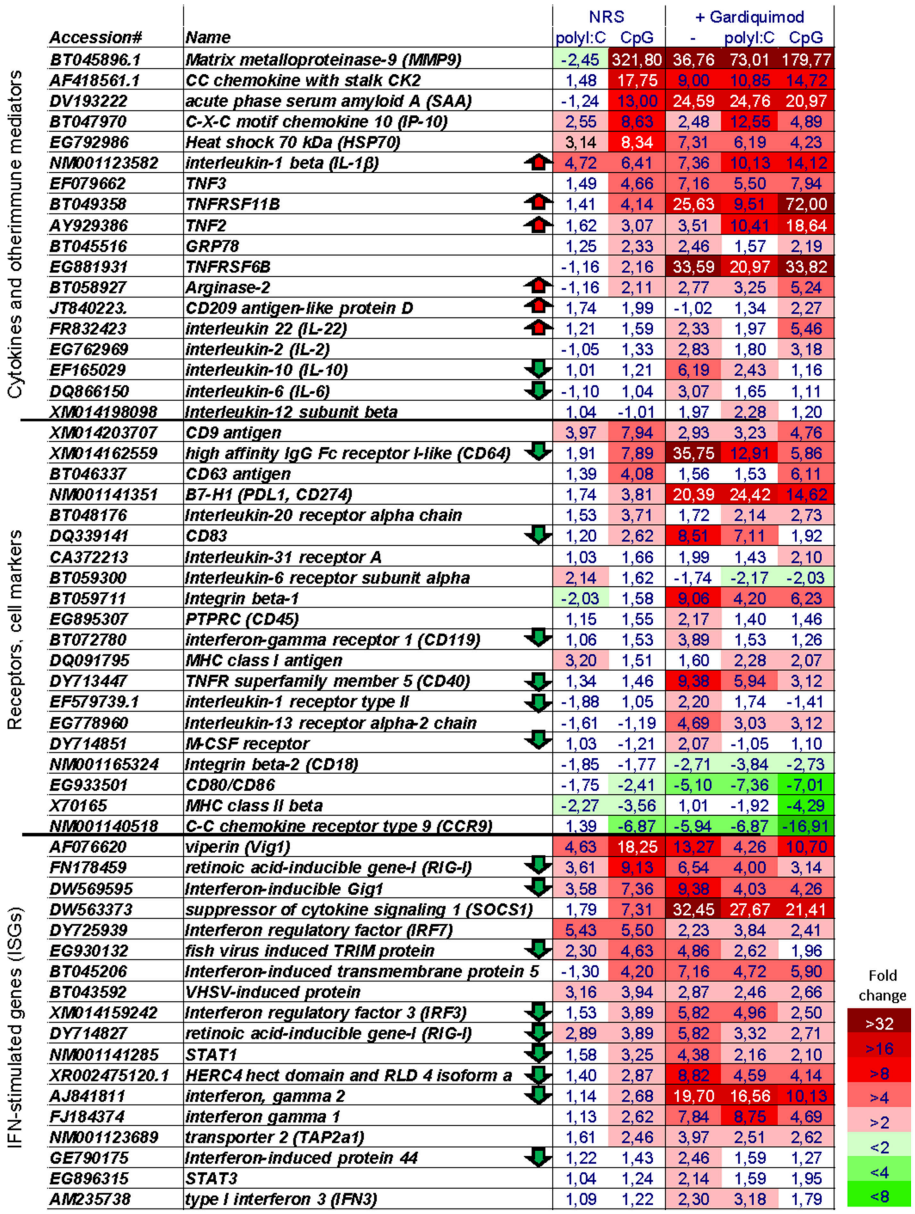


FIGURE 5 | Microarray analysis—transcriptional response of salmon MPs to long term stimulation with polyI:C and CpGs and restimulation with gardiquimod. MPs were left non-stimulated (NS) or stimulated with 2 µM CpGs or 20 µg/ml of polyI:C. After 6 days, samples were restimulated with 1 µg/ml of Gardiquimod and RNA from both non-restimulated (NRS) and restimulated samples was sampled on day 7. Pooled RNA samples of cells from two individuals were analyzed using a salmonid oligonucleotide microarray. Features with fold change values of +2 and −2 as compared to the NS samples were considered up- and downregulated, respectively. The histograms show the total numbers of up- and downregulated features in the different samples. The Venn diagrams show the numbers of common and unique up- and downregulated genes among the samples.

MHCII while the actin levels were barely detectable, thereby confirming the efficiency of the cell surface isolation procedure.

Major SDS PAGE protein bands present in samples of cell surface proteins from non-stimulated MPs and cells treated with CpGs for 7 days were isolated and analyzed using tandem mass spectrometry (MS/MS). Samples from cells of two individuals were run in parallel and consistently regulated bands were selected for the analysis (**Figure 7B**). The analysis identified CD45 in a high molecular weight band that was upregulated by the CpG treatment. Another high molecular weight band which appeared to be downregulated in CpG-treated samples contained clathrin whereas CD18, an integrin involved in cell adhesion, was identified in a major band that did not seem to be regulated by the treatment in any of the two analyzed individuals. The HSP70



	Accession#	Name	NRS polyI:C	NRS CpG	+ Gardiquimod -	+ Gardiquimod polyI:C	+ Gardiquimod CpG
Cytokines and otherimmune mediators	BT045896.1	Matrix metalloproteinase-9 (MMP9)	-2,45	321,80	36,76	73,01	179,77
	AF418561.1	CC chemokine with stalk CK2	1,48	17,75	9,00	10,85	14,72
	DV193222	acute phase serum amyloid A (SAA)	-1,24	13,00	24,59	24,76	20,97
	BT047970	C-X-C motif chemokine 10 (IP-10)	2,55	8,63	2,48	12,55	4,89
	EG792986	Heat shock 70 kDa (HSP70)	3,14	8,34	7,31	6,19	4,23
	NM001123582	interleukin-1 beta (IL-1β) ↑	4,72	6,41	7,36	10,13	14,12
	EF079662	TNF3	1,49	4,66	7,16	5,50	7,94
	BT049358	TNFRSF11B ↑	1,41	4,14	25,63	9,51	72,00
	AY929386	TNF2 ↑	1,62	3,07	3,51	10,41	18,64
	BT045516	GRP78	1,25	2,33	2,46	1,57	2,19
	EG881931	TNFRSF6B	-1,16	2,16	33,59	20,97	33,82
	BT058927	Arginase-2 ↑	-1,16	2,11	2,77	3,25	5,24
	JT840223.	CD209 antigen-like protein D ↑	1,74	1,99	-1,02	1,34	2,27
	FR832423	interleukin 22 (IL-22) ↑	1,21	1,59	2,33	1,97	5,46
	EG762969	interleukin-2 (IL-2)	-1,05	1,33	2,83	1,80	3,18
	EF165029	interleukin-10 (IL-10) ↓	1,01	1,21	6,19	2,43	1,16
	DQ866150	interleukin-6 (IL-6) ↓	-1,10	1,04	3,07	1,65	1,11
	XM014198098	interleukin-12 subunit beta	1,04	-1,01	1,97	2,28	1,20
Receptors, cell markers	XM014203707	CD9 antigen	3,97	7,94	2,93	3,23	4,76
	XM014162559	high affinity IgG Fc receptor I-like (CD64) ↓	1,91	7,89	35,75	12,91	5,86
	BT046337	CD63 antigen	1,39	4,08	1,56	1,53	6,11
	NM001141351	B7-H1 (PDL1, CD274)	1,74	3,81	20,39	24,42	14,62
	BT048176	Interleukin-20 receptor alpha chain	1,53	3,71	1,72	2,14	2,73
	DQ339141	CD83 ↓	1,20	2,62	8,51	7,11	1,92
	CA372213	Interleukin-31 receptor A	1,03	1,66	1,99	1,43	2,10
	BT059300	Interleukin-6 receptor subunit alpha	2,14	1,62	-1,74	-2,17	-2,03
	BT059711	Integrin beta-1	-2,03	1,58	9,06	4,20	6,23
	EG895307	PTPRC (CD45)	1,15	1,55	2,17	1,40	1,46
	BT072780	interferon-gamma receptor 1 (CD119) ↓	1,06	1,53	3,89	1,53	1,26
	DQ091795	MHC class I antigen	3,20	1,51	1,60	2,28	2,07
	DY713447	TNFR superfamily member 5 (CD40) ↓	1,34	1,46	9,38	5,94	3,12
	EF579739.1	interleukin-1 receptor type II ↓	-1,88	1,05	2,20	1,74	-1,41
	EG778960	Interleukin-13 receptor alpha-2 chain	-1,61	-1,19	4,69	3,03	3,12
	DY714851	M-CSF receptor ↓	1,03	-1,21	2,07	-1,05	1,10
	NM001165324	Integrin beta-2 (CD18)	-1,85	-1,77	-2,71	-3,84	-2,73
	EG933501	CD80/CD86	-1,75	-2,41	-5,10	-7,36	-7,01
	X70165	MHC class II beta	-2,27	-3,56	1,01	-1,92	-4,29
	NM001140518	C-C chemokine receptor type 9 (CCR9)	1,39	-6,87	-5,94	-6,87	-16,91
IFN-stimulated genes (ISGs)	AF076620	viperin (Vig1)	4,63	18,25	13,27	4,26	10,70
	FN178459	retinoic acid-inducible gene-I (RIG-I) ↓	3,61	9,13	6,54	4,00	3,14
	DW569595	Interferon-inducible Gig1 ↓	3,58	7,36	9,38	4,03	4,26
	DW563373	suppressor of cytokine signaling 1 (SOCS1)	1,79	7,31	32,45	27,67	21,41
	DY725939	Interferon regulatory factor (IRF7)	5,43	5,50	2,23	3,84	2,41
	EG930132	fish virus induced TRIM protein ↓	2,30	4,63	4,86	2,62	1,96
	BT045206	Interferon-induced transmembrane protein 5	-1,30	4,20	7,16	4,72	5,90
	BT043592	VHSV-induced protein	3,16	3,94	2,87	2,46	2,66
	XM014159242	Interferon regulatory factor 3 (IRF3) ↓	1,53	3,89	5,82	4,96	2,50
	DY714827	retinoic acid-inducible gene-I (RIG-I) ↓	2,89	3,89	5,82	3,32	2,71
	NM001141285	STAT1 ↓	1,58	3,25	4,38	2,16	2,10
	XR002475120.1	HERC4 hect domain and RLD 4 isoform a ↓	1,40	2,87	8,82	4,59	4,14
	AJ841811	interferon, gamma 2 ↓	1,14	2,68	19,70	16,56	10,13
	FJ184374	interferon gamma 1	1,13	2,62	7,84	8,75	4,69
	NM001123689	transporter 2 (TAP2a1)	1,61	2,46	3,97	2,51	2,62
	GE790175	Interferon-induced protein 44 ↓	1,22	1,43	2,46	1,59	1,27
	EG896315	STAT3	1,04	1,24	2,14	1,59	1,95
	AM235738	type I interferon 3 (IFN3)	1,09	1,22	2,30	3,18	1,79

FIGURE 6 | Microarray heat map showing the expression of selected immune genes. The numbers show the "fold change" values as compared to non-stimulated cells. The heat map legend is shown in the lower right corner. Note, that genes of interest have been tentatively assigned to three groups; however, many of them can be assigned to more than one group. Arrows indicate genes whose expression is at least 1.9-fold higher or lower in CpG + Gardiquimod samples as compared to samples stimulated only with Gardiquimod.

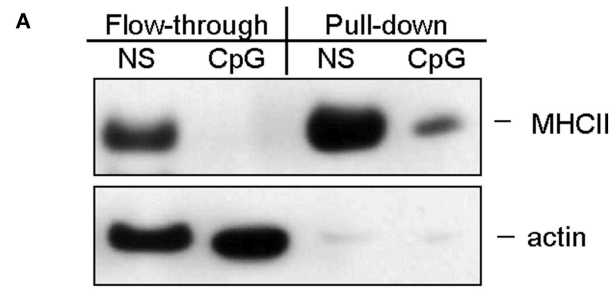
family members GRP78 and HSP70 were identified in bands which appeared to be slightly upregulated by the CpG treatment.

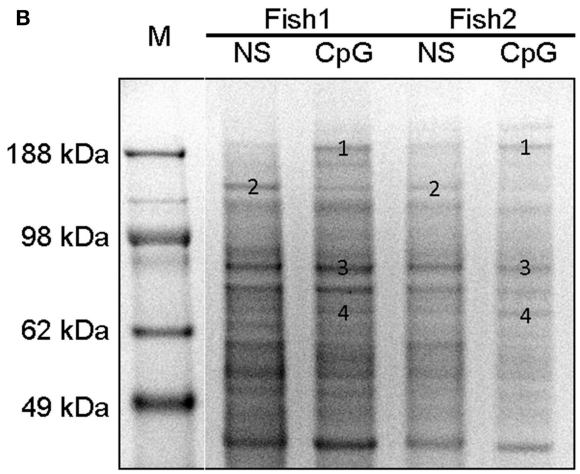
DISCUSSION

In the current study, long-term *in vitro* stimulation (>5 days) with CpGs induced functional and phenotypical differentiation of salmon MPs. Although these cells developed dendritic morphology and an M1-like proinflammatory transcriptional profile, they downregulated their surface MHCII expression, and had an impaired allostimulatory capacity.

The differentiation of MPs into cells with dendritic morphology appeared to correlate with upregulation of proinflammatory genes since cells stimulated in parallel with polyI:C did not exhibit similar morphological changes and had fewer inflammatory mediators upregulated after 7 days of stimulation. At the same time, the polyI:C-stimulated cells had some IFN-inducible genes upregulated at levels compared to, or even exceeding those in CpG-stimulated cells.

The term "dendritic cell" was introduced by Ralf Steinman, reflecting the specific morphology of DCs isolated from peripheral lymphoid organs (9). However, it should be noted that,





Band #	protein	# peptides	Mascot score
1	CD45	13	218
2	Clathrin	30	441
3	CD18	13	598
4	GRP78	3	167
4	HSP70	4	203

FIGURE 7 | Mass spectrometry analysis of cell surface proteins of non-stimulated and CpG-treated salmon MPs. The cells were either left non-stimulated or were stimulated with CpGs for 7 days. Cell surface proteins were labeled with biotin and purified as described in Materials and methods. **(A)** The efficiency of the cell surface protein purification was confirmed with WB analysis. Flow-through and pull-down samples enriched in proteins associated with cell surface from control non-stimulated and CpG-stimulated cells were run on SDS PAGE and protein levels of MHCII-β and actin were detected with polyclonal antibodies. **(B)** Samples enriched in cell surface proteins isolated from cells of two individuals were run in parallel on SDS-PAGE, and stained with Coomassie. Bands of interest were excised, and subjected to MS/MS analysis. The table below the gel image lists identified proteins in bands whose ID numbers are indicated on the gel image.

under specific conditions, macrophages stimulated with LPS and IFN-γ may also adopt a similar morphology (30), characterized by long, branching pseudopodia. Therefore, considering all of the data we have obtained in this study, it would be more pertinent to conclude that the salmon MP cultures stimulated for 7 days with CpGs were enriched in activated M1 macrophages rather than DCs.

As with other types of primary cell cultures, the starting cultures of adherent salmon leukocytes were not homogenous and, most likely, included monocytes and macrophages at different developmental stages. However, the observation that the cells concertedly downregulated MHCII expression and the Ova uptake capacity suggests that the CpG-induced differentiation of these cells was relatively synchronized.

Similar to mammalian DCs, the shape of the CpG-stimulated salmon MPs was quite dynamic as the dendrites retracted and expanded in different directions within minutes. As speculated elsewhere, this property likely contributes to the antigen presenting function of DCs by allowing the APCs to scan a larger area and facilitate the capture of antigens (37). Regardless of the morphological differentiation, in our study, the CpG treatment downregulated the ability of the MPs to endocytose ovalbumin as soon as 24 h and even further at 7 days poststimulation. The fact that the capacity of the cells to take up CpGs was not attenuated indicates that the CpG stimulation affected only specific endocytic pathways, likely mannose receptor- or scavenger receptor-mediated endocytosis.

Upon maturation, DCs upregulate surface MHCII but lose their ability to take up and process soluble antigen (38, 39). In the current work, the downregulation of the capacity of CpG-stimulated MPs to take up ovalbumin may be considered as an indication that these APCs underwent a similar process of maturation. However, the transient upregulation followed by downregulation of surface MHCII expression after 7 days of treatment with CpGs indicated that during cultivation, the cells developed an exhausted or tolerogenic phenotype which was confirmed by the loss of their allostimulatory activity. It is not likely that this was due to reduced viability or a general loss of functionality since the cells retained ability to take up CpGs and to accumulate them in TLR9-positive endocytic compartments. In addition, although the cells responded to restimulation with Gardiquimod by upregulating fewer genes as compared to cell that had not been pretreated, they were still able to upregulate expression of a number of proinflammatory mediators. This indicates that the CpG-pretreated salmon MPs are not exhausted *per se* but, as reported elsewhere, might have been reprogrammed to respond differently to secondary stimuli (37).

Obviously, the MHCII downregulation was due to suppression of MHCII biosynthesis in CpG-stimulated MPs since the MHCII-β protein levels were downregulated not only on the cell surface but also in the whole lysates as demonstrated by the WB analysis. Similarly, stimulation of mouse peritoneal macrophages with CpGs downregulated the biosynthesis and the surface expression of MHCII (40). However, in that study the MHCII downregulation was observed after a relatively short stimulation (18 h) and, unlike in the current work, the treatment did not suppress the antigen uptake capacity of murine macrophages.

It has been shown that human monocytes differentiated into DCs with GM-CSF and IL-4 in the presence of TLR ligands develop a tolerogenic phenotype (41). This was due to downregulation of surface MHCII and upregulation of B7-H1, a suppressor of T-cell activation and a marker for tolerogenic DCs (42). Likewise, we found that the mRNA of *B7-H1*

was upregulated in CpG-treated MPs, while the costimulatory molecule *CD80/CD86* was, on the contrary, downregulated. Furthermore, *TNFRSF6B*, a secreted TNF decoy receptor which is known for its capacity to induce tolerogenic phenotype in DCs and macrophages (43, 44) was also upregulated in these cells. Since in the current study, there was no concurrent treatment with GM-CSF, we cannot claim that we have obtained tolerogenic DCs; nevertheless, our data indicates that at least some of the mechanisms that control the differentiation and the maturation of professional APCs in presence of TLR ligands are conserved between teleosts and mammals.

Gardiquimod is a TLR7/8 ligand and, in the current study, it induced high expression of both proinflammatory genes as well as IFNs and IFN-stimulated genes (ISGs). As mentioned above, in cells pretreated with CpGs and polyI:C, Gardiquimod upregulated fewer genes as compared to non-pretreated cells. Furthermore, the level of upregulation of many genes in the former samples was generally lower as compared to the latter. A possible explanation for this is that the effect of Gardiquimod was likely influenced by autocrine factors. In this regard, it is possible that the attenuated induction of many of the genes we have observed might be due to modulation of IFN and cytokine receptor signaling. For example, *SOCS1,* which was highly upregulated in the CpG–treated cells inhibits the signaling initiated by type I and II IFN as well as cytokines which signal through the common gamma chain subunit of the interleukin (IL)-2 receptor (45). A strong negative regulatory activity on IFNa1 and IFN-γ signaling has also been exhibited by Atlantic salmon SOCS1 (46). It has been found that *SOCS1* expression can be upregulated directly by CpGs through a STAT-independent mechanism, a process which resulted in suppression of IFN-γ-, IL-6-, and GM-CSF-induced STAT1 phosphorylation and prevented the upregulation of MHCII in murine macrophages (47). Furthermore, it has also been demonstrated that TLR-induced SOCS1 expression in DC precursors leads to a blockade of DC differentiation (48).

Another factor that might have been involved in attenuated gene upregulation by autocrine factors is CD45. This is a protein tyrosine phosphatase receptor which, like SOCS1, is involved in negative regulation of cytokine and IFN receptor signaling (49). In the current study, the protein analysis indicated that the CD45 protein was highly expressed on the surface of CpG-treated cells since the molecule was identified in a high molecular weight band upregulated by the CpG stimulation. The Gardiquimod restimulation induced expression of both type I *IFN* and *IFN-γ* and therefore, the attenuated upregulation of ISGs in CpG-pretreated cells might be, at least in part, due to the inhibitory action of proteins such as SOCS1 and CD45 on the autocrine cytokine signaling. On the other hand, the high expression of ISGs in CpG-treated cells may be explained with elevated expression of IFN-regulatory factors (IRFs), such as *IRF3* and *IRF7* which themselves are ISGs. As we have already shown, overexpression of transgenic salmon *IRF3* and *7* in different salmonid cell lines is able to activate ISRE-dependent promoter elements which are essential for the induction of ISGs (50).

In addition to CD45, the surface protein analysis identified clathrin heavy chain in a down-regulated band and GRP78 and HSP70 in a band that appeared to be upregulated by the CpG treatment. Clathrin is a major protein involved in receptor-mediated endocytosis (51) and its downregulation might be related to the suppression of the antigen uptake capacity in CpG-treated cells. GRP78 and HSP70 are both members of the family of the HSP70 heat shock proteins and function in the endoplasmic reticulum as molecular chaperones. In addition, it has been found that these proteins are secreted and have been implicated in suppression of the allostimulatory capacity of APCs (52, 53). Therefore, HSP70 and GRP78 may have contributed to the reduced allostimulatory capacity of salmon MPs stimulated with CpGs. The downregulation of clathrin and the binding of HSP70 and GRP78 to the surface of CpG-treated salmon MPs need to be confirmed using specific antibodies and might be an interesting objective for future studies.

In summary, CpGs induced *in vitro* differentiation of salmon MPs into cells with dendritic morphology, an M1 transcriptional profile but exhausted allostimulatory phenotype and functions. These findings demonstrate that, despite the poor phylogenetic conservation of the growth factors involved in the differentiation of DCs, the major processes that orchestrate the effects of TLR ligands on the development of APCs are conserved between teleosts in mammals. These data also emphasize on the fact that the potent immunostimulatory properties of a TLR ligand would not necessarily translate into enhanced APC functions and highlight the complexity of the activation of fish immune cells by TLR ligands which may be used as potential adjuvants in the aquaculture.

DATA AVAILABILITY

The microarray data presented in this publication has been deposited in the NCBI's Gene Expression Omnibus (GEO, https://www.ncbi.nlm.nih.gov/geo/) and is available under the accession number GSE126993.

AUTHOR CONTRIBUTIONS

DI designed, performed experiments, analyzed data, and prepared the manuscript. JJ participated in experimental design, data analysis, and manuscript writing. LL and HT were involved in cell culture experiments and assisted with manuscript preparation. AK and SJ designed and performed the microarray analysis and assisted with data analysis, and manuscript preparation.

FUNDING

This study was supported by Aquaculture program of The Research Council of Norway (183196/S40 InNoVacc to JJ) and by funding from the Research Council of Norway (Project No.: 230735/F20) to DI.

ACKNOWLEDGMENTS

The authors would like to thank Toril A. Grønset for the mass spectrometry analysis which was performed at The Tromsø University Proteomic Platform.

SUPPLEMENTARY MATERIAL

The Supplementary Material for this article can be found online at: https://www.frontiersin.org/articles/10.3389/fimmu.2019.00378/full#supplementary-material

REFERENCES

1. Hamilos Dl. Antigen presenting cells. *Immunol Res.* (1989) 8:98–117. doi: 10.1007/BF02919073
2. Thery C, Amigorena S. The cell biology of antigen presentation in dendritic cells. *Curr Opin Immunol.* (2001) 13:45–51. doi: 10.1016/S0952-7915(00)00180-1
3. Corsaro C, Scalia M, Leotta N, Mondio F, Sichel G. Characterisation of kupffer cells in some amphibia. *J Anat.* (2000) 196 (*Pt* 2):249–61. doi: 10.1046/j.1469-7580.2000.19620249.x
4. Takahashi K. Development and differentiation of macrophages and related cells: historical review and current concepts. *J Clin Exp Hematop.* (2001) 41:1–31. doi: 10.3960/jslrt.41.1
5. Iliev Db, Liarte Cq, Mackenzie S, Goetz Fw. Activation of rainbow trout (Oncorhynchus mykiss) mononuclear phagocytes by different pathogen associated molecular pattern (Pamp) bearing agents. *Mol Immunol.* (2005) 42:1215–23. doi: 10.1016/j.molimm.2004.11.023
6. Pozzi LA, Maciaszek Jw, Rock Kl. Both dendritic cells and macrophages can stimulate naive Cd8 T cells *in vivo* to proliferate, develop effector function, and differentiate into memory cells. *J Immunol.* (2005) 175:2071–81. doi: 10.4049/jimmunol.175.4.2071
7. Hodgkinson JW, Grayfer L, Belosevic M. Biology of bony fish macrophages. *Biology.* (2015) 4:881–906. doi: 10.3390/biology4040881
8. Grayfer L, Kerimoglu B, Yaparla A, Hodgkinson JW, Xie J, Belosevic M. Mechanisms of fish macrophage antimicrobial immunity. *Front Immunol.* (2018) 9:1105. doi: 10.3389/fimmu.2018.01105
9. Steinman RM, Cohn ZA. Identification of a novel cell type in peripheral lymphoid organs of mice. I. morphology, quantitation, tissue distribution. *J Exp Med.* (1973) 137:1142–62. doi: 10.1084/jem.137.5.1142
10. Steinman RM, Hawiger D, Nussenzweig MC. Tolerogenic dendritic cells. *Annu Rev Immunol.* (2003) 21:685–711. doi: 10.1146/annurev.immunol.21.120601.141040
11. Caux C, Dezutter-Dambuyant C, Schmitt D, Banchereau J. GM-CSF and TNF-Alpha cooperate in the generation of dendritic langerhans cells. *Nature.* (1992) 360:258–61. doi: 10.1038/360258a0
12. Inaba K, Inaba M, Romani N, Aya H, Deguchi M, Ikehara S, et al. Generation of large numbers of dendritic cells from mouse bone marrow cultures supplemented with granulocyte/macrophage colony-stimulating factor. *J Exp Med.* (1992) 176:1693–702. doi: 10.1084/jem.176.6.1693
13. Sallusto F, Lanzavecchia A. Efficient presentation of soluble antigen by cultured human dendritic cells is maintained by granulocyte/macrophage colony-stimulating factor plus interleukin 4 and downregulated by tumor necrosis factor alpha. *J Exp Med.* (1994) 179:1109–18. doi: 10.1084/jem.179.4.1109
14. Weimershaus M, Van Endert P. Preparation of dendritic cells by *in vitro* cultures. *Methods Mol Biol.* (2013) 960:351–7. doi: 10.1007/978-1-62703-218-6_25
15. Zhou Lj, Tedder Tf. Cd14+ blood monocytes can differentiate into functionally mature Cd83+ dendritic cells. *Proc Natl Acad Sci USA.* (1996) 93:2588–92. doi: 10.1073/pnas.93.6.2588
16. Lovy J, Wright GM, Speare DJ. Comparative cellular morphology suggesting the existence of resident dendritic cells within immune organs of salmonids. *Anat Rec.* (2008) 291:456–62. doi: 10.1002/ar.20674
17. Lovy J, Savidant GP, Speare DJ, Wright GM. Langerin/Cd207 positive dendritic-like cells in the haemopoietic tissues of salmonids. *Fish Shellfish Immunol.* (2009) 27:365–8. doi: 10.1016/j.fsi.2009.01.006
18. Aghaallaei N, Bajoghli B, Schwarz H, Schorpp M, Boehm T. Characterization of mononuclear phagocytic cells in medaka fish transgenic for A Cxcr3a:Gfp reporter. *Proc Natl Acad Sci USA.* (2010) 107:18079–84. doi: 10.1073/pnas.1000467107
19. Lugo-Villarino G, Balla KM, Stachura DL, Banuelos K, Werneck MB, Traver D. Identification of dendritic antigen-presenting cells in the zebrafish. *Proc Natl Acad Sci USA.* (2010) 107:15850–5. doi: 10.1073/pnas.1000494107
20. Granja AG, Leal E, Pignatelli J, Castro R, Abos B, Kato G, et al. Identification of teleost skin Cd8alpha+ dendritic-like cells, representing a potential common ancestor for mammalian cross-presenting dendritic cells. *J Immunol.* (2015) 195:1825–37. doi: 10.4049/jimmunol.1500322
21. Soleto I, Fischer U, Tafalla C, Granja AG. Identification of a potential common ancestor for mammalian cross-presenting dendritic cells in teleost respiratory surfaces. *Front Immunol.* (2018) 9:59. doi: 10.3389/fimmu.2018.00059
22. Mckenna HJ, Stocking KL, Miller RE, Brasel K, De Smedt T, Maraskovsky E, et al. Mice lacking Flt3 ligand have deficient hematopoiesis affecting hematopoietic progenitor cells, dendritic cells, and natural killer cells. *Blood.* (2000) 95:3489–97.
23. Keestra AM, De Zoete MR, Bouwman LI, Van Putten JP. Chicken Tlr21 is an innate Cpg DNA receptor distinct from mammalian Tlr9. *J Immunol.* (2010) 185:460–7. doi: 10.4049/jimmunol.0901921
24. Iliev DB, Skjaeveland I, Jorgensen JB. Cpg oligonucleotides bind Tlr9 and Rrm-containing proteins in atlantic salmon (Salmo Salar). *BMC Immunol.* (2013a) 14:12. doi: 10.1186/1471-2172-14-12
25. Iliev DB, Jorgensen SM, Rode M, Krasnov A, Harneshaug I, Jorgensen JB. Cpg-induced secretion of mhciibeta and exosomes from salmon (Salmo Salar) APCS. *Dev Comp Immunol.* (2010) 34:29–41. doi: 10.1016/j.dci.2009.07.009
26. Skjaeveland I, Iliev DB, Zou J, Jorgensen T, Jorgensen JB. A Tlr9 homolog that is up-regulated by Ifn-gamma in atlantic salmon (Salmo salar). *Dev Comp Immunol.* (2008) 32:603–7. doi: 10.1016/j.dci.2007.10.011
27. Iliev DB, Thim H, Lagos L, Olsen R, Jorgensen JB. Homing of antigen-presenting cells in head kidney and spleen - salmon head kidney hosts diverse APC types. *Front Immunol.* (2013b) 4:137. doi: 10.3389/fimmu.2013.00137
28. Jenberie S, Thim HL, Sunyer JO, Skjodt K, Jensen I, Jorgensen JB. Profiling Atlantic salmon B cell populations: Cpg-mediated Tlr-ligation enhances Igm secretion and modulates immune gene expression. *Sci Rep.* (2018) 8:3565. doi: 10.1038/s41598-018-21895-9
29. Krasnov A, Timmerhaus G, Afanasyev S, Jorgensen SM. Development and assessment of oligonucleotide microarrays for atlantic salmon (*Salmo salar* L.). *Comp Biochem Physiol Part D Genomics Proteomics.* (2011) 6:31–8. doi: 10.1016/j.cbd.2010.04.006
30. Ploeger DT, Hosper NA, Schipper M, Koerts JA, De Rond S, Bank Ra. Cell plasticity in wound healing: paracrine factors Of M1/ M2 polarized macrophages influence the phenotypical state of dermal fibroblasts. *Cell Commun Signal.* (2013) 11:29. doi: 10.1186/1478-811X-11-29
31. Strandskog G, Ellingsen T, Jorgensen JB. Characterization Of three distinct Cpg oligonucleotide classes which differ in ability to induce Ifn alpha/beta activity and cell proliferation in Atlantic salmon (*Salmo salar* L.) leukocytes. *Dev Comp Immunol.* (2007) 31:39–51. doi: 10.1016/j.dci.2006.05.004
32. Tureci O, Bian H, Nestle FO, Raddrizzani L, Rosinski JA, Tassis A, et al. Cascades of transcriptional induction during dendritic cell maturation revealed by genome-wide expression analysis. *FASEB J.* (2003) 17:836–47. doi: 10.1096/fj.02-0724com
33. Stamenkovic I, Clark EA, Seed B. A B-lymphocyte activation molecule related to the nerve growth factor receptor and induced by cytokines in carcinomas. *Embo J.* (1989) 8:1403–10. doi: 10.1002/j.1460-2075.1989.tb03521.x
34. Hallek M, Lepisto EM, Slattery KE, Griffin JD, Ernst TJ. Interferon-gamma increases the expression of the gene encoding the beta subunit of the granulocyte-macrophage colony-stimulating factor receptor. *Blood.* (1992) 80:1736–42.

35. Li Y, Lee PY, Kellner ES, Paulus M, Switanek J, Xu Y, et al. Monocyte surface expression of Fcgamma receptor Ri (Cd64), a biomarker reflecting type-I interferon levels in systemic lupus erythematosus. *Arthritis Res Ther.* (2010) 12:R90. doi: 10.1186/ar3017
36. Chang CJ, Sun B, Robertsen B. Adjuvant activity of fish type I interferon shown in a virus DNA vaccination model. *Vaccine.* (2015) 33:2442–8. doi: 10.1016/j.vaccine.2015.03.093
37. Swetman Andersen CA, Handley M, Pollara G, Ridley AJ, Katz DR, Chain BM. Beta1-integrins determine the dendritic morphology which enhances Dc-sign-mediated particle capture by dendritic cells. *Int Immunol.* (2006) 18:1295–303. doi: 10.1093/intimm/dxl062
38. Askew D, Chu RS, Krieg AM, Harding CV. Cpg Dna induces maturation of dendritic cells with distinct effects on nascent and recycling Mhc-Ii antigen-processing mechanisms. *J Immunol.* (2000) 165:6889–95. doi: 10.4049/jimmunol.165.12.6889
39. Garrett WS, Chen LM, Kroschewski R, Ebersold M, Turley S, Trombetta S, et al. Developmental control of endocytosis in dendritic cells by Cdc42. *Cell.* (2000) 102:325–34. doi: 10.1016/S0092-8674(00)00038-6
40. Chu RS, Askew D, Noss EH, Tobian A, Krieg Am, Harding CV. Cpg oligodeoxynucleotides down-regulate macrophage class II Mhc antigen processing. *J Immunol.* (1999) 163:1188–94.
41. Wolfle SJ, Strebovsky J, Bartz H, Sahr A, Arnold C, Kaiser C, et al. Pd-L1 expression on tolerogenic APCs is controlled by Stat-3. *Eur J Immunol.* (2011) 41:413–24. doi: 10.1002/eji.201040979
42. Sumpter TL, Thomson AW. The status Of Pd-L1 (B7-H1) on tolerogenic APCs. *Eur J Immunol.* (2011) 41:286–90. doi: 10.1002/eji.201041353
43. Hsu TL, Chang YC, Chen SJ, Liu YJ, Chiu AW, Chio CC, et al. Modulation of dendritic cell differentiation and maturation by decoy receptor 3. *J Immunol.* (2002) 168:4846–53. doi: 10.4049/jimmunol.168.10.4846
44. Chang YC, Hsu TL, Lin HH, Chio CC, Chiu AW, Chen NJ, et al. Modulation of macrophage differentiation and activation by decoy receptor 3. *J Leukoc Biol.* (2004) 75:486–94. doi: 10.1189/jlb.0903448
45. Linossi EM, Babon JJ, Hilton DJ, Nicholson SE. Suppression of cytokine signaling: the SOCS perspective. *Cytokine Growth Factor Rev.* (2013) 24:241–8. doi: 10.1016/j.cytogfr.2013.03.005
46. Skjesol A, Liebe T, Iliev DB, Thomassen EI, Tollersrud LG, Sobhkhez M, et al. Functional conservation of suppressors of cytokine signaling proteins between teleosts and mammals: atlantic salmon SOCS1 binds to Jak/Stat family members and suppresses type I and II Ifn signaling. *Dev Comp Immunol.* (2014) 45:177–89. doi: 10.1016/j.dci.2014.02.009
47. Dalpke AH, Opper S, Zimmermann S, Heeg K. Suppressors of cytokine signaling (SOCS)-1 and SOCS-3 are induced by CPG-DNA and modulate cytokine responses in APCs. *J Immunol.* (2001) 166:7082–9. doi: 10.4049/jimmunol.166.12.7082
48. Bartz H, Avalos NM, Baetz A, Heeg K, Dalpke AH. Involvement of suppressors of cytokine signaling in toll-like receptor-mediated block of dendritic cell differentiation. *Blood.* (2006) 108:4102–8. doi: 10.1182/blood-2006-03-008946
49. Irie-Sasaki J, Sasaki T, Matsumoto W, Opavsky A, Cheng M, Welstead G, et al. Cd45 is a JAK phosphatase and negatively regulates cytokine receptor signalling. *Nature.* (2001) 409:349–54. doi: 10.1038/35053086
50. Iliev DB, Sobhkhez M, Fremmerlid K, Jorgensen JB. Myd88 interacts with interferon regulatory factor (Irf) 3 and IRF7 in Atlantic salmon (Salmo salar): transgenic SSMYD88 modulates the IRF-induced type I interferon response and accumulates in aggresomes. *J Biol Chem.* (2011) 286:42715–24. doi: 10.1074/jbc.M111.293969
51. Mcmahon HT, Boucrot E. Molecular mechanism and physiological functions of clathrin-mediated endocytosis. *Nat Rev Mol Cell Biol.* (2011) 12:517–33. doi: 10.1038/nrm3151
52. Corrigall VM, Bodman-Smith MD, Brunst M, Cornell H, Panayi Gs. Inhibition of antigen-presenting cell function and stimulation of human peripheral blood mononuclear cells to express an antiinflammatory cytokine profile by the stress protein bip: relevance to the treatment of inflammatory arthritis. *Arthritis Rheum.* (2004) 50:1164–71. doi: 10.1002/art.20134
53. Stocki P, Wang XN, Dickinson AM. Inducible heat shock protein 70 reduces T cell responses and stimulatory capacity of monocyte-derived dendritic cells. *J Biol Chem.* (2012) 287:12387–94. doi: 10.1074/jbc.M111.307579

Conflict of Interest Statement: HT is currently employed by Vaxxinova Norway. AK and SJ were employed at Nofima Marin AS.

The remaining authors declare that the research was conducted in the absence of any commercial or financial relationships that could be construed as a potential conflict of interest.

Copyright © 2019 Iliev, Lagos, Thim, Jørgensen, Krasnov and Jørgensen. This is an open-access article distributed under the terms of the Creative Commons Attribution License (CC BY). The use, distribution or reproduction in other forums is permitted, provided the original author(s) and the copyright owner(s) are credited and that the original publication in this journal is cited, in accordance with accepted academic practice. No use, distribution or reproduction is permitted which does not comply with these terms.

frontiers in Immunology

ORIGINAL RESEARCH
published: 26 March 2019
doi: 10.3389/fimmu.2019.00584

CpG Oligodeoxynucleotides Modulate Innate and Adaptive Functions of IgM$^+$ B Cells in Rainbow Trout

*Rocío Simón, Patricia Díaz-Rosales, Esther Morel, Diana Martín, Aitor G. Granja and Carolina Tafalla**

Fish Immunology and Pathology Laboratory, Animal Health Research Center (CISA-INIA), Madrid, Spain

Oligodeoxynucleotides (ODN) containing unmethylated CpG motifs have been widely postulated as vaccine adjuvants both in mammals and teleost fish. However, to date, the effects that CpGs provoke on cells of the adaptive immune system remain mostly unexplored in fish. Given that rainbow trout (*Oncorhynchus mykiss*) IgM$^+$ B cells from spleen and blood transcribe high levels of toll like receptor 9 (TLR9), the receptor responsible for CpG detection in mammals, in the current work, we have investigated the effects of CpGs on both spleen and blood IgM$^+$ B cells from this species. CpGs were shown to exert strong proliferative effects on both spleen and blood IgM$^+$ B cells, also increasing their survival. The fact that CpGs increase the size of IgM$^+$ B cells, reduce the expression of surface IgM and IgD and up-regulate the number of IgM-secreting cells strongly suggest that IgM$^+$ B cells differentiate to plasmablasts/plasma cells in response to CpG stimulation. Additionally, CpGs were shown to modulate the antigen presenting capacities of trout IgM$^+$ B cells through an increased surface MHC II expression and transcriptional up-regulation of co-stimulatory molecules, although in this case, significant differences were observed between the effects exerted on spleen and blood cells. Similarly, differences were observed between spleen and blood IgM$^+$ B cells when CpG stimulation was combined with B cell receptor (BCR) cross-linking. Finally, CpGs were also shown to affect innate functions of teleost IgM$^+$ B cells such as their phagocytic capacity. These results demonstrate that CpGs regulate many adaptive and innate functions of teleost B cells, supporting their inclusion as adjuvants in novel vaccine formulations.

Keywords: teleost fish, rainbow trout, CpGs, B cells, IgM, phagocytosis

OPEN ACCESS

Edited by:
Brian Dixon,
University of Waterloo, Canada

Reviewed by:
Helen Dooley,
University of Maryland, Baltimore, United States
Stephanie DeWitte-Orr,
Wilfrid Laurier University, Canada

****Correspondence:***
Carolina Tafalla
tafalla@inia.es

Specialty section:
This article was submitted to Comparative Immunology, a section of the journal Frontiers in Immunology

Received: *05 December 2018*
Accepted: *05 March 2019*
Published: *26 March 2019*

Citation:
Simón R, Díaz-Rosales P, Morel E, Martín D, Granja AG and Tafalla C (2019) CpG Oligodeoxynucleotides Modulate Innate and Adaptive Functions of IgM$^+$ B Cells in Rainbow Trout. Front. Immunol. 10:584. doi: 10.3389/fimmu.2019.00584

INTRODUCTION

At the initial phases of an infection, cells of the innate immune system detect pathogens through the recognition of common pathogen-associated molecular patterns (PAMPs) by germline-encoded pattern recognition receptors (PRRs). Among these PRRs, Toll-like receptors (TLRs) constitute a large family of PRRs, expressed either on the cell surface or the luminal side of intracellular vesicles such as endosomes or lysosomes. These receptors are capable of detecting a wide range of pathogen-associated molecules, such as unmethylated DNA, peptidoglycan, dsRNA, ssRNA, or bacterial lipopolysaccharide (LPS) among others (1).

Interestingly, B cells also express a variable range of TLRs that allow them to directly respond to microbial products, in addition to a clonally-rearranged B cell receptor (BCR) that will respond to specific antigens. Thus, this dual expression program provides B cells with the exclusive machinery to integrate at the same time antigen-specific and innate signals (2). However, in mammals, not all B cell subsets express all TLRs and therefore how each of these subsets responds to TLR ligands differs considerably. For example, in humans, naïve B cells express very low levels of TLRs whereas memory B cells constitutively express a wide range of TLRs through which they regulate their proliferation and differentiation (3). In mice, it has been shown that different subsets of B cells express a qualitatively similar but quantitatively different pattern of TLR transcripts, consequently responding differently to stimulation with TLR agonists (4).

In teleost fish, three main subsets of B cells are found in homeostasis. The main subset corresponds to B cells that co-express IgM and IgD on the cell surface (IgM^+ B cells) (5). These cells are found in lymphoid organs (spleen and head kidney), circulating blood, liver, adipose tissue and in mucosal surfaces (6, 7). Remarkably, these cells differ greatly in many aspects with mammalian conventional B2 cells, as they have been shown to share several phenotypic and functional traits of mammalian innate B1 cell populations (5). Additionally, cells that exclusively express IgD on the surface (IgD^+ cells) have been identified in rainbow trout (*Oncorhynchus mykiss*) gills (8) and catfish (*Ictalurus punctatus*) blood (9). Finally, an independent B cell linage that exclusively expresses IgT on the surface (IgT^+ cells) is also present in most fish species (10). IgT is a teleost-exclusive Ig and in the absence of IgA, IgT^+ B cells have been postulated as lymphocytes specialized in mucosal immunity based on the fact that the ratio of IgT^+ B cells to IgM^+ B cells is higher in mucosal surfaces, and because IgT responses to several parasites seemed to be confined to mucosal compartments (10–12).

To date, in teleost, the expression of TLRs has only been studied in IgM^+ B cells. Thus, in rainbow trout, IgM^+ B cells from different systemic and mucosal tissues were shown to transcribe all TLRs identified at that moment in this species (TLR1, TLR2, TLR3, TLR5, TLR7, TLR8, TLR9, and TLR22) (6). In Atlantic salmon (*Salmo salar*), IgM^+ B cells from lymphoid tissues were also shown to transcribe TLR3, TLR9, TLR8a1, TLR21, and TLR22 (13). Among these TLRs, mammalian TLR9 is responsible for the recognition of foreign DNA molecules from bacteria or viruses that contain short sequences of unmethylated CpG dinucleotides (14). The capacity of teleost TLR9 to respond to CpGs has been suggested based mainly on indirect transcriptional studies, however additional research is still required to unequivocally confirm that TLR9 is sensing CpG in these species (15). Based on structural characteristics, three classes of CpGs exist (A, B, and C), all of them with the capacity to stimulate TLR9, but with important differences in the effects they exert on different leukocyte subpopulations (16). In any case, the expression of TLR9 in teleost IgM^+ B cells seems to predict a responsiveness of these cells to CpGs, already demonstrated in Atlantic salmon by Jenberie et al. (13). In that study, it was revealed that the incubation of leukocyte cultures with CpGs up-regulated the transcription of secreted IgM, CD83 and CD40 in IgM^+ B cells. Furthermore, an up-regulation of IgM and MHC II protein levels in sorted IgM^+ B cells was also demonstrated by Western blot (13).

As mentioned above, in mammals, different B cell subsets respond differently to TLR ligation and these differences are also visible in what concerns TLR9 stimulation. Thus, in mice, although follicular B2 cells proliferate to a higher extent in response to CpGs than B1 cell subsets, only B1 and marginal zone (MZ) cells differentiate to plasma cells in response to TLR9 stimulation in the absence of BCR engagement (4). On the other hand, when BCR cross-linking is combined with TLR9 stimulation, murine B2 cells are able to proliferate and differentiate into class-switched plasma cells both *in vitro* and *in vivo* (17). In humans, on the other hand, although naïve B cells have the capacity to proliferate in response to CpGs alone (18), it is IgM^+ memory B cells that are much more responsive to TLR9 stimulation in the absence of BCR engagement (19).

In this context, in the current work, we have expanded our knowledge on how teleost IgM^+ B cells respond to CpGs, by studying the effects of CpGs on a wide range of functions of rainbow trout IgM^+ B cells, including proliferation and survival, IgM secretion, surface expression of Igs and MHC II, phagocytic capacity, and responsiveness to BCR cross-linking. We have performed this study with both splenic and blood IgM^+ B cells, observing important differences in the way that these two cell subsets respond to CpGs. Given that CpGs have been postulated as possible adjuvants to be included in newly designed vaccination strategies for aquacultured fish, our results provide highly valuable information on the capacity that these molecules have to stimulate both innate and adaptive functions of teleost B cells.

MATERIALS AND METHODS

Experimental Fish

Healthy specimens of female rainbow trout (*Oncorhynchus mykiss*) of ∼50–70 g were obtained from Centro de Acuicultura El Molino (Madrid, Spain) and maintained at the animal facilities of the Animal Health Research Center (CISA-INIA, Instituto Nacional de Investigación y Tecnología Agraria y Alimentaria) in an aerated recirculating water system at 16°C with 12:12 h light/dark photoperiod. Fish were fed twice a day with a commercial diet (Skretting, Spain). Before any experimental procedure, fish were acclimatized to laboratory conditions for at least 2 weeks. All of the experiments described comply with the Guidelines of the European Union Council (2010/63/EU) for use of laboratory animals and have been approved by the INIA Ethics committee (Code CEEA PROEX002/17).

Tissue Sampling

Rainbow trout were killed by benzocaine (Sigma) overdose and blood and spleen collected. Blood was extracted with a heparinized needle from the caudal vein and diluted 10 times with Leibovitz medium (L-15, Thermo Fisher Scientific) supplemented with 100 IU/ml penicillin and 100 µg/ml streptomycin (P/S, Thermo Fisher Scientific), 5% fetal calf serum (FCS, Thermo Fisher Scientific) and 10 IU/ml heparin

(Sigma). Spleen was collected and single cell suspensions were obtained using 100 μm nylon cell strainer (BD Biosciences) and L-15 medium supplemented with antibiotics, 5% FCS and heparin. Blood cell suspensions were placed onto 51% Percoll (GE Healthcare) cushions whereas spleen suspensions were placed onto 30/51% discontinuous Percoll density gradients. All gradients were then centrifuged at 500 × *g* for 30 min at 4°C. The interface cells were collected, washed twice in L-15 containing antibiotics and 5% FCS and adjusted to 2×10^6 cells/ml.

Cell Stimulation

Total leukocyte populations from spleen or blood were cultured at 20°C in L-15 medium supplemented with antibiotics and 5% FCS in 24 or 96-well plates (Nunc). Different stimuli were added to the media and cells were incubated for different time periods depending on specific experiments. The phosphorothioate-modified B class CpG oligodeoxynucleotide (ODN) 1668 (InvivoGen) containing one CpG dinucleotide (CpG) (5′-tccatgaCGttcctgatgct-3′) was used at a final concentration of 5 μM after having determined the optimal concentration based on their positive effect on B cell survival, specifically choosing the concentration that provoked the higher B cell survival after 72 h of incubation (data not shown). The non-CpG ODN 1668 (that contains GpC dinucleotides instead of CpGs) (5′-tccatgaGCttcctgatgct-3′) was used as a negative control (non-CpG) at the same concentration. In some experiments, leukocytes were stimulated with an unlabeled monoclonal antibody (mAb) against trout IgM (clone 1.14, mouse IgG1) (20) at a final concentration of 10 μg/ml as previously described (5). Non-stimulated controls were always included.

B Cell Proliferation

The Click-iT Plus EdU Flow Cytometry Assay Kit (Sigma) was used to measure the proliferation of IgM^+ B cells following manufacturer's instructions. Briefly, blood and spleen leukocyte suspensions at a concentration of 2×10^6 cells per ml were incubated in 96-well plates for 3 days at 20°C with different stimuli depending on the specific experiment as described above. Thereafter, 5-ethynyl-2′-deoxyuridine (EdU) was added to the cultures at a final concentration of 1 μM and the cells were incubated for an additional 24 h. After that time, stimulated and unstimulated cells were collected and stained with anti-IgM (1.14) coupled to allophycocyanin (1 μg/ml) for 20 min at 4°C. Whenever cells had been stimulated with anti-IgM, the cells were only labeled with EdU (1 μM) as described above. The incorporation of EdU to the DNA was determined following the manufacturer's instructions and then analyzed by flow cytometry in a FACS Calibur flow cytometer (BD Biosciences) equipped with CellQuest Pro software (BD Biosciences). Flow cytometry analysis was performed with FlowJo V10 (TreeStar).

ELISPOT Analysis

ELISPOT plates containing Inmobilon-P membranes (Millipore) were activated with 70% ethanol for 30 s, coated with an anti-IgM mAb (clone 4C10) at 2 μg/ml in phosphate buffer saline (PBS) and incubated overnight at 4°C. To block non-specific binding to the membrane, plates were then incubated with 2% bovine serum albumin (BSA) in PBS for 2 h at RT. Leukocyte suspensions from spleen or blood of individual fish that had been stimulated with CpG or non-CpG at 5 μM for 72 h at 20°C or left unstimulated in the same conditions were then added to the wells in triplicate at a concentration of 5×10^4 cells per well. After 24 h of incubation at 20°C, cells were washed away five times with PBS and plates blocked again with 2% BSA in PBS for 1 h at RT. After blocking, biotinylated anti-IgM mAb (clone 4C10) was added to the plates and incubated at 1 μg/ml for 1 h at RT. Following additional washing steps (five times in PBS), the plates were developed using streptavidin-HRP (Thermo Scientific) at RT for 1 h, washed again with PBS and incubated with 3-amino-9-ethylcarbazole (Sigma Aldrich) for 30 min at RT in the dark. Substrate reaction was stopped by washing the plates with water. Once the membranes had dried, they were digitally scanned and the number of spots in each well-determined using an AID iSpot Reader System (Autoimmun Diagnostika GMBH).

Flow Cytometry

Blood or spleen leukocytes seeded in 96-well plates at a density of 2×10^6 cells per ml were incubated for 72 h at 20°C with 5 μM CpG, 5 μM non-CpG or media alone. After the incubation period, cells were washed in staining buffer (PBS containing 1% FCS and 0.5% sodium azide) and co-incubated with FITC-conjugated anti-IgM (1.14) (1 μg/ml) and specific mAbs against trout MHC II β-chain (mAb mouse IgG_1 coupled to allophycocyanin, 2 μg/ml) or trout IgD (mAb mouse IgG_1 coupled to allophycocyanin, 10 μg/ml) previously characterized (21, 22). Thereafter, cells were washed twice with the same buffer and analyzed in a FACS Calibur flow cytometer equipped with CellQuest Pro software. Flow cytometry analysis was performed with FlowJo V10. In these cultures, cell survival was estimated determining the percentage of live IgM^+ B cells in the cultures after counterstaining the cells with 1 μg of Propidium iodide (Invitrogen).

Cell Sorting

IgM^+ B cells were isolated from blood and spleen leukocyte cultures by flow cytometry using a BD FACSAria III cell sorter (BD Biosciences). For this purpose, spleen and blood leukocytes were first seeded in 24-well plates at a density of 2×10^6 cells per ml and incubated for 24 h at 20°C with 5 μM CpG, 5 μM non-CpG, or media alone. After that time, cells were collected and incubated for 20 min at 4°C with an anti-IgM (1.14) mAb coupled to allophycocyanin in staining buffer. Following two washing steps, cells were resuspended in staining buffer and IgM^+ B cells isolated based on their FSC/SSC profiles (to exclude the granulocyte gate) and then on the basis of the fluorescence emitted by the anti-IgM antibody coupled to allophycocyanin. Approximately 70.000 IgM^+ B cells and the same amount of IgM^- cells were collected in PBS for subsequent RNA isolation.

To confirm a direct effect of CpGs on IgM^+ B cells, spleen and blood leukocytes were incubated for 20 min at 4°C with a biotinilated Fab fragment of anti-IgM 1.14 (to avoid cell activation) in staining buffer. Following two washing steps, Streptavidin-Phycoerythrin (PE) (BD Pharmingen) was added. After 20 min at 4°C, cells were

resuspended in staining buffer and IgM$^+$ B cells isolated as described above. Sorted IgM$^+$ B cells were then incubated with 5 μM CpG, 5 μM non-CpG, or media alone for 3 days at 20°C. After this time, cells were stained with anti-MHC II mAb coupled to allophycocyanin, counterstained with 0.2 μg/ml DAPI, and analyzed on a FACS Celesta flow cytometer (BD Biosciences).

Real Time PCR Analysis

Total RNA was isolated from FACS isolated IgM$^+$ B cell populations using the Power SYBR Green Cells-to-Ct Kit (Invitrogen) following the manufacturer's instructions. RNA was treated with DNase during the process to remove genomic DNA that might interfere with the PCR reactions. Reverse transcription was also performed using the Power SYBR Green Cells-to-Ct Kit following the manufacturer's instructions. To evaluate the levels of transcription of the different genes, real-time PCR was performed with a LightCycler® 96 System instrument (Roche) using SYBR Green PCR core Reagents (Applied Biosystems) and specific primers previously described (**Table S1**). Samples obtained from individual fish were analyzed in duplicate under the following conditions: 10 min at 95°C, followed by 40 amplification cycles (15 s at 95°C and 1 min at 60°C). A melting curve for each primer set was obtained by reading fluorescence every degree between 60 and 95°C to ensure that only a single PCR product had been amplified. The expression of individual genes was normalized to the relative expression of the housekeeping gene β-actin, and the expression levels were calculated using the 2-ΔCt method, where ΔCt is determined by subtracting the actin value from the target Ct (Ct cut-off set to 38). β-actin was selected as reference gene according to the MIQE guidelines (23) given that no statistical differences were detected among Ct values obtained for β-actin in the different samples. In any case, all results were confirmed using another reference gene, elongation factor 1α (EF-1α). Negative controls with no template and *minus* reverse transcriptase controls were included in all the experiments.

Phagocytic Activity

To analyze the effect of CpGs on the phagocytic capacity of spleen and blood IgM$^+$ B cells, spleen and blood leukocytes were seeded in 24-well plates at a cell density of 2×10^6 cells per well and incubated for 48 h at 20°C with the appropriate stimuli (5 μM CpG, 5 μM non-CpG, or media alone). After 48 h, the cells were collected and resuspended in L-15 medium without serum. The cells were then incubated for 3 h at 20°C with fluorescent beads (FluoSpheres® Microspheres, 1.0 μm, Crimson Red Fluorescent 625/645, 2% solids; Thermo Fisher Scientific) at a cell:bead ratio of 1:10 as described before (24). After the incubation period, cells were harvested by gently pipetting, and non-ingested beads were removed by centrifugation ($100 \times g$ for 10 min at 4°C) over a cushion of 3% (weight/volume) BSA (Fraction V; Fisher Scientific) in PBS supplemented with 4.5% (weight/volume) D-glucose (Sigma). Cells were then resuspended in staining buffer, labeled with anti-IgM-FITC (1.14) (1 μg/ml) and analyzed on a FACS Calibur flow cytometer. In some experiments, cytochalasin B (0.05 μg/ml) was added to the cells immediately before the addition of the beads to verify active phagocytosis. Flow cytometry analysis was performed with FlowJo V10 software.

Statistical Analysis

Statistical analyses were performed to compare values obtained in each experimental group using a two-tailed paired Student's *t* test with Welch's correction when the F test indicated that the variances of both groups differed significantly. The differences between the mean values were considered significant on different degrees, where * means $p \leq 0.05$, ** means $p \leq 0.01$, and *** means $p \leq 0.005$.

RESULTS

CpGs Induce IgM$^+$ B Cell Proliferation and Survival

In mammals, type B CpGs are particularly efficient in promoting the proliferation and survival of naïve B cells in comparison to other stimuli such as poly I:C, LPS, or flagellin (25). Thus, we analyzed the lymphoproliferative effect of CpG ODNs (type B) in both rainbow trout splenocytes and blood leukocytes. Results obtained from these *in vitro* experiments clearly showed that rainbow trout splenic and blood IgM$^+$ B cells significantly proliferated in response to CpG treatment in comparison to the proliferation rates obtained in untreated cultures (Control) or cultures treated with non-CpG ODNs (non-CpG) (**Figures 1A,B**). Thus, both in spleen and in blood, CpGs increased both the percentage of proliferating IgM$^+$ B cells in relation to the total leukocyte population, as well as the percentage of proliferating IgM$^+$ B cells within the IgM$^+$ B cell compartment (**Figures 1A,B**). The fact that non-CpG ODNs did not have a stimulatory effect on lymphocyte proliferation rates strongly suggests that the lymphoproliferative effects exerted by CpGs on IgM$^+$ B cells are mediated through a CpG-specific TLR signaling. Interestingly, CpGs not only increased the percentage of proliferating IgM$^+$ B cells in the cultures (IgM$^+$EdU$^+$ cells) but also the percentage of IgM$^+$ B cells that were not proliferating (IgM$^+$EdU$^-$ cells) (**Figures 1A,B**), suggesting a positive effect of CpGs on IgM$^+$ B cell survival, independent of proliferation. The lymphoproliferative effects exerted by CpGs were not only visible on IgM$^+$ B cells, since IgM$^-$ cells also proliferated significantly in response to CpGs (**Figures 1A,B**). However, in the case of IgM$^-$ cells, non-CpG ODNs were also capable of provoking some degree of proliferation (**Figures 1A,B**), suggesting a less specific effect on these cells. In fact, in blood, IgM$^-$ cells proliferated in response to CpGs at rates that were not significantly different than those observed in response to non-CpG ODNs (**Figure 1B**).

CpGs Down-Regulate the Expression of IgM and IgD on the Surface of Rainbow Trout B Cells

We next studied whether CpG ODNs affected the expression levels of surface IgM and IgD on rainbow trout splenic as well as blood IgM$^+$ B cells. To assess this, we stimulated leukocyte cultures with CpG ODNs, non-CpG ODNs, or media alone for 72 h and afterwards we analyzed the levels of expression of

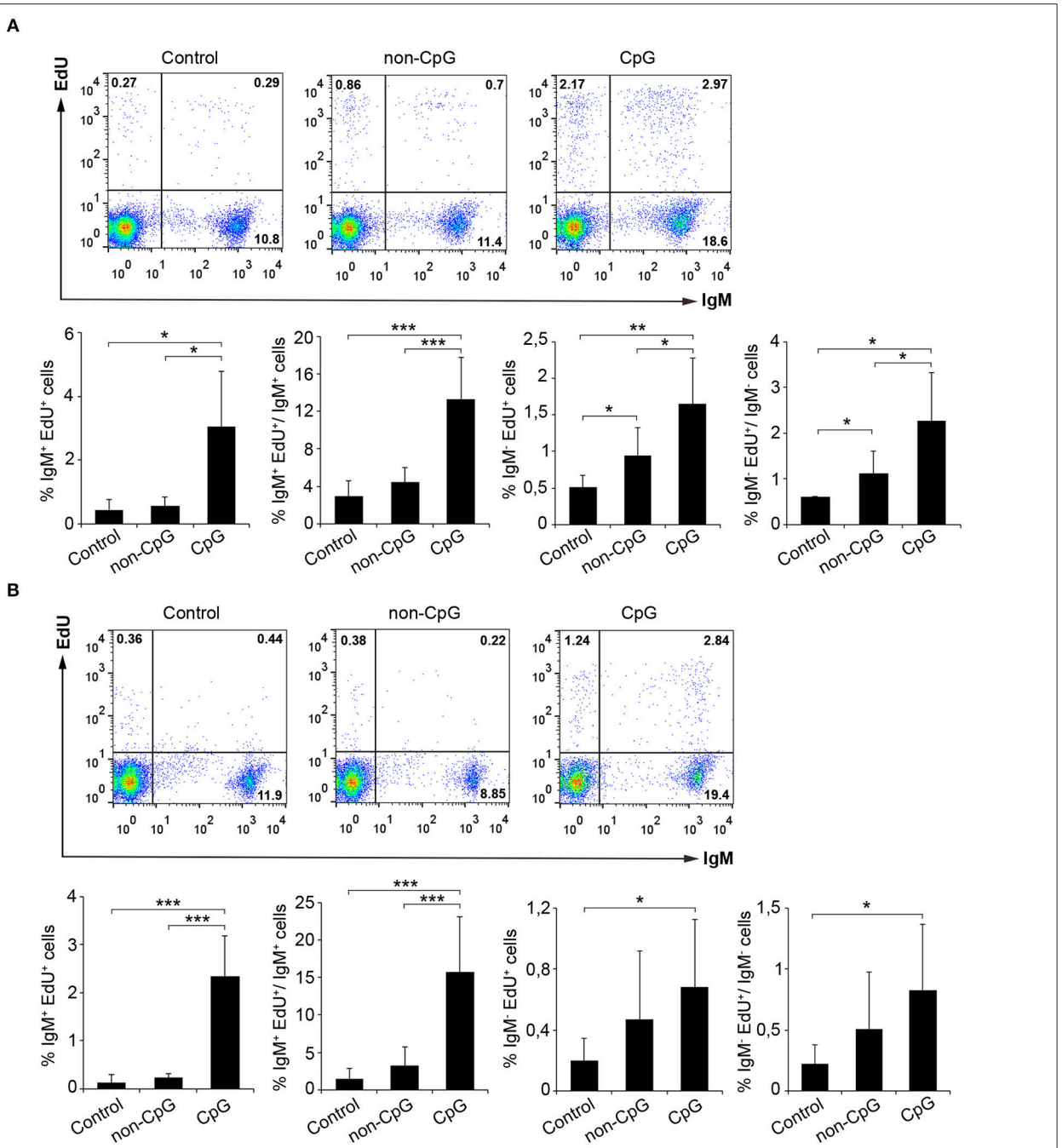


FIGURE 1 | CpGs induce B cell proliferation. The lymphoproliferative effects of CpGs were determined incubating spleen **(A)** or blood **(B)** leukocytes with CpG (5 μM), non-CpG (5 μM) or media alone (Control) during 3 days at 20°C. After this time, cells were labeled with EdU (1 μM) and incubated for a further 24 h. At that point, cells were labeled with anti-IgM mAb and the number of IgM^+ B cells with incorporated EdU (proliferating cells) determined as described in section Materials and Methods. Representative dot plots are included along with graphs showing the quantification of proliferating IgM^+ and IgM^- cells among total leukocytes or the corresponding IgM^+ or IgM^- populations (mean + SD) ($n = 6$ fish). Asterisks denote significantly different values between indicated groups (*$p \leq 0.05$, **$p \leq 0.01$, and ***$p \leq 0.005$).

membrane IgD and IgM by flow cytometry. At this point, it was evident that CpGs exerted a positive effect on IgM^+ B cell survival as the percentage of IgM^+ B cells in splenic or blood cultures increased 1.5 and 2 fold, respectively, in the presence of CpGs (**Figures 2A,D**). Furthermore, the levels of IgD and IgM on the cell surface were significantly reduced in IgM^+ B cells from CpG-treated cultures when compared to untreated cells, both in spleen and in blood (**Figures 2A–F**). Intriguingly, this effect was also observed when cultures were incubated with non-CpG ODNs (**Figures 2A–F**). In any case, this reduction of IgM and

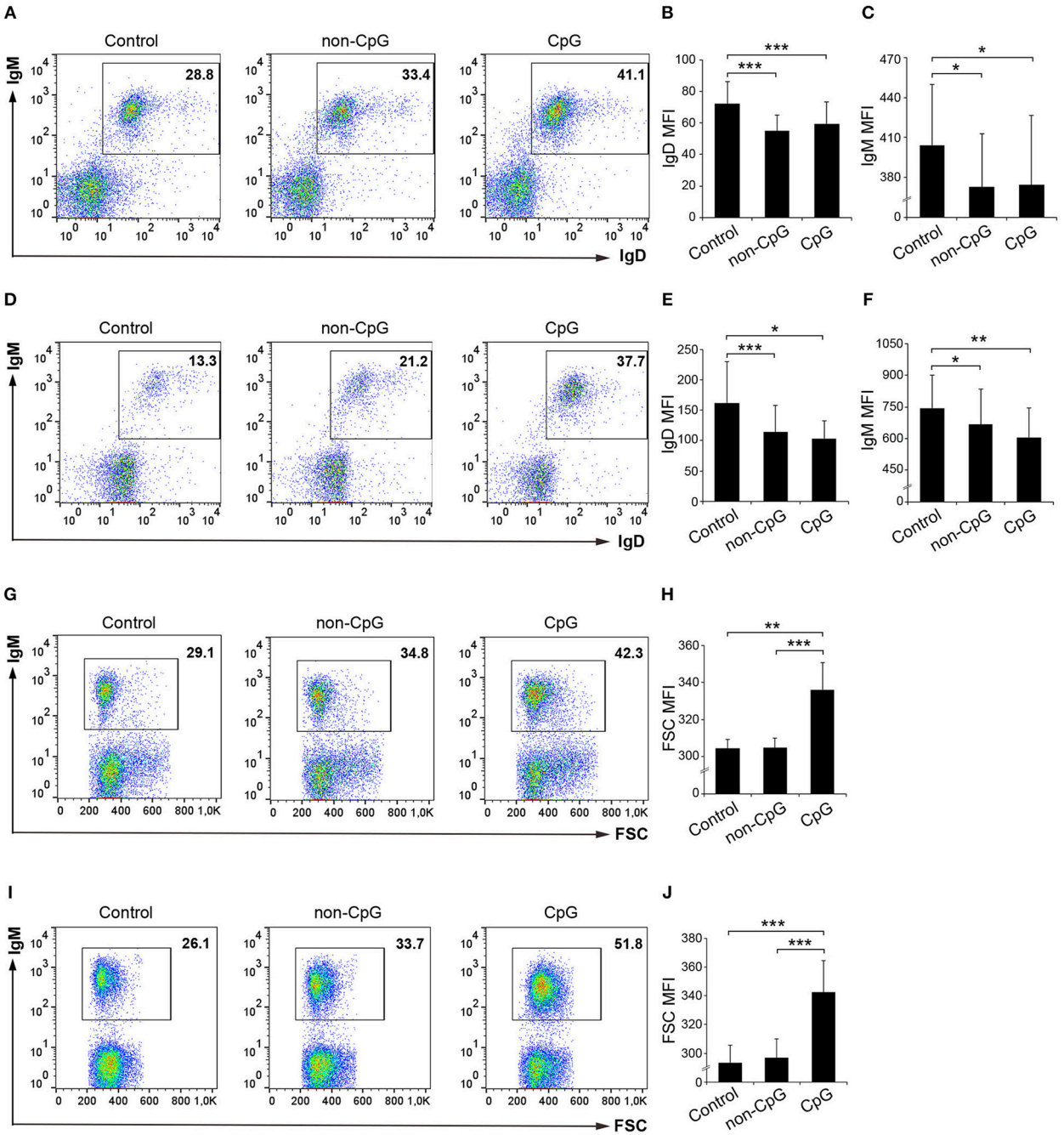


FIGURE 2 | Effect of CpG treatment on IgM and IgD surface expression and size. Spleen and blood leukocytes were incubated with CpG (5 μM), non-CpG (5 μM), or media alone (Control) during 3 days at 20°C. The levels of IgD and IgM surface expression on B cells were then measured via flow cytometry using a specific mAbs in spleen **(A–C)** and blood **(D–F)**. Representative dot plots from spleen **(A)** and blood **(B)** leukocytes are included along with graphs showing mean fluorescence intensity (MFI) values for IgD **(B,E)** and IgM **(C,F)** (mean + SD; $n = 5$ fish). In this experiment, the size of the B cells was also calculated. Representative dot plots from spleen **(G)** and blood **(I)** leukocytes showing the Forward scatter (FSC) of IgM$^+$ B cells are included along with graphs showing the FSC MFI values **(H,J)** (mean + SD; $n = 5$ fish). Asterisks denote significantly different values between indicated groups (*$p \leq 0.05$, **$p \leq 0.01$, and *** $p \leq 0.005$).

IgD surface expression could be indicating a differentiation of naïve B cells to plasmablasts/plasma cells given that throughout this differentiation process B cells lose IgD and reduce their IgM expression on the cell surface both in mammals and in fish (26, 27). As it is also known that throughout this differentiation process IgM$^+$ B cells also increase in size (26, 27), we also studied the effects of CpG on the size of IgM$^+$ B cells. We found a dramatic size increase of spleen and blood IgM$^+$ B cells in response to CpGs (**Figures 2G–J**). In this case, the increase was evident when compared to both untreated IgM$^+$ B cells

and IgM$^+$ B cells from cultures treated with non-CpG ODNs (**Figures 2G–J**), suggesting a specific effect.

In our general experimental design, total leukocytes populations were incubated with CpGs. Thus, it might have been possible that the effects exerted on IgM$^+$ B cells could have been a consequence of an indirect effect by stimulation of another leukocyte subset that secreted cytokines or factors that affected IgM$^+$ B cells upon activation. To rule out this possibility, we performed an additional experiment in which IgM$^+$ B cells were first sorted and then stimulated with CpGs. In this experiment, we confirmed that IgM$^+$ B cells directly sense CpGs. Sorted blood IgM$^+$ B cells stimulated with CpGs had a significantly increased survival rate when compared to IgM$^+$ B cells incubated with non-CpGs or media alone (**Figure S1**). Sorted splenic IgM$^+$ B cells, on the other hand, when stimulated with CpGs, increased their survival rate in comparison to unstimulated controls but not when compared to non-CpG-treated cultures (**Figure S1**). Both blood and spleen IgM$^+$ B cells significantly increased size in comparison to IgM$^+$ B cells incubated with non-CpGs or media alone (**Figure S1**).

CpGs Activate IgM Secretion in Naïve B Cells

In mice, CpGs alone have been shown to induce an increased IgM secretion by promoting the differentiation of innate B1 populations to plasma cells (4). Similarly, in rainbow trout, the incubation of trout spleen and blood leukocytes with CpG ODNs significantly increased the number of IgM-secreting cells after 3 days in comparison to the number of IgM-secreting cells found in non-stimulated or non-CpG treated cultures (non-CpG), as verified in an ELISPOT assay (**Figures 3A,B**).

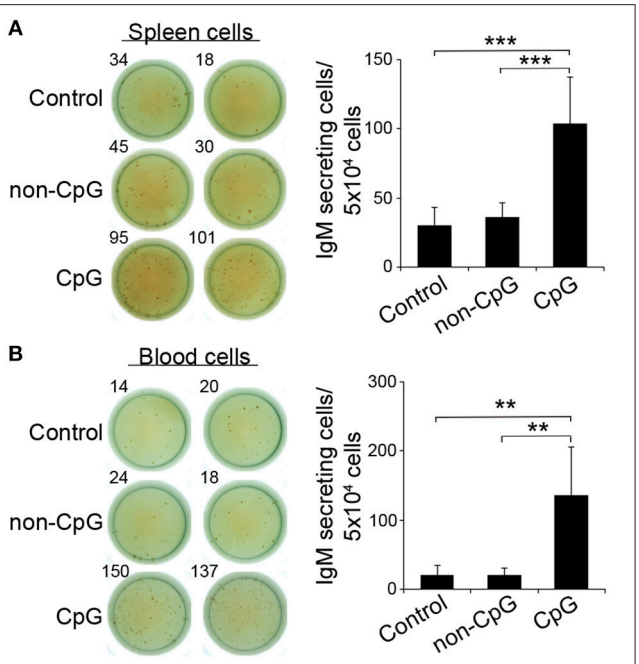


FIGURE 3 | CpGs increase the number of IgM-secreting cells. ELISPOT analysis of IgM-secreting cells in spleen **(A)** and blood **(B)** cultured cells treated with CpG (5 μM), non-CpG (5 μM), or media alone. Cells were cultured with the appropriate stimuli for 48 h and then plated in ELISPOT plates, previously coated with anti-IgM mAb (2 μg/ml) for a further 24 h. After incubation, cells were washed away and a biotinylated anti-IgM mAb (1 μg/ml) was used to detect number of spot forming cells. Duplicates for a representative individual (left) and quantification of spot forming cells (right) from 6 independent fish are shown (mean + SD). Asterisks denote significantly different values between indicated groups (**$p \leq 0.01$ and ***$p \leq 0.005$).

CpGs Up-Regulate the Surface Expression of MHC-II in Naïve Trout B Cells and Induce the Expression of Co-stimulatory Molecules

B cells are professional antigen-presenting cells (APCs) that constitutively express MHC II on the cell surface (28). Furthermore, fish IgM$^+$ B cells, as a consequence of their phagocytic activity, have been postulated as cells with increased presenting capacities than those of mammalian B cells (29). Thus, we also established whether CpGs could affect the expression of MHC II on the surface of rainbow trout splenic and blood IgM$^+$ B cells. Our results clearly show that CpGs significantly increased the levels of surface MHC II on IgM$^+$ B cells from spleen (**Figures 4A–C**). Interestingly, this increase in surface MHC II levels was not visible in splenic IgM$^-$ cells carrying MHC II on the cell surface (**Figure 4C**), which in this organ would mainly account for IgT$^+$ B cells (10). Furthermore, blood IgM$^+$ B cells did not regulate surface MHC II expression in response to CpGs in a significant fashion, given that the values obtained in CpG-treated cultures were not significantly different than those obtained in untreated cultures (**Figures 4D–F**). Despite the differential effect of CpGs on the levels of surface MHC II expression between the two populations studied when total leukocyte cultures were used, CpGs up-regulated the levels of transcription of co-stimulatory molecules in FACS isolated IgM$^+$ B cells from both spleen and blood (**Figures 4G,H**). Thus, stimulation with CpGs provoked that splenic and blood IgM$^+$ B cells upregulated CD83 and CD80/86, a molecule with similar homologies to both mammalian CD80 and CD86 (30) (**Figures 4G,H**). Furthermore, when sorted IgM$^+$ B cells were incubated with CpGs, a significant increase in surface MHC II levels was observed both in splenic and blood IgM$^+$ B cells (**Figure S1**).

CpGs Induce the Phagocytic Activity of IgM$^+$ B Cells

Teleost B cells, similarly to mammalian B1 cell subsets (31), have been shown to have a potent phagocytic activity (32). Therefore, we also investigated if CpG ODNs could have an effect on the capacity of IgM$^+$ B cells to phagocytose microparticles. To analyze this aspect, splenocytes and blood cells were incubated with CpG, non-CpG or with media alone for 48 h. After this time, 1 μm Crimson red-labeled polystyrene beads were added to the cultures and after 3 h of incubation the phagocytic activity of IgM$^+$ B cells determined through flow cytometry.

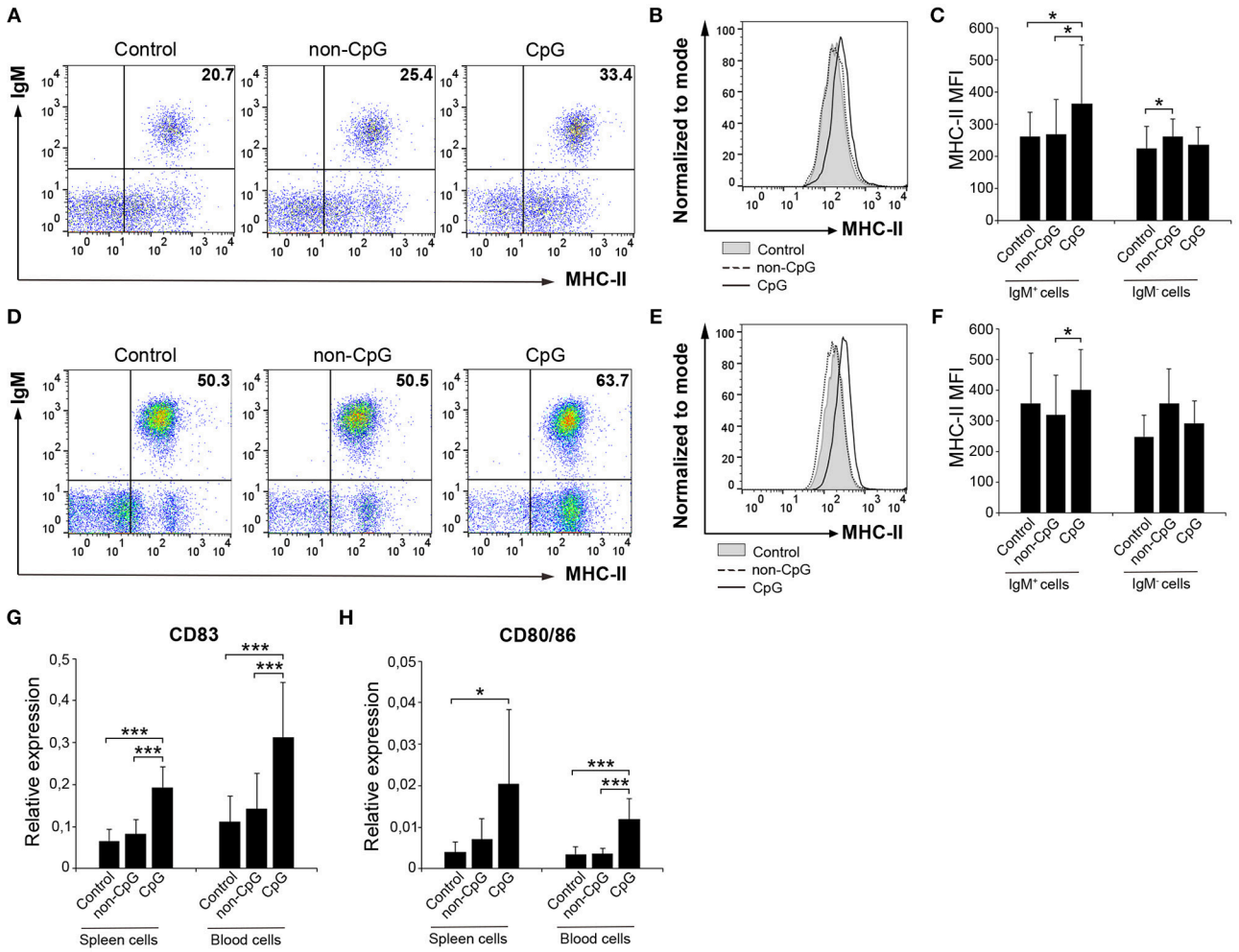


FIGURE 4 | CpGs upregulate MHC-II surface expression and increase the transcription of co-stimulatory molecules. Spleen and blood leukocytes were incubated with CpG (5 μM), non-CpG (5 μM), or media alone (Control) during 3 days at 20°C. The levels of MHC-II expression on the surface of IgM^+ B cells were then measured via flow cytometry using a specific mAb against trout MHC-II. Representative dot plots from spleen **(A)** and blood **(D)** leukocytes are included along with corresponding histograms **(B,E)**. Graphs showing MHC-II MFI values for IgM^+ and IgM^- cells in spleen **(C)** and blood **(F)** are also shown (mean + SD; $n = 7$ fish). Spleen and blood leukocytes were incubated with CpG (5 μM), non-CpG (5 μM), or media alone (Control) for 24 h at 20°C. IgM^+ cells were then isolated by flow cytometry and RNA extracted to determine the levels of transcription of CD83 **(G)** and CD80/86 **(H)** co-stimulatory genes. Gene expression data were normalized against the endogenous control gene β-actin and shown as relative expression (mean + SD; $n = 7$–9 fish). Asterisks denote significantly different values between indicated groups (*$p \leq 0.05$ and ***$p \leq 0.005$).

In spleen, we observed that the pre-stimulation of IgM^+ B cells with CpG ODNs significantly increased the percentage of phagocytic IgM^+ B cells in leukocyte cultures when compared to either unstimulated cultures or cultures treated with non-CpG ODNs (**Figures 5A,C**). Along with this increase in the percentage of phagocytic cells, the mean fluorescence intensity (MFI) of internalized beads in splenic IgM^+ B cells was significantly higher in CpG-treated cells compared to untreated cells (**Figure 5B**), indicating that the average number of particles internalized per IgM^+ B cell was higher when IgM^+ B cells were pre-stimulated. In concordance with this result, we found that the percentage of IgM^+ B cells with a high number of ingested beads (highly phagocytic IgM^+ B cells) was also higher in cultures treated with CpGs in comparison to untreated cultures (**Figure 5D**). Interestingly, in this case, the addition of non-CpG ODNs also increased the percentage of highly phagocytic IgM^+ B cells when compared to untreated cultures (**Figure 5D**). When we analyzed the effects the CpGs had on the IgM^- population from spleen, no significant differences between the values obtained in CpG-treated cultures and those obtained in untreated samples were found (**Figures 5E–G**), although in some cases differences between the values obtained in CpG-treated cultures and those of non-CpG-treated cultures were observed (**Figures 5E,G**).

In blood, the pre-incubation with CpGs also provoked a significant increase in the percentage of IgM^+ B cells with phagocytic capacities (**Figures 6A,C**), in the number of ingested beads per cell (**Figure 6B**) and in the percentage of highly

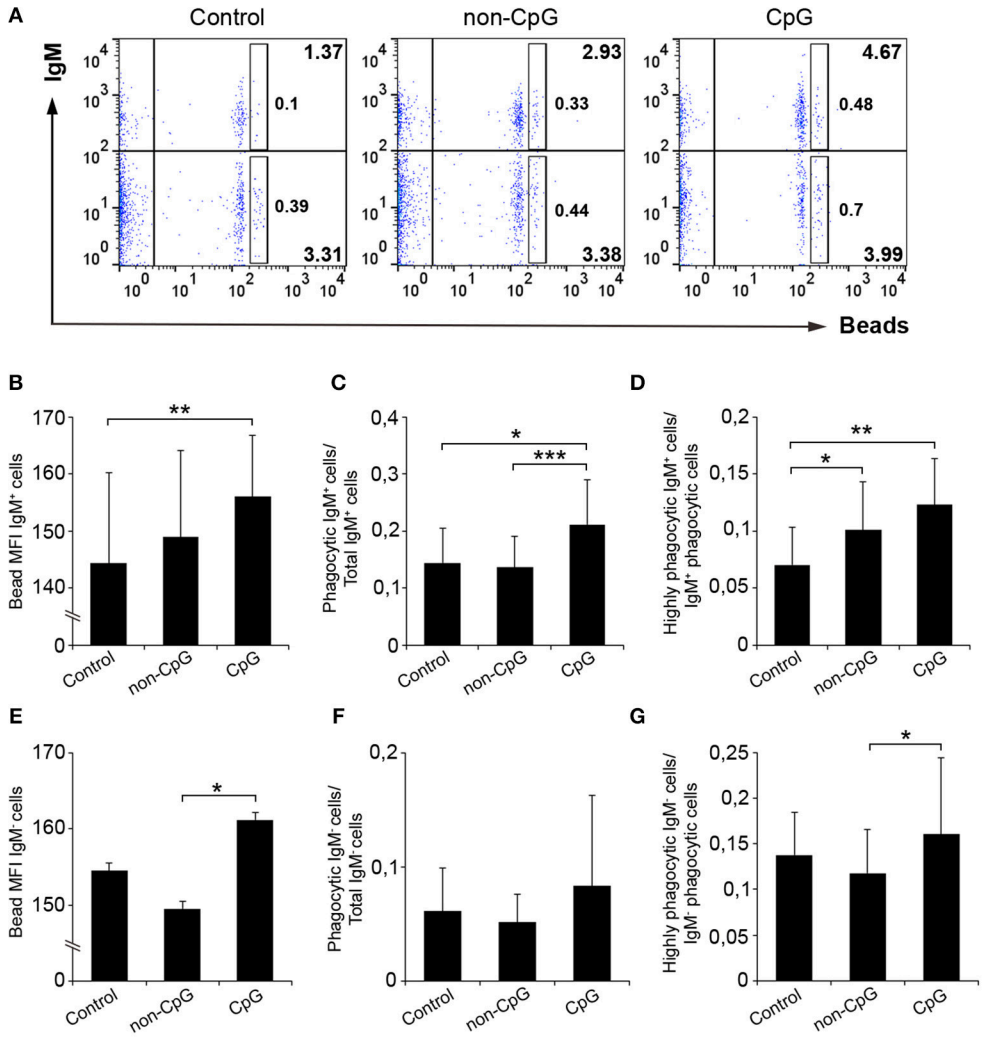


FIGURE 5 | CpGs up-regulate the phagocytic capacities of IgM$^+$ B cells from spleen. Splenocytes were cultured in the presence of CpG, non-CpG, or media alone as previously indicated for 48 h at 20°C. After this time, cells were incubated with Crimson Red fluorescent beads (1 μm diameter) at a ratio of 1:10 (cell/beads) for a further 3 h at 20°C. Non-ingested beads were removed by centrifugation over a cushion of 3% BSA supplemented with 4.5% D-glucose. Cells were then stained with anti-IgM mAb and analyzed by flow cytometry. **(A)** Representative dot plots for each experimental condition are shown. The rectangular areas contain the highly phagocytic IgM$^+$ (upper) or IgM$^-$ (lower) cell sub-populations (cells that have internalized a higher number of beads). Graphs showing the mean fluorescence intensity (MFI) of the internalized beads of IgM$^+$ cells **(B)** or IgM- cells **(E)** (mean + SD; $n = 6$ fish). Graphs showing the ratio between the phagocytic IgM$^+$ cells **(C)** or IgM$^-$ cells **(F)** and the corresponding IgM$^+$ or IgM- populations (mean + SD; $n = 6$ fish). Graphs showing the ratio between the highly IgM$^+$ **(D)** or IgM$^-$ **(G)** phagocytic cells and the corresponding phagocytic population in different conditions (mean + SD; $n = 6$ fish). Asterisks denote significantly different values between indicated groups (*$p \leq 0.05$, **$p \leq 0.01$, and ***$p \leq 0.005$).

phagocytic cells (**Figure 6D**) when compared to both untreated cultures and cultures treated with non-CpG ODNs. No effects were exerted by CpGs on the phagocytic capacities of the IgM$^-$ population in peripheral blood (**Figures 6E–G**).

CpGs Synergize With BCR Cross-Linking in Blood IgM$^+$ Cells

Having established that CpGs induce the proliferation of IgM$^+$ B cells on their own, we decided to analyze whether CpG could synergize with the BCR to induce a higher proliferation rate. To activate the BCR, we incubated the cells with anti-IgM as previously described (5). As reported before (5), the addition of anti-IgM alone was not sufficient to induce the proliferation of trout IgM$^+$ B cells from spleen (**Figures 7A,C**) or blood (**Figures 7B,D**). However, when BCR cross-linking was combined with CpG stimulation, a proliferation rate higher than that observed in cultures stimulated with CpGs alone or with anti-IgM alone was observed in blood (**Figures 7B,D**). This synergistic effect although visible in some fish was not significant in spleen (**Figures 7A,C**).

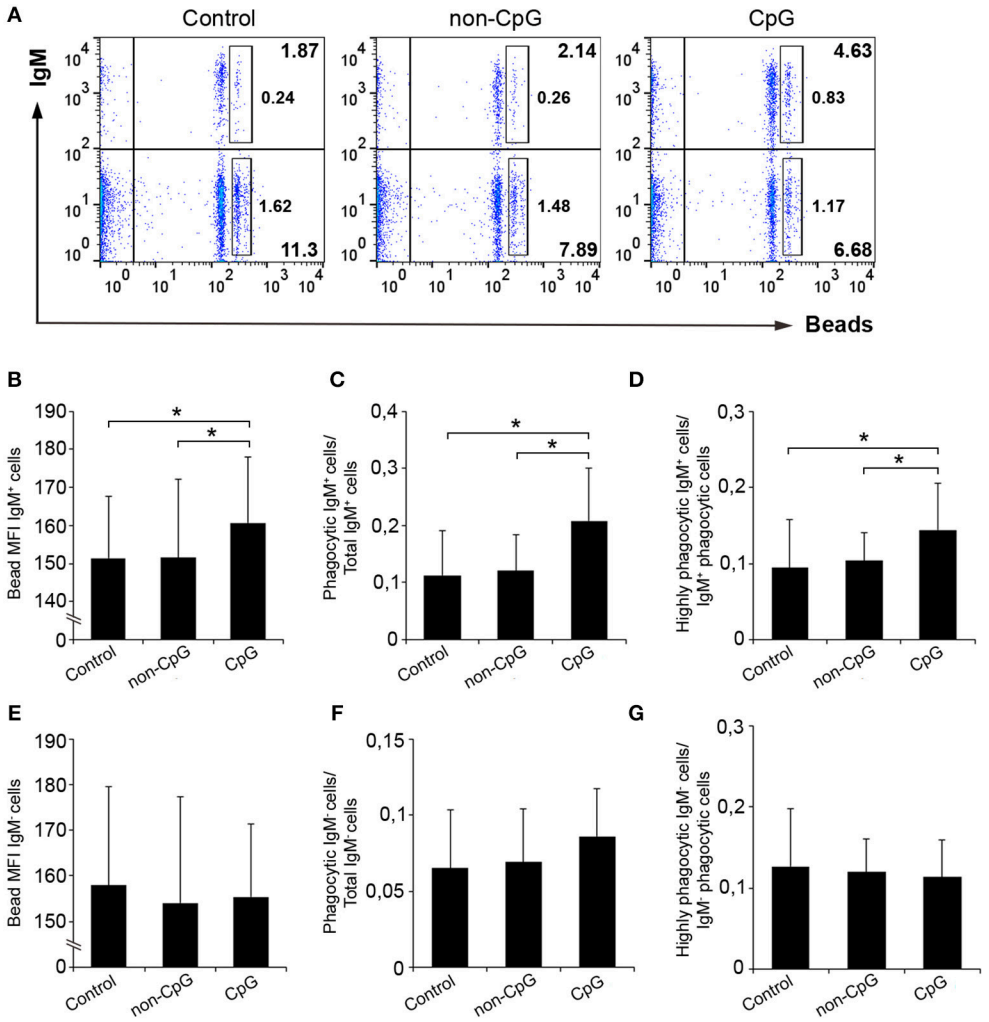


FIGURE 6 | CpGs up-regulate the phagocytic capacities of IgM$^+$ B cells from blood. Blood leukocytes were cultured in the presence of CpG, non-CpG, or media alone as previously indicated for 48 h at 20°C. After this time, cells were incubated with Crimson Red fluorescent beads and non-ingested beads removed as described in the legend of **Figure 5**. **(A)** Representative dot plots for each condition are shown. The rectangular areas contain the highly phagocytic IgM$^+$ (upper) or IgM$^-$ (lower) cell sub-populations (cells that have internalized a higher number of beads). Graphs showing the mean fluorescence intensity (MFI) of the internalized beads of IgM$^+$ cells **(B)** or IgM- cells **(E)** (mean + SD; $n = 6$ fish). Graphs showing the ratio between the phagocytic IgM$^+$ cells **(C)** or IgM$^-$ cells **(F)** and the corresponding IgM$^+$ or IgM- populations (mean + SD; $n = 6$). Graphs showing the ratio between the highly IgM$^+$ **(D)** or IgM$^-$ **(G)** phagocytic cells and the corresponding phagocytic population in different conditions (mean + SD; $n = 6$ fish). Asterisks denote significantly different values between indicated groups ($^*p \leq 0.05$.

DISCUSSION

CpGs have been proposed as promising adjuvants for fish vaccines (33). This presumed adjuvant activity has been ascribed on the basis of the results obtained in CpG-stimulation experiments performed mostly with total leukocyte populations in which cytokine gene expression, cell proliferation or oxygen or nitrogen radical production were measured [reviewed in Carrington and Secombes (34)]. Some of these experiments were carried out with macrophage-enriched populations or macrophage cell lines, thus the effects that CpGs exert on teleost macrophages are well-defined and include an increased antiviral activity, secretion of pro-inflammatory cytokines, and triggering of radical production [reviewed in Carrington and Secombes (34)]. However, the response of cells of the adaptive immune system to CpGs remains largely unknown in teleost. Very recently, Jenberie et al. (13) studied the effect of CpGs on IgM$^+$ B cells from salmon, but the study was mostly based on analyzing the transcription of several immune genes in FACS isolated B cells stimulated or not with CpGs. Although that work confirmed that teleost B cells also react to CpGs, many aspects of how teleost B cells respond to these ODNs rested unexplored. Thus, in order to expand our knowledge on the effects that CpGs have on teleost IgM$^+$ B cells, in the current study we have

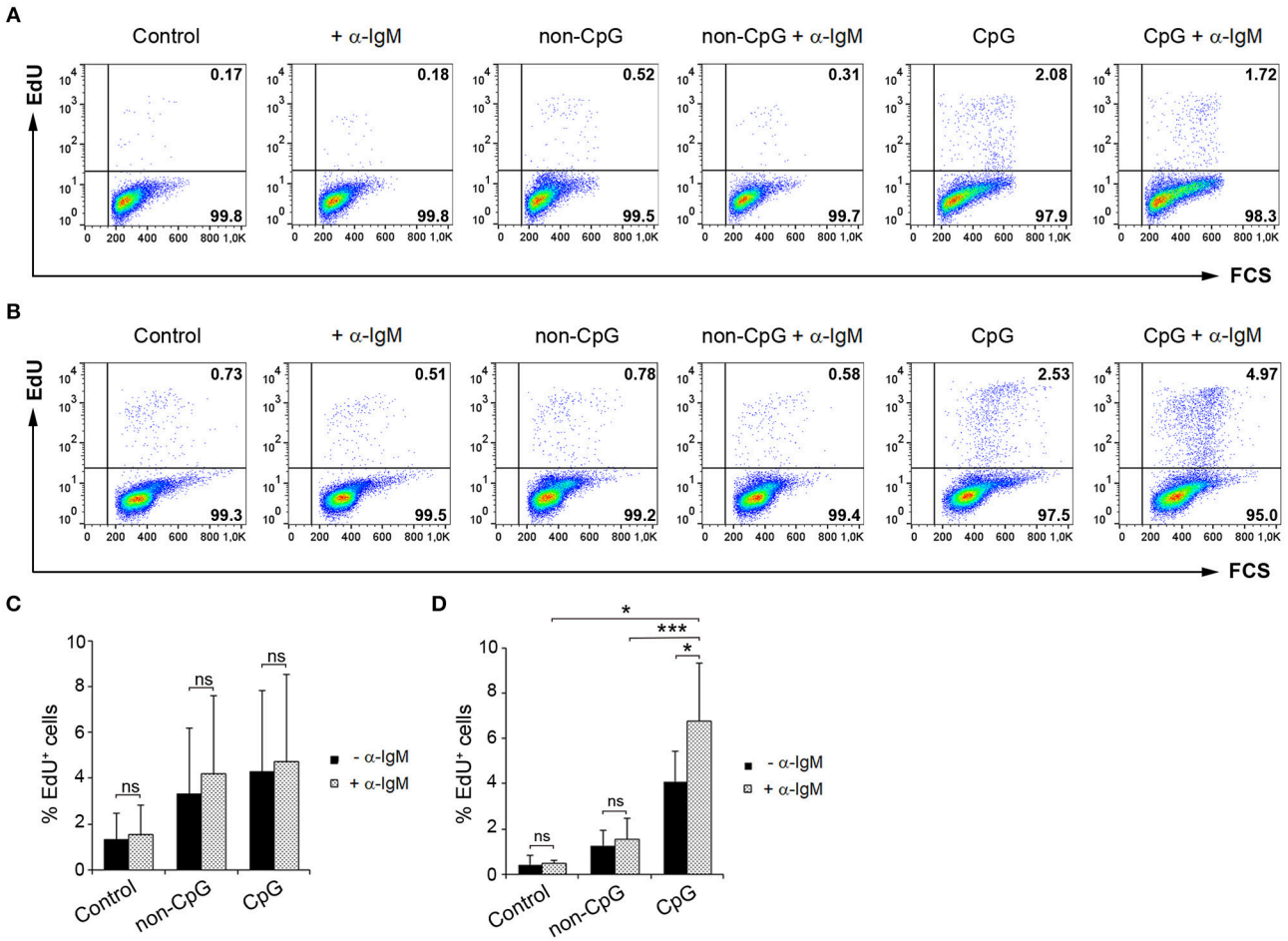


FIGURE 7 | Synergistic effect of CpG and BCR cross-linking on B cell proliferation. Spleen and blood leukocytes were incubated with CpG (5 μM), non-CpG (5 μM), or media alone in the presence or absence of anti-IgM mAb (10 μg/ml) during 3 days at 20°C. After this time, cells were labeled with EdU (1 μM) and incubated for a further 24 h. The percentage of proliferating cells (EdU^+) after the corresponding treatments was evaluated by flow cytometry. Representative dot plots from spleen **(A)** and blood **(B)** leukocytes for each condition are shown. Graphs show the percentage of EdU^+ cells (mean + SD) among spleen **(C)** and blood **(D)** leukocytes (n = 5 fish). Asterisks denote significant differences between cells treated with CpG or non-CpG and/or anti-IgM and their corresponding controls (*$p \leq 0.05$ and ***$p \leq 0.005$).

analyzed how CpGs modulate a wide range of immunological functions of IgM^+ B cells, performing parallel experiments with splenic and blood populations.

As already described for different cytokines such as BAFF (35) or APRIL (36) and TLR ligands such as LPS (24), CpGs increased the survival of trout IgM^+ B cells in cell culture. As occurred with LPS (24) or APRIL (36), this increased survival went along with strong proliferative effects on IgM^+ B cells. In mammals, class B CpGs are particularly efficient in promoting the proliferation of B cells (4, 18, 19, 25, 37), however important differences in CpG-induced proliferation rates have been reported in different studies. Thus, for example, Bernasconi et al. (19) reported that human naïve B cells only proliferated in response to CpGs if the BCR was simultaneously activated, whereas in that study memory B cells were shown to proliferate in response to CpGs alone. On the contrary, other studies have reported high proliferation rates of naïve human B cells stimulated with CpGs alone (18, 25, 38). These differences might be due to the fact that in each of these studies, different CpG ODNs were used. Additionally, differences in source and activation state of the B cells used could also account for the differences observed. In our studies, we compared the effects of CpGs on both spleen (main secondary immune organ) and peripheral blood, but no significant differences were observed in what concerns the effects exerted by CpGs alone on survival or proliferation.

In mice, although the capacity of B1 cells to proliferate in response to CpGs is lower than that of murine B2 cells (4), only B1 and MZ cell populations are capable of differentiating to plasma cells in response to CpG stimulation in the absence of BCR cross-linking (4). This was demonstrated on the basis of augmented IgM secretion, increased CD138 expression and up-regulated transcription of plasma cell-specific markers such as Blimp1 and XBP-1 (4). In the case of rainbow trout, we have demonstrated that CpGs significantly increased the number

of cells secreting IgM. As expected from B cells that were differentiating to plasmablast/plasma cells, an increase in size and a decrease in surface IgD and IgM expression were also evident. However, the fact that Blimp1 transcription is not significantly up-regulated in response to CpGs in isolated IgM^+ B cells from CpG-treated cultures when compared to those of sorted IgM^+ B cells from untreated cultures (data not shown) could be suggesting that CpGs are not able to achieve a complete differentiation of trout B cells to plasma cells. However, we have to take into account that Blimp1 has been designated as a protein required for the development of IgM-secreting cells and the maintenance of long-lived plasma cells in mammals (39), but not in fish. Hence, assuming that the requirements for B cell differentiation will be exactly the same in teleost fish is somehow risky, having established the great differences that exist between fish IgM^+ B cells and mammalian B2 cells (5). Therefore, at this point, we can conclude that CpGs induce the differentiation of IgM^+ B cells to antibody secreting cells (ASCs) as verified by increased IgM secretion, reduction of surface IgM and IgD expression and increased size, but whether these cells reach a full differentiation state should be further investigated. Intriguingly, when determining the effect of CpGs on the levels of surface IgM and IgD we found that non-CpG ODNs provoked a similar effect than that exerted by CpGs, suggesting that these nucleic acids are also recognized by immune cells and can activate the cells to some extent. In mice, non-CpG ODNs were shown to synergize with a specific antigen in stimulating specific B cells to proliferate, to express early activation markers and to activate the NF-κB pathway (40).

In addition to being responsible for the secretion of antibodies, B cells in both mammals and fish are professional antigen presenting cells capable of presenting to T cells antigens they acquire through the BCR in the context of MHC II (28). To investigate whether CpGs could affect antigen presenting capacities of trout B cells, we studied the levels of MHC II surface expression in stimulated and unstimulated cells. We found that IgM^+ B cells from spleen up-regulated the levels of surface MHC II in response to CpGs. Similarly, human B cells treated with CpGs up-regulated MHC II and CD86 expression (18). In salmon, the up-regulation of MHC II in kidney IgM^+ B cells treated with CpGs was demonstrated through Western blot (13). Interestingly, in trout, this effect was not exerted on blood IgM^+ B cells when total leukocyte cultures were incubated with CpGs but were clearly visible when sorted blood IgM^+ B cells were incubated with CpGs. Furthermore, both splenic and blood IgM^+ B cells up-regulated the transcription of co-stimulatory molecules (CD83 and CD80/86) in response to CpGs. In salmon, stimulation of salmon kidney IgM^+ B cells with CpGs alone increased the transcription of CD83 but not that of CD86 (13). In any case, whether the effects on MHC II surface expression are executed on the same population that differentiates toward a plasmablast/ plasma cell should be further explored, as it had been commonly accepted that as B cells differentiate to plasma cells MHC II surface levels decreased (41).

Fish B cells (32), similarly to mammalian B1 cells (31), have the capacity to phagocyte microparticles. This capacity has been related to a high microbicidal activity of fish B cells (32), as well as with a greater capacity to present particulate antigens they acquire through this mechanism (29). Of course this correlates with the fact that fish B cells have been shown to share many functional and phenotypic traits of mammalian B1 populations (5), implicated in the early innate response to pathogens. In this context, we thought of great relevance to determine if CpGs could affect an innate function of trout IgM^+ B cells, such as their phagocytic capacity. Our results demonstrate that CpGs significantly up-regulated the phagocytic capacity of both splenic and blood IgM^+ B cells. These effects of CpGs were evidenced by a higher percentage of B cells with phagocytic capacity, a higher number of beads ingested per cell and a higher percentage of cells with a high number of internalized beads. Interestingly, these effects were exclusively exerted on the IgM^+ population both in spleen and blood, suggesting that phagocytic IgM^- cells do not respond to CpGs as IgM^+ B cells in what refers to their phagocytic capacities. Although it may be possible different cell types are included within the IgM^- phagocytic population, IgT^+ B cells should make up for most of these cells, given that IgT^+ B cells have been described to account for ∼12% of the lymphocyte population in spleen (10). Thus, the effect of CpGs on IgT^+ B cells and whether CpGs affect the phagocytic capacities of mammalian B1 cells are interesting questions that should also be explored in the future.

The fact that human naïve B cells rapidly up-regulate TLR expression after BCR stimulation (19), strongly suggested that BCR signaling can synergize with TLR ligation. As expected, this synergy was demonstrated in human naïve B cells, but not in memory B cells that do not proliferate differently to CpGs when the BCR is simultaneously activated (19). In mice, this synergy between CpGs and BCR cross-linking was also visualized, with effects on both B cell proliferation and Ig secretion (37). In our experiments, we found that although a slight increase in the proliferative response of splenic IgM^+ B cells was observed when anti-IgM and CpGs were combined, a significant synergy between these two signals was only observed in blood IgM^+ B cells. These results demonstrate that CpGs have the capacity to amplify BCR-mediated signals also in teleost, but again point to important differences in the way B cell populations from different organs respond to CpGs.

In conclusion, our results show that CpGs have major effects on a wide range of adaptive and innate functions of IgM^+ B cells from rainbow trout. These include lymphoproliferative effects and positive effects on cell survival. Additionally, experimental evidence point to CpGs provoking the differentiation of some of these IgM^+ B cells to plasmablasts, although whether these cells reach a fully differentiated state or not remains undefined. CpGs were also shown to regulate the antigen presenting properties of IgM^+ B cells and to amplify BCR-mediated signals, although in this case, significant differences in the way splenic and blood IgM^+ B cells responded to the CpGs were found. Finally, CpGs were also shown to modulate innate functions of fish IgM^+ B cells, such as their phagocytic capacity. All these results point to CpGs as excellent adjuvant candidates for novel vaccine formulation designs in aquaculture.

DATA AVAILABILITY

All datasets generated for this study are included in the manuscript and/or the **Supplementary Files**.

AUTHOR CONTRIBUTIONS

RS performed most of the experimental work, with help from PD-R, EM, DM, and AG. CT and RS designed the experiments and wrote the main body of the paper, with contributions from PD-R and AG.

FUNDING

This work was supported by project AGL2017-85494-C2-1-R from the Spanish Ministry of Science, Innovation and Universities (MICINN), by the European Research Council (ERC Consolidator Grant 2016 725061 TEMUBLYM) and by project 2016-T1/BIO-1672 from the Comunidad de Madrid.

ACKNOWLEDGMENTS

We want to thank Dr. Erin Bromage (University of Massachusetts Dartmouth, USA) for providing the mAb against rainbow trout IgD. Dr. Beatriz Abós is also greatly acknowledged for technical help with the ELISPOT and proliferation assays.

SUPPLEMENTARY MATERIAL

The Supplementary Material for this article can be found online at: https://www.frontiersin.org/articles/10.3389/fimmu.2019.00584/full#supplementary-material

REFERENCES

1. Kawai T, Akira S. The roles of TLRs, RLRs and NLRs in pathogen recognition. *Int Immunol.* (2009) 21:317–37. doi: 10.1093/intimm/dxp017
2. Rawlings DJ, Schwartz MA, Jackson SW, Meyer-Bahlburg A. Integration of B cell responses through Toll-like receptors and antigen receptors. *Nat Rev Immunol.* (2012) 12:282–94. doi: 10.1038/nri3190
3. Bernasconi NL, Traggiai E, Lanzavecchia A. Maintenance of serological memory by polyclonal activation of human memory B cells. *Science.* (2002) 298:2199–202. doi: 10.1126/science.1076071
4. Genestier L, Taillardet M, Mondiere P, Gheit H, Bella C, Defrance T. TLR agonists selectively promote terminal plasma cell differentiation of B cell subsets specialized in thymus-independent responses. *J Immunol.* (2007) 178:7779–86. doi: 10.4049/jimmunol.178.12.7779
5. Abos B, Bird S, Granja AG, Morel E, More Bayona JA, Barreda DR, et al. Identification of the first teleost CD5 molecule: additional evidence on phenotypical and functional similarities between fish IgM(+) B cells and mammalian B1 cells. *J Immunol.* (2018) 201:465–80. doi: 10.4049/jimmunol.1701546
6. Abos B, Castro R, Pignatelli J, Luque A, Gonzalez L, Tafalla C. Transcriptional heterogeneity of IgM(+) cells in rainbow trout (*Oncorhynchus mykiss*) tissues. *PLoS ONE.* (2013) 8:e82737. doi: 10.1371/journal.pone.0082737
7. Pignatelli J, Castro R, Gonzalez Granja A, Abos B, Gonzalez L, Jensen LB, et al. Immunological characterization of the teleost adipose tissue and its modulation in response to viral infection and fat-content in the diet. *PLoS ONE.* (2014) 9:e110920. doi: 10.1371/journal.pone.0110920
8. Castro R, Bromage E, Abos B, Pignatelli J, Gonzalez Granja A, Luque A, et al. CCR7 is mainly expressed in teleost gills, where it defines an $IgD^{+}IgM^{-}$ B lymphocyte subset. *J Immunol.* (2014) 192:1257–66. doi: 10.4049/jimmunol.1302471
9. Edholm ES, Bengten E, Stafford JL, Sahoo M, Taylor EB, Miller NW, et al. Identification of two IgD+ B cell populations in channel catfish, *Ictalurus punctatus*. *J Immunol.* (2010) 185:4082–94. doi: 10.4049/jimmunol.1000631
10. Zhang YA, Salinas I, Li J, Parra D, Bjork S, Xu Z, et al. IgT, a primitive immunoglobulin class specialized in mucosal immunity. *Nat Immunol.* (2010) 11:827–35. doi: 10.1038/ni.1913
11. Xu Z, Parra D, Gomez D, Salinas I, Zhang YA, Von Gersdorff Jorgensen L, et al. Teleost skin, an ancient mucosal surface that elicits gut-like immune responses. *Proc Natl Acad Sci USA.* (2013) 110:13097–102. doi: 10.1073/pnas.1304319110
12. Xu Z, Takizawa F, Parra D, Gomez D, Von Gersdorff Jorgensen L, Lapatra SE, et al. Mucosal immunoglobulins at respiratory surfaces mark an ancient association that predates the emergence of tetrapods. *Nat Commun.* (2016) 7:10728. doi: 10.1038/ncomms10728
13. Jenberie S, Thim HL, Sunyer JO, Skjodt K, Jensen I, Jorgensen JB. Profiling Atlantic salmon B cell populations: CpG-mediated TLR-ligation enhances IgM secretion and modulates immune gene expression. *Sci Rep.* (2018) 8:3565. doi: 10.1038/s41598-018-21895-9
14. Pan X, Yue J, Ding G, Li B, Liu X, Zheng X, et al. Leucine-rich repeat 11 of Toll-like receptor 9 can tightly bind to CpG-containing oligodeoxynucleotides, and the positively charged residues are critical for the high affinity. *J Biol Chem.* (2012) 287:30596–609. doi: 10.1074/jbc.M112.396432
15. Pietretti D, Wiegertjes GF. Ligand specificities of Toll-like receptors in fish: indications from infection studies. *Dev Comp Immunol.* (2014) 43:205–22. doi: 10.1016/j.dci.2013.08.010
16. Vollmer J, Weeratna R, Payette P, Jurk M, Schetter C, Laucht M, et al. Characterization of three CpG oligodeoxynucleotide classes with distinct immunostimulatory activities. *Eur J Immunol.* (2004) 34:251–62. doi: 10.1002/eji.200324032
17. Eckl-Dorna J, Batista FD. BCR-mediated uptake of antigen linked to TLR9 ligand stimulates B-cell proliferation and antigen-specific plasma cell formation. *Blood.* (2009) 113:3969–77. doi: 10.1182/blood-2008-10-185421
18. Hartmann G, Krieg AM. Mechanism and function of a newly identified CpG DNA motif in human primary B cells. *J Immunol.* (2000) 164:944–53. doi: 10.4049/jimmunol.164.2.944
19. Bernasconi NL, Onai N, Lanzavecchia A. A role for Toll-like receptors in acquired immunity: up-regulation of TLR9 by BCR triggering in naive B cells and constitutive expression in memory B cells. *Blood.* (2003) 101:4500–4. doi: 10.1182/blood-2002-11-3569
20. Deluca D, Wilson M, Warr GW. Lymphocyte heterogeneity in the trout, *Salmo gairdneri*, defined with monoclonal antibodies to IgM. *Eur J Immunol.* (1983) 13:546–51. doi: 10.1002/eji.1830130706
21. Ramirez-Gomez F, Greene W, Rego K, Hansen JD, Costa G, Kataria P, et al. Discovery and characterization of secretory IgD in rainbow trout: secretory IgD is produced through a novel splicing mechanism. *J Immunol.* (2012) 188:1341–9. doi: 10.4049/jimmunol.1101938
22. Granja AG, Leal E, Pignatelli J, Castro R, Abos B, Kato G, et al. Identification of teleost skin CD8alpha+ dendritic-like cells, representing a potential common ancestor for mammalian cross-presenting dendritic cells. *J Immunol.* (2015) 195:1825–37. doi: 10.4049/jimmunol.1500322
23. Bustin SA, Benes V, Garson JA, Hellemans J, Huggett J, Kubista M, et al. The MIQE guidelines: minimum information for publication of quantitative real-time PCR experiments. *Clin Chem.* (2009) 55:611–22. doi: 10.1373/clinchem.2008.112797
24. Abos B, Wang T, Castro R, Granja AG, Leal E, Havixbeck J, et al. Distinct differentiation programs triggered by IL-6 and LPS in teleost IgM(+) B cells in the absence of germinal centers. *Sci Rep.* (2016) 6:30004. doi: 10.1038/srep30004

25. Jiang W, Lederman MM, Harding CV, Rodriguez B, Mohner RJ, Sieg SF. TLR9 stimulation drives naive B cells to proliferate and to attain enhanced antigen presenting function. *Eur J Immunol.* (2007) 37:2205–13. doi: 10.1002/eji.200636984
26. Shapiro-Shelef M, Calame K. Regulation of plasma-cell development. *Nat Rev Immunol.* (2005) 5:230–42. doi: 10.1038/nri1572
27. Granja AG, Tafalla C. Different IgM(+) B cell subpopulations residing within the peritoneal cavity of vaccinated rainbow trout are differently regulated by BAFF. *Fish Shellfish Immunol.* (2019) 85:9–17. doi: 10.1016/j.fsi.2017.10.003
28. Rodriguez-Pinto D. B cells as antigen presenting cells. *Cell Immunol.* (2005) 238:67–75. doi: 10.1016/j.cellimm.2006.02.005
29. Zhu LY, Lin AF, Shao T, Nie L, Dong WR, Xiang LX, et al. B cells in teleost fish act as pivotal initiating APCs in priming adaptive immunity: an evolutionary perspective on the origin of the B-1 cell subset and B7 molecules. *J Immunol.* (2014) 192:2699–714. doi: 10.4049/jimmunol.1301312
30. Zhang YA, Hikima J, Li J, Lapatra SE, Luo YP, Sunyer JO. Conservation of structural and functional features in a primordial CD80/86 molecule from rainbow trout (*Oncorhynchus mykiss*), a primitive teleost fish. *J Immunol.* (2009) 183:83–96. doi: 10.4049/jimmunol.0900605
31. Parra D, Rieger AM, Li J, Zhang YA, Randall LM, Hunter CA, et al. Pivotal advance: peritoneal cavity B-1 B cells have phagocytic and microbicidal capacities and present phagocytosed antigen to CD4+ T cells. *J Leukoc Biol.* (2012) 91:525–36. doi: 10.1189/jlb.0711372
32. Li J, Barreda DR, Zhang YA, Boshra H, Gelman AE, Lapatra S, et al. B lymphocytes from early vertebrates have potent phagocytic and microbicidal abilities. *Nat Immunol.* (2006) 7:1116–24. doi: 10.1038/ni1389
33. Tafalla C, Bogwald J, Dalmo RA. Adjuvants and immunostimulants in fish vaccines: current knowledge and future perspectives. *Fish Shellfish Immunol.* (2013) 35:1740–50. doi: 10.1016/j.fsi.2013.02.029
34. Carrington AC, Secombes CJ. A review of CpGs and their relevance to aquaculture. *Vet Immunol Immunopathol.* (2006) 112:87–101. doi: 10.1016/j.vetimm.2006.03.015
35. Tafalla C, Gonzalez L, Castro R, Granja AG. B Cell-Activating Factor regulates different aspects of B cell functionality and is produced by a subset of splenic B cells in teleost fish. *Front Immunol.* (2017) 8:295. doi: 10.3389/fimmu.2017.00295
36. Soleto I, Morel E, Martin D, Granja AG, Tafalla C. Regulation of IgM(+) B cell activities by rainbow trout APRIL reveals specific effects of this cytokine in lower vertebrates. *Front Immunol.* (2018) 9:1880. doi: 10.3389/fimmu.2018.01880
37. Krieg AM, Yi AK, Matson S, Waldschmidt TJ, Bishop GA, Teasdale R, et al. CpG motifs in bacterial DNA trigger direct B-cell activation. *Nature.* (1995) 374:546–9. doi: 10.1038/374546a0
38. Huggins J, Pellegrin T, Felgar RE, Wei C, Brown M, Zheng B, et al. CpG DNA activation and plasma-cell differentiation of CD27- naive human B cells. *Blood.* (2007) 109:1611–9. doi: 10.1182/blood-2006-03-008441
39. Martins G, Calame K. Regulation and functions of Blimp-1 in T and B lymphocytes. *Annu Rev Immunol.* (2008) 26:133–69. doi: 10.1146/annurev.immunol.26.021607.090241
40. Wang Y, Krieg AM. Synergy between CpG- or non-CpG DNA and specific antigen for B cell activation. *Int Immunol.* (2003) 15:223–31. doi: 10.1093/intimm/dxg020
41. Yoon HS, Scharer CD, Majumder P, Davis CW, Butler R, Zinzow-Kramer W, et al. ZBTB32 is an early repressor of the CIITA and MHC class II gene expression during B cell differentiation to plasma cells. *J Immunol.* (2012) 189:2393–403. doi: 10.4049/jimmunol.1103371

Conflict of Interest Statement: The authors declare that the research was conducted in the absence of any commercial or financial relationships that could be construed as a potential conflict of interest.

Copyright © 2019 Simón, Díaz-Rosales, Morel, Martín, Granja and Tafalla. This is an open-access article distributed under the terms of the Creative Commons Attribution License (CC BY). The use, distribution or reproduction in other forums is permitted, provided the original author(s) and the copyright owner(s) are credited and that the original publication in this journal is cited, in accordance with accepted academic practice. No use, distribution or reproduction is permitted which does not comply with these terms.

frontiers in Immunology

ORIGINAL RESEARCH
published: 26 April 2019
doi: 10.3389/fimmu.2019.00926

PACAP Is Lethal to *Flavobacterium psychrophilum* Through Either Direct Membrane Permeabilization or Indirectly, by Priming the Immune Response in Rainbow Trout Macrophages

Shawna L. Semple[1], Tania Rodríguez-Ramos[1], Yamila Carpio[2], John S. Lumsden[3], Mario P. Estrada[2] and Brian Dixon[1]**

[1] Department of Biology, University of Waterloo, Waterloo, ON, Canada, [2] Center for Genetic Engineering and Biotechnology, Havana, Cuba, [3] Department of Pathobiology, Ontario Veterinary College, University of Guelph, Guelph, ON, Canada

OPEN ACCESS

Edited by:
Roy Ambli Dalmo, UiT The Arctic University of Norway, Norway

Reviewed by:
Natalia Kasica-Jarosz, University of Warmia and Mazury in Olsztyn, Poland
Joao Carlos dos Reis Cardoso, University of Algarve, Portugal

***Correspondence:**
Mario P. Estrada
mario.pablo@cigb.edu.cu
Brian Dixon
bdixon@uwaterloo.ca

Specialty section:
This article was submitted to Comparative Immunology, a section of the journal Frontiers in Immunology

Received: *06 February 2019*
Accepted: *10 April 2019*
Published: *26 April 2019*

Citation:
Semple SL, Rodríguez-Ramos T, Carpio Y, Lumsden JS, Estrada MP and Dixon B (2019) PACAP Is Lethal to Flavobacterium psychrophilum Through Either Direct Membrane Permeabilization or Indirectly, by Priming the Immune Response in Rainbow Trout Macrophages. Front. Immunol. 10:926. doi: 10.3389/fimmu.2019.00926

Pituitary adenylate cyclase-activating polypeptide (PACAP) is a multifunctional neuropeptide that is widely distributed in mammals and is capable of performing roles as a neurotransmitter, neuromodulator, and vasodilator. This polypeptide belongs to the glucagon/secretin superfamily, of which some members have been shown to act as antimicrobial peptides in both mammalian and aquatic organisms. In teleosts, PACAP has been demonstrated to have direct antimicrobial activity against several aquatic pathogens, yet this phenomenon has never been studied throughout a live bacterial challenge. The present study focuses on the influence of synthetic *Clarias gariepinus* 38 amino acid PACAP on the rainbow trout monocyte/macrophage-like cell line, RTS11, when exposed to the coldwater bacterial pathogen *Flavobacterium psychrophilum*. PACAP was shown to have direct antimicrobial activity on *F. psychrophilum* when grown in both cytophaga broth and cell culture media (L-15). Further, the ability of teleostean PACAP to permeabilize the membrane of an aquatic pathogen, *F. psychrophilum*, was demonstrated for the first time. The viability of RTS11 when exposed to PACAP was also observed using a trypan blue exclusion assay to determine optimal experimental doses of the antimicrobial peptide. This displayed that only concentrations higher than 0.1 μM negatively impacted RTS11 survival. Interestingly, when RTS11 was pre-treated with PACAP for 24 h before experiencing infection with live *F. psychrophilum*, growth of the pathogen was severely inhibited in a dose-dependent manner when compared to cells receiving no pre-treatment with the polypeptide. Relative expression of pro-inflammatory cytokines (IL-1β, TNFα, and IL-6) and PACAP receptors (VPAC1 and PAC1) was also analyzed in RTS11 following PACAP exposure alone and in conjunction with live *F. psychrophilum* challenge. These qRT-PCR findings revealed that PACAP may have a synergistic effect on RTS11 immune function. The results of this study provide evidence that PACAP has immunostimulatory activity on rainbow trout immune

cells as well as antimicrobial activity against aquatic bacterial pathogens such as *F. psychrophilum*. As there are numerous pathogens that plague the aquaculture industry, PACAP may stimulate the teleost immune system while also providing an efficacious alternative to antibiotic use.

Keywords: rainbow trout, antimicrobial peptide, PACAP, RTS11, cytokines, fish pathogen, *Flavobacterium psychrophilum*

INTRODUCTION

Due to the rising demand for fish protein (1), aquaculture has become a necessary means to protect wild populations from irreversible overfishing. As such, it is imperative that these culture systems have a minimal impact on the environment while still being able to provide the high-quality product for market. To attain this goal, alternative methods must be developed to combat infectious disease as this is one of the greatest sources of instability and financial cost in aquaculture. Global losses due to aquatic infections total approximately $6 billion USD (2) and currently, fish farmers have few methods outside of antibiotics to prevent/control outbreaks. With multi-drug resistance continually rising [reviewed by Watts et al. (3), Santos and Ramos (4)], antibiotic use in aquaculture is tightly regulated which often leaves farmers with few options when outbreaks do occur. This problem has led to an increased interest in the development of alternative approaches for disease prevention, including the use of naturally occurring antimicrobial peptides (AMPs).

Antimicrobial peptides are a diverse class of highly conserved molecules that are produced as a first line of defense in multicellular organisms. These small peptides (12–50 amino acids) are essential components of innate immunity capable of antimicrobial activity against a wide range of microbial pathogens [reviewed by Zhang and Gallo (5)], which notably includes multi-drug resistant isolates (6, 7). Most AMPs are cationic amphipathic peptides that function by attacking the negatively charged membranes of microorganisms [reviewed by Mahlapuu et al. (8)]. Based on their secondary structures, AMPs can be characterized as one of four types, β-sheet, α-helix, extended and loop with β-sheet and α-helix being the most common [reviewed by Bahar and Ren (9)]. Functionally, they can be characterized as either membrane disruptive AMPs, causing membrane permeabilization, or nonmembrane disruptive AMPs, which directly passage into cells and act on intracellular targets [reviewed by Kang et al. (10)]. Besides direct destruction of pathogens, AMPS also perform immunomodulatory functions in higher vertebrates [reviewed by Otvos (11)] and as a result are also called "host defense peptides" (HDPs) to emphasize these additional activities. The potential immunomodulatory effects are diverse including stimulation of chemotaxis, immune cell differentiation, initiation of adaptive immunity and stimulation of both pro- and anti- inflammatory cytokines (12–15). Though novel AMPs and their activities are continuously being discovered, one that has gained a lot of interest as a result of its vast pleiotropic effects is pituitary adenylate cyclase activating polypeptide (PACAP).

Initially, PACAP was discovered as a neuropeptide due to its ability to stimulate adenylate cyclase activity in ovine pituitary cell cultures (16). Derived from a 175 amino acid precursor, functional PACAP has two molecular forms. The first has 38 amino acids (PACAP-38) while the other form is truncated containing only 27 residues [PACAP-27, (17, 18)]. Of the two, PACAP-38 is considered to be more bioactive as it has been shown to display 100–1000 times greater potency in stimulating cell proliferation, DNA synthesis and inositol phospholipid turnover in cells (19, 20). Further analysis of PACAP-38 revealed that this peptide shared 68% sequence similarity with vasoactive intestinal polypeptide (VIP), thereby classifying PACAP as a member of the secretin/glucagon/growth hormone-releasing hormone/vasoactive intestinal peptide superfamily (16). As this was the case, it is not surprising that PACAP-38 is able to bind with equal affinity to the same G-coupled protein receptors (GCPRs) as VIP, vasoactive intestinal polypeptide receptor 1 (VPAC1) and vasoactive intestinal polypeptide receptor 2 (VPAC2), while also binding to its own receptor, pituitary adenylate cyclase-activating polypeptide type I receptor [PAC1, (21, 22)]. All three of these receptors have a wide tissue distribution much like the neuropeptides themselves (21, 23, 24). PACAP-38 in particular, displays a broad range of functions in multiple tissue types, including antimicrobial activity, growth, immunomodulation, neural development, anti-tumor activity and metabolism to name a few (25–29). From an evolutionary perspective, the amino acid sequence of PACAP-38 is identical in all mammals with only a few amino acid substitutions when comparing to other species (e.g., frog, salmon, tunicate, etc.). PACAP-38 therefore must play a vital role in physiological function as it has remained essentially unchanged for ∼700 million years (30). This broad functional profile as well as its highly conserved nature has made PACAP-38 an attractive candidate for disease control and therapeutic use in aquaculture.

Though there are numerous pathogens that impact the aquaculture industry, *F. psychrophilum* has proven to be a global threat in the culture of freshwater rainbow trout (*Oncorhynchus mykiss*). This gram-negative bacterial pathogen is the causative agent of bacterial coldwater disease (BCWD) and rainbow trout fry syndrome (RTFS), two separate conditions that can occur depending on the bacterial isolate, geographical location and age of the host (31). These conditions present as either an acute bacteremia primarily in small fish (RTSF) or as a more chronic disease most commonly characterized by an ulcerative dermatitis (BCWD) in larger fish (31, 32). Though variable, mortality resulting from these conditions without intervention generally ranges from 2–30% (33) but in extreme cases can be as high as 50–90% (34–36). Despite concerted efforts to selectively

breed for resistance to *F. psychrophilum* (33, 37–39) and multiple attempts to develop an effective vaccine [reviewed by Gomez et al. (40), Makesh et al. (41), and Hoare et al. (42)], there is little information regarding the pathogenesis of the organism. Based on the data presented thus far, it appears that *F. psychrophilum* has an intricate relationship with the spleen and head kidney macrophages of rainbow trout (43, 44). As such, the spleen monocyte/macrophage-like cell line, RTS11 (45), would be an ideal model system for studying *F. psychrophilum* infections. As a relevant immune cell line, RTS11 could provide further insight regarding the immunomodulatory effects of PACAP-38 as well as its antimicrobial function within an appropriate infection model.

Previous research involving teleostean PACAP-38 has focused on assessing its antimicrobial activity when directly dosing aquatic pathogens (46), the growth/immunomodulatory effects of the peptide alone (47–49), or how viral/bacterial infection can influence gene expression of the peptide and its associated receptors (50). Though these results were promising, there is yet to be a study evaluating the activity of PACAP-38 in a live infection model. Furthermore, the effect of PACAP-38 has never been explored with respect to the industrially relevant pathogen, *F. psychrophilum*. The purpose of this study was to measure and understand the antimicrobial activity of PACAP-38 on *F. psychrophilum* as well as to determine whether PACAP could stimulate a protective immune response in RTS11 cells. Confirming the efficacy of PACAP in an *in vitro* infection model will provide further evidence to support its use in *in vivo* experiments. Additionally, the results of this work could provide valuable insights regarding the efficacy of PACAP-38 during live infections and thus aid in the development of a potential alternative for antibiotic use in aquaculture.

MATERIALS AND METHODS

Maintenance of RTS11

The rainbow trout monocyte/macrophage-like cell line, RTS11 (45), was maintained as described previously by Sever et al. (51).

Peptides

Synthetic PACAP From the Teleost *C. gariepinus*

Clarias gariepinus synthetic PACAP-38 (amino acid sequence of HSDGIFTDSYSRYRKQMAVKKYLAAVLGRRYRQRFRNK, MW of 4.7 kDa) was purchased from CS Bio (Shanghai) Ltd, China with 85% purity.

Synthetic HSP70 Peptide Fragment From Rainbow Trout

A synthetic peptide fragment of rainbow trout HSP70 (amino acid sequence of CGDQARTSSGASSQ, MW of 1.3 kDa) was purchased from Biomatik with 98% purity.

Growth of *F. psychrophilum*

Flavobacterium psychrophilum strain 101 (FPG101) was grown as described previously by Semple et al. (44) with minor adjustments. This bacterial isolate has been characterized as virulent in experimental trials by Jarau et al. (52). Briefly, subcultures of FPG101 glycerol stocks were grown on cytophaga agar (CA) at 14°C and checked for purity. An isolated colony was then used to inoculate 3 mL of cytophaga broth (CB) and grown at 14°C for 72 h. After this time, the OD_{600} of the bacterial growth was consistently between 0.4 and 0.5, indicating a viable bacterial count of 2–5 $\times$ 10^8 CFU/mL. For every culture of FPG101, a standard plate count (SPC) was completed to confirm the anticipated bacterial concentration.

Minimum Inhibitory Concentration (MIC) of *C. gariepinus* PACAP-38 on *F. pyschrophilum*

The MIC of *C. gariepinus* PACAP-38 on FPG101 was assessed by a broth microdilution peptide assay (BMPA) (53). To prepare FPG101 for this assay, 3 mL of CB was inoculated with a single colony and allowed to grow overnight at 14°C. After this time, 1 mL of the growth was centrifuged at 5,000 rpm for 5 min, the supernatant removed, and the pellet resuspended in 4 mL of fresh CB, to have an OD_{600} of 0.1-0.4. Finally, the bacterial suspension was diluted in CB to obtain a final OD of 0.001.

The BMPA was made using a flat-bottom 96-well plate (Fisher Scientific). The plate set up consisted of wells containing 90 μL of bacterial suspension and 10 μL of PACAP at 10 different final concentrations from 5 to 50 μM. In the positive control wells, PACAP was substituted with 10 μL of CB while the negative control wells contained 100 μL of CB only. All PACAP concentrations and controls were tested in triplicates. The bacterial growth was monitored after 3 days of incubation at 14°C, by measuring the change in the absorbance at 600 nm using a microplate reader (BioTek). The growth inhibition curves were generated by plotting the OD at 600 nm and the peptide concentration. The MIC was considered as the lowest concentration of PACAP at which no bacterial growth was detected (an OD_{600} of 0).

RTS11 Exposure Trials

Exposure to PACAP

In 6-well tissue culture plates (ThermoFisher), RTS11 was seeded at 1.5 x 10^6 cells/well in 1.5 mL of L-15 media with no antibiotics and maintained overnight at 14°C. Cells were exposed to PACAP concentrations of either 0.0002 μM, 0.002 μM, 0.02 μM, 0.1 μM, 0.2 μM, 2 μM, 20 μM, or a no PACAP control to a final volume of 4 mL per well. Following this single exposure to PACAP, all experimental plates were returned to the 14°C incubator. On days 1, 2, and 3, the supernatant was collected from experimental wells and adherent cells were mechanically dislodged using a sterile 23 cm cell scraper (ThermoFisher) and added to the supernatant of respective wells. All wells were then washed with 1 mL of phosphate buffered saline (PBS, Gibco) which was also added to the appropriate supernatant/cell mixture. The cells were centrifuged (5 min, 500 $\times$ g, 4°C), washed once with 5 mL of PBS, and the resulting cell pellets were stored at −80°C for future use.

Simultaneous Exposure to Both PACAP and Live *F. psychrophilum*

In a second experiment, RTS11 was exposed to PACAP concentrations of 0.0002 μM, 0.002 μM, 0.02 μM, and 0.1 μM in similar conditions as described above in the first PACAP

trial (section Exposure to PACAP). Prior to the single addition of PACAP, 0.5 mL of FPG101 was added to each well at bacterial concentrations ranging from 1.3–2.0 $\times$ 10^6 CFU/mL (multiplicity of infection [MOI] of 0.7–1.3). Sampling was completed as described above (section Exposure to PACAP).

Pre-treatment With PACAP Followed by Infection With Live *F. psychrophilum*

It was observed that *F. psychrophilum* grew rapidly in wells when exposed to RTS11 simultaneously with PACAP. Because it was possible that PACAP might not be able to influence either RTS11 alone, the *F. psychrophilum* alone, or both due to this rapid growth, PACAP was added to RTS11 wells 24 h before the addition of live *F. psychrophilum*. Otherwise all procedures for sample collection and exposure were identical to those described above in the first PACAP experiment (section Exposure to PACAP).

Survival of RTS11 Following PACAP Exposure

To determine whether PACAP negatively influenced RTS11 viability, the cells were exposed to a single dose of 0.002 μM, 0.02 μM, 0.1 μM, 0.2 μM, 2 μM, 20 μM, or a no PACAP control as described above. On days 1, 2, and 3 following this exposure, the supernatant was collected from experimental wells and any adherent cells were detached using 400 μL of 0.25% trypsin-EDTA (Gibco) and the wells washed with 1 mL of PBS. These trypsinized cells were combined with the collected supernatant which was then centrifuged 500 $\times$ g for 5 min at 4°C. The cell pellet was washed twice with 1 mL of PBS before resuspending in 200 μL of PBS. To determine RTS11 cell viability after exposure to PACAP, a trypan blue (Sigma) exclusion test was performed using a haemocytometer under a phase contrast microscope (Leica). This experiment was repeated three times.

Presence of Viable *F. psychrophilum* in RTS11 Cell Cultures Following PACAP Exposure

In six 6-well plates, quadruple wells of RTS11 cells were exposed to either PACAP and *F. psychrophilum* simultaneously or to 24 h pre-treatment of PACAP prior to the addition of *F. psychrophilum* as described above. All experiments had a MOI of 1. On days 2 and 3 post-infection with live *F. psychrophilum*, 500 μL of the supernatant from each well was removed and serially diluted for an SPC assay to determine the number of viable bacterial cells in the supernatant. Otherwise the RTS11 cells for each day were collected as described above and pellets were frozen at −80°C for future RNA extraction.

Permeabilization Assay

FPG101 was grown as described above for the MIC assay in section Minimum Inhibitory Concentration (MIC) of *C. gariepinus* PACAP-38 on *F. pyschrophilum*. One milliliter of the final bacterial culture was removed and boiled for 20 min to act as a heat-killed control. After boiling, 100 μL of the heat-killed FPG101 was spread onto a CA plate to confirm the absence of viable bacteria.

In a sterile, 96-well BioLite plate (ThermoFisher), 90 μL of live bacterial culture was added to all experimental wells. In triplicate, 10 μL of either PACAP or the synthetic HSP70 peptide fragment to reach final concentrations of 50 μM PACAP, 30 μM PACAP, 0.1 μM PACAP, and 50 μM HSP70. As a live bacteria control, 10 μL of cytophaga broth alone was added to triplicate wells of the live FPG101 culture. As a negative control, 90 μL of heat-killed FPG101 was added to triplicate wells and filled to 100 μL with CB. As a blank, triplicate wells received 100 μL of CB. The assay plate received gentle shaking to mix well contents and was incubated at 14°C for 72 h. Following incubation, each well received 100 μL of 2X BacLight solution (ThermoFisher, L13152) and was incubated in the dark for 15 min. Because the BacLight solution consists of both SYTO 9 (6 μM) and propidium iodide (30 μM), the plate was read at an excitation of 485 nm and an emission of 530 nm for SYTO 9 (green) as well as an excitation of 485 nm and an emission of 630 nm for propidium iodide (red). The reads were completed using a Synergy H1 plate reader (BioTek Instruments). The bacterial fluorescent intensities (F_{cell}) were calculated as a ratio of $F_{cell}530/F_{cell}630$ and presented as the green/red fluorescence ratio.

qRT-PCR

RNA Extraction and cDNA Synthesis

RNA was extracted from RTS11 cell pellets (1.5 $\times$ 10^6 cells) using an RNeasy RNA Extraction Kit (Qiagen) as described by the manufacturer. To remove any contaminating genomic DNA, all RNA samples were treated with DNase I (Thermo Scientific). RNA samples were then quantified using the Take3 plate of a Synergy H1 plate reader (BioTek Instruments) and were stored at −80°C until further use. Complementary DNA (cDNA) was synthesized from 500 ng of total RNA using the qScript cDNA Supermix (Quanta Biosciences) in accordance to the manufacturer's instructions. For a no template control, 500 ng of RNA suspended in 20 uL of DEPC water was included in the cDNA synthesis reaction without reverse transcriptase.

qRT-PCR Reactions

To assess transcript levels of *IL-1β*, *TNFα*, *IL-6*, *PAC1*, and *VPAC1* in RTS11 cells, qRT-PCR analysis was completed. All PCR reactions were 10 μl and contained: 2.5 μl of cDNA (25 ng/μl diluted 1:10 in RNase free water), 2x WISENT ADVANCED™ qPCR mastermix (Wisent), and forward and reverse primers (Sigma Aldrich) to a final working concentration of 0.25 μM. All qPCR reactions were completed on the LightCycler® 480 II (Roche). The sequences for all primer sets are outlined in **Table 1**. Each experimental sample was run in triplicate. For each plate, triplicate wells of a calibrator, no template control and RNA only control were also present. The program used for all qRT-PCR reactions was as follows: pre-incubation at 95°C for 10 min followed by 40 cycles of denaturation at 95°C for 10 sec, annealing at 60°C for 5 s and extension at 72°C for 8 s. A melting curve was completed for every run from 65 to 97°C with a read every 5 s. Product specificity was determined through single PCR melting peaks. All qRT-PCR data was analyzed using the ΔΔCt method and is presented as the average of 3 experimental replicates with the standard deviation. Specifically,

TABLE 1 | Primers used for qRT-PCR analysis of RTS11.

Primer name	Sequence (5′-3′)	References
IL-1β	**F:** CCACAAAGTGCATTTGAAC	(54)
	R: GCAACCTCCTCTAGGTGC	
TNFα	**F:** GTGCAAAAGATACCCACC	(54)
	R: CACTGCACGGTGTCAG	
IL-6	**F:** CTTCTACACGCTATCTCTCACTC	(54)
	R: CGTCTGTCCCGAGCT	
VPAC1	**F:** CAGGTGAAAATTGGTTACACTGTTG	(55)
	R: TAGTTCCTAGTGCAGTGGAGTTTCC	
PAC1	**F:** TGAACCTGTTTGTGTCATTCATTCT	(55)
	R: ACACTCCACAGTGTGTAAGAAGCAG	
EF1α	**F:** CGCACAGTAACACCGAAACTAATTAAGC	(54)
	R: GCCTCCGCACTTGTAGATCAGATG	

gene expression was normalized to the reference gene (EF1α) and expressed as fold change over the day 0 control group where control expression was set to 1.

Statistics

All statistical analyses were completed using the statistical software Statistica version 7 (StatSoft, Tulsa, OK). Prior to the completion of the appropriate statistical test, a normal distribution and equal variance was confirmed. A one-way ANOVA was completed for the growth of *F. psychrophilum* in RTS11 cultures and the permeabilization assay. Whereas, a two-way ANOVA was completed for all qRT-PCR results and analyzing the viability of RTS11 to various PACAP concentrations. The appropriate ANOVA test was then followed by a Fisher's least significant difference (LSD) *post-hoc* test to determine significant differences.

RESULTS

Minimum Inhibitory Concentration (MIC)

The MIC was analyzed using both the preferred growth medium of *F. psychrophilum*, cytophaga broth (CB), and the L-15 cell culture media used to sustain the RTS11 cultures (**Figure 1**). For both CB (**Figure 1A**) and L-15 (**Figure 1B**), the MIC was found to be 30 μM. It appears that PACAP can maintain its antimicrobial function in both media types, thus the function of this peptide could be assessed during *in vitro* live infection experiments with RTS11.

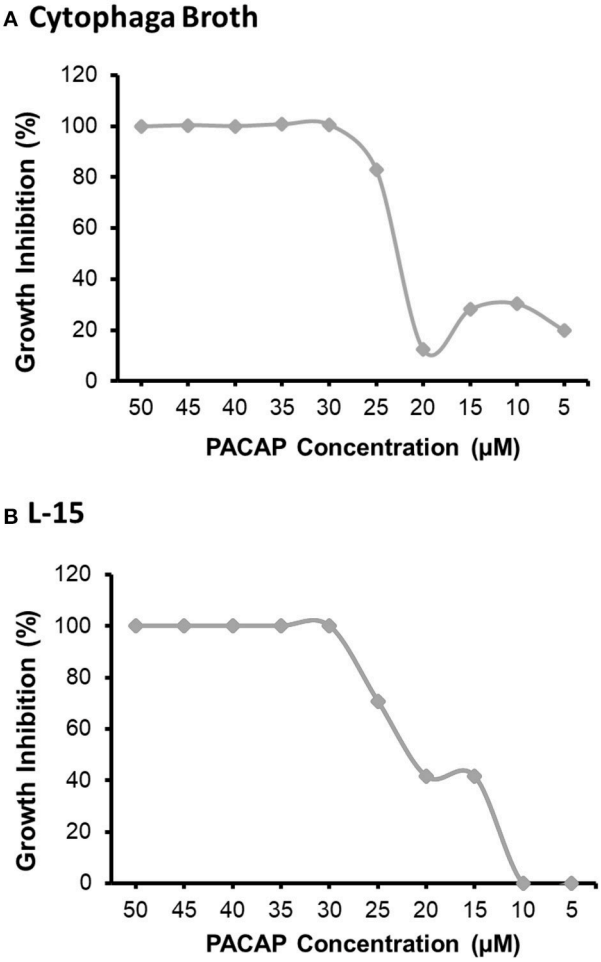


FIGURE 1 | The minimum inhibitory concentration (MIC) of *C. gariepinus* PACAP-38 required to prevent the growth of *F. psychrophilum* alone. The MIC was determined following 3 days of growth in both cytophaga broth **(A)** and in Leibovitz-15 (L-15) cell culture media **(B)**. Each panel represents the results of three independent experiments.

Impact of PACAP Concentrations on RTS11 Survival

Even if PACAP is capable of killing aquatic bacterial pathogens, this ability has reduced value if the peptide negatively impacts the survival of rainbow trout immune cells as well. Based on the six concentrations of PACAP analyzed here (ranging from 0.002–20 μM), only PACAP concentrations of 0.2 μM and higher significantly decreased the viability of RTS11 (**Figure 2**). Furthermore, cell death was only observed on day 2 of exposure. Cell viability was not significantly different between PACAP concentrations on both days 1 and 3 of exposure.

Effect of PACAP on *F. psychrophilum* Growth Throughout RTS11 Infections

When RTS11 was exposed to live *F. psychrophilum* simultaneously with various PACAP concentrations, the number of viable bacteria present in the supernatant was not significantly different when compared to that of the no PACAP control on day 2 (**Figure 3A**). As it was possible that PACAP required time to stimulate a defensive immune state in RTS11, this experiment was repeated but this time the cells were exposed to PACAP concentrations 24 h prior to receiving the infectious dose of *F. psychrophilum*. When using this experimental design, all three concentrations of PACAP (0.002, 0.02, and 0.1 μM) were shown to significantly reduce the number of viable bacteria in the RTS11 on day 2 (**Figure 3B**). This reduction was still observed on day 3 but was only found to be significant in the two higher concentrations of PACAP at 0.02 and 0.1 μM (**Figure 3C**).

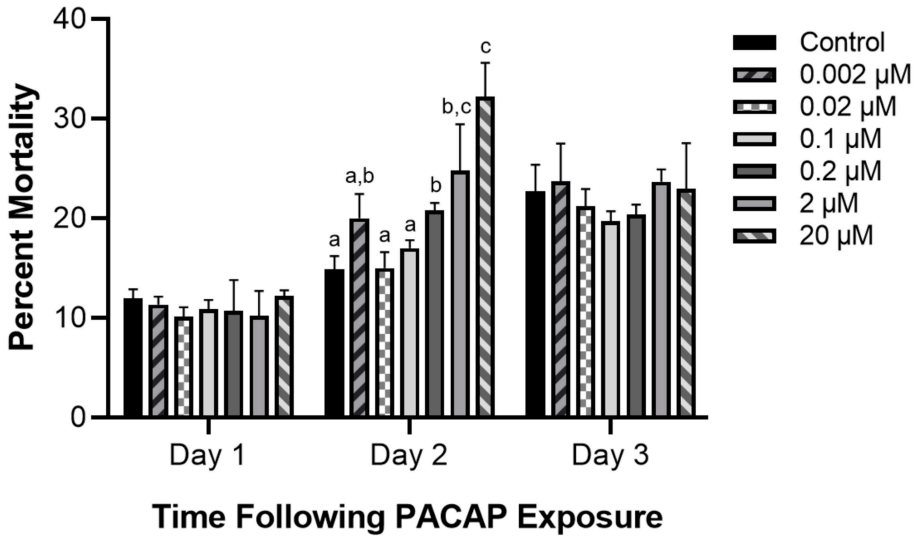


FIGURE 2 | Impact of *C. gariepinus* PACAP-38 on RTS11 viability. RTS11 was exposed to varying concentrations of PACAP ranging from 0–20 μM and the percent mortality of RTS11 was determined for each concentration using a trypan blue assay. This figure represents three independent experiments where a $p < 0.05$ was considered to be significantly different when compared to the no PACAP control for individual timepoints. All vertical error bars represent the standard deviation (SD). Lowercase letters denote significant differences at $p < 0.05$.

Permeabilization of *F. psychrophilum* by PACAP

To establish whether the studied PACAP concentrations were either inducing direct lysis of *F. psychrophilum* or instead stimulating RTS11 to respond to and destroy the bacterial pathogen, a permeabilization assay was performed. At doses comparable to the MIC (50 and 30 μM), PACAP was shown to induce permeabilization of *F. psychrophilum* comparable to that observed when the bacterium was heat-killed (**Figure 4**). Interestingly, this ability was absent when using 0.1 μM of PACAP as, in this case, the bacteria presented reduced permeabilization similar to that of the live *F. psychrophilum* control (**Figure 4**). The permeabilization ability noted here was also specific to PACAP as 50 μM of a synthetic peptide fragment of comparable size (1.3 kDa), HSP70, was not able to permeabilize *F. psychrophilum*.

Influence of *C. gariepinus* PACAP-38 on RTS11 Immune Gene Expression

Exposure to PACAP

To determine whether PACAP alone could stimulate a response in RTS11, the cells were exposed to various concentrations of the peptide (0.002, 0.02, and 0.1 μM) over 4 days. Following this exposure, gene expression of pro-inflammatory cytokines (*IL-1β*, *TNFα*, and *IL-6*) and PACAP receptors (*PAC1* and *VPAC1*) were measured using qRT-PCR. For all three of the pro-inflammatory cytokines measured, a significant difference was only seen on day 2 (**Figures 5A–C**). Furthermore, for *TNFα* and *IL-6*, this significant increase was only observed at the highest PACAP concentration of 0.1 μM. Meanwhile for *IL-1β*, a significant increase occurred at both 0.02 μM and 0.1 μM of PACAP. When regarding the PACAP receptors, there were no significant increases observed for *PAC1* but by day 2, *VPAC1* significantly increased at all of the concentrations studied (**Figures 5D–E**). To confirm that this response was specific to PACAP and not just a property of synthetic peptides in general, RTS11 was also exposed to 0.1 μM of a synthetic peptide fragment of rainbow trout HSP70, which was unable to induce significant expression differences in all of the genes selected for this study (**Figure 5F**).

Exposure to PACAP 24 h Before *F. psychrophilum* Infection

When RTS11 was challenged with live *F. psychrophilum* infection 24 h after exposure to PACAP, there were some interesting differences in transcript expression that were not observed during PACAP exposure alone (**Figure 5**). For *IL-1β* expression, there were no significant differences at 1 and 2 days post-infection when compared to the RTS11 cells exposed to live pathogen alone. However, by day 3 of infection, a significant increase in *IL-1β* transcripts was observed for all three concentrations of PACAP (**Figure 6A**). In comparison, *TNFα* expression was significantly upregulated at day 1, 2, and 3 post-infection but only at 0.1 μM of PACAP, the highest concentration of the AMP (**Figure 6B**). Interestingly, all three concentrations of PACAP showed a significant increase in *IL-6* expression on day 1 post-infection but by day 2 this upregulation was either lost at 0.002 μM or was significantly reduced in the two higher concentrations of PACAP (**Figure 6C**). When compared to the PACAP only expression (**Figure 5**), the PACAP receptors were also influenced differently during pathogen challenge. On day 1 post-infection, *PAC1* showed a significant increase only 0.1 μM (**Figure 6D**). Meanwhile, *VPAC1* showed a significant increase at day 2 in the two higher PACAP concentrations (0.02 and 0.1 μM) and on day 3, all three concentrations of PACAP presented a

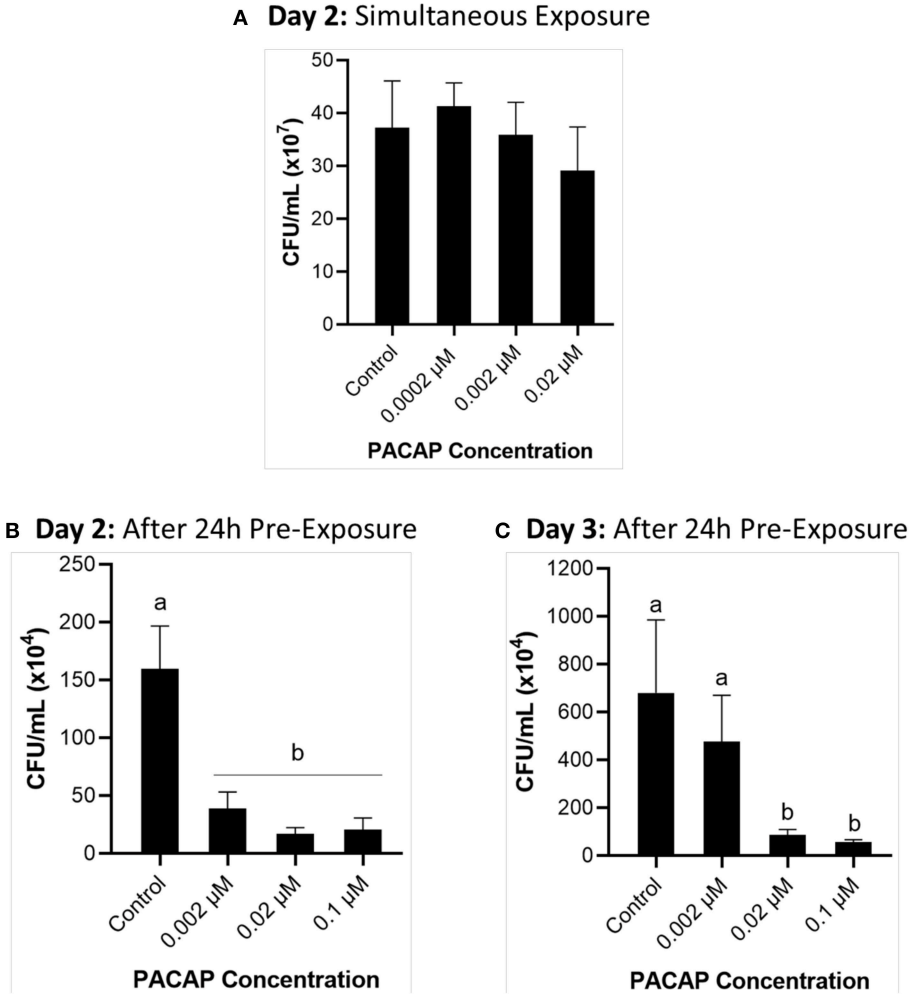


FIGURE 3 | Quantification of *F. psychrophilum* by standard plate count (SPC) of cell culture media during live infection (MOI of 0.7-1.3) of PACAP-treated RTS11. RTS11 was exposed to live *F. psychrophilum* either alone or in combination with *C. gariepinus* PACAP-38 concentrations (0.0002–0.02 μM) and CFU/mL was calculated on day 3 **(A)**. RTS11 pre-treated with PACAP-38 concentrations (0.002–0.1 μM) 24 h before exposure to live *F. psychrophilum* and the CFU/mL was calculated on day 2 post-infection **(B)** and day 3 post-infection **(C)**. Each panel represents the results of three independent experiments where a $p < 0.05$ was considered to be significantly different when compared to the no PACAP control (i.e., RTS11 exposed to only live *F. psychrophilum*). All vertical error bars represent the SD. Lowercase letters denote significant differences at $p < 0.05$.

significant upregulation when compared to the control cells that were exposed to *F. psychrophilum* alone (**Figure 6E**).

DISCUSSION

Influence of PACAP on the Viability of *F. psychrophilum* and RTS11 *in vitro*

Currently aquaculture facilities have very few options outside of antibiotics to combat disease outbreaks. When this is combined with the rising incidence of multi-drug resistance, AMPs such as PACAP are promising alternatives for disease control/prevention. The purpose of this study was to evaluate the antimicrobial activity and immunomodulatory function of PACAP within a live infection model consisting of RTS11 and the coldwater pathogen, *F. psychrophilum*. To assess the efficacy of this proposed system, it was critical to determine the impact that PACAP alone had on both components of the infection model: the host and the bacterium. For several bacterial pathogens, PACAP has been shown to have a direct antimicrobial effect (29, 46) including those of aquatic origin (46). Thus, it was not surprising that PACAP presented a similar result when *F. psychrophilum* was exposed to various concentrations in a preferred growth medium, cytophaga broth. Additionally, the MIC of PACAP was not influenced when *F. psychrophilum* was grown in cell culture media, a substance meant to mimic physiological conditions [reviewed by Yao and Asayama (56)]. This suggests that synthetic PACAP may maintain its antimicrobial effects in some physiological conditions, as may be the case when administered to live organisms. But despite this promising observation, it is important

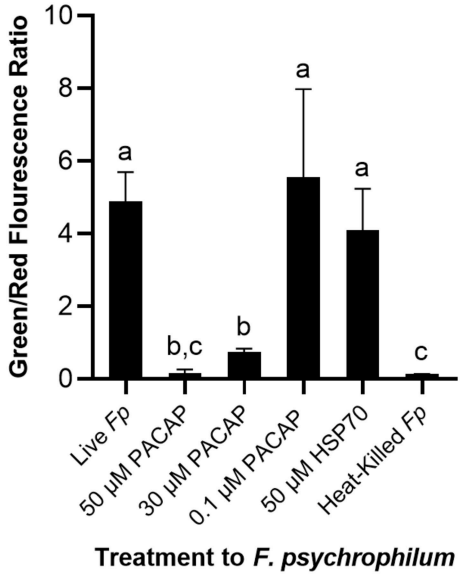


FIGURE 4 | Disruption of *F. psychrophilum* membrane by PACAP-38 of *C. gariepinus*. Live *F. psychrophilum* was grown alone, in the presence of PACAP-38 (50, 30, and 0.1 μM) and in the presence of a control synthetic peptide fragment of comparable size, 50 μM HSP70 (1.3 kDa). As a negative control, heat-killed *F. psychrophilum* was also included. Following a 3 day incubation at 14°C, all experimental wells were exposed to BacLight which would cause live bacterial cells to fluoresce green (SYTO9) and permeabilized cells to fluoresce red (propidium iodide). The ratio of green/red fluorescence was calculated, and this value was compared between conditions. This experiment was replicated four times and the averages are presented as the means + SD. A $p < 0.05$ was considered to be statistically significant. Lowercase letters denote significant differences at $p < 0.05$.

to remember that disease outbreaks in aquaculture settings would differ significantly from microbial culture settings in important ways. Namely the assumption of sterility and the resulting absence of competing microorganisms. As such, concentrations surrounding the observed MIC may not represent an effective therapeutic dose to control/prevent live infection and prove to be suboptimal for the host organism if not properly evaluated.

Aside from their potential as antimicrobials and immunomodulators, AMPs are also praised for potentially having minimal negative effects on mammalian host cells (57) including those of immune origin (58). Quite often this "cell selectivity" is based on the concentration required for the AMP to induce 50% hemolysis in host red blood cells (RBCs). If this concentration is much higher than what is required for the MIC, the peptide is considered to be essentially non-toxic to host cells [reviewed by Matsuzaki (59)]. This has been shown with *C. gariepinus* PACAP-38 when both human and fish RBCs were exposed to the peptide, revealing only RBC lysis at extremely high concentrations (46). Unfortunately, these methods of measurement are not always directly comparable as antimicrobial assays generally use a bacterial concentration of $\sim 5 \times 10^5$ CFU/mL while hemolysis assays use what corresponds to be 6×10^8 cells/mL [reviewed by Matsuzaki (59)]. In fact, when Imura et al. (60) corrected for this concentration difference during their analyses of the antimicrobial peptide magainin, the MIC concentration of 10 μM was enough to completely lyse the host RBCs (60). In the present study, RTS11 was exposed to PACAP wherein higher concentrations (0.2, 2, and 20 μM) had a significantly negative impact on RTS11 viability. Some studies have alluded to the idea that AMPs may be toxic to mammalian cells in the absence of microorganisms (60), thus it is possible that this may also be observed in fish cells. There are important differences between prokaryotic and eukaryotic membranes that may improve the chance that AMPs will preferentially bind to the membrane of microorganisms before host cells (reviewed by 58). Prokaryotic membranes have a high negative charge due to being predominantly composed of phosphatidylglycerol, cardiolipin, or phosphatidylserine, thus have a greater chance of attracting the cationic peptides that are AMPs. In comparison, mammalian cells may be less attractive for AMP penetration as they are enriched in zwitterionic phospholipids resulting in an overall neutral charge [reviewed by Matsuzaki (61) and Huang et al. (62)]. Furthermore, mammalian cell membranes contain cholesterol, something that is absent in prokaryotic membranes. Interestingly, it has been shown that cholesterol can dramatically reduce the activity of AMPs (63) providing another potential layer of protection for mammalian cells. But despite these important differences that may help with membrane selection of AMPs, complete protection of the host cells from AMP-induced cytotoxicity may not be possible at higher AMP concentrations. To even consider PACAP for use as a therapeutic agent in aquaculture settings, the therapeutic dose must not be cytotoxic to the host, whether infected or microbe-free.

Assessing the Ability of PACAP to Inhibit Bacterial Growth During Live Infection of RTS11 Cells

In spite of the value that can be obtained from determining the MIC of PACAP in various culture media, as well as the ideal concentration for survival of host cells, the observed antimicrobial activity is meaningless if it is lost or not effective during live pathogen challenge.

The current study is the first of its kind that has demonstrated the antimicrobial activity of PACAP during an *in vitro* live infection model with an aquatic pathogen. But interestingly, the teleostean version of PACAP was only able to reduce the viable bacterial count of *F. psychrophilum* when RTS11 cells were pre-treated with PACAP for 24 h. It appears that rainbow trout macrophages require time to respond and activate an effective immune response when exposed to *F. psychrophilum*. As obligate poikilotherms, metabolic rates in fish are heavily influenced by their environmental temperature (64, 65). Because cells derived from rainbow trout, a coldwater salmonid, are grown at much lower temperatures than their mammalian counterparts, it may take more time for these cells to respond to stimuli. Indeed this has been shown with both RTS11 and rainbow trout B cells where the chemoattractant ability of the chemokine CK9 strongly increased when the cells were pre-treated with T-independent antigen (66). Likewise, in rainbow trout primary head kidney culture, the cells sometimes required 48 h before an

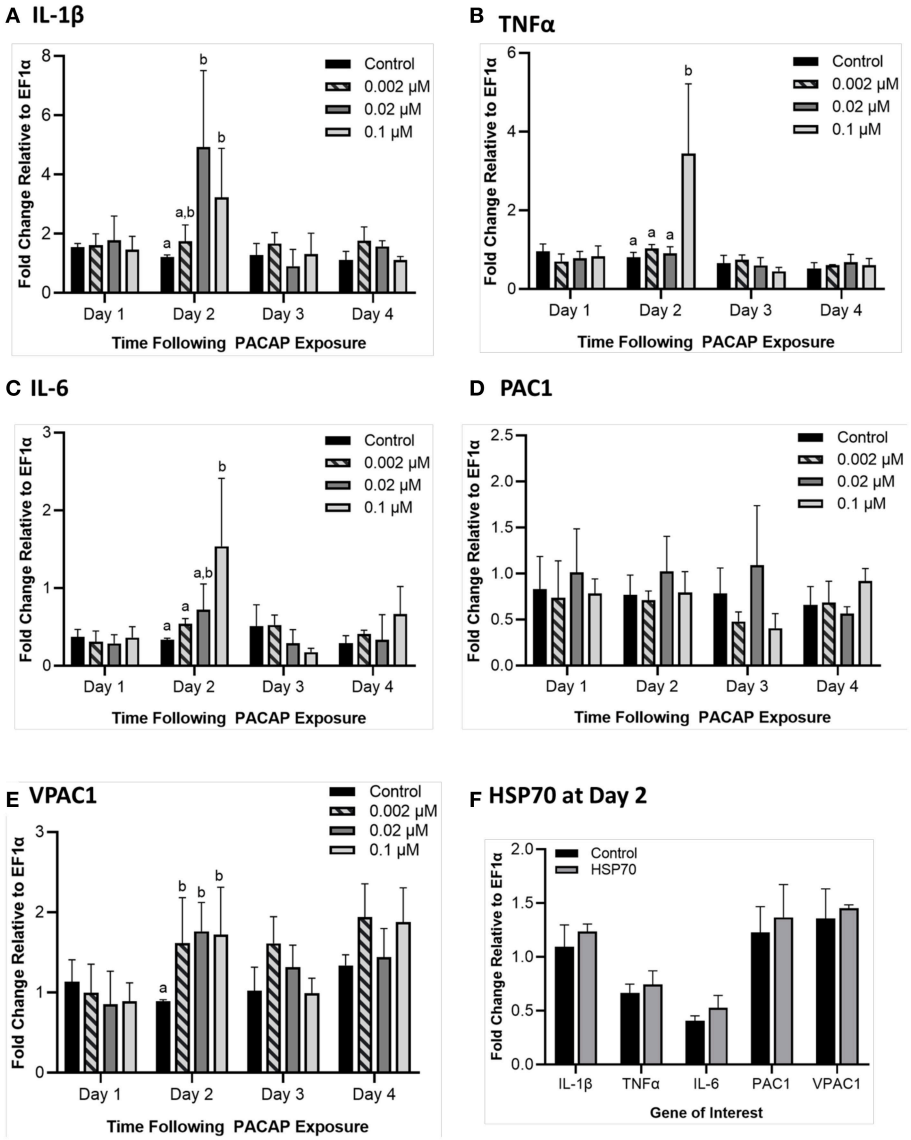


FIGURE 5 | Impact of *C. gariepinus* PACAP-38 (0.002 μM, 0.02 μM and 0.1 μM) on RTS11 pro-inflammatory cytokines and receptors PAC1 and VPAC1 mRNA expression 1–4 days following peptide exposure. Transcript expression of pro-inflammatory cytokines *IL-1β* **(A)**, *TNFα* **(B)** and *IL-6* **(C)** was measured so that the influence of PACAP alone on immune function could be assessed. The present PACAP receptors *PAC1* **(D)** and *VPAC1* **(E)** were also measured to determine whether PACAP could prime RTS11 cells to bind more PACAP. Because 1 day after the pre-exposure appeared to be the only timepoint with significant upregulation due to PACAP, RTS11 was also exposed to 0.1 μM of a synthetic HSP70 peptide fragment control of comparable size (1.3 kDa), for 48 h to confirm that this stimulation was due to PACAP and not a property of synthetic peptides alone **(F)**. All panels represent three independent experiments and are presented as means + SD. A $p < 0.05$ was considered to be statistically significant when compared to the no PACAP control for each timepoint. Lowercase letters denote significant differences at $p < 0.05$.

increase in respiratory burst activity was observed (67). In both of these examples, the immune cells were maintained at 18°C, but in the current study, RTS11 was held at 14°C as this is a relevant temperature at which BCWD occurs (68). Thus, a longer pre-treatment time at this lower temperature may be required depending on the response that is being measured. Though a temperature between 8 and 14°C would be optimal for testing the efficacy of PACAP in protecting rainbow trout from infection with *F. psychrophilum*, there are many infectious diseases that influence the culture of numerous aquatic organisms. As a result, experimental doses with therapeutic AMPs must be tested *in vivo* to ensure that they will provide protection and effective immune stimulation toward relevant pathogens within an applicable temperature range.

Cell culture systems provide a controlled, cost-effective method for exploring numerous biological phenomena, but it is important to recognize the limits of these models. In a cell culture setting, individual cells are directly exposed to the experimental stimulant, without physiological barriers or a complicated cellular milieu to overcome. As a result, *in vitro*

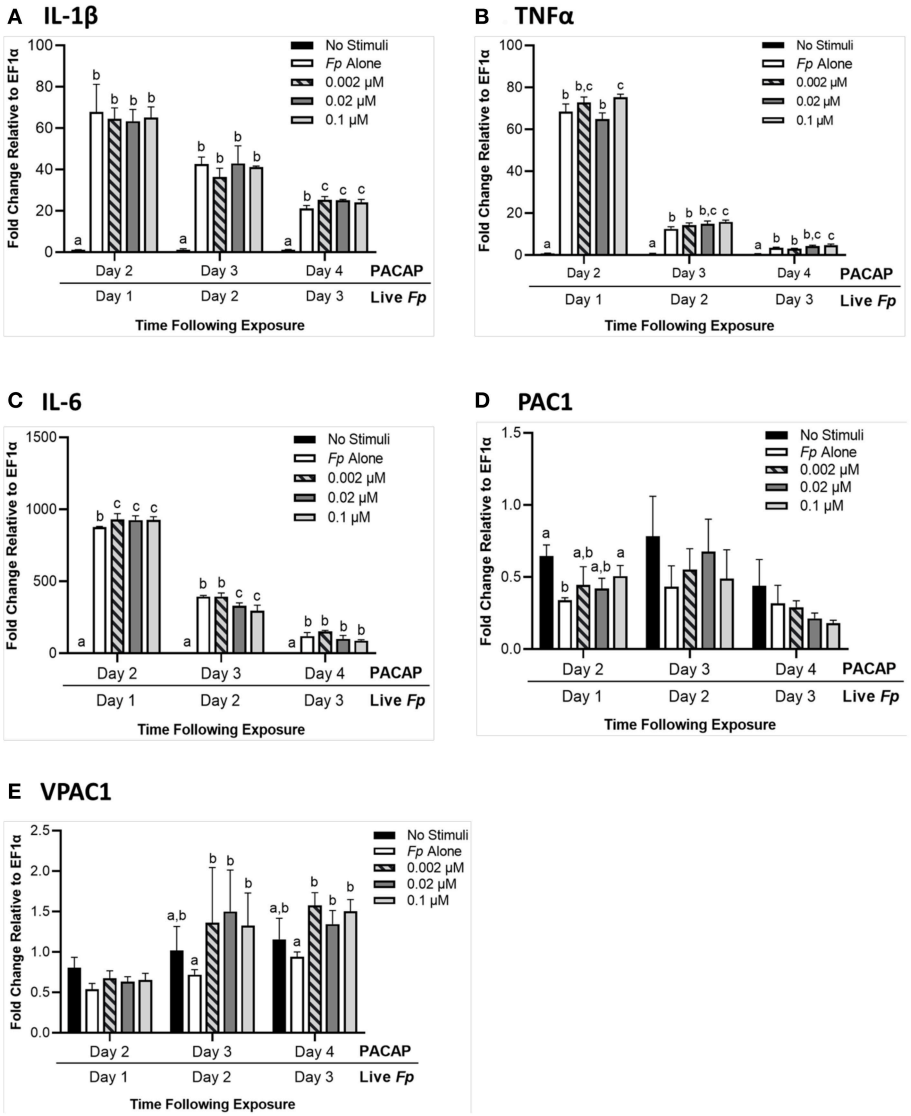


FIGURE 6 | RTS11 transcript expression when challenged with live *F. psychrophilum* following 24 h pre-treatment with PACAP concentrations (0.002, 0.02, and 0.1 μM). RTS11 that was not exposed to PACAP or live *F. psychrophilum* was also included as a no stimuli control. To determine whether PACAP has immunomodulatory effects during live infection, transcripts of the pro-inflammatory cytokines *IL-1β* **(A)**, *TNFα* **(B)** and *IL-6* **(C)** were measured in RTS11 on days 1, 2, and 3 of infection. The PACAP receptors that are found within RTS11, *PAC1* **(D)** and *VPAC1* **(E)** were also assessed throughout the live infection challenge. All panels represent three independent experiments and are presented as means + SD. A $p < 0.05$ was considered to be statistically significant when samples were compared within each timepoint. Lowercase letters denote significant differences at $p < 0.05$.

systems often have much lower doses than what is appropriate within the whole organism. This was displayed when Gotlieb et al. (69) used several methods to isolate and stimulate NK cells revealing that the cells were 10–30 times more susceptible to stress hormones *in vitro* than what was observed when stimulated in plasma, a much more biologically relevant medium. Though the effects of PACAP on fish infections *in vivo* have not yet been explored, there have been several studies to determine the impact of this AMP on growth, immunomodulation and physiology (48, 70–72). One study by Lugo et al. (48) exposed juvenile fish to an average of 4 μg of PACAP per fish, which significantly enhanced tilapia growth. In comparison, with the RTS11 infection model presented here, each well received 1.8 μg or less and antimicrobial activity was still observed. Though the PACAP doses optimized for the current *in vitro* study were very effective, an *in vivo* model would require further optimization to develop an efficacious exposure range.

Confirming the Direct Mode of Action of PACAP on *F. psychrophilum*

When it comes to bacterial pathogens, the consensus regarding AMP function is that they are either membrane disrupting, or non-membrane disrupting [reviewed by Bahar and Ren (9)]. Though PACAP was able to lower the number of viable bacteria

when grown alone in media (for the MIC) and in RTS11 cultures throughout live infection, it was unclear whether this was due to the direct antimicrobial activity of PACAP acting on *F. psychrophilum*. Previous work with mammalian PACAP confirmed for the first time that the peptide was capable of disrupting membranes of relevant terrestrial bacterial pathogens (29). This permeabilization is a common mode of action for α-helical AMPs (73), including PACAP, but until now this ability has not been confirmed for the version of PACAP produced by fish. Previous bioinformatic analysis of PACAP-38 from *C. garipinus* provided evidence that this peptide was very likely to have cell penetrating properties (46). The present study was able to functionally validate the ability of *C. gariepinus* PACAP-38 to permeabilize the membrane of *F. psychrophilum* at concentrations surrounding the MIC. Furthermore, this was an ability specific to PACAP as another synthetic peptide fragment of comparable size from a teleost, HSP70, did not induce permeabilization. Interestingly, at the highest concentration that reduced the viable bacterial count during live infection, 0.1 μM, PACAP was unable to permeabilize the membrane of *F. psychrophilum*. This finding confirmed that at 0.1 μM, one of the many other effects that PACAP may have on teleostean immunity must have been responsible for stimulating RTS11 to destroy and/or slow the growth of the coldwater pathogen.

Understanding the Immunostimulatory Effects of PACAP on RTS11

PACAP has been shown to have immunomodulatory effects on whole fish and in fish cells (46, 70, 71, 74) but this has only been studied in the absence of live infection. Furthermore, there has been limited research regarding the activity of PACAP directly on teleost immune cells. Specifically with RTS11, the immunostimulatory effect of three other α-helical AMPs has been reported (75) but not when dealing with a live bacterial challenge. The present study explores, for the first time, the impact of relevant doses of PACAP on the immune function of RTS11 in both the presence and absence of *F. psychrophilum*. In the absence of bacterial infection, PACAP was shown to stimulate pro-inflammatory cytokine expression 48 h following PACAP treatment as well increasing the expression of one of the PACAP receptors, *VPAC1*. When analyzing PACAP receptor expression in RTS11, it is important to note that only *VPAC1* and *PAC1* receptor genes were measured as it has previously been shown by Lugo et al. (55) that these cells do not express the third receptor gene, *VPAC2*. Lugo et al. (55) also showed that despite *PAC1* presenting the highest constitutive expression in all rainbow trout lymphoid tissues *in vivo*, this was not observed in RTS11 where *VPAC1* presents the greatest expression. As *PAC1* has been found to be a fundamental type I receptor for PACAP this result was unexpected. Nonetheless, the current study validated this finding when *VPAC1* presented significant upregulation following RTS11 stimulation with PACAP while *PAC1* did not. As PACAP was shown to stimulate a slight increase in pro-inflammatory cytokines and upregulate the expression of *VPAC1*, pre-treatment with this AMP may stimulate a protective state within the rainbow trout immune cells.

In itself, the presence of live bacteria would be capable of inducing pro-inflammatory cytokine expression in RTS11. But when this was combined with 24-h pre-treatments with PACAP, infection with *F. psychrophilum* had an effect on transcript expression that was quite different from PACAP alone. Rather than all three of the studied pro-inflammatory cytokines increasing their expression at the same time, each one showed significant upregulation at different time points post-infection when compared to RTS11 exposed to the bacteria alone. The pattern of enhancing inflammatory cytokine production following pre-treatment is similar to that of trained immunity that has been observed in mammalian monocytes and macrophages (76). Quintin et al. (76) showed that when primed with β-glucan prior to exposure to LPS, monocytes and macrophages were able to induce a greater pro-inflammatory response than unprimed cells. Perhaps PACAP has a similar function and is able to prime immune cells to produce a faster, more damaging response when they come into contact with a live pathogen. This would provide an explanation for the observed decrease in viable bacteria following PACAP exposure at doses that were not able to directly permeabilize the membrane of *F. psychrophilum*.

Despite the similarity to trained immunity, the actual function of PACAP in mammalian models appears to be contrary to what has been observed in bony fish. The vast majority of mammalian studies discuss the anti-inflammatory role of PACAP during experimental bacterial infection. These experiments often involve exposure to bacterial products (such as LPS) simultaneously with PACAP, after which various immune parameters are observed (77–79). This has led to the belief that many AMPs, including PACAP, play important anti-inflammatory roles to protect the host from dangerous, over-reactive inflammatory responses (80). Though very valuable, these mammalian studies are not directly comparable to a live, growing infection within an organism or cell culture. Additionally, aside from zebrafish, teleosts appear to be lacking TLR4, which binds and responds to LPS (81, 82). As a result, observations in mammalian study systems may not be directly transferrable to those of fish. The immunostimulatory effect of PACAP on rainbow trout immune cells as observed in this study has been previously reported in head kidney leukocytes derived from another bony fish, the grass carp (71). Wang et al. (71) found that when these immune cells were exposed to bacterial products, PACAP induced inflammatory cytokine expression while having no impact on the expression of the anti-inflammatory cytokine, *IL-10*. When all of this information is taken together, it appears that PACAP may play a different, yet valuable role in the immunomodulation of teleosts when compared to what has been observed in mammals.

CONCLUSIONS

Antimicrobial peptides (AMPs) are promising alternatives to antibiotics in the ongoing battle between aquaculture facilities and infectious agents. One AMP that has received a lot of attention due to its pleiotropic effects in aquatic species is PACAP. The results of the present study revealed that

PACAP derived from the teleost *C. gariepinus* acts as a potent antimicrobial peptide against the causative agent of BCWD, *F. psychrophilum*. Furthermore, its mode of action was confirmed to be permeabilization of the bacterial membrane. When a live infection model was developed with this pathogen and the monocyte/macrophage-like cell line, RTS11, 24 h pre-exposure of PACAP appeared to protect RTS11 by significantly reducing the number of viable bacteria in the culture system. Based on transcript levels of pro-inflammatory cytokines and receptors for the AMP, PACAP was also shown to have an immunostimulatory effect on RTS11 whether exposed to the AMP alone or exposed to both PACAP and live *F. psychrophilum* challenge. Overall, this study was able to provide further validation regarding the antimicrobial effect of PACAP on aquatic pathogens as well as its immunomodulatory activity on teleost immune cells. As a promising candidate for use in aquatic models, future studies should focus on confirming these valuable functions of PACAP throughout live infection models *in vivo*.

AUTHOR CONTRIBUTIONS

SS performed majority of experiments, contributed to experimental design, and wrote the first draft of the manuscript. TR-R performed the remaining experiments, contributed to experimental design and aided in data/statistical analyses. YC and ME provided the synthetic PACAP and contributed to experimental design due to their previous experience studying *C. gariepinus* PACAP function on teleost growth and immunity. JL provided the strain of *F. psychrophilum* and valuable insight regarding appropriate bacterial culture/exposure conditions. BD contributed to experimental design, funding of the project, and writing of the manuscript. All authors contributed to manuscript revisions and approved the final submitted version.

FUNDING

The work presented in this paper was supported by the Natural Science and Engineering Research Council of Canada grant number 217529 and a Canada Research Chair to BD.

ACKNOWLEDGMENTS

The authors would like to acknowledge Dr. Niels Bols for kindly allowing us to use his cell culture facility.

REFERENCES

1. FAO (2018). *The State of World Fisheries and Aquaculture 2018 - Meeting the Sustainable Development Goals*. Rome. Licence: CC BY-NC-SA 3.0 IGO.
2. World Bank (2014). *Reducing Disease Risks in Aquaculture*. World Bank Report #88257-GLB.
3. Watts JEM, Schreier HJ, Lanska L, Hale MS. The rising tide of antimicrobial resistance in aquaculture: sources, sinks and solutions. *Marine Drug.* (2017) 15:E158. doi: 10.3390/md150601580
4. Santos L, Ramos F. Antimicrobial resistance in aquaculture: current knowledge and alternatives to tackle the problem. *Int J Antimicrob Agents.* (2018) 52, 135–143. doi: 10.1016/j.ijantimicag.2018.03.010
5. Zhang L, Gallo RL. Antimicrobial peptides. *Curr Biol.* (2016) 26, PR14–R19. doi: 10.1016/j.cub.2015.11.017
6. Lai Y, Gallo RL. AMPed up immunity: how antimicrobial peptides have multiple roles in immune defense. *Trends Immunol.* (2009) 30, 131–41. doi: 10.1016/j.it.2008.12.003
7. Lee J, Luchian T, Park Y. New antimicrobial peptide kills drug-resistant pathogens without detectable resistance. *Oncotarget.* (2018) 9:15616–34. doi: 10.18632/oncotarget.24582
8. Mahlapuu M, Hakansson J, Ringstad L, Bjorn C. Antimicrobial peptides: an emerging category of therapeutic agents. *Front Cel Infect Microbiol.* (2016) 6:194. doi: 10.3389/fcimb.2016.00194
9. Bahar AA, Ren D. Antimicrobial peptides. *Pharmaceuticals*. (2013) 6:1543–75. doi: 10.3390/ph6121543
10. Kang H, Kim C, Seo CH, Park Y. The therapeutic applications of antimicrobial peptides (AMPs): a patent review. *J Microbiol.* (2017) 55:1–12. doi: 10.1007/s12275-017-6452-1
11. Otvos L. Immunomodulatory effects of anti-microbial peptides. *Acta Microbiol et Immunol Hungar.* (2016) 63:257–77. doi: 10.1556/030.63.2016.005
12. Elssner A, Duncan M, Gavrilin M, Wewers MD. A novel $P2X_7$ receptor activator, the human cathelicidin-derived peptide LL37, induces IL-1β processing and release. *J Immunol.* (2004) 172:4987–94. doi: 10.4049/jimmunol.172.8.4987
13. Yu J, Mookerjee N, Wee K, Bowdish DME, Pistolic J, Li Y, et al. Host defense peptide LL-37, in synergy with inflammatory mediator IL-1β, augments immune responses by multiple pathways. *J Immunol.* (2007) 179:7684–91. doi: 10.4049/jimmunol.179.11.7684
14. Mookherjee N, Brown KL, Bowdish DME, Doria S, Falsafi R, Hokamp K, et al. Modulation of the TLR-mediated inflammatory response by the endogenous human host defense peptide LL-37. *J Immunol.* (2006) 176:2455–64. doi: 10.4049/jimmunol.176.4.2455
15. Di Nardo A, Braff MH, Taylor KR, Na C, Granstein RD, McInturff JE, et al. Cathelicidin antimicrobial peptides block dendritic cell TLR4 activation and allergic contact sensitization. *J. Immunol.* (2007) 178:1829–34. doi: 10.4049/jimmunol.178.3.1829
16. Miyata A, Arimura A, Dahl RR, Minamino N, Uehara A, Jiang L, et al. Isolation of a novel 38 residue-hypothalamic polypeptide which stimulates adenylate cyclase in pituitary cells. *Biochem Biophys Res Commun.* (1989) 164:567–74.
17. Kimura C, Ohkubo S, Ogi K, Hosoya M, Itoh Y, Onda H. A novel peptide which stimulates adenylate cyclase: molecular cloning and characterization of the ovine and human cDNAs. *Biochem Biophy Res Commun*. (1990) 1:81–89.
18. Ogi K, Kimura C, Onda H, Arimura A, Fujino M. Molecular cloning and characterization of cDNA for the precursor of rat pituitary adenylate cyclase activating polypeptide (PACAP). *Biochem Biophy Res Commun.* (1990) 173:1271–9.
19. Deutsch PJ, Sun Y. The 38 amino acid form of pituitary adenylate cyclase activating polypeptide stimulates dual signaling cascadein PC12 cells and promotes neurite growth. *J Biol Chem.* (1992) 267:5108–13
20. Matsumoto H, Koyama C, Sawada T, Koike K, Hirota K, Miyake A. Pituitary folliculo-stallate-like cell line (TtT/GF) responds to novel hypophysiotrophic peptide (pituitary adenylate cyclase-activating peptide), showing increased adenosine 3',5'-monophosphate and interleukin-6 secretion and cell proliferation. *Endocrinology*. (1993) 133:2150–5.
21. Shivers BD, Gorcs TJ, Gottschall PE, Arimura A. Two high affinity binding sites for pituitary adenylate cyclase-activating polypeptide have different tissue distributions. *Endocrinology*. (1991) 128:3055–65. doi: 10.1210/endo-128-6-3055
22. Pisegna JR, Wank SA. Molecular cloning and functional expression of the pituitary adenylate cyclase-activating polypeptide type I receptor. *Biochemistry*. (1993) 90:6345–49.

23. Arimura A, Somogyvari-Vigh A, Miyata A, Mizuno K, Coy DH, Kitada C. Tissue distribution of PACAP as determined by RIA: highly abundant in rat brain and testes. *Endocrinology*. (1991) 129:2787–9.
24. Hashimoto H, Ishihara T, Shigemoto R, Mori K, Nagata S. Molecular cloning and tissue distribution of a receptor for pituitary adenylate cyclase-activating polypeptide. *Neuron*. (1993) 11:333–42. doi: 10.1016/0896-6273(93)90188-W
25. Murakami Y, Koshimura K, Yamauchi K, Nishiki M, Tanaka J, Furuya H, et al. Pituitary adenylate cyclase activating polypeptide (PACAP) stimulates growth hormone release from GH_3 cells through type II PACAP receptor. *Regul Pept*. (1995) 56:35–40.
26. Leyton J, Gozes Y, Pisegna J, Coy D, Purdom S, Casibang M, et al. PACAP(6-38) is a PACAP receptor antagonist for breast cancer cells. *Br Cancer Res Treat*. (1999) 56:177–186.
27. Gray SL, Cummings KJ, Jirik FR, Sherwood NM. Targeted disruption of the pituitary adenylate cyclase-activating polypeptide gene results in early postnatal death associated with dysfunction of lipid and carbohydrate metabolism. *Mol Endocrinol*. (2001) 15:1739–47. doi: 10.1210/mend.15.10.0705
28. Adams BA, Gray SL, Isaac ER, Biaco AC, Vidal-Puig AJ, Sherwood NM. Feeding and metabolism in mice lacking pituitary adenylate cyclase-activating polypeptide. *Endocrinology*. (2008) 149:1571–80. doi: 10.1210/en.2007-0515
29. Starr CG, Maderdrut JL, He J, Coy DH, Wimley WC. Pituitary adenylate cyclase-activating polypeptide is a potent broad-spectrum antimicrobial peptide: structure-activity relationships. *Peptides*. (2018) 104:35–40. doi: 10.1016/j.peptides.2018.04.006
30. Arimura A. Perspectives on pituitary adenylate cyclase activating polypeptide (PACAP) in the neuroendocrine, endocrine, and nervous systems. *Jap J Physiol*. (1998) 48:301–31.
31. Lumsden JS, Young K, Welsh K, MacInnes J, Russell S, Hesami S. Management approaches for coldwater disease caused by *Flavobacterium psychrophilum*. In: *Proceedings of the National Freshwater Aquaculture Symposium*. (2006) p. 111–7.
32. Starliper CE. Bacterial coldwater disease of fishes caused by *Flavobacterium psychrophilum*. *J Adv Res*. (2011) 2:97–108. doi: 10.1016/j.jare.2010.04.001
33. Wiens GD, Palti Y, Leeds TD. Three generations of selective breeding improved rainbow trout (*Oncorhynchus mykiss*) disease resistance against natural challenge with *Flavobacterium psychrophilum* during early life-stage rearing. *Aquaculture*. (2018) 497:414–421. doi: 10.1016/j.aquaculture.2018.07.064
34. Brown LL, Cox WT, Levine RP. Evidence that the causal agent of bacterial cold-water disease *Flavobacterium psychrophilum* is transmitted within salmonid eggs. *Dis Aqua Org*. (1997) 29:213–8.
35. Cipriano RC, Holt RA. *Flavobacterium psychrophilum*, *Cause of Bacterial Cold-Water Disease and Rainbow Trout Fry Syndrome. Fish Disease Leaflet No. 86*. Leetown, WV: United States Dept. of the Interior. U.S. Geological Service, National Fish Health Research Laboratory (2005).
36. Nilsen H, Olsen AB, Vaagnes O, Hellberg H, Bottolfsen K, Skjelstad H, et al. Systemic *Flavobacterium psychrophilum* infection in rainbow trout, *Oncorhynchus mykiss* (Walbaum), farmed in fresh and brackish water in Norway. *J Fish Dis*. (2011) 34:403–8. doi: 10.1111/j.1365-2761.2011.01249.x
37. Silverstein JT, Vallejo RL, Palti Y, Leeds TD, Rexroad CE, Welch TG, et al. Rainbow trout resistance to bacterial cold-water disease is moderately heritable and is not adversely correlated with growth. *J Anim Sci*. (2009) 87:860–7. doi: 10.2527/jas.2008-1157
38. Vallejo RL, Palti Y, Liu S, Evenhuis JP, Gao G, Rexroad III CE, et al. Detection of QTL in rainbow trout affecting survival when challenged with *Flavobacterium psychrophilum*. *Mar Biotechnol*. (2013) 16:349–60. doi: 10.1007/s10126-013-9553-9
39. Marancik D, Gao G, Paneru B, Ma H, Hernandez AG, Salem M, et al. Whole-body transcriptome of selectively bred, resistant-, control-, and susceptible-line rainbow trout following experimental challenge with *Flavobacterium psychrophilum*. *Front Genet*. (2015) 5:453. doi: 10.3389/fgene.2014.00453
40. Gomez E, Mendez J, Cascales D, Guijarro JA. *Flavobacterium psychrophilum* vaccine development: a difficult task. *Microbial Biotechnol*. (2013) 7:414–23. doi: 10.1111/1751-7915.12099
41. Makesh M, Sudheesh PS, Cain KD. Systemic and mucosal immune response of rainbow trout to immunization with an attenuated *Flavobacterium psychrophilum* vaccine strain by different routes. *Fish Shellfish Immunol*. (2015) 44:156–63. doi: 10.1016/j.fsi.2015.02.003
42. Hoare R, Ngo TPH, Adams A. Efficacy of a polyvalent immersion vaccine against *Flavobacterium psychrophilum* and evaluation of immune response to vaccination in rainbow trout fry (*Oncorhynchus mykiss* L.). *Vet Res*. (2017) 48:43. doi: 10.1186/s13567-017-0448-z
43. Nematollahi A, Pasmans F, Haesebrouck F, Decostere A. Early interactions of *Flavobacterium psychrophilum* with macrophages of rainbow trout *Oncorhynchus mykiss*. *Dis Aqua Org*. (2005) 64:23–8. doi: 10.3354/dao064023 .
44. Semple SL, Mulder IM, Rodriguez-Ramos T, Power M, Dixon B. Long-term implantation of acoustic transmitters induces chronic inflammatory cytokine expression in adult rainbow trout (*Oncorhynchus mykiss*). *Vet Immunol Immunopathol*. (2018) 205:1–9. doi: 10.1016/j.vetimm.2018.10.003
45. Ganassin RC, Bols NC. Development of a monocyte/macrophage-like cell line, RTS11, from rainbow trout spleen. *Fish Shellfish Immunol*. (1998) 8:457–76.
46. Lugo JM, Tafalla C, Oliva A, Pons T, Oliva B, Aquilino C, et al. Evidence for antimicrobial and anticancer activity of pituitary adenylate cyclase-activating polypeptide (PACAP) from North African catfish (*Clarias gariepinus*): Its potential use as a novel therapeutic agent in fish and humans. *Fish Shellfish Immunol*. (2019) 86:559–70. doi: 10.1016/j.fsi.2018.11.056
47. Carpio Y, Lugo JM, Leon K, Morales R, Estrada MP. Novel function of recombinant pituitary adenylate cyclase-activating polypeptide as stimulator of innate immunity in African catfish (*Clarias gariepinus*) fry. *Fish Shellfish Immunol*. (2008) 25:439–45. doi: 10.1016/j.fsi.2008.06.004
48. Lugo JM, Oliva A, Morales A, Reyes O, Garay HE, Herrera F, et al. The biological role of pituitary adenylate cyclase-activating polypeptide (PACAP) in growth and feeding behavior in juvenile fish. *J Pept Sci*. (2010) 16:633–43. doi: 10.1002/psc.1275
49. Lugo JM, Carpio Y, Morales R, Roriguez-Ramos T, Ramos L, Estrada MP. First report of the pituitary adenylate cyclase activating polypeptide (PACAP) in crustaceans: conservation of its functions as growth promoting factor and immunomodulator in the white shrimp *Litopenaeus vannamei*. *Fish Shellfish Immunol*. (2013) 35:1788–96. doi: 10.1016/j.fsi.2013.08.028
50. Gorgoglione B, Carpio Y, Secombes CJ, Taylor NGH, Lugo JM, Estrada MP. Viral and bacterial septicaemic infections modulate the expression of PACAP splicing variants and VIP/PACAP receptors in brown trout immune organs. *Fish Shellfish Immunol*. (2015) 47:923–32. doi: 10.1016/j.fsi.2015.10.014
51. Sever L, Vo NTK, Bols NC, Dixon B. Expression of tapasin in rainbow trout tissues and cell lines and up regulation in a monocyte/macrophage cell line (RTS11) by a viral mimic and viral infection. *Devel Comp Immunol*. (2014) 44:86–93. doi: 10.1016/j.dci.2013.11.019
52. Jarau M, Di Natale A, Huber P, MacInnes J, Lumsden JS. Virulence potential of *Flavobacterium psychrophilum* isolates from Ontario, Canada in rainbow trout *Oncorhynchus mykiss* (Walbaum). *J Fish Dis*. (2018). 41:1505–14. doi: 10.1111/jfd.12861.
53. Otvos L, Cudic M. Broth microdilution antibacterial assay of peptides. *Methods Mol Biol*. (2007) 386:309–20. doi: 10.1007/978-1-59745-430-8_12.
54. Semple SL, Kellendonk CJ, Al-Hussinee L, MacInnes JI, Lumsden JS, Dixon B. Serum IgM, MH class IIβ genotype and respiratory burst activity do not differ between rainbow trout families displaying resistance or susceptibility to the coldwater pathogen, *Flavobacterium psychrophilum*. *Aquaculture*. (2018) 483:131–40. doi: 10.1016/j.aquaculture.2017.10.020
55. Lugo JM, Tafalla C, Leceta J, Gomariz RP, Estrada MP. Differential expression pattern of pituitary adenylate cyclase-activating polypeptide (PACAP) alternative splicing variants and its receptors in the immune system of rainbow trout (*Oncorhynchus mykiss*). *Fish Shellfish Immunol*. (2011) 30:734–8. doi: 10.1016/j.fsi.2010.12.008
56. Yao T, Asayama Y. Animal-cell culture media: history, characteristics and current issues. *Reprod Med Biol*. (2017) 16:99–117. doi: 10.1002/rmb2.12024
57. Deslouches B, Phadke SM, Lazarevic V, Cascio M, Islam K, Montelaro RC, et al. *De novo* generation of cationic antimicrobial peptides: influence in length and tryptophan substitution on antimicrobial activity. *Antimicrob Agents Chemother*. (2005) 49:316–22. doi: 10.1128/AAC.49.1.316-322.2005
58. Zhu X, Shan A, Ma Z, Xu W, Wang J, Chou S, et al. Bactericidal efficiency and modes of action of the novel antimicrobial peptide T9W against *Pseudomonas aeruginosa*. *Antimicrobial Agents Chemother*. (2015) 59:3008–17 doi: 10.1128/AAC.04830-14

59. Matsuzaki K. Control of cell selectivity of antimicrobial peptides. *Biochim et Biophy Acta*. (2009) 1788:1687–92. doi: 10.1016/j.bbamem.2008.09.013
60. Imura Y, Choda N, Matsuzaki K. Magainin 2 in action: distinct modes of membrane permeabilization in living bacterial and mammalian cells. *Biophys J*. (2008) 95:5757–65. doi: 10.1529/biophysj.108.133488
61. Matsuzaki K. Why and how are peptide-lipid interactions utilized for self-defense? Magainins and tachyplesins as archetypes. *Biochim et Biophys Acta Biomembran*. (1999) 1462:1–10. doi: 10.1016/S0005-2736(99)00197-2
62. Huang Y, Huang J, Chen Y. Alpha-helical cationic antimicrobial peptides: relationships of structure and function. *Protein Cell*. (2010) 1:143–52. doi: 10.1007/s13238-010-0004-3
63. Matsuzaki K, Sugishita KI, Fujini N, Miyajima K. Molecular basis for membrane selectivity of an antimicrobial peptide, Magainin 2. *Biochemicstry*. (1995) 34, 3423–29. doi: 10.1021/bi00010a034
64. Gillooly JF, Charnov EL, West GB, Savage VM, Brown JH. Effects of size and temperature on developmental time. *Nature*. (2002) 417:70–3. doi: 10.1038/417070a
65. Patterson JT, Mims SD, Wright RA. Effects of body mass and water temperature on routine metabolism of American paddlefish *Polyoden spathula*. *J Fish Biol.* (2013) 82:1269–80. doi: 10.1111/jfb.12066
66. Aquilino C, Granja AG, Castro R, Wang T, Abos B, Parra D, et al. Rainbow trout CK9, a CCL25-like ancient chemokine that attracts and regulates B cells and macrophages, the main antigen presenting cells in fish. *Oncotarget*. (2016) 7:17547–64. doi: 10.18632/oncotarget.8163
67. Novoa B, Figueras A, Ashton I, Secombes CJ. *In vitro* studies on the regulation of rainbow trout (*Oncorhynchus mykiss*) macrophage respiratory burst activity. *Dev Comp Immunol.* (1996) 20:207–16.
68. Holt RA. *Cytophaga Psychrophila the Causative Agent of Bacterial Cold-Water Disease in Salmonid Fish*. PhD Thesis, Corvalis, OR: Oregon State University (1987).
69. Gotlieb N, Rosenne E, Matzner P, Shaashua L, Sorski L, Ben-Eliyahu S. The misleading nature of *in vitro* and *ex-vivo* findings in studying the impact of stress hormones on NK cell cytotoxicity. *Brain Behav Immun.* (2015) 45, 277–86. doi: 10.1016/j.bbi.2014.12.020
70. Lugo JM, Carpio Y, Oliva A, Morales A, Estrada MP. Pituitary adenylate cyclase-activating polypeptide (PACAP): a regulator of the innate and acquired immune functions in juvenile fish. *Fish Shellfish Immunol.* (2010) 29:513–20. doi: 10.1016/j.fsi.2010.05.004
71. Wang X, Wei H, Zhao T, Zhu X, Yang X, Chen D. Evidence for pituitary adenylate cyclase-activating peptide as a direct immunoregulator in teleost head kidney. *Fish Shellfish Immunol.* (2013) 34:265–72. doi: 10.1016/j.fsi.2012.11.002
72. Cardoso JCR, Felix RC, Martins RST, Trindade M, Fonseca VG, Fuentes J. PACAP system evolution and its role in melanophore function in teleost fish skin. *Mol Cell Enodcrinol.* (2015) 411:130–45. doi: 10.1016/j.mce.2015.04.020
73. Sato H, Feix JB. Peptide-membrane interactions and mechanisms of membrane destruction by amphipathic α-helical antimicrobial peptides. *Biochim et Biophys Acta Biomembran*. (2006) 1758:1245–56. doi: 10.1016/j.bbamem.2006.02.021
74. Kasica-Jarosz N, Podlasz P, Kaleczyc J. Pituitary adenylate cyclase-activating polypeptide (PACAP-38) plays an inhibitory role against inflammation induced by chemical damage to zebrafish hair cells. *PLoS ONE*. (2018) 13:e0198180. doi: 10.1371/journal.pone.0198180
75. Chiou PP, Khoo J, Bols NC, Douglas S, Chen TT. Effects of linear cationic α-helical antimicrobial peptides on immune-relevant genes in trout macrophages. *Dev Comp Immunol.* (2006) 30:797–806. doi: 10.1016/j.dci.2005.10.011
76. Quintin J, Saeed S, Martens JHA, Giamarellos-Bourboulis EJ, Ifrim DC, Logie C, et al. *Candida albicans* infection affords protection against reinfection via functional reprogramming of monocytes. *Cell Host Microbe.* (2012) 12:223–32. doi: 10.1016/j.chom.2012.06.006
77. Delgado M, Munoz-Elias EJ, Gomariz RP, Ganea D. VIP and PACAP inhibit IL-12 production in LPS-stimulated macrophages. Subsequent effect on IFNγ synthesis by T cells. *J Neuroimmunol.* (1999) 96, 167–81. doi: 10.1016/S0165-5728(99)00023-5
78. Delgado M, Ganea D. Inhibition of endotoxin-induced macrophage chemokine production by vasoactive intestinal peptide and pituitary adenylate cyclase-activating polypeptide *in vitro* and *in vivo*. *J Immunol.* (2001) 167:966–75. doi: 10.4049/jimmunol.167.2.966
79. Martinez C, Abad C, Delgado M, Arranz A, Juarranz MG, Rodriquez-Hench N, et al. Anti-inflammatory role of septic shock of pituitary adenylate cyclase-activating polypeptide receptor. *Pro Nat Acad Sci USA*. (2002) 99:1053–8. doi: 10.1073/pnas.012367999
80. Delgado M, Munoz-Elias EJ, Gomariz RP, Ganea D. Vasoactive intestinal peptide and pituitary adenylate cyclase-activating polypeptide enhance IL-10 production by murine macrophages: *in vitro* and *in vivo* studies. *J Immunol.* (1999) 162:1707–16.
81. Sepulcre MP, Alcaraz-Perez F, Lopez-Munoz A, Rocz FJ, Meseguer J, Cayuela ML. Evolution of lipopolysaccharide (LPS) recognition and signaling: fish TLR4 does not recognize LPS and negatively regulates NF-kappaB activation. *J Immunol.* (2009) 182:1836–45. doi: 10.4049/jimmunol.0801755
82. Ali A, Rexroad CE, Thorgaard GH, Yao J, Salem M. Characterization of the rainbow trout spleen transcriptome and identification of immune-related genes. *Front. Genet.* (2014) 5:348. doi: 10.3389/fgene.2014.00348

Conflict of Interest Statement: The authors declare that the research was conducted in the absence of any commercial or financial relationships that could be construed as a potential conflict of interest.

Copyright © 2019 Semple, Rodríguez-Ramos, Carpio, Lumsden, Estrada and Dixon. This is an open-access article distributed under the terms of the Creative Commons Attribution License (CC BY). The use, distribution or reproduction in other forums is permitted, provided the original author(s) and the copyright owner(s) are credited and that the original publication in this journal is cited, in accordance with accepted academic practice. No use, distribution or reproduction is permitted which does not comply with these terms.

frontiers in Immunology

ORIGINAL RESEARCH
published: 15 May 2019
doi: 10.3389/fimmu.2019.00869

Immunomodulatory Effects and Induction of Apoptosis by Different Molecular Weight Chitosan Oligosaccharides in Head Kidney Macrophages From Blunt Snout Bream (*Megalobrama amblycephala*)

Changsong Wu[1], *Yishan Dai*[1], *Gailing Yuan*[1,2], *Jianguo Su*[1,2] *and Xiaoling Liu*[1,2]*

[1] *Department of Aquatic Animal Medicine, College of Fisheries, Huazhong Agricultural University, Wuhan, China,* [2] *Hubei Provincial Engineering Laboratory for Pond Aquaculture, Hubei Engineering Technology Research Center for Aquatic Animal Disease Control and Prevention, Wuhan, China*

OPEN ACCESS

Edited by:
Roy Ambli Dalmo, UiT The Arctic University of Norway, Norway

Reviewed by:
Jiong Chen, Ningbo University, China
Michiel Van Der Vaart, Leiden University, Netherlands

***Correspondence:**
Xiaoling Liu
liuxl@mail.hzau.edu.cn

Specialty section:
This article was submitted to Comparative Immunology, a section of the journal Frontiers in Immunology

Received: *20 February 2019*
Accepted: *04 April 2019*
Published: *15 May 2019*

Citation:
Wu C, Dai Y, Yuan G, Su J and Liu X (2019) Immunomodulatory Effects and Induction of Apoptosis by Different Molecular Weight Chitosan Oligosaccharides in Head Kidney Macrophages From Blunt Snout Bream (Megalobrama amblycephala). Front. Immunol. 10:869. doi: 10.3389/fimmu.2019.00869

Prophylactic administration of immunopotentiators has been tested and practiced as one of the most promising disease prevention methods in aquaculture. Chitosan oligosaccharide (COS), as an ideal immunopotentiator, is mainly used as feed additives in aquaculture, and the antimicrobial and immune enhancement effects are highly correlated with molecular weight (MW), but little is known about the mechanisms in teleost. Here, we isolated and purified macrophages in head kidney from blunt snout bream (*Megalobrama amblycephala*), stimulated them with three different MW (∼500 Da, ∼1000 Da and 2000∼3000 Da) COSs, performed RNA-sequencing, global transcriptional analyses, and verification by quantitative real-time PCR (qRT-PCR) and immunofluorescent staining methods. Differential expression gene (DEG) analysis indicated that gene expression patterns are different and the proportion of unique genes are relatively high in different treatment groups. Biological process and gene set enrichment analysis (GSEA) demonstrated that all three COSs activate resting macrophages, but the degrees are different. Weighted gene co-expression network analysis (WGCNA) reflected gene modules correlated to MW, the module hub genes and top GO terms showed the activation of macrophage was positively correlated with the MW, and larger MW COS activated cell death associated GO terms. Further use of the screening and enrichment functions of STRING and Pfam databases discovered that apoptosis-related pathways and protein families were activated, such as the P53 pathway and caspase protein family. qRT-PCR results showed that as the stimulation time extends, the innate immune-related and P53 pathways are gradually activated, and the degree of activation is positively correlated with the stimulation time. In addition, apoptosis was detected by immunofluorescent staining in three groups. Therefore, the use of COS has two sides—it can activate the immune system against pathogen invasion, but with the increase in stimulation time and MW, macrophage apoptosis

is induced, which may be caused by abnormal replication of DNA and excessive inflammation. This study provides a theoretical basis for the rational use of COS as an immunopotentiator in aquaculture.

Keywords: *Megalobrama amblycephala*, Chitosan oligosaccharide, macrophage, transcriptome, apoptosis, P53 pathway

INTRODUCTION

In recent years, with the increasing scale and density of aquaculture industry, infections by a variety of fish pathogens have become more frequent. The negative effects of chemotherapeutants have become increasingly prominent, such as increased resistance of pathogens, decreased cellular, and humoral immune functions of aquatic animals, and drug residues directly threatening human health and safety. Therefore, the prevention and control of aquatic animals from the perspective of immunology have gradually become a research hotspot. Immunopotentiators are a new type of fishery drug that activate the body's immune function and enhance its resistance to infectious diseases (1). Their main immunomodulating mechanism is to act on the cell surface receptors and enable cells to produce cytokines to clear pathogens (2). The application of immunopotentiators is important for controlling fish diseases in aquaculture (3). Chitosan is an important immunopotentiator and is the only alkaline polysaccharide in nature. It has been reported to regulate the function of isolating immune cells *in vitro* (4).

COS, a polymer composed of deacetylated glucosamine units and β-(1-4)-linked N-acetyl-D-glucosamine (GlcNAc), has a polymerization degree (DP) of 2∼20 and an average MW <3,900 Da (5, 6). Due to its water solubility, non-toxicity, superior biocompatibility and adsorption properties, the potential application of COS as dietary supplements or medications has received considerable interest (7). In recent years, more and more research has been devoted to exploring the biological significance of COS application. The results showed that COSs have exhibited versatile biological functions, including anti-oxidative, anti-inflammation anti-microbial, anti-tumor, and anti-coagulant properties (8–10).

Macrophages are critical immune cells that play pivotal roles in both defense and immune homeostasis. Studies have shown that COS is recognized by macrophages and regulates macrophage function as one of the important ways to play an immunomodulatory role (11–13). On the one hand, COS activates resting macrophages to release NO and cytokines. NO has a cytotoxic effect, and a large amount of NO released can kill microorganisms, parasites, and tumor cells (14). Cytokines play an important role in inflammatory response and immune response and regulate both innate and adaptive immunity. It has been reported that COS stimulates resting macrophages to promote the secretion of Th1 cytokines (15). On the other hand, COS can also weaken activated macrophages and inhibit inflammation-related gene secretion (16). In addition, some studies have shown that the biological functions of COS are closely related to MW. COS with DPs of 6–8 (or 4–7 ∼ 5–7) have good antibacterial activity, immunopotentiating effect, and antitumor activity. About 1,700 Da MW COS is suitable for patients with hyperlipidemia; this amount can reduce blood sugar and improve antioxidant ability (17–19). In the study of mammals, the immunoregulatory mechanisms of COS involve the modulation of several important pathways including the suppression of nuclear factor kappa B (NF-κB) and mitogen-activated protein kinases (MAPK), and the activation of AMP-activated protein kinase (AMPK) (20–23). However, the studies of mechanisms are still in the initial stage in bony fish.

In this study, we used three different MW COSs to stimulate the head kidney macrophages of blunt snout bream *in vitro*. Then, the similarities and differences of biological functions of COSs were compared by high-throughput sequencing and bioinformatics analysis. We conducted experimental validation for some important findings. We expected to provide new ideas for the development and utilization of new immunopotentiator in aquaculture.

MATERIALS AND METHODS

Fish Sampling

Blunt snout bream (*M. amblycephala*), ranging from 400 g to 500 g in weight, were obtained from a fish farm located in Hubei Province, China and kept in a recirculating freshwater system at 25–26°C with a natural photoperiod. The animals were fed twice per day with a commercial pellet diet (Haida, Hubei, China) amounting to 3% of body weight. The study was approved by the Institutional Animal Care and Use Ethics Committee of Huazhong Agricultural University.

Isolation of Head-Kidney Macrophages

Blunt snout bream head kidney macrophages were isolated as described previously with slight modifications (24). Briefly, fish were anesthetized with MS222 (Syndel Laboratories, Ltd., Canada) and the head kidney was removed aseptically and passed through a 100 lm mesh (Falcon, Becton Dickinson) in Leibovitz medium (L-15) (Invitrogen, USA) containing 2% fetal bovine serum (FBS) (Gibco, USA) and 200 IU/ml penicillin plus streptomycin (Amresco, USA). The resulting cell suspension was layered onto a 34%/51% Percoll (Pharmacia, Uppsala, Sweden) density gradient and centrifuged at 400 g for 30 min at 4°C. The interface was collected and the cells were washed twice with L-15 at 400 g for 10 min at 4°C before being resuspended to 1×10^7 cells/ml in L-15 containing 10% FBS.

Macrophages Stimulated With COSs and GlcNAc

A total of 2 ml of the macrophage suspension (1×10^7 cells/ml in L-15 containing 10% FBS) was dispensed into each

well of a 6-well plate. After 12 h incubation at 28°C, the non-adherent cells were washed off. COS with MWs ∼500 Da (COS3), ∼1000 Da (COS6), 2000∼3000 Da (COS13-19), and GlcNAc (N-acetyl-D-glucosamine, the monomeric unit of the polymer chitosan) were added to each well (20 μg/ml), respectively (4). PBS was added to each well as the control group. Then, these samples were further incubated for 4, 8, and 16 h at 28°C.

RNA Extraction and cDNA Synthesis

The total RNA from each well was collected with a High Pure RNA Isolation Kit (Roche, Basel, Switzerland) following the manufacturer's instructions. Quality and quantity of the extracted RNA were assessed by electrophoresis in 1% agarose gels and with NanoDrop 2000 spectrometer (Thermo Scientific, USA), using the A260/A280 > 1.8 criterion as the acceptable quality threshold. Approximately 1 μg of total RNA was used to synthesize the first strand cDNA using the PrimeScript® RT reagent Kit with gDNA Eraser (TaKaRa, China) according to the manufacturer's protocols and then stored at −20°C.

cDNA Library Preparation, Illumina Sequencing, and Data Analysis After Stimulation for 4 h

Poly(A)$^+$ RNA was purified from total cellular RNA using poly(dT) oligo-attached magnetic beads, and full-length cDNAs were synthesized with a KAPA Stranded RNA-Seq Library Preparation Kit (Illumina Inc., USA) according to the manufacturer's protocol. The cDNA libraries were sequenced on the Illumina Xten genomic sequencing platform to generate 150-bp paired-end reads, by Wuhan Whbioacme Co. Ltd. Raw reads were first filtered to remove the adaptor and bases of low quality by Trimmomatic (25). Filtered reads were aligned to the *M. amblycephala* genome by HISAT2 (26). The sequencing quality of the raw data and mapped reads ratio after quality control for 15 samples are shown in **Dataset S1**. Although the whole genomic sequence of *M. amblycephala* has been published, the resulting document of gene structure prediction has not been made public (27). Therefore, Geta software was used to make gene structure prediction, and we re-obtained the genomic structure information (**Dataset S2**) and gene sequence (**Dataset S3**) (https://github.com/chenlianfu/geta). Subsequently, the newly obtained protein sequence (**Dataset S4**) was compared with the published sequence using Busco (28). The proportions of homologous genes in the newly predicted and published sequences were 89.7 and 88.2%, respectively. The result show that our prediction is more accurate. Gene expression was quantified with cufflinks, expression values were normalized for library size and differentially expressed genes were considered with DESeq2 (29, 30). All raw data of the results of this article are available in the NCBI Sequence Read Archive Database (http://www.ncbi.nlm.nih.gov/Traces/sra/) under accession number SRP169988.

GO Term and KEGG Pathway Enrichment Analyses

To analyze the potential functions of genes, we first re-annotated the genes of *M. amblycephala*. Briefly, blunt snout bream genes were mapped to multiple public databases such as NCBI non-redundant (NR), Gene Ontology (GO), Swiss-Prot/UniProt, and the Kyoto Encyclopedia of Genes and Genomes (KEGG) databases. Using all the genes as background, we used the numbers of DEGs to calculate the *P*-value (<0.05), which represent the significance of enriched GO terms/KEGG pathways and control the false discovery rate, respectively. The *p*-values were calculated by Fisher's exact test.

Gene Set Enrichment Analysis (GSEA)

To investigate the stimulation effect of COS on various biological function gene sets in macrophages, differences in gene mRNA expression levels of biological functional annotation and pathways between control and COS stimulation groups with different MW were analyzed by GSEA (http://software.broadinstitute.org/gsea/downloads.jsp). For use with GSEA software, the database file (**Dataset S5**) about KEGG pathway enrichment analyses of *M. amblycephala* was built. *P*-value < 0.05 was chosen as the cut-off criteria.

Weighted Gene Co-expression Network Analysis and Protein-Protein Interaction Network Analysis

The weighted correlation network was constructed using the freely accessible R software package as previously described (31, 32). We selected the 10,000 most variant genes for WGCNA analysis. Three different ways can be selected to construct the network and identify modules according to different needs. In our study, the one-step function was used for network construction and detection of consensus modules. The modules were filtered using the following criteria: Pearson $P > 0.8$ and *P*-value < 0.001. Furthermore, we extracted a subnetwork with module genes from the high quality STRING protein interaction database (combined score ≥ 600) (33). Since the STRING database weights and integrates information from numerous sources, including experimental repositories, computational prediction methods, and public text collections, we only parsed the high-quality part of it, hoping to get a convincing interaction subnetwork of our module genes. The subnetwork was illustrated with Gephi (https://gephi.org).

Quantitative Real-Time PCR

Quantitative real-time PCR (qRT-PCR) was used to investigate the target gene expression patterns in different groups and different time points (0 h, 4 h, 8 h, and 16 h) of macrophages after COS stimulation. Primers used for qRT-PCR of this experiment are given in **Table 1**. The qRT-PCR mixture reaction volume was 20 μl, containing 10 μl LightCycler® 480 SYBR Green I Master, 7.4 μl ddH_2O, 0.8 μl of each primer (10 mM), and 1 μl cDNA template. The reactions were performed using LightCycler®480 II (Roche Diagnostics GmbH, USA) according to the procedure as follows: preincubation at 95°C for 5 min, then 40 cycles at

TABLE 1 | Primers used for qRT-PCR in this study.

Gene name	Forward primer (5′-3′)	Reverse primer (5′-3′)	Gene number
ERK1	TCCTGCGAGGGCTGAAATAC	TCCGGTGTGGTCATGTTCTG	MK315044
ERK2	CCCTAAAGCGTTGGACCTGT	AGGTTAAACGGAGCCTCAGC	MK315045
Jnk1	AGCACCCCTACATCAACGTG	CGTTTTTCGTTCGCTCCTCC	MK315047
P38α	TGGGAGCGGATCTCAACAAC	TCAGGCCAGCTGAATGGATG	MK315052
P38β	TGTCGACAAGACCGGGATTC	CTGCTGTGGATGAGGGACTG	MK315053
Fos	GCTGCAAGCTGAAACTGACC	CGATAGGTGAGACGGATGGC	MK315046
Junb	ACTTGAACCTGACGGAACCC	CTTCCTGCTCGTCGGTGATT	MK315048
Jund	AGGAAGAAGCTGCGTAACCG	TTGCTCTCTCAGAACGCTCG	MK315049
NF-κB1	TGGATGGAGGGGCAGATGTA	AAGTGCGCTCAGTTTGCTTG	MK315050
NF-κB2	AACTACCAGTTGAGCGGTGG	GGTCACTGCAGGATTTCCCA	MK315051
TNF-α	CCGCTGCTGTCTGCTTCA	GCCTGGTCCTGGTTCACTCT	HQ696609.1
ATR	GGAGACGGCCAACTTTGAGA	CGAATGAGGTTGCCCTGTCT	MK315042
ATM	CCCGGAGAACCGAATGTTGA	AATCCCTCCAAACGAGCCAG	MK315041
Bax	CCGGCTTGTCATCAAGGCTA	GTGGGGGTGCCAAAATAGGA	MK315043
P53	TGCTGACTGAACAGCCTCAG	GAACTGGACACGTTTTCGCC	MK315040
Caspase3	GGTGGATGCTATGCCTCAGT	CCATTGCGTTGGTTCATGCC	KY006115.1
β-actin	GTGCCAGGTGCCAAGTAGC	AAGCCCAAGATATGCAGGAGT	ADV57164.1

95°C for 5 s, 55°C for 20 s, and 72°C for 20 s. Each sample was tested in triplicate. Specificity of the amplified target gene was assessed using dissociation curve analysis. The target gene relative expression levels vs. the β-actin gene (was selected as the reference gene) was calculated according to the $2^{-\Delta\Delta CT}$ method. To determine the relative fold change of the target gene at different time points, the expression value was normalized using the corresponding control group.

Analysis of Apoptosis by Annexin V-FITC

Annexin V-FITC/PI double staining was used to evaluate cell apoptosis after stimulation for 16 h, strictly following the procedures of the Annexin V-FITC Apoptosis Detection Kit (Beyotime Institute of Biotechnology, China). Briefly, macrophages were seeded in 24-well plates and cultured as before, then treated with COSs (20 μg/ml) for 16 h. After treatments, the cell culture medium was removed, and it was washed once with PBS. We then added 195 μl media binding reagent, 5 μl Annexin V-FITC and 10 μl PI to stain the cells. Finally, cells were incubated at 28°C for 20 min in the dark.

Statistical Analysis

In the present study, data generated by qRT-PCR were presented as the means of three biological replicates ± SE. The statistical significance was assessed by two-tailed independent *t*-test. $P < 0.05$ value was considered to be statistically significant difference and $P < 0.01$ value as extreme difference.

RESULT

Expression of Differentially Expressed Genes (DEGs) After COS Stimulation of Head Kidney Macrophages

We analyzed the DEGs among the control, GlcNAc, COS3, COS6, and COS13-19 groups with DESeq2. Compared with the control group, the COS3, COS6, and COS13-19 groups contained 1005, 986, and 1440 DEGs, respectively (P-value < 0.001). However, there were only 10 DEGs between the control and GlcNAc group, and we think that GlcNAc could not activate resting macrophages (**Figure S1**). These results were clearly visualized by clustering the samples by differential treatment and by constructing a Venn diagram of the DEGs (**Figure 1**). Some DEGs in certain stimulated group were upregulated but in others they were downregulated or showed no difference, like the regions genes in **Figure 1A**. Interestingly, different stimulated groups had different proportions of unique genes in up- or downregulated genes, especially in the COS13-19 group (**Figure 1B**). This may suggest that COSs with different MWs have different effects on macrophages from blunt snout bream head kidney.

Functional Enrichment Analysis of DEGs

There was a clear difference in the number of DEGs between the COS3, COS6, and COS13-19 groups compared with the control. Therefore, we performed Gene Ontology (GO) term and KEGG pathway analysis to filter the biological processes and pathways. The top 15 GO terms (in descending order of the P-value) of the three groups are shown in **Figure 2**. The common enrichment GO terms among the three stimulation groups are defense response, inflammatory response, response to bacterium, response to biotic stimulus, response to external biotic stimulus, and response to other organisms (**Figures 2A–C**). In addition, immune-related responses were enriched in one or two groups, mainly including immune system process (COS6 and COS13-19), regulation of immune system process (COS6), and leukocyte chemotaxis (COS13-19). In the GSEA analysis of KEGG enrichment, the top 10 KEGG pathways (in descending order of the NES) of the three groups are shown (**Figures 2D–F**). Some of the pathways associated with pathogenic infections were significantly enriched, including salmonella infection (COS3 and COS13-19), African trypanosomiasis (COS3), and malaria

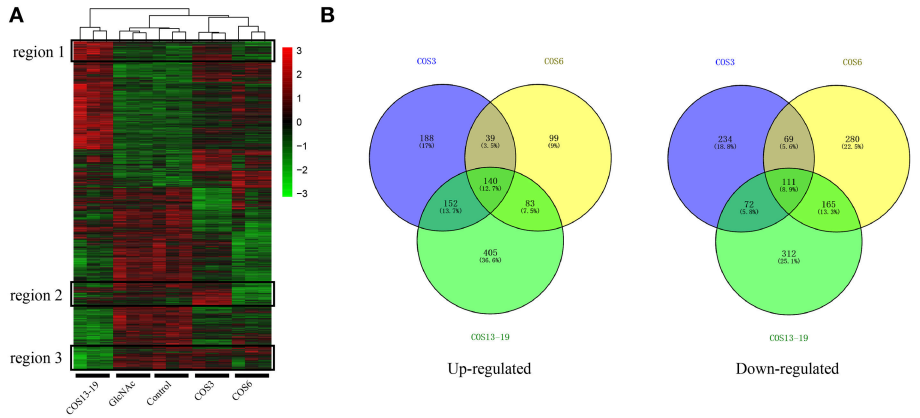


FIGURE 1 | Differentially expressed gene (DEG) analysis of different MW COS-stimulated macrophages ($P < 0.001$). **(A)** A heatmap was used to classify the DEG expression patterns in all groups, the x-axis represents the experimental conditions (4 h). **(B)** Venn diagrams of DEGs in COS3, COS6, and COS13-19 groups. Left panel: up-regulated genes; right panel: down-regulated genes.

(COS3). Immune-related pathways were enriched in COS13-19 groups, such as TNF signaling pathway and Toll-like receptor signaling pathway. Notably, DNA replication was the most prominent pathway in the three groups (**Figure S2**). This may reflect a common characteristic of COS-stimulated macrophages.

Weighted Gene Network Co-expression Analysis of COSs Stimulated Macrophages

Gene co-expression network analysis relies on the assumption that a strong correlation of mRNA expression levels for a group of genes suggests that these genes work cooperatively on features. A gene linkage in a network is simply the number of other genes that are expressed in relation to the gene. The network was initially constructed using the component of the weighted gene co-expression network (WGCNA) method (31, 32). This method has been widely used to construct a weighted gene co-expression network based on absolute Pearson correlation coefficient between gene expression and expression levels to detect gene clusters correlated with a trait (34, 35).

In total, one control group and four treatment groups contained 15 samples, and 10,000 genes were used to construct the gene co-expression network. As 14 is the lowest value that allows obtaining more than 80% similarities in topology models of five groups (**Figure 3A**), a soft threshold of 14 was performed, resulting in the discovery of 17 significant modules (**Figure 3B**). The number and percentage of genes contained in different modules are shown in **Figure 3C**. Among these modules, the cyan and magenta modules were significantly correlated in the COS3 group, the midnightblue and grey60 modules were significantly correlated in the COS6 group, and the blue module was significantly correlated in the COS13-19 group (Pearson $P > 0.8$ and P-value < 0.001, **Figure 3D**). Additionally, gene intramodular analysis of GS and MM in the 5 modules followed. Because GS and MM exhibit significant correlation, the present finding implies that the genes in the module tend to be highly correlated with COS stimulated macrophages, and the magenta, midnightblue and blue modules were the most relevant modules in the COS3, COS6, and COS13-19 groups, respectively (**Figures 3E-G**). This may indicate that these genes contributing to macrophages status in the three groups, so we selected the three modules for further analysis.

Network Construction and Analysis of Selected Modules

The co-expression networks of top ranked genes for the magenta, midnightblue, and blue modules were constructed as shown in **Figures 4A–C**. The 200 strongest connection genes within the blue module were selected to show their connections and confirm hub genes. Within each network, color depth, font sizes, and node sizes are proportional to their connectivity (sum of in-module degrees). To study the biological functions of the magenta, midnightblue and blue modules, we implemented GO term enrichment analysis. For the magenta module, the top 5 enriched GO terms are shown in **Figure 4D**, including peptidyl-proline hydroxylation, protein hydroxylation, single-organism metabolic process, mRNA transport, and oxidationreduction process. Additionally, in **Figure 4A**, the hub genes like EGLN1A, ERO1A, EGLN3, P4HA2, and CPOX were proven to be related to intracellular oxygen concentration. The post-translational formation of 4-hydroxyproline in hypoxia-inducible factor (HIF) alpha proteins is catalyzed by EGLN1A (36). For the midnightblue module, the top 5 GO terms—including the classical pathway of complement activation, negative regulation of MAPK cascade, protein localization to chromatin, leukocyte mediated immunity, and phospholipid transport—were enriched (**Figure 4E**). The hub genes in this module are related to the innate immune system and cell proliferation, such as DUSP2, C1QB, CFP, SPRY4, C1QC, EMILIN1B, WNK4B, ZFP36L1, EGR3, and so on (**Figure 4B**). In the blue module, intracellular signal transduction, MAPK cascade, cell death, death, and programmed cell death GO terms were enriched (**Figure 4F**), as were the hub genes associated with innate immunity and antitumor activity, such as MAP3K12, FMN1, MPX, ABI3A, SLC2A6, TNFAIP2B, DUSP1, NOS2B, JUN, IL1β, and so on

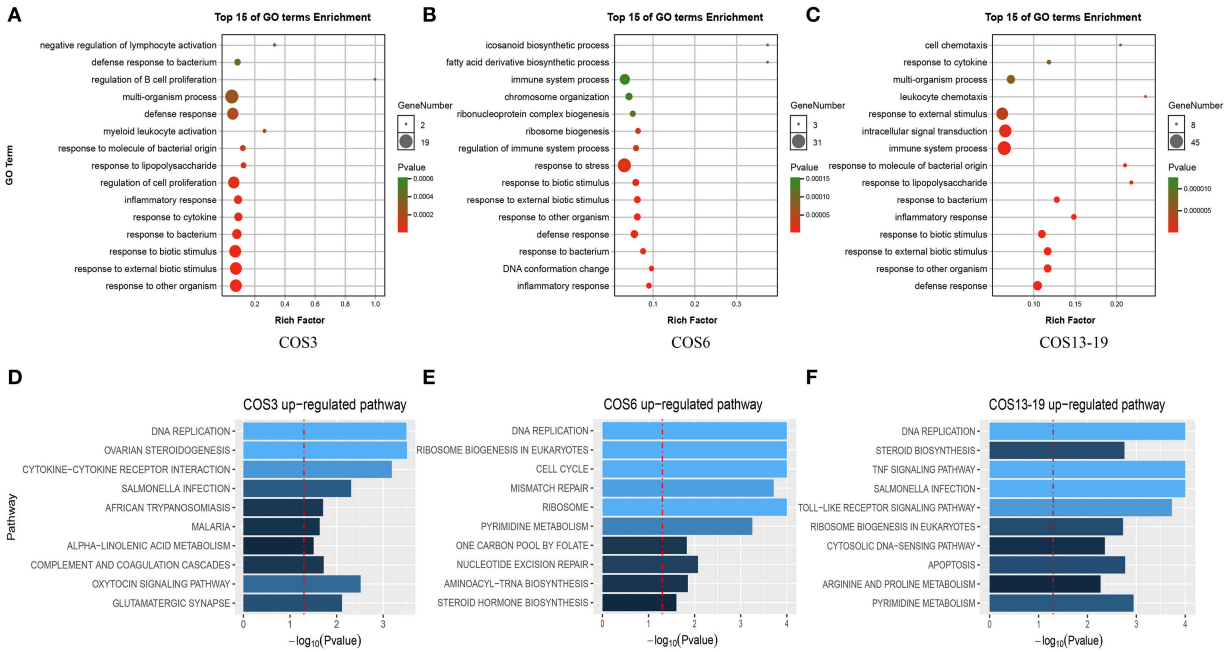


FIGURE 2 | Functional enrichment analysis identified major biological processes and pathways in COS3, COS6, and COS13-19 groups. **(A–C)** GO enrichment analysis of upregulated genes in COS3, COS6, and COS13-19, respectively. **(D–F)** Gene set enrichment analysis (GSEA) of all genes in COS3, COS6, and COS13-19.

(**Figure 4C**). It is worth noting that three GO terms associated with death were significantly enriched in the blue module. In order to further explore the potential function of macrophages stimulated by COS13-19, the biological characteristics of the blue module were examined using existing data on protein-protein interactions, which have been gathered in the publicly available STRING database. We selected the proteins with an interaction score $\geq$ 0.4 in PPI network to perform KEGG pathway enrichment analysis and protein family and domain accurate classification. The top 10 pathways were shown in **Figure 4G**; these pathways were associated with infectious diseases, the immune system, cell growth and death, signal transduction, and metabolism. Interestingly, the enriched results of protein families and domains included caspase recruitment domain, bZIP transcription factor, and PH domain (**Figure 4H**). These results may imply that COS13-19 not only activates the immune system of macrophages, but also regulates cell proliferation and apoptosis through some pathways, such as the FoxO, MAPK, and p53 signaling pathways and cell cycle. Overall, the identification of some genes within the three modules that are known to regulate immune system, cell growth and death, and the gene expression network analysis using the WGCNA approach provides valuable insight into the pathways regulating macrophages which contribute to the COSs stimulated macrophages.

COSs Activated MAPK and NF-κB Signaling Pathways in Blunt Snout Bream Head Kidney Macrophages

In mammalian studies, COS can promote the secretion of cytokines by resting macrophages and play an important role in inflammatory and immune response. The two most studied and identified pathways are the MAPK and NF-κB signaling pathways (4, 15, 37). In our results, the MAPK pathway and NF-κB upstream pathways were enriched. To further evaluate our results, we selected macrophages which qwew stimulated at different time points (4, 8, and 16 h) and key genes in the two pathways for qRT-PCR analysis. As shown in **Figure 5**, ERK1/2, Jnk1, P38α, P38β, Fos, Junb, and Jund are the key genes for MAPK pathway (**Figures 5A-H**). The qRT-PCR results showed that COS could activate the MAPK pathway through p38β at the early stage (4 h) of macrophage stimulation, and then upregulated the other genes. In the NF-κB pathway (**Figures 5I-K**), NF-κB2 was significantly upregulated in the COS6 and COS13-19 groups at 4 h, and the expression of NF-κB1 and inflammatory cytokine TNF-α was upregulated. These results again demonstrate that MAPK and NF-κB signaling pathways are activated in COSs stimulated macrophages.

COS Induced Apoptosis of Macrophages Via P53 Pathway

P53 activation not only leads to cell cycle arrest, but also participates in cell apoptosis, which leads to two distinct results: the former provides the cells with the possibility of initiating repair and reversing the damage. The latter is lethal to cells. Therefore, p53 is considered to be one of the key factors determining cell survival and death (38). In our results, the P53 pathway, cell death-related GO terms, and caspase recruitment domain were enriched. To further verify our results, qRT-PCR and immunofluorescent staining methods were used. These results are shown in **Figure 6**. In the early stages of stimulation (4h), only the ATR and P53

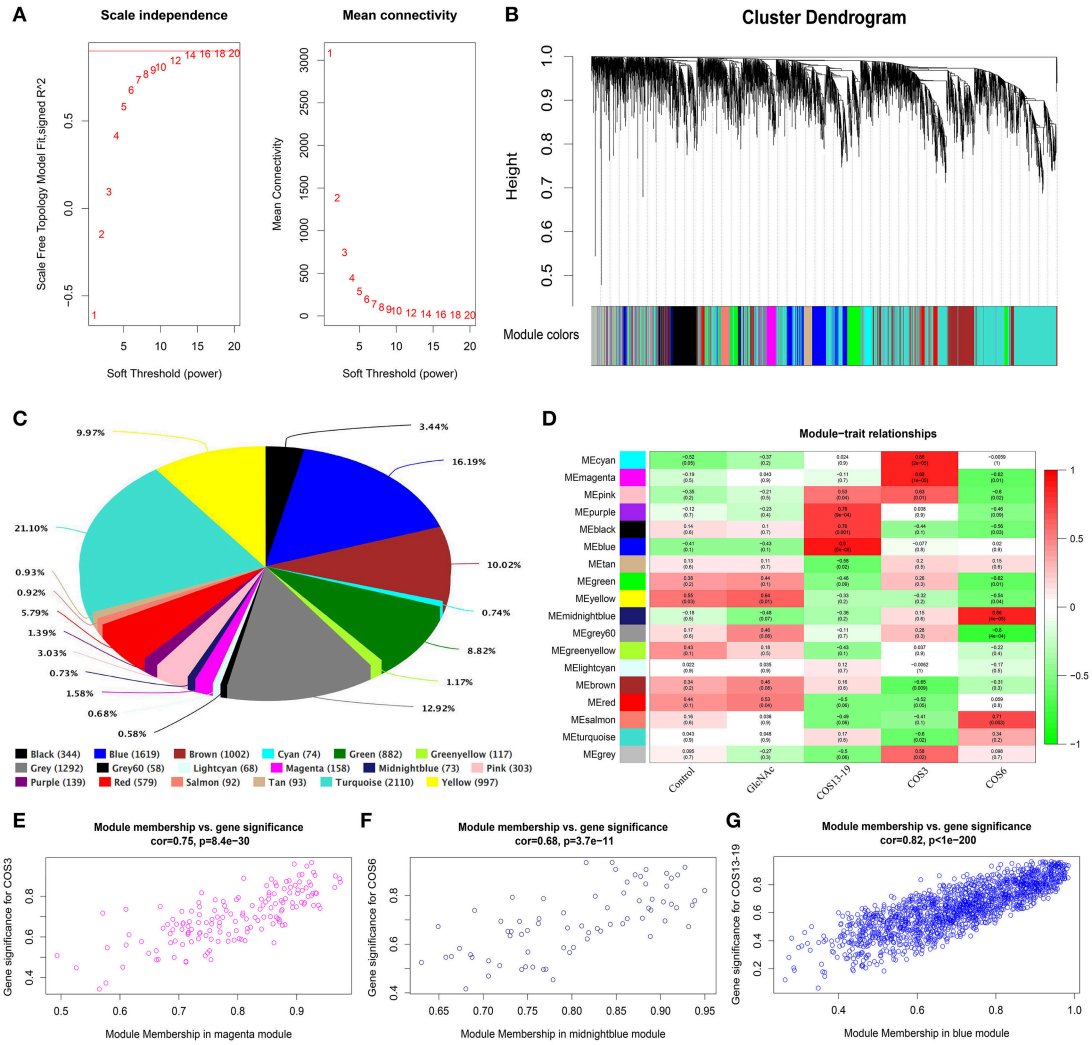


FIGURE 3 | Weighted gene co-expression network analysis (WGCNA) yields behaviorally relevant modules. **(A)** Network topology for different soft-thresholding powers. Numbers in the plots indicate the corresponding soft thresholding powers. The approximate scale-free topology can be attained at the soft-thresholding power of 14. **(B)** Gene dendrogram obtained by clustering the dissimilarity based on consensus topological overlap, with the corresponding module colors indicated by the color row. Each colored row represents a color-coded module which contains a group of highly connected genes. In total, 17 modules were identified. **(C)** Pie chart visualizing the number and percentage of genes in each module. **(D)** Correlation between modules and traits. The upper number in each cell refers to the correlation coefficient of each module in the trait, and the lower number is the corresponding *P*-value. Red represents high adjacency (positive correlation) and green represents low adjacency (negative correlation). **(E–G)** Scatter plots of gene significance (GS) for COS3, COS6, and COS13-19 groups vs. the module membership (MM) in the magenta, midnightblue, and blue modules, respectively. Pearson's r ("cor") and *P*-value as determined by Fisher's z-transformation are indicated above each plot.

genes were significantly upregulated, and Bax and Caspase 3 were subsequently significantly upregulated (**Figures 6A–E**). The results of immunofluorescence staining showed apoptosis occurred after 16 h of stimulation, especially in the COS13-19 group (**Figure 6F** and **Figure S3**). These results implied that COS could promotes macrophage apoptosis through the p53 signaling pathway.

DISCUSSION

Chitosan oligosaccharides (COSs) are natural oligomers derived from chitosan and are the most abundant carbohydrate polymers after cellulose. The biological activities of COSs are dependent on its structural characteristics such as the DP and MW. The higher oligosaccharides (pentamer or larger oligomers) possess various physiological activities such as antimicrobial, antifungal, anti-tumor, radical scavenging, and immuno-stimulating activity (4, 39). In mammalian studies, the immune effects of COS have been studied intensively at the individual and cellular levels. However, the studies in bony fish were mainly focused on feed additives and adjuvants, and the mechanism of action is not clear. Macrophages play important roles in host anti-infection and immune regulation as well. Previous studies have shown that COS is recognized and regulated by macrophages to perform

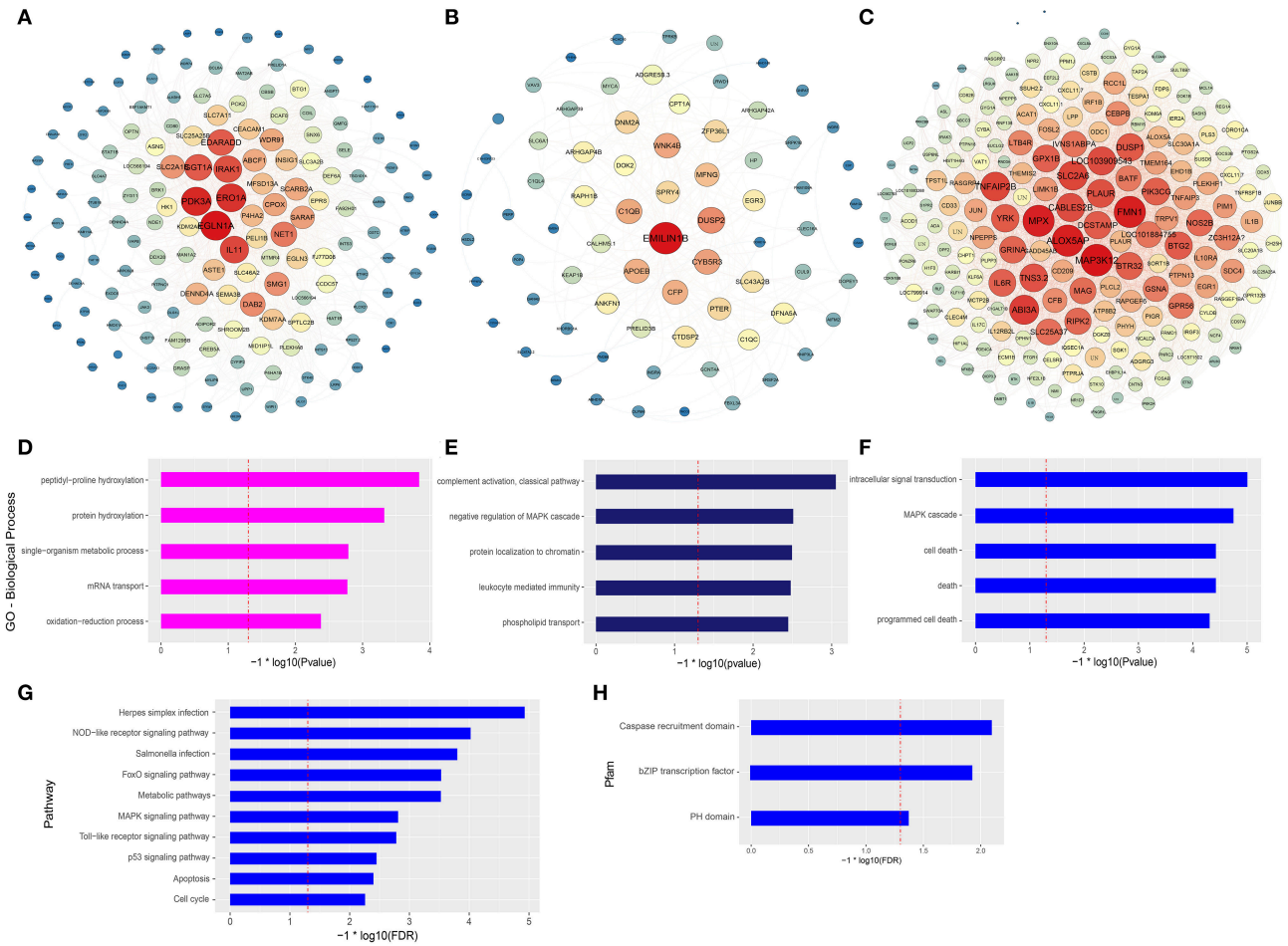


FIGURE 4 | Gene network and enrichment analysis of selected modules. **(A–C)** Top hub genes of the magenta, midnightblue and blue modules are shown. Gene importance was assigned according to circle diameter, and color depth. **(D–F)** GO enrichment analysis of magenta, midnightblue, and blue modules genes. Top 5 GO biological process terms are shown. **(G)** KEGG pathway and **(H)** protein families and domain enrichment analysis of blue module genes screened from the STRING and Pfam databases.

biological functions (12, 40). In this study, we selected COSs with different MWs to stimulate macrophages from blunt snout bream head kidney. Then we studied the stimulation effects at the transcription level by high-throughput sequencing and bioinformatics analysis. We hope to provide theoretical support for the application of COS in the prevention and treatment of bony fish diseases.

In our study, we first demonstrated that GlcNAc could not activate macrophages (10 DEGs) in resting state, and three different MW COSs (COS3, COS6, COS13-19) had a large difference in the number of DEGs after stimulation of macrophages for 4 h. The proportion of up- and downregulated unique genes in the three groups was relatively high. In addition, the genes of different treatment groups had their own unique expression patterns. These results suggest that COSs with different MWs have different biological functions in activating macrophages, which is similar to the study in mammals (4, 41, 42). To investigate the functional similarities and differences of these EDGs in the three groups, biological process GO terms and GSEA KEGG pathway enrichment analysis were used. The results showed that the GO terms' defensive response, inflammatory response, response to bacterium, response to biotic stimulus, response to external biotic stimulus, and response to other organisms were co-activated in the COS3, COS6, and COS13-19 groups. However, the results of GSEA KEGG pathway enrichment showed that the only pathway of co-activation was DNA replication. In addition, COS3 and COS13-19 could activate some infectious disease pathways, COS6 pathways mainly related to DNA replication, and mismatch repair. These results indicated that although COSs have different functions in activating macrophages, they all can activate macrophages to produce inflammation and stress responses in the early stage of stimulation. Notably, DNA replication was the most markedly enriched pathway in the three groups, this may imply that there are other potential biological functions of COSs in stimulating macrophages of blunt snout bream head kidney.

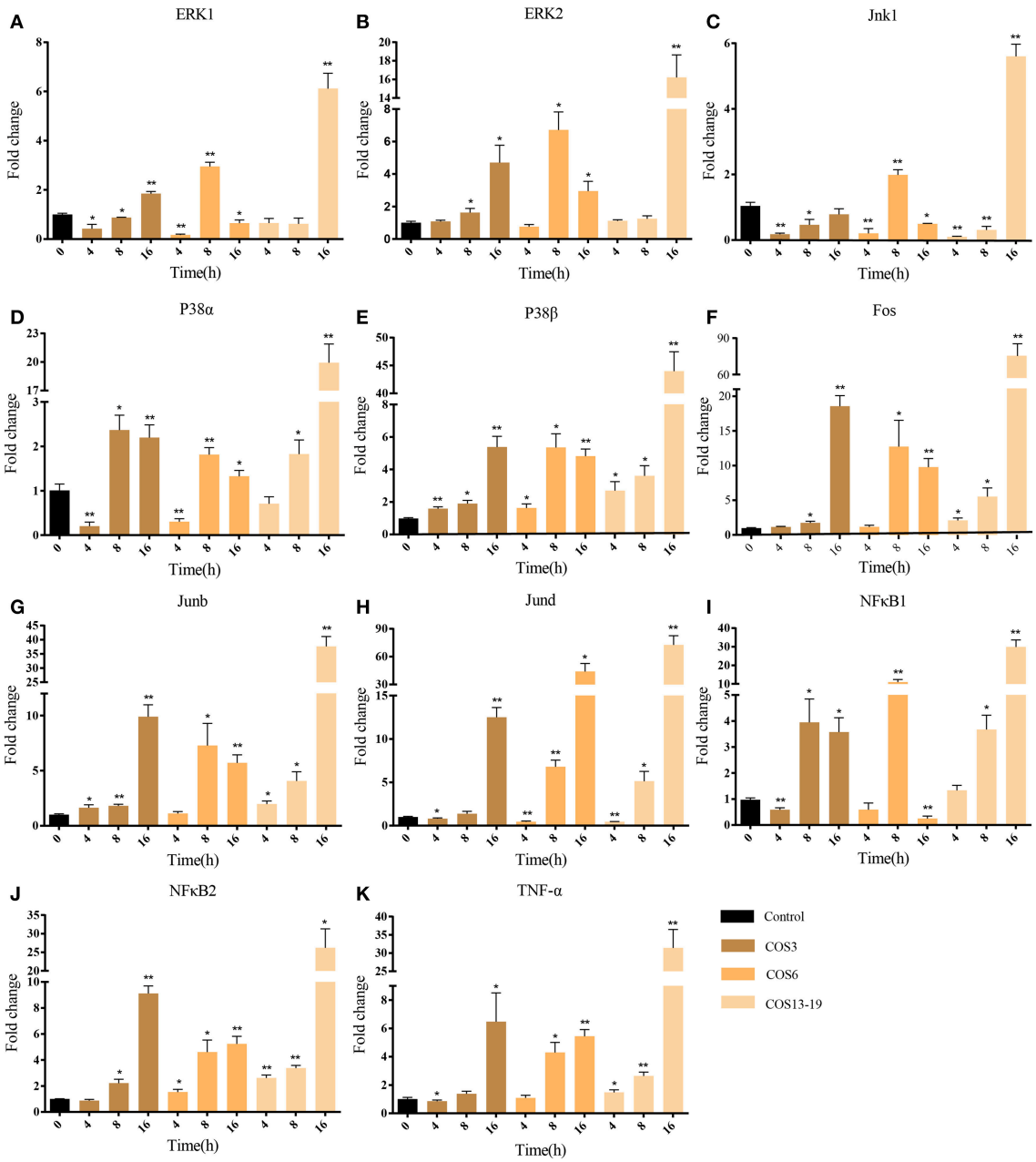


FIGURE 5 | qRT-PCR identified the key gene expressions of the MAPK and NF-κB pathways. **(A–H)** The key genes of the MAPK pathway. **(I–K)** The key genes of NF-κB pathway. The samples were analyzed at 0, 4, 8, and 16 h post-stimulation. β-actin was used as internal reference. Each experiment was executed in triplicate. Data are shown as mean ± SE ($N = 3$). The asterisk indicates significant difference (**$P < 0.01$, *$P < 0.05$) compared with 0 h (set as 1).

Gene co-expression network analysis (WGCNA) is more likely to identify modules containing co-regulatory genes whose encoded proteins are directly involved in structural units (31). In order to continue to study the functional characteristics of COSs, WGCNA analysis was used to determine the most relevant positive-related modules for COS3, COS6, and COS13-19, and respectively, the magenta, midnightblue and blue modules were determined. The core genes of the magenta module are related to oxygen concentration (15), and the GO term enrichment results focus on protein modification, metabolism, nucleic acid transport, and oxygen reduction processes. These results suggest that COS3 has a weak ability to activate the immune system of resting macrophages at the early stage, and is mainly in the oxidative emergency stage to counteract the invasion of foreign substances (13). Innate immune-related GO terms appear in the midnightblue module, whose core genes are mainly related to innate immunity and cell proliferation (43). Interestingly, the GO terms enriched in the blue module are mainly related

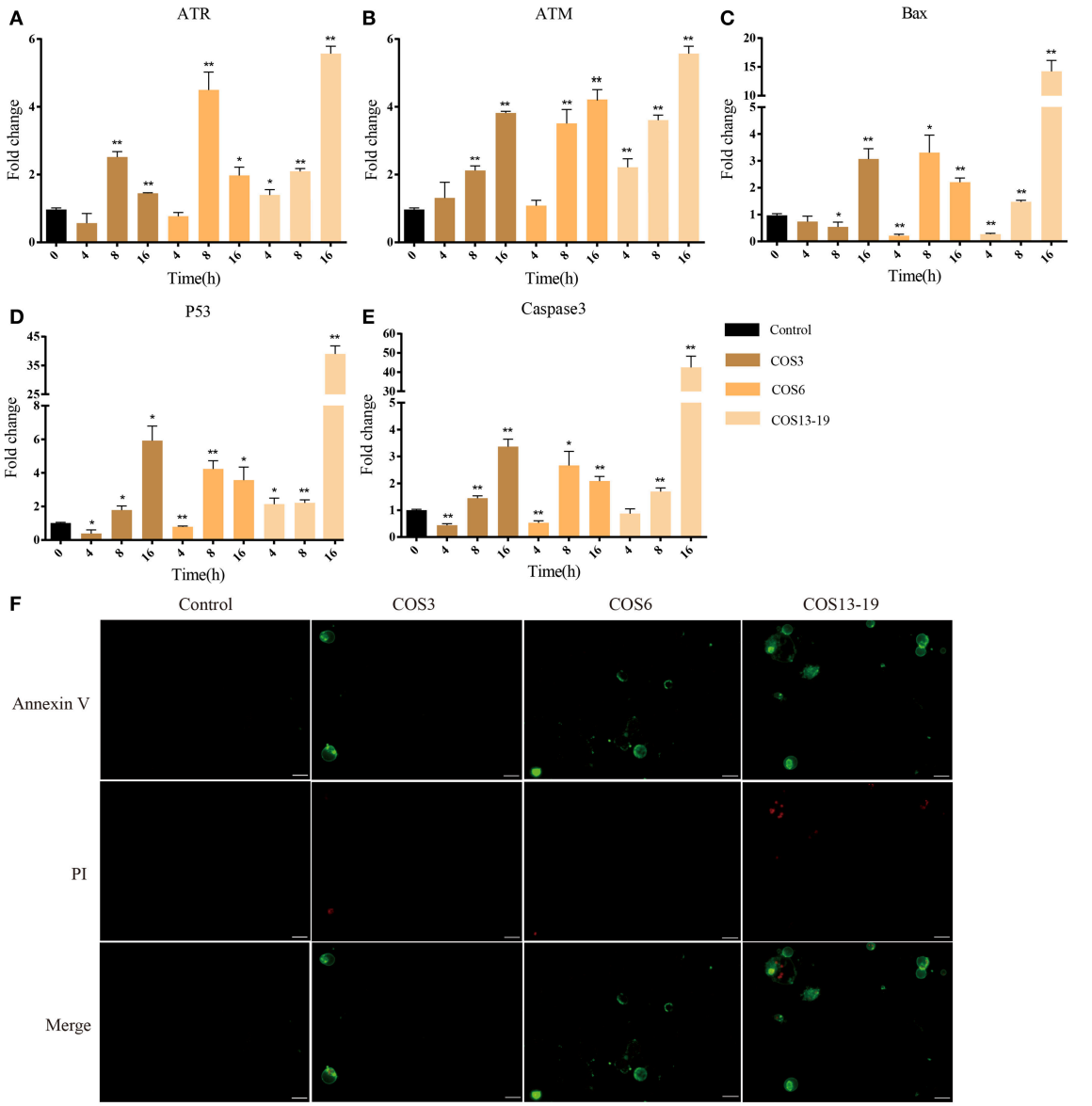


FIGURE 6 | COSs induce apoptosis of blunt snout bream head kidney macrophages via the P53 pathway *in vitro*. **(A–E)** qRT-PCR identified the expression of key genes of the P53 pathway. The samples were analyzed at 0, 4, 8, and 16 h post-stimulation. β-actin was used as internal reference. Each experiment was executed in triplicate. Data were shown as mean ± SE ($N = 3$). The asterisk indicates significant difference (**$P < 0.01$, *$P < 0.05$) compared with 0 h (set as 1). **(F)** Cells were cultured for 16 h at 28°C after stimulation and then stained. Annexin V is the green fluorescent marker, labeling cells in early apoptosis. PI (Propidium Iodide) is the red fluorescent marker, labeling cells in late apoptosis. Bars: 25 μm.

to cell growth and death, and the core genes are related to innate immunity and antitumor activity (43, 44). In order to obtain more accurate pathway and protein families and domain enrichment in the blue module, the STRING database was applied to screen genes with high connectivity in the PPI network. KEGG pathway enrichment results showed that the top 10 pathways were mainly related to infectious diseases, the immune system, cell growth and death, signal transduction and metabolism. Then the Pfam database was used to enrich the domains of screened genes, and three protein families were enriched, namely caspase recruitment domain, bZIP (basic leucine zipper) transcription factor, and PH domain. The caspase protein family is associated with cell death, and caspase 1 and caspase 3 are the key genes of pyroptosis and apoptosis, respectively (45, 46). The bZIP transcription factors are involved in many essential cellular processes, and many are associated with cancer. For example, the activator protein 1 (AP-1) family, which includes the well-known transcription factors c-Fos and c-Jun (enriched in the blue module), is responsible for regulation of cell proliferation and apoptosis (47). Apoptosis and the p53

signaling pathway were enriched in the KEGG pathway, which may imply that the p53 pathway is involved in the apoptosis response of macrophages stimulated by COS13-19. Notably, the cell cycle pathway was also enriched and, combined with the enrichment of the DNA replication pathway of GSEA KEGG analysis, we conjectured that DNA replication activates the P53 pathway, causing macrophage apoptosis (38, 48).

Through bioinformatics analysis, we identified traits associated with three different MW COS-stimulated macrophages in the early stage. The MAPK and NF-κB signaling pathways are the two most widely studied pathways related to inflammation in the application of COSs in mammals (4). In our results, the MAPK and NF-κB upstream signaling pathways were enriched in the COS13-19 group. To verify whether these traits were specific in the COS13-19 group, we extended the stimulation time to 16 hours. MAPK is composed of three downstream mediators including C–Jun N–terminal kinase (JNK), extracellular signal-regulated kinase (ERK1/2) and P38 MAPK. These three mediators promote nuclear translocation of AP-1, which induces the transcription of pro-inflammatory genes (4). Our results showed that p38β was first activated at 4 h, then the other molecules of the MAPK pathway were activated, and the activation intensity increased with the increase of stimulation time. NF-κB2 was first upregulated in the NF-κB pathway, then the downstream TNFα gene was upregulated, and the upregulation was most pronounced in the COS13-19 group. These results indicated that the activation degree of macrophages was positively correlated with the MW and duration of stimulation of COS. This trend was also observed in the subsequent detection of cell apoptosis and the identification of apoptotic pathway genes. ATM and ATR are members of the inositol triphosphate kinase family, which sense different forms of DNA damage (49). ATM plays a "checkpoint" role in double-stranded DNA damage. ATR is responsible for sensing and transmitting other forms of DNA damage, including replication fork damage, DNA cross-linking, and so on. These two genes are relatively independent and cross-talk, co-activating downstream p53 pathway proteins. In the DNA replication pathway, MCM family proteins induce cell apoptosis in terminally differentiated cells (**Figure S1**) (50). Activated macrophages are terminal differentiated cells (51, 52). In our results, ATR and ATM are activated, which may be caused by abnormal replication of DNA, thus activating p53 and downstream proteins, causing cell apoptosis. In addition, the MAPK pathway is important to involve in the initiation of apoptosis. It can be activated by extracellular stimulation to exert biological effects, regulate different cellular functions, and mediate mainly physiological functions such as differentiation, proliferation, and apoptosis. On the one hand, JNK/p38 MAPK signaling activation can increase P53 phosphorylation to regulate the P53 pathway. On the other hand, high expression of AP-1 mainly through bZIP binds DNA to promote the expression of pro-apoptotic genes such as P53, Bax, Fasl, TNF, and so on (22, 53, 54). Apoptosis-related genes in the P53 pathway were significantly upregulated at the late stage of stimulation in three groups (16 h).

In conclusion, we first used high-throughput sequencing and bioinformatics analysis methods to systematically analyze the biological functions of COSs with different MWs on macrophages in teleost. Our results showed that COSs could activate the stress response of macrophages at the early stage, and gradually activate the innate immune response with the increase of stimulation time to resist the invasion of foreign substances, and the activation degree of macrophages was positively correlated with the MW and stimulation time. In addition, we also found that COSs could induce apoptosis of macrophages via the P53 pathway. Firstly, activated macrophages are terminally differentiated cells, and abnormal DNA replication activates ATR and ATM genes to regulate the P53 signaling pathway. Secondly, sustained activation of MAPK pathway genes upregulates P53 expression and phosphorylation, eventually leading to macrophage apoptosis. Inevitably, many immunopotentiators used in fish experiments induce beneficial effects, such as disease protection due to increased cellular and humoral responses. However, attention must be paid to problems such as tolerance, unwanted side effects (e.g., immunosuppression of excessive doses of immunopotentiators) or undesirable effects caused by prolonged use of such compounds.

DATA AVAILABILITY

Publicly available datasets were analyzed in this study. This data can be found here: https://academic.oup.com/gigascience/article/6/7/gix039/3847731.

ETHICS STATEMENT

The study was approved by the Institutional Animal Care and Use Ethics Committee of Huazhong Agricultural University.

AUTHOR CONTRIBUTIONS

XL and CW conceived and designed the experiments. CW and YD performed the experiments and analyzed the data. CW, XL, JS, and GY wrote the manuscript. All authors reviewed the manuscript.

ACKNOWLEDGMENTS

The authors would like to express their appreciation to Tong Chen, Huijie Chen, and Bingbo Lu for collecting blood samples, fish administration, and helpful discussion. This work was supported by the National Natural Science Foundation of China (31772879).

SUPPLEMENTARY MATERIAL

The Supplementary Material for this article can be found online at: https://www.frontiersin.org/articles/10.3389/fimmu.2019.00869/full#supplementary-material

Figure S1 | MA plots provided a global view of all differential genes of GlcNAc **(A)**, COS3 **(B)**, COS6 **(C)**, and COS13-19 **(D)** groups, respectively. The mean of

normalized counts on the x-axis, the log2 fold change on the y-axis. Red dots represent differentially expressed genes ($P < 0.001$) (29).

Figure S2 | Gene set enrichment analysis (GSEA) identified DNA replication pathway was activated in the COS3 **(A)**, COS6 **(B)**, and COS13-19 **(C)** groups. In this plots, genes are ranked by signal/noise ratio according to their differential expression between COS stimulation and control. Genes in the gene set are marked with vertical bars. The normalized enrichment score (NES), nominal *P*-value and FDR are shown in these plots. The heatmap on the right reflects the expression of DNA replication-related genes in different stimulation groups.

Figure S3 | The bright field of immunofluorescence staining. Annexin V is the green fluorescent marker, labeling cells in early apoptosis. PI (Propidium Iodide) is the red fluorescent marker, labeling cells in late apoptosis. Bars: 25 μm.

REFERENCES

1. Su H, Su J. Cyprinid viral diseases and vaccine development. *Fish Shellfish Immunol*. (2018) 83:84–95. doi: 10.1016/j.fsi.2018.09.003
2. Dalmo R. The use of immunostimulants in fish larval aquaculture. *Fish Shellfish Immunol*. (2005) 19:457–72. doi: 10.1016/j.fsi.2005.03.008
3. Sakai M. Current research status of fish Immunostimulants. *Aquaculture*. (1999) 172:63–92. doi: 10.1016/S0044-8486(98)00436-0
4. Muanprasat C, Chatsudthipong V. Chitosan oligosaccharide: Biological activities and potential therapeutic applications. *Pharmacol Therapeut*. (2017) 170:80–97. doi: 10.1016/j.pharmthera.2016.10.013
5. Spindola H, de Sousa V, Santos-Silva A, Pintado M, Malcata F, Carvalho J. Anti-inflammatory activity of chitooligosaccharides *in vivo*. *Mar Drugs*. (2010) 8:1763–8. doi: 10.3390/md8061763
6. Mourya VK, Inamdar NN, Choudhari YM. Chitooligosaccharides: synthesis, characterization and applications. *Poly Sci Series A*. (2011) 53:583–612. doi: 10.1134/s0965545x11070066
7. Velappan S. Recent developments in chitosanase research and its biotechnological applications: a review. *Food Chem*. (2014) 150:392–9. doi: 10.1016/j.foodchem.2013.10.083
8. Yao Q, Zhou D, Mao F. Antioxidant activity of N-carboxymethyl chitosan oligosaccharides. *Bioorg Med Chem Lett*. (2008) 18:5774–6. doi: 10.1016/j.bmcl.2008.09.072
9. Riteau N, Sher A. Chitosan: an adjuvant with an unanticipated STING. *Immunity*. (2016) 44:522–4. doi: 10.1016/j.immuni.2016.03.002
10. Sun T, Zhou D, Xie J, Mao F. Preparation of chitosan oligomers and their antioxidant activity. *Eur Food Res Technol*. (2006) 225:451–6. doi: 10.1007/s00217-006-0439-1
11. Zhang P, Liu W, Peng Y, Han B, Yang Y. Toll like receptor 4 (TLR4) mediates the stimulating activities of chitosan oligosaccharide on macrophages. *Int. Immunopharmacol*. (2014) 23:254–61. doi: 10.1016/j.intimp.2014.09.007
12. Vasconcelos DP, Fonseca AC, Costa M, Amaral IF, Barbosa MA, Aguas AP, et al. Macrophage polarization following chitosan implantation. *Biomaterials*. (2013) 34:9952–9. doi: 10.1016/j.biomaterials.2013.09.012
13. Liu L, Zhou Y, Zhao X, Wang H, Wang L, Yuan G, et al. Oligochitosan stimulated phagocytic activity of macrophages from blunt snout bream (*Megalobrama amblycephala*) associated with respiratory burst coupled with nitric oxide production. *Dev Comp Immunol*. (2014) 47:17–24. doi: 10.1016/j.dci.2014.06.005
14. Jeong H, Koo H, Oh E, Chae H, Kim H, Suh S, et al. Nitric oxide production by high molecular weight water-soluble chitosan via nuclear factor-kappaB activation. *Int J Immunopharmacol*. (2000) 22:923–33. doi: 10.1016/S0192-0561(00)00055-2
15. Nishiyama A, Tsuji S, Yamashita M, Henriksen R, Myrvik Q, Shibata Y. Phagocytosis of N-acetyl-D-glucosamine particles, a Th1 adjuvant, by RAW 264.7 cells results in MAPK activation and TNF-alpha, but not IL-10, production. *Cell Immunol*. (2006) 239:103–12. doi: 10.1016/j.cellimm.2006.04.003
16. Yoon HJ, Moon ME, Park HS, Im SY, Kim YH. Chitosan oligosaccharide (COS) inhibits LPS-induced inflammatory effects in RAW 264.7 macrophage cells. *Biochem Biophys Res Commun*. (2007) 358:954–9. doi: 10.1016/j.bbrc.2007.05.042
17. Phil L, Naveed M, Mohammad IS, Bo L, Bin D. Chitooligosaccharide: An evaluation of physicochemical and biological properties with the proposition for determination of thermal degradation products. *Biomed Pharmacother*. (2018) 102:438–51. doi: 10.1016/j.biopha.2018.03.108
18. Zou P, Yang X, Wang J, Li Y, Yu H, Zhang Y, et al. Advances in characterisation and biological activities of chitosan and chitosan oligosaccharides. *Food Chem*. (2016) 190:1174–81. doi: 10.1016/j.foodchem.2015.06.076
19. Lodhi G, Kim YS, Hwang JW, Kim SK, Jeon YJ, Je JY, et al. Chitooligosaccharide and its derivatives: preparation and biological applications. *BioMed Res Int*. (2014) 2014:654913. doi: 10.1155/2014/654913
20. Muanprasat C, Wongkrasant P, Satitsri S, Moonwiriyakit A, Pongkorpsakol P, Mattaveewong T, et al. Activation of AMPK by chitosan oligosaccharide in intestinal epithelial cells: mechanism of action and potential applications in intestinal disorders. *Biochem Pharmacol*. (2015) 96:225–36. doi: 10.1016/j.bcp.2015.05.016
21. Kim J-H, Kim Y-S, Hwang J-W, Han Y-K, Lee J-S, Kim S-K, et al. Sulfated *Chitosan Oligosaccharides* suppress LPS-induced NO production via JNK and NF-κB Inactivation. *Molecules*. (2014) 19:18232–47. doi: 10.3390/molecules191118232
22. Xia Z, Dickens M, Raingeaud J, Davis R, Greenberg M. Opposing effects of ERK and JNK-p38 MAP kinases on apoptosis. *Science*. (1995) 270:1326–31. doi: 10.1126/science.270.5240.1326
23. Shinohara T, Pantuso T, Tsuji S, Yamashita M, Shinohara S, Myrvik Q, et al. Depletion of cellular cholesterol enhances macrophage MAPK activation by chitin microparticles but not by heat-killed *Mycobacterium bovis* BCG. *Am J Physiol Cell Physiol*. (2008) 295:C341–9. doi: 10.1152/ajpcell.00446.2007
24. Braun-Nesje R, Bertheussen K, Kaplan G, Seljelid R. Salmonid macrophages: separation, *in vitro* culture and characterization. *J Fish Dis*. (1981) 4:141–51. doi: 10.1111/j.1365-2761.1981.tb01118.x
25. Bolger A, Lohse M, Usadel B. Trimmomatic: a flexible trimmer for Illumina sequence data. *Bioinformatics*. (2014) 30:2114–20. doi: 10.1093/bioinformatics/btu170
26. Kim D, Langmead B, Salzberg S. HISAT: a fast spliced aligner with low memory requirements. *Nat Methods*. (2015) 12:357–60. doi: 10.1038/nmeth.3317
27. Liu H, Chen C, Gao Z, Min J, Gu Y, Jian J, et al. The draft genome of blunt snout bream (*Megalobrama amblycephala*) reveals the development of intermuscular bone and adaptation to herbivorous diet. *GigaScience*. (2017) 6:1–13. doi: 10.1093/gigascience/gix039
28. Simao FA, Waterhouse RM, Ioannidis P, Kriventseva EV, Zdobnov EM. BUSCO: assessing genome assembly and annotation completeness with single-copy orthologs. *Bioinformatics*. (2015) 31:3210–2. doi: 10.1093/bioinformatics/btv351
29. Love M, Huber W, Anders S. Moderated estimation of fold change and dispersion for RNA-seq data with DESeq2. *Genome Biol*. (2014) 15:550. doi: 10.1186/s13059-014-0550-8
30. Trapnell C, Williams B, Pertea G, Mortazavi A, Kwan G, van Baren M, et al. Transcript assembly and quantification by RNA-Seq reveals unannotated transcripts and isoform switching during cell differentiation. *Nat Biotechnol*. (2010) 28:511–5. doi: 10.1038/nbt.1621
31. Langfelder P, Horvath S. WGCNA: an R package for weighted correlation network analysis. *BMC Bioinformatics*. (2008) 9:559. doi: 10.1186/1471-2105-9-559
32. Zhang B, Horvath S. A general framework for weighted gene co-expression network analysis. *Stat Appl Genet Mol Biol*. (2005) 4:17. doi: 10.2202/1544-6115.1128
33. Jensen L, Kuhn M, Stark M, Chaffron S, Creevey C, Muller J, et al. STRING 8–a global view on proteins and their functional interactions in 630 organisms. *Nucleic Acids Res*. (2009) 37:D412–6. doi: 10.1093/nar/gkn760
34. Kadarmideen H, Watson-Haigh N, Andronicos N. Systems biology of ovine intestinal parasite resistance: disease gene modules and biomarkers. *Mol Biosyst*. (2011) 7:235–46. doi: 10.1039/c0mb00190b

35. Farber CR. Identification of a gene module associated with BMD through the integration of network analysis and genome-wide association data. *J Bone Miner Res.* (2010) 25:2359–67. doi: 10.1002/jbmr.138
36. Gorres KL, Raines RT. Prolyl 4-hydroxylase. *Crit Rev Biochem Mol Biol.* (2010) 45:106–24. doi: 10.3109/10409231003627991
37. Wu G, Tsai G. Chitooligosaccharides in combination with interferon-gamma increase nitric oxide production via nuclear factor-kappaB activation in murine RAW264.7 macrophages. *Food Chem Toxicol.* (2007) 45:250–8. doi: 10.1016/j.fct.2006.07.025
38. Das S, Boswell S, Aaronson S, Lee S. P53 promoter selection: choosing between life and death. *Cell Cycle.* (2008) 7:154–7. doi: 10.4161/cc.7.2.5236
39. Je JY, Kim SK. Chitooligosaccharides as potential nutraceuticals: production and bioactivities. *Adv Food Nutr Res.* (2012) 65:321–36. doi: 10.1016/B978-0-12-416003-3.00021-4
40. McNelis JC, Olefsky JM. Macrophages, immunity, and metabolic disease. *Immunity.* (2014) 41:36–48. doi: 10.1016/j.immuni.2014.05.010
41. Chen C-L, Wang Y-M, Liu C-F, Wang J-Y. The effect of water-soluble chitosan on macrophage activation and the attenuation of mite allergen-induced airway inflammation. *Biomaterials.* (2008) 29:2173–82. doi: 10.1016/j.biomaterials.2008.01.023
42. Yousef M, Pichyangkura R, Soodvilai S, Chatsudthipong V, Muanprasat C. Chitosan oligosaccharide as potential therapy of inflammatory bowel disease: therapeutic efficacy and possible mechanisms of action. *Pharmacol Res.* (2012) 66:66–79. doi: 10.1016/j.phrs.2012.03.013
43. Tam V, Aderem A. Systems-level analysis of innate immunity. *Ann Rev Immunol.* (2014) 32:547–77. doi: 10.1146/annurev-immunol-032713-120254
44. Corrales L, Gajewski T. Innate immune recognition of cancer. *Ann Rev Immunol.* (2015) 33:445–74. doi: 10.1146/annurev-immunol-032414-112043
45. Yuan J, Najafov A, Py BF. Roles of caspases in necrotic cell death. *Cell.* (2016) 167:1693–704. doi: 10.1016/j.cell.2016.11.047
46. Jorgensen I, Rayamajhi M, Miao EA. Programmed cell death as a defence against infection. *Nat Rev Immunol.* (2017) 17:151–64. doi: 10.1038/nri.2016.147
47. Chan C, Chang M, Wang Y, Chen L, Tsai Y, Lee J, et al. Thrombin activates Ras-CREB/ATF-1signaling and stimulates c-fos, c-jun, and c-myc expression in human gingival fibroblasts. *J Periodontol.* (2008) 79:1248–54. doi: 10.1902/jop.2008.070523
48. Labuschagne C, Vousden K. p53 in survival, death and metabolic health: a lifeguard with a licence to kill. *Nat Rev Mol Cell Biol.* (2015) 16:393–405. doi: 10.1038/nrm4007
49. Shiloh Y. ATM and related protein kinases: safeguarding genome integrity. *Nat Rev Cancer.* (2003) 3:155–68. doi: 10.1038/nrc1011
50. Gao J, Wang Q, Dong C, Chen S, Qi Y, Liu Y. Whole exome sequencing identified MCM2 as a novel causative gene for autosomal dominant nonsyndromic deafness in a chinese family. *PLoS ONE.* (2015) 10:e0133522. doi: 10.1371/journal.pone.0133522
51. Epelman S, Lavine KJ, Randolph GJ. Origin and functions of tissue macrophages. *Immunity.* (2014) 41:21–35. doi: 10.1016/j.immuni.2014.06.013
52. Hashimoto D, Chow A, Noizat C, Teo P, Beasley MB, Leboeuf M, et al. Tissue-resident macrophages self-maintain locally throughout adult life with minimal contribution from circulating monocytes. *Immunity.* (2013) 38:792–804. doi: 10.1016/j.immuni.2013.04.004
53. Jochum W, Passegué E, Wagner E. AP-1 in mouse development and tumorigenesis. *Oncogene.* (2001) 20:2401–12. doi: 10.1038/sj.onc.1204389
54. Lin H, Chen J, Kuo W, Wang C. Chemopreventive properties of Hibiscus sabdariffa L. on human gastric carcinoma cells through apoptosis induction and JNK/p38 MAPK signaling activation. *Chem Biol Interact.* (2007) 165:59–75. doi: 10.1016/j.cbi.2006.10.011

Conflict of Interest Statement: The authors declare that the research was conducted in the absence of any commercial or financial relationships that could be construed as a potential conflict of interest.

Copyright © 2019 Wu, Dai, Yuan, Su and Liu. This is an open-access article distributed under the terms of the Creative Commons Attribution License (CC BY). The use, distribution or reproduction in other forums is permitted, provided the original author(s) and the copyright owner(s) are credited and that the original publication in this journal is cited, in accordance with accepted academic practice. No use, distribution or reproduction is permitted which does not comply with these terms.

frontiers in Immunology

ORIGINAL RESEARCH
published: 06 June 2019
doi: 10.3389/fimmu.2019.01175

Evaluation of a Recombinant *Flavobacterium columnare* DnaK Protein Vaccine as a Means of Protection Against Columnaris Disease in Channel Catfish (*Ictalurus punctatus*)

Miles D. Lange†, Jason Abernathy† and Bradley D. Farmer*

Harry K. Dupree Stuttgart National Aquaculture Research Center, Agricultural Research Service, United States Department of Agriculture, Stuttgart, AR, United States

OPEN ACCESS

Edited by:
Irene Salinas, University of New Mexico, United States

Reviewed by:
Javier Santander, Memorial University of Newfoundland, Canada
James L. Stafford, University of Alberta, Canada

***Correspondence:**
Miles D. Lange
miles.lange@ars.usda.gov

†*Co-first authors*

Specialty section:
This article was submitted to Comparative Immunology, a section of the journal Frontiers in Immunology

Received: *30 October 2018*
Accepted: *08 May 2019*
Published: *06 June 2019*

Citation:
Lange MD, Abernathy J and Farmer BD (2019) Evaluation of a Recombinant Flavobacterium columnare DnaK Protein Vaccine as a Means of Protection Against Columnaris Disease in Channel Catfish (Ictalurus punctatus). Front. Immunol. 10:1175. doi: 10.3389/fimmu.2019.01175

Flavobacterium columnare causes substantial losses among cultured finfish species. The Gram-negative bacterium is an opportunistic pathogen that manifests as biofilms on the host's mucosal surfaces as the disease progresses. We previously demonstrated that the dominant mucosal IgM antibody response to *F. columnare* is to the chaperone protein DnaK that is found in the extracellular fraction. To establish the efficacy of using recombinant protein technology to develop a new vaccine against columnaris disease, we are reporting on two consecutive years of vaccine trials using a recombinant *F. columnare* DnaK protein (rDnaK). In year one, three groups of channel catfish (n = 300) were immunized by bath immersion with a live attenuated *F. columnare* isolate, rDnaK or sham immunized. After 6 weeks, an *F. columnare* laboratory challenge showed a significant increase in survival (>30%) in both the live attenuated and rDnaK vaccines when compared to the non-immunized control. A rDnaK-specific ELISA revealed significant levels of mucosal IgM antibodies in the skin of catfish immunized with rDnaK at 4- and 6-weeks post immunization. In the second year, three groups of channel catfish (n = 300) were bath immunized with rDnaK alone or with rDnaK after a brief osmotic shock or sham immunized. After 6 weeks a laboratory challenge with *F. columnare* was conducted and showed a significant increase in survival in the rDnaK (> 25%) and in rDnaK with osmotic shock (>35%) groups when compared to the non-immunized control. The rDnaK-specific ELISA demonstrated significant levels of mucosal IgM antibodies in the skin of catfish groups immunized with rDnaK at 4- and 6-weeks post immunization. To further understand the processes which have conferred immune protection in the rDnaK group, we conducted RNA sequencing of skin samples from the non-immunized (n = 6) and rDnaK treated channel catfish at 1-week (n = 6) and 6 weeks (n = 6) post immunization. Significantly altered gene expression was identified and results will be discussed. Work to further enhance the catfish immune response

to *F. columnare* rDnaK is underway as this protein remains a promising candidate for additional optimization and experimental trials in a production setting.

Keywords: recombinant protein, bath immersion, *Flavobacterium columnare*, channel catfish, antibody response, RNA sequencing

INTRODUCTION

Flavobacterium columnare, the causative agent of columnaris disease generates substantial mortality during the production of freshwater farmed finfish species (1, 2). Classically, columnaris disease has been shown to predominantly involve the external mucosal surfaces of fish, which can lead to the rapid and widespread destruction of the gills, skin, and fins. *F. columnare* is ubiquitous in the aquatic environment and outbreaks are often triggered during the spring and summer months of the production cycle (3, 4). Intensive rearing of food fish is well-suited for the transmission of *F. columnare* and in these settings the pathogen is opportunistic and outbreaks are common, as fish experience stressors including increased rearing density, unnecessary handling and poor water quality (5–7). As food fish production continues to expand, the frequency of columnaris disease will only continue to increase within the aquaculture industry. The regulation of treatments and resistance to available antibiotics means that alternative methods of disease protection will be required (8).

Many vaccines have been developed and used in the aquaculture industry to prevent expensive losses which occur throughout the production cycle due to a wide variety of infectious diseases (9–12). Some of the earliest fish vaccine preparations were isolated bacterial pathogens that were cultured, killed, and then used to immunize fish to examine their overall immunogenicity (13–16). As we began to understand the nature of adaptive immunity in teleost fish, killed bacterins gave way to live-attenuated bacterial vaccines engineered to cause little or no disease and offer more potential for stimulating the adaptive immune response (17, 18).

Channel catfish has served for many years as a good model for examining teleost immune function (19–22). Studies to evaluate different tissue-derived catfish transcriptomes under different conditions during laboratory challenges have allowed for new insight into the pathogenesis of different Gram-negative bacteria (23–25). Recently our lab characterized the mucosal IgM antibody response in channel catfish to an iron-attenuated *F. columnare* isolate after bath immunization (26). We observed that the DnaK protein was primarily found in the extracellular fraction of different *F. columnare* isolates and was predominantly reactive with mucosal IgM antibodies. The DnaK protein has also been detected in the extracellular fraction of the fish pathogen, *Aeromonas salmonicida*, where the authors classified it as a moonlighting protein and pondered on whether it could be a potential vaccine target (27). Heat shock proteins represent a conserved family of proteins and there is evidence to suggest that these proteins are prominent in activating an adaptive immune response in mammals (28–31).

Recent advances in recombinant protein technology have made the production and subsequent testing of individual immunogens quite effective (32–35). In the current work, we tested the ability of a recombinant *F. columnare* DnaK protein (rDnaK) to induce a catfish mucosal IgM antibody response and to protect against columnaris disease. We also examined molecular mechanisms through which protection may be induced using high-throughput RNA sequencing of a mucosal tissue through multiple weeks post-immunization. These combined results suggest that the *F. columnare* rDnaK protein is a candidate for additional studies to improve and validate these experimental trials in a commercial environment.

MATERIALS AND METHODS

Bacteriology and Extracellular Protein Preparation

F. columnare isolate LV-359-01 was retrieved from frozen glycerol stocks stored at −80°C and streaked onto *F. columnare* Growth Medium (FCGM) (36, 37). After 48 h of growth at 28°C, the isolate was dislodged from the agar using a sterile loop and inoculated into 5 mL of FCGM (starter) overnight at 28°C. The next day the 5 mL starter was placed into 1 L of FCGM and incubated at 28°C for 24 h at 200 RPM. To produce a live bacterin, LV-359-01 was also grown under iron-limiting conditions with FCGM that contained 100 μM of the high-affinity iron chelator 2, 2′-bipyridyl (Sigma-Aldrich, St. Louis, MO). The use of 2, 2′-bipyridyl to attenuate virulence for this isolate of *F. columnare* was an observation made from our previous work (38). For the live bacterin (LV-DP), we subcultured LV-359-01 in FCGM broth under iron limiting conditions for 24 h and used it immediately to bath immunize channel catfish for the Year 1 study. To isolate extracellular proteins, bacterial suspensions were centrifuged using an Eppendorf 5810R at 6,320 × *g* for 20 min. The extracellular portion (ECP) was aspirated into a new tube and centrifuged again for an additional 10 min. The ECP was aspirated and concentrated using 3K MWCO Amicon Ultra-15 centrifugal filter units (EMD Millipore, Billerica, MA). All ECP fractions had a 5% (v/v) protease inhibitor cocktail (Sigma Aldrich, St. Louis, MO) added prior to estimating the total protein concentration using the Coomassie Plus assay kit (ThermoFisher Scientific, Waltham, MA) with bovine serum albumin (Sigma Aldrich, St. Louis, MO) as the standard. Absorbance was read at a wavelength of 595 nm with a BioTek Synergy H1 plate reader operating under Gen5 software (Winooski, VT).

Construction, Expression, and Evaluation of Recombinant *F. columnare* DnaK Protein

To construct the expression vector, we first identified the annotated DnaK protein sequence from the *Flavobacterium columnare* isolate ATCC 49512 genome (AEW86253.1). The full-length nucleotide sequence was submitted for codon optimization, incorporation of restriction sites, *NcoI*, and *XhoI* flanking the coding region, gene synthesis and cloning into pET-28a(+) expression vector with a C-terminal His-tag (Genscript, Piscataway, NJ). During this process the second codon of the DnaK sequence was altered from AGC to GGC for incorporation of the NcoI restriction site. The codon optimized recombinant *F. columnare* DnaK coding sequence which shared 71.4% nucleotide identity (amino acid identity 100% to AEW86253.1 protein sequence) to the *F. columnare* DnaK 49512 genomic clone was verified through Sanger sequencing. The expression vector was transformed into *Escherichia coli* strain BL21 (DE3) (Invitrogen, Carlsbad, CA) on Luria– Bertani (LB) agar supplemented with kanamycin (50 mg/mL) and grown at 37°C. For expression, a recombinant *F. columnare* DnaK clone was retrieved from a frozen glycerol stock stored at −80°C and streaked onto LB agar plate supplemented with kanamycin and grown overnight. A single colony was then cultured overnight in 50 mL of LB broth supplemented with kanamycin. A flask containing 250 mL of fresh LB broth with kanamycin was inoculated with 10 mL of the overnight culture and incubated for 2 h under the same culture conditions. Recombinant protein expression was induced by adding isopropyl thiogalactoside (IPTG) at a 1 mM final concentration and cultured for an additional 2 to 6 h. The rDnaK protein was purified from the *E. coli* pellet under native conditions according to the manufacturer's guidelines (Ni-NTA handbook, Qiagen) using a HisPur Ni-NTA spin column (ThermoFisher Scientific, Waltham, MA). Protein concentration was estimated as described above. Aliquots were dispensed and kept at −20°C until needed. SDS gel electrophoresis was conducted to analyze expressed protein using 10% TGX stain-free gels and buffers of the mini-protean system (Biorad, Hercules, CA). We loaded 5 μg of bacterial lysates or eluted rDnaK protein onto SDS gels with the Precision Plus gel marker (Biorad, Hercules, CA), stained using Simple Blue Safe (ThermoFisher Scientific, Waltham, MA) and visualized using a Biorad ChemiDoc XRS+ gel system operating under Image Lab 3.0 software. The rDnaK protein was excised from the SDS gel and mass spectrometry analysis was conducted as previously described (26).

Bath Immunizations and *F. columnare* Challenges

All channel catfish fingerlings were reared at the Harry K. Dupree Stuttgart National Aquaculture Research Center in Stuttgart, Arkansas, USA.

In year one, 300 catfish in each of three groups (average weight 5 g) were bath immunized under different conditions prior to being stocked into 200 L tanks that received filtered well water and aeration from submerged air stones. Non-immunized control catfish were sham vaccinated, an iron attenuated LV-359-01 (LV-DP) culture was used to bath immunize catfish (calculated dose of 4 x 10^7 CFU/mL), and the recombinant *F. columnare* DnaK protein (rDnaK) was used to bath immunize catfish (100 μg/mL). All bath immunizations were done statically for 30 min with aeration. Fish were maintained on pelleted catfish feed daily (35% protein, 2.5% fat; Delta Western, Indianola, Mississippi).

After 6 weeks, the non-immunized control and two immunized groups were challenged with virulent *F. columnare* LV-359-01 with a calculated dose of 8.5×10^6 CFU/mL. For each group there were three challenge replicates, where catfish ($n = 44$) were stocked into 18 L aquaria containing 10 L of well water. Water was provided through the ultra-low-flow water delivery system at a rate of 30 mL/min (5, 39). An additional tank with catfish ($n = 44$) was used as the non-challenged control. The number of mortalities from each group was recorded twice daily over 6 days for survival curves.

In year two, 300 catfish in each of three groups (average weight 5 g) were bath immunized. Control catfish were sham vaccinated, and rDnaK was used to bath immunize catfish (200 μg/mL). For the third group (rDnaK + salt) a bath immunization occurred just after hyper-osmotic induction. Catfish were first immersed in a 4.5% (w/v) NaCl bath for 2 min and then bath immunized with rDnaK (200 μg/mL). All bath immunizations were done statically for 30 min with aeration.

Six weeks after the bath immunizations, the different groups were challenged (using the same system described above) with virulent *F. columnare* LV-359-01 at a calculated dose of 1.0×10^6 CFU/mL. For each group there were three challenge replicates, where catfish ($n = 40$) were stocked into 18 L aquaria containing 10 L of filtered well water. An additional tank with catfish ($n = 40$) was used as the non-challenged control. The number of mortalities from each group was recorded twice daily over 5 days for survival curves. In all studies, temperature and dissolved oxygen were measured using an YSI Pro20 dissolved oxygen meter (Yellow Springs, Ohio). Each fish culture tank received aeration from submerged air stones and all studies were kept at 12 h light: 12 h dark photoperiod.

Tissue Sampling and ELISAs

In years one and two, catfish from the non-immunized control or immunized groups were sampled at 2, 4, 6, 8, and 10 weeks. In year 2, catfish were also sampled at 1-week post immunization. For tissue sampling, catfish were euthanized in a solution of MS-222 for 10 min (300 mg/L, Syndel USA, Ferndale, WA), and whole blood was collected using 70 μL heparinized capillary tubes (ThermoFisher Scientific, Waltham, MA) from the caudal vein after tail fin removal and then allowed to clot overnight at 4°C. Blood samples were centrifuged at 10,000 × *g* for 10 min using an Eppendorf Minispin; the serum (20–50 μL) was removed and stored at −20°C until needed. After blood collection we proceeded with the preparation of excised skin for tissue culture as described (26). Briefly we wiped down the surface of the skin on both sides with a 70% ethanol solution. Then using sterile instruments, we dissected two consecutive 1.5 mm^2 skin pieces (between the lateral line and dorsal fin), washed

them with Leibovitz's L-15 medium (ThermoFisher Scientific, Waltham, MA), and placed them into 300 μL of complete Leibovitz's L-15 medium (10% FBS, penicillin/streptomycin, amphotericin, gentamicin) in a 48-well plate at 28°C for 24 h. The next day the skin explant tissue culture medium was removed and RNA*later* (ThermoFisher Scientific, Waltham, MA) was added to sufficiently cover the skin explants and stored at −80°C.

We used an indirect ELISA to measure the serum and skin based IgM antibodies as described with some modifications (22, 26). Prior to conducting these ELISA experiments; we established the amount of rDnaK required to bind and generate a consistent OD signal using the DnaK specific mAb 8E2/2 (Enzo Life Sciences, Farmingdale, NY). Pierce 96-well polystyrene plates (ThermoFisher Scientific, Waltham, MA) were coated with 100 μL of 10 μg/mL of *F. columnare* LV-359-01 ECP or 10 μg/mL of rDnaK protein in a sodium bicarbonate buffer. Plates were then rinsed three times with 1x PBS with 0.05% Tween-20 (PBST) and then incubated for 1 h in blocking solution (PBST with 5% milk). One hundred μL of serum (1:100) or skin explant medium (1:4) were further serially diluted to 1:1600 or 1:32 in 1x PBS on the horizontal axis of an antigen-coated ELISA plate and incubated at room temperature for 1 h. Plates were rinsed as above and 100 μL of anti-channel catfish IgM mouse monoclonal 9E1 antibody (40) was added at 1:500 dilution in blocking solution. The anti-trout IgM monoclonal antibody was used as an isotype control (41). After 1 h of incubation at room temperature, plates were washed with PBST and 100 μL of sheep anti-mouse HRP-conjugated IgG (GE Healthcare, Pittsburgh, PA) was diluted 1:5000 in blocking solution and incubated for 30 min at room temperature. Plates were rinsed three times with PBST, and 100 μL of 1-Step Ultra TMB-ELISA substrate solution (Thermo Fisher Scientific, Waltham, MA) was added. The peroxidase reaction was stopped after 20 min with 100 μL of 3M H_2SO_4 and assessed at 490 nm with a BioTek Synergy H1 plate reader operating under Gen5 software (Winooski, VT).

Differences among the serum or skin based *F. columnare* ECP or rDnaK specific IgM antibody levels were evaluated using One-Way ANOVA. Survival data was analyzed using Kaplan-Meier log rank survival analysis. Probabilities of $P < 0.05$ were considered statistically significant. All statistical tests were performed using GraphPad Prism version 7.0 (San Jose, California).

RNA Sequencing of Skin Explants in Year 2

Skin explant tissues from non-immunized catfish ($n = 6$), catfish 1-week after treatment with rDnaK ($n = 6$) and catfish 6 weeks post-treatment with rDnaK ($n = 6$) were randomly selected for transcriptome analyses. Skin explants stored in RNA*later* at −80°C as described were used to create libraries for Illumina (San Diego, CA) high-throughput RNA sequencing (RNAseq). First, total RNA was extracted from each tissue using the Qiagen RNeasy Mini Kit (Germantown, MD) per the manufacturer's recommendation. Total RNA was treated with Amplification Grade DNase I (Sigma-Aldrich, St. Louis, MO) according to the package insert and then precipitated with sodium acetate—ethanol and reconstituted in nuclease-free water. Samples were assessed for quality using the Agilent Bioanalyzer RNA 6000 Nano Kit (Santa Clara, CA), where RNA Integrity Numbers > 8 were considered valid. For each sample, DNase-treated total RNA was standardized to 100 ng by spectrophotometry (Bio-Tek, Winooski, VT) and sequencing libraries were prepared using the NEBNext Ultra II Directional RNA Library Prep Kit for Illumina with the NEBNext Poly(A) mRNA Magnetic Isolation Module (New England Biolabs, Ipswich, MA). Each sample was barcoded using the NEBNext Multiplex Oligos for Illumina, Index Primers Sets 1 and 2 (New England Biolabs). RNAseq libraries were sent to a service provider (Novogene, Sacramento, CA) for 150 bp paired-end sequencing on an Illumina HiSeq X Ten.

Bioinformatics

De-multiplexed, raw reads were provided by the service provider (Novogene). The Trim_Galore! software was used to remove Illumina adapters and trim low-quality ends from each read at a cut-off score of Q20 (42). Bowtie2 was used to align reads against the channel catfish RefSeq transcriptome from the IpCoco_1.2 genome assembly (43). The output from Bowtie2 was piped into the eXpress software using the parameters as recommended by eXpress when using the Bowtie2 aligner and included directional information from the reads (44). Effective read counts for each sample were then used for statistical comparisons by the DESeq2 package of R-bioconductor to generate lists of Differentially Expressed Genes (DEGs) between each control-treatment group. DEG assignment was significant where P-adj < 0.05 and at a fold-change > 1.5. Finally, DEG lists were manually aggregated to the gene-level to provide a final list of candidate genes (45). Raw and processed data along with a complete description of computational methods were submitted to the NCBI Gene Expression Omnibus (GEO) accessible under the accession number GSE121116.

Functional

Enrichment testing was performed on DEG lists to populate gene ontologies (GO). GO categories include Biological Process (BP), Cellular Component (CC), and Molecular Function (MF). The Blast2GO PRO software was used to perform all functional analyses (46). First, the channel catfish RefSeq transcriptome from the IpCoco_1.2 genome assembly was up-loaded into Blast2GO where sequences underwent BLASTx (E-value <1e-3), enzyme commission assignment, InterPro protein sequence analyses along with GO term assignment, where available. Then, each DEG list was evaluated for enrichment first using Fisher's exact test at a False Discovery Rate (FDR < 0.05). To do this, the functionally-annotated catfish transcriptome was used as a "reference set" of genes while the DEG list from each comparison was used as the "test set" of genes in the Blast2GO software. For additional functional information, Gene Set Enrichment Analysis (GSEA) was also performed in the Blast2GO software (47). To do this, differential expression between each comparison of interest was re-analyzed in DESeq2, where a shrinkage estimator (coef=2) was applied. All genes were then ranked by the ratio of significance of expression (p-value) to the direction of fold-change. From this list, the significant DEGs were tabulated along with the corresponding ranking metric for use in GSEA. Each list was evaluated for GO enrichment by 1,000 permutations

using the default settings in Blast2GO but also to include all data (min = 1). As the entire transcriptome (reference set) was functionally characterized in Blast2GO, Fisher's and GSEA analyses were performed using all significant transcripts (test set) for each comparison. Lastly, each significant DEG list was functionally characterized for GO, enzyme commission number, InterPro assessment and KEGG pathway assignment.

qPCR Validation

Select genes were independently assessed via reverse transcription quantitative PCR (RT-qPCR) to validate our RNAseq pipeline. For each comparison, all individual DNase-treated RNA used for RNAseq library creation were also tested using qPCR. Each RNA was re-quantified by spectrophotometry (Bio-Tek) and standardized to 5 ng. The iTaq Universal SYBR Green One-Step Kit (Bio-Rad, Hercules, CA) was used for qPCR reactions. Each reaction contained 2 μL RNA, 5 μL of iTaq universal SYBR Green reaction mix (2x), 0.25 μL of iScript reverse transcriptase, 300 nM of each primer and nuclease-free water up to a total 10 μL volume. RT-qPCR was then performed using a Roche LightCycler 96 System (Indianapolis, IN), with cycling parameters according to the iTaq provided instructions. Technical replicates were performed for each reaction. Negative controls and no reverse transcriptase controls were included in each 96-well plate. Each qPCR was assessed by melting curve analysis. After all reactions, cycle threshold (Ct) values were collected and fold-change between each comparison was determined using the $2^{-\Delta\Delta CT}$ method (48). *P*-values were calculated using a Student's *t*-test. We assessed several sets of published housekeeping gene primer sets (glucuronidase beta, glyceraldehyde-3-phosphate dehydrogenase, alpha tubulin, beta-actin, and 18S ribosomal RNA gene) and found that the 18S ribosomal RNA sets performed the best with skin explant tissue RNA (49–51). Validation primer set sequences are provided (**Table S6**).

RESULTS

Evaluation of Recombinant *Flavobacterium columnare* DnaK Protein

To evaluate the potential of the *F. columnare* DnaK protein as a recombinantly expressed vaccine candidate, the DnaK amino acid sequence was identified among the annotated protein sequences of *F. columnare* isolate ATCC 49512 genome. An alignment of DnaK amino acid sequences from recently released *F. columnare* genomes and protein sequences from other Gram-negative bacteria were compared to that identified in *F. columnare* ATCC 49512 (**Table S1**). The alignment of the DnaK protein sequences showed an average of 99.3% amino acid sequence identity among the different *F. columnare* isolates with lower amino acid sequence identity (∼60%) among the other Gram-negative bacteria. After cloning and expressing the recombinant DnaK protein, Ni-NTA columns were used and provided a highly enriched rDnaK protein which migrated at the expected size (70 kDa). The added time allowed for an increase in protein synthesis between the 4 and 6 h intervals and benefited the overall yield during recombinant expression (**Figure 1**). The eluted rDnaK protein was later confirmed to be *Flavobacterium columnare* ATCC 49512 DnaK protein (AEW86253.1) through mass spectrometry analysis.

Efficacy of Immunization Strategies in Year 1

Six weeks post immunization a laboratory challenge was conducted on the non-immunized control, LV-DP and rDnaK

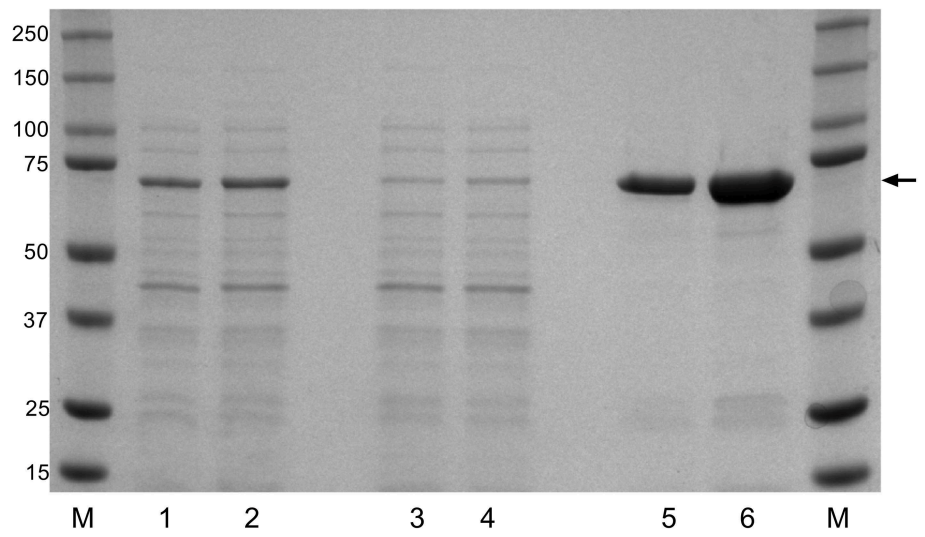


FIGURE 1 | Recombinant expression of *F. columnare* DnaK protein (rDnaK). Coomassie stain of SDS gel of *E. coli* lysates (lanes 1 and 2); Ni-NTA column washes (lanes 3 and 4), and eluted protein fractions (lanes 5 and 6) after 4 or 6 h of IPTG stimulation, respectively. The arrow marks the 70 kDa band representing the approximate size of the eluted rDnaK protein. (M) The pre-stained Precision Plus marker (kDa) was used to estimate molecular mass.

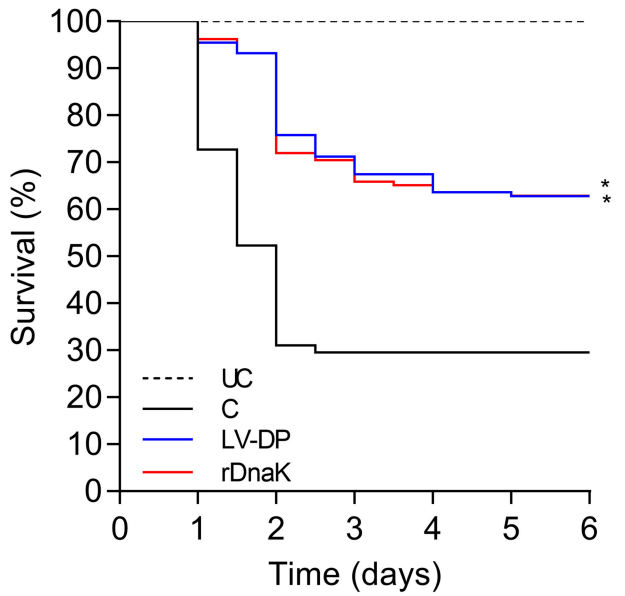


FIGURE 2 | The impact of year-one immunization protocols on the protection of channel catfish against an *F. columnare* laboratory challenge. Kaplan-Meier survival curves of catfish challenged with isolate LV-359-01 over 6 days. The different groups are labeled as indicated in the figure. Data represent cumulative mortality across three replicate tanks per treatment containing 132 fish ($n = 44$/tank). Asterisk(s) denote a significant difference in survival when compared to the non-immunized control group; $^*P < 0.05$.

immunized groups with *F. columnare* LV-359-01. Kaplan-Meier survival analysis showed that 6 days post challenge there was a significantly higher survival rate ($P<0.05$) between the two immunized groups when compared to the non-immunized control (**Figure 2**). There was no significant difference in survival between the immunized groups. The overall survival rate of the immunized groups was 64% while the non-immunized control was 32%. These results indicate that significant protection was achieved in both the LV-DP and rDnaK immunized groups.

Antibody Response to *F. columnare* Extracellular Proteins in Year 1

To evaluate the development of antibodies to the *F. columnare* ECP, the serum of non-immunized and immunized catfish collected at different time points was assessed using an indirect ELISA. The absorbance values showed that individual fish had generated varying amounts of serum IgM antibodies to *F. columnare* ECP (**Figure 3A**). At 2 weeks post immunization the non-immunized control had a mean absorbance value of 0.089 ± 0.01, the LV-DP and rDnaK immunized groups were 0.160 ± 0.06 and 0.145 ± 0.03, respectively. At 4 weeks the LV-DP and rDnaK immunized groups mean absorbance values remained higher than the 2-week control at 0.167 ± 0.07 and 0.115 ± 0.02. There were significantly higher absorbance values ($P < 0.05$) between the two immunized groups at week two and for the LV-DP group at week four. The LV-DP group also had significantly more serum IgM antibodies ($P < 0.05$) that bound to *F. columnare* ECP at week four when compared to the rDnaK group. Over the remaining weeks none of the catfish sampled from either of the two immunized groups generated little more ECP specific serum IgM antibodies than that detected in the non-immunized control. Overall the LV-DP-immunized catfish produced more ECP specific serum antibodies than the rDnaK-immunized fish (with more responsive individuals at weeks four and eight); however, there were no additional significant differences observed between the immunized groups.

Similarly, the humoral immune response of the mucosae was assessed by evaluating the amount of ECP specific IgM antibodies present among the *in vitro* cultured skin explant medium (**Figure 3B**). At 2 weeks, the non-immunized control had a mean absorbance value of 0.071 ± 0.01, while the LV-DP was 0.134 ± 0.06 and rDnaK was 0.076 ± 0.05. The LV-DP group generated a more significant skin IgM antibody response to ECP ($P < 0.05$) than that observed in the control group at weeks 2, 4, 6, 8, and 10. The rDnaK group also generated more significant skin IgM antibody response to ECP than did the non-immunized control at 6 weeks. Interestingly, the LV-DP group generated significantly more ECP specific mucosal IgM antibodies ($P< 0.05$) than did the rDnaK group at weeks 2, 6, and 8. These results indicate that the bath immunization protocols (LV-DP or rDnaK) stimulated different mucosal humoral immune responses, and overall there was a much more substantial immune response with the LV-DP group.

Mucosal Antibody Response to Recombinant *F. columnare* DnaK in Year 1

To establish the level at which mucosal IgM antibodies were specifically generated to the *F. columnare* DnaK protein the skin explant tissue culture medium and an rDnaK specific indirect ELISA were used (**Figure 3C**). Four weeks post immunization the LV-DP immunized group had a mean absorbance of 0.072 ± 0.01 while the rDnaK immunized group was significantly higher at 0.113 ± 0.03 ($P < 0.05$). At 6 weeks LV-DP had generated slightly more rDnaK specific antibodies with a mean absorbance of 0.087 $\pm$ 0.01, while the rDnaK group remained significantly higher with a mean absorbance of 0.177 ± 0.01 ($P < 0.05$). These results indicate that both the LV-DP and rDnaK groups stimulated an *F. columnare* DnaK specific mucosal IgM antibody response albeit at much different levels.

Efficacy of Immunization Strategies in Year 2

In the year two trials to test the efficacy of the recombinant *F. columnare* rDnaK protein vaccine there were two immunized groups (rDnaK and rDnaK + salt), the latter received a brief 4.5% NaCl dip prior to bath immunization. The results to the *F. columnare* laboratory challenge indicated there was a significantly higher survival rate ($P < 0.05$) among the immunized groups when compared to the non-immunized control (**Figure 4**). The overall survival rates of the immunized

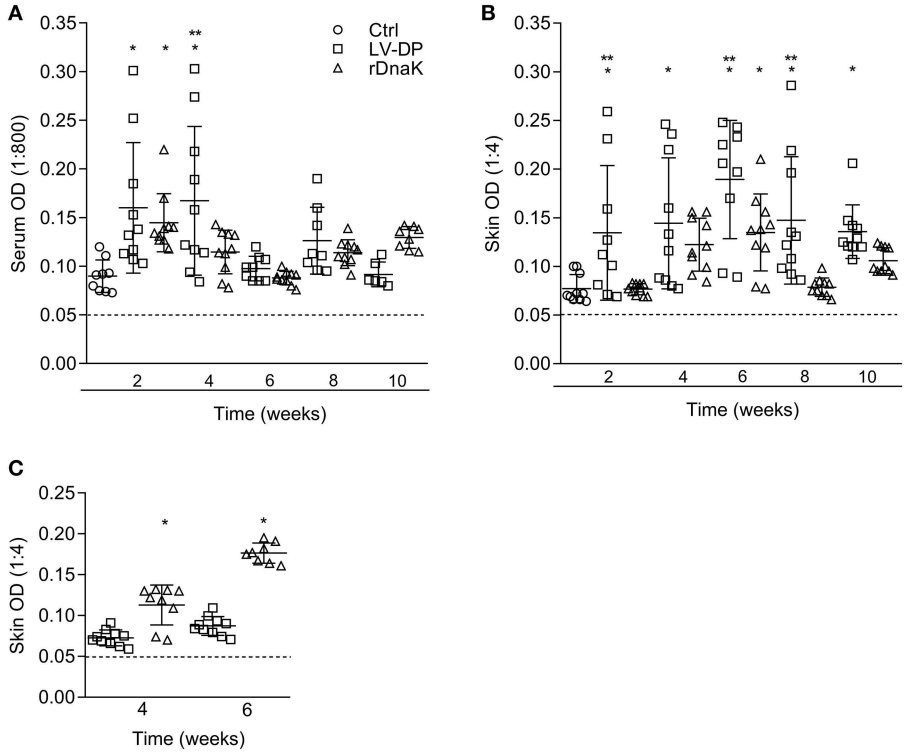


FIGURE 3 | Evaluation of antibodies generated against *F. columnare* ECP and recombinant DnaK protein. The different groups are labeled as indicated in the figure. **(A)** The serum IgM antibody titer (1:800) is the reciprocal of the maximum dilution at which we could reliably detect binding of antibody to *F. columnare* ECP. **(B)** The skin IgM antibody titer (1:4) is the reciprocal of the maximum dilution at which we could reliably detect binding of antibody to *F. columnare* ECP. **(C)** The skin IgM antibody titer (1:4) is the reciprocal of the maximum dilution at which we could reliably detect binding of antibody to *F. columnare* rDnaK. The mean absorbance ± SD for each group is shown as a horizontal line. Asterisk(s) denote a significant difference, $P < 0.05$. (*), indicates a significant difference when compared to the non-immunized control; (**), indicates a significant difference between immunized groups. The dashed line represents the mean background absorbance value observed using an isotype control.

groups were 57% (rDnaK) and 68% (rDnaK + salt) and 31% survival among the non-immunized group. There was no significant difference in survival between the two rDnaK-immunized groups.

Antibody Response to Recombinant *F. columnare* DnaK in Year 2

To evaluate the development of IgM antibodies to recombinant *F. columnare* DnaK protein, the serum of non-immunized and immunized fish was collected at different time points and evaluated using an rDnaK specific indirect ELISA (**Figure 5A**). At 2 weeks post immunization the non-immunized control had a mean absorbance value of 0.093 ± 0.01, the (rDnaK) and (rDnaK + salt) immunized groups were 0.057 ± 0.008 and 0.094 ± 0.01, respectively. Over the next several weeks none of the catfish sampled from either of the two immunized groups generated higher absorbance values than that detected in the non-immunized control indicating little to no serum antibodies were generated to the rDnaK protein.

To establish the level at which mucosal IgM antibodies were generated to rDnaK, skin explant tissue culture medium and an rDnaK specific indirect ELISA were used (**Figure 5B**). At 2 weeks post immunization the non-immunized control had a mean absorbance value of 0.097 ± 0.01, the rDnaK immunized groups were 0.082 ± 0.01 and 0.097 ± 0.01, respectively. The non-immunized control fish never developed rDnaK specific Abs in the skin at the later time points. Both rDnaK immunized groups later generated significantly more skin IgM antibodies to rDnaK ($P < 0.05$) than that observed in the non-immunized group at weeks four and six. The rDnaK group also generated significantly more *F. columnare* rDnaK antibodies ($P < 0.05$) than the (rDnaK + salt) group at 6 weeks. These results indicate both immunized groups stimulated *F. columnare* rDnaK specific mucosal IgM antibody responses.

Differential Gene Expression and Gene Ontology of Skin Explants in Year 2

There was a total of six RNA sequence libraries prepared and sequenced from the skin of individual catfish from the non-immunized control and rDnaK groups (week one and six) for a total of 18 RNAseq libraries. Following the processing of the raw RNA sequencing data and alignment with the *I. punctatus* transcriptome, we conducted comparisons between the control and treatment groups at different

time intervals to establish their gene expression profiles. In each case, the first biological state listed is the base (reference) level. Three comparisons of interest were made including: non-immunized control and rDnaK immunized group (week one), non-immunized control and rDnaK immunized group (week six), and rDnaK (week one) and rDnaK (week six). For each of the three comparisons we identified between 1.0 and 5.5% of the total genes identified among the different transcriptomes as being differentially expressed according to the following cutoff criteria (*P*-adj <0.05, Fold change >1.5). There were 420 differentially expressed genes (DEGs) between the non-immunized control and rDnaK group 1-week post immunization that included 323 upregulated and 96 down regulated genes (**Data Set 1**). There were 579 DEGs between the non-immunized control and the rDnaK group (week six), including 472 upregulated and 106 downregulated genes (**Data Set 2**). There were 52 DEGs identified between the rDnaK groups (week one and six) with 17 upregulated and 35 down regulated genes (**Data Set 3**).

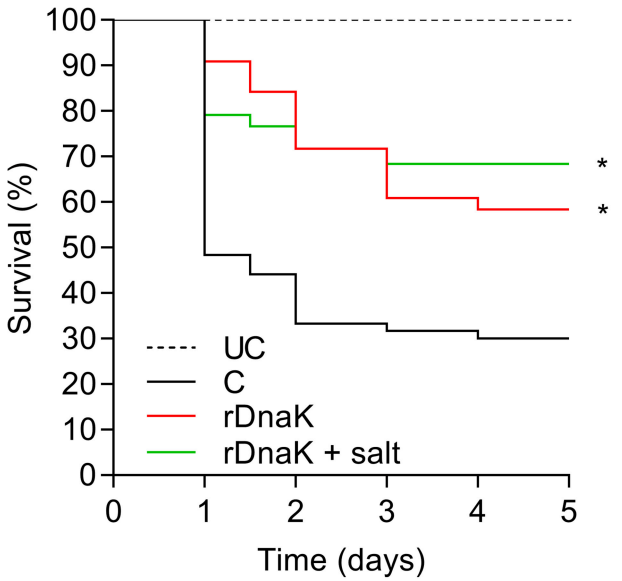


FIGURE 4 | The impact of year-two immunization protocols on the protection of channel catfish against an *F. columnare* laboratory challenge. Kaplan-Meier survival curves of catfish challenged with isolate LV-359-01 over 5 days. The different groups are labeled as indicated in the figure. Data represent cumulative mortality across three replicate tanks per treatment containing 120 fish ($n = 40$/tank). Asterisk(s) denote a significant difference in survival when compared to the non-immunized control group; $^*P < 0.05$.

Gene ontology analyses were performed on the DEGs from each comparison to determine functional enrichment. Among the non-immunized control and rDnaK groups at 1-week post immunization, there were 157 over-represented GO groups: 123 BP, 28 MF, and 6 CC categories. The top five most significant GO names identified in each category are represented by processes such as carbohydrate biosynthesis (GO: 0016051), oxireductase activity (GO: 0016491) and intermediate filament (GO: 0005882) (**Table S2**). The same analysis was conducted between the non-immunized control and the rDnaK group (week 6) resulting in 180 over-represented GO groups: 143 BP, 28 MF, and 9 CC categories (**Table S3**). The top five most significant GO names identified in each category are represented by processes such as ATP generation (GO: 0006757), endopeptidase inhibitor activity (GO: 0004866), and intermediate filament (GO: 0005882). There were no significantly represented GO groups identified among the DEGs of the rDnaK groups (week one and six).

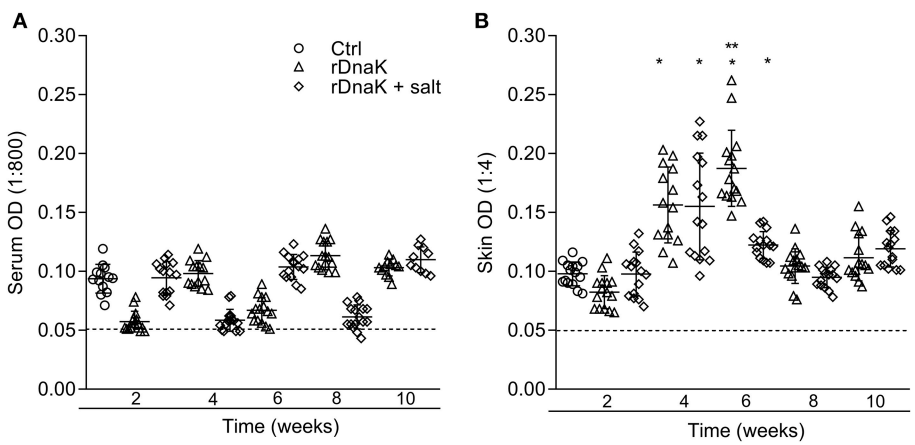


FIGURE 5 | Evaluation of antibodies generated against *F. columnare* recombinant DnaK protein. The different groups are labeled as indicated in the figure. **(A)** The serum IgM antibody titer (1:800) is the reciprocal of the maximum dilution at which we could reliably detect binding of antibody to *F. columnare* rDnaK. **(B)** The skin IgM antibody titer (1:4) is the reciprocal of the maximum dilution at which we could reliably detect binding of antibody to *F. columnare* rDnaK. The mean absorbance ± SD for each group is shown as a horizontal line. Asterisk(s) denote a significant difference, $P < 0.05$. (*), indicates a significant difference when compared to the non-immunized control; (**), indicates a significant difference between immunized groups. The dashed line represents the mean background absorbance value observed using an isotype control.

Identification of Genes Associated With Immune Function in Skin Explants

To evaluate the DEGs that may be involved with skin immune function a GO distribution level 2 analysis was conducted with the top 20 GO terms represented by the non-immunized control and rDnaK group at week one (**Figure S1**). Through this analysis we identified 17 DEGs associated with the GO term immune system process (GO: 0002376) (**Table S4**). Further testing for the representation of enzymes in KEGG pathways identified three genes involved in T-cell differentiation and receptor signaling pathways (maps 04658 and 04660). The GSEA also identified GO terms associated with myeloid leukocyte activation (GO: 0002274) and immune effector process (GO: 00052252).

The same evaluations were then conducted between the non-immunized control and the rDnaK group at week six (**Figure S2**). The DEGs identified 23 genes associated with immune system processes (GO: 0002376) at GO level 2, and seven genes involved in T-cell differentiation and receptor signaling pathways (maps 04658 and 04660) through KEGG analysis (**Table S5**). GSEA identified additional GO terms involved with immunity, including myeloid leukocyte activation (GO: 0002274), regulation of immune effector process (GO: 0002697), cell chemotaxis (GO: 0060326) and leukocyte mediated immunity (GO: 0002443).

Validation of RNA Sequencing

Reverse transcription qPCR was conducted on skin explant RNA samples submitted for library preparation and sequencing. We chose four genes that were both up- and down-regulated among the rDnaK immunized group at different time points for validation of our RNA sequencing analysis (**Table S6**). In all qPCR experiments, average 18S Ct values were within <1 Ct unit of each other among the different RNA samples (**Table S7**). All qPCR data was statistically significant and correlated to the RNA sequencing data (**Table S8**).

DISCUSSION

Columnaris disease continues to be a significant issue among the different production systems of warmwater finfish. *F. columnare* infections principally begin as biofilms on the different mucosal surfaces causing significant damage to the gills and skin (52–54). To avert disease and reduce losses the current study sought to evaluate the potential of the recombinant *F. columnare* DnaK protein to activate a mucosal IgM antibody response in channel catfish and assess the level of protection which could be generated during an *F. columnare* challenge. We were also interested in a time-course assessment of a mucosal tissue to determine potential functional mechanisms involved in this protective immunity.

The use of recombinant protein technology to develop new vaccines is not a new concept and is widely being examined for use in both human and animal health (55–58). Our rationale for choosing this protein was due to a previous study in which DnaK was shown to be the dominant immunogen in the *F. columnare* ECP. The *F. columnare* chaperone protein DnaK was recombinantly expressed, purified and used as a soluble antigen in a bath immersion vaccine. We and others have demonstrated that fish can generate IgM antibodies that are immune-reactive to DnaK proteins found among different Gram-negative bacteria (26, 59). DnaK proteins have also been demonstrated to be highly immunogenic (29, 31, 60). An alignment of DnaK protein sequences among different *F. columnare* genomes indicated a high percentage of amino acid similarity, which led us to hypothesize that the rDnaK protein may induce cross protection between different *F. columnare* isolates.

One of the most important parameters evaluated during vaccine efficacy studies is the ability for the immunogen(s) to confer immune protection against the known pathogen. Previous work in rainbow trout indicated that *F. psychrophilum* heat shock proteins (similar to DnaK chaperone protein) were highly immunogenic but not protective against bacterial cold-water disease (59, 61). The opposite was observed in the current study where 2 years of rDnaK vaccine trials demonstrated that significant protection is achieved after bath immunization. From year-to-year and among the different immunization strategies, we observed very similar increases in survival (∼30%). More importantly in year one we demonstrated that the rDnaK protein can confer protection at a similar rate to live-attenuated bacterial cells and ECP. These results suggest that rDnaK may be a valuable vaccine candidate in providing protection against columnaris disease. We are also confident that the rDnaK immunogen can be further optimized using improved vaccination strategies. Unlike other vaccine trials in fish, the immunization strategies used in this study were performed independent of any conventional adjuvants (62–64). In year two, the use of hyperosmotic induction prior to bath immunization increased overall survival and has been shown by others to have a positive effect on soluble antigen uptake and mucosal antibody production (65). The use of a commercial mucosal adjuvant in tandem with an osmotic shock pre-treatment could prove to be a valued bath immersion vaccine strategy (66, 67).

To evaluate the adaptive immune response, IgM antibodies produced at different time intervals were assessed using a rDnaK-specific ELISA. Similar to what we and others have observed, the use of a soluble antigen to stimulate the external mucosae has generated mucosal IgM antibodies (20, 22, 68). During both vaccine trials rDnaK-specific antibodies were most abundant in the skin during weeks four and six, however all rDnaK-specific antibodies fell to baseline levels by weeks 8 and 10 in the skin of both immunized groups. The overall result is consistent with what we have previously observed (22). Among the later time points it is possible that the limits of detection for the rDnaK-specific ELISA have been reached. As this assay relies on mucosal antibody secretion into the tissue culture medium, a minimum number of antibody-secreting cells would likely need to be present. Perhaps for long term analysis another assay should be performed. In fact others have established through the use of an ELISPOT assay that antibody-secreting cells could be enumerated from lymphocytes isolated from the skin (69). This work showed that the number of antibody-secreting cells remained elevated in the skin for up to 17 weeks after immunization. In later studies, the same group would demonstrate that despite the loss of circulating mucosal antibodies; antibody-secreting cells that were present

in the skin were activated after a significant amount of time and that immune protection was retained (70). Perhaps IgM memory B cells are generated during the bath immunization with rDnaK protein. Clearly the amount of antigen(s), the duration of exposure and antigen complexity will govern the magnitude of antibody responses to individual proteins. Additional testing will need to be performed to determine the longevity of protection among the rDnaK-immunized groups (71).

Analyzing gene expression in the skin of the non-immunized and immunized groups at different time points, we were able to identify DEGs and characterize functionally enriched processes associated with different biosynthetic and transport pathways. The most interesting observation was among the cellular component groups of the rDnaK skin (weeks one and six) which showed an overrepresentation of intermediate filament, intermediate filament cytoskeleton and desmosome (GO groups). The desmosomes are characterized as adhesive intercellular junctions which facilitate skin integrity between individual cells (72). The fish skin is the host's primary barrier to infection and is the frontline defense against infection (73). The integument is vital in its capacity to maintain both structure and regulate the mucosal environment from both friend and foe (74). Li et al. characterized the up- and downregulation of different genes in catfish skin associated with junctional/adhesion groups after an *Aeromonas hydrophila* infection (75). Perhaps during an active mucosal immune response in the skin, the mechanisms which regulate skin integrity and cell infiltration are activated in addition to immune-related genes to ensure that homeostasis is maintained (76).

We also identified candidate genes associated with immune function, and while we don't necessarily have a complete picture of what is occurring in the immunized skin we can make some general observations from our findings. There were molecular processes associated both with immune effector function and regulation of immune effector (rDnaK week one and six) which identified the CD59 glycoprotein-like and matrix metalloproteinase 9 genes, each of which could have a role in innate immune function (77, 78). There were also processes characterized as cell chemotaxis (week six) which identified sphingosine 1-phopshate receptor 4 like, ras-related C3 botulinum toxin substrate 2 and CxC motif chemokine 2-like genes underlying this functional group. Interestingly the cell chemotaxis GO term wasn't enriched at week one, however the sphingosine 1-phopshate receptor 4 like, ras-related C3 botulinum toxin substrate 2 genes were also upregulated. The sphingosine phosphate family of receptors has been implicated in both B and T cell migration in mammals (79, 80).

Lastly, it is evident that B cells were activated and differentiated into rDnaK-specific antibody secreting cells in the skin during the 4 to 6-week interval. A few genes associated with T cell signaling and differentiation (tyrosine-protein kinase Lck-like, protein tyrosine phosphatase, non-receptor type 13, dual specificity phosphatase 14, tyrosine-protein phosphatase non-receptor type 3-like, and 14 kDa phosphohistidine phosphatase-like) were identified in one or both time points and could signify the coordination of T cells in the skin during an adaptive immune response. In general, there is limited information on the fish mucosal T cell response, although different subsets of T cells are likely present in these tissues (66, 81).

The fundamental role of developing a skin cell-mediated immune response and its contribution to overall immune protection against different fish pathogens will need to be further explored. We will continue to investigate the adaptive immune response in fish using conventional immunological assays as well as using genomics technologies to determine optimal conditions for long lasting immunization procedures.

ETHICS STATEMENT

Animal care and experimental protocols were approved by the Stuttgart National Aquaculture Research Center Institutional Animal Care and Use Committee and conformed to USDA Agricultural Research Service Policies and Procedures 130.4 and 635.1.

AUTHOR CONTRIBUTIONS

ML and JA designed the experiments, analyzed the data, and prepared the figures, and drafted the manuscript. ML and BF performed vaccination and challenge studies. JA prepared RNA sequencing libraries and performed the related bioinformatics. All authors contributed to the final manuscript.

FUNDING

These studies were funded under the USDA-ARS Research Project # 6028-32000-007-00D.

ACKNOWLEDGMENTS

We would like to thank Jason Brown for his technical assistance during these studies. We thank the University of Arkansas for Medical Sciences Proteomics Core for high-throughput mass spectrometry analysis. The USDA is an equal opportunity provider and employer. Mention of trade names or commercial products in this publication is solely for the purpose of providing specific information and does not imply recommendation or endorsement by the United States Department of Agriculture.

SUPPLEMENTARY MATERIAL

The Supplementary Material for this article can be found online at: https://www.frontiersin.org/articles/10.3389/fimmu.2019.01175/full#supplementary-material

REFERENCES

1. Welker TL, Shoemaker CA, Arias CR, Klesius PH. Transmission and detection of Flavobacterium columnare in channel catfish Ictalurus punctatus. *Dis Aquat Organ.* (2005) 63:129–38. doi: 10.3354/dao063129
2. Declercq AM, Haesebrouck F, Van den Broeck W, Bossier P, Decostere A. Columnaris disease in fish: a review with emphasis on bacterium-host interactions. *Vet Res.* (2013) 44:27. doi: 10.1186/1297-9716-44-27
3. Arias CR, LaFrentz S, Cai W, Olivares-Fuster O. Adaptive response to starvation in the fish pathogen *Flavobacterium columnare*:

cell viability and ultrastructural changes. *BMC Microbiol.* (2012) 12:266. doi: 10.1186/1471-2180-12-266
4. Mohammed HH, Arias CR. Epidemiology of columnaris disease affecting fishes within the same watershed. *DisAquatOrgan*. (2014) 109:201–11. doi: 10.3354/dao02739
5. Farmer BD, Mitchell AJ, Straus DL. The effect of high total ammonia concentration on the survival of channel catfish experimentally infected with *Flavobacterium columnare*. *J Aquat Anim Health*. (2011) 23:162–8. doi: 10.1080/08997659.2011.616836
6. Olivares-Fuster O, Bullard SA, McElwain A, Llosa MJ, Arias CR. Adhesion dynamics of *Flavobacterium columnare* to channel catfish *Ictalurus punctatus* and zebrafish *Danio rerio* after immersion challenge. *Dis Aquat Organ*. (2011) 96:221–7. doi: 10.3354/dao02371
7. Liu L, Li C, Su B, Beck BH, Peatman E. Short-term feed deprivation alters immune status of surface mucosa in channel catfish (Ictalurus punctatus). *PLoS ONE*. (2013) 8:e74581. doi: 10.1371/journal.pone.0074581
8. Declercq AM, Boyen F, Van den Broeck W, Bossier P, Karsi A, Haesebrouck F, et al. Antimicrobial susceptibility pattern of *Flavobacterium columnare* isolates collected worldwide from 17 fish species. *J Fish Dis.* (2013) 36:45–55. doi: 10.1111/j.1365-2761.2012.01410.x
9. Shoemaker CA, Klesius PH, Evans JJ. Immunization of eyed channel catfish, Ictalurus punctatus, eggs with monovalent *Flavobacterium columnare* vaccine and bivalent *F. columnare* and *Edwardsiella ictaluri* vaccine. *Vaccine*. (2007) 25:1126–31. doi: 10.1016/j.vaccine.2006.09.055
10. Xu DH, Klesius PH, Shoemaker CA. Effect of immunization of channel catfish with inactivated trophonts on serum and cutaneous antibody titers and survival against Ichthyophthirius multifiliis. *Fish Shellfish Immunol*. (2009) 26:614–8. doi: 10.1016/j.fsi.2008.09.015
11. Zhang D, Pridgeon JW, Klesius PH. Vaccination of channel catfish with extracellular products of Aeromonas hydrophila provides protection against infection by the pathogen. *Fish Shellfish Immunol.* (2014) 36:270–5. doi: 10.1016/j.fsi.2013.11.015
12. Xu DH, Moreira GSA, Shoemaker CA, Zhang D, Beck BH. Expression of immune genes in systemic and mucosal immune tissues of channel catfish vaccinated with live theronts of Ichthyophthirius multifiliis. *Fish Shellfish Immunol*. (2017) 66:540–7. doi: 10.1016/j.fsi.2017.05.051
13. Udey LR, Fryer JL. Immunization of fish with bacterins of *Aeromonas salmonicida*. *Mar Fish Rev*. (1978) 40:12–7.
14. Newman SG. Bacterial vaccines for fish. *Ann Rev Fish Dis.* (1993) 145–85. doi: 10.1016/0959-8030(93)90033-8
15. Bader JA, Klesius PH, Vinitnantharat S. Comparison of whole-cell antigens of pressure- and formalin-killed Flexibacter columnaris from channel catfish (Ictalurus punctatus). *Am J Veter Res.* (1997) 58:985–8.
16. Tyler JW, Klesius PH. Protection against enteric septicemia of catfish (Ictalurus punctatus). by immunization with the R-mutant, Escherichia coli (J5). *Am J Veter Res*. (1994) 55:1256–60.
17. Shoemaker CA, Klesius PH, Evans JJ, Arias CR. Use of modified live vaccines in aquaculture. *J World Aquac Soc.* (2009) 40:573–85. doi: 10.1111/j.1749-7345.2009.00279.x
18. LaFrentz BR, Welch TJ, Shoemaker CA, Drennan JD, Klesius PH. Modified LiveEdwardsiella ictaluriVaccine, AQUAVAC-ESC, lacks multidrug resistance plasmids. *J Aquat Anim Health*. (2011) 23:195–9. doi: 10.1080/08997659.2011.642093
19. Lobb CJ, Clem LW. Distinctive subpopulations of catfish serum antibody and immunoglobulin. *MolImmunology*. (1983) 20:811–8. doi: 10.1016/0161-5890(83)90077-9
20. Lobb CJ. Secretory immunity induced in catfish, Ictalurus punctatus, following bath immunization. *Dev Comp Immunol.* (1987) 11:727–38. doi: 10.1016/0145-305X(87)90060-7
21. Lange MD, Waldbieser GC, Lobb CJ. Patterns of receptor revision in the immunoglobulin heavy chains of a teleost fish. *J Immunol*. (2009) 182:5605–22. doi: 10.4049/jimmunol.0801013
22. Lange MD, Webster CD. The effect of temperature on the mucosal IgM antibody response to DNP-KLH in channel catfish (Ictalurus punctatus). *Fish Shellfish Immunol.* (2017) 70:493–7. doi: 10.1016/j.fsi.2017.09.026
23. Li C, Zhang Y, Wang R, Lu J, Nandi S, Mohanty S, et al. RNA-seq analysis of mucosal immune responses reveals signatures of intestinal barrier disruption and pathogen entry following Edwardsiella ictaluri infection in channel catfish, Ictalurus punctatus. *Fish Shellfish Immunol*. (2012) 32:816–27. doi: 10.1016/j.fsi.2012.02.004
24. Sun F, Peatman E, Li C, Liu S, Jiang Y, Zhou Z, et al. Transcriptomic signatures of attachment, NF-kappaB suppression and IFN stimulation in the catfish gill following columnaris bacterial infection. *Dev Comp Immunol.* (2012) 38:169–80. doi: 10.1016/j.dci.2012.05.006
25. Peatman E, Li C, Peterson BC, Straus DL, Farmer BD, Beck BH. Basal polarization of the mucosal compartment in *Flavobacterium columnare* susceptible and resistant channel catfish (Ictalurus punctatus). *MolImmunology*. (2013) 56:317–27. doi: 10.1016/j.molimm.2013.04.014
26. Lange MD, Beck BH, Brown JD, Farmer BD, Barnett LM, Webster CD. Missing the target: DNAk is a dominant epitope in the humoral immune response of channel catfish (Ictalurus punctatus). to *Flavobacterium columnare*. *Fish Shellfish Immunol.* (2016) 51:170–9. doi: 10.1016/j.fsi.2016.02.015
27. Vanden Bergh P, Heller M, Braga-Lagache S, Frey J. The Aeromonas salmonicida subsp. salmonicida exoproteome: global analysis, moonlighting proteins and putative antigens for vaccination against furunculosis. *Proteome Sci*. (2013) 11:44. doi: 10.1186/1477-5956-11-44
28. Amemiya K, Meyers JL, Deshazer D, Riggins RN, Halasohoris S, England M, et al. Detection of the host immune response to Burkholderia mallei heat-shock proteins GroEL and DnaK in a glanders patient and infected mice. *Diagn Microbiol Infect Dis.* (2007) 59:137–47. doi: 10.1016/j.diagmicrobio.2007.04.017
29. Paliwal PK, Bansal A, Sagi SS, Sairam M. Intraperitoneal immunization of recombinant HSP70 (DnaK). of Salmonella Typhi induces a predominant Th2 response and protective immunity in mice against lethal Salmonella infection. *Vaccine*. (2011) 29:6532–9. doi: 10.1016/j.vaccine.2011.07.005
30. Hinode D, Nakamura R, Grenier D, Mayrand D. Cross-reactivity of specific antibodies directed to heat shock proteins from periodontopathogenic bacteria and of human origin [corrected]. *Oral Microbiol Immunol*. (1998) 13:55–8. doi: 10.1111/j.1399-302X.1998.tb00752.x
31. Ratanji KD, Derrick JP, Kimber I, Thorpe R, Wadhwa M, Dearman RJ. Influence of Escherichia coli chaperone DnaK on protein immunogenicity. *Immunology*. (2017) 150:343–55. doi: 10.1111/imm.12689
32. Poobalane S, Thompson KD, Ardo L, Verjan N, Han HJ, Jeney G, et al. Production and efficacy of an Aeromonas hydrophila recombinant S-layer protein vaccine for fish. *Vaccine*. (2010) 28:3540–7. doi: 10.1016/j.vaccine.2010.03.011
33. Nascimento IP, Leite LCC. Recombinant vaccines and the development of new vaccine strategies. *Braz J Med Biol Res.* (2012) 45:1102–11. doi: 10.1590/S0100-879X2012007500142
34. Dash P, Sahoo PK, Gupta PK, Garg LC, Dixit A. Immune responses and protective efficacy of recombinant outer membrane protein R (rOmpR)-based vaccine of Aeromonas hydrophila with a modified adjuvant formulation in rohu (Labeo rohita). *Fish Shellfish Immunol*. (2014) 39:512–23. doi: 10.1016/j.fsi.2014.06.007
35. Liu L, Gong YX, Zhu B, Liu GL, Wang GX, Ling F. Effect of a new recombinant Aeromonas hydrophila vaccine on the grass carp intestinal microbiota and correlations with immunological responses. *Fish Shellfish Immunol*. (2015) 45:175–83. doi: 10.1016/j.fsi.2015.03.043
36. Darwish AM, Farmer BD, Hawke JP. Improved method for determining antibiotic susceptibility of *Flavobacterium columnare* isolates by broth microdilution. *J Aquat Anim Health*. (2008) 20:185–91. doi: 10.1577/H07-047.1
37. Farmer B. Improved methods for the isolation and characterization of *Flavobacterium columnare* (Master's thesis). Baton Rouge, LA: Louisiana State University. (2004).
38. Beck BH, Li C, Farmer BD, Barnett LM, Lange MD, Peatman E. A comparison of high- and low-virulence Flavobacterium columnare strains reveals differences in iron acquisition components and responses to iron restriction. *J Fish Dis.* (2015) 39:259–68. doi: 10.1111/jfd.12343
39. Mitchell A, Farmer B. Evaluation of an ultra-low-flow water delivery system for small experimental tanks. *North Am J Aquac.* (2010) 72:195–200. doi: 10.1577/A09-061.1
40. Miller NW, Bly JE, van GF, Ellsaesser CF, Clem LW. Phylogeny of lymphocyte heterogeneity: identification and separation of functionally distinct

subpopulations of channel catfish lymphocytes with monoclonal antibodies. *Dev Comp Immunol.* (1987) 11:739–47. doi: 10.1016/0145-305X(87)90061-9
41. DeLuca D, Wilson M, Warr GW. Lymphocyte heterogeneity in the trout, Salmo gairdneri, defined with monoclonal antibodies to IgM. *Eur J Immunol.* (1983) 13:546–51. doi: 10.1002/eji.1830130706
42. Martin M. Cutadapt removes adapter sequences from high-throughput sequencing reads. *EMBnet.* (2011) 17:10–2. doi: 10.14806/ej.17.1.200
43. Langmead B, Salzberg SL. Fast gapped-read alignment with Bowtie 2. *Nat Methods.* (2012) 9:357–9. doi: 10.1038/nmeth.1923
44. Roberts A, Pachter L. Streaming fragment assignment for real-time analysis of sequencing experiments. *Nat Methods.* (2013) 10:71–7. doi: 10.1038/nmeth.2251
45. Love MI, Huber W, Anders S. Moderated estimation of fold change and dispersion for RNA-seq data with DESeq2. *Genome Biol.* (2014) 15:1–21. doi: 10.1186/s13059-014-0550-8
46. Gotz S, Garcia-Gomez JM, Terol J, Williams TD, Nagaraj SH, Nueda MJ, et al. High-throughput functional annotation and data mining with the Blast2GO suite. *Nucleic Acids Res.* (2008) 36:3420–35. doi: 10.1093/nar/gkn176
47. Subramaniana A, Tamayo P, Moothaa VK, Mukherjeed S, Eberta BL, Michael A, et al. Gene set enrichment analysis A knowledge-based approach for interpreting genome-wide expression profiles. *Proc Natl Acad Sci USA.* (2005) 102:15545–50. doi: 10.1073/pnas.0506580102
48. Pfaffl MW. A new mathematical model for relative quantification in real-time RT–PCR. *Nucleic Acids Res.* (2001) 29:2003–7. doi: 10.1093/nar/29.9.e45
49. Zhang D, Thongda W, Li C, Zhao H, Beck BH, Mohammed H, et al. More than just antibodies: protective mechanisms of a mucosal vaccine against fish pathogen Flavobacterium columnare. *Fish Shellfish Immunol.* (2017) 71:160–70. doi: 10.1016/j.fsi.2017.10.001
50. Small BC, Murdock CA, Bilodeau-Bourgeois AL, Peterson BC, Waldbieser GC. Stability of reference genes for real-time PCR analyses in channel catfish (Ictalurus punctatus). Tissues under varying physiological conditions. *Comp Biochem Physiol B Biochem Mol Biol.* (2008) 151:296–304. doi: 10.1016/j.cbpb.2008.07.010
51. Zhou T, Li N, Jin Y, Zeng Q, Prabowo W, Liu Y, et al. Chemokine C-C motif ligand 33 is a key regulator of teleost fish barbel development. *Proc Natl Acad Sci USA.* (2018) 115:E5018–27. doi: 10.1073/pnas.1718603115
52. Cai W, De La Fuente L, Arias CR. Biofilm formation by the fish pathogen Flavobacterium columnare: development and parameters affecting surface attachment. *Appl Environ Microbiol.* (2013) 79:5633–42. doi: 10.1128/AEM.01192-13
53. Lange MD, Farmer BD, Declercq AM, Peatman E, Decostere A, Beck BH. Sickeningly Sweet: L-rhamnose stimulates *Flavobacterium columnare* biofilm formation and virulence. *J Fish Dis.* (2017) 40:1613–24. doi: 10.1111/jfd.12629.
54. Lange MD, Farmer BD, Abernathy J. Catfish mucus alters the *Flavobacterium columnare* transcriptome. *FEMS Microbiol Lett.* (2018) 365:1–13. doi: 10.1093/femsle/fny244
55. Grosenbaugh DA, De Luca K, Durand PY, Feilmeier B, DeWitt K, Sigoillot-Claude C, et al. Characterization of recombinant OspA in two different Borrelia vaccines with respect to immunological response and its relationship to functional parameters. *BMC Vet Res.* (2018) 14:312. doi: 10.1186/s12917-018-1625-7
56. Alvarez-Estrada A, Martinez-Martinez S, Martin CG, Garcia-Iglesias MJ, Perez-Martinez C, Yubero-Delgado S, et al. Immunogenic characterization of vaccines based on Haemophilus parasuis Nagasaki strain, OmpP2, OmpP5 and OmpD15, in colostrum-deprived pigs experimentally challenged with the same strain. *Res Vet Sci.* (2018) 119:292–301. doi: 10.1016/j.rvsc.2018.07.009
57. Laird RM, Ma Z, Dorabawila N, Pequegnat B, Omari E, Liu Y, et al. Evaluation of a conjugate vaccine platform against enterotoxigenic Escherichia coli (ETEC), *Campylobacter jejuni* and Shigella. *Vaccine.* (2018) 36:6695–702. doi: 10.1016/j.vaccine.2018.09.052
58. Galeotti M, Romano N, Volpatti D, Bulfon C, Brunetti A, Tiscar PG, et al. Innovative vaccination protocol against vibriosis in *Dicentrarchus labrax* (L.). *juveniles*: improvement of immune parameters and protection to challenge. *Vaccine.* (2013) 31:1224–30. doi: 10.1016/j.vaccine.2012.12.041
59. Sudheesh PS, Lafrentz BR, Call DR, Siems WF, LaPatra SE, Wiens GD, et al. Identification of potential vaccine target antigens by immunoproteomic analysis of a virulent and a non-virulent strain of the fish pathogen *Flavobacterium psychrophilum*. *Dis Aquat Organ.* (2007) 74:37–47. doi: 10.3354/dao074037
60. Delpino MV, Estein SM, Fossati CA, Baldi PC, Cassataro J. Vaccination with Brucella recombinant DnaK and SurA proteins induces protection against Brucella abortus infection in BALB/c mice. *Vaccine.* (2007) 25:6721–9. doi: 10.1016/j.vaccine.2007.07.002
61. Plant KP, LaPatra SE, Cain KD. Vaccination of rainbow trout, *Oncorhynchus mykiss* (Walbaum), with recombinant and DNA vaccines produced to *Flavobacterium psychrophilum* heat shock proteins 60 and 70. *J Fish Dis.* (2009) 32:521–34. doi: 10.1111/j.1365-2761.2009.01008.x
62. Ho PY, Chen YC, Maekawa S, Hu HH, Tsai AW, Chang YF, et al. Efficacy of recombinant protein vaccines for protection against Nocardia seriolae infection in the largemouth bass Micropterus salmoides. *Fish Shellfish Immunol.* (2018) 78:35–41. doi: 10.1016/j.fsi.2018.04.024
63. Trung Cao T, Tsai MA, Yang CD, Wang PC, Kuo TY, Gabriel Chen HC, et al. Vaccine efficacy of glyceraldehyde-3-phosphate dehydrogenase (GAPDH). from Edwardsiella ictaluri against E tarda in tilapia. *J Gen Appl Microbiol.* (2014) 60:241–50. doi: 10.2323/jgam.60.241
64. Sun Y, Liu CS, Sun L. Identification of an Edwardsiella tarda surface antigen and analysis of its immunoprotective potential as a purified recombinant subunit vaccine and a surface-anchored subunit vaccine expressed by a fish commensal strain. *Vaccine.* (2010) 28:6603–8. doi: 10.1016/j.vaccine.2010.07.050
65. Huising M. Increased efficacy of immersion vaccination in fish with hyperosmotic pretreatment. *Vaccine.* (2003) 21:4178–93. doi: 10.1016/S0264-410X(03)00497-3
66. Rombout JH, Yang G, Kiron V. Adaptive immune responses at mucosal surfaces of teleost fish. *Fish Shellfish Immunol.* (2014) 40:634–43. doi: 10.1016/j.fsi.2014.08.020
67. Perez O, Romeu B, Cabrera O, Gonzalez E, Batista-Duharte A, Labrada A, et al. Adjuvants are key factors for the development of future vaccines: lessons from the finlay adjuvant platform. *Front Immunol.* (2013) 4:407. doi: 10.3389/fimmu.2013.00407
68. Valdenegro-Vega VA, Crosbie P, Vincent B, Cain KD, Nowak BF. Effect of immunization route on mucosal and systemic immune response in Atlantic salmon (Salmo salar). *VetImmunol Immunopathol.* (2013) 151:113–23. doi: 10.1016/j.vetimm.2012.10.010
69. Zhao X, Findly RC, Dickerson HW. Cutaneous antibody-secreting cells and B cells in a teleost fish. *DevComp Immunol.* (2008) 32:500–8. doi: 10.1016/j.dci.2007.08.009
70. Findly RC, Zhao X, Noe J, Camus AC, Dickerson HW. B cell memory following infection and challenge of channel catfish with Ichthyophthirius multifiliis. *Dev Comp Immunol.* (2013) 39:302–11. doi: 10.1016/j.dci.2012.08.007
71. Sarkander J, Hojyo S, Tokoyoda K. Vaccination to gain humoral immune memory. *Clin Transl Immunology.* (2016) 5:e120. doi: 10.1038/cti.2016.81
72. Kowalczyk AP, Green KJ. Structure, function, and regulation of desmosomes. *Prog Mol Biol Transl Sci.* (2013) 116:95–118. doi: 10.1016/B978-0-12-394311-8.00005-4
73. Ángeles Esteban M. An overview of the immunological defenses in fish skin. *ISRN Immunol.* (2012) 2012:1–29. doi: 10.5402/2012/853470
74. Kelly C, Salinas I. Under pressure: interactions between commensal microbiota and the teleost immune system. *Front Immunol.* (2017) 8:559. doi: 10.3389/fimmu.2017.00559
75. Li C, Wang R, Su B, Luo Y, Terhune J, Beck B, et al. Evasion of mucosal defenses during Aeromonas hydrophila infection of channel catfish (Ictalurus punctatus) skin. *Dev Comp Immunol.* (2013) 39:447–55. doi: 10.1016/j.dci.2012.11.009
76. Chae YK, Choi WM, Bae WH, Anker J, Davis AA, Agte S, et al. Overexpression of adhesion molecules and barrier molecules is associated with differential infiltration of immune cells in non-small cell lung cancer. *Sci Rep.* (2018) 8:1023. doi: 10.1038/s41598-018-19454-3
77. Parks WC, Wilson CL, Lopez-Boado YS. Matrix metalloproteinases as modulators of inflammation and innate immunity. *Nat Rev Immunol.* (2004) 4:617–29. doi: 10.1038/nri1418

78. Weinstock C, Anliker M, Zabern IV. CD59: a long-known complement inhibitor has advanced to a blood group system. *Immunohematology*. (2015) 31:145–51.
79. Chi H. Sphingosine-1-phosphate and immune regulation: trafficking and beyond. *Trends Pharmacol Sci*. (2011) 32:16–24. doi: 10.1016/j.tips.2010.11.002
80. Rivera J, Proia RL, Olivera A. The alliance of sphingosine-1-phosphate and its receptors in immunity. *Nat Rev Immunol*. (2008) 8:753–63. doi: 10.1038/nri2400
81. Salinas I. The mucosal immune system of teleost fish. *Biology*. (2015) 4:525–39. doi: 10.3390/biology4030525

Conflict of Interest Statement: The authors declare that the research was conducted in the absence of any commercial or financial relationships that could be construed as a potential conflict of interest.

Copyright © 2019 Lange, Abernathy and Farmer. This is an open-access article distributed under the terms of the Creative Commons Attribution License (CC BY). The use, distribution or reproduction in other forums is permitted, provided the original author(s) and the copyright owner(s) are credited and that the original publication in this journal is cited, in accordance with accepted academic practice. No use, distribution or reproduction is permitted which does not comply with these terms.

frontiers in Immunology

ORIGINAL RESEARCH
published: 16 July 2019
doi: 10.3389/fimmu.2019.01641

Recombinant ATPase of Virulent *Aeromonas hydrophila* Protects Channel Catfish Against Motile *Aeromonas* Septicemia

*Hossam Abdelhamed, Michelle Banes, Attila Karsi and Mark L. Lawrence**

Department of Basic Sciences, College of Veterinary Medicine, Mississippi State University, Starkville, MS, United States

Channel catfish farming dominates the aquaculture industry in the United States. However, epidemic outbreaks of motile *Aeromonas* septicemia (MAS), caused by virulent *Aeromonas hydrophila* (vAh), have become a prominent problem in the catfish industry. Although vaccination is an effective preventive method, there is no vaccine available against MAS. Recombinant proteins could induce protective immunity. Thus, in this work, vAh ATPase protein was expressed, and its protective capability was evaluated in catfish. The purified recombinant ATPase protein was injected into catfish, followed by experimental infection with *A. hydrophila* strain ML09-119 after 21 days. Results showed catfish immunized with ATPase exhibited 89.16% relative percent survival after challenge with *A. hydrophila* strain ML09-119. Bacterial concentrations in liver, spleen, and anterior kidney were significantly lower in vaccinated fish compared with the non-vaccinated sham group at 48 h post-infection ($p < 0.05$). Catfish immunized with ATPase showed a significant ($p < 0.05$) higher antibody response compared to the non-vaccinated groups. Overall, ATPase recombinant protein has demonstrated potential to stimulate protective immunity in catfish against virulent *A. hydrophila* infection.

Keywords: ***Aeromonas hydrophila*, motile *Aeromonas* septicemia, aquaculture, recombinant vaccine, catfish**

OPEN ACCESS

Edited by:
Hetron Mweemba Munang'andu, Norwegian University of Life Sciences, Norway

Reviewed by:
Biswajit Maiti, Nitte University, India
Girisha S. Kallappa, Karnataka Veterinary, Animal and Fisheries Sciences University, India

****Correspondence:***
Mark L. Lawrence
lawrence@cvm.msstate.edu

Specialty section:
This article was submitted to Comparative Immunology, a section of the journal Frontiers in Immunology

Received: *31 October 2018*
Accepted: *01 July 2019*
Published: *16 July 2019*

Citation:
Abdelhamed H, Banes M, Karsi A and Lawrence ML (2019) Recombinant ATPase of Virulent Aeromonas hydrophila Protects Channel Catfish Against Motile Aeromonas Septicemia. Front. Immunol. 10:1641. doi: 10.3389/fimmu.2019.01641

INTRODUCTION

Aquaculture is an approximately $1.2 billion industry, and catfish production is a mainstay of the U.S. aquaculture industry, accounting for $386 million in 2016 (1). Disease outbreaks are among the primary limiting factors in catfish production (2). Infectious diseases account for the most significant percentage of losses, with around 65% of the fry and fingerlings lost during production (3). The three bacterial species responsible for most of these losses are *Edwardsiella ictaluri*, *Flavobacterium columnare*, and *Aeromonas hydrophila*. These pathogens are the causative agents of enteric septicemia of catfish (ESC), columnaris disease, and motile *Aeromonas* septicemia (MAS), respectively (4, 5).

Since 2009, a clonal group of *A. hydrophila* strains (referred to as virulent *A. hydrophila* or vAh) has become a major pathogen of farm-raised channel catfish, causing motile *Aeromonas* septicemia (MAS) outbreaks (6). The Aquatic Diagnostic Laboratory at Mississippi State University has reported a continued increase of vAh for the past 5 years. The disease is most common in summer months (7). Estimated losses in ponds with disease outbreaks of vAh infection ranged from 4,000 to 10,000 pounds lost (about 8,000–15,000 fish),

and pond mortality rates can be very high (close to 100%). vAh is distinguishable from previous *Aeromonas* catfish isolates, but it is very similar to an Asian grass carp isolate (8). In the last decade, $60–70 million in losses to the U.S. aquaculture industry have been attributed to MAS outbreaks due to mortalities, lost feeding days, and costs associated with antimicrobial therapy (9).

The lack of preventive measures to control vAh infection has emphasized the need to develop techniques for disease prevention. Recombinant protein technology is a promising technology for development of vaccines against many human and animal pathogens (10, 11). To select potential vAh recombinant protein candidates for use as a vaccine, genomic sequences from vAh strain ML09-119 (CP005966.1) were assembled against the genome of *A. hydrophila* reference strain ATCC 7966^T (NC_008570), revealing that *A. hydrophila* ML09-119, along with all other sequenced vAh strains, contains specific unique outer membrane and secreted proteins (6). These proteins include pilin protein, fimbrial biogenesis outer membrane usher protein, TonB-dependent siderophore receptor protein, TonB-dependent transferrin receptor, OmpA-like protein, and ATPase. We postulate that these proteins could be effective in stimulating protective immunity in catfish against vAh infection.

vAh ATPase has 717 aa and contains two domains. The AAA (ATPases Associated with diverse cellular Activities) domain has 284 aa and is found in the AAA superfamily of ring-shaped P-loop NTPases, which exert their activity through energy-dependent remodeling or translocation of macromolecules (12, 13). The AAA superfamily of ATPases is found in all kingdoms of living organisms and catalyzes many cellular processes in which energy released from ATP hydrolysis is used in molecular remodeling functions (14). In bacteria, ATPases participate in diverse cellular processes including DNA replication, protein degradation, membrane fusion, microtubule severing, peroxisome biogenesis, signal transduction, and regulation of gene expression (15).

The second domain, putative AbiEii toxin domain, is a Type IV toxin-antitoxin (TA) system belonging to the nucleotidyltransferase superfamily (16). It is similar to proteins predicted to be members of the bacterial abortive infection (Abi) system, which enables bacteria to resist bacteriophage infection. Resistance strategies include promoting bacterial death, thus limiting phage replication within a bacterial population. There are 20 or more Abis, and they are predominantly plasmid-encoded lactococcal systems. The putative AbiEii domain is a type of TA system that functions by killing bacteria that lose the plasmid upon division. AbiE phage resistance systems function as novel Type IV TAs and are widespread in bacteria and archaea. Here, we describe the expression and purification of VAh ATPase protein (AHML_21010) and its immune stimulation properties to protect channel catfish against vAh infection.

MATERIALS AND METHODS

Ethics Statement

Catfish experiments were performed according to guidelines of an approved protocol by the Institutional Animal Care and Use Committee at Mississippi State University.

Bacterial Strains, Media, Plasmid, and Reagents

Escherichia coli strains NovaBlue (Novagen, Madison, WI, USA) and BL21 (DE3) (Invitrogen, Carlsbad, CA, USA) were used for cloning and expression, respectively. *E. coli* strains were cultured on Luria–Bertani (LB) agar or broth (Difco, Sparks, MD, USA) and incubated at 37°C throughout the study. *A. hydrophila* strain ML09-119 was cultured in brain heart infusion (BHI) agar or broth (Difco) and incubated at 30°C. Plasmid pET-28a (Novagen) was used as an expression vector. When required, isopropyl-β-D-thiogalactopyranoside (IPTG), kanamycin (Kan, 50 μg/ml), ampicillin (Ap, 100 μg/ml), and colistin (Col, 2.5 μg/ml) (Sigma–Aldrich, Saint Louis, MO, USA) were added to culture media.

Cloning and Expression of ATPase Protein in *E. coli*

The coding region of ATPase (AHML_21010) was amplified from *A. hydrophila* strain ML09-119 genomic DNA by PCR using primers ATPaseF01 (AA**GGATCC**CAAGAGGGTGTTATGTCAGAGC) and ATPaseR01 (AA**GTCGAC**CCTGATGTCCAAGTTCATGTAT). Primers were designed using Primer3 (http://bioinfo.ut.ee/primer3-0.4.0/) based on the ML09-119 genome sequence and synthesized by Sigma-Aldrich. Amplified ATPase region was confirmed by sequencing. For cloning, *Eco*RI and *Sac*I restriction sites (bold letters) were incorporated into primers' 5′ ends. The amplified ATPase coding region (2,160 bp) was cloned into the *Eco*RI and *Sac*I restriction sites in pET-28a. Positive clones were selected on LB Kan plates and verified by colony PCR. ATPase sequence was confirmed using T3 and T7 terminator primers. *E. coli* BL21(DE3) competent bacteria were transformed by positive plasmid using chemical transformation and stored at −80°C in 20% glycerol.

For ATPase protein expression, LB broth containing Kan was inoculated with *E. coli* BL21 (DE3) (1:100) and cultured at 37°C with shaking at 200 rpm until OD_{600} reached 0.6–0.8, after which bacteria were induced with 1 mM IPTG and incubated for 8 more h. Whole bacteria proteins were solubilized in tricine sample buffer (Bio-Rad Laboratories, Hercules, CA, USA) for 5 min at 80°C, and protein separation was conducted using 12% SDS-PAGE to confirm expression of ATPase protein. Whole bacteria proteins from competent *E. coli* BL21 (DE3) and uninduced *E. coli* BL21 with recombinant clone were used as controls.

Purification of Recombinant ATPase Protein

Recombinant ATPase protein containing six histidine tags (His6) was purified by His-Bind resin columns (Novagen). IPTG induced recombinant bacteria were harvested by centrifugation (12,000 x g for 20 min at 4°C), and pellets were lysed using Bug Buster protein extraction reagent (Novagen) with benzonase nuclease and protease inhibitor cocktail set III (Sigma). Soluble fractions were removed by centrifugation, and recombinant ATPase protein was purified from inclusion body pellets by suspending in lysis buffer (Tris-HCl buffer pH 8.0, 6 M urea)

with gentle sonication (4 cycles, 10 s) on ice. After centrifugation, the recombinant protein was loaded onto a resin column (5 mL/column). The resin was washed with wash buffer (0.5 M NaCl, 60 mM imidazole, 20 mM Tris-HCl, pH 7.9), and eluted using elution buffer (1 M imidazole, 0.5 M NaCl, 20 mM Tris-HCl, pH 7.9). Elution fractions were collected for SDS-PAGE analysis. Quantification of the eluted ATPase fractions was determined on a spectrophotometer at 280 nm and Bradford assay (Bio-Rad) according to the supplier's instructions. The identity of recombinant ATPase protein was confirmed by MALDI-TOF mass spectrometry.

Fish Vaccination

Specific pathogen free channel catfish ($n = 300$; mean weight: 68.77 g) were randomly stocked in 15 40-L tanks (20 fish/tank) supplied with flow-through dechlorinated municipal water and continuous aeration. Fish were acclimated for 1 week by feeding twice a day and monitoring water temperature (30°C) and water quality parameters. Fish were assigned to three groups randomly, and each group included five replicate tanks. Group A consisted of intraperitoneal injection of 100 μl of purified ATPase protein at concentration of 250 μg/ml emulsified with non-mineral oil adjuvant Montanide ISA 763 AVG (Seppic, Paris, France) at a ratio of 30:70 protein to adjuvant. Group B included fish injected with 100 μl of sterile phosphate buffered saline (PBS) emulsified with adjuvant, and group C included fish injected with 100 μl sterile PBS (sham-vaccinated). Fish were anesthetized with tricaine methanesulfonate (MS-222; Sigma) before handling.

At 3 weeks post-immunization, catfish were experimentally infected by bath immersion with 2.8×10^{10} CFU/ml of *A. hydrophila* ML09-119 for 6 h at 30°C (17). Bacterial infection dose was chosen based on previous experimental infection doses (8, 18). Bacteria numbers (CFU/ml) in the overnight cultures were determined by plating serial 10-fold dilutions on agar plates followed by viable colony counts. At 48 h post-infection, five fish from each group were euthanatized, and liver, spleen, and anterior kidney tissues were collected aseptically. Tissues were homogenized in 1 ml PBS, and tissue suspensions were diluted serially and spread in triplicate on BHI agar plates. Viable bacterial colonies were enumerated after incubating plates at 37°C for 48 h. The remaining ten fish in each group were monitored daily for 2 weeks to assess relative percent survival (RPS), which is calculated by [1– (% mortality of vaccinated fish / % mortality of control fish)] × 100 (19).

Serum Antibody Response

Before and after immunization, blood was collected from the caudal vein of ten fish per group (two fish per tank), and after clotting the blood overnight at 4°C, serum was obtained by centrifugation at 3500 x g for 10 min.

Antibody titers were determined by enzyme-linked immunosorbent assay (ELISA) as described (20). In the whole-bacteria ELISA, 96-well Immulon™ plates (Bloomington, MN, U.S.A.) were coated with heat-killed whole bacteria (10^8 CFU/ml) overnight at 4°C. For ELISA with purified protein, 96-well plates were coated with 100 μl/well of purified ATPase protein at a concentration of 20 μg/ml in PBS. Subsequently, wells were washed and blocked with 5% nonfat dry milk (Bio-Rad) in PBS for 1 h at room temperature. Wells were washed three times in PBS containing 0.05% Tween-20 (PBS-T). Diluted serum (1:100) was added to each well (50 μl /well), incubated for 1 h at 37°C, and washed with PBS-T. Fifty microliters of a 1:4 dilution of monoclonal antibody 9E1 (anti-catfish Ig) (21, 22) were added to each well. After 1 h incubation at 37°C, plates were washed with PBS-T, and goat anti-mouse antibody conjugate (Fisher Scientific, Pittsburg, PA, USA) was added. Plates were then incubated at room temperature for 1 h and washed. Finally, 100 μl of *p*-nitrophenyl phosphate substrate (Sigma 104 phosphatase substrate) dissolved in 10% diethanolamine buffer was added to each well, and plates were incubated for 45 min at room temperature. Absorbance at 405 nm was measured in an ELISA Microplate Reader (CA, USA). Control wells containing PBS buffer in place of serum were present in each plate and prepared in the same manner. To standardize, average background absorbance for each plate was subtracted from measured absorbance.

Statistical Analysis

The effect of vaccination with ATPase protein on survival of catfish challenged with vAh was assessed with mixed model logistic regression using PROC GLIMMIX in SAS for Windows 9.4 (SAS Institute, Inc., Cary, NC, USA). The number of live catfish in a tank at the end of the trial was the outcome assessed using an events/trials syntax. Protein was the fixed effect assessed in the model. Tank within protein was included as a random effect in the model. The wild-type strain was the referent for comparisons of protein effect.

Effects of ATPase on the number of CFU in fish tissues and on antibody response were assessed by analysis of variance using PROC GLM. Separate models were used to assess CFU in liver, spleen, and anterior kidney as well as the ELISA results. The CFU data were transformed by first adding 1 to each CFU value and then taking the base 10 logarithm. ELISA data were transformed by taking the base 10 logarithm of each value. The distribution of the residuals was evaluated for each model to determine the appropriateness of the statistical model for the data. If the effect of protein was found to be statistically significant, least squares means were compared using the Dunnett adjustment for multiple comparisons with wild-type strain as the referent. A significance level of 0.05 was used for all analyses.

RESULTS

ATPase Protein Purification

The recombinant protein was purified successfully from soluble fraction at 0.2 mg/ml concentration, and amino acid sequences were confirmed by MALDI-TOF mass spectrometry. The SDS-PAGE result indicated the molecular mass of purified ATPase protein was approximately 81.5 kDa (**Figure 1**), which was the same size as the deduced molecular mass based on amino acid composition. Protein identification by peptide sequence using MALDI-TOF mass spectrometry revealed 97% identity of the purified protein to ATPase sequence (accession number: AGM45958).

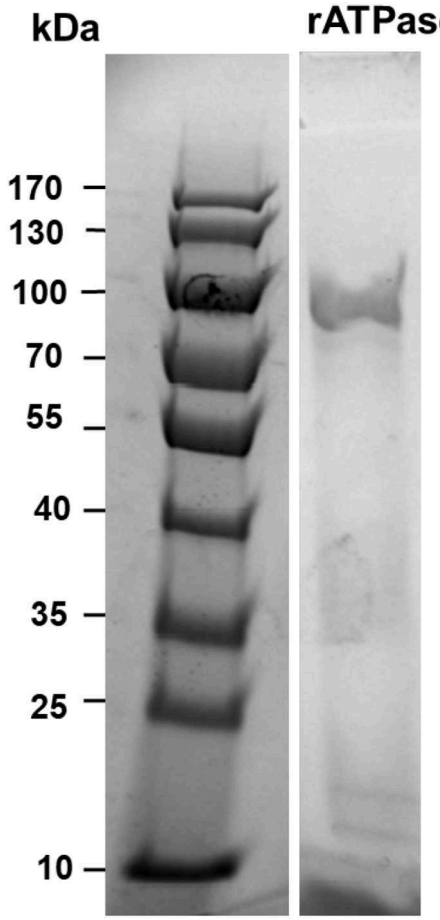


FIGURE 1 | SDS-PAGE with Coomassie blue stain showing purified recombinant ATPase. Molecular weights in kilodaltons are shown for the standard protein marker in the right column. Intervening lanes between the molecular weight marker and the lane containing recombinant ATPase were removed.

Fish Vaccination

Catfish fingerlings immunized with recombinant ATPase protein showed 4.72% mortality (89.16% RPS), which was significantly lower ($p < 0.01$) than both non-vaccinated groups: PBS-adjuvant (29.55% mortality) and PBS-only (43.51% mortality) groups (**Figure 2**).

The mean number of viable bacteria in the liver, spleen, and anterior kidney was significantly lower in fish immunized with recombinant ATPase protein compared to non-vaccinated fish ($p < 0.005$) (**Figure 3**).

Fish Serum Antibody Response

There was no significant difference ($p > 0.05$) in antibody response between recombinant ATPase vaccinated and non-vaccinated catfish when ELISA plates were coated with whole bacteria lysate (**Figure 4A**). In ELISA plates coated with purified protein, significantly higher antibody titers were detected in serum of fish vaccinated with ATPase compared with PBS-only and PBS-adjuvant groups (**Figure 4B**).

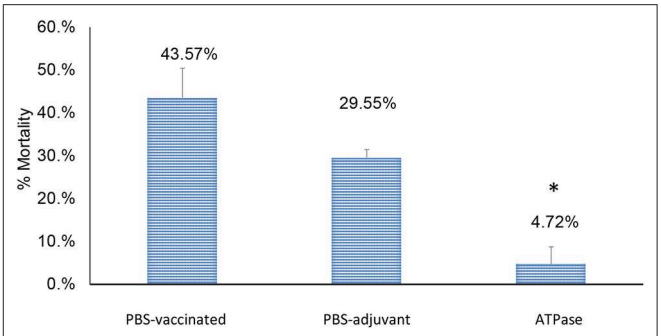


FIGURE 2 | Percent mortalities in catfish vaccinated with recombinant ATPase protein following experimental infection with *A. hydrophila* ML09-119 at 3 weeks post-vaccination. Significant differences between treatments are indicated with asterisks ($p < 0.05$).

DISCUSSION

This study aimed to determine the potential utility of recombinant ATPase protein as a possible vaccine against virulent *A. hydrophila*, an important pathogen responsible for MAS in catfish. Several research groups have identified candidate DNA or recombinant protein vaccines for MAS (23–28), but to date, there is no protective vaccine available against MAS caused by vAh. Previously, we purified four fimbrial proteins (FimA, Fim, MrfG, and FimOM) and three outer membrane proteins (major outer membrane protein OmpA1, TonB-dependent receptor, and transferrin-binding protein A) and assessed their ability to stimulate protective immunity in channel catfish fingerlings against vAh infection (17, 29). In the present study, expression and purification of vAh ATPase protein in *E. coli* were successful, and purified ATPase protein was recovered from the inclusion body.

A. hydrophila strain ML09-119 is representative of the vAh clonal group and exhibits high virulence in channel catfish (8, 30). Intraperitoneal injection of catfish with recombinant ATPase protein elicited a higher survival rate compared with non-immunized fish when challenged with vAh. Vaccination with recombinant ATPase protein also effectively reduced colonization of vAh in liver, spleen, and anterior kidney. No statistically significant difference was observed for antibody production in vaccinated vs. non-vaccinated fish when ELISA plates were coated with whole bacterial lysate. However, significant increase in antibody titer was detected in vaccinated fish when ELISA plates were coated with the purified recombinant protein, indicating that ATPase antigen concentration was insufficient in the whole bacterial lysate to detect ATPase-specific antibodies. In fish, antibody titers do not always correlate with protection (31). Protection generated by ATPase in our experiment could be mediated by antibody, and other factors could contribute such as cell-mediated immunity or innate immune components such as complement, lysozyme, antimicrobial peptides, or acute phase proteins (32–34). Innate immunity was stimulated in grass carp (*Ctenopharyngodon idella*) following immunization with F0F1 ATP synthase subunit beta. This was supported by a significant increase in the

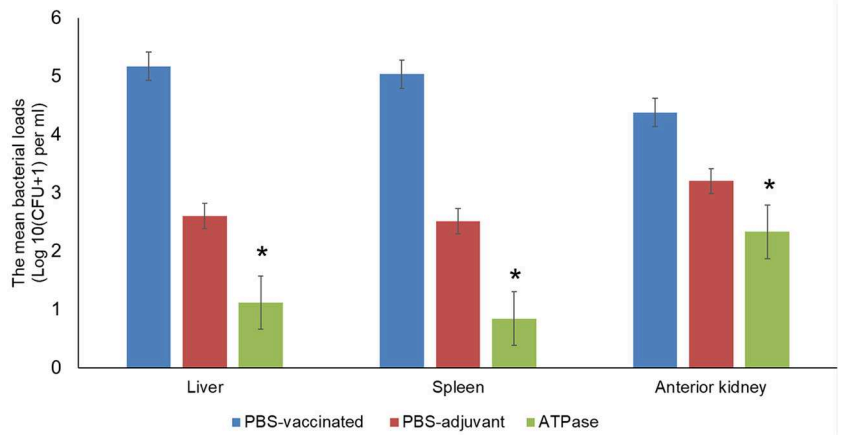


FIGURE 3 | Mean bacterial concentrations (CFU/g) in liver, spleen, and anterior kidney of catfish vaccinated with recombinant ATPase protein at 48 h post-infection with *A. hydrophila* ML09-119. Data are presented as means ± SE ($N = 5$). Significant differences between treatments are indicated with asterisks ($p < 0.05$).

expression of pro-inflammatory cytokine genes in blood plasma, including IL-1β, IL-10, TNF-a, CRP, IFN, and MHC II (33). Innate immune response was significantly increased in rainbow trout (*Oncorhynchus mykiss*) infected with *Yersinia ruckeri* (35).

In some fish diseases, a combination of humoral, cell-mediated, and innate immune responses work in concert to provide protection. Recombinant outer membrane protein C of *Edwardsiella tarda* induced a significant innate immune response and humoral immune response in flounder (*Paralichthys olivaceus*); it also evoked significant protection against *E. tarda* challenge (36). Up-regulation of the immune-related genes encoding lysozyme G, complement factor 4, immunoglobulin M, β2-microglobulin, major histocompatibility complex I and II, and interleukin-1β was observed in Indian major carp *(Labeo rohita)* vaccinated with rOmpR, indicating that humoral, cellular, and innate immunity contribute to the protective response against *A. hydrophila* infection (34). In channel catfish, genes encoding iron homeostasis, transport proteins, complement components, acute phase response, and inflammatory and humoral immune response were upregulated following *E. ictaluri* infection, indicating a multifactorial catfish immune response against this pathogen (32).

Despite the considerable research on function of proteins in the AAA ATPases superfamily, there is not much information about their use as vaccine antigens or contribution to virulence (37). A few studies have utilized ATPase as a vaccine antigen against protozoan parasites in animal models. For example, DNA immunization of mice with Na^+-K^+ATPase from *Strongyloides stercoralis* induced protective immunity and a significant reduction in larval survival, thus suggesting that the Na^+-K^+ATPase may be a good potential target for the immune response (38). Vaccination with a recombinant chlamydial ATPase protein combined with Alum adjuvant resulted in reduction of the number of viable *Chlamydophila pneumoniae* in lungs of mice, indicating that chlamydial ATPase induces protective immunity in mice (39).

Another strategy investigated the use of ATPase for vaccine development in the form of fusion proteins. For example, a surface protein (TcSP2) of *Trypanosoma cruzi* fused to ATPase (ATP) domains of heat shock protein 70 (TcHSP70) induced high antibody titers and increased survival in immunized mice after *T. cruzi* infection (40). Moreover, TcHSP70, as well as an internal fragment of 242 amino acids within the ATPase domain, activated the maturation of dendritic cells macrophages to produce proinflammatory cytokines and chemokines in a mouse model (41).

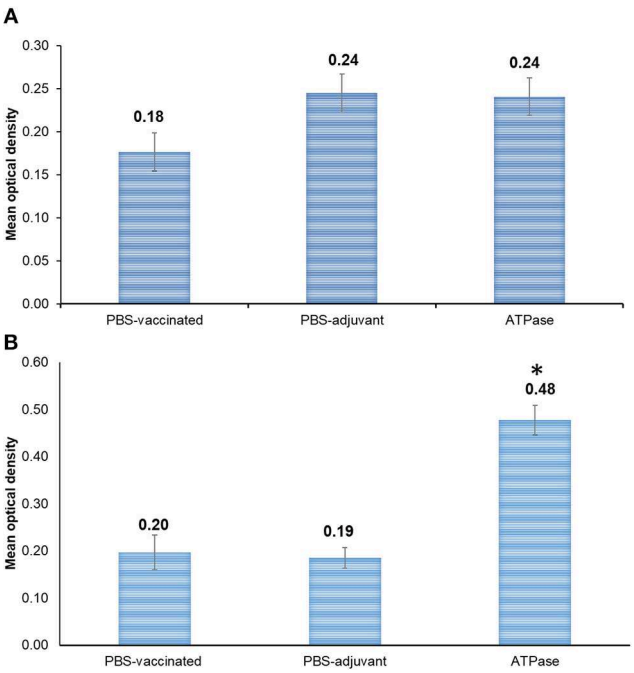


FIGURE 4 | Antibody response in channel catfish serum at day 21 post-vaccination with recombinant ATPase protein. **(A)** Plates were coated with heat-killed whole bacteria. **(B)** Plates were coated with purified ATPase protein. Optical densities at 405 nm are means of 10 fish. Vertical bars denote standard errors of the mean. Significant differences are indicated with asterisks ($p < 0.05$).

No information is available on ATPase as a recombinant antigen in fish or other animals against bacterial pathogen infections. However, some proteins characterized by ATPase activity were successfully used as subunit vaccines against fish bacterial pathogens. For example, heat shock proteins (HSP 60 and HSP 70) have a N-terminal ATPase domain and are usually in an ATP bound state (42, 43). Wilhelm et al. (44) reported protection of salmon (95% RPS) against *Piscirickettsia salmonis* following immunization with HSP as a recombinant vaccine (44), and Sudheesh et al. (45) found that HSP60, HSP70, and two other proteins (ATP synthase and thermolysin) were highly immunogenic proteins against *Flavobacterium psychrophilum* (45).

In conclusion, ATPase was successfully expressed and purified using a pET-28a vector. The recombinant ATPase protein protected catfish against vAh infection and significantly reduced bacterial quantities in catfish tissue, and it stimulated significant antibody titers against the protein. This is the first study to report an ATPase protein as a potential vaccine for a bacterial disease in fish.

ETHICS STATEMENT

Catfish experiments were performed according to guidelines of an approved protocol by the Institutional Animal Care and Use Committee at Mississippi State University.

AUTHOR CONTRIBUTIONS

ML, AK, and HA designed the experiments. ML supervised the overall project. HA performed the laboratory work, analyzed the data, and wrote the manuscript. MB helped with fish experiments and ELIZA. AK and ML reviewed the manuscript.

FUNDING

This work was funded by Agriculture and Food Research Initiative Competitive Grant no. 2013-67015-21313 from the USDA National Institute of Food and Agriculture. Part of HA salary was provided by the Center for Biomedical Research Excellence in Pathogen–Host Interactions, National Institute of General Medical Sciences, National Institutes of Health awarded grant number P20GM103646-05.

ACKNOWLEDGMENTS

We thank Dr. Robert Wills at Mississippi State University for his assistance with statistical analyses. We are grateful for Lionel Genix at SEPPIC INC for providing the adjuvant used in this study. We thank John Harkness for proof reading this manuscript. Finally, we thank Laboratory Animal Resources and Care (LARAC) at the Mississippi State University College of Veterinary Medicine for providing us with SPF catfish.

REFERENCES

1. USDA. *Catfish Production, by the National Agricultural Statistics Service (NASS)*. Agricultural Statistics Board, United States Department of Agriculture (USDA) (2017). Available online at: https://downloads.usda.library.cornell.edu/usda-esmis/files/bg257f046/1v53k047h/fj236430r/CatfProd-02-03-2017.pdf
2. Lewis DH, Plumb JA. Bacterial diseases. In: Plumb JA, editor. *Principal Diseases of Farm Raised Catfish*. South. Coop. Ser. Bull No. 225. (1985). pp. 13–7.
3. Center for Emerging Issues (U.S.). *Assessing Infectious Disease Emergence Potential in the U.S. Aquaculture Industry [electronic resource]: Phase 1, U.S. Aquaculture Industry Profile*. Fort Collins, CO: U.S. Dept. of Agriculture, Animal and Plant Health Inspection Service, Veterinary Services, Center for Emerging Issues (2007).
4. Wagner BA, Wise DJ, Khoo LH, Terhune JS. The epidemiology of bacterial diseases in food-size channel catfish. *J Aquat Anim Health*. (2006) 18:263–72. doi: 10.1577/1548-8667(2002)014<0263:TEOBDI>2.0.CO;2
5. Plumb JA, Hanson LA. Catfish bacterial diseases. In: Plumb JA, Hanson LA, editors. *Health Maintenance and Principal Microbial Diseases of Cultured Fishes*. (2011). p. 275–313. doi: 10.1002/9780470958353.ch11
6. Hemstreet B. An update on *Aeromonas hydrophila* from a fish health specialist for summer 2010. *Catfish J*. (2010) 24.
7. Baumgartner WA, Ford L, Hanson L. Lesions caused by virulent *Aeromonas hydrophila* in farmed catfish (*Ictalurus punctatus* and *I. punctatus* x *I. furcatus*) in Mississippi. *J Vet Diagn Invest*. (2017) 29:747–51. doi: 10.1177/1040638717708584
8. Hossain MJ, Sun D, McGarey DJ, Wrenn S, Alexander LM, Martino ME, et al. An Asian origin of virulent *Aeromonas hydrophila* responsible for disease epidemics in United States-farmed catfish. *MBio*. (2014) 5:e00848–14. doi: 10.1128/mBio.00848-14
9. Dunhua Zhang, De-Hai Xu, Craig Shoemaker, Hemstreet WB. Virulent *Aeromonas hydrophila* in channel catfish. In: *Global Aquaculture Advocate*. (2016). Available online at: https://m.2lua.vn/article/virulent-aeromonas-hydrophila-in-channel-catfish-58744b32e4951993688b456b.html
10. Vishwanath S, McDonald GA, Watkins NG. A recombinant Rickettsia conorii vaccine protects guinea pigs from experimental boutonneuse fever and Rocky Mountain spotted fever. *Infect Immun*. (1990) 58:646–53.
11. Kuzyk MA, Burian J, Machander D, Dolhaine D, Cameron S, Thornton JC, et al. An efficacious recombinant subunit vaccine against the salmonid rickettsial pathogen *Piscirickettsia salmonis*. *Vaccine*. (2001) 19:2337–44. doi: 10.1016/S0264-410X(00)00524-7
12. Iyer LM, Leipe DD, Koonin EV, Aravind L. Evolutionary history and higher order classification of AAA+ ATPases. *J Struct Biol*. (2004) 146:11–31. doi: 10.1016/j.jsb.2003.10.010
13. Frickey T, Lupas AN. Phylogenetic analysis of AAA proteins. *J Struct Biol*. (2004) 146:2–10. doi: 10.1016/j.jsb.2003.11.020
14. Hanson PI, Whiteheart SW. AAA+ proteins: have engine, will work. *Nat Rev Mol Cell Biol*. (2005) 6:519–29. doi: 10.1038/nrm1684
15. Erzberger JP, Berger JM. Evolutionary relationships and structural mechanisms of AAA+ proteins. *Annu Rev Biophys Biomol Struct*. (2006) 35:93–114. doi: 10.1146/annurev.biophys.35.040405.101933
16. Kuchta K, Knizewski L, Wyrwicz LS, Rychlewski L, Ginalski K. Comprehensive classification of nucleotidyltransferase fold proteins: identification of novel families and their representatives in human. *Nucleic Acids Res*. (2009) 37:7701–14. doi: 10.1093/nar/gkp854
17. Abdelhamed H, Nho SW, Turaga G, Banes MM, Karsi A, Lawrence ML. Protective efficacy of four recombinant fimbrial proteins of virulent *Aeromonas hydrophila* strain ML09-119 in channel catfish. *Vet Microbiol*. (2016) 197:8–14. doi: 10.1016/j.vetmic.2016.10.026
18. Abdelhamed H, Ibrahim I, Baumgartner W, Lawrence ML, Karsi A. Characterization of histopathological and ultrastructural changes in channel

catfish experimentally infected with virulent *Aeromonas hydrophila*. *Front Microbiol*. (2017) 8:1519. doi: 10.3389/fmicb.2017.01519
19. Amend DF. Potency testing of fish vaccines. Developments in Biological Standardization. *Sci Res.* (1981) 49:447–54.
20. Waterstrat PR, Ainsworth AJ, Capley G. *In vitro* responses of channel catfish, *Ictalurus punctatus*, neutrophils to *Edwardsiella ictaluri*. *Dev Comp Immunol*. (1991) 15:53–63. doi: 10.1016/0145-305X(91)90047-3
21. Lobb CJ, Clem LW. Fish lymphocytes differ in the expression of surface immunoglobulin. *Dev Comp Immunol*. (1982) 6:473–9. doi: 10.1016/S0145-305X(82)80033-5
22. Miller NW, Bly JE, van Ginkel F, Ellsaesser CF, Clem LW. Phylogeny of lymphocyte heterogeneity: identification and separation of functionally distinct subpopulations of channel catfish lymphocytes with monoclonal antibodies. *Dev Comp Immunol*. (1987) 11:739–47. doi: 10.1016/0145-305X(87)90061-9
23. Wang N, Yang Z, Zang M, Liu Y, Lu C. Identification of Omp38 by immunoproteomic analysis and evaluation as a potential vaccine antigen against *Aeromonas hydrophila* in Chinese breams. *Fish Shellfish Immunol*. (2013) 34:74–81. doi: 10.1016/j.fsi.2012.10.003
24. Maiti B, Shetty M, Shekar M, Karunasagar I. Evaluation of two outer membrane proteins, Aha1 and OmpW of *Aeromonas hydrophila* as vaccine candidate for common carp. *Vet Immunol Immunopathol*. (2012) 149:298–301. doi: 10.1016/j.vetimm.2012.07.013
25. Wu L, Jiang YN, Tang Q, Lin HX, Lu CP, Yao HC. Development of an *Aeromonas hydrophila* recombinant extracellular protease vaccine. *Microb Pathog*. (2012) 53:183–8. doi: 10.1016/j.micpath.2012.07.007
26. Khushiramani RM, Maiti B, Shekar M, Girisha SK, Akash N, Deepanjali A, et al. Recombinant *Aeromonas hydrophila* outer membrane protein 48 (Omp48) induces a protective immune response against *Aeromonas hydrophila* and *Edwardsiella tarda*. *Res Microbiol*. (2012) 163:286–91. doi: 10.1016/j.resmic.2012.03.001
27. Yeh HY, Klesius PH. Over-expression, purification and immune responses to *Aeromonas hydrophila* AL09-73 flagellar proteins. *Fish Shellfish Immunol*. (2011) 31:1278–83. doi: 10.1016/j.fsi.2011.09.016
28. Guan R, Xiong J, Huang W, Guo S. Enhancement of protective immunity in European eel (*Anguilla anguilla*) against *Aeromonas hydrophila* and *Aeromonas sobria* by a recombinant *Aeromonas* outer membrane protein. *Acta Biochim Biophys Sin.* (2011) 43:79–88. doi: 10.1093/abbs/gmq115
29. Abdelhamed H, Ibrahim I, Nho SW, Banes MM, Wills RW, Karsi A, et al. Evaluation of three recombinant outer membrane proteins, OmpA1, Tdr, and TbpA, as potential vaccine antigens against virulent *Aeromonas hydrophila* infection in channel catfish (*Ictalurus punctatus*). *Fish Shellfish Immunol*. (2017) 66:480–6. doi: 10.1016/j.fsi.2017.05.043
30. Tekedar HC, Waldbieser GC, Karsi A, Liles MR, Griffin MJ, Vamenta S, et al. Complete genome sequence of a channel catfish epidemic isolate, *Aeromonas hydrophila* strain ML09-119. *Genome Announc*. (2013) 1:e00755-13. doi: 10.1128/genomeA.00755-13
31. Ellis AE. Immunity to bacteria in fish. *Fish Shellfish Immunol*. (1999) 9:291–308. doi: 10.1006/fsim.1998.0192
32. Peatman E, Baoprasertkul P, Terhune J, Xu P, Nandi S, Kucuktas H, et al. Expression analysis of the acute phase response in channel catfish (*Ictalurus punctatus*) after infection with a Gram-negative bacterium. *Dev Comp Immunol*. (2007) 31:1183–96. doi: 10.1016/j.dci.2007.03.003
33. Luo Z, Fu J, Li N, Liu Z, Qin T, Zhang X, et al. Immunogenic proteins and their vaccine development potential evaluation in outer membrane proteins (OMPs) of *Flavobacterium columnare*. *Aquaculture Fish*. (2016) 1:1–8. doi: 10.1016/j.aaf.2016.10.002
34. Dash P, Sahoo PK, Gupta PK, Garg LC, Dixit A. Immune responses and protective efficacy of recombinant outer membrane protein R (rOmpR)-based vaccine of *Aeromonas hydrophila* with a modified adjuvant formulation in rohu (*Labeo rohita*). *Fish Shellfish Immunol*. (2014) 39:512–23. doi: 10.1016/j.fsi.2014.06.007
35. Raida MK, Buchmann K. Innate immune response in rainbow trout (*Oncorhynchus mykiss*) against primary and secondary infections with *Yersinia ruckeri* O1. *Dev Com Immunol*. (2009) 33:35–45. doi: 10.1016/j.dci.2008.07.001
36. Liu F, Tang X, Sheng X, Xing J, Zhan W. *Edwardsiella tarda* outer membrane protein C: an immunogenic protein induces highly protective effects in flounder (*Paralichthys olivaceus*) against Edwardsiellosis. *Int J Mol Sci*. (2016) 17:1117. doi: 10.3390/ijms17071117
37. Snider J, Thibault G, Houry WA. The AAA+ superfamily of functionally diverse proteins. *Genome Biol*. (2008) 9:216. doi: 10.1186/gb-2008-9-4-216
38. Kerepesi LA, Keiser PB, Nolan TJ, Schad GA, Abraham D, Nutman TB. DNA immunization with Na+-K+ ATPase (Sseat-6) induces protective immunity to larval Strongyloides stercoralis in mice. *Infect Immun*. (2005) 73:2298–305. doi: 10.1128/IAI.73.4.2298-2305.2005
39. Szabó AM, Sipák Z, Miczák A, Faludi I. ABC transporter ATPase of Chlamydophila pneumoniae as a potential vaccine candidate. *Acta Microbiol Immunol Hung*. (2013) 60:11–20. doi: 10.1556/AMicr.60.2013.1.2
40. Carabarin-Lima A, González-Vázquez MC, Baylon-Pacheco L, Patricia-Talamas R. Immunization with the recombinant surface protein rTcSP2 alone or fused to the CHP or ATPase domain of TcHSP70 induces protection against acute *Trypanosoma cruzi* Infection. *J Vaccin Vaccinat*. (2010) 1:130. doi: 10.4172/2157-7560.1000110
41. Planelles L, Thomas M, Pulgar M, Maranon C, Grabbe S, Lopez MC. Trypanosoma cruzi heat-shock protein-70 kDa,alone or fused to the parasite KMP11 antigen, induces functional maturation of murine dendritic cells. *Immunol Cell Biol*. (2002) 80:241–7. doi: 10.1046/j.1440-1711.2002.01081.x
42. Flaherty KM, DeLuca-Flaherty C, McKay DB. Three-dimensional structure of the ATPase fragment of a 70K heat-shock cognate protein. *Nature*. (1990) 346:623–8. doi: 10.1038/346623a0
43. Chamberlain LH, Burgoyne RD. Activation of the ATPase activity of heat-shock proteins Hsc70/Hsp70 by cysteine-string protein. *Biochem J*. (1997) 322:853–8. doi: 10.1042/bj3220853
44. Wilhelm V, Soza C, Martinez R, Rosemblatt M, Burzio LO, Valenzuela PD. Production and immune response of recombinant Hsp60 and Hsp70 from the salmon pathogen *Piscirickettsia salmonis*. *Biol Res*. (2005) 38:69–82. doi: 10.4067/S0716-97602005000100009
45. Sudheesh PS, LaFrentz BR, Call DR, Siems WF, LaPatra SE, Wiens GD, et al. Identification of potential vaccine target antigens by immunoproteomic analysis of a virulent and a non-virulent strain of the fish pathogen *Flavobacterium psychrophilum*. *Dis Aquat Organ*. (2007) 74:37–47. doi: 10.3354/dao074037

Conflict of Interest Statement: The authors declare that the research was conducted in the absence of any commercial or financial relationships that could be construed as a potential conflict of interest.

Copyright © 2019 Abdelhamed, Banes, Karsi and Lawrence. This is an open-access article distributed under the terms of the Creative Commons Attribution License (CC BY). The use, distribution or reproduction in other forums is permitted, provided the original author(s) and the copyright owner(s) are credited and that the original publication in this journal is cited, in accordance with accepted academic practice. No use, distribution or reproduction is permitted which does not comply with these terms.

frontiers in Immunology

ORIGINAL RESEARCH
published: 22 August 2019
doi: 10.3389/fimmu.2019.01991

Metabolites-Enabled Survival of Crucian Carps Infected by *Edwardsiella tarda* in High Water Temperature

Ming Jiang[1,2], *Zhuang-gui Chen*[3], *Jun Zheng*[4] *and Bo Peng*[1,2,3,5]*

[1] State Key Laboratory of Bio-Control, Higher Education Mega Center, School of Life Sciences, Sun Yat-sen University, Guangzhou, China, [2] Laboratory for Marine Biology and Biotechnology, Qingdao National Laboratory for Marine Science and Technology, Qingdao, China, [3] Department of Pediatrics, The Third Affiliated Hospital of Sun Yat-sen University, Guangzhou, China, [4] Faculty of Health Sciences, University of Macau, Macau, China, [5] Southern Marine Science and Engineering Guangdong Laboratory, Zhuhai, China

OPEN ACCESS

Edited by:
Carolina Tafalla, Instituto Nacional de Investigación y Tecnología Agraria y Alimentaria (INIA), Spain

Reviewed by:
Caroline Fossum, Swedish University of Agricultural Sciences, Sweden
Javier Santander, Memorial University of Newfoundland, Canada

***Correspondence:**
Bo Peng
pengb26@mail.sysu.edu.cn

Specialty section:
This article was submitted to Comparative Immunology, a section of the journal Frontiers in Immunology

Received: *30 April 2019*
Accepted: *06 August 2019*
Published: *22 August 2019*

Citation:
Jiang M, Chen Z, Zheng J and Peng B (2019) Metabolites-Enabled Survival of Crucian Carps Infected by Edwardsiella tarda in High Water Temperature. Front. Immunol. 10:1991. doi: 10.3389/fimmu.2019.01991

Temperature is one of the major factors that affect the outbreak of infectious disease. Lines of evidences have shown that virulence factors can be controlled by thermo-sensors in bacterial pathogens. However, how temperature influences host's responses to the pathogen is still largely unexplored, and the study of this might pave the way to develop strategies to manage pathogenic bacterial infection. In the present study, we show that finfish *Carassius carassius*, the crucian carp that is tolerant to a wide range of temperatures, is less susceptible to bacterial infection when grown in 20°C than in 30°C. The different responses of *C. carassius* to bacterial infection could be partially explained by the distinct metabolisms under the specific temperatures: *C. carassius* shows elevated tricarboxylic acid cycle (TCA cycle) but decreased taurine and hypotaurine metabolism as well as lower biosynthesis of unsaturated fatty acids at 30°C. The decreased abundance of palmitate, threonine, and taurine represents the most characteristic metabolic feature. Consistently, exogenous palmitate, threonine, or taurine enhances the survival of *C. carassius* to bacterial infection at 30°C in a dose-dependent manner. This effect could be attributed to the inhibition on the TCA cycle by the three metabolites. This notion is further supported by the fact that low concentration of malonate, a succinate dehydrogenase inhibitor, increases the survival of *C. carassius* at 30°C as well. On the other hand, addition of the three metabolites rescued the decreased expression of pro-inflammatory cytokines including TNF-α1, TNF-α2, IL-1β1, IL-1β2, and lysozyme at 30°C. Taken together, our results revealed an unexpected relationship between temperature and metabolism that orchestrates the immune regulation against infection by bacterial pathogens. Thus, this study shed light on the modulation of finfish physiology to fight against bacterial infection through metabolism.

Keywords: water temperature, bacterial infection, *Carassius carassius*, metabolome, innate immunity

INTRODUCTION

Climate is one of the most important environmental factors that influences the spread of communicable diseases prone to their epidemic (1). The outbreak of bacterial infectious disease depends on not only the pathogenicity of the bacteria but also many environmental factors, including the temperature changes. In aquaculture, infections mostly occur in spring and fall when the water temperature is between 22 and 30°C (2). The outbreak of bacterial infectious diseases depends on at least two determining factors: (1) the multiple strategies of pathogens to sense the environmental perturbations and fluctuations as cues to adjust their growth, development and pathogenesis. It is well established that the elevated temperature promotes the expression of virulence genes like type III secretion system, temperature-sensitive hemagglutinin, adhesins, and other virulence regulators in the species of *Edwardsiella*, *Vibrio*, and *Aeromonas* (2–6); (2) the fish's immune responses to pathogens that affected by residential water temperature. It has long been shown that the elevated temperature negatively affected fish's immune responses to vaccination and reduced the phagocytosis to bacterial pathogens (7). However, the interplay between temperature and host immune response is still largely unexplored (8, 9).

In aquaculture, infectious disease caused by bacteria is the major cause of mortalities that result in huge economic loss (10). A good research model to investigate the relationship between temperature and host immune responses might contribute to the control of infectious diseases in aquaculture and is thus highly needed. Crucian carp *Carassius auratus* is one of the most extensively cultured freshwater fish throughout the world, reaching 2.2 million tons in the year of 2010 (11). Furthermore, crucian carp is a potential model to study genome evolution and physiological adaptation as it has exhibited a striking capacity to cope with the low level of oxygen and a wide range of ambient temperatures (11, 12). The capability of crucian carp to adapt to versatile environments suggests that it is an ideal model to investigate the impacts of environmental factors on the immune responses of fish to pathogens (13).

Edwardsiella tarda, a zoonotic Gram-negative pathogen, infects a broad range of hosts including fish, amphibians, reptiles, and mammals, and causes edwardsiellosis (14–16). *E. tarda* represents a critical pathogen that causes huge economic and biomasses loss in aquaculture (17, 18). The outbreak of edwardsiellosis can lead to massive fish death in a short period. The infected fish shows abnormal swimming behavior, including spiral movement and floating near the water surface (19–22). Epidemiological investigation of the outbreak of *E. tarda* indicates that infection usually occurs when environmental conditions are imbalanced, such as higher water temperature, poor water quality, and high organic content (23, 24). Teleost, including crucian carps and striped bass, are ectotherm, whose body temperature is largely influenced by the water temperature. Consistently, it has different physiology or metabolism at different environmental conditions (25–28). Since metabolism is linked to immunity, it is not astonishing that bacterial infections occur more frequently at certain environmental conditions (29–32). However, the interplay among water temperature, metabolism and immunity is not well understood. The elucidation of such relationship might be useful for the development of a new strategy to fight against bacterial infection at high temperatures.

Metabolomics provides a "top-down," integrated view of biochemistry in complex organisms that could be used to profile the metabolic response to internal and external environments. Crucial biomarkers identified from the metabolomics data could be used to reprogram the metabolome (33, 34). Antibiotic-resistant bacteria and antibiotic-sensitive bacteria have a distinct metabolome, and the crucial metabolic biomarkers can reprogram the antibiotic-resistant bacteria to become sensitive to antibiotics again, shedding light on a new strategy to manage bacterial antibiotic-resistance (33, 35–38). Similarly, tilapia showed distinct responses to *Streptococcus agalactiae* infection when grown at 20, 25, and 30°C. The metabolomics profiling of liver extract from tilapia grown at different temperatures showed that they have different metabolic responses. L-Proline, one of the crucial biomarkers, decreases along with the increasing temperatures. Interestingly, exogenous L-Proline promotes the survival of tilapias to *S. agalactiae* at 30°C (39). These results indicate that metabolic modulation is a novel approach to promote fish survival against bacterial infection at higher temperature (40–42). However, the underlying mechanism is still unknown.

In the present study, we adopted crucian carp and *E. tarda* as the research model to investigate the interplay of temperature, metabolism, and immunity. By challenging crucian carp with *E. tarda*, we found that crucian carp grown at 20°C, the optimum temperature, was more resistant to bacterial infection than those grown at 30°C. The profiling of the metabolome in fish grown at these two different environmental conditions identified three crucial biomarkers, palmitate, threonine, and taurine, which can be used to reprogram the metabolome of crucian carp and make the fish less susceptible to bacterial infection. More importantly, these three metabolites increase the expression of innate immune genes that are known to promote inflammation to kill pathogens.

RESULTS

Crucian Carps Grown at Different Temperatures Show Distinct Susceptibility to *E. tarda* Infection

To investigate how temperature affects host's susceptibility to bacterial infection, crucian carps *Carassius carassius*, cultured at 20 or 30°C, were challenged with 1×10^5 CFU *E. tarda* EIB202. Upon infection by *E. tarda*, the cumulative survival rates of *C. carassius* grown at 20°C were 76%, compared to 30% grown at 30°C (**Figure 1**). This result indicates that crucian carps cultured at 30°C are more susceptible to *E. tarda* infection than those cultured at 20°C.

Water Temperature Affects Metabolomes of Crucian Carps

Hosts adjusted their metabolism to adapt to different temperatures that have profound effects on their capability to cope with bacterial infection (39). We apply GC-MS-based

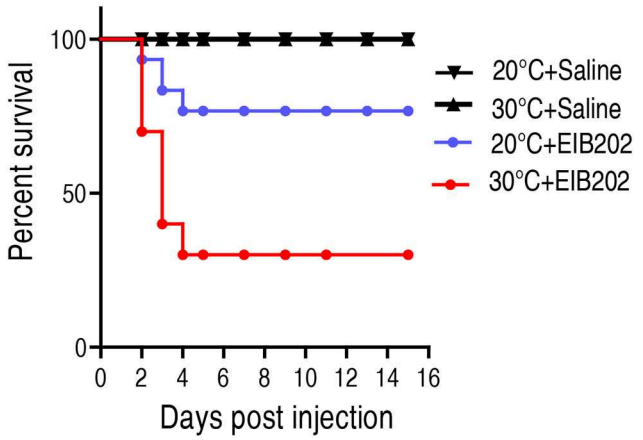


FIGURE 1 | The survival of crucian carp to *E. tarda* infection cultured at 20 and 30°C. *C. carassius* ($n = 30$ per group) were acclimated at 20 or 30°C for 7 days before bacterial challenge. For bacterial infection, *C. carassius* were injected with 10 μl 1×10^5 CFU/fish *E. tarda* or 10 μl saline solution as negative control. Accumulative death was monitored for a total of 15 days.

metabolomics to investigate the metabolic differences between the *C. carassius* that were acclimated at 20 and 30°C for 7 days. Spleens are removed, homogenized, and the metabolites were extracted for non-targeted metabolomic analysis (**Figure S1**). For each spleen sample, two technical replicates were adopted. In total, 48 GC-MS data sets were generated. After data processing, 56 metabolites with different abundances were identified, followed by categorization into carbohydrates (35%), lipids (27%), amino acids (24%), nucleotides (7%), and others (7%) (**Figure 2A**). Among the 56 metabolites, 33 metabolites were reduced in the *C. carassius* grown at 30°C. Interestingly, the abundance of the metabolites belonging to the category of lipids were all decreased in fish cultured at 30°C (**Figure 2B**). A heat map of the metabolites of different abundances was generated and was shown in **Figure 2C**. Z-score varied between −17 and 24 at 30°C as compared to 20°C. The abundance of 17 metabolites were increased and 33 metabolites were decreased from samples in fish grown at 30°C (**Figure 2D**). These data suggest that *C. carassius* mounts metabolic shift when cultured at different temperatures.

Metabolic Pathways Being Affected in *C. carassius* Cultured at 30°C

Enriched metabolic pathways are crucial for the understanding of the key events during metabolic shift (43). Thus, the identified 56 metabolites with different abundance were analyzed by pathway enrichment analysis using an online software (http://www.metaboanalyst.ca). Thirteen metabolic pathways were identified. Valine, leucine, and isoleucine biosynthesis was the pathway mostly affected, followed by glycine, serine and threonine metabolism, alanine, aspartate and glutamate metabolism, methane metabolism, arginine and proline metabolism, taurine and hypotaurine metabolism, and TCA cycle. (**Figure 3A**). Among the 13 enriched metabolic pathways, three pathways, namely, taurine and hypotaurine metabolism, TCA cycle, and biosynthesis of unsaturated fatty acids, were of special interest because the abundance of metabolites in taurine and hypotaruine metabolism and biosynthesis of unsaturated fatty acids were all decreased, while the abundance of metabolites in the TCA cycle was increased in fish grown at 30°C (**Figure 3B**). These results indicate that *C. carassius* compromises taurine and hypotaurine metabolism and biosynthesis of unsaturated fatty acids but boosts the TCA cycle to cope with the temperature stress. This adaptation may make the fish more susceptible to bacterial infection.

Taurine, Palmitic Acid, and Threonine Were the Crucial Biomarkers to Distinguish *C. carassius* Cultured at 20 or 30°C

To identify the crucial metabolites cultured at 20 and 30°C, orthogonal partial least square discriminant analysis (OPLS-DA) was conducted to recognize the sample patterns. The two groups were distributed in two quarters. Component t[1] separated 30°C group from 20°C group (**Figure 4A**) and Component t[1] differentiated variability within groups. Discriminating variables were shown as S-plot (**Figure 4B**) where cut-off values were set as grater or equal to 0.05 and 0.5 for absolute value of covariance p and correlation p(corr), respectively. Nineteen biomarkers screened by component t[1] were shown in **Figure 4B** (font in red). Among the 19 metabolites, the abundance of 9 metabolites were decreased in the group grown at 20°C, in which taurine, threonine, and palmitic acid showed the most significant difference. Taurine and palmitic acid are important components belonging to the taurine and hypotaurine metabolism and the biosynthesis of unsaturated fatty acids, respectively. Threonine belongs to the pathway with the second most impact (**Figure 3A**). Thus, taurine, palmitic acid, and threonine were the crucial biomarkers that distinguish the group cultured at 20 or 30°C. The scatter map of taurine, threonine, and palmitic acid were shown in **Figure 4C**.

The TCA Cycle Was Upregulated in *C. carassius* Cultured at 30°C

We constructed the metabolic pathways affected by the water temperature in **Figure 5A**, where metabolites with increased and decreased abundance are highlighted in red and blue, respectively. Our results showed that the abundances of all the identified metabolites of the TCA were increased (**Figures 3B**, **5A**), implying that TCA cycle may play important roles in addition to taurine, threonine, and palmitic acid. To explore this possibility, we measured the activity of the enzymes of the TCA cycle, including pyruvate dehydrogenase (PDH), succinate dehydrogenase (SDH), α-ketoglutarate dehydrogenase (α-KGDH), and malic dehydrogenase (MDH). As shown in **Figure 5B**, the activities of PDH, SDH, α-KGDH, and MDH were higher in 30°C than those in 20°C: 7.18 ± 1.01 U/mg vs. 9.66 ± 1.34 U/mg for PDH; 25.99 ± 3.86 U/mg vs. 35.73 ± 1.86 U/mg for SDH; 8.27 ± 1.11 U/mg vs. 11.41 ± 1.14 U/mg for α-KGDH; and

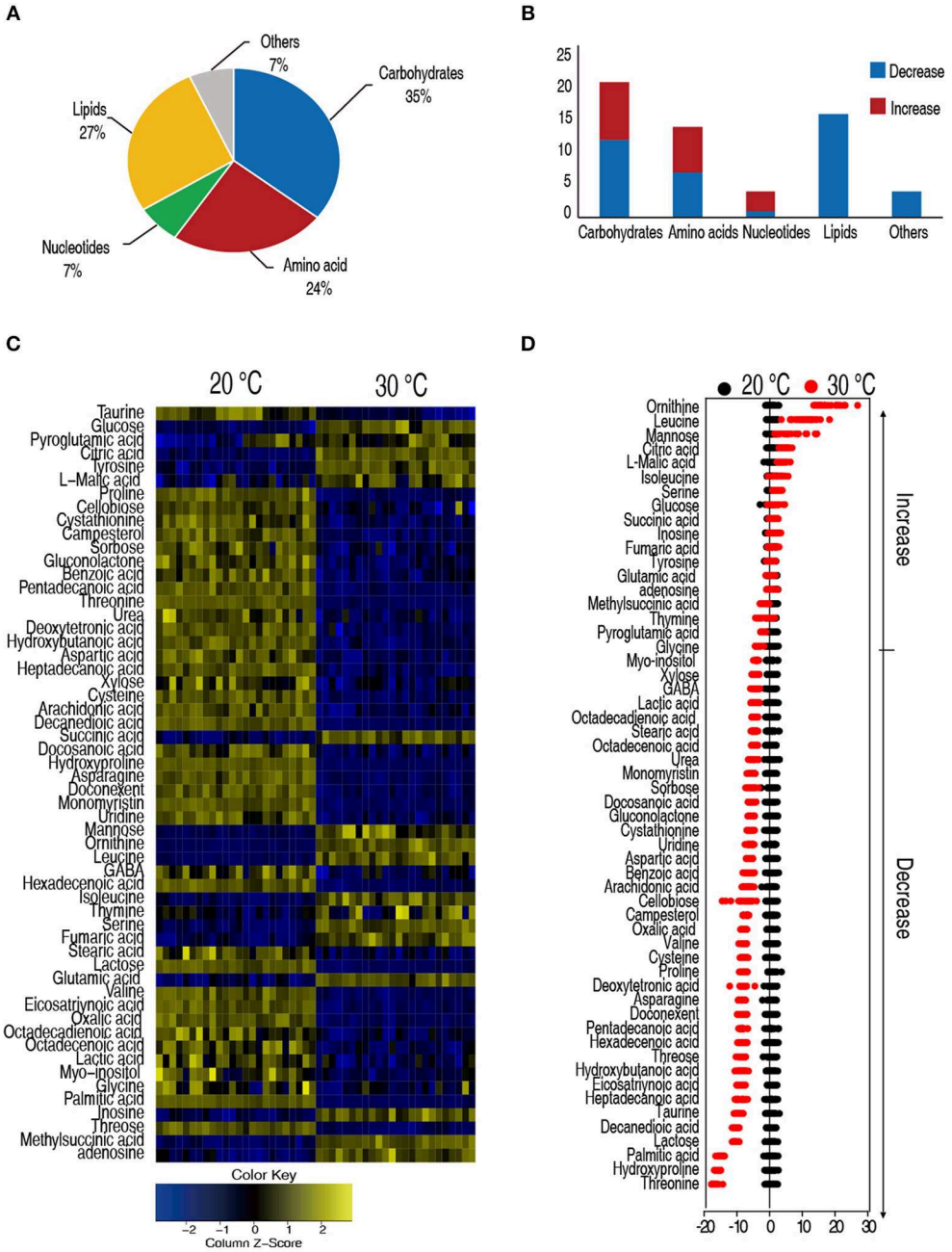
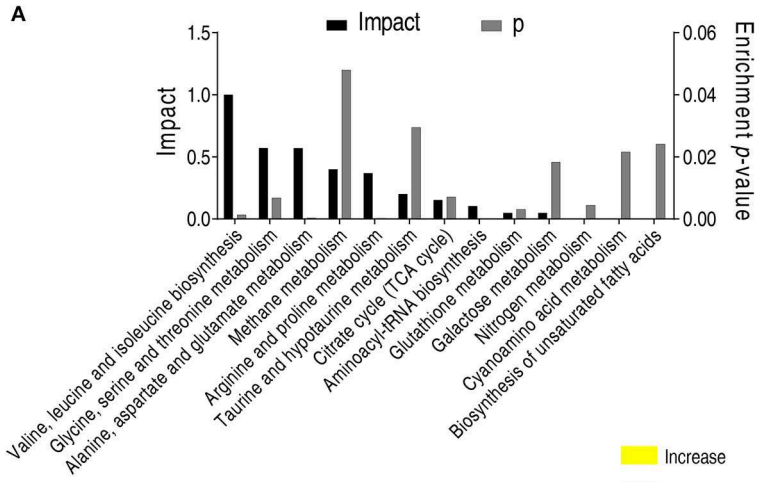


FIGURE 2 | *C. carassius* cultured at 20 and 30°C had a different metabolism. **(A)** Categories of the different metabolites. Fifty six metabolites with different abundance were searched against in KEGG for their categories, and the pie chart was generated in Excel 2010 (Microsoft, USA). **(B)** The number of metabolites of different abundance in each category as shown in **(A)**. **(C)** Heat map of unsupervised hierarchical clustering of different metabolites (row). Yellow and blue indicate increase and decrease of the metabolites scaled to mean and standard deviation of row metabolite level, respectively, (see color scale) **(D)** Z scores (standard deviation from average) of metabolites identified from 30 to 20°C, which are corresponding to the data shown in **(C)**. Each point represents one technical repeat of metabolite.

16.41 ± 2.03 U/mg vs. 21.55 ± 1.69 U/mg for MDH, respectively (the percentage change and statistical significance were listed in **Table 1**). The increased abundance of the key metabolites in the TCA cycle, including succinate, malate, citrate, and fumarate, indicates that TCA cycle is upregulated at 30°C as to 20°C.

Decreased Metabolites Are Key to Survival of Fish to Bacterial Challenge at 30°C

We hypothesized that the increase of taurine, threonine, and palmitic acid in *C. carassius* may promote fish survival of bacterial challenge at 30°C. To test this, fish was intraperitoneally injected



B

Valine, leucine and isoleucine biosynthesis

	20C°	30C°
Threonine	148935.2715	93645.87239
Leucine	727376.5772	1244730.719
Valine	3051141.113	2472395.33
Isoleucine	881147.5881	1079701.829

Citrate cycle (TCA cycle)

	20C°	30C°
Succinic acid	599482.0567	758430.6878
L-Malic acid	1836795.64	2201947.769
Citric acid	1190596.953	2098234.718
Fumaric acid	4624049.85	5616507.856

Alanine, aspartate and glutamate metabolism

	20C°	30C°
Aspartic acid	431790.1413	288656.7686
Glutamic acid	3154119.209	4503866.354
GABA	931309.0164	817748.7406
Asparagine	895795.2375	585831.7655
Fumaric acid	4624049.85	5616507.856
Succinic acid	599482.0567	758430.6878

Glycine, serine and threonine metabolism

	20C°	30C°
Serine	4325236.65	5908047.979
Cystathionine	1288007.791	1107733.709
Glycine	19766546.75	19256642.07
Threonine	148935.2715	93645.87239
Cysteine	562905.4538	384407.4982

Arginine and proline metabolism

	20C°	30C°
Ornithine	593716.0572	1272232.872
Aspartic acid	431790.1413	288656.7686
Glutamic acid	3154119.209	4503866.354
Proline	1868043.578	1491788.513
Hydroxyproline	752988.8086	581565.3258
GABA	931309.0164	817748.7406
Fumaric acid	4624049.85	5616507.856
Urea	176190.0141	139342.8037

Aminoacyl-tRNA biosynthesis

	20C°	30C°
Asparagine	895795.2375	585831.7655
Cysteine	562905.4538	384407.4982
Glycine	19766546.75	19256642.07
Aspartic acid	431790.1413	288656.7686
Serine	4325236.65	5908047.979
Isoleucine	881147.5881	1079701.829
Leucine	727376.5772	1244730.719
Valine	3051141.113	2472395.33
Tyrosine	1528312.607	2270771.811
Threonine	148935.2715	93645.87239
Proline	1868043.578	1491788.513
Glutamic acid	3154119.209	4503866.354

Taurine and hypotaurine metabolism

	20C°	30C°
Cysteine	562905.4538	384407.4982
Taurine	56336073.11	48536758.26

Biosynthesis of unsaturated fatty acids

	20C°	30C°
Docosanoic acid	663919.9194	564343.9311
Palmitic acid	8111446.284	6434605.654
Stearic acid	5659052.574	4921529.223
Arachidonic acid	504113.0184	344621.9904
Doconexent	890250.1072	659126.0717

Glutathione metabolism

	20C°	30C°
Cysteine	562905.4538	384407.4982
Glutamic acid	3154119.209	4503866.354
Glycine	19766546.75	19256642.07
Ornithine	593716.0572	1272232.872
Pyroglutamic acid	30906510.01	32991893.61

Galactose metabolism

	20C°	30C°
Lactose	6021054.545	5117811.892
Glucose	26545625.69	33012565.74
Mannose	761020.4153	1093843.066
Myo-inositol	18248548.01	17216682.56

Nitrogen metabolism

	20C°	30C°
Glutamic acid	3154119.209	4503866.354
Cystathionine	1288007.791	1107733.709
Glycine	19766546.75	19256642.07

Methane metabolism

	20C°	30C°
Glycine	19766546.75	19256642.07
Serine	4325236.65	5908047.979

Cyanoamino acid metabolism

	20C°	30C°
Glycine	19766546.75	19256642.07
Serine	4325236.65	5908047.979

FIGURE 3 | Pathway enrichment analysis of metabolites with different abundance. **(A)** Pathway enrichment analysis of different metabolites. Metabolites demonstrating different abundance were analyzed by pathway enrichment analysis using online software (http://www.metaboanalyst.ca). Significant enriched pathways are selected to plot ($p < 0.05$). **(B)** Abundance of metabolites in the enriched pathways listed in **(A)**. The metabolites in fish grown at 30°C were compared to that at 20°C. Different metabolites highlighted in yellow and blue indicate increased and decreased abundance, respectively.

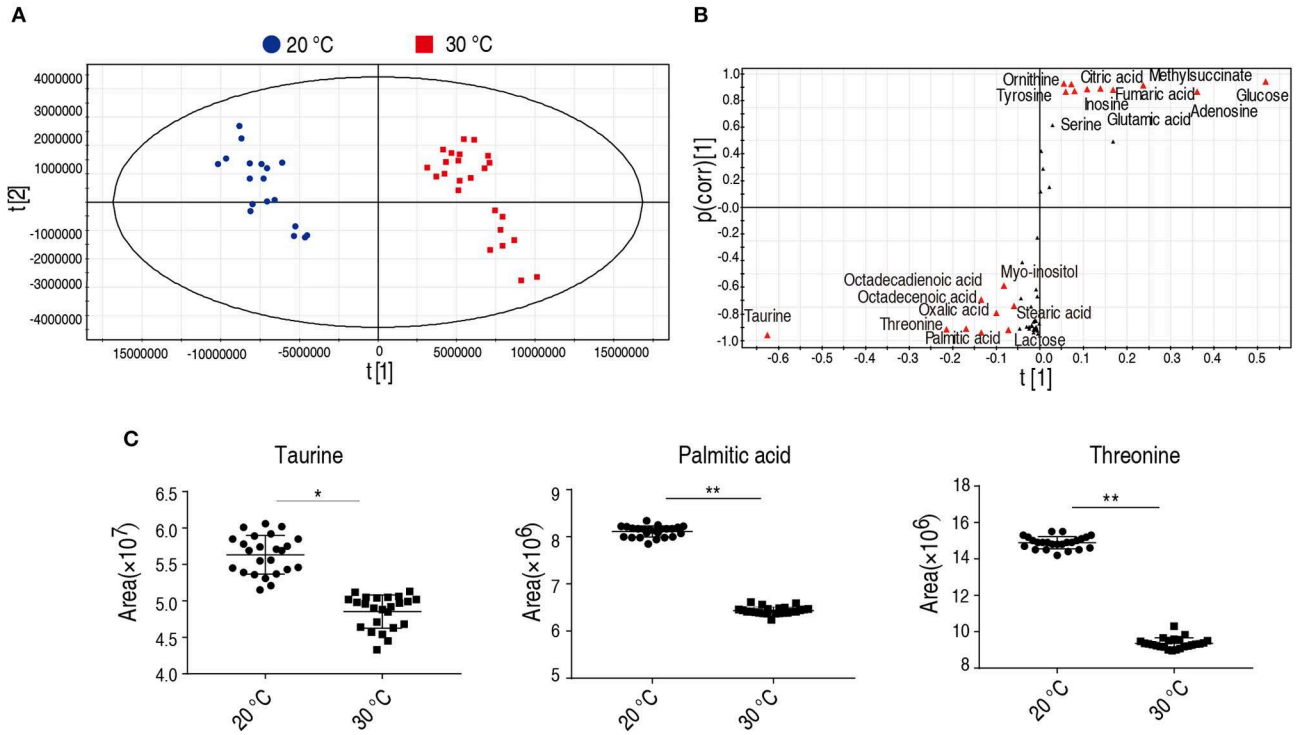


FIGURE 4 | Identification of crucial biomarkers. **(A)** The PCA analysis of metabolites with difference abundance in fish grown at the 30 and 20°C to investigate intergroup difference. Each dot represents the technique replicates in the plot. The metabolites with difference abundance in fish grown at 30 and 20°C were separated by the independent factors t[1]. **(B)** S-plot, generated by OPLS-DA, to identify different metabolites of intragroup as from t[1] in **(A)**. Each triangle represents individual metabolite. The potential biomarkers are highlighted in red for metabolites whose *p* value is ≥0.05 and 0.5 for absolute value of covariance *p* and correlation *p* (corr), respectively. **(C)** Crucial biomarkers represent the metabolism of fish grown between 30 and 20°C. The abundance of the three crucial biomarkers, taurine, threonine, and palmitic acid, are compared between 20 and 30°C and presented as scatter plot. Each dot represents individual replicate. $^{*}p < 0.05$; $^{**}p < 0.01$.

with taurine (50, 100, and 200 μg), threonine (125, 250, and 500 μg), or palmitic acid (3.5, 7, and 14 μg), followed by the challenge with *E. tarda*. Our results showed that the three metabolites had a protective effect on bacterial infection in a dose-dependent manner (**Figure 6A**).

To further address the metabolic basis of how the three metabolites protect fish against bacterial infection, we measured the enzymatic activities of PDH, SDH, α-KGDH, MDH in the TCA cycle after metabolite administration. Exogenous administration of taurine and palmitic acid significantly reduced the enzymatic activity of PDH in fish (from 6.18 ± 0.25 U/mg to 5.01 ± 0.52 U/mg by taurine; from 6.41 ± 0.63 U/mg to 4.87 ± 0.52 U/mg by palmitic acid), α-KGDH (from 7.05 ± 0.17 U/mg to 4.81 ± 0.72 U/mg by taurine; from 6.09 ± 0.57 U/mg to 2.51 ± 0.31 U/mg by palmitic acid), SDH (from 28.56 ± 2.00 U/mg to 16.91 ± 1.75 U/mg by taurine; from 30.80 ± 0.52 U/mg to 12.90 ± 0.79 U/mg by palmitic acid), and MDH (from 19.29 ± 0.95 U/mg to 15.0 ± 1.15 U/mg by taurine; from 18.04 ± 0.87 U/mg to 13.38 ± 0.81 U/mg by palmitic acid) (**Figure 6B**; **Tables 2**, **3**). While exogenous threonine decreased the activity of α-KGDH from 7.05 ± 0.17 to 5.73 ± 0.61, and of SDH from 28.56 ± 2.00 to 21.77 ± 1.89 U/mg, but had no effect on the activities of PDH and MDH (**Figure 6B**; **Table 4**). These results suggested that exogenous taurine and palmitic acid may downregulate TCA cycle to promote *C. carassius* survival from *E. tarda* infection at 30°C. To further validate the role of attenuated TCA cycle in fish survival, we treated *C. carassius* with a low concentration of malonate, an inhibitor of SDH, and found that fish survival was increased in 20% (**Figure 6C**). Therefore, the attenuation of the TCA cycle by taurine and palmitic acid, threonine or inhibitors of SDH promotes fish survival from bacterial infection at 30°C.

Taruine and Palmitic Acid Promote the Expression of Innate Immune Genes

To investigate whether the crucial biomarkers exert their effects through adjusting the fish immunity, we quantified the transcriptional level of 13 innate immune genes, including TNF-α1, TNF-α2, IL-1β1, IL-1β2, lysozyme, nfkbiab, IL-11, TLR9, TLR2, IFN-γ1-1, IFN-γ1-2, and complement component C3. Interestingly, the transcriptional level of TNF-α1, TNF-α2, IL-1β1, IL-1β2, and lysozyme were decreased when *C. carassius* was cultured at 30°C, but they can be quickly increased upon treatment with taurine, palmitic acid, and threonine (**Figures 7A,B**). The transcriptional expressions of TLR2, IFN-γ1-1, IFN-γ1-2, and C3 were also further boosted when the metabolites were supplemented (**Figures 7A,B**). Furthermore, all of these three metabolites downregulated the expression of IL-11 (**Figures 7A,B**). These results indicated that the three crucial biomarkers regulate innate immune response to fight against the infection at 30°C.

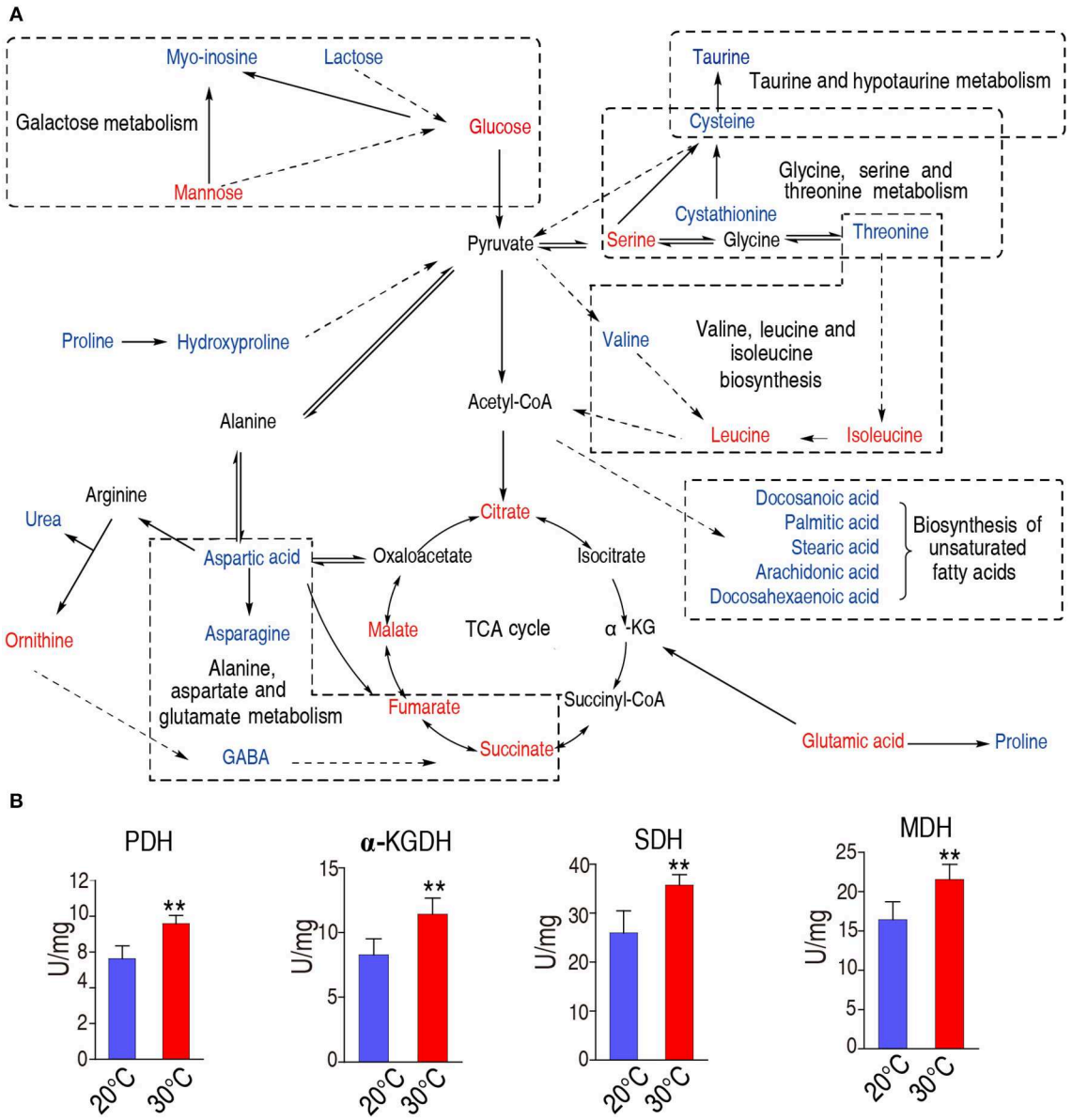


FIGURE 5 | Metabolic network of metabolites of different abundance, and activity of the TCA cycle. **(A)** Integrated metabolic network in relation to different metabolites. Different metabolites are searched against KEGG, and the metabolic network was reconstructed with ChemDraw Pro 18. The red and blue stand for the increased and decreased metabolites in fish grown at 30°C, respectively. **(B)**The enzymatic activity of PDH, α-KGDH, SDH, and MDH of spleen from fish grown at 30 and 20°C were quantified. Spleens were removed, lysed and extracted for enzyme analysis, and the data were shown as histogram. The significant differences are analyzed by non-parametric Kruskal-Wallis one-way analysis with Dunn multiple comparison *post hoc* test. $^{**}p < 0.01$ indicates statistic significant.

DISCUSSION

Environmental temperature affects fish host immune responses to microbial infection (44). Several endemic diseases of salmonids are more prevalent and difficult to control with the increase of water temperature (44). One reason is that the increase in water temperatures are likely to enhance the susceptibility of fish to disease and the likelihood of disease emergence (44). That temperature shift alters the immune status of *Cyprinus carpio* advanced fingerlings, while persistent sub-lethal exposure to chlorine augments temperature induced immunosuppression (26). Multiple acute temperature stress affects leucocyte populations and antibody responses in the common carp, *Cyprinus carpio L.* (27). Water temperature affects metabolism and metabolome in fish (39, 45). L-Proline, a crucial biomarker identified from temperature shift, increased the survival of tilapias infected by *Streptococcus agalactiae* in high water temperature (39). Our results further demonstrated that water temperature alters crucian carp metabolism, orchestrating innate immunity to cope with bacterial infection.

Insights gained on the metabolome-mediated mechanisms may provide new therapeutic methods for the treatment of infections or preventive measures against the future outbreaks of bacterial infection.

The first core finding in the present study showed that high temperature disrupts the normal flow of the TCA cycle, making the host vulnerable to bacterial infection. The activated TCA cycle is a characteristic metabolic feature at high temperature as confirmed by the elevated activities of enzymes in pyruvate metabolism and the TCA cycle. More importantly, the inhibition of the TCA cycle promoted fish survival during bacterial infection. Therefore, the enhanced TCA cycle is critical for crucian carps to survive at higher water temperature.

The second core finding shows that the crucial biomarkers not only promote the survival of crucian carps cultured at 30°C, but also rescue the expression of innate immune genes that are repressed at 30°C. Specifically, palmitic acid, threonine, and taurine restored the expressions of TNF-α1, TNF-α2, IL-1β1, IL-1β2, and lysozyme, which were reduced at 30°C. In addition, nfkbiab, TLR9, TLR3, IL-11, and C3 were also regulated

TABLE 1 | Enzyme activity of PDH, α-KGDH, SDH, and MDH of spleen at 30 and 20°C.

Enzyme name	20°C (U/mg)	30°C (U/mg)	Percentage of change (%)
PDH	7.18 ± 1.01	9.66 ± 1.34	34.5**
α-KGDH	8.27 ± 1.11	11.41 ± 1.14	37.8**
SDH	25.99 ± 3.86	35.73 ± 1.86	37.8**
MDH	16.41 ± 2.03	21.55 ± 1.69	31.2**

*Values are represented as Means ± SEM. **p < 0.01.*

TABLE 2 | Enzyme activity of PDH, α-KGDH, SDH, and MDH of spleen at 30°C in the presence of taurine.

Enzyme name	Saline control	Taurine	Percentage of change (%)
PDH	6.18 ± 0.25	5.01 ± 0.52	18.9**
α-KGDH	7.05 ± 0.17	4.81 ± 0.72	31.8**
SDH	28.56 ± 2.00	16.91 ± 1.75	40.7**
MDH	19.29 ± 0.95	15.0 ± 1.15	22.3**

*Values are represented as Means ± SEM. **p < 0.01.*

TABLE 3 | Enzyme activity of PDH, α-KGDH, SDH, and MDH of spleen at 30°C in the presence of palmitic acid.

Enzyme name	10% BSA control	Palmitic acid + 10% BSA	Percentage of change (%)
PDH	6.41 ± 0.63	4.87 ± 0.52	23.9**
α-KGDH	6.09 ± 0.57	2.51 ± 0.31	58.7**
SDH	30.80 ± 0.52	12.90 ± 0.79	58.1**
MDH	18.04 ± 0.87	13.38 ± 0.81	25.8**

*Values are represented as Means ± SEM. **p < 0.01.*

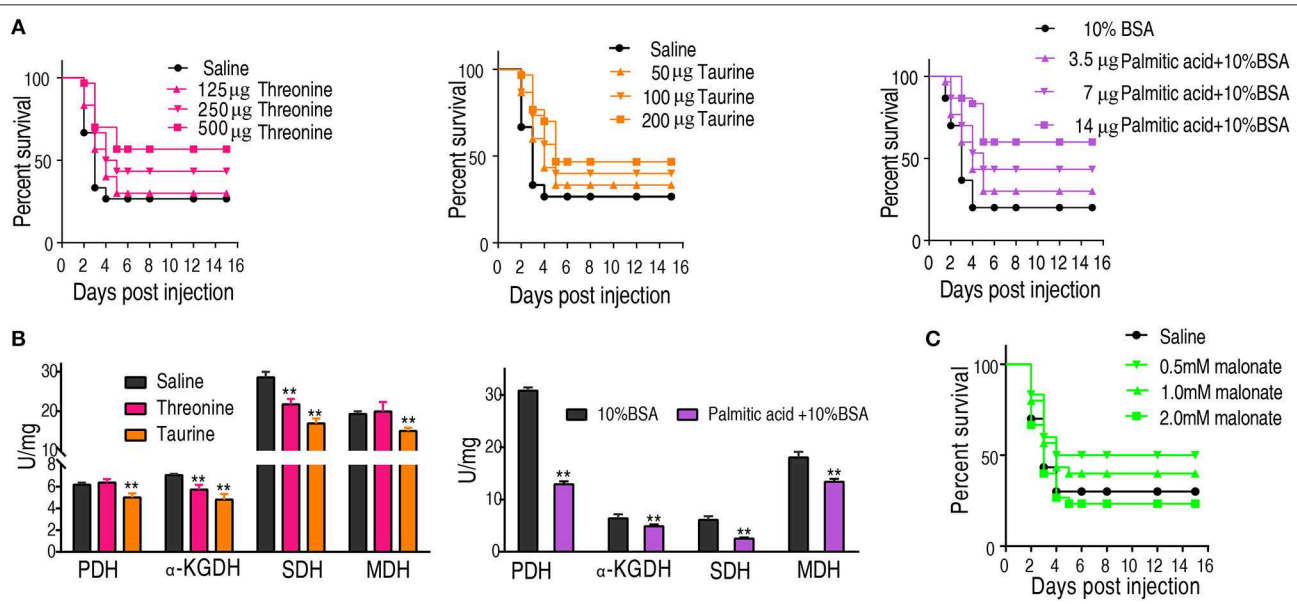


FIGURE 6 | Crucial biomarkers modulate the metabolism of crucian carps and promote their survival against bacterial infections. **(A)** The survival of crucian carps in the presence of crucial biomarkers upon *E. tarda* infection. *C. carassius* was treated with saline control or different dose crucial biomarkers at 30°C for 3 days, followed by bacterial challenge through intraperitoneal injection (1×10^5 CFU). The accumulative fish death was monitored for a total of 15 days' post-infection ($n = 30$ per group). **(B)** Activity of PDH, alpha-KGDH, SDH, and MDH of spleen in the presence of crucial biomarkers (200 μg taurine, 500 μg threonine, or 14 μg palmitic acid plus 10% BSA). Values are means ± SEM($n = 6$ per group), and statistic difference is analyzed with non-parametric Kruskal-Wallis one-way analysis with Dunn multiple comparison *post hoc* test. **$p < 0.01$. **(C)** Percent survival of crucial carps in the presence of malonate. *C. carassius* was treated with malonate at different doses for 12 h followed by *E. tarda* challenge through intraperitoneal injection (1×10^5 CFU). The accumulative fish death was monitored for a total of 15 days post-infection ($n = 30$ per group).

by the three metabolites. Therefore, our data provide direct evidence that these crucial metabolites, identified from water temperature-mediated metabolomes, regulate innate immune response. Among the genes of innate immunity, only 13 genes were selected as they are the only genes available for crucian carps in GeneBank, categorized to B-Jellyroll cytokines (TNF-α1 and TNF -α2), β-Trefoil cytokines (IL-1β1 and IL-1β2), Type I α helical cytokines (IL-11), Type II α helical cytokines (IFN-γ1-1 and IFN-γ1-2), TLR family (TLR 2, TLR 3, and TLR 9), lysozyme, complement system (C3), and nfkbiab (46). The function of B-Jellyroll cytokines, also called the TNF superfamily cytokines in fish, is similar to their mammalian counterparts that are expressed at early stage of bacterial infection (47). TNF-α plays a critical role in regulating inflammation by promoting phagocytosis, increasing the expression of immune genes and generation of bacterial-killing reactive oxygen species, and leukocyte homing, proliferation and migration in fish like trout (47–49). IL-1β, which belongs to the β-Trefoil cytokines, was the first interleukin identified in boy and cartilaginous fish (50). It is usually produced once the cells are activated by pattern recognition receptors (51). IL-1β plays a diverse pro-inflammatory roles that increases the number of phagocytes, phagocytic, and lysozyme activity, modulating the

TABLE 4 | Enzyme activity of PDH, α-KGDH, SDH, and MDH of spleen at 30°C in the presence threonine.

Enzyme	Saline control	Threonine	Percentage of change
PDH	6.18 ± 0.25	6.38 ± 0.43	3.2$^{n.s.}$
a-KGDH	7.05 ± 0.17	5.73 ± 0.61	18.7**
SDH	28.56 ± 2.00	21.77 ± 1.89	23.7**
MDH	19.29 ± 0.95	19.93 ± 3.43	3.3$^{n.s.}$

*Values are represented as Means ± SEM. **$p < 0.01$; n.s., no significance.*

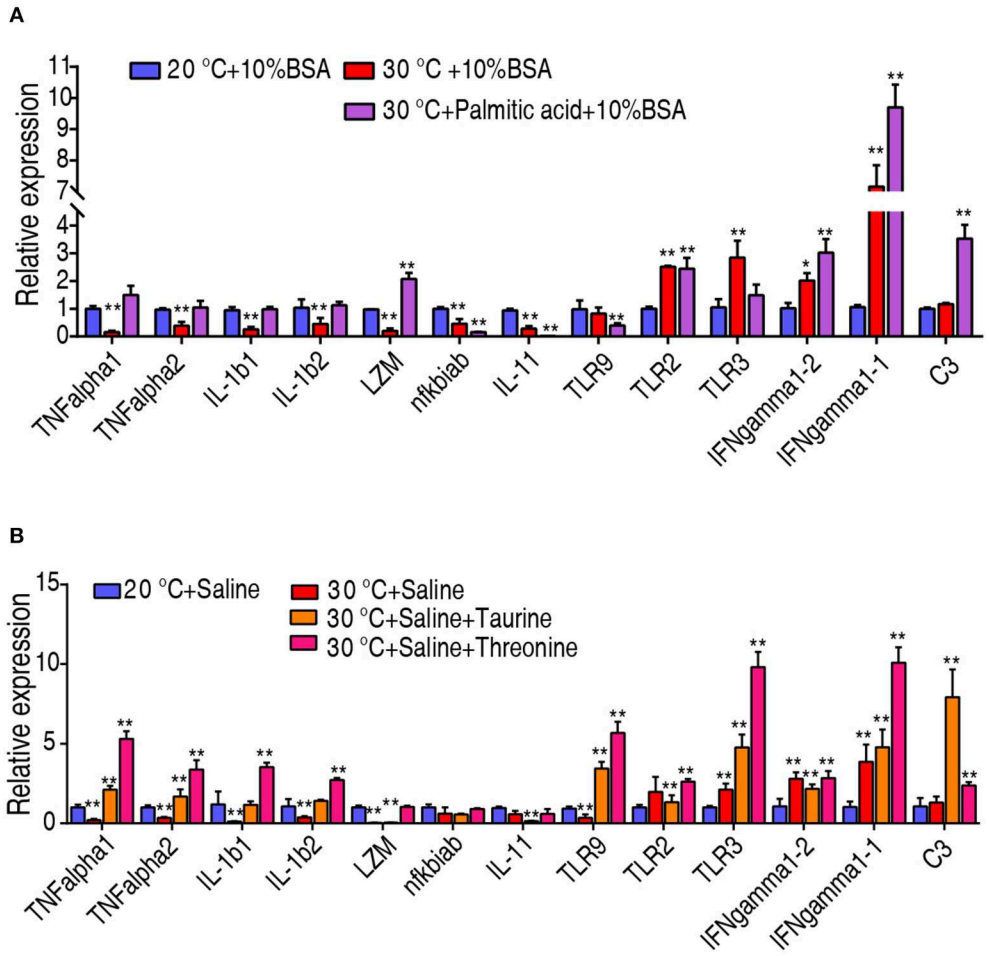


FIGURE 7 | Crucial biomarkers modulate the innate immune responses of fish at 30°C. **(A,B)** qRT-PCR for cytokine genes of *C. carassius* treated with control (saline or 10% BSA) or crucial biomarkers (200 μg taurine, 500 μg threonine, or 14 μg palmitic acid plus 10% BSA) for 3 days following *E. tarda* challenge through intraperitoneal injection (1×10^3 CFU). The spleens were collected 12 h post-injection for RNA extraction and qRT-PCR. Values are means ± SEM from six biological replicates. *$p < 0.05$; **$p < 0.01$.

IL-17 family for antimicrobial activity and enhancing antibody production when co-administrated with bacterial vaccine (52–56). The TLR family are conserved cell membrane receptors that recognize pathogen-associated molecular pattern or damage-associated molecular patterns, and they function in fish species to initiate an immune response (57–59). The complement system and lysozyme are innate molecules to target bacterial cells for cell lysis by disrupting the cell membrane. They mount a non-specific immune response and represent maternal immunity from fish embryo stage, and thus are important for fish survival during bacterial infection (60). Therefore, the innate immune response was compromised by crucian carp at high temperature, but it can be rescued through metabolic reprogramming.

In addition, palmitate, threonine, and taurine protect crucian carps from *E. tarda* infection at 30°C, possibly by inhibition of the TCA cycle. More importantly, the three metabolites exhibit similar impacts on the TCA cycle and innate immune responses. These results suggest that the TCA cycle related to the innate immunity.

In summary, the present study identifies important metabolites that could promote the fish survival upon bacterial infection at 30°C, a higher water temperature than their optimum water temperature. We showed that crucian carps grown at 30°C demonstrated a metabolome that is characterized by the enhanced TCA cycle but a reduced abundance of palmitate, threonine, and taurine. Importantly, exogenous palmitate, threonine, and taurine slightly inhibit the TCA cycle and restore the altered innate immune responses repressed at the higher temperature. These results indicate that higher water temperature reduces the survival of crucian carps via metabolism, which can be reprogramed through crucial biomarkers.

MATERIALS AND METHODS

Ethics Statement

This study was conducted in accordance with the recommendations in the Guide for the Care and Use of Laboratory Animals of the National Institutes of Health and maintained according to the standard protocols. All experiments were approved by the Institutional Animal Care and Use Committee of Sun Yat-sen University (Animal welfare Assurance Number: 16).

Bacteria Strains and Fish

Edwardsiedlla tarda EIB202 is a virulent strain isolated from the outbreak of farmed turbot and is a generous gift from Dr. Yuanxin Zhang (61). EIB202 was grown in Luria-Bertani (LB) broth or 1% LB agar plate.

Crucian carp, *C. carassius,* (body length: 3 ± 0.5 cm, body weight: 2 ± 0.2 g) was obtained from Crucian Carp Breeding Corporation (Guangzhou, P.R. China). *C. carassius* was free of *Edwardsiedlla* infection through microbiological detection. *C. carassius* was normally reared in 50 L water tanks equipped with Closed Recirculating Aquaculture Systems, and the maintaining physico-chemical parameters were: dissolved oxygen: 6–7 mg/L, carbon dioxide content: <10 mg/L, pH value: 7.0–7.5, nitrogen content: 1–2 mg/L, and nitrite content: 0.1–0.3 mg/L. These animals were cultured under this condition for 2 weeks before experimental manipulation and were fed twice daily with commercial fish feed (38% crude protein, 6% crude fat, and 16% crude ash related to wet matter, 7% crude fiber and 8% moisture, based on NRC recommendations, at a ratio of 3% of body weight per day) on a 12 h/12 h rhythm of light and darkness photoperiod always. The tank was cleaned once a day by siphoning up the food debris and feces. To accommodate *C. carassius* to different temperatures, the water temperature was gradually changed until the fish were adapted to constant temperature at 20 or 30°C. The water quality was monitored regularly.

Bacterial Challenge

To prepare *E. tarda* EIB202 for bacterial infection, a single colony was picked up from agar plate and grown in LB medium overnight. The overnight culture was diluted into fresh LB medium at 1:100 and grown with shaking at 200 rpm at 30°C until OD_{600} of the culture reached 1.0. Cells were pelleted by centrifugation and washed with 0.85% saline solution three times and suspended in saline solution.

For bacterial infection, each *C. carassius* cultured at 20 or 30°C was intraperitoneally injected with 10 μl 1×10^5 CFU bacterial suspension or saline only ($n = 30$ for each treatment). These crucian carps were observed for symptoms twice daily for 15 days for accumulative death.

Sample Preparation for GC-MS Analysis

Sample preparation was carried out as described previously (32). *C. carassius* cultured at 20 or 30°C were euthanized in ice slush (5 parts ice/1 part water, 0–4°C) for at least 10 min following cessation of gill movement, and left in the ice water for a total of 20 min after cessation of all movement to ensure death by hypoxia following the guidelines of NIH. *C. carassius* were rinsed with distilled water and then wiped thoroughly with sterilized gauze. Spleens were removed ascetically, where 25 mg of spleens were cut and immensed immediately in 1 mL cold methanol. Then, the samples were sonicated for 5 min at 10W-power setting at Ultrasonic Processor (JY92-IIDN, SCIENTZ), followed by centrifugation at 12,000 × g in 4°C for 10 min. The supernatant was collected and 10 μl 0.1 mg/ml ribitol (Sigma) was added as the internal standard. The supernatant was concentrated in a rotary vacuum centrifuge device (LABCONCO). The dried polar extracts were incubated with 80 μl methoxy amination hydrochloride (20 mg/ml pyridine) for 90 min at 37°C, followed by an addition of 80 μl N-methyl-N-trimethylsilyltrifluoroacetamide (MSTFA) (Sigma) and incubated for another 30 min at 37°C. Finally, the resulted samples were cooled down to room temperature prior to mass spectrometry analysis.

Gas Chromatography-Mass Spectrometry (GC-MS) Analysis

GC-MS analysis was carried out with a variation on the two-stage techniques as described previously (32). In brief, 1 μL derivatized sample was injected into a DBS-MS column using splitless injection, and analysis was carried out by Agilent 7890A

GC equipped with an Agilent 5975C VL MSD detector (Agilent Technologies). The initial temperature of the GC oven was held at 85°C for 5 min followed by an increase to 270°C at a rate of 15°C min^{-1} then held for 5 min. Helium was used as carrier gas and the flow was kept at 1 mL min^{-1} constantly. The MS was operated in a range of 50–600 m/z. For each sample, two technical replicates were prepared to confirm the reproducibility of the reported procedures.

Exogenous Administration of Taurine, Threonine or Palmitic Acid and Bacterial Challenge

C. carassius ($n = 330$) was randomly divided into five groups, including three metabolite groups ($n = 90$ per group), and two control groups ($n = 30$ per group), and acclimatized for 7 days at 30°C. For the three metabolites groups, *C. carassius* was intraperitoneally injected with taurine (Sigma) at three doses (50, 100, or 200 μg per fish; $n = 30$ for each dose), threonine (Sigma) at three doses (125, 250, or 500 μg per fish; $n = 30$ for each dose), or palmitic acid (Sigma) at three doses (3.5, 7.0, or 14.0 μg per fish; $n = 30$ for each dose). For the two control groups, they were either injected with saline only ($n = 30$) as a control to taurine and threonine groups, or with 10% bovine serum albumin (Sigma) as a control to palmitic acid group. The injection was conducted once daily for 3 days. Afterwards, *C. carassius* was challenged by intraperitoneal injection of *E. tarda* EIB202 with a dose of 10 μl 1×10^5 CFU/fish, and the fish mortality was observed for 15 days for accumulative death.

To quantify the transcriptional level of innate immune genes by qRT-PCR, *C. carassius* was intraperitoneally injected with taurine (200 μg per fish; $n = 20$), threonine (500 μg per fish; $n = 20$), or palmitic acid (14 μg per fish; $n = 20$) once daily for 3 days. Then, *C. carassius* were challenged with *E. tarda* EIB202 with a dose of 10 μl 1×10^3 CFU per fish. The spleens were aseptically removed and collected 12 h post-infection as stated above for RNA isolation.

TABLE 5 | Primers used for QRT-PCR analysis.

Gene	Primer	Sequence (5′-3′)
Actin	Forward	gggatgggacagaaggacag
	Reverse	acgcagctcgttgtagaagg
Tubulin	Forward	ctgctgggaactctattgtc
	Reverse	ctccaggtctacaaacacag
GAPDH	Forward	tgacccctccagtatgacca
	Reverse	gagggcctcctcaataccaa
TNFalpha1	Forward	tcacgctcaacaagtctcag
	Reverse	tggtcctttctccagtaaag
TNFalpha2	Forward	ccgctgtctgcttcacatt
	Reverse	ggccttggaagtgacattt
IL-1b1	Forward	atgcgctgctcaacttcat
	Reverse	ctggcccttattttgttgag
IL-1b2	Forward	caaagcgatcctcttcattt
	Reverse	attcgggtcatcagttttaa
IL-11	Forward	ttcgagtggctgaacagaac
	Reverse	aggcccagtcacagaagagc
TLR-2	Forward	cttagatgggctcactcatc
	Reverse	gggtgggagacatctttaag
TLR-3	Forward	tagatgccagctacaactcttt
	Reverse	ggctccccaattaacttcag
TLR-9	Forward	gccaacccatgttatcagtc
	Reverse	ggtgtcgcagatttttaaga
IFNgamma1-1	Forward	ctacgggtcctgaaagactt
	Reverse	gcctgggaagtagttttctc
IFNgamma1-2	Forward	tctggggagtatgcttgttga
	Reverse	gcctgggaagtagttttcttg
nfkbiab	Forward	cagtttggcgcagacatt
	Reverse	gcgcctttgctgattagaag
LZM	Forward	tgtgtctgatgtggctgtgc
	Reverse	tgcacacatagttgccaagtga
C3	Forward	tggggatggatctgaaaca
	Reverse	tgcccatgatgaggtacga

Measurement of Enzyme Activity

Enzyme activities were measured as described previously (37, 62). In brief, spleens freshly removed from fish were rinsed with pre-cooled 1 × PBS, resuspended in lysate buffer, and disrupted by sonication for 5 mins at 10W power setting. Following centrifugation, the supernatant, defined as the total protein, was transferred to a new tube, and the protein concentration in the supernatant was determined by Bradford assay. The total proteins of 100 μg were applied for pyruvate dehydrogenase or α-ketoglutarate dehydrogenase assay, and 250 μg of total proteins for succinate dehydrogenase or malate dehydrogenase assays. The enzymatic assay was conducted by mixing an equal volume of the protein sample and reaction buffer to a final volume of 200 μL in 96-well plate. The plate was further incubated at 37°C for 15 min, and the absorbance was read at 570 nm on a microplate reader. The enzyme activity was calculated by plotting against the standard curve. The reaction mixtures are as follows: PDH reaction mixture: 0.5 mM 3-(4,5-di methyl thiazol-2-yl)-2,5-diphenyltetrazolium bromide (MTT) (Sangon Biotech), 1 mM $MgCl_2$ (Sigma), 6.5 mM phenazine methosulfate (PMS) (Sangon Biotech), 0.2 mM thiamine pyrophosphate (TPP) (Sangon Biotech), and 2 mM sodium pyruvate (Sigma) and 50 mM phosphate buffered saline (PBS) (Invitrogen); KGDH reaction mixture: 0.5 mM MTT, 1 mM $MgCl_2$, 6.5 mM PMS, 0.2 mM TPP, 2 mM α-ketoglutaric acid sodium salt (Sigma) and 50 mM PBS; SDH reaction mixture: 0.5 mM MTT, 13 mM PMS, 5 mM sodium succinate (Sigma), and 50 mM PBS; MDH reaction mixture: 0.5 mM MTT, 13 mM PMS, 50 mM malic acid disodium salt (Sigma), and 50 mM PBS.

RNA Isolation and qRT-PCR

Total RNA was isolated with Trizol (Invitrogen, USA) and quantified by Nanodrop (Thermo Scientific). Reverse transcription-PCR (qRT-PCR) was carried out using Prime-Script™ RT reagent Kit with gDNA eraser (Takara, Japan)

with 1 μg of total RNA according to manufacturer's instructions. The experiment was performed in six biological replicates.

qRT-PCR was performed with a LightCycler-480 (Roche, Germany) using SYBR Premix Ex Taq II Kits (Takara, Japan) following the manufacture's instruction. The experiment was performed in six biological replicates. Primers for each gene were listed in **Table 5**, and each primer pair was specific. *Actin, tubulin and GAPDH* genes were chosen as the internal control. The relative expression of each gene was determined by comparative threshold cycle method ($2^{-\Delta\Delta CT}$ method).

Data Processing and Statistical Analysis

For the GC-MS data analysis, metabolites from the GC-MS spectra were identified by searching against National Institute of Standards and Technology (NIST) library used the software of NIST MS search 2.0. The resulting data matrix was normalized using the concentrations of added internal standards, which were subsequently removed so that the data could be used for modeling consisted of the extracted compound. Peak areas of all identified metabolites were normalized by ribitol as internal standard. Statistical difference of metabolites in each sample was obtained by Kruskal–Wallis test and Mann–Whitney test using SPSS 23.0 (IBM Corp, USA). Z-score and hierarchical clustering were used to analyze the normalization area. Hierarchical clustering was completed in the R platform (https://cran.r-project.org). Multivariate statistical analysis included principal component analysis (PCA) and orthogonal partial least square discriminant analysis (OPLS-DA) implemented with SIMCA 12.0 (Umetrics, Umeå, Sweden).

For the data analysis of qRT-PCR and enzyme activity, non-parametric Kruskal-Wallis one-way analysis with Dunn multiple comparison *post hoc* test was used, SPSS 23.0, $p < 0.05$ was considered significant.

DATA AVAILABILITY

All datasets generated for this study are included in the manuscript and/or the **Supplementary Files**.

ETHICS STATEMENT

This study was conducted in accordance with the recommendations in the Guide for the Care and Use of Laboratory Animals of the National Institutes of Health and maintained according to the standard protocols. All experiments were approved by the Institutional Animal Care and Use Committee of Sun Yat-sen University (Animal welfare Assurance Number: 16).

AUTHOR CONTRIBUTIONS

BP conceptualized and designed the project and wrote the manuscript. MJ and ZC performed the experiments. MJ and JZ performed the data analysis. BP, MJ, ZC, and JZ interpreted the data. All the authors reviewed the manuscript.

FUNDING

This work was sponsored by grants from the National Key R&D Research program of China (2016YFD0501307), NSFC project (31822058, 31672656, 31872602), and the Fundamental Research Funds for the Central Universities (18lgzd14).

SUPPLEMENTARY MATERIAL

The Supplementary Material for this article can be found online at: https://www.frontiersin.org/articles/10.3389/fimmu.2019.01991/full#supplementary-material

REFERENCES

1. Connolly MA. *A Field Manual-Communicable Disease Control in Emergencies*. WHO (2005).
2. Shapiro RS, Cowen LE. Thermo control of microbial development and virulence: molecular mechanism of microbial temperature sensing. *mBio*. (2012) 3:e00238-12. doi: 10.1128/mBio.00238-12
3. Hu YH, Zhou HZ, Jin QW, Zhang J. The serine protease autotransporter Tsh contributes to the virulence of *Edwarsiella tarda*. *Vet Microbiol*. (2016) 189:68–74. doi: 10.1016/j.vetmic.2016.04.021
4. Awan F, Dong Y, Wang N, Liu J, Ma K, Liu Y. The fight for invincibility: environmental stress response mechanism and *Aeromonas hydrophila*. *Microb Pathog*. (2018) 116:135–45. doi: 10.1016/j.micpath.2018.01.023
5. Huang L, Guo L, Xu L, Qin Y, Zhao L, Su Y, et al. The role of rpoS in the regulation of *Vibrio alginolyticus* virulence and the response to diverse stresses. *J Fish Dis*. (2019) 42:703–12. doi: 10.1111/jfd.12972
6. Yao Z, Guo Z, Wang Y, Li W, Fu Y, Lin Y, et al. Integrated succinylome and metabolome profiling reveals crucial role of S-ribosylhomocystein lysase in quorum sensing and metabolism of *Aeromonas hydrophila*. *Mol Cell Proteomics*. (2019) 18:200–15. doi: 10.1074/mcp.RA118.001035
7. Avtalion RR, Willian Clem L. Environmental control of the immune response in fish. *Crit Rev Environ Sci Tech*. (1981) 11:163–88. doi: 10.1080/10643388109381687
8. Greenspan SE, Bower DS, Roznik EA, Pike DA, Marantelli G, Alford RA, et al. Infection increases vulnerability to climate change via effects on host thermal tolerance. *Sci Rep*. (2017) 7:9349. doi: 10.1038/s41598-017-09950-3
9. Hector TE, Sqro CM, Hall MD. Pathogen exposure disrupts an organism's ability to cope with thermal stress. *Glob Change Biol*. (2019) 1–13. doi: 10.1111/gcb.14713
10. Wang Y, Wang X, Ali F, Li Z, Fu Y, Yang X, et al. Comparative extracellular proteomics of *Aeromonas hydrophila* reveals iron-regulated secreted proteins as potential vaccine candidates. *Front Immunol*. (2019) 10:256. doi: 10.3389/fimmu.2019.00256
11. Liao XL, Cheng L, Xu P, Lu GQ, Wachholtz M, Sun XW, et al. Transcriptome analysis of crucian carp (*Carassius auratus*), an important aquaculture and hypoxia-tolerant species. *PLoS ONE*. (2013) 8:e62308. doi: 10.1371/journal.pone.0062308
12. Sollid J, Weber RE, Nilsson GE. Temperature alters the respiratory surface area of crucian carp *Carassius carassius* and goldfish *Carassius auratus*. *J Exp Biol*. (2005) 208:1109–16. doi: 10.1242/jeb.01505
13. Rhee JS, Jeong CB, Kim DH, Kim IIC, Lee YS, Lee CL, et al. (2014). Immune gene discovery in the crucian carp *Carassius auratus*. *Fish Shellfish Immunol*. 36:240–51. doi: 10.1016/j.fsi.2013.11.009
14. Liu XJ, Zhu WC, Su YB, Guo C, Zeng ZH, Li H, et al. Characterization of ampicillin-stressed proteomics and development of a direct method for

detecting drug-binding proteins in *Edwardsiella tarda*. *J Proteomics*. (2015) 116:97–105. doi: 10.1016/j.jprot.2014.12.018
15. Ling SH, Wang XH, Xie L, Lim TM, Leung KY. Use of green fluorescent protein (GFP) to study the invasion pathways of *Edwardsiella tarda* in *in vivo* and *in vitro* fish models. *Microbiology*. (2000) 146:7–19. doi: 10.1099/00221287-146-1-7
16. Xu T, Zhang XH. *Edwardsiella tarda*: an intriguing problem in aquaculture. *Aquaculture*. (2014) 431:129–35. doi: 10.1016/j.aquaculture.2013.12.001
17. Li Z, Liu X, Liu J, Zhang K, Yu H, He Y, et al. Transcriptome profiling based on protein-protein interaction networks provides a core set of genes for understanding blood immune response mechanisms against *Edwardsiella tarda* infection in Japanese flounder (*Paralichthys olivaceus*). *Dev Comp Immunol*. (2018) 78:100–13. doi: 10.1016/j.dci.2017.09.013
18. Katharios P, Kalatzis PG, Kokkari C, Pavlidis M, Wang Q. Characterization of a highly virulent *Edwardsiella anguillarum* strain isolated from Greek aquaculture, and a spontaneously induced prophage therein. *Front Microbiol*. (2019) 10:141. doi: 10.3389/fmicb.2019.00141
19. Meyer FP, Bullock GL. *Edwardsiella tarda*, a new pathogen of channel catfish (*Ictalurus punctatus*). *Appl Microbiol*. (1973) 25:155–6.
20. Miyazaki T, Kaige N. Comparative histopathology of edwardsiellosis in fishes. *Fish Pathol*. (1985) 20:219–27. doi: 10.3147/jsfp.20.219
21. John AM, Prakash JA, Simon EG, Thomas N. *Edwardsiella tarda* sepsis with multiple liver abscesses in a patient with Cushing's syndrome. *Indian J Med Microbiol*. (2012) 30:352–4. doi: 10.4103/0255-0857.99503
22. Miniero DY, Xavier de Oliverir MG, Paulo Vieira Cunha M, Soares Franco L, Pulecio Santos SL, Zanolli Moreno L, et al. *Edwardsiella tarda* outbreak affecting fishes and aquatic birds in Brazil. *Vet Q*. (2018) 38:99–105. doi: 10.1080/01652176.2018.1540070
23. Woo PTK, Bruno DW. Fish diseases and disorders. Volume 3, viral, bacterial and fungal infections. In: Evans JJ, Klesius PH, Plumb JA, Shoemaker CA, editors. *Edwardsiella septicaemias*. 2nd ed. Wallingford: CABI International (2010). p. 512–534.
24. Park SB, Aoki T, Jung TS. Pathogenesis of and strategies for preventing *Edwardsiella tarda* infection in fish. *Vet Res*. (2012) 43:67. doi: 10.1186/1297-9716-43-67
25. Kim JH, Park HJ, Kim KW, Hwang IK, Kim DH, Oh CW, et al. Growth performance, oxidative stress, and non-specific immune responses in juvenile sablefish, *Anoplopoma fimbria*, by changes of water temperature and salinity. *Fish Physiol Biochem*. (2017) 43:1421–31. doi: 10.1007/s10695-017-0382-z
26. Verma AK, Pal AK, Manush SH, Das T, Dalvi RS, Chandrachoodan PP, et al. Persistent sub-lethal chlorine exposure augments temperature induced immunosuppression in *Cyprinus carpio* advanced fingerlings. *Fish Shellfish Immunol*. (2007) 22:547–55. doi: 10.1016/j.fsi.2006.08.001
27. Engelsma MY, Hougee S, Nap D, Hofenk M, Rombout JH, van Muiswinkel WB, et al. Multiple acute temperature stress affects leucocyte populations and antibody responses in common carp, *Cyprinus carpio* L. *Fish Shellfish Immunol*. (2003) 15:397–410. doi: 10.1016/S1050-4648(03)00006-8
28. Le Morvan C, Deschaux P, Troutaud D. Effects and mechanisms of environmental temperature on carp (*Cyprinus carpio*)anti-DNP antibody response and non-specific cytotoxic cell activity: a kinetic study. *Dev Comp Immunol*. (1996) 20:331–40. doi: 10.1016/S0145-305X(96)00027-4
29. Zhao XL, Wu CW, Peng XX, Li H. Interferon-α2b against microbes through promoting biosynthesis of unsaturated fatty acids. *J Proteome Res*. (2014) 13:4155–63. doi: 10.1021/pr500592x
30. Chen XH, Liu SR, Peng B, Li D, Cheng ZX, Zhu JX, et al. Exogenous L-valine promotes phagocytosis to kill multidrug-resistant bacterial pathogens. *Front Immunol*. (2017) 8:207. doi: 10.3389/fimmu.2017.00207
31. Zeng ZH, Du CC, Liu SR, Li H, Peng XX, Peng B. Glucose enhances tilapia against *Edwardsiella tarda* infection through metabolome reprogramming. *Fish Shellfish Immunol*. (2017) 61:34–43. doi: 10.1016/j.fsi.2016.12.010
32. Jiang M, Gong QY, Lai SS, Cheng ZX, Chen ZG, Zheng J, et al. Phenylalanine enhances innate immune response to clear ceftazidime-resistant *Vibrio alginolyticus* in *Danio rerio*. *Fish Shellfish Immunol*. (2019) 84:912–9. doi: 10.1016/j.fsi.2018.10.071
33. Peng B, Su YB, Li H, Han Y, Guo C, Tian YM, et al. Exogenous alanine or/and glucose plus kanamycin kills antibiotic-resistant bacteria. *Cell Metab*. (2015) 21:249–61. doi: 10.1016/j.cmet.2015.01.008
34. Su YB, Peng B, Han Y, Li H, Peng XX. Fructose restores susceptibility of multidrug-resistant *Edwardsiella tarda* to kanamycin. *J Proteome Res*. (2015) 14:1612–20. doi: 10.1021/pr501285f
35. Cheng ZX, Ma YM, Li H, Peng XX. N-acetylglucosamine enhances survival ability of tilapias infected by *Streptococcus iniae*. *Fish Shellfish Immunol*. (2014) 40:524–30. doi: 10.1016/j.fsi.2014.08.008
36. Su YB, Peng B, Li H, Cheng ZX, Zhang TT, Zhu JX, et al. The pyruvate cycle increases aminoglycosides efficacy and provides respiratory energy in bacteria. *Proc Natl Acad Sci USA*. (2018) 115:E1578–87. doi: 10.1073/pnas.1714645115
37. Yang J, Zeng ZH, Yang MJ, Cheng ZX, Peng XX, Li H. NaCl promotes antibiotic resistance by reducing redox states in *Vibrio alginolyticus*. *Environ Microbiol*. (2018) 20:4022–36. doi: 10.1111/1462-2920.14443
38. Liu SR, Peng XX, Li H. Metabolic mechanism of ceftazidime resistance in *Vibrio alginolyticus*. *Infect Drug Resist*. (2019) 12:417–29. doi: 10.2147/IDR.S179639
39. Zhao XL, Han Y, Ren ST, Ma YM, Li H, Peng XX. L-proline increases survival of tilapias infected by *Streptococcus agalactiae* in higher water temperature. *Fish Shellfish Immunol*. (2015) 44:33–42. doi: 10.1016/j.fsi.2015.01.025
40. Ma YM, Yang MJ, Wang S, Li H, Peng XX. Liver functional metabolomics discloses an action of L-leucine against *Streptococcus iniae* infection in tilapias. *Fish Shellfish Immunol*. (2015) 45:414–21. doi: 10.1016/j.fsi.2015.04.037
41. Chen XH, Zhang BW, Li H, Peng XX. Myo-inositol improves the host's ability to eliminate balofloxacin-resistant *Escherichia coli*. *Sci Rep*. (2015) 5:10720. doi: 10.1038/srep10720
42. Wu CW, Zhao XL, Wu XJ, Wen C, Li H, Chen XH, et al. (2015). Exogenous glycine and serine promote growth and antifungal activity of *Penicillium citrinum* W1 from the south-west Indian Ocean. FEMS Microbiol. *Letter*. 362:fnv040. doi: 10.1093/femsle/fnv040
43. Maudsley S, Chadwick W, Wang L, Zhou Y, Martin B, Park SS. Bioinformatic approaches to metabolic pathway analysis. *Methods Mol Biol*. (2011) 756:99–130. doi: 10.1007/978-1-61779-160-4_5
44. Marcos-López M, Gale P, Oidtmann BC, Peeler EJ. Assessing the impact of climate change on disease emergence in freshwater fish in the United Kingdom. *Transbound Emerg Dis*. (2010) 57:293–304. doi: 10.1111/j.1865-1682.2010.01150.x
45. Gandar A, Laffaille P, Canlet C, Tremblay-Franco M, Gautier R, Perrault A, et al. Adaptive response under multiple stress exposure in fish: from the molecular to individual level. *Chemosphere*. (2017) 188:60–72. doi: 10.1016/j.chemosphere.2017.08.089
46. Zou J, Secombes CJ. The function of fish cytokines. *Biology*. (2016) 5:E23. doi: 10.3390/biology5020023
47. Zou J, Peddie S, Scapigliati G, Zhang Y, Bols NC, Ellis AE, et al. Functional characterization of the recombinant tumor necrosis factors in rainbow trout, *Oncorhynchus mykiss*. *Dev Comp Immunol*. (2003) 27:813–22. doi: 10.1016/S0145-305X(03)00077-6
48. Boecke A, Sieger D, Neacsu CD, Kashkar H, Krönke M. Factor associated with neutral sphingomyelinase activity mediates navigational capacity of leukocytes responding to wounds and infection: live imaging studies in zebrafish larvae. *J Immunol*. (2012) 189:1559–66. doi: 10.4049/jimmunol.1102207
49. Lu XJ, Chen Q, Yang GJ, Chen J. The TNFα converting enzyme (TACE) from ayu (*Plecoglossus altivelis*) exhibits TNFα shedding activity. *Mol Immunol*. (2015) 63:497–504. doi: 10.1016/j.molimm.2014.10.010
50. Bird S, Wang T, Zou J, Cunningham C, Secombes CJ. The first cytokine sequence within cartilaginous fish: IL-1 beta in the small spotted catshark (*Scyliorhinus canicula*). *J Immunol*. (2002) 168:3329–40. doi: 10.4049/jimmunol.168.7.3329
51. Vojtech LN, Scharping N, Woodson JC, Hansen JD. Roles of inflammatory caspases during processing of zebrafish interleukin-1β in *Francisella noatunensis* infection. *Infect Immun*. (2012) 80:2878–85. doi: 10.1128/IAI.00543-12
52. Hong S, Peddie S, Campos-Pérez JJ, Zou J, Secombes CJ. The effect of intraperitoneally administered recombinant IL-1beta on immune parameters and resistance to *Aeromonas salmonicida* in the rainbow trout (*Oncorhynchus mykiss*). *Dev Comp Immunol*. (2003) 27:801–12. doi: 10.1016/S0145-305X(03)00056-9

53. Wang X, Li C, Thongda W, Luo Y, Beck B, Peatman E. Characterization and mucosal responses of interleukin 17 family ligand and receptor genes in channel catfish *Ictalurus punctatus*. *Fish Shellfish Immunol*. (2014) 38:47–55. doi: 10.1016/j.fsi.2014.02.020
54. Taechavasonyoo A, Hirono I, Kondo H. The immune-adjuvant effect of Japanese flounder *Paralichthys olivaceus* IL-1β. *Dev Comp Immunol*. (2013) 41:564–8. doi: 10.1016/j.dci.2013.07.003
55. Yamasaki M, Araki K, Maruyoshi K, Matsumoto M, Nakayasu C, Moritomo T, et al. Comparative analysis of adaptive immune response after vaccine trials using live attenuated and formalin-killed cells of *Edwardsiella tarda* in ginbuna crucian carp (*Carassius auratus langsdorfii*). *Fish Shellfish Immunol*. (2015) 45:437–42. doi: 10.1016/j.fsi.2015.04.038
56. Cheng ZX, Chu X, Wang SN, Peng XX, Li H. Six genes of ompA family shuffling for development of polyvalent vaccines against *Vibrio alginolyticus* and *Edwardsiella tarda*. *Fish Shellfish Immunol*. (2018) 75:308–15. doi: 10.1016/j.fsi.2018.02.022
57. Matzinger P. The danger model: a renewed sense of self. *Science*. (2002) 296:301–5. doi: 10.1126/science.1071059
58. Medzhitov R. Recognition of microorganisms, activation of the immune response. *Nature*. (2007) 449:819–26. doi: 10.1038/nature06246
59. Rebl A, Goldammer T, Seyfert HM. Toll-like receptor signaling in body fish. *Vet Immunol Immunopathol*. (2010) 134:139–50. doi: 10.1016/j.vetimm.2009.09.021
60. Wang Z, Zhang S. The role of lysozyme and complement in the antibacterial activity of zebrafish (*Danio rerio*) egg cytosol. *Fish Shellfish Immunol*. (2010) 29:773–7. doi: 10.1016/j.fsi.2010.07.002
61. Wang QY, Yang MJ, Xiao JF, Wu HZ, Wang X, Lv YZ, et al. Genome sequence of the versatile fish pathogen *Edwardsiella tarda* provides insights into its adaptation to braod host ranges and intracellular niches. *PLos ONE*. (2009) 4:e7646. doi: 10.1371/journal.pone.0007646
62. Ma Y, Guo C, Li H, Peng XX. Low abundance of respiratory nitrate reductase is essential for *Escherichia coli* in resistance to aminoglycoside and cephalosporin. *J Proteomics*. (2013) 87:78–88. doi: 10.1016/j.jprot.2013.05.019

Conflict of Interest Statement: The authors declare that the research was conducted in the absence of any commercial or financial relationships that could be construed as a potential conflict of interest.

Copyright © 2019 Jiang, Chen, Zheng and Peng. This is an open-access article distributed under the terms of the Creative Commons Attribution License (CC BY). The use, distribution or reproduction in other forums is permitted, provided the original author(s) and the copyright owner(s) are credited and that the original publication in this journal is cited, in accordance with accepted academic practice. No use, distribution or reproduction is permitted which does not comply with these terms.

frontiers in Immunology

ORIGINAL RESEARCH
published: 06 September 2019
doi: 10.3389/fimmu.2019.02119

Detection of Salmonid IgM Specific to the *Piscine Orthoreovirus* Outer Capsid Spike Protein Sigma 1 Using Lipid-Modified Antigens in a Bead-Based Antibody Detection Assay

Lena Hammerlund Teige[1], *Subramani Kumar*[1,2], *Grethe M. Johansen*[1], *Øystein Wessel*[1], *Niccolò Vendramin*[3], *Morten Lund*[4,5], *Espen Rimstad*[1], *Preben Boysen*[1] *and Maria K. Dahle*[4]*

[1] *Department of Food Safety and Infection Biology, Norwegian University of Life Sciences, Oslo, Norway,* [2] *Stem Cell and Cancer Biology Lab, Centre for Biotechnology, Anna University, Chennai, India,* [3] *National Institute of Aquatic Resources, Technical University of Denmark, Lyngby, Denmark,* [4] *Department of Fish Health, Norwegian Veterinary Institute, Oslo, Norway,* [5] *PatoGen, Alesund, Norway*

OPEN ACCESS

Edited by:
Irene Salinas, University of New Mexico, United States

Reviewed by:
Kevin R. Maisey, Centro de Biotecnología Acuícola, Universidad de Santiago de Chile, Chile
Kim Dawn Thompson, Moredun Research Institute, United Kingdom

***Correspondence:**
Maria K. Dahle
maria.dahle@vetinst.no

Specialty section:
This article was submitted to Comparative Immunology, a section of the journal Frontiers in Immunology

Received: *10 April 2019*
Accepted: *22 August 2019*
Published: *06 September 2019*

Citation:
Teige LH, Kumar S, Johansen GM, Wessel Ø, Vendramin N, Lund M, Rimstad E, Boysen P and Dahle MK (2019) Detection of Salmonid IgM Specific to the Piscine Orthoreovirus Outer Capsid Spike Protein Sigma 1 Using Lipid-Modified Antigens in a Bead-Based Antibody Detection Assay. Front. Immunol. 10:2119. doi: 10.3389/fimmu.2019.02119

Bead-based multiplex immunoassays are promising tools for determination of the specific humoral immune response. In this study, we developed a multiplexed bead-based immunoassay for the detection of Atlantic salmon (*Salmo salar*) antibodies against *Piscine orthoreovirus* (PRV). Three different genotypes of PRV (PRV-1, PRV-2, and PRV-3) cause disease in farmed salmonids. The PRV outer capsid spike protein σ1 is predicted to be a host receptor binding protein and a target for neutralizing and protective antibodies. While recombinant σ1 performed poorly as an antigen to detect specific antibodies, N-terminal lipid modification of recombinant PRV-1 σ1 enabled sensitive detection of specific IgM in the bead-based assay. The specificity of anti-PRV-1 σ1 antibodies was confirmed by western blotting and pre-adsorption of plasma. Binding of non-specific IgM to beads coated with control antigens also increased after PRV infection, indicating a release of polyreactive antibodies. This non-specific binding was reduced by heat treatment of plasma. The same immunoassay also detected anti-PRV-3 σ1 antibodies from infected rainbow trout. In summary, a refined bead based immunoassay created by N-terminal lipid-modification of the PRV-1 σ1 antigen allowed sensitive detection of anti-PRV-1 and anti-PRV-3 antibodies from salmonids.

Keywords: Atlantic salmon (*Salmo salar* L.), antibody, IgM, bead-based immunoassay, *Piscine orthoreovirus* (PRV), heart and skeletal muscle inflammation, heat inactivated plasma

INTRODUCTION

Atlantic salmon (*Salmo salar* L.) aquaculture has become an intensive and large-scale industry, and control of infectious diseases is an increasingly important task. Infectious diseases may be counteracted by vaccination, however, vaccine development against viral diseases in Atlantic salmon has not been straightforward, and few commercially available, efficient virus vaccines, are in use (1). An associated challenge has been to identify good correlates of protection, i.e., assays that can predict protective immunity (2). Important here are assays for detection of specific antibodies.

Bead-based multiplex immunoassays, such as the Luminex xMAP technology, have been successfully used to detect mammalian antibodies for more than a decade (3–5). This method has the potential to detect specific antibodies against several antigens simultaneously, and can be used to identify antibodies directed against a wide range of antigens in one sample using small amounts of antigens and sample material. According to producers, the cost of the xMAP assay is about half the cost of the same analysis using an Enzyme-Linked Immunosorbent Assays (ELISA) (www.bio-rad.com/webroot/web/pdf/lsr/literature/6313.pdf). The possibility to measure multiple analytes in the same sample further decrease the cost of each analysis. In addition to this, the xMAP assay is time-saving, can be used with much smaller sample volumes, uses around 1/50 the amount of capture antigen and offers broader dynamic range and higher sensitivity (3, 6, 7). The first bead-based multiplex immunoassays made to detect virus-specific antibodies in farmed Atlantic salmon were created and published in 2017 (8).

In mammals, the dominating circulating antibody isotype is IgG, while IgM is generally of lower affinity and comparatively more polyreactive (9); hence most assays to detect mammalian specific antibody responses target IgG. In contrast, the dominating isotype in teleost fish serum is IgM (10), requiring antibody responses to be measured within this compartment. The limited specificity of IgM is expected to give rise to detection of unspecific targets in fish, experienced as false positives in an antibody assay. Serology, i.e., detecting previous exposure to specific pathogen antigen by antibody repertoires, has not been widely used in aquaculture, but is commonly used for humans and in terrestrial animal husbandry for diagnosis and surveillance purposes. ELISAs with whole viral particles or recombinant viral proteins as capture antigen and neutralization bioassays have been used for diagnostics in aquaculture (11–15), but these methods require relatively large volumes of sample material and are time-consuming and costly when analyzing for antibodies against multiple target antigens.

Piscine orthoreovirus (PRV) belongs to the genus *Orthoreovirus* in the family *Reoviridae,* which have a segmented double-stranded RNA genome enclosed in a double-layered icosahedral capsid. Different PRV genotypes cause diseases in farmed salmonids; including PRV-1 mediated heart and skeletal muscle inflammation (HSMI) in Atlantic salmon (16, 17), PRV-2 mediated erythrocytic inclusion body syndrome (EIBS) in coho salmon (*Onchorhynchus kisutchi*) in Japan (18), and PRV-3 mediated anemia and HSMI-like heart pathology in rainbow trout (*Onchorhynchus mykiss*) in Europe (19–22).

HSMI is one of the most prevalent diseases in farmed Atlantic salmon in Norway (16, 23, 24), and is reported from farmed salmon in several other countries as well (25–27). During the course of HSMI in Atlantic salmon, the virus peak occurs after replication in the red blood cells (24). This is followed by infection of myocytes (28), which is associated with inflammation in the heart- and skeletal red muscles (16, 17, 29). Typical histopathological signs include epi-, endo- and myocarditis, myositis, and necrosis of myocardium and red skeletal muscle (30). Mortality from HSMI varies from 0 to 20% in a net-pen, but near 100% of the fish show histopathological changes (31). Experiments have associated HSMI with reduced tolerance to hypoxic stress, which may increase mortality (32). PRV-1 is ubiquitous in farmed Atlantic salmon a few months after sea entry, presumably due to a combination of virus, host and management factors such as infectivity, host susceptibility, amounts of shedding, farms size, density of farms, and persistence of infection (33). Persistence of PRV-1 has also been associated with melanized foci in white skeletal muscle (34).

PRV-3 can infect both rainbow trout and Atlantic salmon, but with a slower replication rate and less heart pathology in salmon (20). The virus has been detected in farmed salmonids in several European countries and Chile (22, 25, 35, 36), and in wild seatrout (*Salmo trutta*) and Atlantic salmon in Norway (37). PRV-3 has an 80–90% nucleotide and amino acid sequence identity to PRV-1, and rabbit antisera raised against PRV-1 proteins cross-reacts with PRV-3 proteins (35). Secondary structure predictions also support a high conservation of protein structure between homologous PRV-1 and PRV-3 proteins (35).

The information on protein structure and function in PRV is limited. *Mammalian orthoreovirus* (MRV) has been extensively studied, and based on strong conservation of secondary structure, is used as a model for predicting PRV structure and infection cycle. Based on sequence homology to MRV and other reoviruses, a PRV particle is predicted to consist of nine proteins forming the inner and outer capsids, and there are three additional non-structural proteins involved in the replication process in the infected cell (38). In MRV, trimers of the σ1 protein form spikes in the outer capsid and is the cell attachment protein and serotype determinant (39–41). Genetic analysis of PRV indicate that σ1 is the cell attachment protein for PRV as well (38). Monoclonal antibodies directed against MRV σ1 have been shown to be neutralizing (42).

Bead-based multiplex immunoassays using recombinant outer capsid μ1c and virus-factory μNS proteins were recently used to demonstrate PRV-specific IgM in plasma from experimentally PRV-1-infected Atlantic salmon (8) and PRV-3-infected rainbow trout (21). Recombinant PRV σ1 was also tested (8), but failed to bind antibodies from plasma efficiently. The PRV σ1 spike protein is particularly interesting, as it is likely to be the receptor binding protein, and antibodies directed against epitopes on σ1 could be virus neutralizing and protective.

Common bacterial expression systems can synthetize misfolded proteins or proteins without the correct post-translational modifications. This is a likely explanation of why the previously tested PRV σ1 failed at binding antibodies in the immunoassay. Lipid modification is a natural part of post-translational modifications of proteins targeting the outer or inner membrane in gram negative bacteria (43). The lipid-modification and membrane localization can contribute to a more correct conformation of the recombinant protein compared to cytosolic production. Bacterial lipid modification is controlled via an N-terminal signal peptide in the prolipoprotein. Through the secretory and twin-arginine translocation (Sec and Tat) pathways (44), three consecutive enzymatic steps lead to modification of a cysteine residue in the signal peptide, turning

it into N-acyl S-diacylglyceryl cysteine (45). In addition to affecting the protein conformation, lipid modification can also help proteins attach to hydrophobic surfaces, like the polystyrene plastic in ELISA plates, in the right conformation via their hydrophobic lipid part. This is a potential way of improving a diagnostic immunoassay (46, 47). In this manner, an ELISA using the ICP11 protein of shrimp white spot syndrome virus (WSSV) was recently optimized using bacterial lipid modification (46).

We targeted recombinant PRV σ1 for the bacterial lipid modification system by fusing it to an N-terminal peptide containing the Tat prolipoprotein signaling sequence in the pG-TL vector, thereby targeting it for modification with an N-acyl-S-diacylglyceryl moiety (48). By coupling this modified antigen (LM-PRVσ1) to beads in the multiplex immunoassay, we were able to detect specific antibodies against PRV σ1. Here, we demonstrate the Atlantic salmon antibody response against PRV-1 σ1, and the cross-reactivity with rainbow trout antibodies against PRV-3 σ1.

MATERIALS AND METHODS

Experimental PRV-1 Infection Trial and Blood Sampling in Atlantic Salmon

Plasma for antibody detection was collected from infected and uninfected groups of Atlantic salmon (SalmoBreed strain) from a PRV-1 challenge trial described in detail in Lund et al. (32). The trial was approved by the Norwegian Animal Research Authority and performed in accordance with the recommendations of the current animal welfare regulations: FOR-1996-01-15-23 (Norway).

In brief, seawater-adapted Atlantic salmon from the SalmoBreed strain (Bergen, Norway), confirmed negative for PRV and other pathogenic viruses, were kept in filtered and UV-irradiated brackish water (25‰ salinity), 12°C (±1°C) with continuous light. At Day 0, shedder fish ($N = 235$) were anesthetized (benzocaine chloride, 50 mg/L, Apotekproduksjon AS, Oslo, Norway), i.p. injected with 0.1 ml of an inoculum made from pelleted blood cells collected from a previous PRV trial (49). The virus in this material (PRV NOR2012-V3621) originates from a Norwegian field outbreak in 2012, and have been purified, characterized and used to prove causality between PRV and HSMI (17). A high level of PRV RNA was previously indicated in this material (PRV RTqPCR Ct 17.3 using a 100 ng RNA input), and the material was previously aliquoted in several batches and frozen for use in future trials (32, 49). Injected fish were placed in an experimental fish tank (1,000 L), and an equal number of naïve cohabitants was added. An identical control tank contained the same total number of uninfected fish. The infection trial lasted for 15 weeks. Ten cohabitant fish and ten control fish were sampled at 0, 4, 7, 10, 12, and 15 weeks, respectively, during which PRV infection was verified by RTqPCR, and HSMI by histological examination (32).

For sampling, the fish were euthanized by bath immersion with benzocaine chloride (200 mg/L water) (Apotekproduksjon AS, Oslo, Norway). Blood was collected from the caudal vein using lithium heparin-coated vacutainers (BD Vacutainer) with 20 G Venoject needles and centrifuged (3,000 rpm, 10 min, 4°C) for collection of plasma. The plasma samples were stored at −20°C.

Field Samples From Rainbow Trout

In January 2018, a recirculating aquaculture system farm in Jutland, Denmark, rearing rainbow trout experienced clinical disease associated with PRV-3. The Danish isolate of PRV-3 described in Dhamotharan et al. (35) was detected in heart and spleen samples from clinically affected fish by qPCR described in Finstad et al. (24), Blood samples were collected from the caudal vein of survivor fish ($N = 16$) in a raceway where clinical disease had occurred 2 months earlier.

Experimental PRV-3 Infection Trial and Blood Sampling in Rainbow Trout

The blood/plasma samples from rainbow trout was from a previously published challenge trial (20). In short, Specific Pathogen free (SPF) rainbow trout of 32 g in average were either i.p. injected with 0.1 ml of challenge inoculum or challenged by 1:1 cohabitation with the injected fish (cohabitants). The challenge inoculum was pooled rainbow trout blood (diluted 1:4 v/v in L-15 medium) from a pilot challenge study, which represented the first passage in experimental fish (20). The original material was collected from three individual fish from a rainbow trout hatchery outbreak in Norway in 2014 (19), and the PRV-3 isolate (NOR060214) has been purified, fully sequenced (35), and used in two previous experimental trials (20, 21). Blood samples were collected from eight fish sampled at 8 and 10 weeks after infection, and from eight uninfected control fish.

Construction of Plasmids for Recombinant Unmodified and Lipid-Modified PRV Protein Production

The unmodified recombinant PRV-1 σ1 and μ1c proteins were produced in *E. coli* from pcDNA3 as described by Finstad et al. (28). For lipid modified protein production, the complete open reading frame of PRV-1 σ1 gene target was obtained through PCR amplification from pcDNA3/PRV σ1 [NOR050607 (38)] using PfuUltra II Fusion HS DNA Polymerase (Agilent, Santa Clara, CA, USA). The gene specific forward and reverse primers used for amplification contained BamHI and EcoRI restriction sites at the N- and C-terminus, respectively. The PCR amplicon was resolved in 1% (w/v) agarose gel electrophoresis alongside 1 kbp DNA ladder (Fermentas Life Sciences, Germany) (**Figure S1A**) and purified according to instructions for the NucleoSpin® Gel and PCR Clean-up kit (MACHEREY-NAGEL, Düren, Germany). The DNA eluates were quantified using a Nanodrop Spectrophotometer (Thermo Fisher, Wilmington, DE, USA) and cloned into the digested pG-T-LM vector containing the Tat signaling peptide (**Figure S1B**), as described earlier (48), using the In-Fusion HD cloning system (Clontech, Mountain View, CA, USA). All the recombinant constructs were screened by colony PCR using gene and vector specific primers, and further confirmed by DNA sequencing (ATCG, Toronto, Canada). The resulting

recombinant construct was named pGT-LM/PRVσ1. The lipid modification process is previously described in detail for the WSSV-ICP11 protein (48).

To be used as control antigen in this study, the unmodified and lipid modified ISAV-FP protein were produced in the same manner as the previously published WSSV-ICP11 protein (41), which was also used as a control antigen here. In brief, the complete open reading frame of the ISAV-FP gene was PCR amplified (777 bp) using gene specific primers with Nde1/EcoR1 and BamH1/ EcoR1 restriction sites at the N- and C-terminus, respectively. The targeted ISAV-FP PCR amplicons were digested using respective endonucleases. The amplicons were cloned into pET28a and pGT-LM vectors for targeted unmodified and lipid-modified protein expression, respectively. The unmodified and lipid-modified clones were verified by restriction digestion and sequencing. The expression vectors were named pET28a- ISAV-FP (unmodified) and pGT-LM-ISAV-FP (lipid- modified).

Expression of Proteins in *E. coli*

Both unmodified and lipid-modified recombinant constructs were transformed into the *E. coli* strain, GJ1158 (Genei, Bangalore, India) for protein expression. Transformants confirmed to contain the correct plasmid sequence were inoculated into 10 ml LB medium containing 100 μg/ml ampicillin, and incubated (200 rpm, 37°C) until absorbance reached 0.6 at 600 nm. Protein production was induced by adding 1 mM Isopropyl β-D-1-thiogalactopyranoside (IPTG), and the bacterial culture was given a 4 h post-induction time (200 rpm, 37°C). The induced bacteria were harvested by centrifugation (3,000 × g, 5 min), washed twice with 0.9% saline and re-suspended in 1X phosphate buffered saline. Lysed recombinant bacteria (25 μl) were analyzed by gel electrophoresis and western blotting for recombinant lipid modified protein expression using anti-his antibodies (**Figure S2**).

Purification of Recombinant Lipid-Modified Proteins

The pelleted bacteria were re-suspended in 50 mM Sodium phosphate pH 8.0/300 mM NaCl and lysed with lysozyme (Thermo Fisher Scientific) at a final concentration 100 μg/mL for 1 h at 4°C, followed by sonication. The membrane fraction was harvested by centrifugation at 150,000 × g for 1 h at 4°C. The membrane pellet was re-suspended in lysis buffer and solubilized with 1% Sodium lauroyl sarcosinate (also known as sarkosyl) buffer (Sigma Aldrich, St. Louis, MO, USA), followed by centrifugation (1 h, 100,000 × g, 4°C). The proteins contained a 6x Histidine tag, which was utilized for purification using immobilized metal affinity chromatography (IMAC). The supernatants containing solubilized membrane proteins were loaded on a Tris-carboxymethyl ethylene diamine (TED) column pre-charged with Ni2+ ion and pre-equilibrated with equilibration buffer (MACHEREY-NAGEL). The column was then washed with wash buffer containing 5 mM imidazole. The column bound-proteins were eluted with purification buffer (50 mM NaH_2PO_4, 300 mM NaCl, pH 8.0) supplemented with 25–50 mM imidazole. The protein eluates were analyzed using Criterion precast gels (4–12%) (Bio-Rad) (**Figure 1A**).

Bead-Based Assay

MagPlex®-C Microspheres (Luminex Corp., Austin, TX, USA) #12, #21, #27, #29, #34, #36, #44, #62, and #64 were coated with antigens using the Bio-Plex Amine Coupling Kit (Bio-Rad, Hercules, CA, USA) according to the manufacturer's instructions. The N-Hydroxysulfosuccinimide sodium salt and N-(3-Dimethylaminopropyl)-N'-ethylcarbod used for the coupling reaction were both Sigma-Aldrich. For each coupling reaction, 6-24 μg of recombinant protein was used. Proteins used were PRV σ1, lipid modified PRV σ1 (LM-PRVσ1), lipid modified WSSV ICP11 (LM-WSSV-ICP11) unmodified infectious salmon anemia virus fusion protein (ISAV-FP), lipid modified ISAV-FP (LM-ISAV-FP) and the hapten-carrier DNP-keyhole limpet hemocyanin (DNP-KLH) (Calbiochem, Merck, Darmstadt, Germany), which represents a model antigen to estimate non-specific antibodies (50). The bead concentrations were determined using Countess automated cell counter (Invitrogen, Carlsbad, CA, USA). Coupled beads were stored in black Eppendorf tubes at 4°C for up to 10 weeks. All incubations were performed at room temperature, protected from light on a HulaMixer rotator (Thermo Fisher Scientific) at 15 rpm.

The immunoassay was performed as described earlier (8). Briefly, Bio-Plex Pro™ Flat Bottom Plates (Bio-Rad) were used. Beads were diluted in PBS containing 0.5% BSA (Rinderalbumin; Bio-Rad Diagnostics GmbH, Dreieich, Germany) and 0.05% azide (Merck, Darmstadt, Germany) (PBS+) and 2,500 beads of each bead number were added to each well. AntiSalmonid-IgH monoclonal antibody (clone IPA5F12) (Cedarlane, Burlington, Ontario, Canada) diluted 1:400 in PBS+ was used as an unconjugated anti-IgM heavy chain monoclonal antibody. Biotinylated goat AntiMouse IgG2a antibody (Southern Biotechnology Association, Birmingham, AL, USA) diluted 1:1,000 in PBS+ was used as a secondary antibody and Streptavidin-PE (Invitrogen) diluted 1:50 in PBS+ as the reporter flourochrome. Plates were read using a Bio-Plex 200 (Bio-Rad). The DD-gate was set to 5,000–25,000, and between 20 and 100 beads from each population were read from each well. The reading was carried out using a low PMT target value. Results were analyzed using the Bio-Plex Manager 5.0 and 6.1 (Bio-Rad).

SDS-PAGE and Western Blotting

Western blotting was used to confirm antibody binding to the specific proteins. Protein samples with the recombinant unmodified PRV-1 proteins μ1c and σ1 used previously (8), LM-PRVσ1, LM-WSSV-ICP11, ISAV-FP, and LM-ISAV-FP were analyzed. Protein concentrations were determined using a NanoDrop ND-1000 spectrophotometer (Thermo Fischer Scientific). From the proteins above, 0.6 μg protein was diluted to 35 μl with dH_2O. 2.5 μl Reducing Agent (Bio-Rad) and 12.5 μl Sample Buffer (Bio-Rad) was added, and the mix was heated to 95°C for 5 min before separation by gel electrophoresis (SDS-PAGE) in a 4–12% Bis-Tris Criterion™ XT PreCast

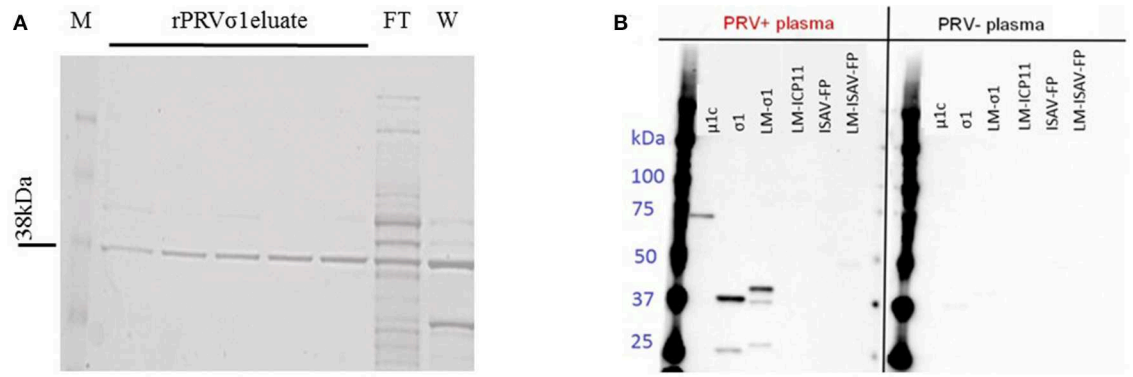


FIGURE 1 | Production of lipid modified PRV proteins. **(A)** SDS-PAGE profile showing the purified lipid-modified PRVσ1 (M-Marker, FT-Flow through, and W-Wash). Eluates 1–2 with 25 mM imidazole and 3–5 with 50 mM imidazole elution. **(B)** Specificity of plasma IgM to PRV antigens. Proteins used in the multiplex immunoassay were analyzed by western blotting. Left panel incubated with plasma from PRV-infected Atlantic salmon (pooled sample from 10 to 15 wpc) and right panel incubated with plasma from control fish (pooled samples from the same challenge trial) as primary antibody.

Gel (Bio-Rad). Precision Plus Protein Standard (Bio-Rad) was used to confirm protein size. After the gel electrophoresis, the protein was transferred to membrane using a Trans-Blot midi transfer pack (Bio-Rad). The membrane was blocked in PBS with 0.001% Tween 20 (EMD Millipore) and 5% skim milk powder (Merck) for 1 h before incubation with pooled plasma from PRV negative salmon or PRV infected salmon (0 wpc and 10–15 wpc from the PRV-1 challenge trial) diluted 1:100 overnight at 4°C on a roller. The membrane was washed 4 × 15 min, and then incubated with Anti-Salmonid IgH antibody (clone IPA5F12) (1:500) for 1 h in room temperature. The washing was repeated and the membrane was incubated with Anti-Mouse IgG-HRP ECL peroxidase-labeled Anti-Mouse antibody, NA931VS (GE Healthcare, Buckinghamshire, UK) (1:50,000) and Precision Protein StrepTactinHRP (Bio-Rad) (0.7 μl in 10 ml) for 1 h at room temperature. All antibodies were diluted in PBS with 0.001% Tween 20 and 1% skim milk powder, and all washing were done with in PBS with 0.001% Tween 20. The signal was developed using ECL Prime Western Blotting Detection Reagent (GE Healthcare) and detected on Bio-Rad Chemidoc XRS.

Heat Treatment and Adsorption of Plasma

Aiming to eliminate background binding of plasma to non-PRV proteins, the plasma was heated to temperatures from 30 to 56°C for 5–60 min. This is in line with previously used protocols for salmon plasma complement inactivation (51, 52).

To demonstrate PRV σ1 specificity, PRV-1 positive plasma (from 12 to 15 wpc in the PRV-1 challenge trial) was adsorbed against beads coated with lipid-modified and non-lipid-modified proteins. In addition to antigens described earlier, beads coated with PRV μNS expressed in insect cells (8, 53) and *E. coli* protein (background) coated beads described earlier (8) were included in the experiment. Pooled heat-treated plasma (48°C for 20 min) was diluted 1:200, and 50 μl of each plasma sample was added to a 96 well-plate and incubated with beads. The beads used were coated with PRVσ1 PRVμ1c, PRVμNS, LM-WSSV-ICP11, LM-PRVσ1, ISAV-FP, or LM-ISAV-FP. Coated beads of each bead type (100,000 in 50 μl) or 50 μl PBS without beads were added per well. Incubation was done on a shaker at 500 rpm in room temperature and protected from light for 3 h. After incubation, the beads were removed using a magnetic separator, and bead-free plasma was transferred to a new plate and stored overnight at 4°C. The plasma was analyzed the next day using Bio-Plex 200 and Bioplex manager 6.1 with DNP-KLH, LM-WSSV-ICP11, LM-PRVσ1, ISAV-FP, and LM-ISAV-FP coated beads.

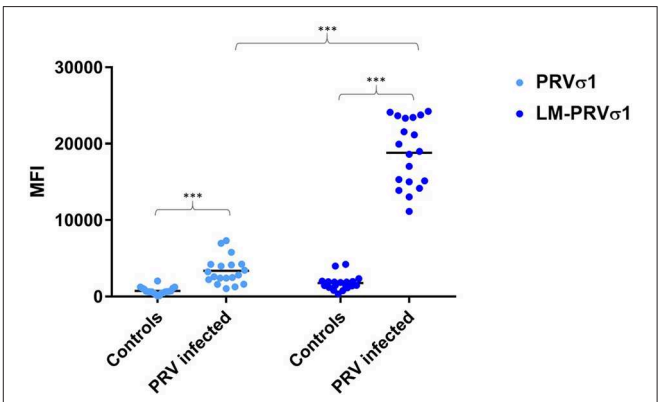


FIGURE 2 | Increased detection of anti-σ1 using lipid modified antigen. Comparison between beads coated with σ1 and beads coated with LM-σ1 when used in the immunoassay to analyze plasma from PRV-infected Atlantic salmon (12–15 wpc) and controls. Significant difference between infected and control fish, and between different antigens when used to analyse infected fish samples are indicated by asterisks (Mann-Whitney test).

Statistical Analysis

A non-parametric Mann-Whitney unpaired rank test was performed between groups in **Figure 2**, between control groups and infected groups at all time points in **Figure 3** and between LM-PRVσ1 and the other proteins in **Figure 5A**. All statistical

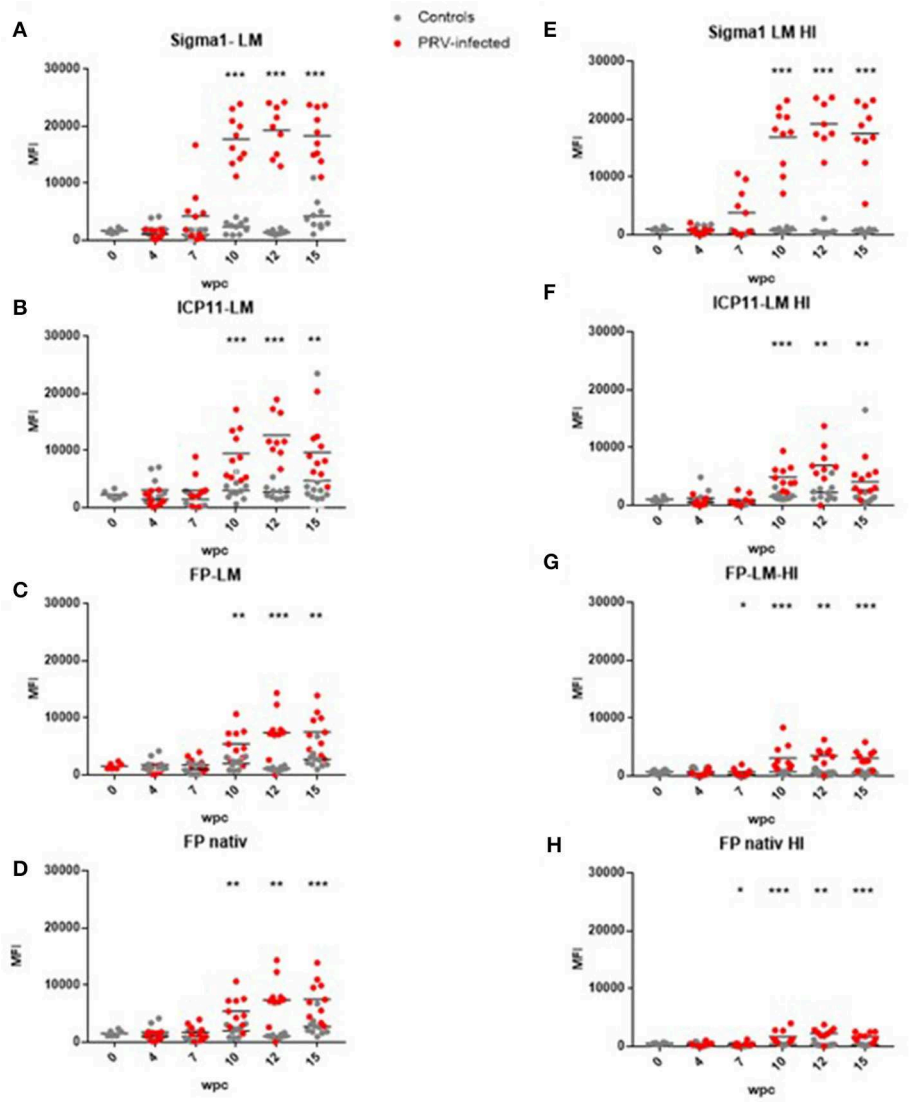


FIGURE 3 | Antibody detection in untreated and heat-treated plasma. **(A)** LM-PRVσ1 on untreated plasma. **(B)** LM-WSSV-ICP11 on untreated plasma. **(C)** LM-ISAV-FP on untreated plasma. **(D)** ISAV-FP on untreated plasma. **(E)** LM-PRVσ1 on heat-treated plasma. **(F)** LM-WSSV-ICP11 on heat-treated plasma. **(G)** LM-ISAV-FP on heat-treated plasma. **(H)** ISAV-FP on heat-treated plasma. Significant difference between groups are indicated by asterisks (Mann-Whitney test).

analyses were performed with the help of GraphPad Prism 7.03 (GraphPad Software Inc., USA).

RESULTS

Production and Purification of Lipid Modified PRV σ1

The lipid modified LM-PRVσ1 was cloned and produced in *E. coli*, and found to be located in the outer membrane of the bacteria, as confirmed through sub-cellular fractionation and western-immunoblotting (**Figure S2**). The LM-PRVσ1 was purified in a detergent-free form in a single step using immobilized metal affinity chromatography (IMAC), as previously described (48). The protein was successfully purified and a band was detected at the expected size of 38 kDa (**Figure 1A**, **Figure S3A**).

Confirmation of Anti PRV Antibody Specificity Through Immunoblotting

To show the formation of anti-PRV σ1 antibodies in PRV-infected fish, recombinant PRV σ1 protein with or without lipid modification along with PRV-1 μ1c were immunoblotted using plasma from PRV-1 infected and uninfected Atlantic salmon as a source of primary antibody. IgM binding to proteins corresponding in size to PRV σ1 and LM-PRVσ1, as well as PRVμ1c was confirmed in plasma from PRV infected fish. No

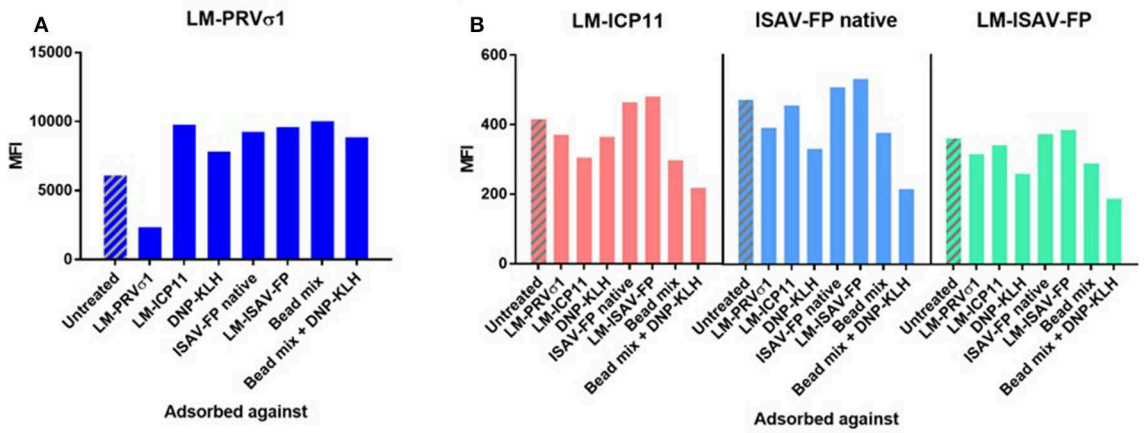


FIGURE 4 | Pre-adsorption of heat-treated pooled plasma from PRV-infected fish against antigens indicate specificity of anti-PRVσ1 antibodies. Measured on beads coupled with **(A)** LM-PRVσ1 and **(B)** non-PRV control proteins.

binding to the control antigens LM-WSSV-ICP11, LM-ISAV-FP, or ISAV-FP were observed (**Figure 1B**, **Figure S3B**). This confirms the presence of antibodies binding to σ1 in plasma from PRV-infected fish.

Lipid-Modified PRV σ1 Coated on Luminex xMAP Beads Can Be Used to Detect Anti-PRV Antibodies

Compared to unmodified PRV-1 σ1, the lipid modified PRV σ1 protein coated on xMAP beads bound the antibodies produced after PRV infection more effectively, as indicated by significantly higher levels of mean fluorescence intensity (MFI) in the luminex assay (**Figure 2**).

Anti-PRV-1 σ1 antibodies were then measured in plasma originating from a PRV-1 infection trial. In this trial, anti-PRV σ1 antibody levels increased from week 7 after PRV infection and reached a plateau at 10–15 wpc (**Figure 3A**).

Test of Binding Specificity Using Lipid-Modified Control Proteins

Other lipid-modified and unmodified proteins were tested to confirm that the antibodies binding to LM-PRVσ1 were specific for the virus protein and not targeting the N-terminal lipid modification. The control proteins used were lipid modified ICP11 from WSSV, and unmodified and lipid modified ISAV-FP. When testing the control antigens on plasma from the PRV-1 challenge trial, we observed an increase in antibodies binding to both unmodified and lipid modified proteins from week 10 after PRV challenge (**Figures 3B–D**).

Effects of Heat Treatment and Pre-adsorption of Plasma on Binding Specificity

After heat treatment of plasma to eliminate background binding to non-PRV proteins, 48°C for 20 min was found as optimal (**Figures S4A,B**). Using these treatment conditions, antibody binding to LM-PRVσ1 beads decreased using plasma from control fish, but not when using plasma from infected fish, indicating antigen specificity after infection (**Figure 3E**). For the non-PRV proteins, antibody binding decreased after heat treatment when using plasma from both infected and uninfected fish (**Figures 3F–H**). When heat-treated and untreated plasma from controls from the same individuals, sampled 12 and 15 wpc, were run on the same plate (to avoid plate-to-plate variation), the binding to LM-PRVσ1-coated beads decreased for all control fish after heat treatment. For infected fish, the antibody binding to LM-PRVσ1 decreased in some individuals and increased in others after heat treatment (**Figure S4C**).

To further evaluate the antigen specificity of the antibodies, pooled plasma was pre-adsorbed with beads coated with the specific antigens, as well as mixes of antigen-coated beads. The binding to LM-PRVσ1-coated beads decreased only after pre-adsorption of plasma with LM-PRVσ1 beads, but increased after adsorption with any of the other beads coated with LM-modified or unmodified proteins, including the hapten-carrier conjugate DNP-KLH (**Figure 4A**). Less changes were seen when analyzing binding to LM-WSSV-ICP11, LM-ISAV-FP, or ISAV-FP after adsorption, but decreases in binding were seen especially after adsorption with DNP-KLH and bead mixes (**Figure 4B**).

Anti-PRV-3 σ1 Antibodies Bind to PRV-1 σ1 LM-Coated Beads

Heat-treated plasma samples from a field outbreak of PRV-3 were analyzed using beads coated with LM-PRVσ1 as well as PRV μ1c, PRV μNS and *E. coli* protein (background) coated beads. Results show that antibody binding (MFI) to LM-PRVσ1 was significantly higher than binding to PRV μNS coated beads, PRV μ1c-coated beads as well as *E. coli* protein (background) coated beads (**Figure 5A**). LM-PRVσ1 and LM-WSSV-ICP11 beads were tested on heat-treated plasma and blood from naïve and PRV-3 infected rainbow trout. The IgM binding to LM-PRVσ1-coated beads was low in naïve fish, whereas MFI levels above 20,000 was obtained from week 10 after infection (**Figure 5B**)

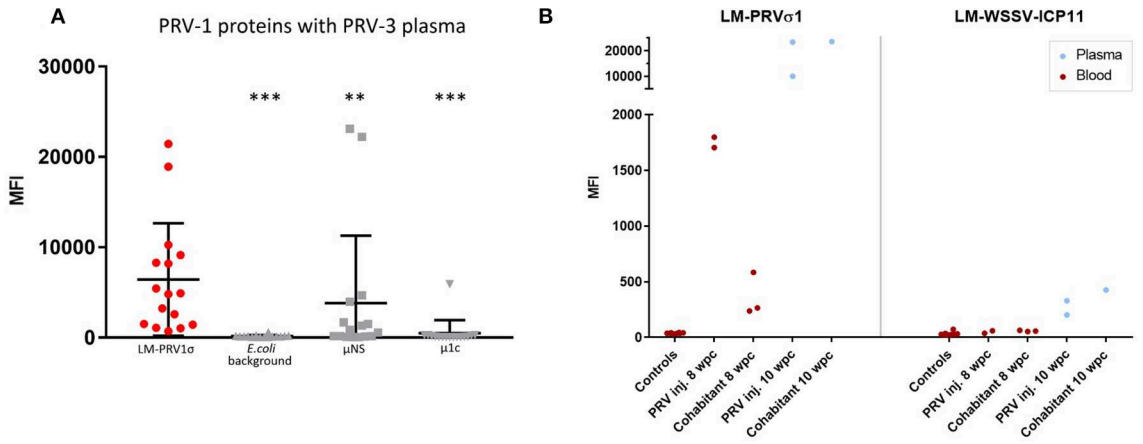


FIGURE 5 | Detection of cross-binding antibodies induced by PRV3 infection in rainbow trout. **(A)** Field samples from a PRV-3 outbreak in rainbow trout analyzed with LM-PRVσ1, μNS, and μ1c (PRV-1) coupled beads in the immunoassay. Significant difference between MFI of LM-PRVσ1 beads and the other beads are indicated by asterisks (Mann-Whitney test). **(B)** MFI from blood and plasma samples from individuals experimentally infected with PRV and uninfected controls using LM-PRVσ1 and LM-WSSV-ICP11 coupled beads. All samples were heat-treated.

Only low levels (MFI up to 426) of antibodies binding to LM-WSSV-ICP11 beads were detected (**Figure 5B**). An alignment between the σ1 amino acid sequences of PRV-1 NOR050607 coated on the beads and PRV-3 NOR060214 used in the PRV-3 infection trial revealed 81% identity (**Figure S5A**). The N-terminal was the least variable part of the protein, whereas several areas of variation were found in the central and C-terminal part. The last two AA in the C-terminal are hydrophobic in PRV-1, but hydrophilic in PRV-3. The PRV-3 sequence was 1 amino acid longer due to an inserted glycine at position 39. An antigenicity plot indicated minor differences in the antigenicity pattern between the two PRV genotypes (**Figure S5B**).

DISCUSSION

Since the σ1 protein from MRV is known for its role in receptor binding and cell entry (39, 41), and is a primary target for neutralizing antibodies (40, 54), σ1 was predicted as a promising target for neutralizing antibodies against PRV. Virus neutralization assays have been successfully used for other salmonid viruses, including the salmonid alphavirus (SAV) (55). However, no such assays have been developed for PRV, as the virus has resisted cultivation in cell lines. So far, primary erythrocytes are the only cells where PRV is reported to replicate for more than one passage *ex vivo* (56), and even in erythrocytes the consistency of replication is too low to allow the establishment of a neutralization assay. Because of this, other assays for detection of anti-PRV antibodies are attractive.

In our former development of bead based multiplex immunoassays for detection of PRV-specific antibodies we were able to detect specific IgM targeting PRV-1 μ1c and μNS proteins in Atlantic salmon plasma, but not IgM directed against the PRV-1 spike protein σ1 (8). The PRV-3 genotype has been found associated with disease in several European countries after its initial discovery in Norwegian farmed rainbow trout. In a recently published challenge trial (21), antibodies against PRV-3 μ1c were detected at low levels using a bead-based assay coated with PRV-1 μ1c. This study demonstrates that sensitive detection of anti-PRV σ1 antibodies in Atlantic salmon and anti-PRV-3 σ1 antibodies in rainbow trout was obtained through N-terminal lipid modification of the recombinant PRV σ1 antigen (LM-PRVσ1) prior to use in the bead-based immunoassay.

Lipid modification using a bacterial prolipoprotein signaling sequence have previously been put forward as a desired strategy for inducing a potential adjuvant effect to a vaccine antigen (48). In this case, we tested if the lipid-modification of recombinant PRV σ1 coated on beads could promote detection of PRV σ1-specific antibodies, and found that the lipid modification indeed led to increased antibody detection. A similar improvement of antigen-antibody interaction has been associated with increased hydrophobic anchorage of N-terminal lipid-modified antigens in other studies (47, 48). A possible reason for the improved IgM detection obtained by PRV σ1 lipid-modification is a stabilization of σ1 mimicking the conformation and/or orientation in the intact virus with the N-terminal bound to the surface and the C-terminal exposed (57). This orientation is likely to improve the exposure of the correct epitopes for detection by antibodies, including neutralizing antibodies.

For control of antigen specificity, the lipid modified ICP11 protein from the shrimp virus WSSV (58), and the fusion protein (FP) of ISAV (59), with and without lipid modification, was tested. The experimental fish had not been previously exposed to these viral proteins, as the trial fish were tested negative for ISAV (32), and WSSV is a crustacean virus (60). Nevertheless, we detected IgM binding to these proteins in salmonid plasma in uninfected fish, and this binding increased significantly during the

course of PRV infection. We also detected binding to LM-PRVσ1 in control fish not previously exposed to PRV. This background binding could be explained by polyreactive antibodies present in control fish, with increasing levels induced by the PRV infection. An induction of polyreactive antibodies after infection has been described in fish (50, 61, 62) and mammals (9).

Heat treatment of plasma at more than 43°C for as little as 5 min removed most of the background binding in control fish without reducing the specific interaction with lipid-modified PRV σ1 in infected fish, clearly indicating that PRV σ1-specific antibodies were detected. Binding to the non-PRV proteins was reduced by heat treatment, but not completely removed, and was still significantly higher in infected fish than in control fish. In contrast to the rigid structure of the classic antibody model, it has been hypothesized that polyreactive antibodies have more flexible antigen binding sites and are able to change conformation to accommodate different antigens (9). It is conceivable that heat treatment might negatively affect this flexibility or that the polyreactive antibodies is more heat-labile than the specific antibodies for other unknown reasons. Whether background binding was caused by polyreactive antibodies alone or secondary via other plasma factors, requires further study. As the lipid-modified signaling peptide fused to the PRV σ1 N-terminal is a natural part of gram negative bacterial membrane proteins (43), previous exposure to and acquired immunity against it cannot be completely ruled out. However, results from adsorption against other lipid-modified proteins indicate that antibodies detected on the LM-PRVσ1-coated beads do not bind to the acylated N-terminal peptide, but specifically to PRV σ1. Together the effects of heat treatment and pre-adsorption of plasma strongly suggest an increase in the formation of polyreactive antibodies during a PRV infection, whereas antibodies binding to the LM-PRVσ1 coated beads are PRV σ1 specific.

In the PRV-1 trial in Atlantic salmon analyzed here, PRV RNA peaked in cohabitant fish at 7 weeks post-introduction of virus shedders and histopathological changes consistent with HSMI were most prominent after 10 weeks (32). Anti-PRV σ1 IgM was produced 7 weeks after the initial exposure of experimental fish to PRV shedders, which corresponds to 3 weeks after the first detection of PRV in blood from these fish (32). This timing resembles our previous observations on production of IgM targeting the PRV μ1 and μNS proteins (8). In both the trial analyzed here, and the trial analyzed with bead based immunoassay previously (8), a reduction in HSMI lesions was observed in the time after the specific IgM production reached a maximum level, and could indicate a protective effect. Antibody-mediated protection against viruses represent the humoral arm of the adaptive immune system, but cellular protection mediated by T-lymphocytes may be equally important. Results from earlier PRV infection trials have indicated a role of cytotoxic (CD8+) T-cell mediated protection (29, 63). In particular, recruitment of immune cells to the PRV-infected heart has been associated with a reduction in PRV-infected cardiomyocytes (24, 28). This suggests a possible role for both humoral and cellular immune mechanisms in clearing of the PRV infection in the heart, and we should be careful with drawing conclusions based on correlation between specific antibody production and protection from HSMI. PRV is a virus that persists in blood cells after infection (33, 64). Viral RNA persisted in blood throughout this trial as well, showing the insufficiency of the humoral immune response to eradicate virus from blood. The IgM level stayed elevated through the duration of this study (15 weeks). Since PRV-1 causes a persistent infection in Atlantic salmon, the virus-specific IgM response can be expected to be of longer duration than shown here. Longer trials should be performed to clarify the long-term antibody production level.

We have demonstrated that LM-PRVσ1 provide a more sensitive assay for PRV-3 antibody detection than μ1c, and is more suitable for identifying populations previously exposed to PRV-3 and effects of potential vaccines. The LM-PRVσ1 assay worked in both PRV-1 infected Atlantic salmon and PRV-3 infected rainbow trout and the PRVμ1c assay worked in PRV-1 infected Atlantic salmon only (except in one fish). Multiplexing these assays can potentially be used to distinguish between infections with PRV-1 and PRV-3 in a population. PRV-1 and PRV-3 have 80.1% nucleotide and a 90.5% amino acid identity [(35); **Figure S5A**]. The similarity is somewhat higher in the N-terminal compared to the protein body and C-terminal head. Several of the amino acid differences represent significant alterations in the side chain charges or polarity, which may affect 3D structure or protein-protein interaction. The two very last C-terminal amino acids differs, containing hydrophobic side chains (isoleucines, I) in PRV-1 and polar/charged side chains [Threonine (T), arginine (R)] in PRV-3, which is likely to lead to structure and antibody epitope differences. The amino acid differences within the core of PRV σ1 differ, but clearly not enough to hamper the antibody cross-binding capacity. The functional importance of these differences are difficult to predict, as the amino acid identity between the PRV-1/-3 σ1 sequences and the MRV σ1 sequence are only approximately 21% (38). MRV σ1 is considerably larger (459 AA compared to 314 AA for PRV-1 σ1), and the extended sequence of MRV is located both in the N-and C-terminal. Based on structural analyses on MRV σ1 (54, 57, 65), it is the N-terminal tail which inserts into the virion, the body which contains the motif for sialic acids/glucans, and the C-terminal head domain which binds the target cell receptor, junctional adhesion-molecule-A (JAM-A). Neutralizing antibody binding has been localized to the C-terminal head domain (54). This part of σ1 is truncated in all PRV genotypes compared to MRV, and functional and interaction prediction *in silico* is not straightforward. The only conserved motif predicted in PRV (both genotype 1 and 3) is the glucan/sialic acid biding motif (38, 66).

In contrast to PRV-1, which establish a persistent infection that can be detected in the host up to a year after infection (64), PRV-3 is cleared from infected rainbow trout (20, 21), and an immunoassay to identify immunized populations could be particularly useful. A still open question is the duration of the specific humoral response to infection, and the possibility to identify vaccinated or previously exposed populations after more than 15 weeks.

Recently, two PRV vaccine trials using whole virus vaccines and DNA vaccines, respectively, showed partial protection of Atlantic salmon from HSMI (67, 68). In order to optimize such trials, assays that can reveal true correlates of protective immune responses against PRV are useful. Sensitive immunoassays that require small volumes of minimal-invasive samples are attractive for aquaculture. Using this bead-based detection assay, 1 μl plasma in 100-fold dilution is sufficient for providing sensitive antibody detection, and through multiplexing, a larger repertoire of pathogen-specific antibodies can be analyzed simultaneously. The potential of bead–based analyses is that not only antibody detection, but also pathogen detection and detection of other molecular markers can be obtained in concert in the same sample. As also put forward by others (69), this analytic method has a great future potential in aquacultural diagnostics.

DATA AVAILABILITY

The datasets generated for this study are available on request to the corresponding author.

AUTHOR CONTRIBUTIONS

LT: study conception and design, acquisition of data, analysis, interpretation of data, drafting, revising, and approving the manuscript. SK: study design, acquisition of data, analysis, interpretation of data, drafting, revising, and approving the manuscript. GJ: acquisition of data, analysis, interpretation of data, revising, and approving the manuscript. ØW: interpretation of data, revising, and approving the manuscript. NV and ML: sample collection, interpretation of data, revising, and approving the manuscript. ER: study conception and design, revising, and approving the manuscript. PB: study design, interpretation of data, revising, and approving the manuscript. MD: study conception and design, analysis, interpretation of data, drafting, revising, and approving the manuscript.

FUNDING

This study was supported by the Research Council of Norway, grants 237315/E40 (ViVaFish) and 280847/E40 (ViVaAct), and by internal PhD-grant from the Norwegian University of Life Sciences.

ACKNOWLEDGMENTS

We thank our colleagues at the Norwegian University of Life Sciences, Elisabeth Furuseth Hansen for technical assistance and Anne Storset for ideas and helpful discussions.

SUPPLEMENTARY MATERIAL

The Supplementary Material for this article can be found online at: https://www.frontiersin.org/articles/10.3389/fimmu.2019.02119/full#supplementary-material

REFERENCES

1. Brudeseth BE, Wiulsrod R, Fredriksen BN, Lindmo K, Lokling KE, Bordevik M, et al. Status and future perspectives of vaccines for industrialised fin-fish farming. *Fish Shellfish Immunol.* (2013) 35:1759–68. doi: 10.1016/j.fsi.2013.05.029
2. Munang'andu HM, Evensen O. Correlates of protective immunity for fish vaccines. *Fish Shellfish Immunol.* (2019) 85:132–40. doi: 10.1016/j.fsi.2018.03.060
3. Powell RL, Ouellette I, Lindsay RW, Parks CL, King CR, McDermott AB, et al. A multiplex microsphere-based immunoassay increases the sensitivity of SIV-specific antibody detection in serum samples and mucosal specimens collected from rhesus macaques infected with SIVmac239. *Bio Res Open Access.* (2013) 2:171–8. doi: 10.1089/biores.2013.0009
4. Guigue N, Menotti J, Hamane S, Derouin F, Garin YJ. Performance of the BioPlex 2200 flow immunoassay in critical cases of serodiagnosis of toxoplasmosis. *Clin Vaccine Immunol.* (2014) 21:496–500. doi: 10.1128/CVI.00624-13
5. Koffi D, Toure AO, Varela ML, Vigan-Womas I, Beourou S, Brou S, et al. Analysis of antibody profiles in symptomatic malaria in three sentinel sites of Ivory Coast by using multiplex, fluorescent, magnetic, bead-based serological assay (MAGPIX). *Malar J.* (2015) 14:509. doi: 10.1186/s12936-015-1043-2
6. Baker HN, Murphy R, Lopez E, Garcia C. Conversion of a capture ELISA to a Luminex xMAP assay using a multiplex antibody screening method. *J Vis Exp.* (2012):4084. doi: 10.3791/4084
7. Wang H, Cong F, Guan J, Xiao L, Zhu Y, Lian Y, et al. Development of a sensitive and specific xMAP assay for detection of antibodies against infectious laryngotracheitis and bronchitis viruses. *Virol J.* (2018) 15:146. doi: 10.1186/s12985-018-1048-x
8. Teige LH, Lund M, Haatveit HM, Rosaeg MV, Wessel O, Dahle MK, et al. A bead based multiplex immunoassay detects *Piscine orthoreovirus* specific antibodies in Atlantic salmon (*Salmo salar*). *Fish Shellfish Immunol.* (2017) 63:491–9. doi: 10.1016/j.fsi.2017.02.043
9. Notkins AL. Polyreactivity of antibody molecules. *Trends Immunol.* (2004) 25:174–9. doi: 10.1016/j.it.2004.02.004
10. Hordvik I. Immunoglobulin isotypes in Atlantic salmon, *Salmo salar*. *Biomolecules*. (2015) 5:166–77. doi: 10.3390/biom5010166
11. Munang'andu HM, Fredriksen BN, Mutoloki S, Dalmo RA, Evensen O. Antigen dose and humoral immune response correspond with protection for inactivated infectious pancreatic necrosis virus vaccines in Atlantic salmon (*Salmo salar* L). *Vet Res.* (2013) 44:7. doi: 10.1186/1297-9716-44-7
12. Kim HJ, Park JS, Kwon SR. Development of a stringent ELISA protocol to evaluate anti-viral hemorrhagic septicemia virus-specific antibodies in olive flounder Paralichthys olivaceus with improved specificity. *J Microbiol.* (2015) 53:481–5. doi: 10.1007/s12275-015-5101-9
13. Kibenge MT, Opazo B, Rojas AH, Kibenge FS. Serological evidence of infectious salmon anaemia virus (ISAV) infection in farmed fishes, using an indirect enzyme-linked immunosorbent assay (ELISA). *Dis Aquat Organ.* (2002) 51:1–11. doi: 10.3354/dao051001
14. Mikalsen AB, Sindre H, Torgersen J, Rimstad E. Protective effects of a DNA vaccine expressing the infectious salmon anemia virus hemagglutinin-esterase in Atlantic salmon. *Vaccine.* (2005) 23:4895–905. doi: 10.1016/j.vaccine.2005.05.025
15. Rocha A, Fernandez-Alonso M, Mas V, Perez L, Estepa A, Coll JM. Antibody response to a fragment of the protein G of VHS rhabdovirus in immunised trout. *Vet Immunol Immunopathol.* (2002) 86:89–99. doi: 10.1016/S0165-2427(02)00016-8

16. Palacios G, Lovoll M, Tengs T, Hornig M, Hutchison S, Hui J, et al. Heart and skeletal muscle inflammation of farmed salmon is associated with infection with a novel reovirus. *PLoS ONE.* (2010) 5:e11487. doi: 10.1371/journal.pone.0011487
17. Wessel O, Braaen S, Alarcon M, Haatveit H, Roos N, Markussen T, et al. Infection with purified *Piscine orthoreovirus* demonstrates a causal relationship with heart and skeletal muscle inflammation in Atlantic salmon. *PLoS ONE.* (2017) 12:e0183781. doi: 10.1371/journal.pone.0183781
18. Takano T, Nawata A, Sakai T, Matsuyama T, Ito T, Kurita J, et al. Full-genome sequencing and confirmation of the causative agent of erythrocytic inclusion body syndrome in coho salmon identifies a new type of *Piscine orthoreovirus*. *PLoS ONE.* (2016) 11:e0165424. doi: 10.1371/journal.pone.0165424
19. Olsen AB, Hjortaas M, Tengs T, Hellberg H, Johansen R. First description of a new disease in rainbow trout (*Oncorhynchus mykiss* (Walbaum)) similar to heart and skeletal muscle inflammation (HSMI) and detection of a gene sequence related to *Piscine Orthoreovirus* (PRV). *PLoS ONE.* (2015) 10:e0131638. doi: 10.1371/journal.pone.0131638
20. Hauge H, Vendramin N, Taksdal T, Olsen AB, Wessel O, Mikkelsen SS, et al. Infection experiments with novel *Piscine orthoreovirus* from rainbow trout (*Oncorhynchus mykiss*) in salmonids. *PLoS ONE.* (2017) 12:e0180293. doi: 10.1371/journal.pone.0180293
21. Vendramin N, Kannimuthu D, Olsen AB, Cuenca A, Teige LH, Wessel Ø, et al. *Piscine orthoreovirus* subtype 3 (PRV-3) causes heart inflammation in rainbow trout (*Oncorhynchus mykiss*). *Vet Res.* (2019) 50:14. doi: 10.1186/s13567-019-0632-4
22. Adamek M, Hellmann J, Flamm A, Teitge F, Vendramin N, Fey D, et al. Detection of *Piscine orthoreoviruses* (PRV-1 and PRV-3) in Atlantic salmon and rainbow trout farmed in Germany. *Transbound Emerg Dis.* (2019) 66:14–21. doi: 10.1111/tbed.13018
23. Kongtorp RT, Kjerstad A, Taksdal T, Guttvik A, Falk K. Heart and skeletal muscle inflammation in Atlantic salmon, *Salmo salar* L: a new infectious disease. *J Fish Dis.* (2004) 27:351–8. doi: 10.1111/j.1365-2761.2004.00549.x
24. Finstad OW, Dahle MK, Lindholm TH, Nyman IB, Lovoll M, Wallace C, et al. *Piscine orthoreovirus* (PRV) infects Atlantic salmon erythrocytes. *Vet Res.* (2014) 45:35. doi: 10.1186/1297-9716-45-35
25. Godoy MG, Kibenge MJ, Wang Y, Suarez R, Leiva C, Vallejos F, et al. First description of clinical presentation of *Piscine orthoreovirus* (PRV) infections in salmonid aquaculture in Chile and identification of a second genotype (Genotype II) of PRV. *Virol J.* (2016) 13:98. doi: 10.1186/s12985-016-0554-y
26. Ferguson HW, Kongtorp RT, Taksdal T, Graham D, Falk K. An outbreak of disease resembling heart and skeletal muscle inflammation in Scottish farmed salmon, *Salmo salar* L., with observations on myocardial regeneration. *J Fish Dis.* (2005) 28:119–23. doi: 10.1111/j.1365-2761.2004.00602.x
27. Di Cicco E, Ferguson HW, Schulze AD, Kaukinen KH, Li S, Vanderstichel R, et al. Heart and skeletal muscle inflammation (HSMI) disease diagnosed on a British Columbia salmon farm through a longitudinal farm study. *PLoS ONE.* (2017) 12:e0171471. doi: 10.1371/journal.pone.0171471
28. Finstad OW, Falk K, Lovoll M, Evensen O, Rimstad E. Immunohistochemical detection of *Piscine reovirus* (PRV) in hearts of Atlantic salmon coincide with the course of heart and skeletal muscle inflammation (HSMI). *Vet Res.* (2012) 43:27. doi: 10.1186/1297-9716-43-27
29. Mikalsen AB, Haugland O, Rode M, Solbakk IT, Evensen O. Atlantic salmon reovirus infection causes a CD8 T cell myocarditis in Atlantic salmon (*Salmo salar* L.). *PLoS ONE.* (2012) 7:e37269. doi: 10.1371/journal.pone.0037269
30. Kongtorp RT, Taksdal T, Lyngoy A. Pathology of heart and skeletal muscle inflammation (HSMI) in farmed Atlantic salmon *Salmo salar*. *Dis Aquat Organ.* (2004) 59:217–24. doi: 10.3354/dao059217
31. Kongtorp RT, Halse M, Taksdal T, Falk K. Longitudinal study of a natural outbreak of heart and skeletal muscle inflammation in Atlantic salmon, *Salmo salar* L. *J Fish Dis.* (2006) 29:233–44. doi: 10.1111/j.1365-2761.2006.00710.x
32. Lund M, Dahle MK, Timmerhaus G, Alarcon M, Powell M, Aspehaug V, et al. Hypoxia tolerance and responses to hypoxic stress during heart and skeletal muscle inflammation in Atlantic salmon (*Salmo salar*). *PLoS ONE.* (2017) 12:e0181109. doi: 10.1371/journal.pone.0181109
33. Haatveit HM, Wessel O, Markussen T, Lund M, Thiede B, Nyman IB, et al. Viral protein kinetics of *Piscine orthoreovirus* infection in atlantic salmon blood cells. *Viruses.* (2017) 9:49. doi: 10.3390/v9030049
34. Bjorgen H, Wessel O, Fjelldal PG, Hansen T, Sveier H, Saebo HR, et al. *Piscine orthoreovirus* (PRV) in red and melanised foci in white muscle of Atlantic salmon (*Salmo salar*). *Vet Res.* (2015) 46:89. doi: 10.1186/s13567-015-0244-6
35. Dhamotharan K, Vendramin N, Markussen T, Wessel O, Cuenca A, Nyman IB, et al. Molecular and antigenic characterization of *Piscine orthoreovirus* (PRV) from Rainbow Trout (*Oncorhynchus mykiss*). *Viruses.* (2018) 10:E170. doi: 10.3390/v10040170
36. Bohle H, Bustos P, Leiva L, Grothusen H, Navas E, Sandoval A, et al. First complete genome sequence of *Piscine orthoreovirus* variant 3 infecting Coho salmon (*Oncorhynchus kisutch*) farmed in Southern Chile. *Genome Announc.* (2018) 6:e00484. doi: 10.1128/genomeA.00484-18
37. Garseth AH, Moldal T, Gasnes SK, Hjortaas MJ, Sollien VP, Gjevre AG. Piscine orthoreovirus-3 is prevalent in wild seatrout (*Salmo trutta* L.) in Norway. *J Fish Dis.* (2019) 42:391–6. doi: 10.1111/jfd.12943
38. Markussen T, Dahle MK, Tengs T, Lovoll M, Finstad OW, Wiik-Nielsen CR, et al. Sequence analysis of the genome of *Piscine orthoreovirus* (PRV) associated with heart and skeletal muscle inflammation (HSMI) in Atlantic salmon (*Salmo salar*). *PLoS ONE.* (2013) 8:e70075. doi: 10.1371/annotation/746a9036-0e54-4a9a-ab16-adb108a3a227
39. Lee PW, Hayes EC, Joklik WK. Protein sigma 1 is the reovirus cell attachment protein. *Virology.* (1981) 108:156–63. doi: 10.1016/0042-6822(81)90535-3
40. Weiner HL, Fields BN. Neutralization of reovirus: the gene responsible for the neutralization antigen. *J Exp Med.* (1977) 146:1305–10. doi: 10.1084/jem.146.5.1305
41. Barton ES, Forrest JC, Connolly JL, Chappell JD, Liu Y, Schnell FJ, et al. Junction adhesion molecule is a receptor for reovirus. *Cell.* (2001) 104:441–51. doi: 10.1016/S0092-8674(01)00231-8
42. Tyler KL, Mann MA, Fields BN, Virgin HWt. Protective anti-reovirus monoclonal antibodies and their effects on viral pathogenesis. *J Virol.* (1993) 67:3446–53.
43. Madan Babu M, Leena Priya M, Anthonymuthu TS, Madera M, Gough J, Aravind L, et al. A Database of Bacterial Lipoproteins (DOLOP) with functional assignments to predicted lipoproteins. *J Bacteriol.* (2006) 188:2761–73. doi: 10.1128/JB.188.8.2761-2773.2006
44. Sargent F, Berks BC, Palmer T. Pathfinders and trailblazers: a prokaryotic targeting system for transport of folded proteins. *FEMS Microbiol Lett.* (2006) 254:198–207. doi: 10.1111/j.1574-6968.2005.00049.x
45. Sankaran K, Wu HC. Lipid modification of bacterial prolipoprotein. Transfer of diacylglyceryl moiety from phosphatidylglycerol. *J Biol Chem.* (1994) 269:19701–6.
46. Murugan V, Sankaran K. Bacterial lipid modification of ICP11 and a new ELISA system applicable for WSSV infection detection. *Mar Biotechnol.* (2018) 20:375–84. doi: 10.1007/s10126-018-9815-7
47. Kamalakkannan S, Murugan V, Jagannadham MV, Nagaraj R, Sankaran K. Bacterial lipid modification of proteins for novel protein engineering applications. *Protein Eng Des Sel.* (2004) 17:721–9. doi: 10.1093/protein/gzh087
48. Kumar S, Balamurali MM, Sankaran K. Bacterial lipid modification of proteins requires appropriate secretory signals even for expression - implications for biogenesis and protein engineering. *Mol Membr Biol.* (2014) 31:183–94. doi: 10.3109/09687688.2014.943819
49. Lund M, Rosaeg MV, Krasnov A, Timmerhaus G, Nyman IB, Aspehaug V, et al. Experimental *Piscine orthoreovirus* infection mediates protection against pancreas disease in Atlantic salmon (*Salmo salar*). *Vet Res.* (2016) 47:107. doi: 10.1186/s13567-016-0389-y
50. Lund H, Bakke AF, Sommerset I, Afanasyev S, Schriwer G, Thorisdottir A, et al. A time-course study of gene expression and antibody repertoire at early time post vaccination of Atlantic salmon. *Mol Immunol.* (2019) 106:99–107. doi: 10.1016/j.molimm.2018.12.018
51. Lamas J, Ellis AE. Atlantic salmon (*Salmon salar*) neutrophil responses to *Aeromonas salmonicida*. *Fish Shellfish Immunol.* (1994) 4:201–19. doi: 10.1006/fsim.1994.1019
52. Rosaeg MV, Lund M, Nyman IB, Markussen T, Aspehaug V, Sindre H, et al. Immunological interactions between *Piscine orthoreovirus* and Salmonid alphavirus infections in Atlantic salmon. *Fish Shellfish Immunol.* (2017) 64:308–19. doi: 10.1016/j.fsi.2017.03.036

53. Haatveit HM, Nyman IB, Markussen T, Wessel O, Dahle MK, Rimstad E. The non-structural protein muNS of *Piscine orthoreovirus* (PRV) forms viral factory-like structures. *Vet Res.* (2016) 47:5. doi: 10.1186/s13567-015-0302-0
54. Dietrich MH, Ogden KM, Katen SP, Reiss K, Sutherland DM, Carnahan RH, et al. Structural insights into reovirus sigma1 interactions with two neutralizing antibodies. *J Virol.* (2017) 91:e01621-16.. doi: 10.1128/JVI.01621-16
55. Graham DA, Rowley HR, Frost P. Cross-neutralization studies with salmonid alphavirus subtype 1-6 strains: results with sera from experimental studies and natural infections. *J Fish Dis.* (2014) 37:683–91. doi: 10.1111/jfd.12167
56. Wessel O, Olsen CM, Rimstad E, Dahle MK. *Piscine orthoreovirus* (PRV) replicates in Atlantic salmon (*Salmo salar* L.) erythrocytes *ex vivo*. *Vet Res.* (2015) 46:26. doi: 10.1186/s13567-015-0154-7
57. Nibert ML, Dermody TS, Fields BN. Structure of the reovirus cell-attachment protein: a model for the domain organization of sigma 1. *J Virol.* (1990) 64:2976–89.
58. Wang HC, Wang HC, Ko TP, Lee YM, Leu JH, Ho CH, et al. White spot syndrome virus protein ICP11: a histone-binding DNA mimic that disrupts nucleosome assembly. *Proc Natl Acad Sci USA*. (2008) 105:20758–63. doi: 10.1073/pnas.0811233106
59. Aspehaug V, Mikalsen AB, Snow M, Biering E, Villoing S. Characterization of the infectious salmon anemia virus fusion protein. *J Virol.* (2005) 79:12544–53. doi: 10.1128/JVI.79.19.12544-12553.2005
60. Verbruggen B, Bickley LK, van Aerle R, Bateman KS, Stentiford GD, Santos EM, et al. Molecular mechanisms of white spot syndrome virus infection and perspectives on treatments. *Viruses.* (2016) 8:E23. doi: 10.3390/v8010023
61. Magnadottir B. Innate immunity of fish (overview). *Fish Shellfish Immunol.* (2006) 20:137–51. doi: 10.1016/j.fsi.2004.09.006
62. Sinyakov MS, Dror M, Zhevelev HM, Margel S, Avtalion RR. Natural antibodies and their significance in active immunization and protection against a defined pathogen in fish. *Vaccine.* (2002) 20:3668–74. doi: 10.1016/S0264-410X(02)00379-1
63. Johansen LH, Dahle MK, Wessel O, Timmerhaus G, Lovoll M, Rosaeg M, et al. Differences in gene expression in Atlantic salmon parr and smolt after challenge with *Piscine orthoreovirus* (PRV). *Mol Immunol.* (2016) 73:138–50. doi: 10.1016/j.molimm.2016.04.007
64. Garver KA, Johnson SC, Polinski MP, Bradshaw JC, Marty GD, Snyman HN, et al. *Piscine orthoreovirus* from Western North America is transmissible to Atlantic salmon and sockeye salmon but fails to cause heart and skeletal muscle inflammation. *PLoS ONE.* (2016) 11:e0146229. doi: 10.1371/journal.pone.0146229
65. Kirchner E, Guglielmi KM, Strauss HM, Dermody TS, Stehle T. Structure of reovirus σ1 in complex with its receptor junctional adhesion molecule-A. *PLoS Pathogens.* (2008) 4:e1000235. doi: 10.1371/journal.ppat.1000235
66. Reiter DM, Frierson JM, Halvorson EE, Kobayashi T, Dermody TS, Stehle T. Crystal structure of reovirus attachment protein sigma1 in complex with sialylated oligosaccharides. *PLoS Pathogens.* (2011) 7:e1002166. doi: 10.1371/journal.ppat.1002166
67. Wessel O, Haugland O, Rode M, Fredriksen BN, Dahle MK, Rimstad E. Inactivated *Piscine orthoreovirus* vaccine protects against heart and skeletal muscle inflammation in Atlantic salmon. *J Fish Dis.* (2018) 41:1411–9. doi: 10.1111/jfd.12835
68. Haatveit HM, Hodneland K, Braaen S, Hansen EF, Nyman IB, Dahle MK, et al. DNA vaccine expressing the non-structural proteins of *Piscine orthoreovirus* delay the kinetics of PRV infection and induces moderate protection against heart -and skeletal muscle inflammation in Atlantic salmon (*Salmo salar*). *Vaccine.* (2018) 36:7599–608. doi: 10.1016/j.vaccine.2018.10.094
69. Adams A, Thompson KD. Recent applications of biotechnology to novel diagnostics for aquatic animals. *Rev Sci Tech.* (2008) 27:197–209. doi: 10.20506/rst.27.1.1792

Conflict of Interest Statement: The authors declare that the research was conducted in the absence of any commercial or financial relationships that could be construed as a potential conflict of interest.

Copyright © 2019 Teige, Kumar, Johansen, Wessel, Vendramin, Lund, Rimstad, Boysen and Dahle. This is an open-access article distributed under the terms of the Creative Commons Attribution License (CC BY). The use, distribution or reproduction in other forums is permitted, provided the original author(s) and the copyright owner(s) are credited and that the original publication in this journal is cited, in accordance with accepted academic practice. No use, distribution or reproduction is permitted which does not comply with these terms.

frontiers in Immunology

REVIEW
published: 21 July 2020
doi: 10.3389/fimmu.2020.01362

Application of Outer Membrane Protein-Based Vaccines Against Major Bacterial Fish Pathogens in India

Biswajit Maiti[1], Saurabh Dubey[2], Hetron Mweemba Munang'andu[2]*, Iddya Karunasagar[3], Indrani Karunasagar[1,3] and Øystein Evensen[2]**

[1] Nitte University Centre for Science Education and Research, Mangaluru, India, [2] Department of Paraclinical Sciences, Faculty of Veterinary Medicine, Norwegian University of Life Sciences, Oslo, Norway, [3] NITTE (Deemed to be University), Mangaluru, India

OPEN ACCESS

Edited by:
Geert Wiegertjes, Wageningen University and Research, Netherlands

Reviewed by:
Bo Peng, Sun Yat-sen University, China
Kim Dawn Thompson, Moredun Research Institute, United Kingdom
Michiel Van Der Vaart, Leiden University, Netherlands

***Correspondence:**
Biswajit Maiti
maiti.b@nitte.edu.in
Hetron Mweemba Munang'andu
hetroney.mweemba.munangandu@nmbu.no
Øystein Evensen
oystein.evensen@nmbu.no

Specialty section:
This article was submitted to Comparative Immunology, a section of the journal Frontiers in Immunology

Received: 29 February 2020
Accepted: 28 May 2020
Published: 21 July 2020

Citation:
Maiti B, Dubey S, Munang'andu HM, Karunasagar I, Karunasagar I and Evensen Ø (2020) Application of Outer Membrane Protein-Based Vaccines Against Major Bacterial Fish Pathogens in India. Front. Immunol. 11:1362. doi: 10.3389/fimmu.2020.01362

Aquaculture is one of the fastest-growing food-producing sectors in the world. However, its growth is hampered by various disease problems due to infectious microorganisms, including Gram-negative bacteria in finfish aquaculture. Disease control in aquaculture by use of antibiotics is not recommended as it leads to antibiotic residues in the final product, selection, and spread of antibiotic resistance in the environment. Therefore, focus is on disease prevention by vaccination. All Gram-negative bacteria possess surface-associated outer membrane proteins (OMPs), some of which have long been recognized as potential vaccine candidates. OMPs are essential for maintaining the integrity and selective permeability of the bacterial membrane and play a key role in adaptive responses of bacteria such as solute and ion uptake, iron acquisition, antimicrobial resistance, serum resistance, and bile salt resistance and some adhesins have virulence attributes. Antigenic diversity among bacterial strains even within the same bacterial species has constrained vaccine developments, but OMPs that are conserved across serotypes could be used as potential candidates in vaccine development, and several studies have demonstrated their efficacy and potential as vaccine candidates. In this review, we will look into the application of OMPs for the design of vaccines based on recombinant proteins, subunit vaccines, chimeric proteins, and DNA vaccines as new-generation vaccine candidates for major bacterial pathogens of fish for sustainable aquaculture.

Keywords: outer membrane proteins (OMPs), vaccination, fish, aquaculture, fish pathogens

INTRODUCTION

Asia accounts for more than 80% of the global aquaculture production of which India is the third largest producer (1, 2). Indian aquaculture has enormous potential and contributes significantly to the country's economy and its foreign exchange earnings. Finfishes are the most cultured species in the world, and India is no exception, contributing to 68% of world food fish aquaculture production with the other groups being molluskan shellfish (oyster, clam, mussel, and scallop), crustaceans (shrimps and prawns), and other fishes (1). A half of global food fish consumption comes from aquaculture. However, there is a need to improve management practices in order to reduce the disease burden and usage of drugs for disease treatment.

Although aquaculture is fast growing in Asian countries such as India, the largest proportion of fish farming is done by low-resource farmers in earthen ponds and floating cages in rivers and lakes whose environmental conditions support the survival of opportunistic pathogenic bacteria that cause disease in fish. Implementation of biosecurity measures is mostly low while the use of antibiotics is high, posing the danger of drug resistance (3–5). As such, vaccination is considered to be the most effective environmentally friendly disease control strategy. However, the most prevalent diseases infecting the top farmed fish species in each country guide the choice and priority of vaccine development. India being a country mostly producing carp, pathogens infecting top farmed carp species would be a priority for fish vaccines. Another confounding factor is the choice of vaccine delivery system as to whether vaccines should be administered by injection, orally, or immersion, which is guided by factors such the cost of vaccination, labor input, stress on fish, and other factors. Hence, the objective of this review is to bring into perspective the major fish species farmed in India together with major pathogens that need vaccine development. We also wanted to highlight the shortcomings of whole cell inactivated (WCI) and attenuated live vaccines used elsewhere that have paved way to research on the use of outer membrane protein (OMP) vaccines in Indian aquaculture. Herein, we provide an up-to-date status of ongoing research on OMP vaccines being developed against major pathogens infecting the top-farmed fish species in Indian aquaculture.

FISH AQUACULTURE: PRESENT STATUS

Food and nutritional security are being addressed through aquaculture due to stagnation of capture fisheries. In 2016, total global production of fish, crustaceans, mollusks, and other aquatic animals reached 170.9 million tons (MT) in which a large volume (>88%) was utilized for human consumption (1, 2). Global aquaculture is a fast-growing vital sector for the production of high-protein food, having an average annual growth rate of 5.8% during 2001–2016 (6). In India, aquaculture is a rapidly growing fisheries sector with an annual growth rate of over 7% of which freshwater aquaculture contributed 95% of the total annual production of 5.77 mt (MT) by 2017 (7). As discussed by Jayasankar (8), advances in carp breeding technologies and traditional polyculture system have contributed to increased production of the three India major carp species, namely, catla (*Catla catla*), rohu (*Labeo rohita*), and mrigal (*Cirrhinus mrigala*), accounting for 70–75% of total freshwater production. This is followed by the culture of three exotic carp species comprising of common carp (*Cyprinus carpio*), silver carp (*Hypophthalmichthys molitrix*), and grass carp (*Ctenopharyngodon idella*) that account for 20–30% of freshwater fish species. The increase in stocking density brought about by intensified farming systems led to increased output from 500 to 600 kg/ha to 3,000 kg/ha, resulting in fish farmers achieving higher production levels of 6–8 t/ha/year, while national average output increased from 50 kg/ha/year in 1974–1975 to about 2,135 kg/ha/year in 1994–1995 and 2,270 kg/ha/year in 2003–2004 (9, 10). Due to the contribution of public and private hatcheries in the production of about 40 billion fry in 2017, it is projected that by 2020, total carp production would exceed 15 mt due to intensive farming systems supported by high stocking densities (8). This increasing trend in stocking density could be contributing to the increase in disease outbreaks as a result of the increase in the disease transmission index as well as induction of stress predisposing fish to various infections.

MAJOR BACTERIAL FISH PATHOGENS IN INDIA

The major diseases of finfish in Indian aquaculture are caused by bacterial infections (7, 11). Viral pathogens like tilapia lake virus (TiLV) (12), nodavirus (13), Koi herpesvirus virus (KHV) (14), and red sea bream iridovirus (RSBIV) (15, 16) are not pathogens of top farmed fish species in India. The major parasite-causing disease in fish in India is *Ichthyophthirius mulifiliis* (11) whose impact is not severe compared to bacterial pathogens. Overall, viral and parasitic diseases cause less economic losses unlike bacterial diseases that cause an adverse economic impact, calling for the urgent need of protective vaccines (17). The most prevalent bacterial pathogens in Indian aquaculture belong to the genera *Aeromonas*, *Edwardsiella*, *Vibrio*, and *Flavobacterium*, infecting the top farmed fish species (11, 18). **Table 1** shows fish species infected by these bacteria and their occurrence during different stages of the fish production cycles. Other pathogenic bacterial genera that are associated with fish diseases in India include *Streptococcus*, *Pseudomonas*, and *Mycobacterium*.

Aeromonads belong to the family *Aeromonadaceae*, and the most common species associated with fish diseases in India are *Aeromonas hydrophila* (24, 25), *Aeromonas sobria* (26, 27), *Aeromonas caviae* (28), and *Aeromonas veronii* (29). They are natural inhabitants of aquatic environments such as freshwater, estuarine, and infrequently marine waters (25). These pathogens cause hemorrhagic septicemia, tail-rot (or fin-rot), red sore, ulcerative disease, dropsy, asymptomatic septicemia, exophthalmos, and ulceration in different fish species (30).

Vibriosis is one of the most critical fish diseases caused by members of the genus *Vibrio* that are ubiquitous in aquatic environments. The disease affects both cold-water and warmwater fish species, including sea bass, carp, catfish, salmon, flounder, and eel across the world. In India, the *Vibrio* species known to cause diseases include *Vibrio anguillarum*, *Vibrio alginolyticus*, *Vibrio parahaemolyticus*, *Vibrio ordalii*, and *Vibrio vulnificus* of which classical vibriosis is mostly caused by *V. anguillarum* (20, 31).

Another important genus is *Edwardsiella*, which is ubiquitous in aquatic environments and is responsible for high mortality in several commercial fish species including carp, catfish, and tilapia in India. Previous studies have shown that the most common *Edwardsiella* species infecting fish in India was *Edwardsiella tarda* (22) as the causative agent of septicemia in warmwater fish species, especially catfish. It also causes fish gangrene, emphysematous putrefactive disease, red disease, and enteric septicemia in carp, catfish, and several other fish species (32, 33).

TABLE 1 | Major bacterial diseases causing fish diseases in Indian aquaculture.

Bacteria	Disease name	Fish spp.	Symptom	Stage of fish	References
Aeromonas hydrophila	Motile aeromonad septicemia	Indian carp fish (catla, rohu, and mrigal)	Hemorrhagic and ulcerative lesion on the skin, fins, head	All stages	(11, 19–21)
Edwardsiella spp.	Edwardsiellosis	Indian carp fish (catla, rohu, and mrigal) and other cat fishes	Ulcerative abscesses in internal organs, rectal protrusion	Mostly fry and fingerlings	(11, 20–23)
Vibrio anguillarum	Vibriosis	Catla, rohu, mrigal, and sea bass	Hemorrhagic septicemia	All stages	(11, 20, 21)
Flavobacterium columnare	Columnaris disease	Catla, rohu, mrigal, common carp, and other species	Gasping, lethargic, gill looks discolored with trapped material	All stages	(11, 20, 21)

However, in a recent study, we showed that piscine *Edwardsiella* isolates from 10 fish species in India belonged to *Edwardsiella piscicida* and *Edwardsiella anguillarum* (34). Therefore, it is likely that all fish isolates previously classified as *E. tarda* were either *E. piscicida* or *E. anguillarum*.

Among the *Flavobacterium*, *Flavobacterium columnare* is the most common isolate and often associated with columnaris in farmed catfish (Clarias batrachus), carp (*C. carpio*), rohu (*L. rohita*), catla (*C. catla*), and other fish species (35, 36). Other *Flavobacterium* species reported to cause disease in fish in India include *Flavobacterium* aquaticum, *Flavobacterium* granuli, *Flavobacterium* hercynium, and *Flavobacterium* terrae (35).

The common denominator for all these bacteria species is that they ubiquitously live in water and are able to survive under different environmental conditions (25, 37–40) becoming pathogenic as fish become vulnerable to infection when predisposing factors such as high stocking densities that stress fish leading to immunosuppression favor infection establishment. Therefore, the increase in stocking density aimed at increasing productivity in Indian aquaculture discussed in the section *Fish Aquaculture: Present Status* could be contributing to the increase in disease outbreaks caused by these bacteria species.

DISEASE PREVENTION THROUGH VACCINATION

Intensive aquaculture systems where single or multiple fish species are cultured at high densities facilitate high transmission of pathogens between individual fish. Although biosecurity measures that include quarantine, sanitation, and disinfection as well as the use of probiotics, disease-free brood stock, immunostimulants, and quality feed have been shown to reduce disease transmission, these measures do not always ensure total elimination of infectious agents. On the other hand, use of antibiotics poses the risk of selection of drug resistance in pathogens, making the treatment ineffective, spread of resistance determinants to other bacteria (41), and antibiotic residues in food (42). To prevent the recurrence of disease outbreaks and widespread use of antibiotics in aquatic environments in India, the most environment-friendly practical approach would be vaccination. For example, vaccination of Atlantic salmon (*Salmo salar* L.) against pathogens such as *Aeromonas salmonicida* and *Vibrio salmonicida* for more than 30 years contributed to a significant reduction of antibiotics use in Norway from nearly 50,000 kg of antibiotics in 1987 to <1,000–2,000 kg in 1997 (43).

Vaccines in aquaculture are either administered by injection, oral route, or immersion. Advantages of oral and immersion vaccine delivery systems are that they are less labor intensive, uses the natural route of pathogen exposure, and less stressful on fish, while vaccination by injection is labor intensive, bypasses the natural route of pathogen exposure, and is stressful on fish. However, vaccination by injection guarantees delivery of the same antigen dose to all fish, while immersion and oral vaccine delivery do not (44). Vaccines administered by injection require high labor costs for individual handling, which is expensive for the majority of low-resource fish farmers in India. On the contrary, vaccine delivery by immersion or oral does not require high labor costs because fish are vaccinated in bulk at the same time orally through feed or by immersion in vaccine-containing water. The major predicament with vaccine delivery by immersion is that practically it cannot be done in open water in ponds or cages floating in rivers and lakes. On the other hand, the major drawback with oral vaccination is that vaccines administered by ingestion are degraded in the acidic environment of the stomach/foregut before they reach the intestine where they are potentially taken up by cells of the innate immune system for local antigen presentation or transport to major immune organs (kidney/spleen) (45). There are few oral vaccines licensed to date (46), and new approaches using new technologies such as poly D, L lactic-co-glycolic acid (PLGA) nanoparticle vaccines that can protect antigens against low pH degradation in the stomach/gut are considered better alternatives.

CHOICE OF VACCINE CANDIDATE: OUTER MEMBRANE PROTEINS

Traditionally, fish vaccines are made of live-attenuated or WCI vaccines (47, 48). WCI bacterial vaccines are prepared by chemical or heat inactivation of bacteria, and they account for the largest proportion of commercial vaccines used in aquaculture worldwide (49). They are safe because they are not infectious ("killed") but have the disadvantage of being less immunogenic, needing adjuvants to produce long-term

protective immunity (49). They elicit humoral immune responses that to a lesser extent confer protection against intracellular replicating bacteria such as *A. hydrophila, Edwardsiella* spp., or *Piscirickettsia* sp. because they do not induce cell-mediated immune (CMI) responses needed to eliminate intracellularly replicating bacteria (50). In contrast, live attenuated vaccines are highly immunogenic and have the ability to evoke both humoral and CMI responses needed to eliminate extra- and intracellular bacteria, but they pose the danger of reversion to virulence (50). DNA vaccines meet challenges of genetically modified organism (GMO) regulations; although the vaccines by themselves are not considered GMOs, vaccinated fish are considered GMOs under certain conditions. In the case of Indian aquaculture where intracellular replicating bacteria such as *A. hydrophila* and *Edwardsiella* spp. account for a large proportion of pathogens infecting top farmed fish species, there is a need for vaccines able to evoke both humoral and CMI responses. Currently, there are no licensed attenuated live vaccines against diseases caused by these pathogens. Hence, the use of genetically engineered vaccines using immunogenic proteins such as OMPs encoded in carrier vectors able to evoke both humoral and CMI responses is considered to be a better alternative.

Several studies show that bacterial OMPs have the potential to serve as vaccine candidates for immunization against bacteria infecting fish (49). OMPs are the essential component of outer membranes and are found in many prokaryotes (bacteria) as well as in specific organelles like mitochondria, chloroplasts (51) of eukaryotic cells, possibly even in archaea (52). In general, about 2–3% of the total bacterial genes encode OMPs in Gram-negative bacteria (53). They are made of β-barrel structures that contain 8–22 β-strands, which are antiparallel to each other and tilted strongly on the barrel axis (54). They are shaped in different forms such as monomers, homo-dimers, and/or homo-trimers in the outer membrane of which more than a dozen OMP structures have been resolved. As shown in **Figure 1**, the structural layout of OMPs shows that the C and N-terminal ends of OMPs are directed toward the periplasm, while surface loops (marked as L1, L2, L3, and so on) are located on the outermost exterior where they are exposed to the outside environment. Several studies have shown that the surface periplasmic that turns together with surface loops of OMPs have more sequence variations than the β-sheet strands, which are conserved in most bacteria species (51, 55). For example, Braun and Cole (56) found a low amino acid sequence similarity of the periplasmic turns and surface loops (54%) while β-sheets similarity was higher (74%) among OmpA proteins of *Serratia marcescens*. The strategic location of surface loops being exposed to the exterior surface render them ideal for interaction with host cells while their sequence differences could account for antigenic diversity within bacterial species (57). As such, OMPs are considered potential vaccine candidates since they are (i) highly immunogenic due to their exposed epitopes on the bacterial outer cell surface and (ii) highly conserved among different serovars and within Gram-negative bacteria (58–63). Suffice to point out that some OMPs also work as adhesins facilitating the attachment and penetration of bacteria into the host cells, thereby contributing to virulence (58–63). In addition, OMPs carry pathogen-associated molecular patterns (PAMPs) such as lipopolysaccharide (LPS) recognized by pathogen recognition receptors (PRRs) found on host cells such as monocytes, macrophages, neutrophils, and dendritic cells involved in antigen uptake, processing, and presentation to cells of the adaptive immune system for induction of long-term protective immunity. Overall, this supports the use of OMPs as ideal vaccine candidates for both intra- and extracellular bacteria that are endemic in Indian aquaculture. As shown in **Table 1**, various OMPs have been used for vaccine development against various pathogens infecting different fish species in India.

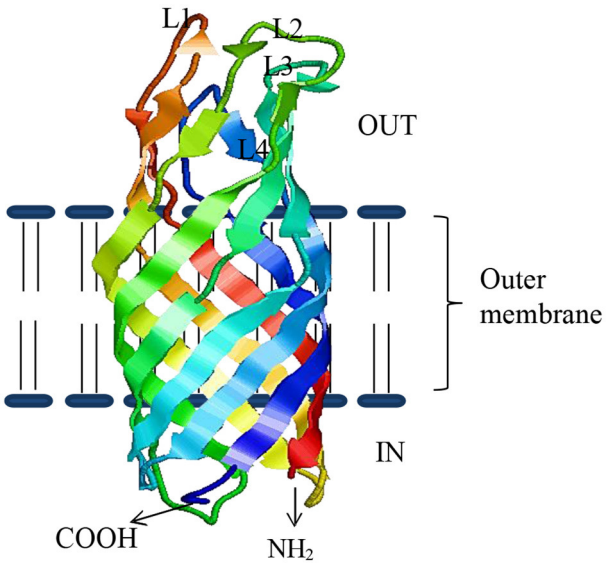


FIGURE 1 | The β-sheeted architecture of OmpW protein of *A. hydrophila*. Four outside exposed loops of the protein are indicated as L1–L4, respectively.

DEVELOPMENT OF VACCINE CANDIDATES THROUGH EPITOPE MAPPING

Epitope mapping of antigenic proteins recognized by B and T cells is crucial for optimal vaccine design. One approach suggested by Rappuoli (64) is to use reverse vaccinology in which several molecules are screened using *in silico* analysis to identify potential vaccine candidates (65). **Figure 2** illustrates the use of reverse vaccinology in vaccine design. In India, various studies have been conducted aimed at identifying bacterial antigenic proteins using *in silico* analysis as shown in **Table 2**. Nucleotide or genome sequence of several OMPs can be retrieved from the databases for *in silico* analysis. There are several bioinformatics tools available used to identify open reading frames (ORFs) encoding putative *omp* genes while the basic local alignment search tool (BLAST) (http://blast.ncbi.nlm.nih.gov/Blast.cgi) of the National Center for Biotechnology Information (NCBI) can be used for sequence verification. After predicting ORFs encoding the putative *omp* genes, the next step is to apply a battery of algorithms designed to extract as much information

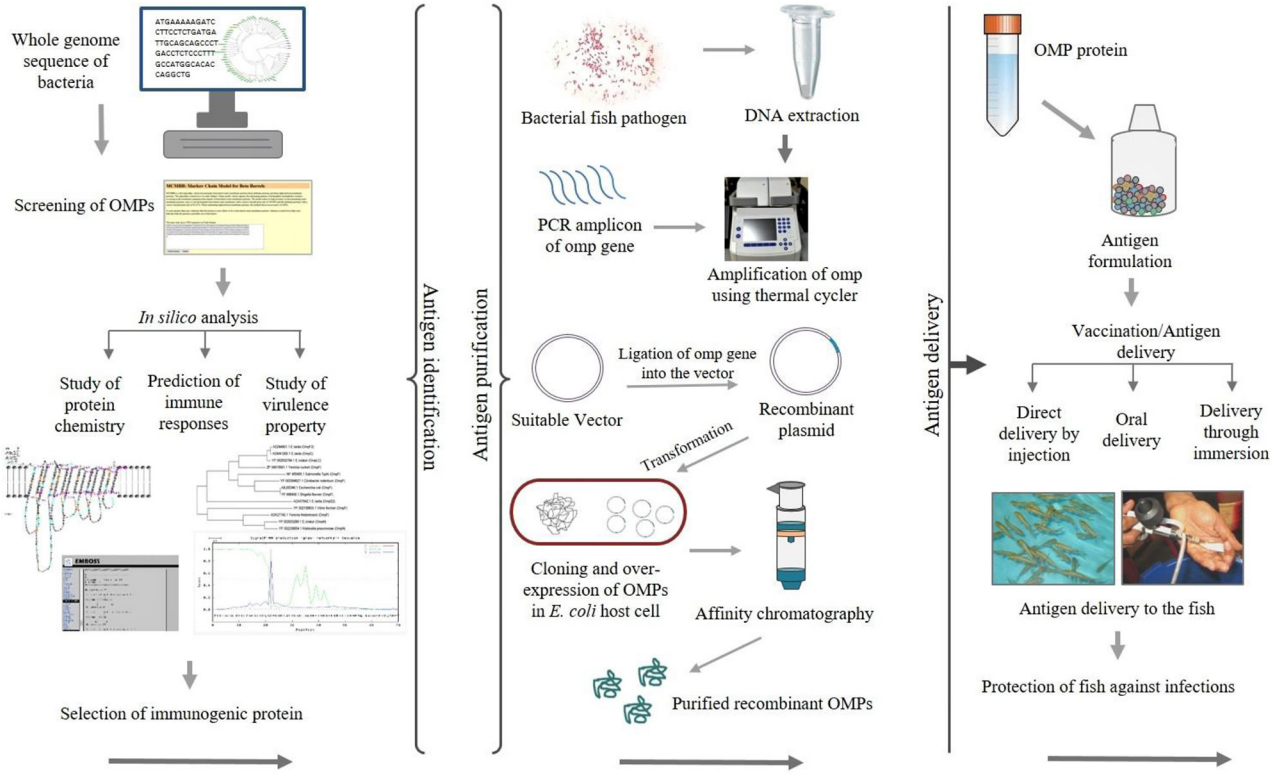


FIGURE 2 | Schematic diagram showing the application of recombinant outer membrane proteins (OMPs) through a reverse vaccinology approach.

about the ORF as possible, including tentative molecular weight, pI, and hydrophobic nature of the protein. In general, OMPs include signal peptide required for translocation from the cytoplasm to the outer membrane of cells. The SignalP 5.0 server (http://www.cbs.dtu.dk/services/SignalP/) (83) offers a platform based on a combination of several artificial neural networks that can predict the presence of signal peptides and identify the cleavage sites in proteins. The number of domains and motifs can be found with the help of a domain finder and motif finder. Further, beta-barrel OMPs can be predicted and two-dimensional topology can be analyzed using the online software PRED-TMBB (http://bioinformatics.biol.uoa.gr/PRED-TMBB) (84). The degree of immunogenicity associated with specific OMPs can be predicted using various tools such as the EMBOSS server (http://bioinfo.nhri.org.tw/gui/) (85), which is one of the popular online sites used for the determination of antigenic sites present in the protein. The presence of B- and T-cell epitopes can be identified in OMP sequences using different software. For example, the locations of linear B-cell epitopes in the OMP sequence can be identified by the BepiPred server (http://www.cbs.dtu.dk/services/BepiPred/) (86) that uses a combination of hidden Markov model and propensity scale methods. The commonly used T-cell epitope predicting tool like NetCTL (http://www.cbs.dtu.dk/services/NetCTL/) (87) identifies protein sequences using major histocompatibility complex (MHC) class I binding prediction of 12 MHC supertypes including the supertypes A26 and B39. Peptide–MHC class I binding can be predicted using NetMHC server (http://www.cbs.dtu.dk/services/NetMHC/) (88) that works on artificial neural networks (ANNs) and weight matrices.

Another approach used for epitope mapping that has gained precedent in recent years is whole-genome sequencing (WGS) of pathogens used to identify new antigens. Together with recombinant DNA technology, WGS has contributed to improving OMP vaccine design, while protein sequence comparison has proved to be a powerful tool used to identify immunogenic proteins that are broadly protective against variant pathogen strains. For example, Dubey et al. (34) used protein sequence comparison and phylogenetic analysis to show that the OmpW of *E. piscicida* and *E. anguillarum* had high similarity, suggesting that a common antigen can be used against isolates from different fish species and geographical areas in Asia.

RECOMBINANT ANTIGEN DELIVERY SYSTEM FOR OUTER MEMBRANE PROTEIN VACCINES

Genetically engineered vaccines are made of purified recombinant proteins or subunit of proteins expressed in heterologous vectors (89). The main advantage of recombinant vaccines is safety because they only contain the antigenic protein and not the entire pathogens. Moreover, genetically engineered vaccines help remove undesired harmful antigens or cleave

TABLE 2 | Outer membrane protein (OMP)-based vaccination studies conducted in India against major bacterial fish pathogens.

Type of vaccine	Targeted OMP(s)	Antigen formulations	Bacterial species	Fish species	Method Ag delivery	RPS (%)	References
Mixed protein	Total OMPs	With or without adjuvants	*A. hydrophila*	Goldfish (*C. auratus*)	I/p	NC (70*)	(66)
Mixed protein	Total OMPs	Mixed with adjuvant	*E. tarda*	Rohu (*L. rohita*)	I/p	100	(67)
Mixed protein	Total OMPs	Mixed with saline	*A. hydrophila*	Goldfish (*C. auratus*)	ND	ND	(68)
Mixed protein	Total OMPs	PLGA microparticle encapsulated	*A. hydrophila*	Rohu (*L. rohita*)	I/p	ND	(69)
Mixed protein	Total OMPs	PLA and PLGA nanoparticle encapsulated	*A. hydrophila*	Rohu (*L. rohita*)	I/p	NC (80 and 75*)	(70)
Mixed protein	Total OMPs	Alginate-chitosan-PLGA encapsulated	*A. hydrophila*	Rohu (*L. rohita*)	I/p	NC	(71, 72)
Subunit protein	OmpTS	Mixed with adjuvant	*A. hydrophila*	Rohu (*L. rohita*)	I/p	57	(73, 74)
Subunit protein	OmpK	Mixed with adjuvant	*V. anguillarum*	Rohu (*L. rohita*)	I/p	67.8	(75)
Subunit protein	OmpR	Mixed with adjuvant	*A. hydrophila*	Rohu (*L. rohita*)	I/p	NC	(76)
Subunit protein	Omp48	Mixed with saline	*A. hydrophila* and *E. tarda*	Rohu (*L. rohita*)	I/m	69 and 60, respectively	(77)
Subunit protein	OmpA	Mixed with saline	*E. tarda*	Common carp	I/p	54.3	(78)
Subunit protein	Aha1 and OmpW	Mixed with saline	*A. hydrophila*	Common carp	I/p	52 and 71, respectively	(58, 59)
Subunit protein	OmpW	PLGA nanoparticle encapsulated	*A. hydrophila*	Rohu (*L. rohita*)	Oral delivery	80	(79)
Subunit protein	OmpA	Chitosan nanoparticle encapsulated	*E. tarda*	Fringed-lipped peninsula carp (*L. fimbriatus*)	Oral delivery	NC (PCSP: 73)	(80)
DNA vaccine	Omp38	Chitosan microparticle encapsulated	*V. anguillarum*	Asian sea bass (*L. calcarifer*)	Oral delivery	46	(81)
DNA vaccine	Omp38	Mixed with saline	*V. anguillarum*	Sea bass (*L. calcarifer*)	I/m	55.6	(82)

**% of survival; ND, not done; NC, not calculated.*
RPS, relative percent survival; PCSP, post-challenge survival proportions; PLGA, poly D, L lactic-co-glycolic acid; PLA, polylactic acid.

out epitopes that stimulate T-suppressor cells. The common genetically engineered vaccines used for delivery of OMPs and other antigens in aquaculture are subunit and DNA vaccines.

Outer Membrane Proteins as a Subunit Vaccine

In recent years, recombinant OMPs are widely tested as subunit vaccines for various pathogens in different fish species since they are highly immunogenic and they are considered safe because they only contain the antigen proteins and not the entire pathogen (59, 65, 71, 77–80, 90–105). Subunit vaccines either (i) are made of specific targeted epitopes identified from total OMPs using technologies such *in silico* analysis or mass spectrometry (**Table 2**) or (ii) use total OMP expressed in recombinant expression vectors (**Table 3**).

In India, Maji et al. (68) fractionated the *A. hydrophila* OMP using gel permeation and ion-exchange chromatography and generated 10 fractions of which two of the fractionated antigens made of 23-kDa and 57-kDa polypeptides had higher sero-reactivity than the crude OMP. In another study, Kumar et al. (67) used isoelectric focusing (IEF) followed by two-dimensional polyacrylamide gel electrophoresis (PAGE) and mass spectrophotometry to identify two immunogenic proteins (OMP assembly factor YaeT and GroEL) from *E. tarda* OMP that produced 100% protection after challenge in vaccinated rohu. Sharma and Dixit (106) used *in silico* analysis to eliminate nonspecific binding epitopes and selectively identified four immunodominant B-cell epitopes of the *A. hydrophila* OmpF that were highly immunogenic. They showed that the region harboring 66–80 aa residues of the OmpF had the highest reactivity in ELISA, clearly indicating that the OmpF epitope$_{66-80}$ was the most potent vaccine candidate against *A. hydrophila*. In another study, Sharma and Dixit (108) used a bioinformatic algorithm to show that the linear B-cell epitopes covering 143–175 aa of *A. hydrophila* OmpC had the highest cross reactivity with the parent OmpC protein. Antibody

TABLE 3 | *In silico* vaccine designing study conducted in India to control fish pathogens.

Type of vaccine	Targeted OMP(s)	Name of bacteria pathogen	Conclusion from analysis	References
Subunit vaccine	OmpC	*A. hydrophila*	Promising vaccine candidate	(106)
Subunit vaccine	LamB	*A. hydrophila*	A porin protein, useful as a vaccine candidate	(107)
Subunit vaccine	OmpF	*A. hydrophila*	OmpF epitope in fusion with a carrier protein, promising vaccine candidate	(108)
Subunit vaccine	TolC	*E. tarda* and *F. columnare*	Good vaccine candidate	(109)
Subunit vaccine	OmpW	*E. tarda*	An adhesin molecule, potential vaccine candidate	(63)
Subunit vaccine	OmpN	*E. ictaluri*	A porin protein, useful as a vaccine candidate	(110)
Subunit vaccine	OmpK and OmpU	*V. anguillarum*	Potential vaccine candidate	(65)

isotyping, cytokine ELISA, and cytokine array analysis revealed a Th2 skewed immune response. Mahendran et al. (109) used *in silico* immunoinformatics to identify T-cell epitopes with binding interaction between *E. tarda* TolC and *F. columnare* FCOLo peptides of OMPs with MHC-I alleles. Altogether, these studies show that specific immunogenic proteins can be identified targeting B- and T-cell epitopes from total/crude OMPs for use in vaccine design.

The majority of OMP subunit vaccines are made of entire ORFs of total OMPs expressed and purified from heterologous vectors (**Table 3**). Bader et al. (111) showed that total OMP extracted from *Edwardsiella ictaluri* had low protection in channel catfish vaccinated with 3.13 or 6.25 μg of OMP, but a higher dose of OMP (12.5 μg) produced higher protection [relative percent survival (RPS) = 67.5]. Khushiramani et al. (73, 74) showed that the *A. hydrophila* OmpTS produced 57% survival in rohu after challenge. Similarly, Wang et al. (112) compared the protective ability of a 20-kDa protein of *A. hydrophila* OmpW with a kDa adhesin protein (Aha1) of *A. hydrophila* in common carp (*C. carpio*) and showed that the rOmpW (RPS = 71%) had superior protection over the Aha1 (RPS = 52%) after challenge (59). In another study, Khushiramani et al. (77) showed that the rOmp48 produced high protection in rohu against multiple fish pathogens viz *A. hydrophila* (RPS = 69%) and *E. tarda* (RPS = 60%), indicating that Omp48 could be used against multiple pathogens. A study by Maiti et al. (78) reported RPS = 54.3% in common carp using vaccinated rOmpA after challenge with *E. tarda*. Similarly, Hamod et al. (75) showed high protection (RPS = 67.8%) in adult rohu vaccinated with a rOmpK subunit vaccine after challenge with *Vibrio anguillarum*. Dash et al. (76) showed that a rOmpR vaccine adjuvanted with mineral oil produced 54 and 90% survival in rohu after challenge with *A. hydrophila* at 56 and 140 days post vaccination, respectively. In the same study, Dash et al. (76) used the same rOmpR vaccine with a modified adjuvant of mineral oil mixed with phosphate buffered saline (PBS) at equal volumes (1:1 ratio) and showed protection of 67 and 87% after challenge with *A. hydrophila* at 56 and 140 days post vaccination, respectively. Put together, these studies show that OMP vaccines are being developed against major fish pathogens such as *A. hydrophila*, *E. tarda*, and *V. anguillarum* (**Table 1**) and that vaccine efficacy trials are mostly done in fish species such as rohu, common carp, and channel catfish that are among the top farmed species in the Indian aquaculture. In addition, these studies also show that different OMPs such as OmpA, OmpK, OmpR, OmpW, OmpTS, and Omp48 are being used in the design of subunit vaccines in India.

Outer Membrane Protein Encoding Genes for DNA Vaccines

Another important vaccination approach used for the delivery of OMP antigens is the use of plasmid vectors to produce DNA vaccines able to transcribe and translate the immunogenic OMP genes intracellularly (113). DNA vaccines possess several advantages over WCI vaccines such as the stimulation of both humoral and CMI responses (50, 114, 115) unlike WCI vaccines that only stimulate humoral responses (49). Moreover, DNA vaccines do not require the potentiation effect of adjuvants unlike WCI vaccines that have been shown to have severe side effects caused by adjuvants incorporated in vaccine formulations (116). In addition, DNA vaccines do not pose the danger of reversion to virulence unlike live attenuated vaccine that pose the risk of reverting to virulence. However, there are some drawbacks associated with DNA vaccination of which the most important is the possibility of integration of plasmid DNA into the host genome, which pose the danger of being transferred to other aquatic organisms and humans (117). Other difficulties include the cost of preparation and method of administration. In India, a porin gene encoding 38-kDa major OMP (Omp38) of *V. anguillarum* was used to construct a DNA vaccine for immunization of sea bass (*Lates calcarifer*) administered by intramuscular injection by Kumar et al. (82). After challenge with *V. anguillarum*, vaccinated sea bass was protected (RPS = 55.6%) unlike the control group that had high mortality. In another trial, Asian sea bass vaccinated using a DNA vaccine showed moderate protection (RPS = 46%) after challenge with *V. anguillarum* (81). Overall, there are few studies on OMP-based DNA vaccine compared to those with subunit vaccines for fish carried out in India so far.

BIODEGRADABLE NANOPARTICLE DELIVERY SYSTEMS

PLGA, polylactic acid (PLA), and chitosan are polymers, commonly used for vaccine delivery as nanoparticles

because of their biodegradable nontoxic properties (118–120). Moreover, they are easy to produce and are relatively affordable. They are attractive for oral vaccination because they easily adsorb to epithelial cells and penetrate the mucosal barrier where they are taken up by antigen-presenting cells (APCs). And as such, they can be bioengineered to enhance their adsorption on mucosal cells. Cellular uptake of PLGA nanoparticles is widely documented as shown that they are easily engulfed by various phagocytic cells such as monocytes, macrophages, neutrophils, and dendritic cells that serve as APCs leading to activation of cells of the adaptive immune system for induction of long-term protective immunity (121–126). They protect the vaccines from degradation, and they have been shown to have some potentiation effect able to enhance their uptake and enable slow release of antigens at deposition sites (127–129). Put together, these attributes render use of biodegradable nanoparticles as a better option for oral delivery of OMP vaccines than feed-coated oral vaccines.

Behera et al. (69) used PLGA microparticle for delivery *A. hydrophila* OMPs in rohu in which they observed an increase in several innate immune parameters such as respiratory burst, lysozyme, and complement activity alongside an increase in long-term expression of antibody responses against *A. hydrophila* in rohu. In another study, Behera et al. (72) showed 90% survival in rohu vaccinated with *A. hydrophila* OMP PLGA microsphere vaccine than in control fish vaccinated with OMPs that had 100% mortality after challenge with *A. hydrophila*. Similarly, Rauta and Nayak (70) showed high antibody responses and survival in rohu vaccinated with PLA-OMP (80%) and PLGA-OMP (75%) nanoparticles after challenge with *A. hydrophila*. Dubey et al. (79) immunized rohu using OmpW encapsulated in PLGA nanoparticles by oral vaccination and showed a dose-dependent protective immunity in which fish vaccinated with a low antigen dose had 48.3% survival while fish vaccinated with a high antigen dose had 73.3 % after challenge with *A. hydrophila*. In another study, Dubey et al. (80) showed that the OmpA encapsulated in chitosan nanoparticles (73.3%) had superior protection over WCI vaccine (48.3%) in *Labeo fimbriatus* after challenge with *E. tarda*. In general, studies on biodegradable nanoparticle fish vaccines are increasing in India because of safety and ease of administration orally through feed and absence of side effects. On the other hand, WCI vaccine formulations with adjuvants such as mineral oils have been linked to side effects in fish (116).

CHALLENGES IN DEVELOPING OUTER MEMBRANE PROTEIN VACCINES

While OMPs have proved to be protective antigens ideal for vaccine development, there are several factors that make the design of fish vaccines using OMPs a challenge. For example, the surface loops that encode epitopes for B-cell binding have been shown to be highly divergent for some bacterial species, making it difficult to choose antigens with a broad protective ability against variant strains for use in different ecosystems. One of the challenges in bioengineering of OMP vaccines is LPS detoxification. LPS activates the innate immune system via Toll-like receptor (TLR)4 of which excessive TLR4 activation causes endotoxicity, leading to excessive inflammatory cytokine expression (130). While Zollinger et al. (131) described detoxification of LPS using a detergent extraction process, other scientists have used bioengineering techniques for LPS detoxification (132, 133). Leitner et al. (134) showed that genetic modification of LPS lipid A of *Vibrio cholerae* detoxified the LPS activity and elicited the production of highly protective antibodies, while Watkins et al. (135) detoxified LPS by producing truncated LPS containing lipid IVa instead of full LPS. Endotoxicity of LPS encoded in OMPs used for fish vaccine design has not been determined, and this poses a threat in the safety of OMPs used for fish vaccines. Another challenge in OMP-based vaccines is selecting epitopes able to evoke both humoral and CMI responses. OMP surface antigens encode epitopes specific for B-cell binding (136), while luminal antigens shielded inside β-sheets have been shown to be skewed toward CMI responses (137). The challenge is to identify luminal peptides suitable for producing T-cell vaccines. While OMPs are, by themselves, potent adjuvants able to activate the innate immune system through interaction between their PAMPs and host TLRs, they require additional conventional adjuvants to sustain long-term activation of the innate immune system of which the choice of adjuvant can be a challenge especially for oral vaccines (138, 139).

CONCLUSION

OMPs are essential molecules of Gram-negative bacteria as they play various roles including adaptation, immunogenicity, and pathogenesis of bacterium. They possess epitopes essential for binding to B and T lymphocytes, rendering them to be ideal vaccine candidates for both extra- and intra-cellular replicating bacteria. And as shown herein, they have been widely used in vaccine development for the Indian aquaculture, which has a high prevalence of both extra- and intracellular replicating bacterial pathogens such as *Edwardsiella* spp., *Aeromonads*, *Vibrio* spp., and *Flavobacterium* spp. The quest to develop safe vaccines that do not pose the danger of reversion to virulence, such as live attenuated vaccines, coupled with the need for vaccines able to evoke both humoral and CMI responses, unlike WCI vaccines, has extended the search for protective vaccines to include OMPs in vaccine development. Evidence obtained through work carried out by several groups in India reveals that OMPs are potent immunogenic molecules able to provide significant protection in fish when delivered as subunit, DNA, or PLGA/chitosan nanoparticle vaccines. Despite so, there is a need for optimization of several factors such as the choice of antigen delivery systems whether to use intra- or extra-cellular delivery as well as whether to use oral, immersion, or injectable vaccine delivery systems and to develop prime-boost vaccination regimes that confer the highest protection throughout the fish production cycle. Nonetheless, this review shows that OMP subunit, DNA, and PLGA/chitosan nanoparticle vaccines could

form a large proportion of future vaccines for fish bacterial diseases in India.

AUTHOR CONTRIBUTIONS

BM conceptualized the initial draft of the manuscript. SD and HM conceived and reviewed the manuscript. ØE, IdK, and InK revised the manuscript. All authors read and approved publication of the manuscript.

FUNDING

This study was supported by the Department of Science and Technology (DST), Government of India, through the Indo-Norway joint project (INT/NOR/RCN/BIO/P-01/2018) and through the project "Biotechnology applied for controlling diseases in aquaculture in Norway and India" funded by the Research Council of Norway (grant 283566).

REFERENCES

1. FAO. *FAO Yearbook: Fishery and Aquaculture Statistics, 2016* (2018).
2. FAO. *The State of World Fisheries and Aquaculture 2018-Meeting the Sustainable Development Goals* (2018).
3. John N, Abdulla MH. Prevalence, distribution and drug resistance of motile aeromonads in freshwater ornamental fishes. *Indian J Fish.* (2012) 59:161–4.
4. Sahoo P, Swaminathan TR, Abraham TJ, Kumar R, Pattanayak S, Mohapatra A, et al. Detection of goldfish haematopoietic necrosis herpes virus (Cyprinid herpesvirus-2) with multi-drug resistant *Aeromonas hydrophila* infection in goldfish: first evidence of any viral disease outbreak in ornamental freshwater aquaculture farms in India. *Acta Tropica.* (2016) 161:8–17. doi: 10.1016/j.actatropica.2016.05.004
5. Singh AK, Rathore G, Singh V, Mani I, Singh RK, Mishra SK, et al. Bacterial resistance to oxytetracycline in different life stages of Indian freshwater carp aquaculture system. *Int J Microbiol.* (2009) 1:25–34. doi: 10.9735/0975-5276.1.1.25-34
6. Fisheries F. *World Aquaculture 2010: Food and Agriculture Organization of the United Nations* (2011).
7. Novotny L, Dvorska L, Lorencova A, Beran V, Pavlik I. Fish: a potential source of bacterial pathogens for human beings. *A review. J Vet Med.* (2004) 49:343–58. doi: 10.17221/5715-VETMED
8. Jayasankar P. Present status of freshwater aquaculture in India-A review. *Indian J Fish.* (2018) 65:157–65. doi: 10.21077/ijf.2018.65.4.81300-20
9. Katiha PK, Jena J, Pillai N, Chakraborty C, Dey MM. Inland aquaculture in India: past trend, present status and future prospects. *Aquacult Econ Manag.* (2005) 9:237–64. doi: 10.1080/13657300590961573
10. Katiha PK, editor. Freshwater aquaculture in India: Status, potential and constraints. In: *National Centre for Agricultural Economics and Policy Research, Workshop Proceedings*. New Delhi (2000). p. 98–108.
11. Mishra SS, Rakesh D, Dhiman M, Choudhary P, Debbarma J, Sahoo S, et al. Present status of fish disease management in freshwater aquaculture in India: state-of-the-art-review. *J Aquacult Fish.* (2017) 1:003. doi: 10.24966/AAF-5523/100003
12. Behera B, Pradhan P, Swaminathan T, Sood N, Paria P, Das A, et al. Emergence of tilapia lake virus associated with mortalities of farmed Nile tilapia *Oreochromis niloticus* (Linnaeus 1758) in India. *Aquaculture.* (2018) 484:168–74. doi: 10.1016/j.aquaculture.2017.11.025
13. Azad I, Shekhar M, Thirunavukkarasu A, Poornima M, Kailasam M, Rajan J, et al. Nodavirus infection causes mortalities in hatchery produced larvae of *Lates calcarifer*: first report from India. *Dis Aquat Organ.* (2005) 63:113–8. doi: 10.3354/dao063113
14. Swaminathan TR, Kumar R, Dharmaratnam A, Basheer V, Sood N, Pradhan P, et al. Emergence of carp edema virus in cultured ornamental koi carp, *Cyprinus carpio* koi, in India. *J Gen Virol.* (2016) 97:3392–9. doi: 10.1099/jgv.0.000649
15. Girisha S, Puneeth T, Nithin M, Kumar BN, Ajay S, Vinay T, et al. Red sea bream iridovirus disease (RSIVD) outbreak in Asian seabass (*Lates calcarifer*) cultured in open estuarine cages along the west coast of India: First report. *Aquaculture.* (2020) 520:734712. doi: 10.1016/j.aquaculture.2019.734712
16. Sivasankar P, John KR, George MR, Mageshkumar P, Manzoor MM, Jeyaseelan MJP. Characterization of a virulent ranavirus isolated from marine ornamental fish in India. *Virusdisease.* (2017) 28:373–82. doi: 10.1007/s13337-017-0408-2
17. Nayak SK. Current status of *Aeromonas hydrophila* vaccine development in fish: an Indian perspective. *Fish Shellfish Immunol.* (2020) 100:283–99. doi: 10.1016/j.fsi.2020.01.064
18. Das MK, Das RK. A review of the fish disease epizootic ulcerative syndrome in India. *Environ Ecol.* (1993) 11:134–45.
19. Karunasagar I, Rosalind GM, Gopal Rao K. *Aeromonas hydrophila* septicaemia of Indian major carps in some commercial fish farms of West Godavari District, Andhra Pradesh. *Curr Sci (Bangalore).* (1989) 58:1044–5.
20. Mukherjee SC. *Fish Diseases in India, Their Causes and Control Measures - Winter School on Recent Advances in Diagnosis and Management of Diseases in Mariculture, 7th to 27th November 2002, Course Manual.* Central Marine Fisheries Research Institute, Cochin, India (2002).
21. Das BK. *Bacterial Diseases of fish.* Fish Health management, National Training Programme. Central Institute of Freshwater Aquaculture, Bhubaneswar, India (2011).
22. Kumar P, Adikesavalu H, Abraham TJ. Prevalence of *Edwardsiella tarda* in commercially important finfish and shellfish of Bihar and West Bengal, India. *J Coast Life Med.* (2016) 4:30–5. doi: 10.12980/jclm.4.2016apjtd-2014-0184
23. Surendraraj A, Farvin KS, Yathavamoorthi R, Thampuran N. Enteric bacteria associated with farmed freshwater fish and its culture environment in Kerala, India. *Res J Microbiol.* (2009) 4:334–44. doi: 10.3923/jm.2009.334.344
24. Shome R, Shome B, Ram N. Study of virulence factors of *Aeromonas hydrophila* isolates causing acute abdominal dropsy and ulcerative diseases in Indian major carps. *Indian J Fish.* (1999) 46:133–40.
25. Janda JM, Abbott SL. Evolving concepts regarding the genus *Aeromonas*: an expanding panorama of species, disease presentations, and unanswered questions. *Clin Infect Dis.* (1998) 27:332–44. doi: 10.1086/514652
26. Dar G, Kamili A, Chishti M, Dar S, Tantry T, Ahmad F. Characterization of *Aeromonas sobria* isolated from Fish Rohu (*Labeo rohita*) collected from polluted pond. *J Bacteriol Parasitol.* (2016) 7:3. doi: 10.4172/2155-9597.1000273
27. Das A, Rathore A, Janani C, Hemanth C, Balakrishnan R. Diagnosis of motile *Aeromonas sobria* from cat fishes with septicemia by PCR. *IOSR J Appl Phys.* (2013) 2:87–91. doi: 10.9790/2380-0268791
28. Thomas J, Madan N, Nambi K, Majeed SA, Basha AN, Hameed ASS. Studies on ulcerative disease caused by *Aeromonas caviae*-like bacterium in Indian catfish, *Clarias batrachus* (Linn). *Aquaculture.* (2013) 376:146–50. doi: 10.1016/j.aquaculture.2012.11.015
29. Sreedharan K, Philip R, Singh ISB. Characterization and virulence potential of phenotypically diverse *Aeromonas veronii* isolates recovered from moribund freshwater ornamental fishes of Kerala, India. *Antonie Van Leeuwenhoek.* (2013) 103:53–67. doi: 10.1007/s10482-012-9786-z
30. Karunasagar I, Rosalind GM, Gopal Rao K. *Aeromonas hydrophila* septicaemia of Indian major carps in some commercial fish farms of West Godavari District, Andhra Pradesh. *Curr Sci (Bangalore).* (1989) 58:1044–5.
31. Das B. *Bacterial Diseases of Fish*. Fish Health management, National Training Programme. Central Institute of Freshwater Aquaculture, Bhubaneswar, India. (2011).
32. Egusa S. Some bacterial diseases of freshwater fishes in Japan. *Fish Pathol.* (1976) 10:103–14. doi: 10.3147/jsfp.10.103
33. Meyer F, Bullock G. *Edwardsiella tarda*, a new pathogen of channel catfish (*Ictalurus punctatus*). *Appl Microbiol.* (1973) 25:155. doi: 10.1128/AEM.25.1.155-156.1973

34. Dubey S, Maiti B, Kim SH, Sivadasan SM, Kannimuthu D, Pandey PK, et al. Genotypic and phenotypic characterization of *Edwardsiella* isolates from different fish species and geographical areas in Asia: implications for vaccine development. *J Fish Dis.* (2019) 42:835–50. doi: 10.1111/jfd.12984
35. Verma DK, Rathore G. New host record of five *Flavobacterium* species associated with tropical fresh water farmed fishes from North India. *Braz J Microbiol.* (2015) 46:969–76. doi: 10.1590/S1517-838246420131081
36. Prasad Y, Kumar D, Sharma AK. Lytic bacteriophages specific to *Flavobacterium columnare* rescue catfish, *Clarias batrachus* (Linn.) from columnaris disease. *J Environ Biol.* (2011) 32:161–8.
37. Gao X, Pi D, Chen N, Li X, Liu X, Yang H, et al. Survival, virulent characteristics, and transcriptomic analyses of the pathogenic *Vibrio anguillarum* under starvation stress. *Front Cell Infect Microbiol.* (2018) 8:389. doi: 10.3389/fcimb.2018.00389
38. Parveen S, Islam MS, Huq A. Abundance of *Aeromonas* spp. in river and lake waters in and around Dhaka, Bangladesh. *J Diarrhoeal Dis Res.* (1995) 13:183–6.
39. Holmes P, Niccolls LM, Sartory DP. The ecology of mesophilic *Aeromonas* in the aquatic environment. In: Austin B, Altwegg M, Gosling PJ, Joseph S, editors. *The Genus Aeromonas*. West Sussex: Wiley (1996). p. 127–50.
40. Welker TL, Shoemaker CA, Arias CR, Klesius PH. Transmission and detection of *Flavobacterium columnare* in channel *catfish Ictalurus punctatus*. *Dis Aquat Organ*. (2005) 63:129–38. doi: 10.3354/dao063129
41. Karunasagar I, Pai R, Malathi G, Karunasagar I. Mass mortality of *Penaeus monodon* larvae due to antibiotic-resistant *Vibrio harveyi* infection. *Aquaculture.* (1994) 128:203–9. doi: 10.1016/0044-8486(94)90309-3
42. Bower C, Daeschel M. Resistance responses of microorganisms in food environments. *J Int J Food Microbiol.* (1999) 50:33–44. doi: 10.1016/S0168-1605(99)00075-6
43. Sommerset I, Krossøy B, Biering E, Frost P. Vaccines for fish in aquaculture. *Expert Rev Vaccines*. (2005) 4:89–101. doi: 10.1586/14760584.4.1.89
44. Munang'andu HM, Evensen Ø. Correlates of protective immunity for fish vaccines. *Fish Shellfish Immunol.* (2019) 85:132–40. doi: 10.1016/j.fsi.2018.03.060
45. Martín-Martín A, Simón R, Abós B, Díaz-Rosales P, Tafalla C. Rainbow trout mount a robust specific immune response upon anal administration of thymus-independent antigens. *Dev Comp Immunol.* (2020) 109:103715. doi: 10.1016/j.dci.2020.103715
46. Embregts CW, Forlenza M. Oral vaccination of fish: lessons from humans and veterinary species. *Dev Comp Immunol.* (2016) 64:118–37. doi: 10.1016/j.dci.2016.03.024
47. Hirst ID, Ellis AE. Iron-regulated outer membrane proteins of *Aeromonas salmonicida* are important protective antigens in Atlantic salmon against furunculosis. *Fish Shellfish Immunol.* (1994) 4:29–45. doi: 10.1006/fsim.1994.1004
48. Karunasagar I, Ali A, Otta S. Immunization with bacterial antigens: infections with motile aeromonads. *Dev Biol Stand.* (1997) 90:135–41.
49. Munang'andu HM, Mutoloki S, Evensen Ø. Non-replicating vaccines. In: Gudding R, Lillehaug A, Evensen Ø, editors. *Fish Vaccination*. West Sussex: Wiley Blackwell (2014). p. 22–32.
50. Munang'andu HM. Intracellular bacterial infections: a challenge for developing cellular mediated immunity vaccines for farmed fish. *Microorganisms.* (2018) 6:33. doi: 10.3390/microorganisms6020033
51. Schulz GE. β-barrel membrane proteins. *Curr Opin Struct Biol.* (2000) 10:443–7. doi: 10.1016/S0959-440X(00)00120-2
52. Nikaido H. Molecular basis of bacterial outer membrane permeability revisited. *Microbiol Mol Biol Rev.* (2003) 67:593–656. doi: 10.1128/MMBR.67.4.593-656.2003
53. Wimley WC. The versatile β-barrel membrane protein. *Curr Opin Struct Biol.* (2003) 13:404–11. doi: 10.1016/S0959-440X(03)00099-X
54. Bond PJ, Sansom MS. The simulation approach to bacterial outer membrane proteins. *Mol Membr Biol.* (2004) 21:151–61. doi: 10.1080/0968760410001699169
55. Schulz GE. The structure of bacterial outer membrane proteins. *Biochim Biophys Acta.* (2002) 1565:308–17. doi: 10.1016/S0005-2736(02)00577-1
56. Braun G, Cole ST. DNA sequence analysis of the *Serratia marcescens* ompA gene: implications for the organisation of an enterobacterial outer membrane protein. *Mol Gen Genet.* (1984) 195:321–8. doi: 10.1007/BF00332766
57. Koebnik R, Locher KP, Van Gelder P. Structure and function of bacterial outer membrane proteins: barrels in a nutshell. *Mol Microbiol.* (2000) 37:239–53. doi: 10.1046/j.1365-2958.2000.01983.x
58. Maiti B, Raghunath P, Karunasagar I, Karunasagar I. Cloning and expression of an outer membrane protein OmpW of *Aeromonas hydrophila* and study of its distribution in *Aeromonas* spp. *J Appl Microbiol.* (2009) 107:1157–67. doi: 10.1111/j.1365-2672.2009.04296.x
59. Maiti B, Shetty M, Shekar M, Karunasagar I, Karunasagar I. Evaluation of two outer membrane proteins, Aha1 and OmpW of *Aeromonas hydrophila* as vaccine candidate for common carp. *Vet Immunol Immunopathol.* (2012) 149:298–301. doi: 10.1016/j.vetimm.2012.07.013
60. Vàzquez-Juárez RC, Romero MJ, Ascencio F. Adhesive properties of a LamB-like outer-membrane protein and its contribution to *Aeromonas veronii* adhesion. *J Appl Microbiol.* (2004) 96:700–8. doi: 10.1111/j.1365-2672.2004.02177.x
61. Vazquez-Juarez RC, Gomez-Chiarri M, Barrera-Saldaña H, Hernandez-Saavedra N, Dumas S, Ascencio F. Evaluation of DNA vaccination of spotted sand bass (Paralabrax maculatofasciatus) with two major outer-membrane protein-encoding genes from *Aeromonas veronii*. *Fish Shellfish Immunol.* (2005) 19:153–63. doi: 10.1016/j.fsi.2004.12.007
62. Ebanks RO, Goguen M, McKinnon S, Pinto DM, Ross NW. Identification of the major outer membrane proteins of *Aeromonas salmonicida*. *Dis Aquat Organ.* (2005) 68:29–38. doi: 10.3354/dao068029
63. Neema M, Karunasagar I. *In silico* homology modeling and epitope prediction of outer membrane protein OMP W, a potential vaccine candidate against *Edwardsiella tarda*. *Int J Curr Microbiol Appl Sci.* (2018) 41:1349–58. doi: 10.20546/ijcmas.2018.703.319
64. Rappuoli R. Reverse vaccinology. *Curr Opin Microbiol.* (2000) 3:445–50. doi: 10.1016/S1369-5274(00)00119-3
65. Baliga P, Shekar M, Venugopal MN. Potential outer membrane protein candidates for vaccine development against the pathogen *Vibrio anguillarum*: a reverse vaccinology based identification. *J Curr Microbiol.* (2018) 75:368–77. doi: 10.1007/s00284-017-1390-z
66. Viji VT, Deepa K, Velmurugan S, Donio MBS, Jenifer JA, Babu MM, et al. Vaccination strategies to protect goldfish *Carassius auratus* against *Aeromonas hydrophila* infection. *J Dis Aquat Organ.* (2013) 104:45–57. doi: 10.3354/dao02581
67. Kumar G, Rathore G, El-Matbouli M. Outer membrane protein assembly factor YaeT (omp85) and GroEL proteins of *Edwardsiella tarda* are immunogenic antigens for *Labeo rohita* (Hamilton). *J Fish Dis.* (2014) 37:1055–9. doi: 10.1111/jfd.12205
68. Maji S, Mali P, Joardar SN. Immunoreactive antigens of the outer membrane protein of *Aeromonas hydrophila*, isolated from goldfish, *Carassius auratus* (Linn.). *Fish Shellfish Immunol.* (2006) 20:462–73. doi: 10.1016/j.fsi.2005.06.003
69. Behera T, Nanda P, Mohanty C, Mohapatra D, Swain P, Das B, et al. Parenteral immunization of fish, *Labeo rohita* with Poly D, L-lactide-co-glycolic acid (PLGA) encapsulated antigen microparticles promotes innate and adaptive immune responses. *Fish Shellfish Immunol.* (2010) 28:320–5. doi: 10.1016/j.fsi.2009.11.009
70. Rauta PR, Nayak B. Parenteral immunization of PLA/PLGA nanoparticle encapsulating outer membrane protein (Omp) from *Aeromonas hydrophila*: evaluation of immunostimulatory action in *Labeo rohita* (rohu). *Fish Shellfish Immunol.* (2015) 44:287–94. doi: 10.1016/j.fsi.2015.02.007
71. Zhang Y-q, Zhang T-t, Li J-n, Liu X-l, Li L. Design and evaluation of a tandemly arranged outer membrane protein U (OmpU) multi-epitope as a potential vaccine antigen against *Vibrio mimicus* in grass carps (*Ctenopharyngodon idella*). *Vet Immunol Immunopathol.* (2014) 160:61–9. doi: 10.1016/j.vetimm.2014.03.016
72. Behera T, Swain P. Alginate-chitosan-PLGA composite microspheres induce both innate and adaptive immune response through parenteral immunization in fish. *Fish Shellfish Immunol.* (2013) 35:785–91. doi: 10.1016/j.fsi.2013.06.012

73. Khushiramani R, Girisha SK, Karunasagar I, Karunasagar I. Cloning and expression of an outer membrane protein ompTS of *Aeromonas hydrophila* and study of immunogenicity in fish. *Protein Expr Purif.* (2007) 51:303–7. doi: 10.1016/j.pep.2006.07.021
74. Khushiramani R, Girisha SK, Karunasagar I, Karunasagar I. Protective efficacy of recombinant OmpTS protein of *Aeromonas hydrophila* in Indian major carp. *Vaccine.* (2007) 25:1157–8. doi: 10.1016/j.vaccine.2006.10.032
75. Hamod MA, Nithin MS, Shukur YN, Karunasagar I, Karunasagar I. Outer membrane protein K as a subunit vaccine against V. *anguillarum*. *Aquaculture.* (2012) 354-355:107–10. doi: 10.1016/j.aquaculture.2012.03.033
76. Dash P, Sahoo P, Gupta P, Garg L, Dixit AJF. Immune responses and protective efficacy of recombinant outer membrane protein R (rOmpR)-based vaccine of *Aeromonas hydrophila* with a modified adjuvant formulation in rohu (*Labeo rohita*). *Fish Shellfish Immunol.* (2014) 39:512–23. doi: 10.1016/j.fsi.2014.06.007
77. Khushiramani RM, Maiti B, Shekar M, Girisha SK, Akash N, Deepanjali A, et al. Recombinant *Aeromonas hydrophila* outer membrane protein 48 (Omp48) induces a protective immune response against *Aeromonas hydrophila* and *Edwardsiella tarda*. *Res Microbiol.* (2012) 163:286–91. doi: 10.1016/j.resmic.2012.03.001
78. Maiti B, Shetty M, Shekar M, Karunasagar I, Karunasagar I. Recombinant outer membrane protein A (OmpA) of *Edwardsiella tarda*, a potential vaccine candidate for fish, common carp. *Microbiol Res.* (2011) 167:1–7. doi: 10.1016/j.micres.2011.02.002
79. Dubey S, Avadhani K, Mutalik S, Sivadasan S, Maiti B, Paul J, et al. *Aeromonas hydrophila* OmpW PLGA nanoparticle oral vaccine shows a dose-dependent protective immunity in rohu (*Labeo rohita*). *Vaccines.* (2016) 4:21. doi: 10.3390/vaccines4020021
80. Dubey S, Avadhani K, Mutalik S, Sivadasan S, Maiti B, Girisha S, et al. *Edwardsiella tarda* OmpA encapsulated in chitosan nanoparticles shows superior protection over inactivated whole cell vaccine in orally vaccinated fringed-lipped peninsula carp (*Labeo fimbriatus*). *Vaccines.* (2016) 4:40. doi: 10.3390/vaccines4040040
81. Kumar SR, Ahmed VI, Parameswaran V, Sudhakaran R, Babu VS, Hameed ASS. Potential use of chitosan nanoparticles for oral delivery of DNA vaccine in Asian sea bass (*Lates calcarifer*) to protect from *Vibrio* (*Listonella*) *anguillarum*. *Fish Shellfish Immunol.* (2008) 25:47–56. doi: 10.1016/j.fsi.2007.12.004
82. Kumar SR, Parameswaran V, Ahmed VPI, Musthaq SS, Hameed ASS. Protective efficiency of DNA vaccination in Asian seabass (*Lates calcarifer*) against *Vibrio anguillarum*. *Fish Shellfish Immunol.* (2007) 23:316–26. doi: 10.1016/j.fsi.2006.11.005
83. Nielsen H, Tsirigos KD, Brunak S, von Heijne G. A brief history of protein sorting prediction. *Protein J.* (2019) 38:200–16. doi: 10.1007/s10930-019-09838-3
84. Bagos PG, Liakopoulos TD, Spyropoulos IC, Hamodrakas SJ. PRED-TMBB: a web server for predicting the topology of β-barrel outer membrane proteins. *Nucleic Acids Res.* (2004) 32:W400–W4. doi: 10.1093/nar/gkh417
85. Kolaskar A, Tongaonkar PC. A semi-empirical method for prediction of antigenic determinants on protein antigens. *FEBS Lett.* (1990) 276:172–4. doi: 10.1016/0014-5793(90)80535-Q
86. Larsen JEP, Lund O, Nielsen M. Improved method for predicting linear B-cell epitopes. *Immunome Res.* (2006) 2:2. doi: 10.1186/1745-7580-2-2
87. Larsen MV, Lundegaard C, Lamberth K, Buus S, Lund O, Nielsen M. Large-scale validation of methods for cytotoxic T-lymphocyte epitope prediction. *BMC Bioinform.* (2007) 8:424. doi: 10.1186/1471-2105-8-424
88. Andreatta M, Nielsen M. Gapped sequence alignment using artificial neural networks: application to the MHC class I system. *Bioinformatics.* (2016) 32:511–7. doi: 10.1093/bioinformatics/btv639
89. Hansson M, Nygren PA, Ståhl S. Design and production of recombinant subunit vaccines. *Biotechnol Appl Biochem.* (2000) 32:95–107. doi: 10.1042/BA20000034
90. SongLin G, PanPan L, JianJun F, JinPing Z, Peng L, LiHua D. A novel recombinant bivalent outer membrane protein of *Vibrio vulnificus* and *Aeromonas hydrophila* as a vaccine antigen of American eel (*Anguilla rostrata*). *Fish Shellfish Immunol.* (2015) 43:477–84. doi: 10.1016/j.fsi.2015.01.017
91. Luo Z, Fu J, Li N, Liu Z, Qin T, Zhang X, et al. Immunogenic proteins and their vaccine development potential evaluation in outer membrane proteins (OMPs) of *Flavobacterium columnare*. *J Aquacult Fish.* (2016) 1:1–8. doi: 10.1016/j.aaf.2016.10.002
92. Nguyen HT, Nguyen TTT, Chen YC, Vu-Khac H, Wang PC, Chen SC. Enhanced immune responses and effectiveness of refined outer membrane protein vaccines against *Vibrio harveyi* in orange-spotted grouper (*Epinephelus coioides*). *J Fish Dis.* (2018) 41:1349–58. doi: 10.1111/jfd.12828
93. Wang E, Qin Z, Yu Z, Ai X, Wang K, Yang Q, et al. Molecular characterization, phylogenetic, expression, and protective immunity analysis of OmpF, a promising candidate immunogen against *Yersinia ruckeri* infection in channel catfish. *J Front Immunol.* (2018) 9:2003. doi: 10.3389/fimmu.2018.02003
94. Ningqiu L, Junjie B, Shuqin W, Xiaozhe F, Haihua L, Xing Y, et al. An outer membrane protein, OmpK, is an effective vaccine candidate for *Vibrio harveyi* in Orange-spotted grouper (*Epinephelus coioides*). *Fish Shellfish Immunol.* (2008) 25:829–33. doi: 10.1016/j.fsi.2008.09.007
95. Cai S-H, Yaol S-Y, Lu Y-S, Wu Z-H, Jian J-C, Wang B. Immune response in *Lutjanus erythropterus* induced by the major outer membrane protein (OmpU) of *Vibrio alginolyticus*. *Dis Aquat Organ.* (2010) 90:63–8. doi: 10.3354/dao02206
96. Cai SH, Lu YS, Wu ZH, Jian JC. Cloning, expression of *Vibrio alginolyticus* outer membrane protein-OmpU gene and its potential application as vaccine in crimson snapper, *Lutjanus erythropterus* Bloch. *J Fish Dis.* (2013) 36:695–702. doi: 10.1111/jfd.12036
97. Wang Q, Chen J, Liu R, Jia J. Identification and evaluation of an outer membrane protein OmpU from a pathogenic *Vibrio harveyi* isolate as vaccine candidate in turbot (*Scophthalmus maximus*). *Lett Appl Microbiol.* (2011) 53:22–9. doi: 10.1111/j.1472-765X.2011.03062.x
98. Lun J, Xia C, Yuan C, Zhang Y, Zhong M, Huang T, et al. The outer membrane protein, LamB (maltoporin), is a versatile vaccine candidate among the Vibrio species. *Vaccine.* (2014) 32:809–15. doi: 10.1016/j.vaccine.2013.12.035
99. Liu F, Tang X, Sheng X, Xing J, Zhan W. *Edwardsiella tarda* outer membrane protein C: an immunogenic protein induces highly protective effects in flounder (*Paralichthys olivaceus*) against edwardsiellosis. *Int J Mol Sci.* (2016) 17:1117. doi: 10.3390/ijms17071117
100. Yang Q, Pan Y-L, Wang K-Y, Wang J, He Y, Wang E-L, et al. OmpN, outer membrane proteins of *Edwardsiella ictaluri* are potential vaccine candidates for channel catfish (*Ictalurus punctatus*). *Mol Immunol.* (2016) 78:1–8. doi: 10.1016/j.molimm.2016.08.011
101. Abdelhamed H, Ibrahim I, Nho SW, Banes MM, Wills RW, Karsi A, et al. Evaluation of three recombinant outer membrane proteins, OmpA1, Tdr, and TbpA, as potential vaccine antigens against virulent *Aeromonas hydrophila* infection in channel catfish (*Ictalurus punctatus*). *Fish Shellfish Immunol.* (2017) 66:480–6. doi: 10.1016/j.fsi.2017.05.043
102. Yadav SK, Sahoo PK, Dixit A. Characterization of immune response elicited by the recombinant outer membrane protein OmpF of *Aeromonas hydrophila*, a potential vaccine candidate in murine model. *Mol Biol Rep.* (2014) 41:1837–48. doi: 10.1007/s11033-014-3033-9
103. Le H, LiHua D, JianJun F, Peng L, SongLin G. Immunogenicity study of an expressed outer membrane protein U of *Vibrio vulnificus* in Japanese eel (*Anguilla japonica*). *J Appl Microbiol.* (2018) 125:1642–54. doi: 10.1111/jam.14068
104. He L, Wu L, Lin P, Zhai S, Guo S, Xiao Y, et al. First expression and immunogenicity study of a novel trivalent outer membrane protein (OmpII-UA) from *Aeromonas hydrophila*, *Vibrio vulnificus* and *Edwardsiella anguillarum*. *Aquaculture.* (2020) 519:734932. doi: 10.1016/j.aquaculture.2020.734932
105. Guo S, He L, Wu L, Xiao Y, Zhai S, Yan Q. Immunization of a novel bivalent outer membrane protein simultaneously resisting *Aeromonas hydrophila*, *Edwardsiella anguillarum* and *Vibrio vulnificus* infection in European eels (*Angullia angullia*). *Fish Shellfish Immunol.* (2020) 97:46–57. doi: 10.1016/j.fsi.2019.12.044
106. Sharma M, Dixit A. Identification and immunogenic potential of B cell epitopes of outer membrane protein OmpF of *Aeromonas hydrophila* in translational fusion with a carrier protein. *Appl Microbiol Biotechnol.* (2015) 99:6277–91. doi: 10.1007/s00253-015-6398-3

107. Upadhyaya T, Singh RK, Upadhyaya T, Singh RK, Dixit A. Molecular cloning and sequence analysis of lamB encoding outer membrane maltose-inducible porin of *Aeromonas hydrophila*: full length research paper. *DNA Seq.* (2007) 18:302–6. doi: 10.1080/10425170701248608
108. Sharma M, Dixit A. Immune response characterization and vaccine potential of a recombinant chimera comprising B-cell epitope of *Aeromonas hydrophila* outer membrane protein C and LTB. *Vaccine.* (2016) 34:6259–66. doi: 10.1016/j.vaccine.2016.10.064
109. Mahendran R, Jeyabaskar S, Sitharaman G, Michael RD, Paul AV. Computer-aided vaccine designing approach against fish pathogens *Edwardsiella tarda* and *Flavobacterium columnare* using bioinformatics softwares. *Drug Des Dev Ther.* (2016) 10:1703. doi: 10.2147/DDDT.S95691
110. Neema M, Karunasagar I, Karunasagar I. Structural and functional characterization of outer membrane protein N in *Edwardsiella ictaluri*: a bioinformatic approach. *Intl J Pharm Sci Res.* (2011) 2:13–26.
111. Bader JA, Shoemaker CA, Klesius PH. Immune response induced by N-lauroylsarcosine extracted outer-membrane proteins of an isolate of Edwardsiella ictaluri in channel catfish. *Fish Shellfish Immunol.* (2004) 16:415–28. doi: 10.1016/j.fsi.2003.07.003
112. Wang N, Yang Z, Zang M, Liu Y, Lu C. Identification of Omp38 by immunoproteomic analysis and evaluation as a potential vaccine antigen against *Aeromonas hydrophila* in Chinese breams. *Fish Shellfish Immunol.* (2013) 34:74–81. doi: 10.1016/j.fsi.2012.10.003
113. Liu MA. DNA vaccines: a review. *J Intern Med.* (2003) 253:402–10. doi: 10.1046/j.1365-2796.2003.01140.x
114. Munang'andu HM, Evensen Ø. A review of intra-and extracellular antigen delivery systems for virus vaccines of finfish. *J Immunol Res.* (2015) 2015:960859. doi: 10.1155/2015/960859
115. Yamasaki M, Araki K, Nakanishi T, Nakayasu C, Yamamoto A. Role of $CD4^+$ and $CD8\alpha^+$ T cells in protective immunity against *Edwardsiella tarda* infection of ginbuna Crucian carp, *Carassius auratus* langsdorfii. *Fish Shellfish Immunol.* (2014) 36:299–304. doi: 10.1016/j.fsi.2013.11.016
116. Mutoloki S, Alexandersen S, Evensen Ø. Sequential study of antigen persistence and concomitant inflammatory reactions relative to side-effects and growth of Atlantic salmon (*Salmo salar* L.) following intraperitoneal injection with oil-adjuvanted vaccines. *Fish Shellfish Immunol.* (2004) 16:633–44. doi: 10.1016/j.fsi.2003.10.002
117. Rogan D, Babiuk L. Novel vaccines from biotechnology. *Rev Sci Tech.* (2005) 24:159. doi: 10.20506/rst.24.1.1561
118. Makadia HK, Siegel SJ. Poly lactic-co-glycolic acid (PLGA) as biodegradable controlled drug delivery carrier. *Polymers.* (2011) 3:1377–97. doi: 10.3390/polym3031377
119. Akagi T, Baba M, Akashi M. Biodegradable nanoparticles as vaccine adjuvants and delivery systems: regulation of immune responses by nanoparticle-based vaccine. *Polym Nanomed.* (2011) 247:31–64. doi: 10.1007/12_2011_150
120. Borchard G, Esmaeili F, Heuking S. Chitosan-based delivery systems for mucosal vaccination. In: Sarmento B, Das Nevas J, editors. *Chitosan-Based Systems for Biopharmaceuticals: Delivery, Targeting Polymer Therapeutics.* John Wiley & Sons, Ltd. (2012). p. 211–24.
121. Newman KD, Elamanchili P, Kwon GS, Samuel J. Uptake of poly(D,L-lactic-co-glycolic acid) microspheres by antigen-presenting cells in vivo. *J Biomed Mater Res.* (2002) 60:480–6. doi: 10.1002/jbm.10019
122. Prior S, Gander B, Blarer N, Merkle HP, Subirá MaL, Irache JM, et al. *In vitro* phagocytosis and monocyte-macrophage activation with poly(lactide) and poly(lactide-co-glycolide) microspheres. *Eur J Pharm Sci.* (2002) 15:197–207. doi: 10.1016/S0928-0987(01)00218-4
123. Diwan M, Elamanchili P, Lane H, Gainer A, Samuel J. Biodegradable nanoparticle mediated antigen delivery to human cord blood derived dendritic cells for induction of primary T cell responses. *J Drug Target.* (2003) 11:495–507. doi: 10.1080/10611860410001670026
124. Elamanchili P, Lutsiak CME, Hamdy S, Diwan M, Samuel J. "Pathogen-mimicking" nanoparticles for vaccine delivery to dendritic cells. *J Immunother.* (2007) 30:378–95. doi: 10.1097/CJI.0b013e31802cf3e3
125. Waeckerle-Men Y, Groettrup M. PLGA microspheres for improved antigen delivery to dendritic cells as cellular vaccines. *Adv Drug Deliv Rev.* (2005) 57:475–82. doi: 10.1016/j.addr.2004.09.007
126. Desai MP, Labhasetwar V, Walter E, Levy RJ, Amidon GL. The Mechanism of uptake of biodegradable microparticles in caco-2 cells is size dependent. *Pharm Res.* (1997) 14:1568–73. doi: 10.1023/A:1012126301290
127. Calvo P, Remuñan-López C, Vila-Jato JL, Alonso MJ. Chitosan and chitosan/ethylene oxide-propylene oxide block copolymer nanoparticles as novel carriers for proteins and vaccines. *Pharm Res.* (1997) 14:1431–6. doi: 10.1023/A:1012128907225
128. Panyam J, Dali MM, Sahoo SK, Ma W, Chakravarthi SS, Amidon GL, et al. Polymer degradation and *in vitro* release of a model protein from poly (D, L-lactide-co-glycolide) nano-and microparticles. *J Control Release.* (2003) 92:173–87. doi: 10.1016/S0168-3659(03)00328-6
129. Sahana D, Mittal G, Bhardwaj V, Kumar MR. PLGA nanoparticles for oral delivery of hydrophobic drugs: influence of organic solvent on nanoparticle formation and release behavior *in vitro* and *in vivo* using estradiol as a model drug. *J Pharm Sci.* (2008) 97:1530–42. doi: 10.1002/jps.21158
130. Fitzgerald KA, Rowe DC, Golenbock DT. Endotoxin recognition and signal transduction by the TLR4/MD2-complex. *Microbes Infect.* (2004) 6:1361–7. doi: 10.1016/j.micinf.2004.08.015
131. Zollinger W, Mandrell R, Altieri P, Berman S, Lowenthal J, Artenstein MS. Safety and immunogenicity of a *Neisseria meningitidis* type 2 protein vaccine in animals and humans. *J Infect Dis.* (1978) 137:728–39. doi: 10.1093/infdis/137.6.728
132. Zariri A, Pupo E, Van Riet E, Van Putten JP, van der Ley P. Modulating endotoxin activity by combinatorial bioengineering of meningococcal lipopolysaccharide. *Sci Rep.* (2016) 6:36575. doi: 10.1038/srep36575
133. Zariri A, van der Ley P. Biosynthetically engineered lipopolysaccharide as vaccine adjuvant. *Expert Rev Vaccines.* (2015) 14:861–76. doi: 10.1586/14760584.2015.1026808
134. Leitner DR, Feichter S, Schild-Prüfert K, Rechberger GN, Reidl J, Schild S, et al. Lipopolysaccharide modifications of a cholera vaccine candidate based on outer membrane vesicles reduce endotoxicity and reveal the major protective antigen. *Infect Immun.* (2013) 81:2379–93. doi: 10.1128/IAI.01382-12
135. Watkins HC, Rappazzo CG, Higgins JS, Sun X, Brock N, Chau A, et al. Safe recombinant outer membrane vesicles that display M2e elicit heterologous influenza protection. *Mol Ther.* (2017) 25:989–1002. doi: 10.1016/j.ymthe.2017.01.010
136. Gerritzen MJ, Martens DE, Wijffels RH, van der Pol L, Stork M. Bioengineering bacterial outer membrane vesicles as vaccine platform. *Biotechnol Adv.* (2017) 35:565–74. doi: 10.1016/j.biotechadv.2017.05.003
137. Galen JE, Curtiss R 3rd. The delicate balance in genetically engineering live vaccines. *Vaccine.* (2014) 32:4376–85. doi: 10.1016/j.vaccine.2013.12.026
138. Apostólico JdS, Lunardelli VAS, Coirada FC, Boscardin SB, Rosa DS. Adjuvants: classification, modus operandi, and licensing. *J Immunol Res.* (2016) 2016:1459394. doi: 10.1155/2016/1459394
139. Munang'andu HM, Mutoloki S, Evensen Ø. An overview of challenges limiting the design of protective mucosal vaccines for finfish. *Front Immunol.* (2015) 6:542. doi: 10.3389/fimmu.2015.00542

Conflict of Interest: The authors declare that the research was conducted in the absence of any commercial or financial relationships that could be construed as a potential conflict of interest.

Copyright © 2020 Maiti, Dubey, Munang'andu, Karunasagar, Karunasagar and Evensen. This is an open-access article distributed under the terms of the Creative Commons Attribution License (CC BY). The use, distribution or reproduction in other forums is permitted, provided the original author(s) and the copyright owner(s) are credited and that the original publication in this journal is cited, in accordance with accepted academic practice. No use, distribution or reproduction is permitted which does not comply with these terms.

Advantages of publishing in Frontiers

OPEN ACCESS
Articles are free to read for greatest visibility and readership

FAST PUBLICATION
Around 90 days from submission to decision

HIGH QUALITY PEER-REVIEW
Rigorous, collaborative, and constructive peer-review

TRANSPARENT PEER-REVIEW
Editors and reviewers acknowledged by name on published articles

Frontiers
Avenue du Tribunal-Fédéral 34
1005 Lausanne | Switzerland

Visit us: www.frontiersin.org
Contact us: info@frontiersin.org | +41 21 510 17 00

REPRODUCIBILITY OF RESEARCH
Support open data and methods to enhance research reproducibility

DIGITAL PUBLISHING
Articles designed for optimal readership across devices

FOLLOW US
@frontiersin

IMPACT METRICS
Advanced article metrics track visibility across digital media

EXTENSIVE PROMOTION
Marketing and promotion of impactful research

LOOP RESEARCH NETWORK
Our network increases your article's readership